Environmental Assessment of the Alaskan Continental Shelf

Annual Reports of Principal Investigators for the year ending March 1981

Volume III: Effects of Contaminants

U.S. DEPARTMENT OF COMMERCE
National Oceanic & Atmospheric Administration
Office of Marine Pollution Assessment

U.S. DEPARTMENT OF INTERIOR
Bureau of Land Management

Annual Reports of Principal Investigators

1981

Environmental Assessment of the Alaskan Continental Shelf

Annual Reports of Principal Investigators for the year ending March 1981

Volume III: Effects of Contaminants

U.S. DEPARTMENT OF COMMERCE
National Oceanic & Atmospheric Administration
Office of Marine Pollution Assessment

U.S. DEPARTMENT OF INTERIOR
Bureau of Land Management

The facts, conclusions and issues appearing in these reports are based on interim results of an Alaskan environmental studies program managed by the Outer Continental Shelf Environmental Assessment Program (OCSEAP) of the National Oceanic and Atmospheric Administration (NOAA), U.S. Department of Commerce, and primarily funded by the Bureau of Land Management (BLM), U.S. Department of Interior, through interagency agreement.

TABLE OF CONTENTS

Volume 3: Effects of Contaminants

Annual Report

Contract No. NA80RAC00018
Research Unit No. 597

Multivariate Analysis of Petroleum Weathering in the Marine Environment - Sub Arctic

Submitted by:

James R. Payne, Bruce E. Kirstein, Randolph E. Jordan, G. Daniel McNabb, Jr., James L. Lambach, Marck Frydrych, William J. Paplawsky, Gary S. Smith, Paul J. Mankiewicz, Robert T. Redding, Daniel M. Baxter, Robert E. Spenger, Robert F. Shokes, and David J. Maiero

James R. Payne, Principal Investigator
Division of Environmental Chemistry and Geochemistry
Science Applications, Inc.
La Jolla, California 92038

November 5, 1981

TABLE OF CONTENTS

TABLE OF CONTENTS (Continued)

TABLE OF CONTENTS (Continued)

LIST OF TABLES

LIST OF TABLES (Continued)

LIST OF TABLES (Continued)

LIST OF TABLES (Continued)

LIST OF FIGURES

LIST OF FIGURES (Continued)

LIST OF FIGURES (Continued)

LIST OF FIGURES (Continued)

LIST OF FIGURES (Continued)

LIST OF FIGURES (Continued)

LIST OF FIGURES (Continued)

LIST OF FIGURES (Continued)

LIST OF FIGURES (Continued)

LIST OF FIGURES (Continued)

ACKNOWLEDGMENTS

This report represents the sustained efforts of many people in various capacities over a period of many months. Various consultants have contributed greatly to this report. N. L. Guinasso of Texas A&M provided initial guidance and review of existing oil-weathering models. Professor D. Mackay of the University of Toronto has contributed extensively through his decade of experience in oil-weathering, and we draw upon this vast experience for mass transfer, slick spreading and water-in-oil emulsification. Professor S. Middleman of the University of California at San Diego contributed extensively on the topics of diffusion coefficients and the state of mixedness of an oil slick. His contributions are presented in Sections 4.6.2 and 4.6.3. Dr. Fred Su at SAI provided some of the detailed mathematical derivations involving component-specific transport phenomena. Gas chromatography/mass spectrometry analyses were completed by John Nemmers and Norm Flynn. Drs. Osmond Holm-Hansen and Farooq Azam of Scripps Institute of Oceanography have been instrumental in the development and execution of experiments designed to examine the microbial degradation of spilled petroleum under simulated environmental conditions.

Logistics support in conducting the sub-arctic field and laboratory programs at Kasitsna Bay was provided by Russ Gaegel, resident manager of the Kasitsna Bay, Alaska, NOAA-facility. Beth Heffernan, Karen Meyers and Marinee Payne also provided laboratory assistance at Kasitsna Bay.

The photographic prints and reproductions of all capillary gas chromatograms presented in this report were prepared by Larry Haines. Suzanne Goldman, Mabel O'Byrne and Mary Williams produced the final copy of this report on the word-processor, and along with Erika Franklin aided in its final reproduction and compilation. Cheryl Fish typed the original draft manuscipts, prepared many of the figures and tables presented, and provided overall management of the production of the report in its final form.

These people are all extended a special note of thanks; the efforts put forth by each were far above ordinary expectations.

1.0 INTRODUCTION

Oil is a complex mixture of hydrocarbons and heterocyclic molecules which, when introduced into the marine environment, undergoes differential dissolution and evaporation, adsorption onto particulate material, photo-oxidation and biological degradation. Additionally, oil as a bulk material is subject to the combined processes of dispersion into the water column and the formation of water-in-oil emulsions (mousse). The magnitude of these processes and their varying rates are dependent upon the specific chemical materials involved and on such "environmental" factors as turbulence, air and water temperature, particulate type and concentration, oil composition, light intensity, and microbial composition and abundance. The purpose of this program has been to investigate the physical and chemical changes which occur to spilled petroleum in the marine environment as a result of the combined actions of these abiotic and biotic factors. Among the processes being examined and quantified are: evaporation, dissolution, microbial oxidation, photo-chemical oxidation, emulsification (mousse formation), adsorption onto particulate material, and the influence of a commercial dispersant on these processes.

Our investigations have been designed to provide qualitative and quantitative information on the fates of specific compounds during oceanic weathering. Ultimately, the goal of this program is to generate a combined component-specific and pseudo-component (boiling point or distillation "cut") model to simulate and predict spilled petroleum behavior as a result of physical/chemical weathering. These models are being developed to encompass specific compound partitioning as well as overall oil mass balance considerations, and they are being tested with observed chemical changes from laboratory and field experiments. The algorithms which make up the computerized model can then be used in a predictive manner to determine the time-dependent chemical compositions and properties of real or simulated oil spills. When coupled to trajectory models, such a physical-chemical weathering model should allow environmental managers to better estimate the impacts from real and

hypothetical oil spill situations. Furthermore, a thorough understanding of the time-dependent compositions and concentrations of spilled petroleum mixtures (including their marine weathering products) will aid in extrapolating the findings from biological effects experiments to real environmental situations.

While this study was initially designed to be an experimental and modeling effort confined to SAI's La Jolla facilities, it was feasible to expand the program to include field studies in the Alaskan subarctic environment of NOAA's Kasitsna Bay laboratory facilities near Homer. At this facility, experiments designed to simulate and quantify open ocean evaporation, dissolution, and microbial and photochemical oxidation processes have been ongoing. Also, in conjunction with other NOAA contractors (Drs. Griffiths and Morita; RU190), experiments designed to evaluate the long-term chemical fate of fresh and weathered oil in sub-tidal sediments have been conducted.* During the most recent field studies at Kasitsna Bay (summer 1981) experiments to examine the long-term chemical fate of fresh oil and mousse in different intertidal regimes were also begun.

As part of our ongoing research into the mechanisms of marine oil weathering, SAI scientists and engineers have continued to participate in several NOAA and BLM-sponsored reviews including: MARINE OIL POLLUTION: FEDERAL PROGRAM REVIEW, conducted for the Inter-agency Committee on Ocean Pollution Research, Development and Monitoring (COPRDM), held in Boulder, Colorado, September 1980; the St. George Basin Synthesis meetings held in Anchorage, Alaska, April 1981; and the National Academy of Sciences Review and Update on the Fate of Petroleum in the Marine Environment, to be held in November, 1981. Background papers were prepared for each of these sessions and are available.

*Since the information on long-term fate of sedimented oil is pertinent to the overall goals of this program, the results of our efforts with Griffiths and Morita are included as Appendix C of this report.

Many of the results from our multivariant petroleum weathering program have been discussed in detail in interim and progress reports and, therefore, will be repeated herein only as necessary to provide continuity among the key topics being addressed. This report is intended to be an independent document summarizing the program's activities to date, however, it relies in part on the interested expert having access to the preceding progress reports, which have been provided to NOAA's technical monitor. This "annual" report consists of major sections which deal with the modeling and experimental activities as well as updates on our progress in understanding the separate and net effects that the various weathering mechanisms have on spilled oil composition and component distribution.

2.0 TOPICAL SUMMARY OF PROGRAM ACTIVITIES

The following outline presents the major program segments and their activities to date in order to provide an overview of the multivariant analysis approach which has been used to generate physical properties data on oil weathering and to formulate an oil weathering simulation model. As mentioned previously, detailed results from many of these activities have been presented in several progress reports; these are contained, along with more recent accomplishments, in subsequent discussions herein in varying levels of detail as needed to present the program's achievements to date.

Oil Weathering Model Development

- Mechanisms for handling laboratory and field derived compound specific data have been developed. Time-series reduced gas chromatographic data on specific observed compound concentrations in oil and water have been compared directly to computer-model predictions.

- All reduced gas chromatographic data from oil, water and SPM samples analyzed in La Jolla and/or NOAA's laboratory facility at Kasitsna Bay, Alaska, are now incorporated into SAI's DEC-10 computer which is being used for the oil weathering model. Observed vs predicted component-specific weathering alterations can be evaluated for a wide variety of field and laboratory "environmental" conditions.

- It has become apparent that two submodels - one which is component-specific and one which "weathers" oil in pseudo-components (distillation cuts) - are required to give adequate mass/volume and viscosity/density predictions in addition to providing component concentration information. Algorithms for both approaches have been developed and are presented in this report.

- Pertinent compound-specific and distillation-cut physical property parameter requirements have been defined (Henry's law constants, diffusivities and mass transfer coefficients), and experiments have been conducted to provide needed data.

- Algorithms have been developed to model the following oil weathering processes:

- Compound-specific evaporation and dissolution in laboratory stirred tanks.

- Pseudo-compound evaporation from ocean surface using various literature sources for mass transfer coefficients.

- Compound-specific evaporation from a semi-infinite slick.

- Compound-specific evaporation from a finite slick.

- Compound-specific dissolution from a semi-infinite slick.

- Computer codes have been written for all the algorithms which are currently in final form. These are being used to compare experimental with theoretical projections, with refinement continuing as necessary.

Oil Characterization

- Liquid-solid column chromatography (L/C) fractionation, capillary gas chromatography (GC), capillary gas chromatography/mass spectrometry (GC/MS), synchronous-scanning UV-fluorescence, distillation cut, viscosity and trace element data were obtained on four selected crude oils (Murban, Cook Inlet, Prudhoe Bay, and Wilmington Crude).

- Prudhoe Bay crude was selected for further analysis and oil weathering studies.

Weathering Processes Investigated Using Prudhoe Bay Crude Oil

- Experiments have been undertaken to obtain laboratory and field rate data on the following oil weathering processes.

  - Compound-specific evaporation/dissolution as a function of temperature and the presence or absence of a commercial dispersing agent (Corexit 9527).

  - Microbial degradation as a function of nutrient concentrations, the presence or absence of oil, microbial population dynamics, and the source of water (La Jolla vs. Kasitsna Bay) for continuous flow indoor and outdoor aquaria.

  - Water-in-oil emulsion (mousse) formation as measured by emulsion stability, kinematic viscosity and density in mousse generated in an ambient-environment outdoor wave tank constructed at Kasitsna Bay.

- Static equilibrium experiments have been undertaken to determine:

  - Liquid-liquid partition coefficients of individual components between oil and seawater as a function of temperature (data required for dissolution algorithms of computer model).

  - Partition coefficients of individual oil components between seawater and five representative suspended particulate material types isolated from selected Cook Inlet sediments (required for oil/SPM interaction algorithms).

  - Effect of oil on selected SPM sinking rates as a function of particle type and seawater/oil temperature.

  - Identification of microbial oxidation products by GC/MS analyses (with and without prior derivatization). Rate data on oxidation product formation are being obtained from flow-through rate experiments referred to above.

- Limited photochemical oxidation experiments have been conducted using simulated irradiation of oil/seawater and oil/seawater/dispersant mixtures in quartz tubes; numerious oxidation products have been tentatively identified by GC/MS analysis.*

Kasitsna Bay Laboratory

- To obtain more valid oil weathering process data representing the subarctic marine environment, a certain amount of field experimentation is necessary to evaluate the effects of specific parameters such as microbial population densities, variable air/water temperature gradients, ambient nutrient and SPM levels, solar radiation input, rainfall, snowfall and other similar factors which cannot be properly simulated in laboratory environments. Recognizing this, after the laboratory and modeling activities had begun in La Jolla, NOAA and SAI investigators designed a major project expansion which would utilize NOAA's Kasitsna Bay, Alaska, facility. A geochemistry laboratory was established there by SAI chemists and indoor and outdoor aquaria and test tank facilities were constructed.

- All necessary facilities improvements were completed in August 1980 and oil weathering studies in the outdoor and indoor aquaria were initiated in September 1980. Several outdoor tanks were allowed to undergo long-term subarctic ambient weathering

*Due to limitations in resources, further investigation of this area has been postponed to subsequent periods of the program.

from October 1980 through April 1981. Periodic samples from the outdoor flow-through systems were collected; and the analyses of these and the other samples collected during the Spring 1981 (April) field program are presented. An additional set of outdoor experiments evaluating evaporation/dissolution and microbial processes were initiated to evaluate seasonal (Spring/Summer) perturbations to oil weathering behavior, and results from these studies are also considered.

- The Kasitsna Bay facility was re-occupied in August 1981 and during the Summer/Fall 1981 program, further additions were undertaken and completed, providing a 2,500 liter outdoor wave tank to allow more realistic simulation of subarctic, open ocean oil weathering in the presence of 6- to 10-inch standing- and breaking-wave turbulence. Additional details on the wave tank experiments, extensive summer/fall microbial degradation experiments, oil/suspended particulate material interaction studies and *in situ* chemical weathering studies of stranded oil in selected intertidal regimes are presented herein.

3.0 OIL CHARACTERIZATION

At the onset of the program, four crude oils (representative of a wide variety of oil types) including two crudes produced in Alaska, were selected for detailed chemical analyses. The ultimate purpose of this investigation was to select one of the four crudes for additional detailed weathering characterizations. Crude oils are a naturally occurring complex mixture of organic and inorganic compounds, and the properties of a given crude are dependent upon the original depositional environment, the hydrocarbon sources and the degree of post-depositional maturation and migration. In general, most crudes can be classified into three categories:

- paraffin-based, exemplified by the continental crudes of the mid-United States,
- asphalt-based such as crudes produced in California and the Gulf of Mexico coast of the United States,
- mixed-base crudes such as those from the Middle East and Alaska.

Since the objective of this program is to arrive at a computer model which is applicable to a wide variety of crude petroleums it might be advantageous to select at least one crude from each of the three classes (i.e., paraffin, asphaltic and mixed base). However, the paraffin-based crudes of the first category are not as likely to be involved in contamination of the marine environment, and these crudes have relatively low levels of aromatic compounds, which include the most toxic constituents of crude oil. For these reasons paraffin-based crudes were not included in this study.

Table 3-1 presents gross characterization parameters of the four selected crude oils examined in this study. These include: 1) a relatively high API gravity (lower specific gravity) Murban crude which is designated as an intermediate type or mixed-base crude - this particular crude oil has less sulfur and asphaltic material than most other Middle-East crudes (Evaluation of the World's Important Crudes, 1973); 2) a slightly lower API gravity crude

TABLE 3-1. GROSS CHARACTERIZATIONS OF FOUR SELECTED WHOLE CRUDE OILS.

Crude Oil	API* Gravity	Specific Gravity g/ml	Viscosity(100°F)* Kinematic cST	Viscosity(100°F)* Saybolt SUS	Pour Pt** °F	% Asphalt***	Ni **** ppm	V **** ppm	S **** %	N **** %
Murban, Aba Dhabi	40.5*	0.829	2.8	35.9	-20	7	3.0	9.9	0.96	0.10
Cook Inlet, Alaska	35.4	0.848	17	85	-15	12	1.3	0.47	0.09	0.11
Prudhoe Bay, Alaska	27.0	0.893	19	84	-10	23	13.5	28.3	0.98	0.27
Wilmington, Calif.	19.4	0.938	100	470	<5*	24	100	80.6	1.8	0.83

Sources:

* Coleman, et al. 1978

** Evaluation of Worlds Important Crudes, 1973

*** Calculated from Conradson carbon value, Coleman et al., 1978

**** Ni, V, S, and N: this study

from Cook Inlet, Alaska, which is representative of oils produced in the sub-arctic environment and which by nature of its production and transport might be expected to be released at sea; 3) a lower API gravity Prudhoe Bay crude oil which would have a high probability of release in arctic regimes during production and in sub-arctic environments during transport and storage; and 4) a low API gravity crude from Wilmington, CA. The data in Table 3-1 illustrate that as the API gravity decreases (density increases) the viscosities of the whole crudes generally increase and the pour points are observed to rise. Percent asphalt content is also observed to increase in going from the higher to lower API gravity crudes selected. Nickel, vanadium, sulfur and nitrogen contents are more variable among the crudes (data generated as part of this study); however, general increases in trace element concentrations are also observed in the trend from higher to lower API gravities. These considerations are important in that asphalts and the presence of trace elements such as nickel, vanadium and sulfur have been implicated in stabilization of water-in-oil emulsions (PAYNE, 1981) and as such, their presence or absence might also be a factor in selecting one representative crude for additional oil weathering studies.

In addition to the whole-crude physical property characterizations and trace element data presented in Table 3-1, each of these four oils was further characterized by separation into aliphatic, aromatic and polar fractions by liquid-solid (silica gel) column chromatography (see Methods, Appendix B), and each fraction was then examined by fused silica capillary column gas chromatography (flame ionization detector) and capillary column gas chromatograph/mass spectrometry (GC/MS). Figures 3-1 through 3-4 present the capillary column gas chromatograms obtained on the fractionated Murban, Cook Inlet, Prudhoe Bay and Wilmington Crude Oils, respectively. As the figures illustrate, the first three crudes are characterized by a regularly repeating series of n-alkanes and branched and cyclic hydrocarbons in the aliphatic fraction, whereas the Wilmington crude is characterized only by a large Unresolved Complex Mixture (UCM). Likewise, the aromatic fractions from Murban, Cook Inlet, and Prudhoe Bay crudes are very similar (Figures 3-1B

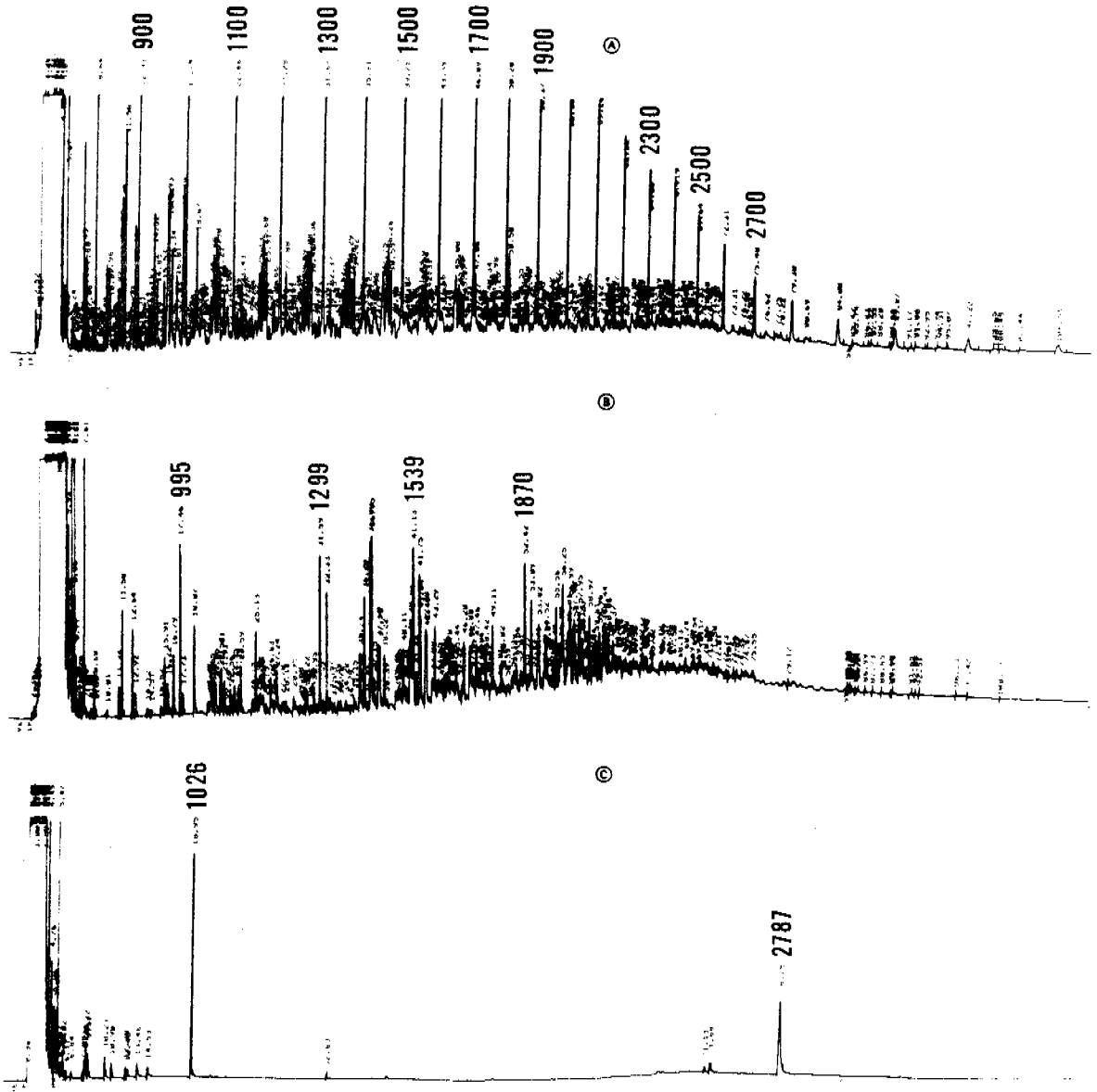

FIGURE 3-1. FLAME IONIZATION DETECTOR CAPILLARY GAS CHROMATOGRAMS OBTAINED ON L/C FRACTIONATED MURBAN CRUDE OIL: (A) ALIPHATIC FRACTION (F1); (B) AROMATIC FRACTION (F2); (C) POLAR FRACTION (F3). (KOVAT RETENTION INDICES ARE SHOWN ABOVE SELECTED PEAKS).

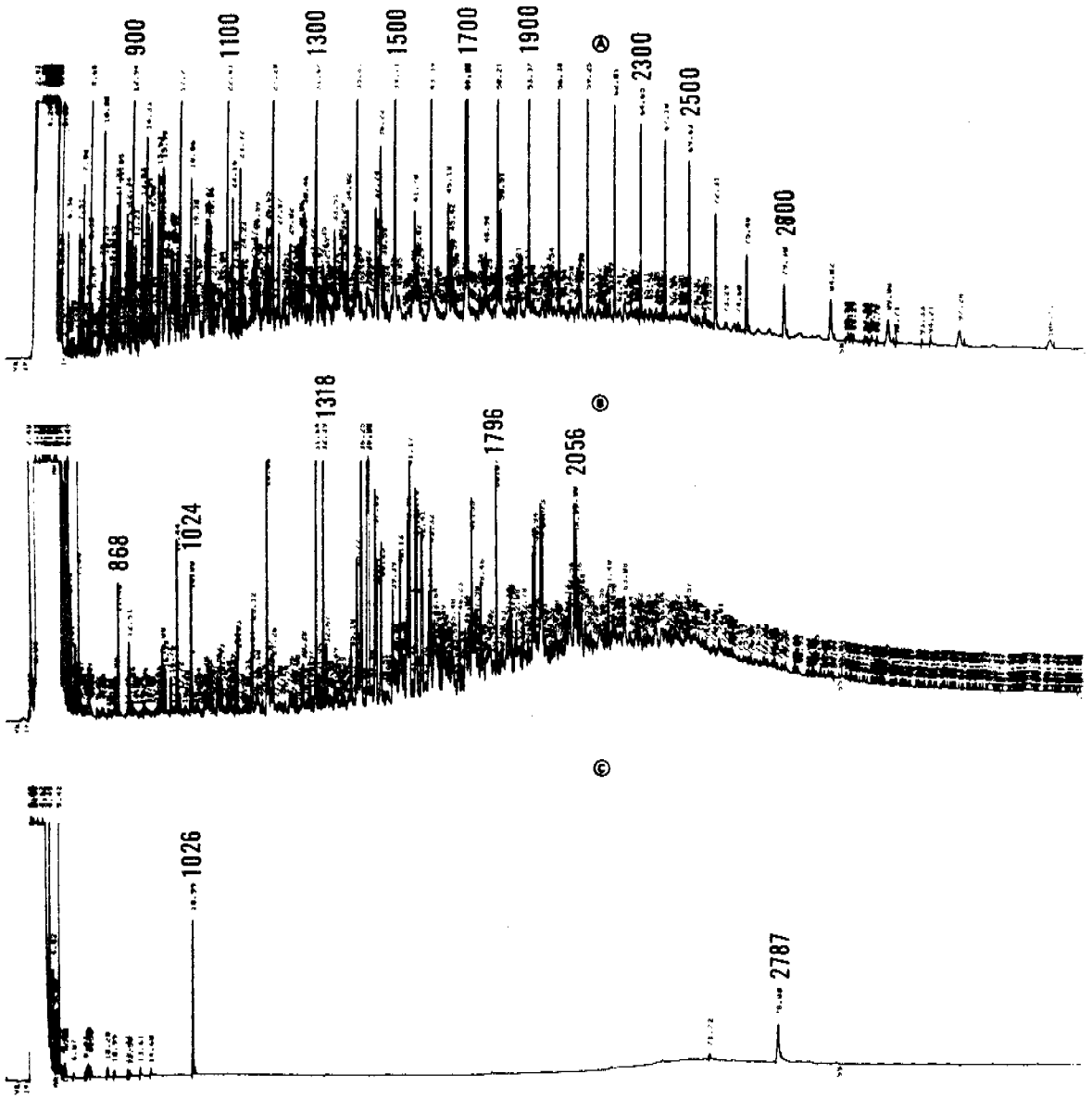

FIGURE 3-2. FLAME IONIZATION DETECTOR CAPILLARY GAS CHROMATOGRAMS OBTAINED ON L/C FRACTIONATED COOK INLET CRUDE OIL: (A) ALIPHATIC FRACTION (F1); (B) AROMATIC FRACTION (F2); (C) POLAR FRACTION (F3). (KOVAT RETENTION INDICES ARE SHOWN ABOVE SELECTED PEAKS).

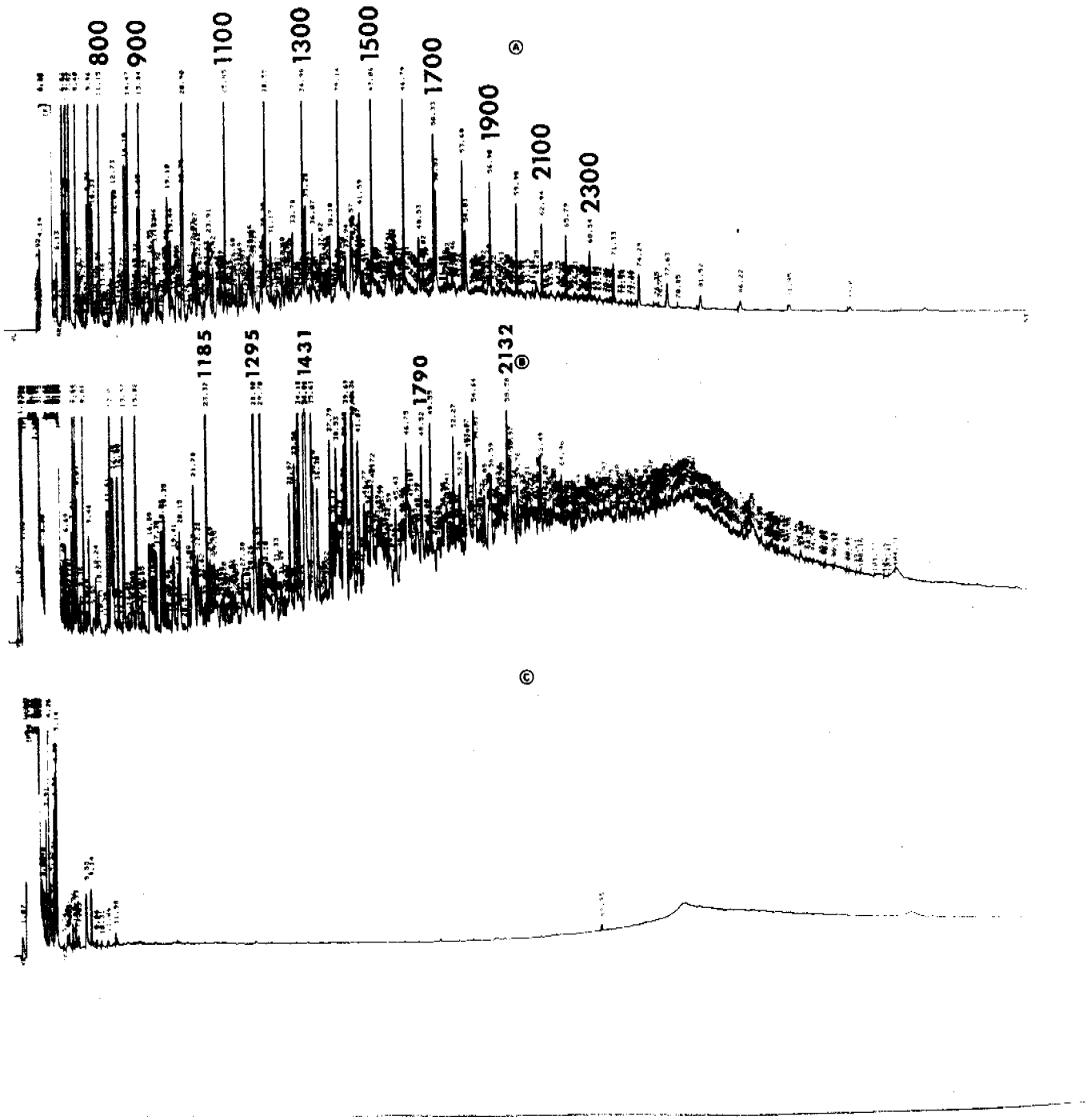

FIGURE 3-3. FLAME IONIZATION DETECTOR CAPILLARY GAS CHROMATOGRAMS OBTAINED ON L/C FRACTIONATED PRUDHOE BAY CRUDE OIL: (A) ALIPHATIC FRACTION (F1); (B) AROMATIC FRACTION (F2); (C) POLAR FRACTION (F3). (KOVAT RETENTION INDICES ARE SHOWN ABOVE SELECTED PEAKS).

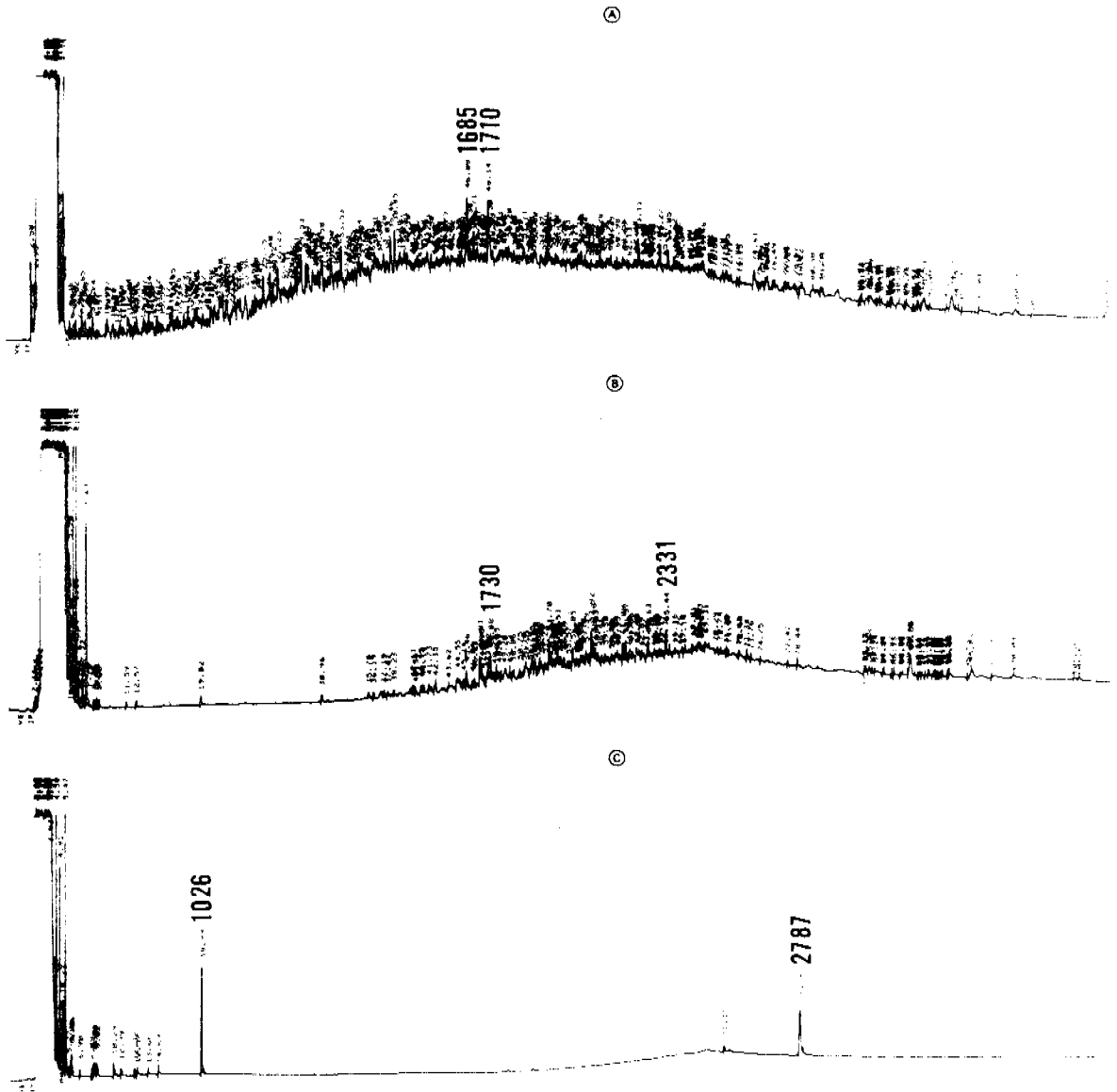

FIGURE 3-4. FLAME IONIZATION DETECTOR CAPILLARY GAS CHROMATOGRAMS OBTAINED ON L/C FRACTIONATED WILMINGTON CRUDE OIL: (A) ALIPHATIC FRACTION (F1); (B) AROMATIC FRACTION (F2); (C) POLAR FRACTION (F3). (KOVAT RETENTION INDICES ARE SHOWN ABOVE SELECTED PEAKS).

through 3-3B). The Wilmington crude oil aromatic distribution, however, is skewed to the higher molecular weight compounds. Polar components in the third fraction are observed to be limited in all four of these oils.

Gravimetric data obtained on the aliphatic and aromatic fractions and computer reduced compound-specific concentrations (organized by Kovat retention indices, Kovat 1958) are presented in Tables 3-2 and 3-3 for Murban crude; Tables 3-4 and 3-5 for Cook Inlet crude; Tables 3-6 and 3-7 for Prudhoe Bay crude and Tables 3-8 and 3-9 for Wilmington crude. Compound concentrations for the limited number of components present in the polar (F3) fractions from each oil are shown in Table 3-10. These data were generated on SAI's DEC-10 computer using our compound-specific data reduction program, and such data provide the basis for additional compound-specific weathering phenomena as will be discussed in detail in the next section "Oil Weathering Processes".

Figure 3-5 presents the reconstructed ion GC/MS chromatogram obtained on the aromatic fraction from Prudhoe Bay crude oil, and the individual aromatic components tentatively identified in this fraction are numbered on the chromatogram and listed in Table 3-11. Similar GC/MS data were obtained on the other crudes, however, comparative differences among the crudes can be better illustrated by graphic output such as that shown in Figures 3-6 through 3-8, rather than by tabulated compound identifications and concentrations.

Figure 3-6 presents the individual n-alkane concentrations for Murban crude, Cook Inlet crude and Prudhoe Bay crude, with the inset showing the relative concentrations of isoprenoid compounds in each of these oils. In that the Wilmington crude was not represented by an evenly repeating series of n-alkanes, aliphatic concentrations for that crude are not presented in Figure 3-6. The Cook Inlet crude and Prudhoe Bay crude show very similar trends. whereas the Murban crude is clearly characterized by relatively higher concentrations of the lower molecular weight hydrocarbons.

TABLE 3-2. MURBAN CRUDE OIL CONCENTRATIONS FOR ALIPHATIC FRACTION.

FRACTION=1 HP-RUN-DATE=10/22/1981 HP-RUN-NO= 37 HP-BOT-NO= 13

PEAK NUMBER	RETENTION TIME	KOVAT INDEX	KOVAT SUBGROUP	KOVAT GROUP	RESPONSE FACTOR	CONCENTRATION TOTAL
1.00	5.2180	0	0	0	1.440	1026.4
2.00	5.3900	0	0	0	1.440	195.91
3.00	7.4300	0	0	0	1.440	1079.7
4.00	7.6800	0	0	0	1.440	482.57
5.00	7.8400	0	0	0	1.440	279.37
6.00	8.6400	800	0	0	1.440	4477.0
7.00	9.7400	826	0	0	1.440	499.65
8.00	9.9600	831	0	0	1.440	504.46
9.00	10.920	853	0	0	1.440	468.62
10.0	11.560	868	0	0	1.440	3614.0
11.0	12.620	893	0	0	1.440	1145.9
12.0	12.930	900	0	0	1.440	6541.1
13.0	13.740	917	0	0	1.440	195.56
14.0	14.110	926	0	0	1.440	552.50
15.0	14.330	929	0	0	1.440	547.88
16.0	14.520	933	0	0	1.440	1266.2
17.0	14.850	940	0	0	1.440	850.38
18.0	15.530	953	0	0	1.440	971.73
19.0	16.340	970	0	0	1.440	1566.6
20.0	16.810	980	0	0	1.440	717.81
21.0	17.030	984	0	0	1.440	255.17
22.0	17.490	994	0	0	1.440	1678.0
23.0	17.790	1000	0	0	1.440	6646.0
24.0	18.870	1022	0	0	1.440	864.00
25.0	20.340	1052	0	0	1.440	780.98
26.0	20.580	1057	0	0	1.440	744.32
27.0	20.720	1060	0	0	1.440	353.39
28.0	20.900	1064	0	0	1.440	820.30
29.0	22.000	1086	0	0	1.440	760.69
30.0	22.660	1100	0	0	1.440	7770.6
31.0	23.430	1117	0	0	1.440	618.52
32.0	23.650	1121	0	0	1.440	314.78
33.0	23.870	1126	0	0	1.440	436.31
34.0	24.250	1134	0	0	1.440	296.63
35.0	24.440	1139	0	0	1.440	318.87
36.0	24.620	1147	0	0	1.440	483.82
37.0	25.190	1155	0	0	1.440	1258.0
38.0	25.400	1159	0	0	1.440	623.50
39.0	25.600	1164	0	0	1.440	1013.7
40.0	25.910	1170	0	0	1.440	714.59
41.0	26.200	1177	0	0	1.440	202.50
42.0	26.660	1187	0	0	1.440	530.62
43.0	26.870	1191	0	0	1.440	198.05
44.0	27.280	1200	0	0	1.430	7768.1
45.0	27.880	1213	0	0	1.440	588.59
46.0	28.510	1228	0	0	1.440	208.44
47.0	29.040	1240	0	0	1.440	222.20
48.0	29.670	1258	0	0	1.440	449.88
49.0	30.080	1263	0	0	1.440	877.04
50.0	30.360	1270	0	0	1.440	450.92
51.0	30.790	1279	0	0	1.450	286.46
52.0	31.230	1289	0	0	1.450	233.33
53.0	31.670	1300	0	0	1.450	8169.3
54.0	32.370	1316	0	0	1.440	535.79
55.0	32.650	1323	0	0	1.430	587.82
56.0	33.040	1333	0	0	1.420	276.92
57.0	33.520	1344	0	0	1.420	490.39
58.0	33.760	1350	0	0	1.410	232.95
59.0	34.080	1358	0	0	1.410	460.04
60.0	34.290	1363	0	0	1.400	725.68
61.0	34.580	1370	0	0	1.400	734.22
62.0	34.820	1376	0	0	1.390	695.01
63.0	35.810	1400	0	0	1.380	6548.0
64.0	36.220	1410	0	0	1.390	451.27
65.0	37.750	1449	0	0	1.440	645.58
66.0	38.080	1458	0	0	1.450	310.20
67.0	38.260	1462	0	0	1.460	807.97
68.0	38.550	1470	0	0	1.470	747.11
69.0	39.710	1500	0	0	1.510	6913.3
70.0	41.490	1548	0	0	1.500	637.40
71.0	41.690	1553	0	0	1.500	412.29
72.0	42.040	1563	0	0	1.500	787.86
73.0	42.310	1570	0	0	1.500	361.98
74.0	43.080	1591	0	0	1.500	194.35
75.0	43.390	1600	0	0	1.500	5925.5
76.0	45.080	1648	0	0	1.550	1821.5
77.0	45.420	1658	0	0	1.560	489.04
78.0	45.600	1663	0	0	1.560	291.18
79.0	45.870	1670	0	0	1.570	376.65
80.0	46.890	1700	0	0	1.600	5527.8
81.0	47.060	1710	0	0	1.500	497.15
82.0	48.340	1743	0	0	1.560	757.28
83.0	48.980	1763	0	0	1.540	315.69
84.0	49.250	1771	0	0	1.530	204.46
85.0	50.200	1800	0	0	1.510	4193.8
86.0	50.500	1815	0	0	1.440	632.91
87.0	51.550	1842	0	0	1.780	651.36
88.0	52.020	1857	0	0	1.880	294.55
89.0	52.200	1863	0	0	1.920	296.29
90.0	52.460	1871	0	0	1.970	418.88
91.0	53.370	1900	0	0	2.160	5078.5
92.0	56.380	2000	0	0	1.560	3791.2
93.0	57.490	2038	0	0	1.580	310.88
94.0	58.490	2071	0	0	1.590	219.71
95.0	59.260	2100	0	0	1.610	3161.2
96.0	60.340	2139	0	0	1.620	210.90
97.0	61.270	2172	0	0	1.640	321.56
98.0	62.020	2200	0	0	1.650	2950.3
99.0	63.000	2237	0	0	1.660	423.33
100.	64.650	2300	0	0	1.740	2698.1
101.	65.590	2337	0	0	1.700	211.89

FRACTION=1 HP-RUN-DATE=10/22/1981 HP-RUN-NO= 37 HP-BOT-NO= 13

PEAK NUMBER	RETENTION TIME	KOVAT INDEX	KOVAT SUBGROUP	KOVAT GROUP	RESPONSE FACTOR	CONCENTRATION TOTAL
102.	67.190	2400	0	0	1.630	2226.7
103.	68.040	2434	0	0	1.650	216.63
104.	69.440	2500	0	0	1.670	1925.0
105.	70.500	2532	0	0	1.680	213.54
106.	72.310	2600	0	0	1.720	1895.1
107.	75.480	2708	0	0	2.560	2243.8
108.	76.620	2729	0	0	2.320	294.62
109.	79.300	2800	0	0	1.770	1302.8
110.	84.000	2900	0	0	1.850	1046.3
111.	85.740	2929	0	0	1.870	258.29
112.	89.870	3000	0	0	1.920	866.60
113.	97.220	3100	0	0	2.630	1028.1
114.	106.51	3200	0	0	2.320	662.13
115.	106.51	3200	0	0	2.520	.00000

TOTAL RESOLVED HYDROCARBON = 154001.4
TOTAL UNRESOLVED HYDROCARBON = 155808.5
RESPONSE FACTOR AV. FOR C ~ 1000 TO 3000 FOR UCM = 1.714239
RATIO: RESOLVED/UNRESOLVED = 0.988402

SUM OF THE N-ALKANES = 75961.44
SUM OF THE EVEN N-ALKANES = 38150.2
SUM OF THE ODD N-ALKANES = 37811.24

RATIO: (PRISTANE+PHYTANE)/(N-ALKANES) = 1.487679E-2
RATIO: ODD/EVEN N-ALKANES = 0.991115
RATIO: PRISTANE/C-17 = 8.993653E-2
RATIO: PHYTANE/C-18 = 0.150916
RATIO: PRISTANE/PHYTANE = 0.785492
RATIO: (N-ALKANES)/(BRANCHED HYDROCARBONS) = 0.973365

Weight Distribution of Murban Crude by Fraction

Fraction	Weight (mg/g)
1	369
2	123
3	53.3

TABLE 3-3. MURBAN CRUDE OIL CONCENTRATIONS FOR AROMATIC FRACTION.

FRACTION:2 HP-RUN-DATE:10/22/1981 HP-RUN-NO: 38 HP-BGT-NO: 15

PEAK NUMBER	RETENTION TIME	KOVAT INDEX	KOVAT SUBGROUP	KOVAT GROUP	RESPONSE FACTOR	CONCENTRATION TOTAL
1.00	5.0780	0	0	0	1.440	22366.
2.00	5.1900	0	0	0	1.440	7550.2
3.00	5.2900	0	0	0	1.440	21893.
4.00	5.3400	0	0	0	1.440	11195.
5.00	5.4400	0	0	0	1.440	15563.
6.00	5.5300	0	0	0	1.440	18429.
6.50	5.6200	700	0	0	.0000	.00000
7.00	5.8600	708	0	0	1.440	1816.5
8.00	5.9380	711	0	0	1.440	106.15
9.00	6.3680	726	0	0	1.440	878.19
10.0	6.5600	733	0	0	1.440	41.969
11.0	6.6300	735	0	0	1.440	332.76
12.0	6.7700	740	0	0	1.440	43.073
12.5	8.4900	800	0	0	.0000	.00000
13.0	7.6100	780	0	0	1.440	282.57
14.0	11.240	863	0	0	1.440	59.163
15.0	11.500	871	0	0	1.440	199.52
16.0	12.640	895	0	0	1.440	163.78
16.5	12.840	900	0	0	.0000	.00000
17.0	12.920	902	0	0	1.440	43.927
18.0	15.910	963	0	0	1.440	158.62
19.0	16.220	969	0	0	1.440	64.858
20.0	16.290	981	0	0	1.440	126.05
21.0	17.460	999	0	0	1.440	352.77
21.5	17.710	1000	0	0	.0000	.00000
22.0	17.730	1000	0	0	1.440	44.710
23.0	18.870	1029	0	0	1.440	221.95
24.0	20.290	1093	0	0	1.440	81.222
25.0	21.050	1068	0	0	1.440	57.632
26.0	21.930	1086	0	0	1.440	94.191
27.0	22.560	1098	0	0	1.440	65.244
27.5	22.600	1100	0	0	.0000	.00000
28.0	22.950	1108	0	0	1.440	76.890
29.0	23.390	1117	0	0	1.440	67.528
30.0	23.590	1121	0	0	1.440	103.48
31.0	24.750	1146	0	0	1.440	55.852
32.0	25.130	1155	0	0	1.440	234.02
33.0	26.630	1187	0	0	1.440	67.137
34.0	27.240	1206	0	0	1.430	122.79
35.0	28.950	1239	0	0	1.440	47.257
36.0	30.996	1284	0	0	1.450	77.553
37.0	31.390	1299	0	0	1.450	830.37
38.0	31.620	1300	0	0	1.450	.00000
39.0	32.130	1317	0	0	1.440	290.31
40.0	32.670	1325	0	0	1.430	37.539
41.0	35.760	1399	0	0	1.380	158.27
42.0	35.760	1400	0	0	1.380	.00000
43.0	36.200	1411	0	0	1.390	338.86
44.0	36.820	1427	0	0	1.410	282.00
45.0	36.950	1430	0	0	1.420	206.19
46.0	37.150	1435	0	0	1.420	46.474
47.0	37.600	1447	0	0	1.440	120.51
48.0	37.750	1451	0	0	1.440	85.203
49.0	38.220	1463	0	0	1.460	117.97
50.0	39.660	1500	0	0	1.510	.00000
51.0	40.110	1512	0	0	1.510	143.78
52.0	40.790	1530	0	0	1.510	119.26
53.0	40.940	1534	0	0	1.510	126.10
54.0	41.130	1539	0	0	1.510	320.19
55.0	41.440	1548	0	0	1.500	83.104
56.0	41.750	1556	0	0	1.500	136.32
57.0	42.380	1573	0	0	1.500	60.466
58.0	43.020	1590	0	0	1.500	66.804
59.0	43.290	1598	0	0	1.500	161.38
60.0	43.360	1600	0	0	1.500	.00000
61.0	43.650	1608	0	0	1.510	71.931
62.0	44.270	1626	0	0	1.530	69.228
63.0	44.450	1631	0	0	1.530	41.585
64.0	45.440	1659	0	0	1.560	84.789
65.0	46.200	1681	0	0	1.580	132.38
66.0	46.800	1698	0	0	1.600	105.74
67.0	46.860	1700	0	0	1.600	.00000
68.0	47.080	1710	0	0	1.500	.00000
69.0	47.460	1716	0	0	1.580	196.08
70.0	48.420	1746	0	0	1.560	97.316
71.0	49.110	1767	0	0	1.540	186.79
72.0	50.020	1795	0	0	1.510	55.686
73.0	50.180	1800	0	0	1.510	.00000
74.0	50.510	1815	0	0	1.440	.00000
75.0	51.110	1829	0	0	1.700	45.577
76.0	51.290	1835	0	0	1.730	74.174
77.0	51.560	1843	0	0	1.790	52.425
78.0	52.010	1857	0	0	1.880	101.06
79.0	52.420	1870	0	0	1.970	470.68
80.0	53.090	1892	0	0	2.100	402.54
81.0	53.340	1900	0	0	2.160	.00000
82.0	53.820	1915	0	0	2.060	215.10
83.0	54.520	1939	0	0	1.920	106.13
84.0	54.670	1944	0	0	1.890	60.789
85.0	55.300	1964	0	0	1.770	75.466
86.0	55.560	1973	0	0	1.720	275.57
87.0	56.000	1988	0	0	1.630	73.068
88.0	56.250	1996	0	0	1.580	367.74
89.0	56.360	2000	0	0	1.560	.00000
90.0	56.810	2015	0	0	1.570	92.288
91.0	56.990	2021	0	0	1.570	231.47
92.0	57.400	2036	0	0	1.580	107.14
93.0	57.950	2055	0	0	1.590	237.79
94.0	58.970	2090	0	0	1.600	275.58
95.0	59.240	2100	0	0	1.610	.00000
96.0	59.610	2113	0	0	1.610	184.98

FRACTION:2 HP-RUN-DATE:10/22/1981 HP-RUN-NO: 38 HP-BGT-NO: 15

PEAK NUMBER	RETENTION TIME	KOVAT INDEX	KOVAT SUBGROUP	KOVAT GROUP	RESPONSE FACTOR	CONCENTRATION TOTAL
97.0	59.960	2126	0	0	1.620	239.34
98.0	60.440	2143	0	0	1.620	133.64
99.0	60.860	2158	0	0	1.630	137.60
100.	61.370	2177	0	0	1.640	140.03
101.	61.860	2195	0	0	1.640	58.671
102.	61.990	2200	0	0	1.650	.00000
103.	62.180	2205	0	0	1.650	63.213
104.	62.440	2217	0	0	1.660	56.003
105.	64.320	2288	0	0	1.730	99.906
106.	64.630	2300	0	0	1.740	.00000
107.	66.910	2389	0	0	1.640	52.644
108.	67.170	2400	0	0	1.630	.00000
109.	68.740	2464	0	0	1.660	48.519
110.	69.540	2497	0	0	1.670	62.154
111.	69.610	2500	0	0	1.670	.00000
112.	71.580	2573	0	0	1.700	46.185
113.	72.300	2600	0	0	1.720	.00000
114.	73.440	2700	0	0	2.560	.00000
115.	79.280	2800	0	0	1.770	.00000
116.	84.000	2900	0	0	1.850	.00000
117.	89.860	3000	0	0	1.920	.00000
118.	97.230	3100	0	0	2.630	.00000
119.	106.49	3200	0	0	2.320	.00000

TOTAL RESOLVED HYDROCARBON = 111[illegible].1
TOTAL UNRESOLVED HYDROCARBON = 31[illegible].35
RESPONSE FACTOR AV. FOR C - 1500 TO 3100 FOR UCM = 1.[illegible]
RATIO: RESOLVED/UNRESOLVED = 3.590606

SUM OF THE N-ALKANES = 122.7935
SUM OF THE EVEN N-ALKANES = 122.7935
SUM OF THE ODD N-ALKANES = 0

RATIO: (PRISTANE+PHYTANE)/(N-ALKANES) = 0
RATIO: ODD/EVEN N-ALKANES = 0
RATIO: PRISTANE/C-17 = 0
RATIO: PHYTANE/C-18 = 0
RATIO: PRISTANE/PHYTANE = 0
RATIO: (N-ALKANES)/(BRANCHED HYDROCARBONS) = 1.098496E-3

TABLE 3-4. COOK INLET CRUDE OIL CONCENTRATIONS FOR ALIPHATIC FRACTION.

FRACTION:1 HP-RUN-DATE:10/21/1981 HP-RUN-NO: 31 HP-BOT-NO: 1 FRACTION:1 HP-RUN-DATE:10/21/1981 HP-RUN-NO: 31 HP-BOT-NO: 1

PEAK NUMBER	RETENTION TIME	KOVAT INDEX	KOVAT SUBGROUP	KOVAT GROUP	RESPONSE FACTOR	CONCENTRATION TOTAL	PEAK NUMBER	RETENTION TIME	KOVAT INDEX	KOVAT SUBGROUP	KOVAT GROUP	RESPONSE FACTOR	CONCENTRATION TOTAL
2.00	5.0500	0	0	0	1.440	1236.4	103.	39.710	1500	0	0	1.510	6685.5
3.00	5.1400	0	0	0	1.440	3096.1	104.	40.050	1509	0	0	1.510	447.67
4.00	5.2000	0	0	0	1.440	7834.8	105.	41.480	1548	0	0	1.500	551.48
5.00	5.3500	0	0	0	1.440	1986.5	106.	41.700	1554	0	0	1.500	932.17
6.00	5.5100	0	0	0	1.440	249.29	107.	42.020	1562	0	0	1.500	562.93
7.00	5.8000	700	0	0	1.440	2538.0	108.	42.290	1570	0	0	1.500	232.27
8.00	6.3600	719	0	0	1.440	509.92	109.	43.390	1600	0	0	1.500	9339.2
9.00	7.0100	759	0	0	1.440	617.92	110.	45.100	1648	0	0	1.550	1865.6
10.0	7.6300	764	0	0	1.440	147.39	111.	45.420	1657	0	0	1.560	756.45
11.0	7.7600	768	0	0	1.440	409.47	112.	45.590	1662	0	0	1.560	271.47
12.0	7.9400	774	0	0	1.440	1028.8	113.	45.660	1670	0	0	1.570	225.35
13.0	8.4800	790	0	0	1.440	186.35	114.	46.900	1700	0	0	1.600	4452.8
14.0	8.6000	797	0	0	1.440	239.55	115.	47.080	1710	0	0	1.500	3129.7
15.0	8.6800	800	0	0	1.440	1712.3	116.	48.340	1743	0	0	1.560	539.57
16.0	8.8900	805	0	0	1.440	306.56	117.	48.980	1762	0	0	1.540	641.31
17.0	9.5300	820	0	0	1.440	203.21	118.	49.250	1770	0	0	1.530	160.10
18.0	9.7900	826	0	0	1.440	457.30	119.	50.210	1800	0	0	1.510	3465.1
19.0	10.080	831	0	0	1.440	1549.5	120.	50.510	1815	0	0	1.440	1085.1
20.0	10.730	848	0	0	1.440	497.27	121.	51.530	1841	0	0	1.780	389.20
21.0	10.930	853	0	0	1.440	806.74	122.	52.010	1856	0	0	1.680	223.88
22.0	11.330	862	0	0	1.440	1751.6	123.	52.810	1863	0	0	1.920	272.53
23.0	11.550	867	0	0	1.440	2241.4	124.	53.110	1891	0	0	2.100	587.96
24.0	12.340	886	0	0	1.440	570.09	125.	53.370	1900	0	0	2.160	4624.1
25.0	12.630	893	0	0	1.440	836.68	126.	55.270	1963	0	0	1.780	103.31
26.0	12.940	900	0	0	1.440	5395.7	127.	56.380	2000	0	0	1.560	3046.8
27.0	13.230	906	0	0	1.440	611.81	128.	57.500	2039	0	0	1.580	176.43
28.0	13.360	909	0	0	1.440	202.75	129.	58.250	2100	0	0	1.610	2912.4
29.0	13.830	918	0	0	1.440	796.79	130.	61.280	2173	0	0	1.640	198.28
30.0	14.110	924	0	0	1.440	607.16	131.	61.490	2181	0	0	1.640	210.20
31.0	14.330	929	0	0	1.440	1863.5	132.	62.010	2200	0	0	1.650	2668.8
32.0	14.510	933	0	0	1.440	1241.1	133.	64.650	2300	0	0	1.740	2613.3
33.0	14.860	940	0	0	1.440	1377.1	134.	65.110	2318	0	0	1.720	240.29
34.0	15.090	945	0	0	1.440	286.06	135.	67.180	2400	0	0	1.630	2171.3
35.0	15.530	956	0	0	1.440	1712.3	136.	69.630	2500	0	0	1.670	1794.5
36.0	15.860	960	0	0	1.440	186.36	137.	72.310	2600	0	0	1.720	1916.9
37.0	15.980	963	0	0	1.440	369.79	138.	75.480	2700	0	0	2.560	2245.0
38.0	16.890	982	0	0	1.440	273.42	139.	79.300	2800	0	0	1.770	1238.9
39.0	17.020	984	0	0	1.440	356.85	140.	86.020	2980	0	0	1.850	1136.3
40.0	17.160	987	0	0	1.440	335.92	141.	89.880	3000	0	0	1.920	984.75
41.0	17.440	993	0	0	1.440	1313.7	142.	97.280	3100	0	0	2.630	989.35
42.0	17.770	1000	0	0	1.440	6695.2	143.	106.52	3200	0	0	2.320	530.60
43.0	18.160	1008	0	0	1.440	588.12	144.	106.52	3200	0	0	2.520	.00000
44.0	18.320	1011	0	0	1.440	279.23							
45.0	18.660	1022	0	0	1.440	2294.7							
46.0	19.300	1031	0	0	1.440	1008.5							
47.0	19.670	1039	0	0	1.440	162.95							
48.0	19.990	1046	0	0	1.440	164.25							
49.0	20.320	1052	0	0	1.440	254.38							
50.0	20.470	1056	0	0	1.440	334.91							
51.0	20.550	1057	0	0	1.440	162.66							
52.0	20.680	1060	0	0	1.440	444.21							
53.0	20.860	1064	0	0	1.440	1056.2							
54.0	21.170	1070	0	0	1.440	360.05							
55.0	21.620	1079	0	0	1.440	109.26							
56.0	21.870	1084	0	0	1.440	287.08							
57.0	22.040	1088	0	0	1.440	329.09							
58.0	22.630	1100	0	0	1.440	7113.8							
59.0	23.160	1111	0	0	1.440	1252.1							
60.0	23.400	1117	0	0	1.440	587.10							
61.0	23.600	1121	0	0	1.440	213.39							
62.0	23.920	1128	0	0	1.440	1655.6							
63.0	24.230	1134	0	0	1.440	840.32							
64.0	24.460	1139	0	0	1.440	431.57							
65.0	25.170	1155	0	0	1.440	911.25							
66.0	25.390	1159	0	0	1.440	621.41							
67.0	25.590	1164	0	0	1.440	784.67							
68.0	25.900	1170	0	0	1.440	328.22							
69.0	26.250	1178	0	0	1.440	146.67							
70.0	26.650	1186	0	0	1.440	1012.6							
71.0	26.860	1191	0	0	1.440	674.61							
72.0	27.260	1200	0	0	1.430	7804.0							
73.0	27.630	1207	0	0	1.440	245.19							
74.0	27.870	1213	0	0	1.440	425.99							
75.0	28.340	1224	0	0	1.440	279.52							
76.0	28.510	1228	0	0	1.440	309.80							
77.0	29.020	1239	0	0	1.440	659.24							
78.0	29.870	1258	0	0	1.440	274.39							
79.0	30.060	1263	0	0	1.440	882.64							
80.0	30.460	1272	0	0	1.450	467.51							
81.0	30.780	1279	0	0	1.450	316.81							
82.0	30.970	1284	0	0	1.450	158.26							
83.0	31.220	1289	0	0	1.450	565.67							
84.0	31.670	1300	0	0	1.450	7596.8							
85.0	31.970	1307	0	0	1.440	381.35							
86.0	32.350	1316	0	0	1.440	670.89							
87.0	32.670	1324	0	0	1.430	451.64							
88.0	33.300	1339	0	0	1.420	185.11							
89.0	33.510	1344	0	0	1.420	1142.6							
90.0	34.080	1358	0	0	1.410	356.34							
91.0	34.290	1363	0	0	1.400	521.84							
92.0	34.580	1370	0	0	1.400	361.59							
93.0	34.820	1376	0	0	1.390	1148.1							
94.0	35.520	1392	0	0	1.380	357.53							
95.0	35.810	1400	0	0	1.380	6183.5							
96.0	36.820	1425	0	0	1.410	215.04							
97.0	37.740	1449	0	0	1.440	1846.8							
98.0	38.080	1458	0	0	1.450	276.84							
99.0	38.220	1461	0	0	1.460	1647.4							
100.	38.550	1470	0	0	1.470	619.79							
101.	38.840	1477	0	0	1.460	252.12							
102.	39.350	1490	0	0	1.500	224.17							

TOTAL RESOLVED HYDROCARBON = 179155.5
TOTAL UNRESOLVED HYDROCARBON = 211498.7
RESPONSE FACTOR AV. FOR C - 700 TO 2900 FOR UCM = 1.701876
RATIO: RESOLVED/UNRESOLVED = 0.847076

SUM OF THE N-ALKANES = 70600.05
SUM OF THE EVEN N-ALKANES = 35349.81
SUM OF THE ODD N-ALKANES = 35250.23

RATIO: (PRISTANE+PHYTANE)/(N-ALKANES) = 0.0596988
RATIO: ODD/EVEN N-ALKANES = 0.997183
RATIO: PRISTANE/C-17 = 0.702859
RATIO: PHYTANE/C-18 = 0.311339
RATIO: PRISTANE/PHYTANE = 2.884348
RATIO: (N-ALKANES)/(BRANCHED HYDROCARBONS) = 0.650359

Weight Distribution of Cook Inlet Crude by Fraction

Fraction	Weight (mg/g)
1	803
2	64.6
3	127

TABLE 3-5. COOK INLET CRUDE OIL CONCENTRATIONS FOR AROMATIC FRACTION.

FRACTION=2 HP-RUN-DATE=10/21/1981 HP-RUN-NO= 32 HP-SGT-NO= 3

PEAK NUMBER	RETENTION TIME	KOVAT INDEX	KOVAT SUBGROUP	KOVAT GROUP	RESPONSE FACTOR	CONCENTRATION TOTAL
1.00	5.1500	0	0	0	1.440	2491.7
2.00	5.2100	0	0	0	1.440	792.16
2.50	5.6200	700	0	0	.0000	.00000
3.00	5.7500	705	0	0	1.440	2473.2
4.00	6.2300	721	0	0	1.440	1439.9
5.00	6.4200	728	0	0	1.440	150.45
6.00	7.0300	749	0	0	1.440	45.534
7.00	7.4400	763	0	0	1.440	422.83
7.50	8.4900	800	0	0	.0000	.00000
8.00	11.080	860	0	0	1.440	24.567
9.00	11.430	868	0	0	1.440	158.93
9.50	12.840	900	0	0	.0000	.00000
10.0	12.310	893	0	0	1.440	133.41
11.0	15.880	962	0	0	1.440	93.352
12.0	16.190	969	0	0	1.440	91.254
13.0	16.760	980	0	0	1.440	54.587
14.0	17.440	994	0	0	1.440	286.82
14.5	17.710	1000	0	0	.0000	.00000
15.0	18.880	1024	0	0	1.440	262.96
16.0	20.280	1053	0	0	1.440	33.044
17.0	21.930	1086	0	0	1.440	69.648
18.0	22.680	1100	0	0	1.440	27.983
18.5	22.600	1108	0	0	.0000	.00000
19.0	23.420	1118	0	0	1.440	65.698
20.0	23.630	1122	0	0	1.440	81.521
21.0	24.510	1141	0	0	1.440	33.662
22.0	24.750	1146	0	0	1.440	40.122
23.0	25.600	1165	0	0	1.440	40.225
24.0	26.180	1177	0	0	1.440	23.415
25.0	26.640	1186	0	0	1.440	410.90
26.0	26.870	1192	0	0	1.440	39.855
27.0	27.240	1200	0	0	1.430	.00000
28.0	27.260	1208	0	0	1.430	75.094
29.0	28.500	1228	0	0	1.440	28.949
30.0	28.960	1239	0	0	1.440	40.922
31.0	29.360	1248	0	0	1.440	28.678
32.0	29.600	1253	0	0	1.440	36.598
33.0	30.970	1285	0	0	1.450	49.908
34.0	31.620	1300	0	0	1.450	.00000
35.0	31.640	1300	0	0	1.490	1203.7
36.0	31.950	1307	0	0	1.440	54.634
37.0	32.390	1318	0	0	1.440	732.28
38.0	32.670	1325	0	0	1.430	87.609
39.0	33.490	1345	0	0	1.420	34.429
40.0	34.290	1364	0	0	1.400	20.120
41.0	34.990	1381	0	0	1.390	26.759
42.0	35.180	1385	0	0	1.390	85.650
43.0	35.760	1400	0	0	1.380	.00000
44.0	35.770	1400	0	0	1.380	241.85
45.0	36.250	1412	0	0	1.390	427.73
46.0	36.880	1428	0	0	1.410	571.49
47.0	37.020	1432	0	0	1.420	225.48
48.0	37.630	1447	0	0	1.440	257.14
49.0	37.770	1451	0	0	1.440	38.288
50.0	38.250	1463	0	0	1.460	281.57
51.0	38.810	1478	0	0	1.480	22.044
52.0	39.390	1493	0	0	1.500	142.30
53.0	39.660	1500	0	0	1.510	.00000
54.0	39.740	1502	0	0	1.510	72.082
55.0	40.130	1512	0	0	1.510	173.73
56.0	40.590	1525	0	0	1.510	62.959
57.0	40.820	1531	0	0	1.510	55.243
58.0	40.960	1535	0	0	1.510	144.61
59.0	41.170	1540	0	0	1.510	229.77
60.0	41.860	1558	0	0	1.500	26.979
61.0	41.780	1557	0	0	1.500	91.616
62.0	42.410	1574	0	0	1.500	498.40
63.0	43.140	1594	0	0	1.500	164.99
64.0	43.320	1598	0	0	1.500	189.26
65.0	43.360	1600	0	0	1.500	.00000
66.0	43.640	1608	0	0	1.510	70.557
67.0	44.310	1627	0	0	1.530	74.776
68.0	44.490	1632	0	0	1.530	47.388
69.0	45.000	1644	0	0	1.550	35.506
70.0	45.170	1651	0	0	1.550	38.891
71.0	45.480	1660	0	0	1.560	69.522
72.0	46.230	1682	0	0	1.580	97.685
73.0	46.490	1689	0	0	1.590	45.581
74.0	46.840	1699	0	0	1.600	180.54
75.0	46.860	1700	0	0	1.600	.00000
76.0	47.080	1710	0	0	1.500	.00000
77.0	47.160	1709	0	0	1.590	35.004
78.0	47.530	1720	0	0	1.580	293.69
79.0	47.900	1731	0	0	1.570	52.290
80.0	48.460	1748	0	0	1.550	154.86
81.0	49.030	1765	0	0	1.540	29.367
82.0	49.240	1771	0	0	1.530	21.953
83.0	49.740	1786	0	0	1.520	40.629
84.0	50.070	1796	0	0	1.510	323.08
85.0	50.180	1800	0	0	1.510	.00000
86.0	50.510	1815	0	0	1.840	.00000
87.0	50.630	1814	0	0	1.600	29.517
88.0	51.140	1830	0	0	1.700	93.925
89.0	51.320	1836	0	0	1.740	26.118
90.0	51.600	1844	0	0	1.800	62.087
91.0	52.080	1860	0	0	1.900	136.38
92.0	52.320	1867	0	0	1.950	64.794
93.0	52.590	1876	0	0	2.000	38.983
94.0	52.780	1882	0	0	2.040	93.215
95.0	53.260	1897	0	0	2.140	59.833
96.0	53.340	1900	0	0	2.160	.00000

FRACTION=2 HP-RUN-DATE=10/21/1981 HP-RUN-NO= 32 HP-SGT-NO= 3

PEAK NUMBER	RETENTION TIME	KOVAT INDEX	KOVAT SUBGROUP	KOVAT GROUP	RESPONSE FACTOR	CONCENTRATION TOTAL
97.0	53.750	1913	0	0	2.070	209.93
98.0	53.940	1919	0	0	2.040	221.00
99.0	54.200	1926	0	0	1.990	28.330
100.	54.570	1940	0	0	1.910	173.10
101.	54.730	1946	0	0	1.880	125.83
102.	55.050	1953	0	0	1.860	25.295
103.	56.080	1990	0	0	1.610	88.162
104.	56.360	2000	0	0	1.560	.00000
105.	57.130	2026	0	0	1.570	38.463
106.	58.000	2056	0	0	1.590	295.17
107.	58.170	2062	0	0	1.590	120.36
108.	58.360	2069	0	0	1.590	60.395
109.	58.680	2080	0	0	1.600	23.171
110.	59.080	2094	0	0	1.600	68.066
111.	59.240	2100	0	0	1.610	.00000
112.	59.300	2102	0	0	1.610	31.437
113.	59.550	2111	0	0	1.610	53.660
114.	60.560	2148	0	0	1.630	89.155
115.	61.150	2169	0	0	1.630	58.386
116.	61.400	2178	0	0	1.640	125.11
117.	61.900	2196	0	0	1.640	51.497
118.	61.990	2200	0	0	1.650	.00000
119.	63.080	2241	0	0	1.690	93.961
120.	64.620	2299	0	0	1.740	25.774
121.	64.630	2300	0	0	1.740	.00000
122.	66.840	2387	0	0	1.650	73.826
123.	67.170	2400	0	0	1.630	.00000
124.	67.270	2404	0	0	1.640	38.015
125.	69.570	2498	0	0	1.670	61.089
126.	69.610	2500	0	0	1.670	.00000
127.	72.300	2600	0	0	1.720	.00000
128.	72.610	2616	0	0	1.650	61.907
129.	75.370	2697	0	0	2.540	37.175
130.	75.440	2700	0	0	2.560	.00000
131.	76.580	2729	0	0	2.330	42.131
132.	79.280	2800	0	0	1.770	.00000
133.	84.000	2900	0	0	1.850	.00000
134.	89.860	3000	0	0	1.920	.00000
135.	97.230	3100	0	0	2.630	.00000
136.	106.49	3200	0	0	2.320	.00000

TOTAL RESOLVED HYDROCARBON = 20856.13
TOTAL UNRESOLVED HYDROCARBON = 32399.1
RESPONSE FACTOR AV. FOR C = 1500 TO 3100 FOR UCM = 1.803576
RATIO: RESOLVED/UNRESOLVED = 0.643726

SUM OF THE N-ALKANES = 0
SUM OF THE EVEN N-ALKANES = 0
SUM OF THE ODD N-ALKANES = 0

RATIO: (PRISTANE+PHYTANE)/(N-ALKANES) = 0
RATIO: ODD/EVEN N-ALKANES = 0
RATIO: PRISTANE/C-17 = 0
RATIO: PHYTANE/C-18 = 0
RATIO: PRISTANE/PHYTANE = 0
RATIO: (N-ALKANES)/(BRANCHED HYDROCARBONS) = 0

TABLE 3-6. PRUDHOE BAY CRUDE OIL CONCENTRATIONS FOR ALIPHATIC FRACTION.

PEAK NUMBER	RETENTION TIME	KOVAT INDEX	KOVAT SUBGROUP	KOVAT GROUP	RESPONSE FACTOR	CONCENTRATIO TOTAL
1.00	6.2700	0	0	0	1.900	222.26
2.00	6.4600	0	0	0	1.900	503.98
3.00	7.4000	700	0	0	1.900	772.90
4.00	8.7600	750	0	0	1.900	220.44
5.00	8.9900	759	0	0	1.900	1211.2
6.00	9.2900	770	0	0	1.900	191.87
7.00	9.8300	790	0	0	1.900	68.820
8.00	10.110	800	0	0	1.900	1672.0
9.00	11.080	821	0	0	1.900	30.366
10.0	11.350	827	0	0	1.900	93.765
11.0	11.650	833	0	0	1.900	198.99
12.0	11.790	836	0	0	1.900	107.53
13.0	12.470	851	0	0	1.900	31.594
14.0	12.640	855	0	0	1.900	46.322
15.0	13.030	863	0	0	1.900	593.76
16.0	13.410	871	0	0	1.900	1829.6
17.0	14.200	888	0	0	1.900	32.568
18.0	14.560	896	0	0	1.900	215.27
19.0	14.750	900	0	0	1.900	1000.3
20.0	15.150	908	0	0	1.900	41.800
21.0	15.610	917	0	0	1.900	29.476
22.0	15.800	921	0	0	1.900	253.08
23.0	16.130	927	0	0	1.900	24.606
24.0	16.310	931	0	0	1.900	19.959
25.0	16.430	933	0	0	1.900	147.04
26.0	16.820	941	0	0	1.900	173.72
27.0	17.620	957	0	0	1.900	193.63
28.0	17.840	961	0	0	1.900	50.313
29.0	17.990	964	0	0	1.900	385.73
30.0	18.320	971	0	0	1.900	464.17
31.0	18.980	984	0	0	1.900	525.15
32.0	19.620	997	0	0	1.900	233.64
33.0	19.780	1000	0	0	1.900	806.36
34.0	20.320	1011	0	0	1.900	32.441
35.0	20.470	1014	0	0	1.900	57.809
36.0	20.800	1023	0	0	1.900	143.15
37.0	21.110	1027	0	0	1.900	245.25
38.0	21.470	1034	0	0	1.900	176.60
39.0	21.690	1039	0	0	1.900	110.11
40.0	22.150	1048	0	0	1.900	59.166
41.0	22.480	1055	0	0	1.900	160.00
42.0	22.740	1060	0	0	1.900	525.59
43.0	23.270	1071	0	0	1.900	181.56
44.0	23.750	1081	0	0	1.900	32.780
45.0	23.870	1083	0	0	1.900	27.952
46.0	24.030	1086	0	0	1.900	44.593
47.0	24.190	1089	0	0	1.900	149.12
48.0	24.710	1100	0	0	1.900	1540.3
49.0	25.070	1106	0	0	1.900	31.424
50.0	25.240	1111	0	0	1.900	35.194
51.0	25.480	1117	0	0	1.900	169.07
52.0	25.680	1121	0	0	1.900	22.708
53.0	25.980	1127	0	0	1.900	140.61
54.0	26.270	1133	0	0	1.900	205.11
55.0	26.470	1138	0	0	1.900	82.415
56.0	26.630	1141	0	0	1.900	84.914
57.0	27.040	1150	0	0	1.900	101.47
58.0	27.360	1157	0	0	1.900	55.861
59.0	27.470	1159	0	0	1.900	57.131
60.0	27.690	1164	0	0	1.900	146.53
61.0	28.000	1171	0	0	1.900	306.20
62.0	28.430	1180	0	0	1.900	41.080
63.0	28.650	1184	0	0	1.900	288.49
64.0	29.060	1193	0	0	1.900	190.33
65.0	29.370	1200	0	0	1.880	1241.8
66.0	29.980	1213	0	0	1.890	272.23
67.0	30.630	1228	0	0	1.890	90.111
68.0	30.840	1233	0	0	1.890	56.531
69.0	31.240	1242	0	0	1.900	72.615
70.0	31.680	1252	0	0	1.900	244.49
71.0	31.960	1258	0	0	1.900	94.603
72.0	32.170	1263	0	0	1.900	165.13
73.0	32.370	1272	0	0	1.910	495.52
74.0	33.410	1292	0	0	1.910	25.825
75.0	33.760	1300	0	0	1.920	1247.9
76.0	34.010	1306	0	0	1.920	371.69
77.0	34.280	1311	0	0	1.920	46.336
78.0	34.500	1317	0	0	1.930	75.993
79.0	34.780	1324	0	0	1.930	270.40
80.0	35.730	1347	0	0	1.940	264.84
81.0	36.170	1358	0	0	1.940	109.84
82.0	36.380	1363	0	0	1.950	181.73
83.0	36.660	1370	0	0	1.950	96.982
84.0	36.920	1376	0	0	1.950	294.29
85.0	37.290	1385	0	0	1.960	24.823
86.0	37.630	1393	0	0	1.960	98.436
87.0	37.890	1400	0	0	1.960	1258.7
88.0	38.200	1407	0	0	1.970	91.772
89.0	38.630	1419	0	0	1.990	158.12
90.0	39.240	1434	0	0	2.010	169.79
91.0	39.790	1448	0	0	2.020	35.920
92.0	39.930	1452	0	0	2.030	102.34
93.0	40.160	1458	0	0	2.030	32.132
94.0	40.310	1462	0	0	2.040	210.76
95.0	40.630	1470	0	0	2.050	147.10
96.0	41.040	1480	0	0	2.060	31.088
97.0	41.780	1500	0	0	2.080	1485.5
98.0	42.080	1508	0	0	2.080	57.090
99.0	42.520	1520	0	0	2.090	67.564
100.	42.740	1526	0	0	2.090	29.778
101.	43.390	1542	0	0	2.090	34.977

PEAK NUMBER	RETENTION TIME	KOVAT INDEX	KOVAT SUBGROUP	KOVAT GROUP	RESPONSE FACTOR	CONCENTRATIC TOTAL
102.	43.560	1548	0	0	2.090	115.13
103.	43.870	1557	0	0	2.090	166.07
104.	44.110	1563	0	0	2.090	50.379
105.	44.540	1575	0	0	2.090	28.248
106.	44.820	1583	0	0	2.100	99.971
107.	45.440	1600	0	0	2.100	1111.4
108.	45.640	1605	0	0	2.110	50.216
109.	46.030	1617	0	0	2.140	52.106
110.	46.350	1626	0	0	2.170	77.078
111.	46.660	1635	0	0	2.190	36.170
112.	47.150	1649	0	0	2.230	248.75
113.	47.418	1662	0	0	2.260	189.16
114.	47.900	1670	0	0	2.280	120.60
115.	48.910	1700	0	0	2.340	995.66
116.	49.110	1710	0	0	3.250	639.29
117.	49.980	1732	0	0	2.290	66.746
118.	50.340	1743	0	0	2.260	160.17
119.	50.640	1752	0	0	2.250	45.434
120.	50.836	1758	0	0	2.230	24.929
121.	51.000	1763	0	0	2.220	61.740
122.	51.690	1784	0	0	2.180	51.411
123.	52.210	1800	0	0	2.140	823.03
124.	52.530	1815	0	0	2.270	532.36
125.	53.340	1835	0	0	2.280	32.259
126.	53.556	1842	0	0	2.310	91.029
127.	54.470	1871	0	0	2.420	49.604
128.	55.140	1892	0	0	2.500	66.152
129.	55.370	1900	0	0	2.530	753.89
130.	55.640	1909	0	0	2.550	30.201
131.	57.100	1957	0	0	2.690	46.463
132.	58.328	2000	0	0	2.816	842.36
133.	59.520	2039	0	0	2.990	154.89
134.	60.530	2074	0	0	3.150	145.79
135.	61.260	2100	0	0	3.270	810.26
136.	63.020	2163	0	0	3.570	76.649
137.	63.690	2187	0	0	3.690	55.736
138.	64.040	2200	0	0	3.750	832.65
139.	65.030	2236	0	0	3.860	98.829
140.	65.730	2263	0	0	3.930	99.231
141.	66.720	2300	0	0	4.040	716.71
142.	69.310	2400	0	0	4.660	726.08
143.	70.990	2461	0	0	4.610	52.956
144.	72.830	2526	0	0	4.588	643.89
145.	73.010	2532	0	0	4.730	81.040
146.	73.860	2561	0	0	4.860	118.35
147.	75.010	2600	0	0	5.030	596.84
148.	76.180	2631	0	0	5.900	103.93
149.	77.840	2690	0	0	6.640	108.77
150.	78.466	2700	0	0	7.760	583.16
151.	82.520	2800	0	0	5.960	361.19
152.	87.480	2900	0	0	6.440	195.04
153.	89.230	2928	0	0	6.840	147.81
154.	93.580	3000	0	0	7.120	272.89
155.	101.11	3100	0	0	9.630	309.68
156.	110.59	3200	0	0	8.830	287.33
157.	110.59	3200	0	0	9.650	.00000

TOTAL RESOLVED HYDROCARBON = 48856.59
TOTAL UNRESOLVED HYDROCARBON = 152022.6
RESPONSE FACTOR AV. FOR C = 1200 TO 3140 FOR UCM = 4.222611
RATIO=RESOLVED/UNRESOLVED = 0.276507

SUM OF THE N-ALKANES = 15937.11
SUM OF THE EVEN N-ALKANES = 8266.371
SUM OF THE ODD N-ALKANES = 7670.736

RATIO:(PRISTANE+PHYTANE)/(N-ALKANES) = 7.351608E-2
RATIO: ODD/EVEN N-ALKANES = 0.927945
RATIO: PRISTANE/C-17 = 0.648078
RATIO: PHYTANE/C-18 = 0.646825
RATIO: PRISTANE/PHYTANE = 1.200857
RATIO:(N-ALKANES)/(UNRESOLVED HYDROCARBONS) = 0.1660588

Weight Distribution of Prudhoe Bay Crude by Fraction

Fraction	Weight (mg/g)
1	879
2	75
3	60

TABLE 3-7. PRUDHOE BAY CRUDE OIL CONCENTRATIONS FOR AROMATIC FRACTION.

FRACTION=2 HP-RUN-DATE= 9/22/1981 HP-RUN-NO= 72 HP-SOT-NO= 9

PEAK NUMBER	RETENTION TIME	KOVAT INDEX	KOVAT SUBGROUP	KOVAT GROUP	RESPONSE FACTOR	CONCENTRATION TOTAL
1.00	5.0700	0	0	0	1.720	198.48
1.50	5.1400	700	0	0	.0000	.00000
2.00	5.2400	704	0	0	1.720	30.523
3.00	5.3200	708	0	0	1.720	1050.7
4.00	5.5900	719	0	0	1.720	259.24
5.00	5.7200	725	0	0	1.720	40.506
6.00	6.9500	761	0	0	1.720	1362.9
7.00	6.6500	765	0	0	1.720	31.096
8.00	7.1300	786	0	0	1.720	29.295
9.00	7.2600	792	0	0	1.720	89.482
9.50	7.4500	800	0	0	.0000	.00000
10.0	7.4900	800	0	0	1.720	53.026
11.0	7.6600	805	0	0	1.720	26.549
12.0	10.040	861	0	0	1.720	474.62
13.0	10.390	870	0	0	1.720	1794.1
13.5	11.470	900	0	0	.0000	.00000
14.0	11.910	915	0	0	1.720	68.746
15.0	12.870	929	0	0	1.720	118.78
16.0	14.830	964	0	0	1.720	50.858
17.0	14.270	954	0	0	1.720	220.08
18.0	14.680	963	0	0	1.720	736.48
19.0	14.970	969	0	0	1.720	309.65
20.0	15.530	980	0	0	1.720	299.91
21.0	16.160	993	0	0	1.720	926.74
21.5	16.480	1000	0	0	.0000	.00000
22.0	17.040	1012	0	0	1.720	60.596
23.0	17.600	1023	0	0	1.720	452.93
24.0	18.240	1036	0	0	1.720	55.931
25.0	19.030	1053	0	0	1.720	304.08
26.0	19.250	1057	0	0	1.720	96.556
27.0	19.380	1060	0	0	1.720	75.039
28.0	19.770	1068	0	0	1.720	168.90
29.0	20.340	1080	0	0	1.720	326.51
30.0	20.680	1087	0	0	1.720	261.53
31.0	20.970	1093	0	0	1.720	31.137
31.5	21.320	1100	0	0	.0000	.00000
32.0	21.410	1102	0	0	1.720	25.859
33.0	21.630	1107	0	0	1.720	23.976
34.0	23.190	1140	0	0	1.720	164.11
35.0	23.480	1147	0	0	1.720	210.96
36.0	23.820	1154	0	0	1.720	152.70
37.0	24.050	1159	0	0	1.720	58.427
38.0	24.260	1164	0	0	1.720	124.06
39.0	24.500	1169	0	0	1.720	127.45
40.0	24.670	1177	0	0	1.720	85.472
41.0	25.290	1188	0	0	1.720	520.45
42.0	25.540	1191	0	0	1.720	27.436
43.0	25.710	1195	0	0	1.720	92.759
44.0	25.930	1200	0	0	1.720	139.14
45.0	25.940	1200	0	0	1.720	.00000
46.0	26.160	1205	0	0	1.720	27.690
47.0	26.450	1211	0	0	1.720	21.965
48.0	27.130	1227	0	0	1.720	171.69
49.0	27.670	1239	0	0	1.720	106.25
50.0	28.010	1247	0	0	1.720	100.41
51.0	28.240	1252	0	0	1.720	91.939
52.0	28.650	1262	0	0	1.720	76.356
53.0	28.950	1269	0	0	1.720	184.60
54.0	29.410	1279	0	0	1.720	57.255
55.0	29.600	1283	0	0	1.720	60.048
56.0	30.200	1297	0	0	1.720	1259.5
57.0	30.300	1300	0	0	1.720	.00000
58.0	30.560	1306	0	0	1.710	77.748
59.0	30.940	1315	0	0	1.700	737.95
60.0	31.270	1323	0	0	1.690	149.48
61.0	31.880	1338	0	0	1.670	46.904
62.0	32.140	1344	0	0	1.660	46.813
63.0	32.620	1356	0	0	1.650	25.049
64.0	32.870	1362	0	0	1.640	47.891
65.0	33.260	1372	0	0	1.630	30.491
66.0	33.760	1384	0	0	1.610	125.32
67.0	34.330	1398	0	0	1.600	176.99
68.0	34.410	1400	0	0	1.590	.00000
69.0	34.500	1402	0	0	1.600	33.488
70.0	34.780	1409	0	0	1.610	530.99
71.0	35.390	1425	0	0	1.630	359.91
72.0	35.510	1428	0	0	1.630	171.79
73.0	35.920	1438	0	0	1.640	25.701
74.0	36.160	1445	0	0	1.650	183.98
75.0	36.290	1448	0	0	1.650	40.603
76.0	36.770	1460	0	0	1.670	277.89
77.0	37.350	1475	0	0	1.690	84.677
78.0	37.940	1490	0	0	1.710	155.97
79.0	38.290	1500	0	0	1.720	.00000
80.0	38.320	1500	0	0	1.720	138.36
81.0	38.670	1510	0	0	1.710	209.85
82.0	39.110	1522	0	0	1.710	61.565
83.0	39.350	1528	0	0	1.710	76.088
84.0	39.480	1532	0	0	1.710	67.565
85.0	39.660	1537	0	0	1.700	163.18
86.0	39.980	1546	0	0	1.700	50.688
87.0	40.270	1554	0	0	1.700	360.57
88.0	40.910	1571	0	0	1.690	382.99
89.0	41.580	1589	0	0	1.680	83.018
90.0	41.790	1595	0	0	1.680	105.44
91.0	41.950	1600	0	0	1.680	.00000
92.0	42.140	1605	0	0	1.700	23.659
93.0	42.800	1624	0	0	1.770	65.828
94.0	42.990	1629	0	0	1.790	56.629
95.0	43.430	1642	0	0	1.830	51.286
96.0	43.970	1656	0	0	1.890	30.977

FRACTION=2 HP-RUN-DATE= 9/22/1981 HP-RUN-NO= 72 HP-SOT-NO= 9

PEAK NUMBER	RETENTION TIME	KOVAT INDEX	KOVAT SUBGROUP	KOVAT GROUP	RESPONSE FACTOR	CONCENTRATION TOTAL
97.0	44.550	1674	0	0	1.950	23.596
98.0	44.730	1678	0	0	1.960	75.040
99.0	44.870	1683	0	0	1.980	24.234
100.	45.300	1696	0	0	2.020	26.795
101.	45.430	1700	0	0	2.040	.00000
102.	45.630	1710	0	0	2.200	106.89
103.	45.980	1715	0	0	1.990	179.71
104.	46.320	1727	0	0	1.960	80.158
105.	46.590	1735	0	0	1.930	24.762
106.	46.890	1744	0	0	1.900	102.48
107.	47.340	1764	0	0	1.850	202.37
108.	48.450	1791	0	0	1.760	198.88
109.	48.720	1800	0	0	1.740	.00000
110.	49.066	1815	0	0	1.700	.00000
111.	49.560	1826	0	0	1.990	66.389
112.	49.800	1836	0	0	2.070	83.400
113.	50.010	1841	0	0	2.130	43.110
114.	50.820	1866	0	0	2.380	227.38
115.	50.980	1871	0	0	2.430	36.169
116.	51.170	1878	0	0	2.480	33.366
117.	51.470	1887	0	0	2.570	131.40
118.	51.670	1893	0	0	2.630	61.880
119.	51.860	1900	0	0	2.690	.00000
120.	52.110	1908	0	0	2.630	98.167
121.	52.290	1914	0	0	2.580	102.84
122.	52.910	1935	0	0	2.410	184.63
123.	53.060	1940	0	0	2.370	75.793
124.	53.940	1969	0	0	2.130	72.737
125.	54.290	1997	0	0	1.900	25.529
126.	54.850	2008	0	0	1.890	.00000
127.	55.140	2018	0	0	1.890	22.683
128.	55.860	2035	0	0	1.890	26.987
129.	56.290	2050	0	0	1.900	218.64
130.	56.500	2057	0	0	1.900	67.069
131.	56.670	2063	0	0	1.900	28.102
132.	57.010	2075	0	0	1.900	52.511
133.	57.340	2087	0	0	1.900	119.85
134.	57.660	2098	0	0	1.910	45.880
135.	57.710	2100	0	0	1.910	.00000
136.	58.280	2120	0	0	1.900	63.868
137.	59.440	2163	0	0	1.880	67.191
138.	59.700	2172	0	0	1.880	112.23
139.	60.160	2189	0	0	1.870	26.102
140.	60.440	2200	0	0	1.870	.00000
141.	60.500	2202	0	0	1.870	45.016
142.	61.930	2256	0	0	1.870	67.085
143.	63.040	2298	0	0	1.870	23.278
144.	63.070	2300	0	0	1.870	.00000
145.	63.680	2324	0	0	1.830	23.384
146.	65.570	2400	0	0	1.700	.00000
147.	67.740	2489	0	0	1.660	29.996
148.	67.990	2500	0	0	1.650	.00000
149.	69.240	2552	0	0	1.650	41.619
150.	70.370	2600	0	0	1.650	.00000
151.	70.590	2607	0	0	1.700	25.283
152.	73.130	2700	0	0	2.300	.00000
153.	76.440	2800	0	0	1.660	.00000
154.	80.580	2900	0	0	1.680	.00000
155.	85.500	3000	0	0	1.830	.00000
156.	91.750	3100	0	0	3.440	.00000

TOTAL RESOLVED HYDROCARBON = 22520.58
TOTAL UNRESOLVED HYDROCARBON = 36649.98
RESPONSE FACTOR AV. FOR C =1400 TO 3200 FOR UCM = 1.961737
RATIO: RESOLVED/UNRESOLVED = 0.614148

SUM OF THE N-ALKANES = 0
SUM OF THE EVEN N-ALKANES = 0
[illegible] N-ALKANES = 0

TABLE 3-8. WILMINGTON CRUDE OIL CONCENTRATIONS FOR ALIPHATIC FRACTION.

FRACTION#1 HP-RUN-DATE:10/21/1981 HP-RUN-NO: 34 HP-BOT-NO: 7

PEAK NUMBER	RETENTION TIME	KOVAT INDEX	KOVAT SUBGROUP	KOVAT GROUP	RESPONSE FACTOR	CONCENTRATION TOTAL
1.00	5.0100	0	0	0	1.440	540.78
2.00	5.1600	0	0	0	1.440	17470.
3.00	5.3200	0	0	0	1.440	1414.6
4.00	5.7900	0	0	0	1.440	1043.3
5.00	15.120	0	0	0	1.440	82.352
6.00	16.460	0	0	0	1.440	76.485
7.00	16.650	0	0	0	1.440	91.486
8.00	17.790	1000	0	0	1.440	77.525
9.00	18.210	1009	0	0	1.440	78.936
10.0	19.060	1027	0	0	1.440	92.822
11.0	19.670	1040	0	0	1.440	82.797
12.0	20.900	1066	0	0	1.440	145.77
13.0	21.400	1076	0	0	1.440	111.46
14.0	21.710	1083	0	0	1.440	80.644
15.0	23.200	1115	0	0	1.440	77.228
16.0	23.460	1120	0	0	1.440	80.198
17.0	23.960	1131	0	0	1.440	317.45
18.0	24.640	1145	0	0	1.440	109.53
19.0	24.900	1151	0	0	1.440	102.62
20.0	25.750	1169	0	0	1.440	225.82
21.0	26.400	1182	0	0	1.440	172.95
22.0	26.720	1189	0	0	1.440	167.45
23.0	27.230	1200	0	0	1.430	236.43
24.0	28.520	1229	0	0	1.440	106.79
25.0	29.530	1252	0	0	1.440	139.65
26.0	30.010	1263	0	0	1.440	143.62
27.0	31.580	1300	0	0	1.450	139.56
28.0	33.270	1340	0	0	1.420	75.580
29.0	33.530	1346	0	0	1.410	205.90
30.0	34.210	1362	0	0	1.400	83.654
31.0	35.760	1400	0	0	1.380	.00000
32.0	36.910	1426	0	0	1.410	128.37
33.0	37.780	1446	0	0	1.440	117.04
34.0	38.090	1453	0	0	1.450	122.81
35.0	38.460	1462	0	0	1.460	255.28
36.0	38.850	1471	0	0	1.470	249.05
37.0	40.100	1500	0	0	1.510	85.394
38.0	42.500	1600	0	0	1.500	93.802
39.0	44.520	1647	0	0	1.550	140.10
40.0	46.080	1685	0	0	1.580	287.25
41.0	46.300	1690	0	0	1.590	113.54
42.0	46.710	1700	0	0	1.600	153.16
43.0	48.140	1710	0	0	1.500	350.08
44.0	50.200	1800	0	0	1.510	102.09
45.0	51.710	1815	0	0	1.440	127.47
46.0	53.340	1900	0	0	2.160	.00000
47.0	56.030	2000	0	0	1.560	101.49
48.0	57.160	2035	0	0	1.580	62.645
49.0	59.240	2100	0	0	1.610	.00000
50.0	63.110	2200	0	0	1.650	279.55
51.0	65.270	2300	0	0	1.740	117.53
52.0	66.050	2400	0	0	1.630	160.37
53.0	69.610	2500	0	0	1.670	.00000
54.0	72.300	2600	0	0	1.720	.00000
55.0	74.610	2700	0	0	2.560	362.38
56.0	79.280	2800	0	0	1.770	.00000
57.0	84.000	2900	0	0	1.850	.00000
58.0	91.530	3000	0	0	1.920	213.71
59.0	96.368	3049	0	0	2.270	325.16
60.0	97.230	3100	0	0	2.630	.00000
61.0	100.76	3138	0	0	2.520	138.29
62.0	106.49	3200	0	0	2.320	.00000

TOTAL RESOLVED HYDROCARBON = 28358.51
TOTAL UNRESOLVED HYDROCARBON = 179475
RESPONSE FACTOR AV. FOR C - 1000 TO 3100 FOR UCM = 1.762911
RATIO: RESOLVED/UNRESOLVED = 0.157569

SUM OF THE N-ALKANES = 2023.472
SUM OF THE EVEN N-ALKANES = 1185.446
SUM OF THE ODD N-ALKANES = 838.0259

RATIO: (PRISTANE+PHYTANE)/(N-ALKANES) = 0.236606
RATIO: ODD/EVEN N-ALKANES = 0.706929
RATIO: PRISTANE/C-17 = 2.285708
RATIO: PHYTANE/C-18 = 1.248612
RATIO: PRISTANE/PHYTANE = 2.746258
RATIO: (N-ALKANES)/(BRANCHED HYDROCARBONS) = 7.623572E-2

Weight Distribution of Wilmington Crude by Fraction

Fraction	Weight (mg/g)
1	205
2	335
3	204

TABLE 3-9. WILMINGTON CRUDE OIL CONCENTRATIONS FOR AROMATIC FRACTION.

FRACTION:2 HP-RUN-DATE:10/21/1981 HP-RUN-NO: 35 HP-BOT-NO: 9

PEAK NUMBER	RETENTION TIME	KOVAT INDEX	KOVAT SUBGROUP	KOVAT GROUP	RESPONSE FACTOR	CONCENTRATION TOTAL
1.00	5.3500	0	0	0	1.440	273.42
2.00	5.6000	0	0	0	1.440	507.48
2.50	5.6200	700	0	0	.0000	.00000
3.00	5.8200	705	0	0	1.440	2570.7
4.00	5.9000	706	0	0	1.440	170.29
5.00	6.3600	717	0	0	1.440	1402.1
6.00	6.6400	724	0	0	1.440	584.55
7.00	7.6300	746	0	0	1.440	442.19
8.00	27.240	1200	0	0	1.430	.00000
9.00	31.620	1300	0	0	1.450	.00000
10.0	35.760	1400	0	0	1.380	.00000
11.0	39.660	1500	0	0	1.510	.00000
12.0	43.360	1600	0	0	1.500	.00000
13.0	44.550	1634	0	0	1.530	232.30
14.0	46.810	1698	0	0	1.600	103.07
15.0	46.860	1700	0	0	1.600	.00000
16.0	47.080	1710	0	0	1.500	.00000
17.0	47.860	1730	0	0	1.570	100.29
18.0	50.180	1800	0	0	1.510	.00000
19.0	50.510	1815	0	0	1.440	.00000
20.0	53.340	1900	0	0	2.160	.00000
21.0	53.700	1911	0	0	2.080	200.20
22.0	56.050	1989	0	0	1.620	189.65
23.0	56.360	2000	0	0	1.560	.00000
24.0	57.390	2035	0	0	1.580	113.34
25.0	57.920	2054	0	0	1.580	144.18
26.0	59.240	2100	0	0	1.610	.00000
27.0	61.090	2167	0	0	1.630	156.63
28.0	61.370	2177	0	0	1.640	113.98
29.0	61.990	2200	0	0	1.650	.00000
30.0	64.630	2300	0	0	1.740	.00000
31.0	65.440	2331	0	0	1.710	101.68
32.0	67.170	2400	0	0	1.630	.00000
33.0	69.610	2500	0	0	1.670	.00000
34.0	72.300	2600	0	0	1.720	.00000
35.0	75.440	2700	0	0	2.560	.00000
36.0	79.280	2800	0	0	1.770	.00000
37.0	84.000	2900	0	0	1.850	.00000
38.0	89.860	3000	0	0	1.920	.00000
39.0	97.230	3100	0	0	2.630	.00000
40.0	106.49	3200	0	0	2.320	.00000

TOTAL RESOLVED HYDROCARBON = 7446.003
TOTAL UNRESOLVED HYDROCARBON = 67236.01
RESPONSE FACTOR AV. FOR C = 1600 TO 3100 FOR UCM = 1.821669
RATIO: RESOLVED/UNRESOLVED = 0.1107443

SUM OF THE N-ALKANES = 0
SUM OF THE EVEN N-ALKANES = 0
SUM OF THE ODD N-ALKANES = 0

RATIO: (PRISTANE+PHYTANE)/(N-ALKANES) = 0
RATIO: ODD-EVEN N-ALKANES = 0
RATIO: PRISTANE/C-17 = 0
RATIO: PHYTANE/C-18 = 0
RATIO: PRISTANE/PHYTANE = 0
RATIO: (N-ALKANES)/(BRANCHED HYDROCARBONS) = 0

TABLE 3-10. POLAR (F3) FRACTION COMPONENTS FOR THE FOUR SELECTED CRUDES.

Murban Crude Oil Concentrations for Polar Fraction

Retention Time (min)	Kovat	Concentration (µg/g)
18.95	1026	121.
78.75	2787	116.

Cook Inlet Crude Oil Concentrations for Polar Fraction

Retention Time (min)	Kovat	Concentration (µg/g)
18.99	1026	151.
78.80	2787	111.

Prudhoe Bay Crude Oil Concentrations for Polar Fraction

Retention Time (min)	Kovat	Concentration (µg/g)
5.14	640	64.4
8.55	806	49.6
9.14	861	28.4

Wilmington Crude Oil Concentrations for Polar Fraction

Retention Time (min)	Kovat	Concentration (µg/g)
18.99	1026	211.
78.76	2787	224.

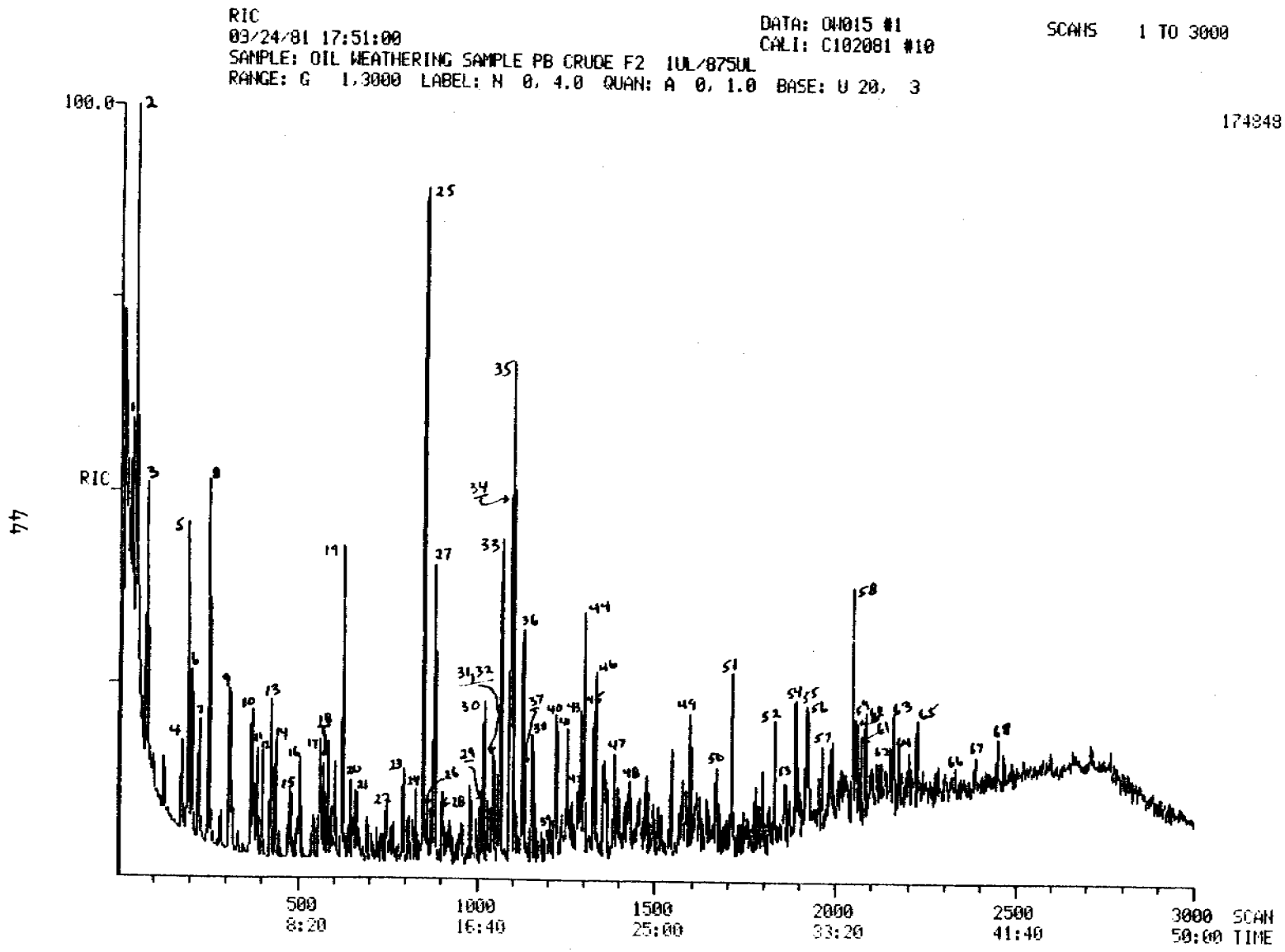

FIGURE 3-5. RECONSTRUCTED ION CHROMATOGRAM (RIC) GENERATED FROM GC/MS ANALYSES OF THE AROMATIC FRACTION (F2) OF PRUDHOE BAY CRUDE OIL. IDENTIFICATIONS OF THE NUMBERED PEAKS ARE PRESENTED IN TABLE 3-11.

TABLE 3-11. GC/MS IDENTIFICATIONS OF SELECTED COMPONENTS IN THE AROMATIC FRACTION OF PRUDHOE BAY CRUDE OIL (SEE FIGURE 3-5).

1	ethylbenzene
2	p-xylene
3	o-xylene
4	n-propylbenzene
5	ethylmethylbenzene
6	trimethylbenzene
7-9	C_3 benzenes
10	methylpropylbenzene
11-13	C_4 benzenes
14	ethyldimethylbenzene
15	C_4 benzene
16	tetramethylbenzene
17	unsaturated C_4 benzene (possibly a methylindane)
18	C_4 benzene
19	naphthalene
20,21	unsaturated C_5 benzenes (possibly C_2 indanes)
22	unsaturated C_6 benzene (possibly a C_2 tetralin)
23,24	C_6 benzenes
25	2-methylnaphthalene
26	unsaturated C_6 benzene (possibly a C_2 tetralin)
27	1-methylnaphthalene
28	unsaturated C_6 benzene (possibly a C_2 tetralin)
29	C_7 benzene
30	biphenyl
31	2-ethylnaphthalene
32	1-ethylnaphthalene
33-38	dimethylnaphthalenes
39	C_3 naphthalene
40	methylbiphenyl
41	2-isopropylnaphthalene
42	1-isopropylnaphthalene
43-46	trimethylnaphthalenes
47	fluorene
48	dimethylbiphenyl
49	methylfluorene
50	dibenzothiophene
51	phenanthrene
52,53	methyldibenzothiophenes
54-56	methylphenanthrenes
57	C_2 napthothiophenes
58-61	dimethylphenanthrenes
62-65	C_3 phenanthrenes
66	benzonaphthothiophene
67	chrysene or benz (a)anthracene
68	phthalate ester

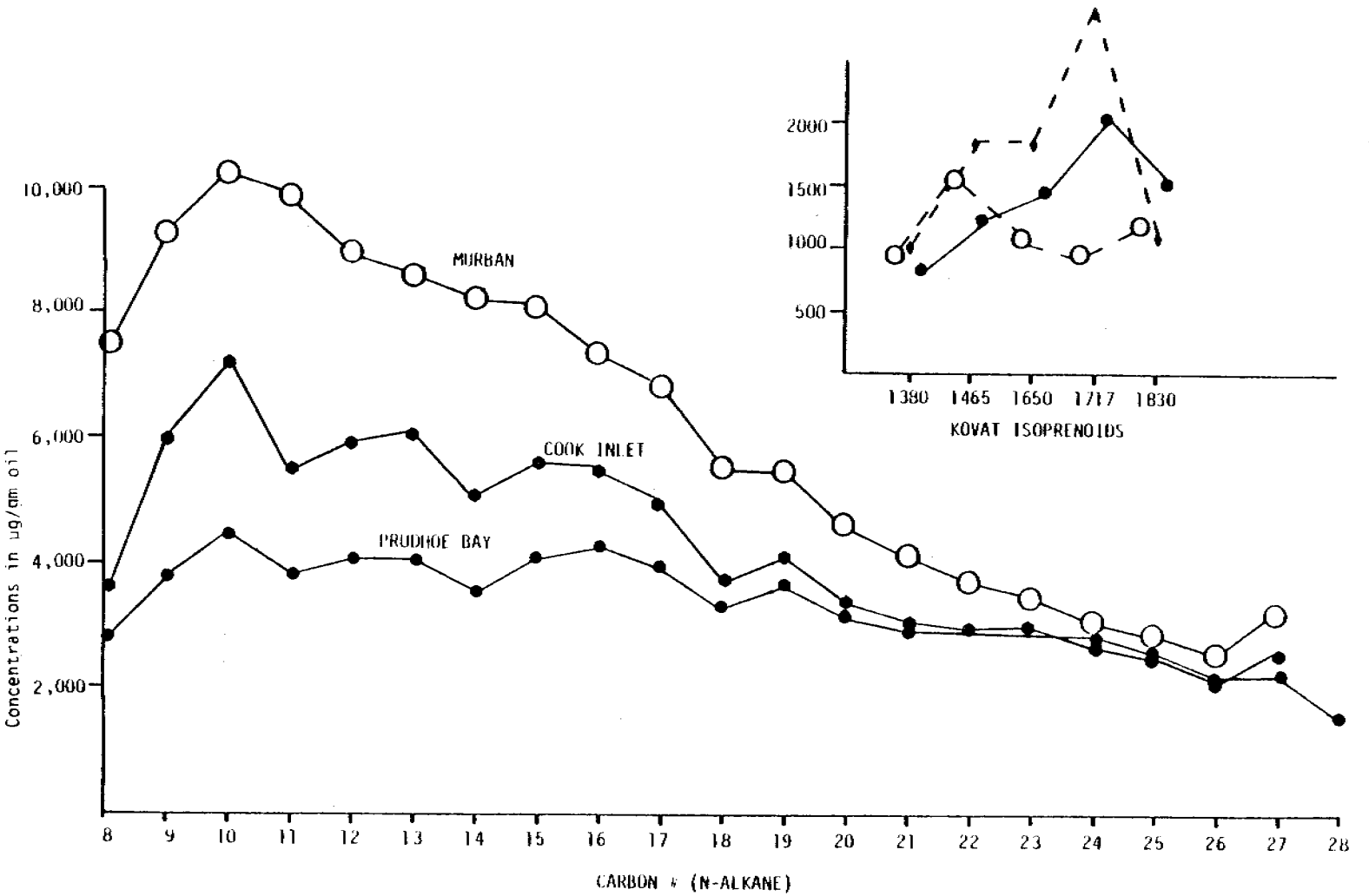

FIGURE 3-6. ALIPHATIC (n-alkane and isoprenoid) CARBON DISTRIBUTIONS FOR PRUDHOE BAY, COOK INLET AND MURBAN (middle east) CRUDE OILS.

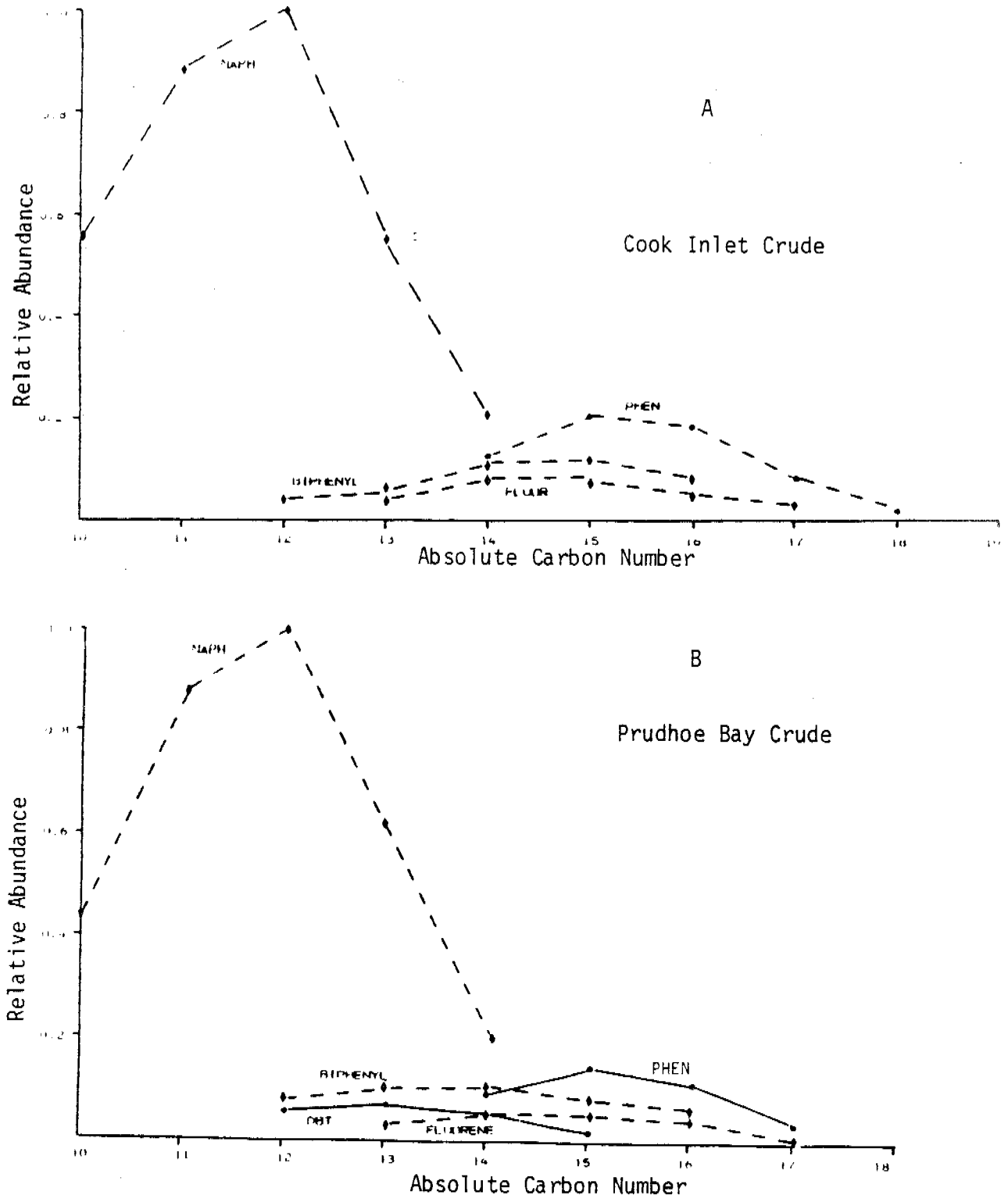

FIGURE 3-7. RELATIVE ABUNDANCE PLOTS FROM SELECTIVE ION MONITORING (GCMS) OF THE MAJOR ALKYL SUBSTITUTED AROMATIC SERIES DETECTED IN COOK INLET (TOP) AND PRUDHOE BAY (BOTTOM) OILS. (NAPH - naphthalene; PHEN- phenanthrenes; DBT - dibenzothiophenes; FLUOR - fluorenes)

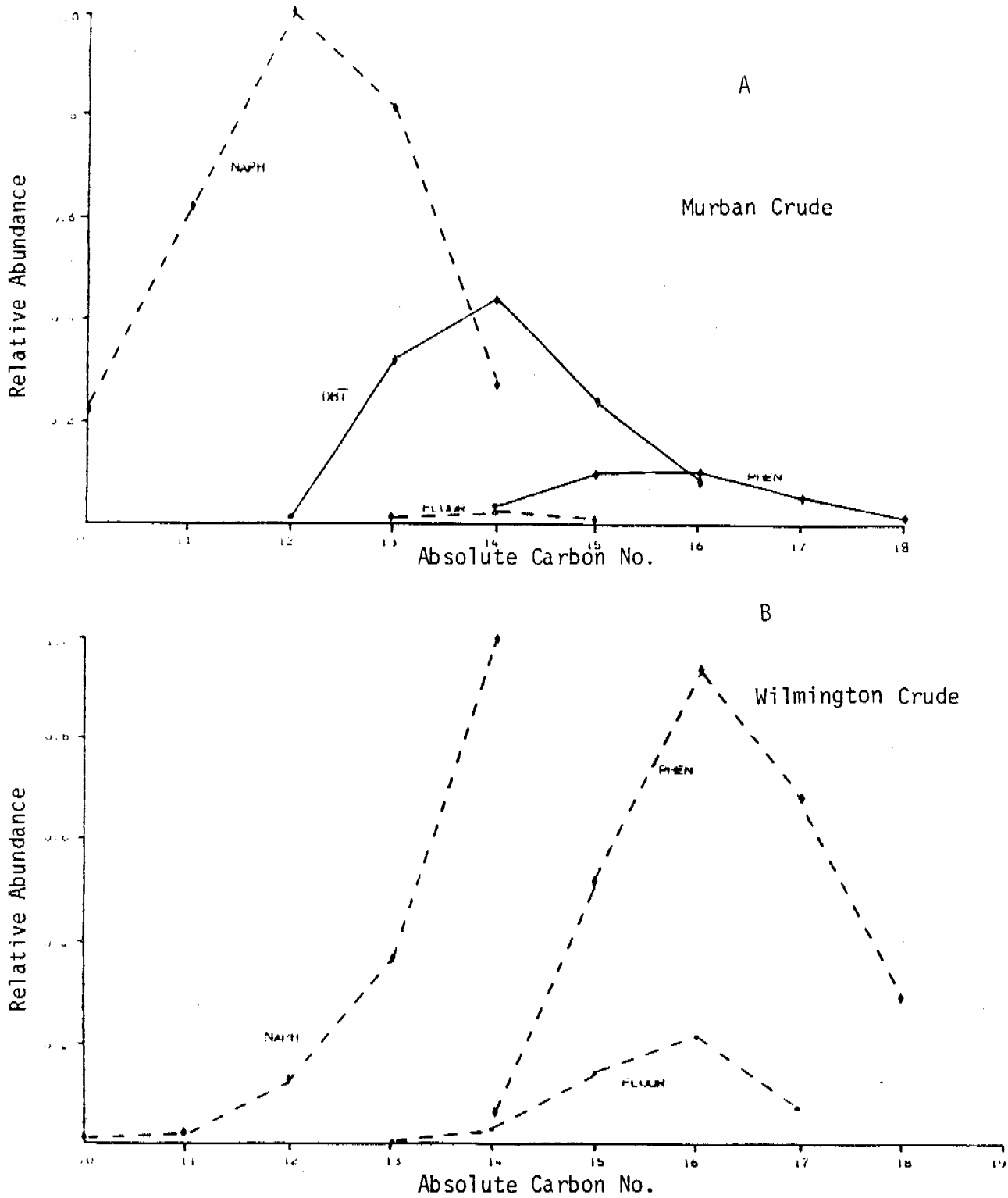

FIGURE 3-8. RELATIVE ABUNDANCE PLOTS FROM SELECTIVE ION MONITORING (GCMS) OF THE MOLECULAR ION FOR THE MAJOR ALKYL SUBSTITUTED AROMATIC SERIES DETECTED IN THE MURBAN (TOP) AND LONG BEACH (BOTTOM) CRUDE OILS. (Abbreviations as in Figure 3-7)

Even more striking similarities of the two Alaskan crude oils are depicted in Figure 3-7, which shows the relative abundance of alkyl-substituted polynuclear aromatic (PNA) hydrocarbons as derived from selected ion monitoring GC/MS analyses. Figure 3-7A presents the relative abundance of the PNAs for Cook Inlet crude and Figure 3-7B presents the same data for Prudhoe Bay crude oil. It should be noted that in these oils, as in many other crudes, the alkyl-substituted polynuclear aromatic compounds are predominant over the non-substituted parent compounds. In Figure 3-7 the parent hydrocarbon is denoted by the first data point nearest the origin of the Absolute Carbon Number coordinate, and the degree of alkyl-substitution is then shown to increase with, for example, 11 representing methylnaphthalene, 12 representing dimethylnaphthalene, etc. In comparing Prudhoe Bay and Cook Inlet crudes it can be seen that the relative abundance of alkyl-substituted naphthalenes are nearly identical, and similar trends are observed for biphenyl, fluorene and phenanthrene. In this instance, Cook Inlet crude shows some evidence of slightly higher relative levels of alkyl-substituted phenanthrene. Of these two oils, only Prudhoe Bay crude oil contained significant concentrations of the alkyl-substituted sulfur-heteroaromatic dibenzothiophenes. This is also reflected in the difference in weight percent sulfur of the two crudes as shown by the data in Table 3-1. Figure 3-8 presents the relative abundance plots for the alkyl-substituted polynuclear aromatic hydrocarbons in Murban Crude and Wilmington crude. The alkyl-substituted naphthalene composition of Murban crude is similar to that observed for the two Alaskan crudes; however, this oil contains significantly higher levels of alkyl-substituted dibenzothiophenes, and again the weight percent sulfur in the crude is somewhat higher. The alkyl-substituted naphthalene distribution for Wilmington crude is significantly different from the other three oils considered, and of the four crudes it has the highest relative abundance of phenanthrene and fluorene.

Interestingly, there were no significant levels of dibenzothiophene detected. BALL and RALL (1962) have shown that the sulfur content of the low-boiling (up to 250°C) fractions of Wilmington crude is predominantly in

the form of alkyl thiophenes and saturated cyclic sulfides. The bulk of the sulfur-containing components, however, were in the residue and were not characterized in that study. It should be noted from the data in Table 3-1 that the Wilmington crude also had the highest levels of the trace elements nickel and vanadium.

Another significant feature of the relative abundance plots for aliphatic and aromatic hydrocarbons is that the crudes with higher API gravities (lower specific gravities) also tend to have higher relative concentrations of the lower molecular weight, and less dense, aliphatic and aromatic hydrocarbons. That is, the Wilmington crude with the lowest API gravity is not represented by lower molecular weight aliphatic materials and the aromatic fractions are skewed towards the more highly alkyl-substituted phenanthrenes and fluorenes. As the data in Table 3-1 illustrate, the lower API gravity crudes also tend to have higher weight percent asphalts.

Synchronous scanning spectrofluorometry has also been used to characterize the polynuclear aromatic hydrocarbons content of crude oil and sediments and waters exposed to crude oils (WAKEHAM, 1977; GORDON et al., 1976; VO-DINH et al., 1978; BOEHM and FIEST, 1980) and this technique was also used in our studies to characterize the four selected crude oils examined. Families of aromatic hydrocarbons can be revealed by this method (LLOYD, 1971) and synchronous scan UV fluorescence spectra of the four crudes are shown in Figures 3-9, 3-10 and 3-11. These spectra were obtained on a Perkin-Elmer model MPF-44A high performance fluorescence spectrofluorometer with the exitation and emission monochromoters offset by 30 nm. The combined excitation emission spectra were obtained over the range of 230 to 600 nm. In general, monocyclic aromatic hydrocarbons emit most strongly in the 280 to 290 nm region, dicyclic aromatics such as alkyl-substituted naphthalenes emit at about 310 to 320 nm; 3 and 4 ring aromatics emit in the range of 340 to 380 nm and compounds with greater than 5 rings emit in the range of 400 to 470 nm.

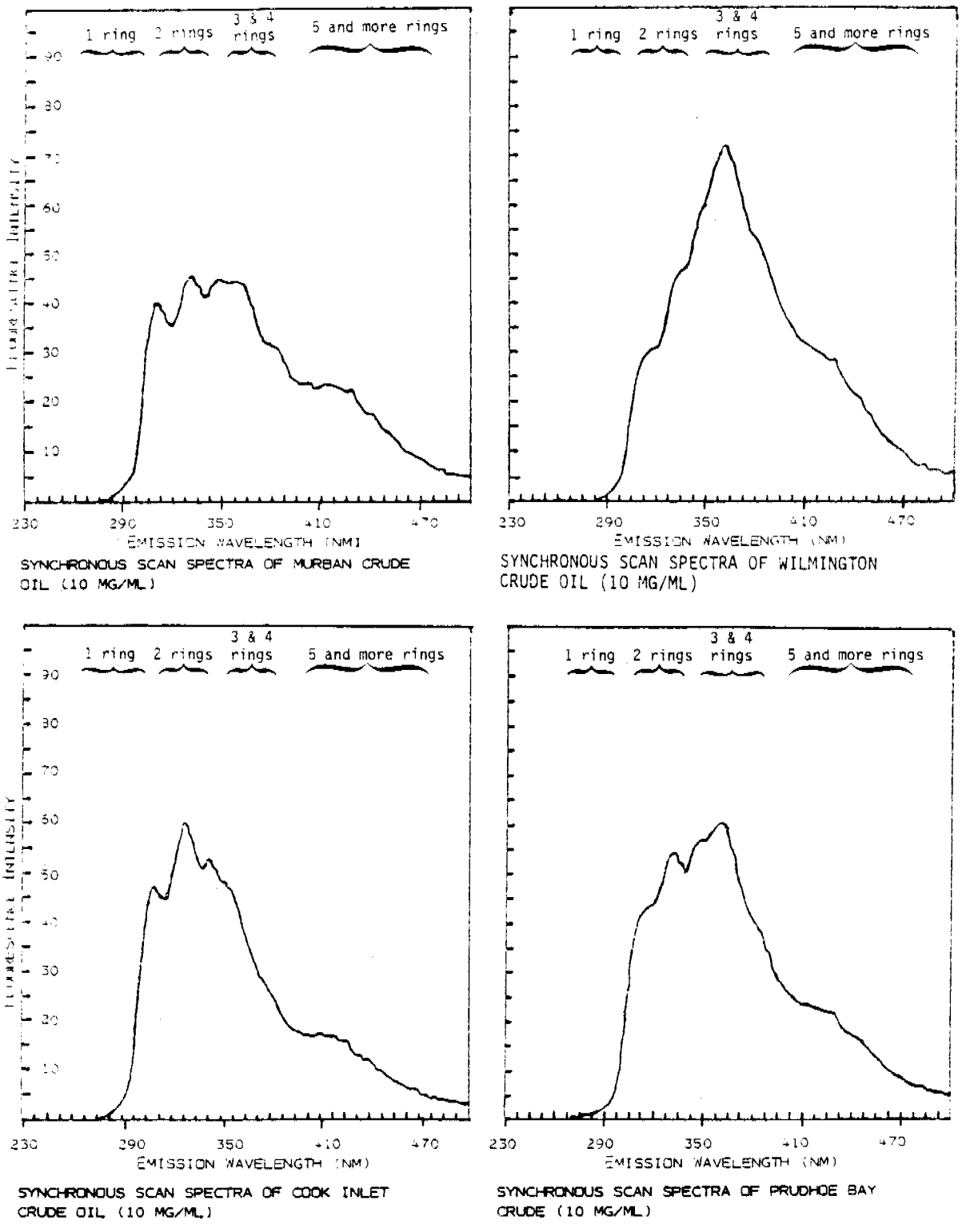

FIGURE 3-9. SYNCHRONOUS SCAN UV FLUORESCENCE SPECTRUM OF 10 mg/ml CONCENTRATION OF THE FOUR SELECTED CRUDE OILS.

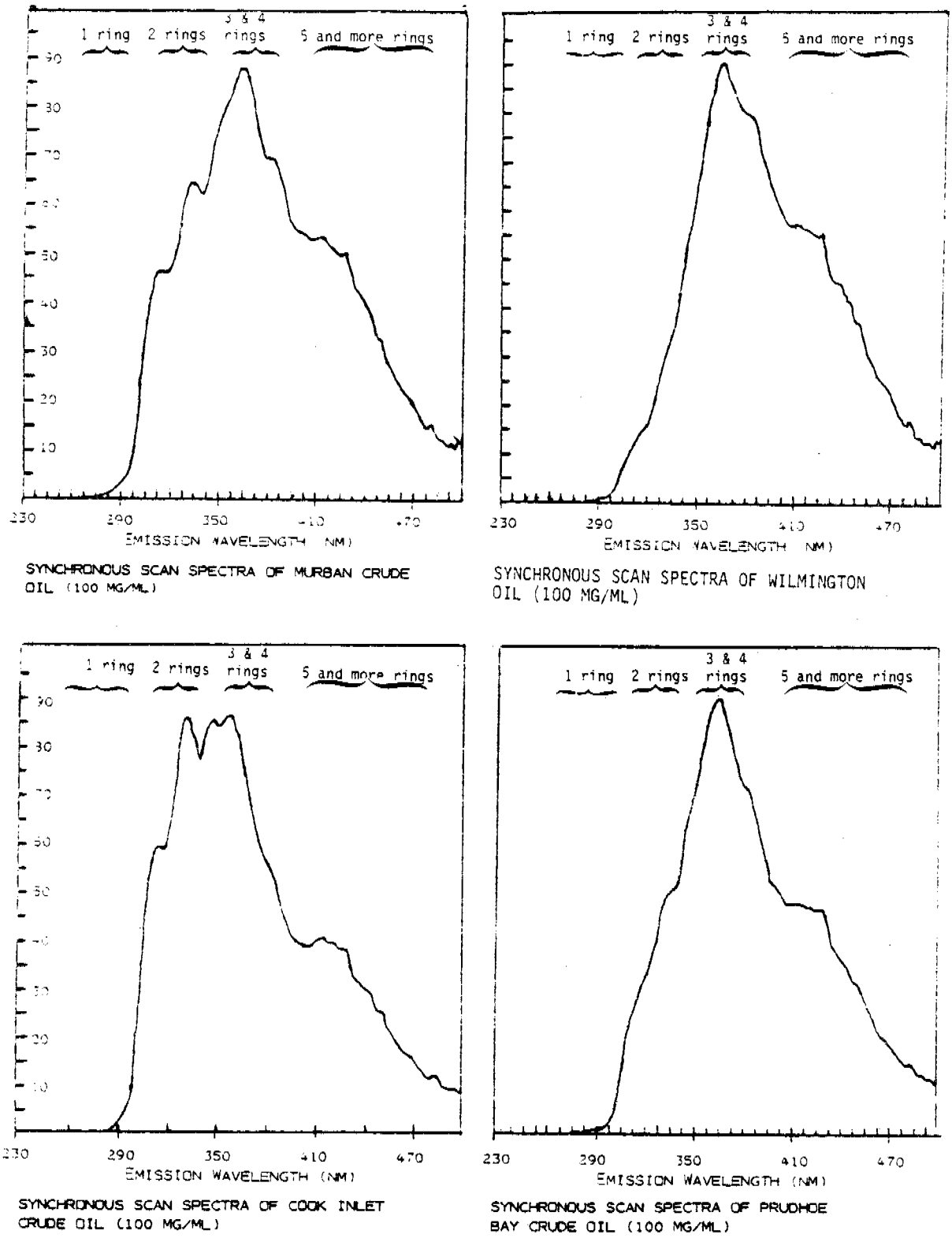

FIGURE 3-10. SYNCHRONOUS SCAN UV FLUORESCENCE SPECTRUM OF 100 mg/ml CONCENTRATIONS OF THE FOUR SELECTED CRUDE OILS.

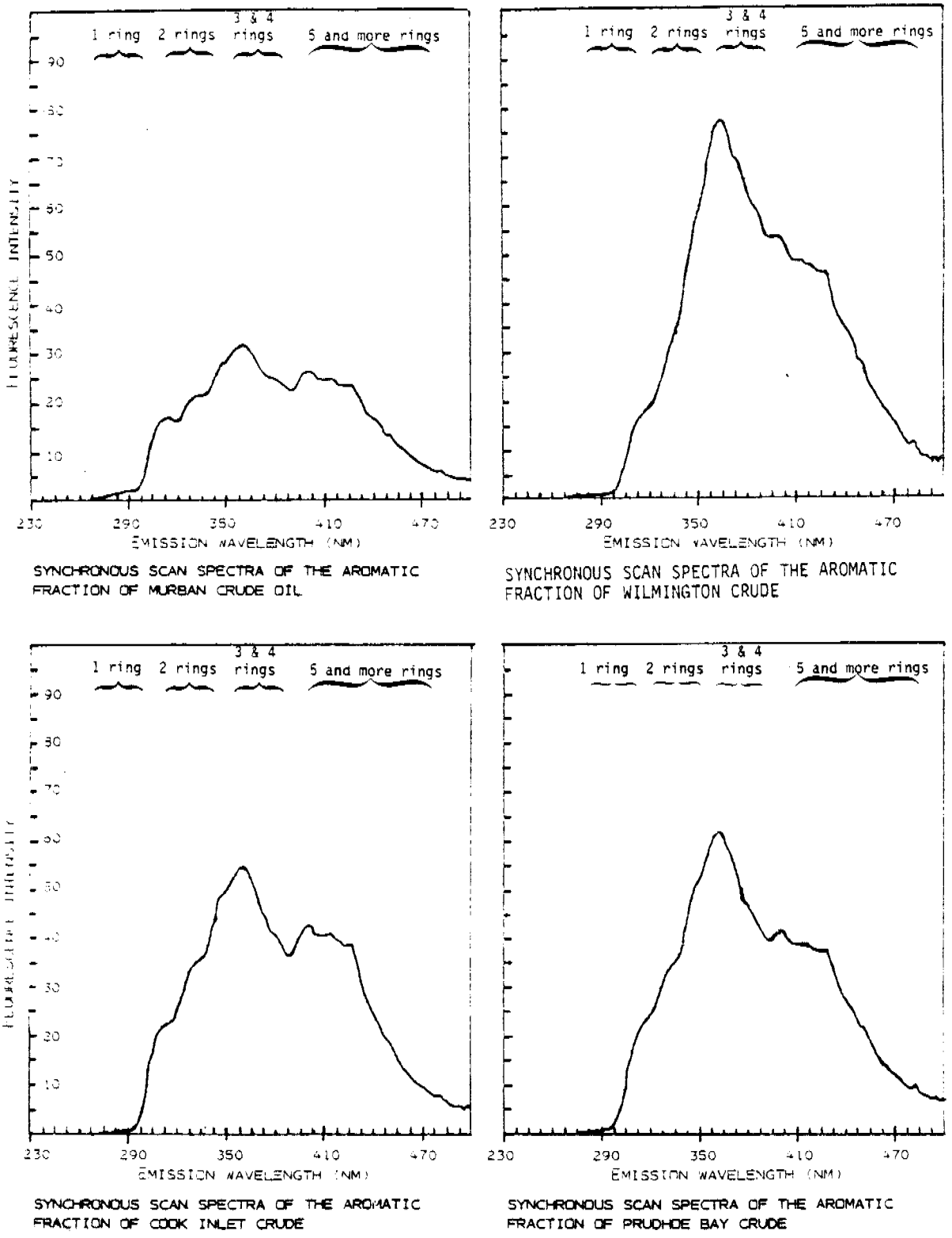

FIGURE 3-11. SYNCHRONOUS SCAN UV FLUORESCENCE SPECTRUM OF THE AROMATIC FRACTIONS OF THE FOUR SELECTED CRUDE OILS.

The four crudes shown in Figure 3-9 were scanned at concentrations of 10 mg/ml in spectral grade cyclohexane and the spectra shown in Figure 3-10 were obtained at concentrations of 100 mg/ml. It can be seen from the spectra presented in Figures 3-9 and 3-10 that at lower concentrations better fluorescence resolution for the small ringed compounds is obtained at the lower wavelengths. At higher concentrations, greater fluorescence and resolution is observed for the 4 and 5 ring compounds, reflecting the effective energy transfer processes which occur at higher concentrations (JOHN and SOUTAR, 1976; VO-DIDH et al.)

From the spectra of the whole crude oil samples it appears that Cook Inlet and Murban crude oils contain a higher abundance of 2 and 3 ring aromatic compounds with Prudhoe Bay crude being intermediate and Wilmington having the lowest relative abundance of these compounds. As noted above, these compositional differences are also illustrated by the relative abundance PNA plots presented in Figures 3-7 and 3-8. The 4 and 5 ring aromatics appears to be more concentrated in the Wilmington and Murban crude oils. Figure 3-11 presents the synchronous scan UV-fluorescence spectra obtained on the aromatic fractions of each of the selected oils, and while the results are similar to those obtained for the unfractionated oils, a slight relative increase in fluorescence from the 3, 4, and 5 ring compounds can be observed.

While component-specific data are necessary for developing an oil weathering model, additional data are also required to enable a mass balance approach describing the state of an actively weathering oil slick. As was discussed in the previous sections on modeling, it is not possible to develop a mass balance model of oil weathering if only specific organic compounds, or even confined groups of compounds, are considered. Thus, to obtain information on the overall mass balance for various spilled crude oils, fractional distillation data are required of the type routinely used in the petroleum industry for overall oil characterizations. With such an approach, compounds can be grouped into pseudo-component classes based on their boiling points,

and cumulative percent compositional data can be obtained on crudes as a function of the true boiling point distillation curve. Tables 3-12 through 3-15 present the fractional-distillation cut data (COLEMAN et al, 1978) for Murban, Cook Inlet, Prudhoe Bay and Wilmington crudes, respectively. The percent composition of each fractional cut is presented by boiling point, and the cumulative volume percent and API gravity of each distillation cut are also given. From this data, it can be seen that cumulative percent distilled can vary significantly from oil to oil, and it is also possible to see how different oil compositions are skewed to higher or lower molecular weight components. Note that the relative percent of nondistillable residue increases from Murban crude (19.1%) to Cook Inlet (25.6%) to Prudhoe Bay crude (36.3%) to Wilmington crude (53.3%) in line with the relative compositions of higher molecular weight materials, percent asphalt and (to a general extent) Kinematic and Saybolt viscosities. Not surprisingly, a relatively smooth decreasing trend in API gravity is also observed with each distillate cut. Figure 3-12 presents the true boiling point distillation curves showing the cumulative volume percent of each crude distilled vs. true boiling point in °F up to the limit of the nondistillable stillpot residual. Similar plots will be utilized extensively with the development of the pseudo component oil weathering model, and predicted vs. observed (as derived from capillary GC data) distillation curves will be used to compare oil weathering model output and observed field data.

In examining the detail from Tables 3-12 through 3-15, and the curves presented in Figure 3-12, it can be seen that significant portions of each of the crudes occur in the non-distillable residuum with boiling points above 790°F. Thus, while Murban and Cook Inlet crudes have 80% and 71% distillable components, Prudhoe Bay crude oil and Wilmington crude oil have distillable fractions consisting of only 62.6% and 46.3% of the starting oil, respectively. The steepness of the boiling point distillation temperature vs. percent distilled curves in Figure 3-12 also shows the relative differences in percent higher molecular weight non-boiling components. That is, the steeper the

TABLE 3-12. FRACTIONAL DISTILLATION DATA ON MURBAN BAB-BU HASA ABU DHABI CRUDE OIL.

Fraction No.	Cut Temp °F	Volume Percent	Cumulative Percent	°API 60°F	Cumulative % Based on Total Distillable Only
1	122	1.7	1.7	96.7	2.1
2	167	2.9	4.6	86.2	5.7
3	212	4.9	9.5	70.6	11.8
4	257	6.0	15.5	62.3	19.4
5	302	6.7	22.2	55.7	27.7
6	347	6.4	28.6	51.6	35.7
7	392	5.7	34.3	48.5	42.8
8	437	5.6	39.9	45.6	49.8
9	482	5.9	45.8	43.0	57.2
10	527	4.9	50.7	40.0	63.3
11	580	5.7	56.4	35.8	70.4
12	638	5.6	62.0	34.0	77.4
13	685	6.5	68.5	30.0	85.5
14	738	6.0	74.5	28.4	93.0
15	790	5.6	80.1	26.6	100

% Non-distillable residuum: 19.1; cumulative % 99.2; °API 16.7

% Asphalt in residuum: 30

TABLE 3-13. FRACTIONAL DISTILLATION DATA ON COOK INLET, ALASKA CRUDE OIL (McArthur River Field).

Fraction No.	Cut Temp °F	Volume Percent	Cumulative Percent	°API 60°F	Cumulative % Based on Total Distillable Only
1	122	2.4	2.4	89.2	3.4
2	167	2.5	4.9	77.2	6.9
3	212	5.9	10.8	65.0	15.1
4	257	6.1	16.9	59.5	23.7
5	302	5.1	22.0	55.4	30.8
6	347	5.2	27.2	50.8	38.1
7	392	4.9	32.1	46.5	45.0
8	437	5.1	37.2	43.0	52.2
9	482	5.2	42.4	39.6	59.5
10	527	5.0	47.4	37.0	66.5
11	580	3.3	50.7	32.8	71.1
12	638	5.2	55.9	31.3	78.4
13	685	7.0	62.9	28.7	88.2
14	738	4.2	67.1	26.6	94.1
15	790	4.2	71.3	25.0	100

% Non-distillable residuum: 25.6; cumulative % 96.9: °API 11.6

% Asphalt in residuum: 35

TABLE 3-14. FRACTIONAL DISTILLATION DATA ON PRUDHOE BAY, ALASKA CRUDE OIL.

Fraction No.	Cut Temp °F	Volume Percent	Cumulative Percent	°API 60°F	Cumulative % Based on Total Distillable Only
1	122	-	-	-	-
2	167	2.1	2.1	72.7	3.4
3	212	2.6	4.7	64.2	7.5
4	257	3.5	8.2	56.7	13.1
5	302	3.6	11.8	51.6	18.8
6	347	3.7	15.5	47.6	24.8
7	392	3.5	19.0	45.2	30.4
8	437	4.3	23.3	41.5	37.2
9	482	4.8	28.1	37.8	44.9
10	527	5.0	33.1	34.8	52.9
11	580	2.8	35.9	30.6	57.3
12	638	6.5	42.4	29.1	67.7
13	685	6.8	49.2	26.2	78.6
14	738	6.0	55.2	24.0	88.2
15	790	7.4	62.6	22.5	100

% Non-distillable residuum: 36.3; cumulative % 98.9; °API 11.4

% Asphalt in residuum: 57

TABLE 3-15. FRACTIONAL DISTILLATION DATA ON WILMINGTON, CALIFORNIA CRUDE OIL.

Fraction No.	Cut Temp °F	Volume Percent	Cumulative Percent	°API 60°F	Cumulative % Based on Total Distillable Only
1	122	-	-	-	-
2	167	-	-	-	-
3	212	2.3	2.3	68.6	5.0
4	257	2.4	4.7	58.7	10.2
5	302	2.4	7.1	53.0	15.3
6	347	2.5	9.6	48.1	20.7
7	392	2.8	12.4	43.2	26.8
8	437	3.6	16.0	38.8	34.6
9	482	4.4	20.4	35.4	44.1
10	527	5.3	25.7	32.3	55.5
11	580	4.7	30.4	26.8	65.7
12	638	6.3	36.7	24.5	79.3
13	685	4.1	40.8	22.3	88.1
14	738	5.5	46.3	20.3	100
15	790	*	-		

% Non-distillable residuum: 53.5; cumulative % 99.6; °API 8.9

% Asphalt in residuum: 42

* Distillation discontinued at 740°F

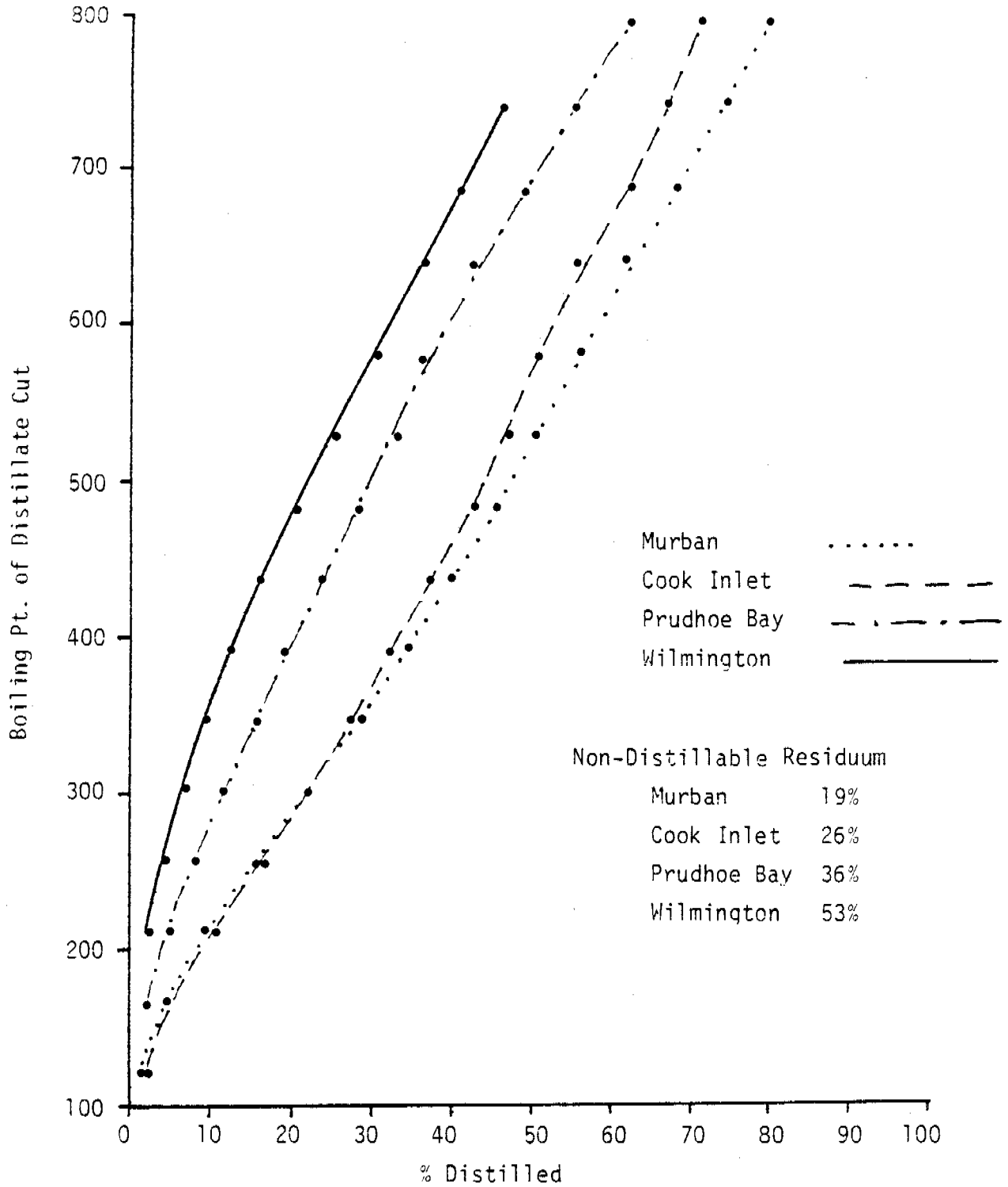

FIGURE 3-12. BOILING POINT DISTILLATION CURVES FOR THE FOUR SELECTED CRUDE OILS STUDIED.

curve in Figure 3-12 the more components present boiling above 790°F. Figure 3-13 shows the cumulative boiling point distributions for the four crudes based on the total distillable fractions only. That is, it is a temperature vs. percent distilled curve for the fraction of the oil which can be distilled below 790°F, and thus, the weight of each distillate cut has been normalized to the overall weight of the total distillate obtained. What this data shows is that at a given temperature less total material of the distillable fraction has been distilled for Prudhoe Bay and Wilmington crude vs Murban and Cook Inlet crude, and this again reflects the somewhat higher molecular weight component concentrations of the Prudhoe Bay and Wilmington crude oils.

Selection of Prudhoe Bay Crude Oil for Further Oil Weathering Studies

Based on the results just presented, Prudhoe Bay crude oil was selected as being the best candidate for extensive sub-arctic weathering studies. Prudhoe Bay crude oil has an API gravity somewhat lower than the Murban or Cook Inlet crudes, yet its aliphatic fraction is represented by an evenly repeating series of alkanes (unlike the Wilmington crude) which facilitates examination of microbial degradation processes. Also, Prudhoe Bay crude oil has a relatively high percent asphaltic fraction and intermediate levels of nickel, vanadium, sulfur and nitrogen, making it an ideal oil for extended studies investigating the formation of water-in-oil emulsions or mousse (PAYNE, 1981). As demonstrated by the synchronous scan UV fluorescence data and the selected ion monitoring relative abundance plots for the polynuclear aromatic hydrocarbons, Prudhoe Bay crude oil is intermediate in overall aromatic hydrocarbon composition. On this basis, the Prudhoe Bay crude is a good representative selection for toxicity determinations on weathered crude oil. Finally, while both Cook Inlet crude oil and Prudhoe Bay crude oil have a higher potential of being released in sub-arctic environments, the selection of Prudhoe Bay crude over Cook Inlet crude was supported by the fact that it contains relatively higher levels of the alkyl-substituted dibenzothiophenes.

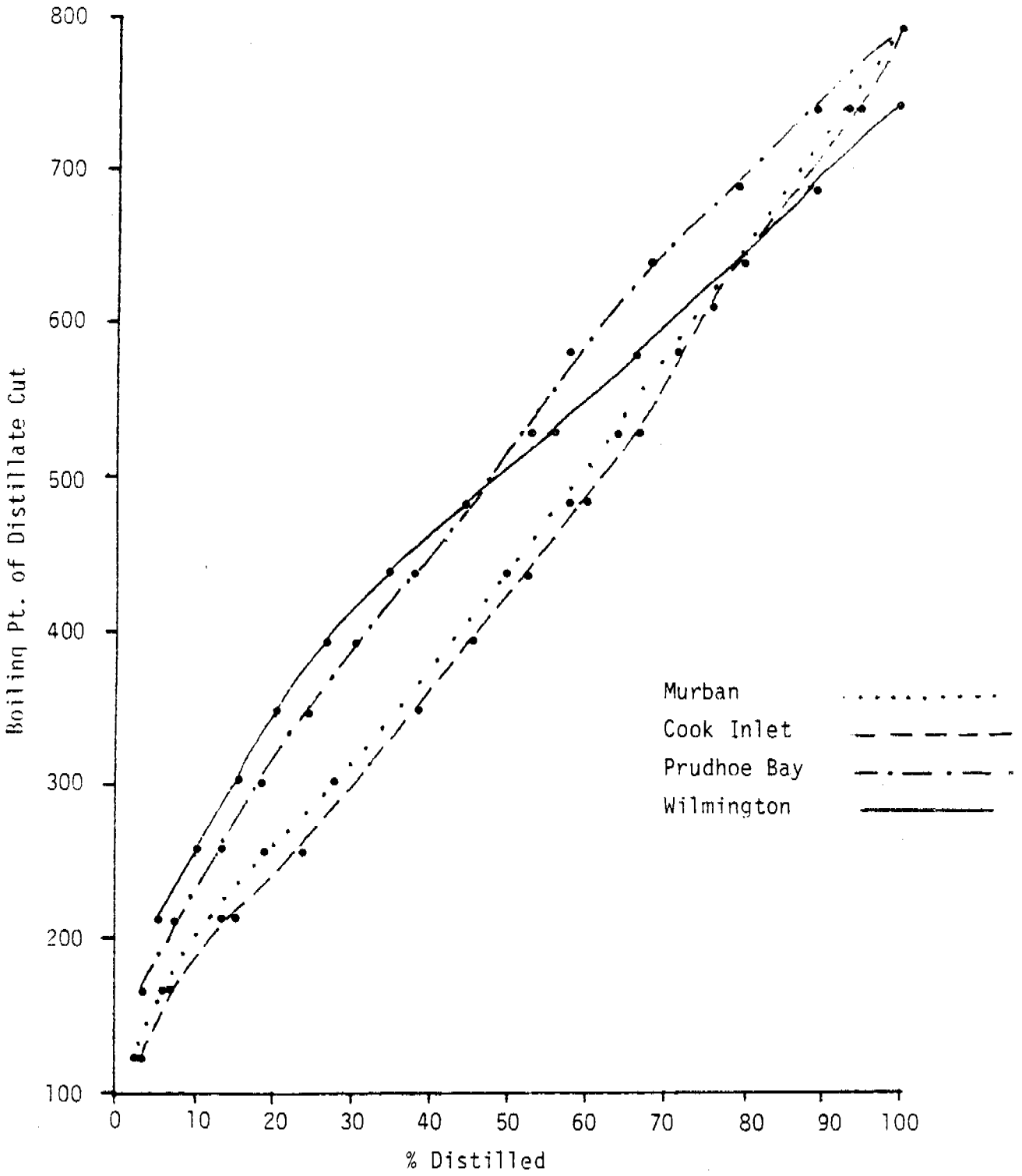

FIGURE 3-13. CUMULATIVE BOILING POINT DISTILLATION CURVES FOR THE TOTAL DISTILLABLE FRACTIONS OF THE FOUR CRUDE OILS STUDIED.

4.0 OIL WEATHERING MODEL DEVELOPMENT

The objectives for a mathematical model of oil weathering on the ocean surface are to temporally predict both the mass of oil remaining in the slick and the chemical composition and physical properties of the oil slick. These two objectives require that oil composition be described in terms of both specific components and component categories, or "pseudocompounds." Pseudocomponent classification has been widely used in the petroleum industry to describe crude oil because of the inherent interest in bulk oil characteristics and accounting for total mass. A specific-component description is of more interest to describing spilled oil as a changing source of foreign chemicals to an aquatic ecosystem, but the complexity of oil composition makes it impractical to keep track of bulk oil mass in terms of individual components.

The mathematical models presented in this report are in various stages of development and computerization. The most developed to date are those describing the evaporation and dissolution processes, and present for the first time a coupling of the two types of material balance models (specific- and pseudo-component) in a form that will provide environmental predictions. These models incorporate the concepts of interfacial mass transfer, the considerations of both mechanically well-stirred and stagnant oil phases, the effects of slick spreading, and the boundary conditions imposed on the oil by the environment. In addition, these models include descriptive predictions of specific compound concentrations in the air and water columns in contact with a slick or other spilled oil phase.

Both portions of the model require distinct and independent mathematical formulations. In order to predict the mass of oil remaining in a slick as a function of time, a method of characterizing the bulk oil with respect to the various transport processes that alter and dissipate oil must be utilized. The total oil mass cannot be characterized by its individual components because of their number and complexity, and the limitations of analysis. To compensate for these limitations, the pseudo-component approach "cuts" oil into a number of fractions, assigning appropriate physical properties to each.

In attempting to predict the mass of oil remaining in a slick, the two most important mass transport processes to consider are evaporation and dissolution. Of these two, evaporation appears to have the greater influence, certainly over short time scales, making vapor pressure an especially important oil characteristic. Adequate description of the dissolution process, on the other hand, requires water solubility information. The pseudo-component approach to describe these processes is to cut the oil into a number of fractions based on properties of distillation fractions.

The pseudo-component approach, which is that taken in virtually all previous efforts to model oil weathering, is singularly useful for providing total material balances with time for spilled oil (especially for slicks). However, this approach does not predict the time-dependent material balance for specific chemical components. In order to obtain component-specific information, component specific physical properties (e.g., solubilities, vapor pressures and other phase partitioning parameters) must be used. There have been no other functional component specific models developed previously. Ironically, most of the data generated when an actual oil spill has occurred have been component-specific concentrations across phase boundaries.

Although evaporation and dissolution are the oil-weathering processes of most importance during the initial stages of a spill, other longer-term weathering processes destroy and produce compounds to a degree that is important to any component-specific model. In the case of autoxidation, a compound may chemically react to become an aldehyde, ketone, alcohol or carboxylic acid, all of which are more soluble in the water column than are the precursor hydrocarbon compounds. Similarly, metabolites of microbial degradation have physical properties markedly different from their corresponding parent compounds. Such "fringe" processes, which are not unimportant, are typically more complex than are the evaporation and dissolution processes, increasing the complexity of their mathematical descriptions.

In discussing the segments of the model which follow, three basic aspects have been considered for each oil weathering process:

(1) physical properties (of bulk oil and specific components)

(2) mass balance equations (for specific components and pseudo-components)

(3) environmental parameters (which the oil encounters upon being spilled)

Physical properties include the thermodynamic and transport characteristics required to describe a particular process. In the cases of evaporation and dissolution, thermodynamic properties are the vapor pressures, Henry's law coefficients, solubilities, and mixing rules, while the transport properties include diffusivities, viscosities and, again, mixing rules.

4.1 Pseudo-Component Marine Evaporation of Oil

Predicting the quantity of oil in the slick as a function of time requires that a total mass balance approach be used. It is not possible to write a total material balance for crude oil by using component specific information. If one tries to use component specific information, it soon becomes apparent that all the components in crude oil will never be identified, thus precluding an accounting of the total mass of the oil. No predictive equations have ever been successfully developed based on specific components where the purpose of prediction was a total mass balance for oil.

The question then is raised as to how one uses bulk properties of the oil to make specific predictions? The petroleum industry refers to these bulk properties of oil as "characterization parameters". The characterization of an oil must be done with respect to a specific prediction as the objective. For example, when the prediction (process design or mathematical model) is a process that involves vapor-liquid transport, the characteristic parameters are then vapor pressures or partial pressures. When the prediction is the performance of a catalytic reformer where naphthas are converted to aromatics,

the characteristics required on the catalytic reformer feedstock are combined contents of paraffins-olefins-naphthas-aromatics, referred to as PONA. Kinetic equations use PONA values as starting concentrations along with kinetic constants to predict the product from the catalytic reforming process. Both these examples illustrate a pseudo-component model, sometimes referred to as a "lumped" model.

In predicting the mass of oil remaining in an oil slick as a function of time as evaporation proceeds, characterization of the oil must be with respect to vapor pressure. An overall mass balance utilizes the vapor pressure and environmental parameters to predict loss of oil and, therefore, mass of oil remaining in the slick. The following discussion considers: 1) the procedure for characterizing crude oils with respect to pseudo-component vapor pressures and 2) the pertinent equations for the overall mass balance as they apply to the use of the overall oil weathering model.

4.1.1 Pseudo-Component Characterization of Crude Oil

The standard inspections on a crude oil include distillation, density of the distillate cuts, and viscosity of the distillate cuts. There are virtually no component-specific data that can be obtained which will allow adequate prediction of the bulk properties of the oil. The standard distillation data come from either a true boiling point distillation or an ASTM (American Society for Test and Materials) D-86 distillation; both are carried out at one atmosphere total pressure. Each of these distillations can be carried out at 10 mm Hg total pressure to obtain information on the less volatile fractions of the oil.

Either distillation is conducted in a manner such that the distillate fractions are collected separately (i.e., the fraction distilling at 50 to 75°C is physically separated from the fraction distilling at 75 to 100°C). The total number of fractions collected is usually five to seven, but can be as many as 20. Characteristic data for the distillate fractions include the

temperatures at the beginning and end of each fraction (or "cut"), sometimes in the form of a continuous curve of temperature vs percent distillate. The API (American Petroleum Institute) gravity for each cut is then measured, as is occasionally the viscosity of each cut.

Given the boiling point (1 atm) and API gravity of each cut (or pseudo-component), the vapor pressure of the cut as a function of temperature can be calculated. First, the molecular weight and critical temperature of the cut are calculated according to the following correlation (FALLON and WATSON, 1944):

$$y = C_1 + C_2X_1 + C_3X_2 + C_4X_1X_2 + C_5X_1^2 + C_6X_2^2 \qquad (4.1)$$

where X_1 is the boiling point (°F) at one atmosphere, X_2 is the API gravity, and the constants C_1 to C_5 have the values indicated in Table 4-1. Similarly, the critical temperature can be calculated from the same equation form using the indicated constant values in Table 4-1.

Next the equivalent paraffin carbon number is calculated according to (GAMSON and WATSON, 1944):

$$N_c = (MW - 2)/14 \qquad (4.2)$$

The critical volume is then calculated according to:

$$V_c = (1.88 + 2.44N_c)/0.044 \qquad (4.3)$$

TABLE 4-1. CORRELATION EQUATION CONSTANTS FOR THE CHARACTERIZATION OF NARROW BOILING PETROLEUM FRACTIONS (see text for equation form).

PROPERTY	C_1	C_2	C_3	C_4	C_5	C_6
Molecular weight $t_b \leq 500°F$	6.241E+01	-4.595E-02	-2.836E-01	3.256E-03	4.578E-04	5.279E-04
Molecular weight $t_b > 500$	4.268E+02	-1.007	-7.491	1.380E-02	1.047E-03	2.621E-02
Critical temperature to ≤ 500	4.055E+02	1.337	-2.662	-2.169E-03	-4.943E-04	1.454E-02
Critical temperature $t_b > 500$	4.122E+02	1.276	-2.865	-2.888E-03	-3.707E-04	2.288E-02
b'	1.237E-02	2.516E-01	4.039E-02	-4.024E-02	-----	-----
Kinematic vis, cs @ 122°F API ≤ 35	-4.488E-01	-9.344E-04	1.583E-02	-5.219E-05	5.2688-06	1.536E-04
Kinematic vis, cs @ 122°F API > 35	-6.019E-01	1.793E-03	-3.159E-03	-5.1E-06	9.067E-07	3.522E-05

and the critical pressure is calculated from:

$$P_c = \frac{20.8T_c}{(v_c - 8)} + P_c' \tag{4.4}$$

where P_c' = 10 to (correct the critical pressure correlation from a strictly paraffinic mixture to a naphtha-aromatic-paraffin mixture). Next a parameter (b) is calculated according to

$$b = b' - 0.02 \tag{4.5}$$

where

$$b' = C_1 + C_2N_c + C_3N_c^2 + C_4N_c^3 \tag{4.6}$$

and the values of the constants C_1 to C_4 are indicated in Table 4-1.

A final parameter designated as A is then calculated according to:

$$A = \frac{T_{r_b}}{T_{r_b} - 1} \left\{ \log_{10} (P_{r_b}) + \exp \left[-20(T_{r_b} - b)^2 \right] \right\} \tag{4.7}$$

where T_{r_b} and P_{r_b} are the reduced temperature and pressure at the normal boiling point. The vapor pressure equation which can be used down to 10 mm Hg is:

$$\log_{10} P_r = \frac{-A(1 - T_r)}{T_r} - \exp \left[-20(T_r - b)^2 \right] \tag{4.8}$$

where A, b, T_c and P_c were determined from the normal boiling point and API gravity of the cut. The temperature at which the vapor pressure is 10 mm Hg can be obtained by the root-finding algorithm of Newton-Raphson.

Below 10 mm Hg, the vapor pressure is calculated according to the Clausius-Clapeyron equation as follows (GAMSON and WATSON, 1944):

$$\ln \frac{P_2}{P_1} = \frac{\lambda_o}{RT_c} \int_{T_{r_1}}^{T_{r_2}} \frac{(1 - T_r)^{0.38}}{T_r^2} \, dT_r \qquad (4.9)$$

and is based on the law which states the ratio of the heat of vaporization, λ, to $(1 - T_r)^{0.38}$ is a constant at any temperature. The latent heat of vaporization is calculated from the slope of the natural log of the vapor pressure equation with respect to the temperature at the temperature where the vapor pressure is 10 mm Hg. Thus, in the above equation, P_2 is the 10 mm Hg vapor pressure at the temperature, T_r, previously determined.

A sample calculation for the characterization of Prudhoe Bay crude oil is presented in Tables 4-2 and 4-3A. Table 4-2 presents the standard inspections (COLEMAN, 1978; PPC, 1973) for the crude and is the starting point for the characterization calculations. Note that the distillation in Table 4-2 was conducted at 40 mm Hg for cuts 11 to 15. Thus, these cut temperatures must be corrected to one atmosphere (API, 1976). Table 4-3A presents the computer generated output along with the corrected cut temperatures, and a calculation of the vapor pressures at an environmental temperature of 55°F. The characterizations of Cook Inlet, Murban, and Wilmington crudes are presented in Tables 4-3B to 4-3D, and the vapor pressures calculated from these characterizations are presented in Table 4-3E for all four crudes.

TABLE 4-2. STANDARD INSPECTIONS FOR PRUDHOE BAY CRUDE OIL (COLEMAN, 1978).

Item 9
Sample 71011

IDENTIFICATION

Prudhoe Bay field
Sadlerochit, Triassic
8,890 - 9,008 feet

Alaska
North Slope

GENERAL CHARACTERISTICS

Gravity, specific, 0.893 Gravity, ° API, 27.0 Pour point, ° F., 15
Sulfur, percent, 0.82 Color, brownish black
Viscosity, Saybolt Universal at 77° F, 111 sec; 100° F, 84 sec Nitrogen, percent, 0.230

DISTILLATION, BUREAU OF MINES ROUTINE METHOD

Steam 1—Distillation at atmospheric pressure, 741 mm. Hg
First drop, 81 ° F.

Fraction No.	Cut temp. ° F	Percent	Sum, percent	Sp. gr. 60/60° F.	° API 60° F.	C. I.	Refractive index, n_D at 20° C.	Specific dispersion	S. U. vis. 100° F.	Closed test, ° F
1	122									
2	167	2.1	2.1	0.693	72.7	–	1.38591	127.9		
3	212	2.6	4.7	.723	64.2	23	1.40312	139.0		
4	257	3.5	8.2	.752	56.7	27	1.41922	141.9		
5	302	3.6	11.8	.775	51.6	30	1.43082	147.0		
6	347	3.7	15.5	.790	47.6	31	1.43922	149.6		
7	392	3.5	19.0	.801	45.2	30	1.44626	152.1		
8	437	4.3	23.3	.818	41.5	33	1.45528	154.7		
9	482	4.8	28.1	.836	37.8	36	1.46565	157.0		
10	527	5.0	33.1	.851	34.8	38	1.47467	160.5		
Steam 2—Distillation continued at 40 mm. Hg										
11	398	2.8	35.9	0.873	30.6	45	1.48218	161.5	40	10
12	437	6.5	42.4	.881	29.1	45	1.48650	168.6	45	30
13	482	6.8	49.2	.897	26.2	49	1.49477	169.4	58	50
14	527	6.0	55.2	.910	24.0	52			93	70
15	572	7.4	62.6	.919	22.5	53			176	90
Residuum		36.3	98.9	.990	11.4					

Carbon residue, Conradson: Residuum, 11.6 percent; crude, 4.7 percent. Residuum: Sulfur, percent, – Nitrogen, percent, –

APPROXIMATE SUMMARY

	Percent	Sp. gr.	° API	Viscosity
Light gasoline	4.7	0.710	67.9	
Total gasoline and naphtha	19.0	0.762	54.2	
Kerosene distillate	4.3	.818	41.5	
Gas oil	18.4	.860	33.1	
Nonviscous lubricating distillate	11.0	.887-.911	28.0-23.9	50-100
Medium lubricating distillate	8.1	.911-.922	23.9-22.0	100-200
Viscous lubricating distillate	1.8	.922-.924	22.0-21.6	Above 200
Residuum	36.3	.990	11.4	
Distillation loss	1.1			

TABLE 4-3A. SUMMARY OF THE TBP CUTS CHARACTERIZATION FOR PRUDHOE BAY, ITEM 9, SAMPLE 71011.

SUMMARY OF TBP CUTS CHARACTERIZATION FOR: PRUDHOE BAY, ITEM 9, SAMPLE 71011

	TB	API	VOL	MW	TC	PC	VC	A	B	T10	VIS	NC	NS
1	1.670E+02	7.270E+01	2.120E+00	8.921E+01	9.310E+02	3.030E+01	3.002E+02	3.227E+00	1.976E-01	4.604E+02	4.144E-01	3	1
2	2.120E+02	6.420E+01	2.629E+00	1.016E+02	9.862E+02	3.654E+01	4.370E+02	3.311E+00	2.111E-01	4.959E+02	4.919E-01	3	1
3	2.570E+02	5.670E+01	3.539E+00	1.139E+02	1.040E+03	3.514E+01	4.860E+02	3.391E+00	2.220E-01	5.315E+02	6.006E-01	3	1
4	3.020E+02	5.160E+01	3.640E+00	1.270E+02	1.091E+03	3.365E+01	5.410E+02	3.493E+00	2.341E-01	5.677E+02	7.474E-01	3	1
5	3.470E+02	4.760E+01	3.741E+00	1.431E+02	1.139E+03	3.218E+01	6.015E+02	3.612E+00	2.440E-01	6.044E+02	9.433E-01	3	1
6	3.920E+02	4.520E+01	3.539E+00	1.607E+02	1.184E+03	3.062E+01	6.713E+02	3.767E+00	2.554E-01	6.420E+02	1.200E+00	3	1
7	4.370E+02	4.150E+01	4.340E+00	1.779E+02	1.230E+03	2.942E+01	7.396E+02	3.909E+00	2.643E-01	6.796E+02	1.555E+00	3	1
8	4.820E+02	3.780E+01	4.853E+00	1.960E+02	1.276E+03	2.834E+01	8.111E+02	4.059E+00	2.724E-01	7.176E+02	2.046E+00	3	1
9	5.270E+02	3.480E+01	5.056E+00	2.125E+02	1.323E+03	2.760E+01	8.765E+02	4.170E+00	2.789E-01	7.551E+02	2.603E+00	3	1
10	5.900E+02	3.060E+01	2.831E+00	2.429E+02	1.382E+03	2.615E+01	9.969E+02	4.424E+00	2.890E-01	8.097E+02	3.309E+00	3	1
11	6.400E+02	2.910E+01	6.572E+00	2.736E+02	1.423E+03	2.481E+01	1.119E+03	4.609E+00	2.974E-01	8.540E+02	5.367E+00	3	1
12	6.850E+02	2.620E+01	6.876E+00	2.980E+02	1.464E+03	2.390E+01	1.218E+03	4.892E+00	3.032E-01	8.949E+02	9.239E+00	3	1
13	7.350E+02	2.400E+01	6.067E+00	3.320E+02	1.506E+03	2.297E+01	1.350E+03	5.177E+00	3.097E-01	9.411E+02	1.812E+01	3	1
14	7.900E+02	2.250E+01	7.402E+00	3.757E+02	1.547E+03	2.100E+01	1.523E+03	5.501E+00	3.166E-01	9.943E+02	4.046E+01	3	1
15	8.500E+02	1.140E+01	3.670E+01	6.000E+02	0.000E+00	0.000E+00	0.000E+00	0.000E+00	0.000E+00	0.000E+00	1.810E+02	0	0

TB = NORMAL BOILING TEMPERATURE, DEG F
API = API GRAVITY
VOL = VOLUME PER CENT OF TOTAL CRUDE
MW = MOLECULAR WEIGHT
TC = CRITICAL TEMPERATURE, DEG RANKINE
PC = CRITICAL PRESSURE, ATMOSPHERES
VC = CRITICAL VOLUME, CC/MOLE
A AND B ARE PARAMETERS IN THE VAPOR PRESSURE EQUATION
T10 IS THE TEMPERATURE IN DEG R WHERE THE VAPOR PRESSURE IS 10 MM HG
VIS IS THE KINEMATIC VISCOSITY IN CENTISTOKES AT 122 DEG F
NC = ERROR CODE, SHOULD BE LESS THAN 20
NS = ERROR CODE, SHOULD BE EQUAL TO 1
IGNORE THE ERROR CODES FOR COMPONENT NUMBER 15
CRUDE OIL CHARACTERIZATION AND PSEUDOCOMPONENT EVAPORATION MODEL
IDENTIFICATION: PRUDHOE BAY, ITEM 9, SAMPLE 71011

VAPOR PRESSURE IN ATMOSPHERES AT 3.200E+01 DEG F

	VP
1	3.704E-02
2	1.086E-02
3	2.584E-03
4	5.643E-04
5	1.123E-04
6	1.965E-05
7	3.176E-06
8	4.635E-07
9	6.603E-08
10	3.052E-09
11	1.049E-10
12	1.422E-11
13	5.662E-13
14	8.024E-15

TABLE 4-3B.

SUMMARY OF TBP CUTS CHARACTERIZATION FOR: COOK INLET, ALASKA
TYPE 7, SAMPLE 72025

	TB	API	SPGR	VOL	MW	TC	PC	VC	A	B	T10	VIS	NC	NS
1	1.22E+02	8.92E+01	6.30E-01	2.40E+00	7.80E+01	8.75E+02	4.01E+01	3.44E+02	3.15E+00	1.03E-01	4.25E+02	3.74E-01	3	1
2	1.67E+02	7.72E+01	6.66E-01	2.58E+00	9.07E+01	9.27E+02	3.77E+01	3.94E+02	3.25E+00	1.99E-01	4.61E+02	4.20E-01	3	1
3	2.12E+02	6.50E+01	7.08E-01	6.09E+00	1.02E+02	9.84E+02	3.64E+01	4.38E+02	3.32E+00	2.12E-01	4.96E+02	4.92E-01	3	1
4	2.57E+02	5.95E+01	7.20E-01	6.30E+00	1.16E+02	1.04E+03	3.47E+01	4.93E+02	3.42E+00	2.24E-01	5.32E+02	5.99E-01	3	1
5	3.02E+02	5.54E+01	7.44E-01	5.26E+00	1.31E+02	1.08E+03	3.30E+01	5.52E+02	3.55E+00	2.36E-01	5.69E+02	7.41E-01	3	1
6	3.47E+02	5.08E+01	7.63E-01	5.37E+00	1.46E+02	1.13E+03	3.16E+01	6.13E+02	3.67E+00	2.47E-01	6.05E+02	9.38E-01	3	1
7	3.92E+02	4.65E+01	7.81E-01	5.06E+00	1.62E+02	1.18E+03	3.04E+01	6.77E+02	3.79E+00	2.56E-01	6.43E+02	1.19E+00	3	1
8	4.37E+02	4.30E+01	7.97E-01	5.26E+00	1.80E+02	1.23E+03	2.92E+01	7.47E+02	3.94E+00	2.65E-01	6.80E+02	1.54E+00	3	1
9	4.82E+02	3.96E+01	8.13E-01	5.37E+00	1.98E+02	1.27E+03	2.81E+01	8.21E+02	4.10E+00	2.73E-01	7.19E+02	2.02E+00	3	1
10	5.27E+02	3.70E+01	8.25E-01	5.16E+00	2.14E+02	1.32E+03	2.72E+01	8.91E+02	4.23E+00	2.80E-01	7.56E+02	2.67E+00	3	1
11	5.80E+02	3.28E+01	8.47E-01	8.41E+00	2.41E+02	1.37E+03	2.61E+01	9.91E+02	4.43E+00	2.89E-01	8.02E+02	2.97E+00	3	1
12	6.36E+02	3.13E+01	8.54E-01	5.37E+00	2.79E+02	1.42E+03	2.45E+01	1.14E+03	4.75E+00	2.99E-01	8.55E+02	5.05E+00	3	1
13	6.85E+02	2.87E+01	8.68E-01	7.22E+00	3.67E+02	1.46E+03	2.35E+01	1.25E+03	4.99E+00	3.05E-01	8.97E+02	8.67E+00	3	1
14	7.30E+02	2.66E+01	8.80E-01	4.33E+00	3.45E+02	1.50E+03	2.24E+01	1.40E+03	5.33E+00	3.12E-01	9.47E+02	1.72E+01	3	1
15	7.90E+02	2.50E+01	8.89E-01	4.33E+00	3.87E+02	1.54E+03	2.14E+01	1.57E+03	5.73E+00	3.18E-01	9.98E+02	3.65E+01	3	1
16	8.50E+02	1.16E+01	9.72E-01	2.64E+01	6.00E+02	0.00E+00	0.00E+00	0.00E+00	0.00E+00	0.00E+00	0.00E+00	1.79E+02	0	0

TB = NORMAL BOILING TEMPERATURE, DEG F
API = API GRAVITY
VOL = VOLUME PER CENT OF TOTAL CRUDE
MW = MOLECULAR WEIGHT
TC = CRITICAL TEMPERATURE, DEG RANKINE
PC = CRITICAL PRESSURE, ATMOSPHERES
VC = CRITICAL VOLUME, CC/MOLE
A AND B ARE PARAMETERS IN THE VAPOR PRESSURE EQUATION
T10 IS THE TEMPERATURE IN DEG R WHERE THE VAPOR PRESSURE IS 10 MM HG
VIS IS THE KINEMATIC VISCOSITY IN CENTISTOKES AT 122 DEG F
NC = ERROR CODE, SHOULD BE LESS THAN 20
NS = ERROR CODE, SHOULD BE EQUAL TO 1
IGNORE THE ERROR CODES FOR COMPONENT NUMBER 16

TABLE 4.3-C.

SUMMARY OF TBP CUTS CHARACTERIZATION FOR: MURBAN, ABU DHABI
ITEM 99999, SAMPLE 99999

	TB	API	SPGR	VOL	MW	TC	PC	VC	A	B	T10	VIS	NC	NS
1	1.22E+02	9.67E+01	6.10E-01	1.71E+00	7.95E+01	8.73E+02	3.95E+01	3.50E+02	3.16E+00	1.85E-01	4.25E+02	3.93E-01	3	1
2	1.67E+02	8.62E+01	6.39E-01	2.92E+00	9.39E+01	9.21E+02	3.67E+01	4.07E+02	3.29E+00	2.03E-01	4.62E+02	4.35E-01	3	1
3	2.12E+02	7.06E+01	6.88E-01	4.94E+00	1.05E+02	9.78E+02	3.50E+01	4.49E+02	3.37E+00	2.14E-01	4.97E+02	4.96E-01	3	1
4	2.57E+02	6.23E+01	7.18E-01	6.05E+00	1.17E+02	1.03E+03	3.42E+01	5.00E+02	3.46E+00	2.26E-01	5.33E+02	5.90E-01	3	1
5	3.02E+02	5.57E+01	7.43E-01	6.75E+00	1.31E+02	1.08E+03	3.30E+01	5.51E+02	3.55E+00	2.36E-01	5.69E+02	7.41E-01	3	1
6	3.47E+02	5.16E+01	7.60E-01	6.45E+00	1.47E+02	1.13E+03	3.15E+01	6.16E+02	3.68E+00	2.47E-01	6.06E+02	9.31E-01	3	1
7	3.92E+02	4.85E+01	7.73E-01	5.75E+00	1.64E+02	1.18E+03	3.01E+01	6.85E+02	3.83E+00	2.57E-01	6.43E+02	1.10E+00	3	1
8	4.37E+02	4.56E+01	7.85E-01	5.65E+00	1.83E+02	1.22E+03	2.88E+01	7.59E+02	4.00E+00	2.67E-01	6.81E+02	1.52E+00	3	1
9	4.82E+02	4.30E+01	7.97E-01	5.95E+00	2.03E+02	1.26E+03	2.76E+01	8.38E+02	4.19E+00	2.75E-01	7.20E+02	1.90E+00	3	1
10	5.27E+02	4.00E+01	8.11E-01	4.94E+00	2.22E+02	1.31E+03	2.67E+01	9.13E+02	4.29E+00	2.82E-01	7.57E+02	2.61E+00	3	1
11	5.80E+02	3.58E+01	8.31E-01	5.75E+00	2.48E+02	1.36E+03	2.56E+01	1.02E+03	4.50E+00	2.91E-01	8.04E+02	3.71E+00	3	1
12	6.36E+02	3.40E+01	8.40E-01	5.65E+00	2.87E+02	1.41E+03	2.40E+01	1.17E+03	4.84E+00	3.01E-01	8.57E+02	4.82E+00	3	1
13	6.85E+02	3.00E+01	8.61E-01	6.55E+00	3.12E+02	1.45E+03	2.33E+01	1.27E+03	5.04E+00	3.06E-01	8.98E+02	5.39E+00	3	1
14	7.36E+02	2.84E+01	8.70E-01	6.05E+00	3.53E+02	1.49E+03	2.21E+01	1.43E+03	5.41E+00	3.13E-01	9.49E+02	1.62E+01	3	1
15	7.96E+02	2.66E+01	8.80E-01	5.65E+00	3.95E+02	1.53E+03	2.11E+01	1.60E+03	5.83E+00	3.19E-01	1.00E+03	3.42E+01	3	1
16	8.50E+02	1.67E+01	9.39E-01	1.93E+01	6.00E+02	0.00E+00	0.00E+00	0.00E+00	0.00E+00	0.00E+00	0.00E+00	1.35E+02	0	0

TB = NORMAL BOILING TEMPERATURE, DEG F
API = API GRAVITY
VOL = VOLUME PER CENT OF TOTAL CRUDE
MW = MOLECULAR WEIGHT
TC = CRITICAL TEMPERATURE, DEG RANKINE
PC = CRITICAL PRESSURE, ATMOSPHERES
VC = CRITICAL VOLUME, CC/MOLE
A AND B ARE PARAMETERS IN THE VAPOR PRESSURE EQUATION
T10 IS THE TEMPERATURE IN DEG R WHERE THE VAPOR PRESSURE IS 10 MM HG
VIS IS THE KINEMATIC VISCOSITY IN CENTISTOKES AT 122 DEG F
NC = ERROR CODE, SHOULD BE LESS THAN 20
NS = ERROR CODE, SHOULD BE EQUAL TO 1
IGNORE THE ERROR CODES FOR COMPONENT NUMBER 16

TABLE 4-3D.

SUMMARY OF TBP CUTS CHARACTERIZATION FOR: WILMINGTON, CALIFORNIA
TITLE 94, SAMPLE 71052

	TB	API	SPGR	VOL	MW	TC	PC	VC	A	B	T10	VIS	NC	NS
1	2.12E+02	6.80E+01	6.95E-01	2.30E+00	1.04E+02	9.80E+02	3.59E+01	4.45E+02	3.35E+00	2.13E-01	4.97E+02	4.94E-01	3	1
2	2.57E+02	5.87E+01	7.31E-01	2.40E+00	1.15E+02	1.04E+03	3.48E+01	4.91E+02	3.41E+00	2.24E-01	5.32E+02	5.99E-01	3	1
3	3.02E+02	5.30E+01	7.54E-01	2.40E+00	1.29E+02	1.09E+03	3.34E+01	5.45E+02	3.51E+00	2.35E-01	5.68E+02	7.45E-01	3	1
4	3.47E+02	4.81E+01	7.74E-01	2.51E+00	1.44E+02	1.14E+03	3.21E+01	6.03E+02	3.62E+00	2.45E-01	6.05E+02	9.42E-01	3	1
5	3.92E+02	4.32E+01	7.96E-01	2.81E+00	1.59E+02	1.19E+03	3.10E+01	6.63E+02	3.73E+00	2.54E-01	6.41E+02	1.21E+00	3	1
6	4.37E+02	3.80E+01	8.17E-01	3.61E+00	1.75E+02	1.24E+03	2.99E+01	7.27E+02	3.85E+00	2.60E-01	6.78E+02	1.58E+00	3	1
7	4.82E+02	3.54E+01	8.33E-01	4.41E+00	1.93E+02	1.28E+03	2.87E+01	7.98E+02	4.00E+00	2.71E-01	7.16E+02	2.08E+00	3	1
8	5.27E+02	3.23E+01	8.49E-01	5.31E+00	2.09E+02	1.33E+03	2.80E+01	8.61E+02	4.12E+00	2.77E-01	7.54E+02	2.02E+00	3	1
9	5.80E+02	2.68E+01	8.79E-01	4.71E+00	2.29E+02	1.39E+03	2.72E+01	9.40E+02	4.26E+00	2.85E-01	7.98E+02	3.20E+00	3	1
10	6.38E+02	2.45E+01	8.92E-01	6.31E+00	2.59E+02	1.44E+03	2.57E+01	1.06E+03	4.52E+00	2.94E-01	8.49E+02	5.86E+00	3	1
11	6.85E+02	2.23E+01	9.04E-01	4.11E+00	2.86E+02	1.48E+03	2.47E+01	1.17E+03	4.74E+00	3.00E-01	8.91E+02	1.04E+01	3	1
12	7.36E+02	2.03E+01	9.16E-01	5.51E+00	3.20E+02	1.52E+03	2.36E+01	1.30E+03	5.03E+00	3.08E-01	9.40E+02	2.16E+01	3	1
13	8.56E+02	8.90E+00	9.91E-01	5.36E+01	6.00E+02	0.00E+00	0.00E+00	0.00E+00	0.00E+00	0.00E+00	0.00E+00	2.10E+02	0	0

TB = NORMAL BOILING TEMPERATURE, DEG F
API = API GRAVITY
VOL = VOLUME PER CENT OF TOTAL CRUDE
MW = MOLECULAR WEIGHT
TC = CRITICAL TEMPERATURE, DEG RANKINE
PC = CRITICAL PRESSURE, ATMOSPHERES
VC = CRITICAL VOLUME, CC/MOLE
A AND B ARE PARAMETERS IN THE VAPOR PRESSURE EQUATION
T10 IS THE TEMPERATURE IN DEG R WHERE THE VAPOR PRESSURE IS 10 MM HG
VIS IS THE KINEMATIC VISCOSITY IN CENTISTOKES AT 122 DEG F
NC = ERROR CODE, SHOULD BE LESS THAN 20
NS = ERROR CODE, SHOULD BE EQUAL TO 1
IGNORE THE ERROR CODES FOR COMPONENT NUMBER 13

TABLE 4-3E.

CRUDE OIL CHARACTERIZATION AND PSEUDOCOMPONENT EVAPORATION MODEL
IDENTIFICATION: PRUDHOE BAY, ALASKA

VAPOR PRESSURE IN ATMOSPHERES AT 5.540E+01 DEG F

	VP
1	7.751E-02
2	2.440E-02
3	6.852E-03
4	1.644E-03
5	3.617E-04
6	7.046E-05
7	1.283E-05
8	2.115E-06
9	3.394E-07
10	3.193E-08
11	1.556E-09
12	1.255E-10
13	4.983E-12
14	1.264E-13

CRUDE OIL CHARACTERIZATION AND PSEUDOCOMPONENT EVAPORATION MODEL
IDENTIFICATION: COOK INLET, ALASKA

VAPOR PRESSURE IN ATMOSPHERES AT 5.540E+01 DEG F

	VP
1	2.280E-01
2	7.673E-02
3	2.430E-02
4	6.680E-03
5	1.561E-03
6	3.402E-04
7	6.809E-05
8	1.217E-05
9	1.945E-06
10	3.071E-07
11	2.770E-08
12	1.275E-09
13	9.292E-11
14	3.248E-12
15	7.181E-14

CRUDE OIL CHARACTERIZATION AND PSEUDOCOMPONENT EVAPORATION MODEL
IDENTIFICATION: MURBAN, ABU DHABI

VAPOR PRESSURE IN ATMOSPHERES AT 5.540E+01 DEG F

	VP
1	2.279E-01
2	7.565E-02
3	2.368E-02
4	6.517E-03
5	1.555E-03
6	3.350E-04
7	6.459E-05
8	1.110E-05
9	1.657E-06
10	2.699E-07
11	2.295E-08
12	1.031E-09
13	7.944E-11
14	2.403E-12
15	4.950E-14

CRUDE OIL CHARACTERIZATION AND PSEUDOCOMPONENT EVAPORATION MODEL
IDENTIFICATION: WILMINGTON, CALIFORNIA

VAPOR PRESSURE IN ATMOSPHERES AT 5.540E+01 DEG F

	VP
1	2.389E-02
2	6.728E-03
3	1.613E-03
4	3.583E-04
5	7.427E-05
6	1.411E-05
7	2.361E-06
8	3.822E-07
9	4.110E-08
10	2.372E-09
11	1.997E-10
12	9.010E-12

4.1.2 Pseudo-Component Evaporation Model on the Ocean Surface

The evaporation model which predicts the oil remaining in a slick is derived from the physical properties of the oil cuts and a total material balance. From the previous discussion a number of pseudo-components are defined. For each pseudo-component the vapor pressure, molecular weight and initial quantity are known, and a material balance can be written to include each:

$$\frac{dM_i}{dt} = -K_p A X_i P_i^* \quad \text{for } i = 1, 2, \ldots\ldots\ldots \text{total number of components} \tag{4.10}$$

where it is assumed that the oil slick is well stirred and a pseudo-Raoult's law applies as the mixing rule. In this rate equation, M_i is the number of moles of component i in the oil slick, P_i^* is the vapor pressure at the prevailing environmental temperature, A is the area of the slick, K_p is an over-all mass-transfer coefficient based on partial pressure driving forces, and x_i is the mole fraction of component i in the slick. The differential equations are all coupled through the mole fraction term where the total number of moles appears in the denominator.

The over-all mass-transfer coefficient can be calculated two different ways. One way is the approach of MACKAY and MATSUGU, 1976:

$$K = 0.0292\ U^{0.78}\ \chi^{-0.11}\ Sc^{-0.67} \tag{4.11}$$

where U is the wind velocity in m/hr, X is the slick diameter (assumes circular slick), and Sc is the Schmidt number (2.7). This expression is a correlation and is the proper mass transfer coefficient to multiply by the partial pressure to obtain the rate.

Implicit in the rate equation for the i-th component is the assumption that the partial pressure in the bulk atmosphere is zero. It can then be seen that the mass transfer coefficient above takes into account an averaging effect whereby the evaporation rate on the downwind portion of the slick is lower than the upwind portion due to the fact that P_i becomes finite in the air immediately over the oil slick in the direction of the wind.

Another approach to calculating overall mass transfer coefficients is that of TREYBAL, 1955, and LISS, 1974:

$$\frac{1}{K} = \frac{1}{k_g} + \frac{H^*}{k_\ell} \tag{4.12}$$

where k_g is the individual gas-phase mass-transfer coefficient, k_ℓ is the individual liquid-phase mass-transfer coefficient and H* is the Henry's law coefficient which is defined by:

$$P_i \equiv H^* x_i \tag{4.13}$$

The units on k_g for a partial pressure driving force are typically moles/(m^2 hr atm), the units on k for a mole fraction driving force is moles/(m^2 hr), and the units on H* are atm. The individual mass transfer coefficients, k_ℓ and k_g, must then be obtained from actual data in a manner similar to that used to deduce K in equation (4.11).

The other bulk property of interest for the oil slick is its viscosity. When oil is spilled on the ocean surface, the viscosity is low enough so that mixing occurs and the well-mixed oil-phase assumption is valid. However, as evaporation occurs the viscosity increases because the low-viscosity fractions are removed. The viscosity "blending" relationship used to predict the bulk viscosity as a function of composition is:

$$\ln\mu_{mix} = \sum_{i=1} x_i \ln\mu_i \quad \text{for } i = 1, 2, \ldots\ldots \tag{4.14}$$

Therefore, in order to predict viscosity as a function of time the viscosity of the individual fraction from the distillation characterization must be known. If these data are not available then the viscosity of the cut can be estimated from the correlation form indicated in equation (4.1) where the predicted quantity is $\log_{10}$ of the kinematic viscosity at 122°F in centistokes and the constants C_1 to C_5 are presented in Table 4-1 (HOUGEN, 1965). The viscosity for each cut can then be scaled with respect to temperature according to (GOLD, 1969):

$$\ln \frac{\mu}{\mu_o} = 5.2 \times 10^{-4}\left(\frac{1}{T} - 0.00172\right) \tag{4.15}$$

where T is in degrees R (Rankine scale). This viscosity equation does not take into account water-in-oil emulsion (mousse) formation (MACKAY, 1980).

The area for mass transfer in equation (4.10) is calculated from the rate at which the oil spreads on the water surface. Considerable research has been devoted to the spreading of oil on the water surface, however, many of the resulting models are still relatively elementary. We have relied on the MACKAY, 1980 version.

Oil is assumed to spread in thick and thin slicks, with the thick slick feeding the thin slick. Using arguments based on observation, the area of the thin slick is given by:

$$\frac{dA_1}{d_t} = k_1 A_1^{1/3} \exp\left[-k_2/Z\right] \tag{4.16}$$

where A_1, is the area, k_1 and k_2 are constants and Z is the thickness of the thick slick. The thick slick area is given by:

$$\frac{dA_2}{d_t} = k_3 Z^{1.33} A_2 - k_4 A_1 / Z \qquad (4.17)$$

where A_2 is the area of the thick slick and k_3 and k_4 are constants. The area and thickness are related by the mass (moles) of oil in the slick and the bulk density, and the oil remaining in the slick is obtained from the previous differential equations describing the pseudo-component material balances.

Constants for the above equations are $k_1 = 1$, $k_2 = 0.0015$, $k_3 = 150$ and $k_4 = 1 \times 10^{-6}$. The units on the variables are meters and seconds. The thick oil slick is assumed to have an initial thickness of 2 cm and the thin slick area is assumed to be 8 times the thick area. The thin oil slick thickness is set at 1 micrometer.

The evaporation model just described could be used to predict mass transfer from a spilled oil mass over any time period. However, it is known through observation that an oil slick eventually becomes rigid and is not well-stirred at longer (greater than a few days) time intervals. Therefore, we have established a criterion to guage when a slick becomes rigid based on bulk viscosity (presently a value of 1000 centipoises is being used). A more sophisticated approach would be to include information on the sea state and the Reynold's stress at the air-sea interface; however, such data are difficult to come by in quantitative form.

Equations (4.1) through (4.17) represent the pseudo-component mathematical model describing the weathering of an oil slick due to evaporation. The material balance approach incorporates physical properties, mass balance, and the effect of environmental conditions. Figure 4-1 summarizes the flow of information that occurs in this model.

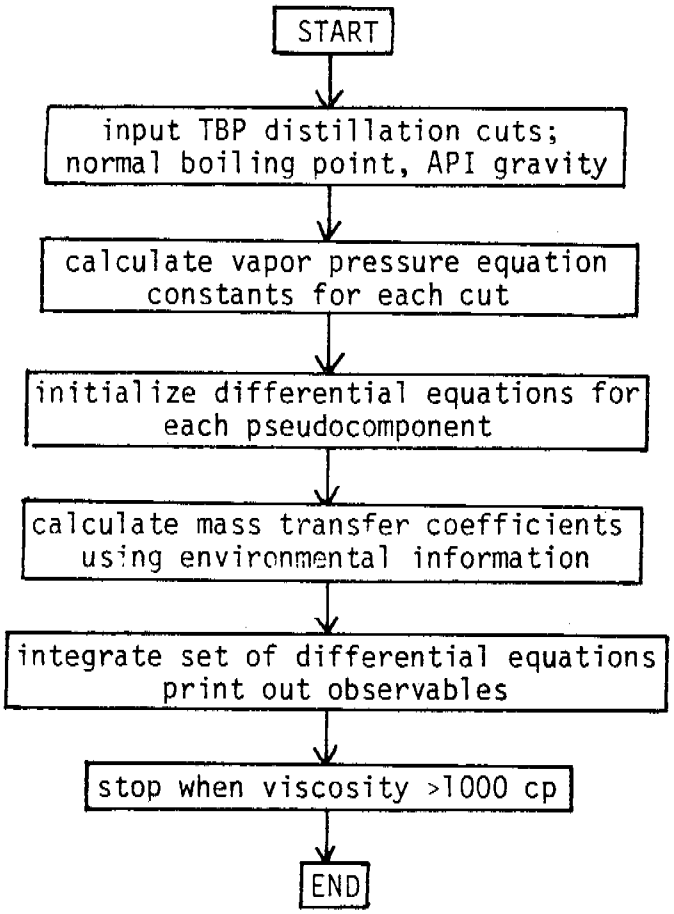

FIGURE 4-1. CALCULATION STEPS FOR PREDICTING SLICK MASS DUE TO EVAPORATION USING PSEUDOCOMPONENTS.

The results of an evaporation calculation for Prudhoe Bay crude oil are presented in Figures 4-2 and 4-3, and in Appendix A. Figure 4-2 presents the starting distillation curve (at time zero) and curves at other times up to 500 hours. Figure 4-3 presents the predicted gas-chromatograph curve where the residuum has been deleted and the curves renormalized. These results were obtained for a mass-transfer coefficient calculated from the MACKAY and MATSUGU (1976) correlation for a 10 knot wind.

When an oil slick becomes "rigid" due to increasing viscosity, the components leave the slick by diffusion, but mathematically the slick can still appear to be well-stirred. Section 4.6.3 presents a discussion for a criterion to determine when internal circulation in an oil slick ceases. In order for an oil slick to appear well-stirred when in fact it is a slab, the diffusivity, the convective mass transfer coefficient, the Henry's law coefficient and the slick thickness must satisfy a certain relation. The following section presents a discussion of this relation, which is called the mass-transfer "Biot" number, and how the modeling mathematics can be simplified by evaluating this relationship.

4.2 The Influence of Mechanical State on an Oil Slick

In essentially all of the previously published modeling work on oil weathering by the processes of evaporation and dissolution, the oil phase has been modeled as a well-stirred phase, resulting in a decaying exponential expression. Another modeling assumption which might be applied to an oil phase is that diffusion controls the mass transfer of components, at least under certain conditions. The well-stirred oil assumption is not universally appropriate since there can be conditions under which an oil phase is stagnant and not mechanically stirred. However, if the rate of evaporation (or dissolution) is the rate limiting step, then the concentration gradients in the oil phase can "keep up" with the evaporation rate at the surface and the oil phase appears well-stirred (i.e., no concentration gradients exist). The rate of evaporation or dissolution can be expected to be rate limiting when the

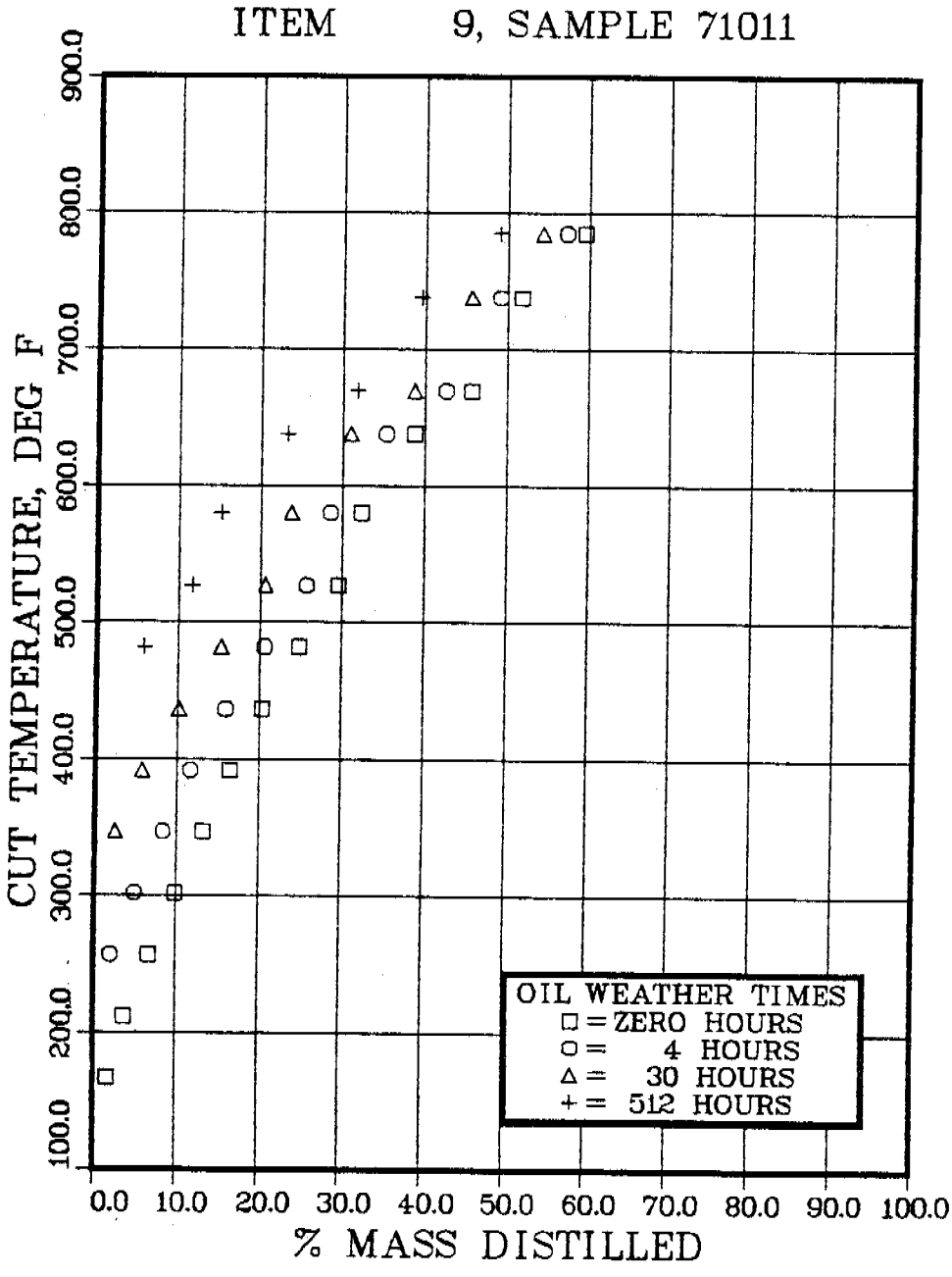

FIGURE 4-2. PREDICTED TOTAL DISTILLATION CURVES FOR WEATHERED OIL AT 55°F.

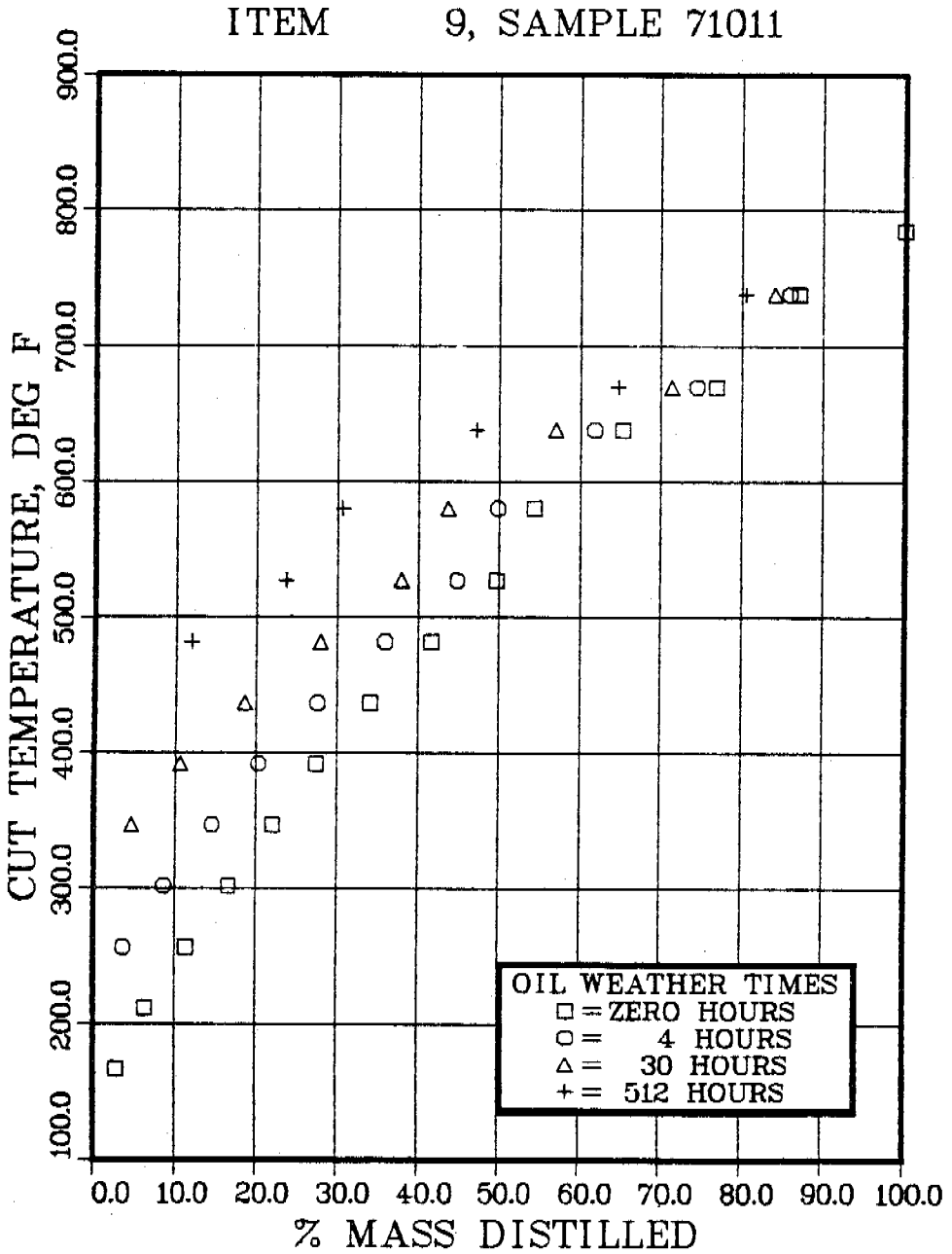

FIGURE 4-3. PREDICTED GC DISTILLATION CURVES FOR WEATHERED OIL AT 55°F.

partial pressure or solubility of the component of interest is quite small, or when a crust or skin has formed on the oil surface.

The following discussion examines a criterion for invoking the well-stirred oil phase assumption by invoking results from corresponding heat transfer problems. This criterion is then examined for the physical properties of the components of interest for evaporation from an oil slick. Finally, the results of a numerical experiment are presented which demonstrate that a decaying exponential model can fit the data from an evaporation experiment where the evaporation is diffusion controlled within the bulk oil phase.

4.2.1 Modeling Assumptions

In heat transfer problems involving flat plates and a surface heat transfer coefficient, there are two problem solutions termed the "thin" and "thick" plate solutions. A thin plate does not have sufficient internal thermal resistance relative to the surface resistance to support temperature gradients. In other words, the surface resistance to heat transfer is much greater than the internal resistance. As a result the temperature of a thin plate is essentially uniform and the thin plate problem solution is the same as that obtained for a well-stirred phase comprising the plate. A particular plate can be classified as thermally thick or thin according to the Biot number (ROHSENOW and HARTNETT, 1973) which is:

$$Bi \equiv \frac{h\delta}{K} \qquad \text{(dimensionless)} \tag{4.18}$$

where h is the surface conductance, δ is the plate thickness and K is the thermal conductivity. Roughly, for a flat plate with the convective boundary condition:

$$\text{thin, } Bi < 0.1 \; ; \quad \text{thick, } Bi > 0.1 \tag{4.19}$$

The Biot number as defined above is the same as H in the solutions for the temperatures of a well-stirred fluid in contact with a slab with "radiation" boundary conditions (JAEGER, 1945).

The corresponding Biot number for mass transfer problems involving flat plates is obtained by examining the following equations for heat and mass transfer:

$$-K \left.\frac{dT}{dx}\right|_{x=0} = h(T_m - T) \tag{4.20}$$

where T is the temperature of the solid at the interface and T_m is the temperature of the convective medium. The corresponding equation for mass transfer is:

$$-\mathscr{D} \left.\frac{dc}{dx}\right|_{x=0} = h(C_m - C_m^*) \tag{4.21}$$

where $\mathscr{D}$ is the diffusion coefficient in the slab, C is the concentration in the slab at the interface, C_m is the concentration of the convective medium, C_m^* is the hypothetical concentration of the convective medium in equilibrium with C, and h is now the convective mass-transfer coefficient. The equilibrium relationship required is assumed to be a Henry's law type expressed as:

$$C_m^* = \xi C \tag{4.22}$$

Equations (4.21) and (4.22) are not in the same form because of the equilibrium relationship that exists in the mass transfer case. However, making the change of variable $C_m^* = \xi C$ in the later equation yields:

$$-\mathscr{D}\frac{dc}{dx}\bigg|_{x=0} = \xi h(\bar{C}_m - C) \tag{4.23}$$

Now, compared to the heat transfer Biot number, the Biot mass-transfer number becomes:

$$Bi(mass) = \frac{h\xi\delta}{\mathscr{D}} \tag{4.24}$$

In order to use the Biot number criterion to determine if an oil slick is diffusion-controlled, the quantity ξ in the Henry's law expression is required. The following calculation illustrates the assumptions and data required to calculate ξ. The starting point for the calculation is:

$$C_a = \xi C_\ell \tag{4.25}$$

where C_a is the concentration in the air, gm/cc; C_ℓ is the concentration in the liquid, gm/cc; and ξ is dimensionless.

In the absence of experimental measurements of ξ, a conventional Raoult's law is assumed:

$$P_i = x_i P_{vp} \tag{4.26}$$

where P_i is the partial pressure of component i, x_i is the mole fraction, and P_{vp} is the pure component vapor pressure. In order to use this expression, it must be assumed that:

$$C_a = \left[\frac{M_i}{RT}\right] P_{vp} \left[\frac{M_o}{\rho_o} \frac{1}{M_i}\right] C_\ell \qquad (4.27)$$

where M_i is the molecular weight of the component of interest, M_o is the mean molecular weight of the oil, and P_{vp} is the bulk oil density. The quantity RT/M_i converts C_a to partial pressure and the quantity $M_o/(P_{vp}M_i)$ converts C_ℓ to mole fraction; thus recovering Raoult's law as used here. The dimensionless Henry's law constant sought becomes:

$$\xi \equiv \frac{P_{vp}M_o}{\rho_o RT} \qquad (4.28)$$

which has units of (gm-mole i)/(gm-mole oil) and is unitless according to the use of mole fraction in Raoult's law.

In order to illustrate the calculation of the Biot mass-transfer number, the vapor pressures for hydrocarbons containing 6 to 18 carbon atoms can be predicted from (BUTLER, 1975):

$$P_i = \exp\,[10.94 - 1.06N_i] \qquad (4.29)$$

where P_i is the vapor pressure in mm Hg at 20°C and N_i is the number of carbon atoms. The quantity ξ becomes:

$$\xi = \frac{\exp\,[10.94 - 1.06N_i]\, M_o}{760\rho_o RT} \qquad (4.30)$$

Assuming a mean molecular weight for the oil of 300 gms/gm-mole and a bulk oil density of 0.8 gm/cm^3, Equation (4.30) becomes:

$$\xi = 2 \times 10^{-5} \exp [10.94 - 1.06N_i] \tag{4.31}$$

at 20°C, and the above can be used to calculate the Biot mass-transfer number.

In order to calculate the Biot mass-transfer number, the diffusivity of the component of interest, the convective mass-transfer coefficient and oil thickness must be estimated. For the diffusivity a value of 10^{-6} cm^2/sec is used (REID, 1977); a slick thickness of 0.5 cm, and for the convective mass-transfer coefficient a value of 1000 cm/hr (0.28 cm/sec; LISS, 1974). The Biot mass-transfer number becomes:

$$Bi \equiv 1.4 \times 10^{-5} \xi \tag{4.32}$$

or, using the expression for :

$$Bi = 2.8 \exp [10.94 - 1.06N_i] \tag{4.33}$$

Table 4-4 presents the Biot mass transfer number for hydrocarbons containing 6 to 20 carbon atoms. This table indicates that the "thin" plate solution (i.e., the well-stirred phase assumption) is satisfactory, and that it can be used for hydrocarbons $n\text{-}C_{14}$ and higher in carbon number. Thus, for these compounds the evaporation rate is so small that the diffusion transport rate can "keep up," and the concentration profiles within the oil are "flat." However, for hydrocarbons containing 13 carbon atoms or less, the evaporation rate is much greater than the diffusion rate. As a result concentration profiles can be present in the oil phase and the well-stirred oil-phase assumption should not be used.

It is important to recognize the assumptions used to calculate the Biot mass-transfer number. The diffusivity assumed is 10^{-6} cm^2/sec, and it is

TABLE 4-4. BIOT MASS TRANSFER NUMBER ($\mathcal{D}=10^{-6}$ cm^2/sec, $\delta=0.5$ cm, h=1000 cm/hr, T=20°C).

N_i (carbon atoms)	Bi (dimensionless)	
6	273	
7	94	
8	33	
9	11	
10	4	
11	1.4	
12	0.5	
13	0.16	diffusion controlled (convection>diffusive rate)
14	0.05	(diffusive rate>convective)
15	0.02	well-stirred
16	0.006	
17	0.002	
18	0.0008	
19	0.0003	
20	0.0001	

conceivable that a value of 10^{-7} to 10^{-9} cm^2/sec is real. Since the diffusivity appears in the denominator of the Biot mass transfer number, all the values presented in Table 4-4 could increase accordingly. Also there are no data available to determine the real value of the equilibrium constant, ξ, and it is not readily known how close to reality the calculated values are.

4.2.2 Material Transport Under Diffusion-Controlled Evaporation

The previous discussion presents information on the criterion for the assumption of a well-stirred oil phase for modeling the evaporation oil-weathering process. It was pointed out that many assumptions were required to perform the calculation of the Biot mass transfer number and these assumptions definitely require refinement. However, whether or not the evaporation process is diffusion-controlled it must be recognized that experimentally the well-stirred oil phase model, which is a decaying exponential, appears to fit the observed data quite well. Therefore, it is worthwhile to examine the mathematics of a diffusion controlled slab from which components are evaporating and compare the observable variable with a first order decay law. The observable variable is the concentration of the component of interest in the air stream, or the bulk average concentration in the fluid, as a function of time.

The numerical experiment performed here was that of calculating the theoretical air phase concentration of a component evaporating from a diffusion-controlled slab, and then fitting by least squares a decaying exponential to the "data".

The concentration profiles in a diffusion controlled slab from which a component of interest is evaporating are (CARSLAW and JAEGER, 1959):

$$\frac{C}{C_o} = \frac{4}{\pi} \sum_{n=1}^{\infty} \frac{(-1)^{n+1}}{(2n-1)} \cos\left\{\frac{(2n-1)\pi x}{2\ell}\right\} \exp\left[-\frac{(2n-1)^2\pi^2\theta}{4}\right] \qquad (4.34)$$

where C_o is the initial concentration throughout and θ is the dimensionless time: $\mathcal{D}t/\ell^2$. The evaporation rate, and hence the concentration of the component of interest in an air stream above the surface, is the derivative of the above expression evaluated at the evaporating surface. The derivative need not be multiplied by the area and diffusivity since these quantities only "scale" the calculated concentration, and thus the calculated concentration in the air stream is in arbitrary units.

The results of this numerical experiment are presented in Figures 4-4 through 4-6. In each of the figures the fitting curve, which is $A*\exp[-k\theta]$, has four symbols marking it, and the theoretical curve is the one with no symbols running from a dimensionless time of 0.1 to 1.5. In Figure 4-4 the fitted curve covers one e-folding time; i.e., the time required for the theoretical curve to decrease by 1/e = 0.367, beginning at $\theta = 0.1$. In Figures 4-5 and 4-6 the fitted curves cover two and three e-folding times, respectively.

The result of this numerical experiment is that the fitted $A*\exp[-k\theta]$ curves cannot be distinguished in a laboratory experiment from the theoretical curve. In other words, performing a laboratory experiment on evaporation, fitting the data to $A*\exp[-k\theta]$, and obtaining an apparently good fit of the data is not sufficient to draw a conclusion about which mechanism is controlling.

The results of this numerical experiment can be used to obtain a single exponential expression to predict the decay of the air-phase concentration above a diffusion-controlled slab in the following way. Note that over the range of dimensionless time from 0.1 to 1.5 the "k" in the exponential fit is about -2.5. Thus, $\exp[-kt]$ where $k = 2.5\mathcal{D}t/\ell^2$, and t is time in seconds, provides a good fit to the data over the range of the independent variable examined.

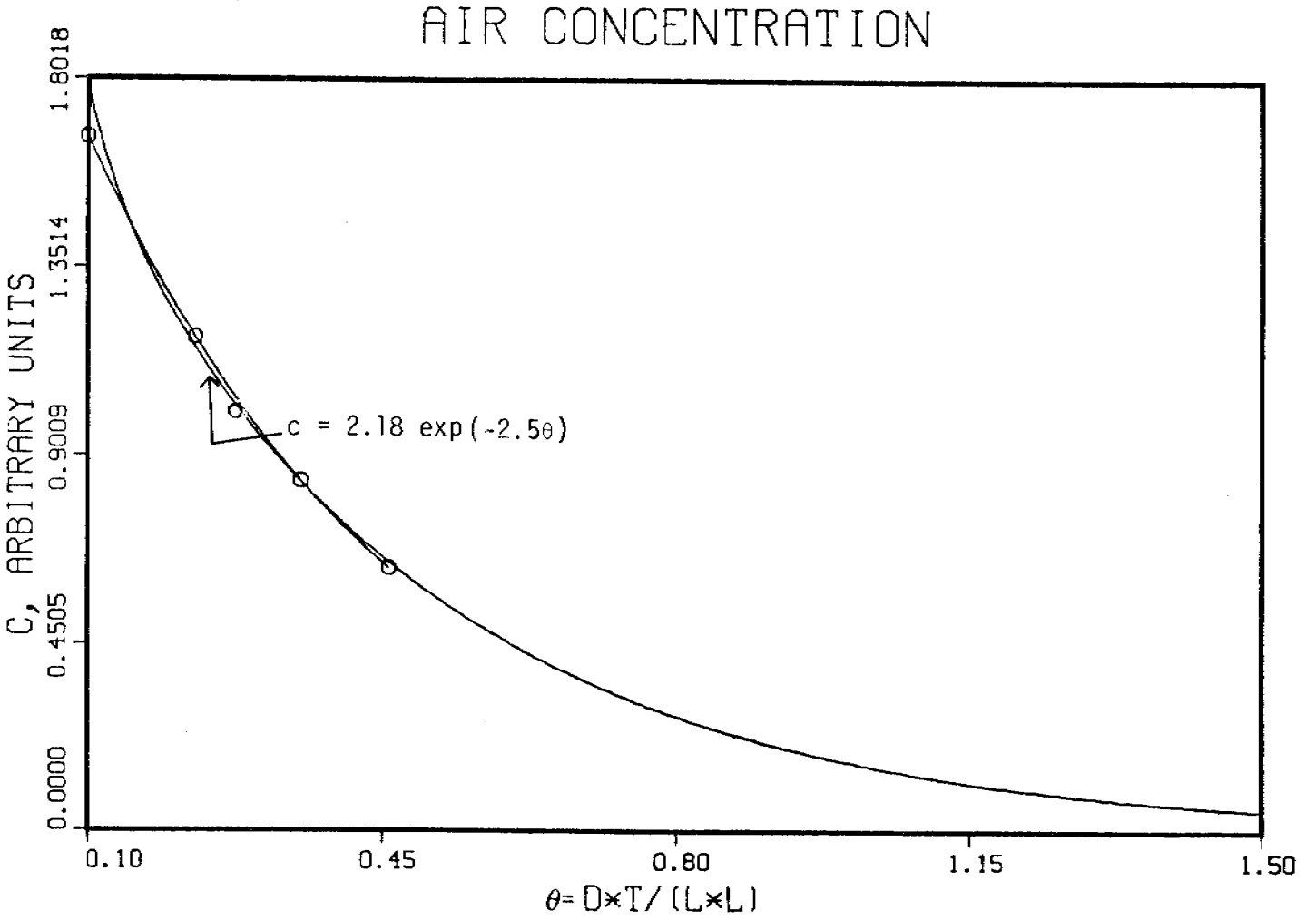

FIGURE 4-4. THEORETICAL AIR CONCENTRATION OF AN EVAPORATING COMPONENT ABOVE A DIFFUSION CONTROLLED SLAB AND A LEAST SQUARES EXP(-kθ).

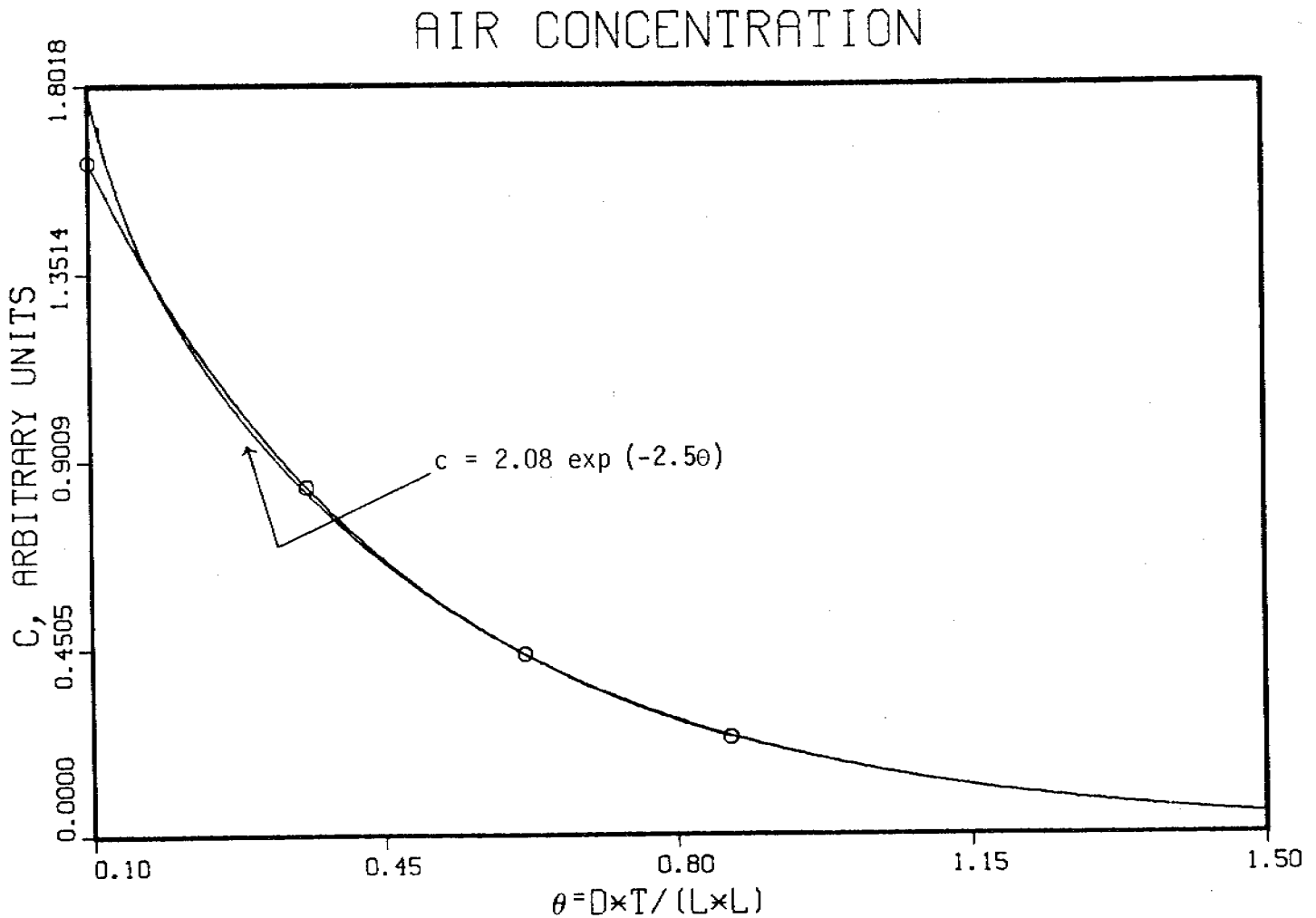

FIGURE 4-5. THEORETICAL AIR CONCENTRATION OF AN EVAPORATING COMPONENTS ABOVE A DIFFUSION CONTROLLED SLAB AND A LEAST SQUARES EXP(-kθ)

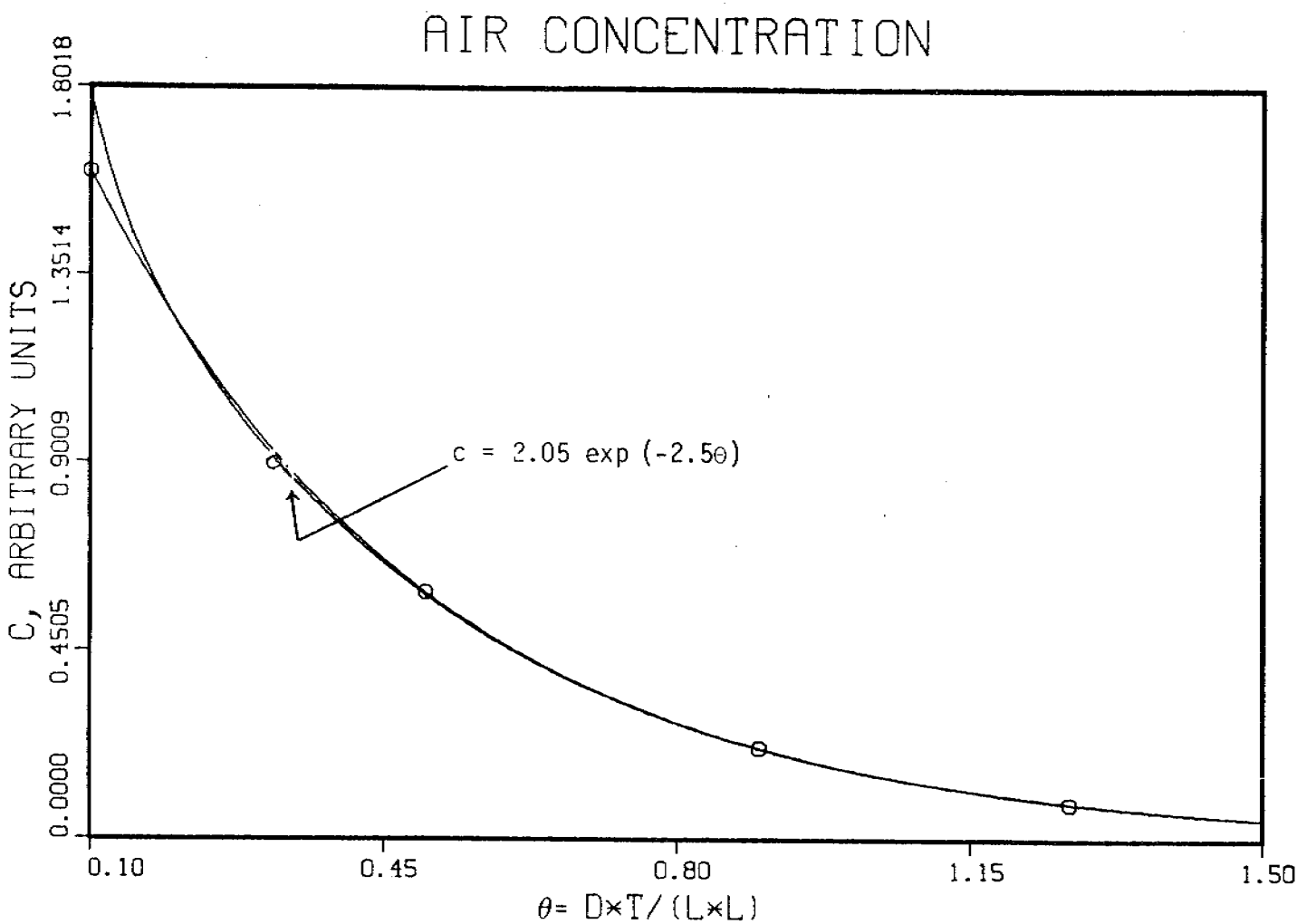

FIGURE 4-6. THEORETICAL AIR CONCENTRATION OF AN EVAPORATING COMPONENT ABOVE A DIFFUSION CONTROLLED SLAB AND A LEAST SQUARE EXP (-kθ).

These discussions have presented criteria to determine if an evaporating oil slick should be modeled as a well-stirred or stagnant phase. The method for that determination has been based on the Biot mass-transfer number in much the same way the presence of laminar flow is based on the Reynolds number. However, the data required to calculate the Biot mass-transfer number are not readily available, and estimates of these data must be made.

The primary reason for wanting to know if the oil phase is well-stirred or stagnant is that each of these states require different data and equations for model development. If an oil slick is diffusion-controlled, wind speed will not affect the average, time-dependent composition of the diffusing component in the oil mass. On the other hand, if the oil phase is well-stirred the wind speed will have an affect on the average composition of the oil.

Even though an oil phase can be diffusion controlled, it has been demonstrated that a decaying exponential will fit the air phase concentration data quite well. Thus, if an experiment is conducted to determine if evaporation from an oil slick is occurring from a well-stirred phase, it is necessary to obtain a good fit to the data but not sufficient to distinguish a well-stirred from a diffusion-controlled phase.

4.3 Component-Specific Evaporation from a Finite Oil Slick

The component-specific approach to model the evaporation process cannot predict the total mass of oil remaining in a slick. This approach can yield component-specific concentrations in the oil as a function of time when coupled to a pseudo-component overall material balance. For each specific component the rate of loss of component i from the slick takes the same form as a pre-defined pseudo-component:

$$\frac{dC_i}{dt} = -KAH_iC_i \quad \text{for } i = 1, 2, \ldots\ldots\ldots \tag{4.35}$$

where C_i is the concentration of component i in the oil, H_i is the Henry's law coefficient for the i-th component, and K and A are the same as those used in the pseudo-component equations. There is no "closure" on the total mass of oil remaining in the slick when the above equation is used because the index i does not include all species. Therefore, the closure of the material balance can be handled in any of three ways:

1) ignore the decreasing slick mass and integrate equation (4.35) directly;

2) decrease the slick mass for those compounds for which a differential equation is written;

3) use the pseudo-component material balance to calculate a total slick mass and use this information in the differential equation.

Using the last approach, the rate of loss of component i from the slick is written the same as before but now with the concentration C_i as:

$$C_i = g_i/M_T \tag{4.36}$$

where g_i is the mass of i and M_T is the total mass of oil. M_T is calculated from the pseudo-component differential equations.

This approach to component-specific evaporation modeling will predict an increase in concentration with respect to time for those compounds with very low or essentially zero vapor pressures. While approach 2) above would also do the same, the error in predicting the total mass of oil remaining in the slick is not known, and it is believed the pseudo-component prediction will yield the best results when coupled to the component-specific model.

4.4 Component-Specific Evaporation from a Semi-Infinite Oil Slick

The foregoing discussion on evaporation of components, from an oil slick does not take into account the fact that the partial pressure in the air of all the components being transported from the oil through evaporation will not necessarily be zero. For example, when the Henry's law coefficient of a compound is very low, it takes only a very small amount of it to saturate the air, which is the case with a very volatile compound such as naphthalene. Also, since the air above an oil slick is not of infinite "volume" due to finite turbulent diffusivities which form transport boundaries, it is necessary to consider the effects of these conditions on component-specific transport.

Consider an oil slick being continuously emitted from a point source onto the ocean surface as shown in Figure 4-7. This slick is referred to as the semi-infinite slick. By writing differential material balances for both the oil and air phases the following set of equations describes the evaporation of component i:

$$U_a \frac{\partial C_a}{\partial x} = \bar{\bar{\mathscr{D}}}_z \frac{\partial^2 C_a}{\partial z^2} \tag{4.37}$$

$$C_a(x) = 0 \quad \text{at} \quad Z = \infty \tag{4.38}$$

$$C_a(Z) = 0 \quad \text{at} \quad x = 0 \tag{4.39}$$

$$\frac{dC_H}{dx} = \frac{H\bar{\mathscr{D}}_z}{\bar{U}_o \delta} \left.\frac{dC_a}{dz}\right|_{z=0} \tag{4.40}$$

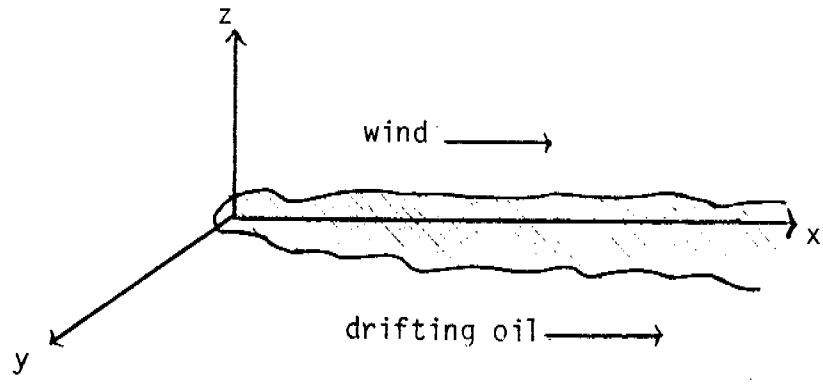

FIGURE 4-7. CONTINUOUS OIL SLICK WITH ORIGIN AT x = o; SURFACE IS IN y-x PLANE

$$\frac{dC_H}{dx} = - \frac{K_o}{\bar{U}_o \delta} \left[C_H - C_a \Big|_{z=0} \right] \tag{4.41}$$

$$C_H = HC_i \quad \text{at} \quad x = 0 \tag{4.42}$$

where C is the concentration of the species of interest with the subscipt "a" denoting the air, H denoting the oil, i denotes the X = 0 concentration, U_a is the mean wind speed, $\bar{\mathcal{D}}_z$ is the turbulent diffusivity in the air, H is the Henry's law coefficient, U_o is the oil velocity, δ is the slick thickness, and K_o is the over-all mass-transfer coefficient. This derivation essentially follows that of SUTTON (1943) in which the evaporation of water from lakes was studied. A modification of Sutton's derivation was made here where the over-all mass-transfer coefficient was introduced so that the results of other researchers can be utilized. The width of the slick does not appear in the above equations as a result of the assumption that the slick width is constant. This assumption will generally be valid only in the case where the oil is emitted to the surface slowly.

Equations (4.37) through (4.42) can be solved by Laplace transforms. The quantity of interest is the concentration of a specific component in the oil, and the solution is:

$$\frac{C}{C_o} = \frac{1}{\alpha} \exp\left[kx\alpha^2\right] \operatorname{erfc}\left[\alpha\sqrt{kx}\right] + \frac{1}{\beta} \exp\left[kx\beta^2\right] \operatorname{erfc}\left[\beta\sqrt{kx}\right] \tag{4.43}$$

where α and β are the roots of:

$$q^2 + \frac{\tilde{H}}{K} q + \frac{\tilde{H}}{k} = 0 \tag{4.44}$$

which may be complex. The other terms are defined as:

$$\tilde{H} = \frac{K_o}{\bar{U}_o \delta} \tag{4.45}$$

and

$$K \equiv \frac{H\bar{\mathcal{D}}_z}{\bar{U}_o \delta} \tag{4.46}$$

and

$$k \equiv \frac{\bar{U}_a}{\bar{\mathcal{D}}_z} \tag{4.47}$$

This model for a semi-infinite oil slick will not predict an increase in concentration with respect to time for the less volatile compounds in the oil phase due to the fact that an over-all material balance is not considered here as it is in the pseudo-component model. However, the above model will predict what combinations of parameters are important in invoking the zero air phase concentration assumption. Equations 4.43 through 4.47 show that the oil-phase concentration can be adequately predicted by assuming a zero air-phase partial pressure for small distances from the oil release point. However, for large distances from the oil release point, the zero air-phase partial-pressure assumption is not always adequate to predict the oil-phase concentrations and the above equations must be used.

Figures 4-8 and 4-9 present the calculations of the relative concentration of a specific compound in a semi-infinite oil slick for the parameters indicated in the figure legends. Also presented in these figures is the oil concentration when a zero partial pressure for this species is assumed to exist in the air phase. For the case of a 10 knot wind, the error introduced in assuming a zero partial pressure is approximately a factor of 10 at a downwind distance of one kilometer. This error rapidly increases with distance and thus shows that the zero-partial-pressure assumption should not be used, but that equations 4.43 through 4.47 must be used to predict the oil-phase concentration as a function of downwind distance for the parameters specified. The case of a 40 knot wind is presented in Figure 4-8 and shows that the error at one kilometer is essentially zero and does not become significant until 5 kilometers. This result is expected because a strong wind lowers the partial pressure above the slick. For less than a 10 knot wind the error in assuming a zero partial pressure will be quite large. These results are being used to determine when the zero partial-pressure assumption can (or can not) be involved.

4.5 Component-Specific Dissolution from a Semi-Infinite Oil Slick

The dissolution of specific components from an oil slick into the water column is described mathematically in much the same way as evaporation. However, dissolution accounts for only a small reduction of the slick mass compared to evaporation. The pertinent physical property required to describe dissolution is the liquid-liquid partition coefficient which is the analogy of Henry's law for evaporation.

Unfortunately there is no characterization process for dissolution that can be applied to the bulk oil in the same manner that distillation is used to characterize the oil with respect to evaporation. There have been two attempts to classify the oil into pseudo-components with respect to solubility, one by YANG and WANG (1977), but was not carried through to the quantitative stage, and another due to MACKAY (1980) where only two major "cuts" were

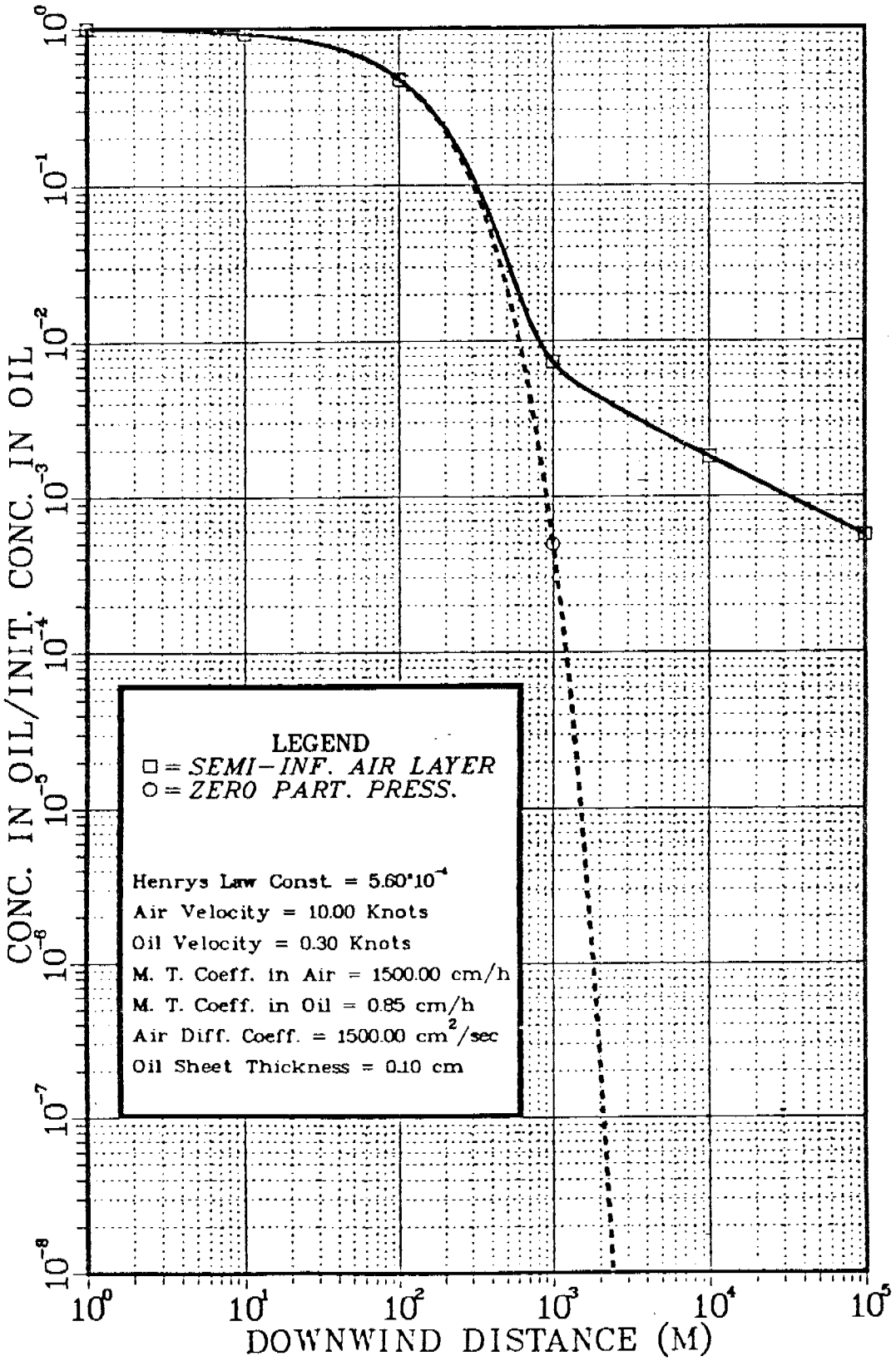

FIGURE 4-8. PREDICTED OIL-PHASE CONCENTRATION IN A SEMI-INFINITE OIL SLICK FOR A 10 KNOT WIND.

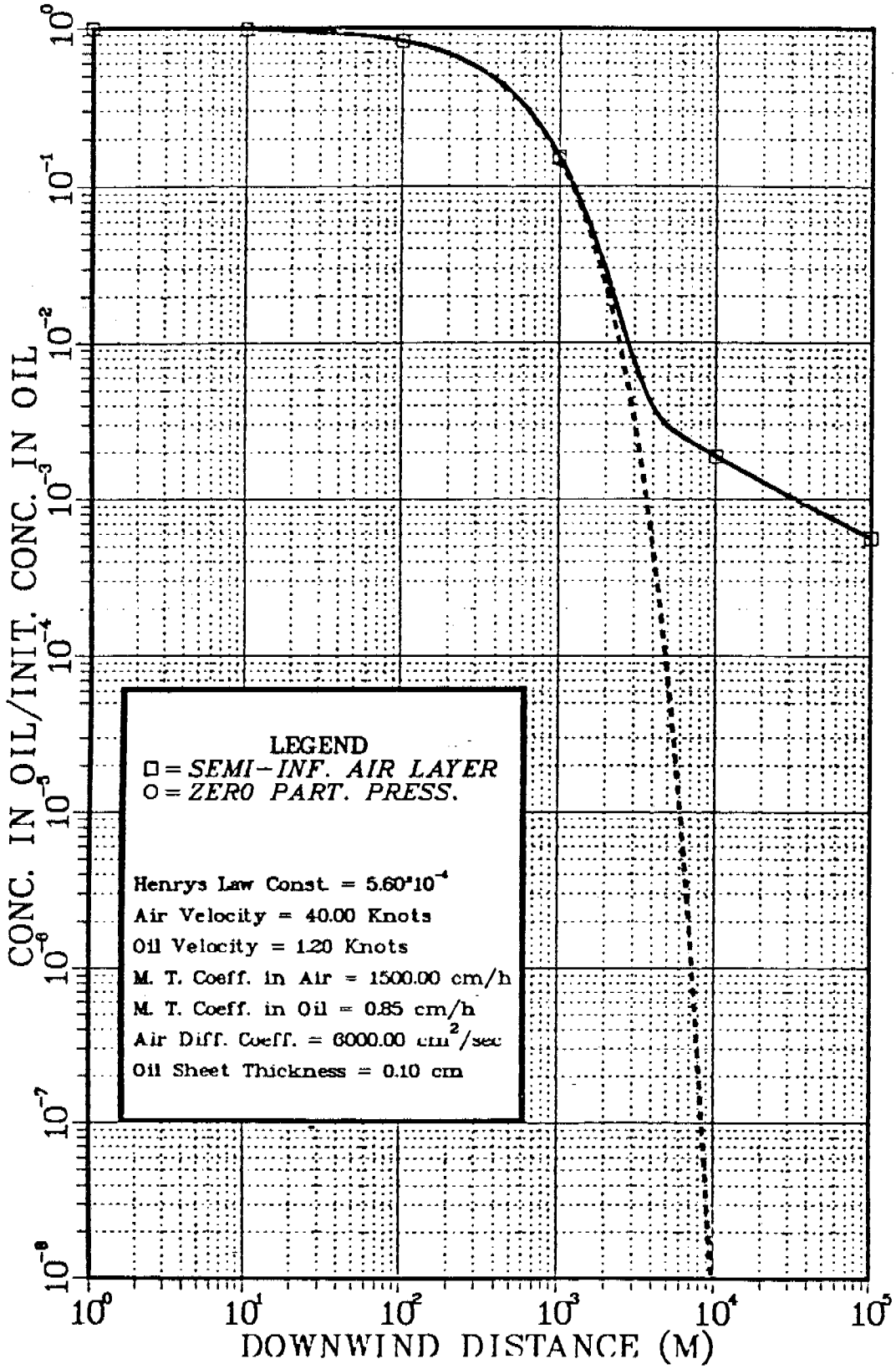

FIGURE 4-9. PREDICTED OIL-PHASE CONCENTRATION IN A SEMI-INFINITE OIL SLICK FOR A 40 KNOT WIND.

recognized. Since dissolution apparently accounts for a relatively small mass loss from the slick, an independent component-specific approach to dissolution is being utilized in our model.

Required physical property data required are liquid-liquid partition coefficients, referred to in the content of our work as m-values. It must be emphasized that pure component solubility data alone are not useful in obtaining m-values, because these types of data only yield information about the chemical potential of the species in the aqueous phase. What is needed along with pure component solubility data is the chemical potential of the species in the oil phase. Henry's law data coupled with solubility and vapor pressure data will provide a computed m-value through calculation, while liquid-liquid equilibrium experiments measure the m-value directly.

The dissolution oil weathering process is used to calculate species concentrations in the water column, not to account for the mass balance of the oil slick itself. The appropriate equations for a well-stirred slick with the coordinate reference shown in Figure 4-10 are:

$$\frac{\partial C_w}{\partial t} = \bar{\mathcal{D}}_w \frac{\partial^2 C_w}{\partial x^2} \tag{4.48}$$

$$C_w(x) = 0 \quad \text{at} \quad t = 0 \tag{4.49}$$

$$\frac{dC_w}{dx} = 0 \quad \text{at} \quad x = \ell, \; t > 0 \tag{4.50}$$

$$\frac{dC_m}{dt} = \frac{\bar{\mathcal{D}}_w}{m\delta} \frac{dC_w}{dx} \quad \text{at} \quad x = 0, \; t > 0 \tag{4.51}$$

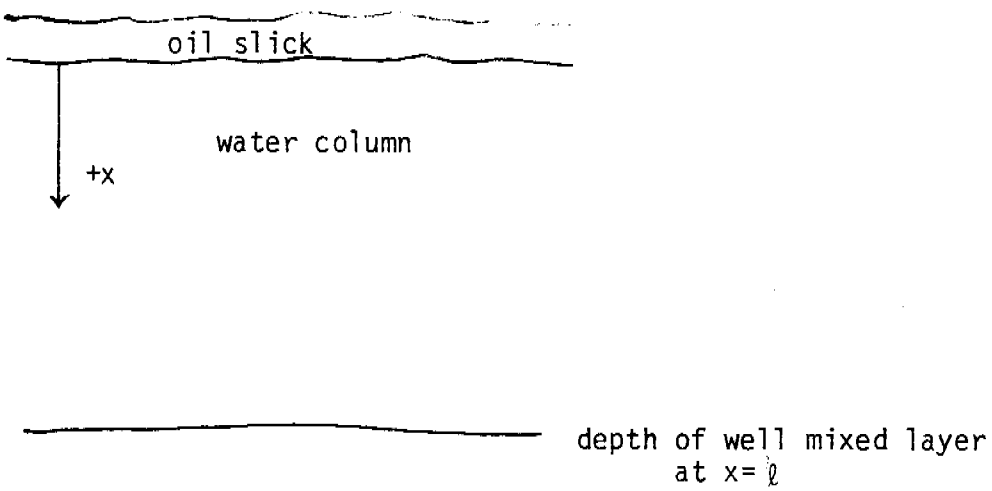

FIGURE 4-10. ILLUSTRATION OF COORDINATE FRAME FOR DISSOLUTION OF HYDROCARBONS INTO WATER COLUMN.

$$\frac{dC_m}{dt} = -\frac{K_o}{\delta}[C_m - C_w] \quad \text{at} \quad x = 0 \tag{4.52}$$

$$C_m = C_m^\circ \quad \text{at} \quad t = 0 \tag{4.53}$$

where C_w is the concentration of the species of interest in the water column, C_m is the concentration of the species of interest in the oil divided by the partition coefficient m, m is defined as the concentration in the oil divided by the concentration in the water at equilibrium, $\bar{\mathcal{D}}_w$ is the turbulent diffusivity in the water column, δ is the slick thickness, K_o is the over-all mass-transfer coefficient, and C_m^o is the initial C_m concentration in the oil.

The types of compounds to which the above problem solution will be applied are presented in Table 4-5 (MACKAY and SHIU, 1977). These compounds represent the polynuclear aromatic hydrocarbons which are likely to have the significant environmental toxic effects. The solutions represented by the above equations apply only strictly for the case where there is no evaporation. This condition is approximated when there is a crust on the oil or the dissolution rate is much greater than the evaporation rate. Likewise, the solution to the corresponding evaporation problem applies only strictly for the case where there is no dissolution, which is approximated when the evaporation rate is much greater than the dissolution rate. When evaporation and dissolution are both important, a "three-slab" problem results; however, this particular condition would be unlikely in a mathematical sense.

4.6 Comprehensive Aspects of Model Development

The previous discussions on model development did not include water-in-oil dispersions or microbial processes. The current plan for bringing these oil-weathering processes into the model is to incorporate the direction provided by MACKAY (1980) for the dispersion and mousse formation processes and the findings of the current microbial work as it becomes available.

TABLE 4-5. COMPOUNDS OF IMPORTANCE IN AQUATIC ENVIRONMENT (MACKEY & SHIU, 1977).

Compd	Solubilities, Exptl, mg/L	Solubilities, Exptl, x_w, mole fraction $\times 10^9$
Indan, C_9H_{10}	109.1 ± 1.02	16650
Naphthalene, $C_{10}H_8$	31.7 ± 0.26	4460
1-Methylnaphthalene, $C_{11}H_{10}$	28.5 ± 0.3	3550
2-Methylnaphthalene, $C_{11}H_{10}$	25.4 ± 0.2	3220
1,3-Dimethylnaphthalene, $C_{12}H_{12}$	8.0 ± 0.5	920
1,4-Dimethylnaphthalene, $C_{12}H_{12}$	11.4 ± 0.1	1310
1,5-Dimethylnaphthalene, $C_{12}H_{12}$	3.38 ± 0.04	377
2,3-Dimethylnaphthalene, $C_{12}H_{12}$	3.0 ± 0.01	347
2,6-Dimethylnaphthalene, $C_{12}H_{12}$	2.0 ± 0.02	233
1-Ethylnaphthalene, $C_{12}H_{12}$	10.7 ± 0.3	1240
1,4,5-Trimethylnaphthalene, $C_{13}H_{14}$	2.1 ± 0.1	215
Biphenyl, $C_{12}H_{10}$	7.0 ± 0.06	815
Acenaphthlene, $C_{12}H_{10}$	3.93 ± 0.014	459
Fluorene, $C_{13}H_{10}$	1.98 ± 0.04	214
Phenanthrene, $C_{14}H_{10}$	1.29 ± 0.07	130
Anthracene, $C_{14}H_{10}$	0.073 ± 0.005	7.57
2-Methylanthracene, $C_{15}H_{12}$	0.039 ± 0.004	3.67
9-Methylanthracene, $C_{15}H_{12}$	0.261 ± 0.002	24.4
9,10-Dimethylanthracene, $C_{16}H_{14}$	0.056 ± 0.0005	4.90
Pyrene, $C_{16}H_{14}$	0.135 ± 0.005	12.0
Fluoranthene, $C_{16}H_{10}$	0.26 ± 0.002	22.8
1,2-Benzofluorene, $C_{17}H_{10}$	0.045 ± 0.0012	3.75
2,3-Benzofluorene, $C_{17}H_{10}$	0.0020 ± 0.00003	0.956
Chrysene, $C_{18}H_{12}$	0.0020 ± 0.00017	0.158
Triphenylene, $C_{18}H_{12}$	0.043 ± 0.00013	3.39
Naphthacene, $C_{18}H_{12}$	0.00057 ± 0.00003	0.037
1,2-Benzanthracene, $C_{18}H_{12}$	0.014 ± 0.0002	1.10
7,12-Dimethyl-1,2-benzanthracene, $C_{20}H_{16}$	0.061 ± 0.0006	4.26
Perylene, $C_{20}H_{12}$	0.0004 ± 0.00002	0.0283
3,4-Benzopyrene, $C_{20}H_{12}$	0.0038 ± 0.00031	0.273
3-Methylcholanthrene, $C_{21}H_{16}$	0.0029 ± 0.000021	0.192
Benzo[g,h,i]perylene, $C_{22}H_{12}$	0.00026 ± 0.00001	0.0173
Coronene, $C_{24}H_{12}$	0.00014 ± 0.00002	0.00856

The logic involved in performing a calculation utilizing both pseudo-component and specific-component models is shown in Figure 4-11. The most important mass balance calculation is the pseudo-component evaporation process from which the slick mass and viscosity are obtained. Dissolution is not assumed to significantly affect slick mass. In parallel to the pseudo-component evaporation process, the component-specific evaporation and dissolution processes are calculated. These calculations proceed initially assuming a well-stirred slick state and continue until the viscosity reaches some prespecified value at which the slick becomes rigid. At this point the diffusion equation is used to calculate component specific concentrations according to the previous discussion of the Biot mass-transfer number.

4.6.1 Measurement of Henry's Law Coefficient

The need for specific thermodynamic information to describe interphase mass transport was presented in the discussions of component-specific evaporation and dissolution. The vapor-liquid equilibrium data required are called Henry's law coefficients (H). The Henry's law coefficient pertains to that portion of the phase equilibrium diagram where the ratio of phase concentrations is constant, which is the case when the concentration of the species of interest in one phase is small (e.g., oxygen in water).

Henry's law coefficients appear in the flux expressions and the overall mass-transfer coefficients which describe interphase mass transfer. The reason for the appearance of H in the flux expression is that a concentration difference between two phases is not sufficient information to identify in which direction mass will transfer. If the system is not at equilibrium, mass will transfer in the direction toward equilibrium. The information required to determine which way mass will transfer is the chemical potential of the species in each phase because the chemical potential is the potential for mass transfer. The Henry's law coefficient provides the method to map the concentration in one phase to the same chemical potential basis as the other phase. By using H, the correct driving force can be written for mass transfer.

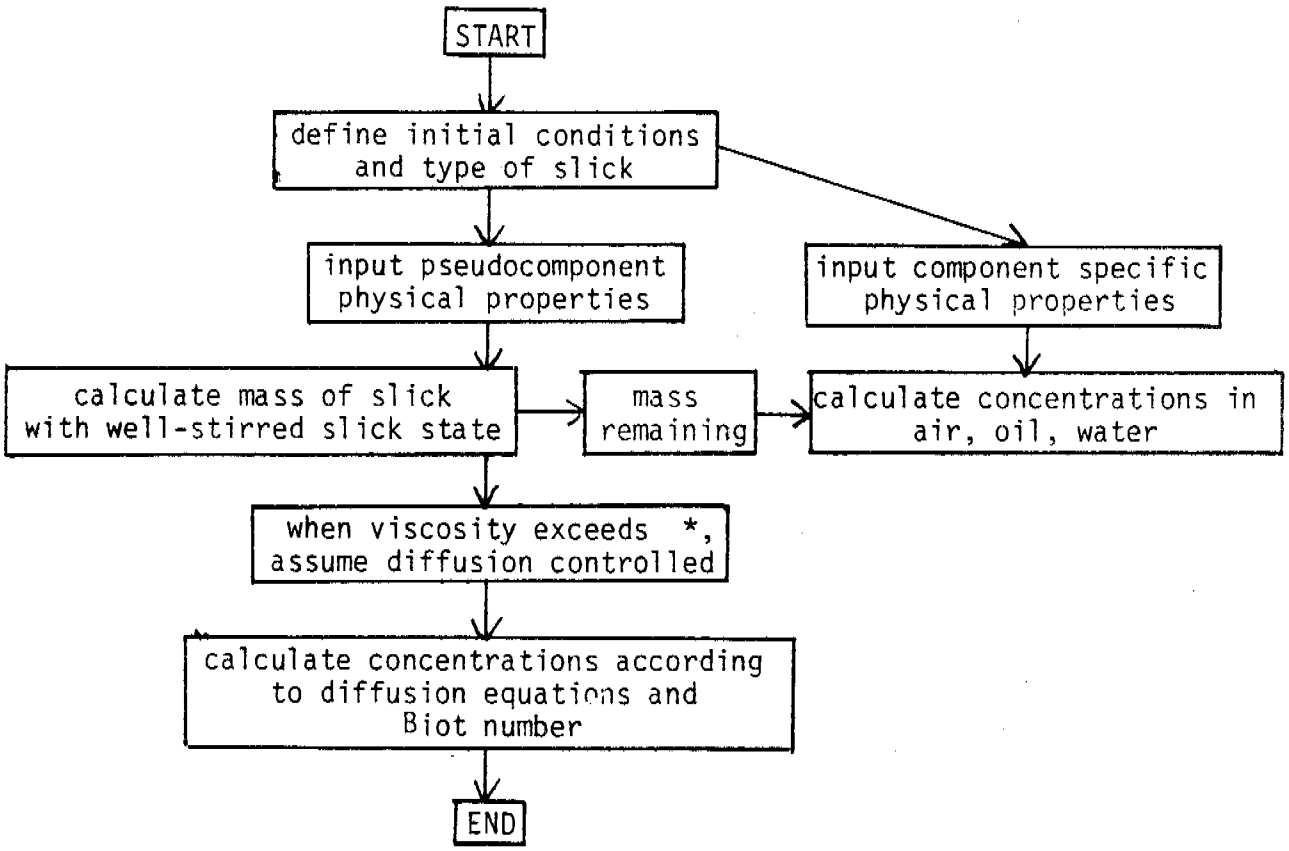

FIGURE 4-11. LOGIC FOR USING PSEUDOCOMOPNENT AND SPECIFIC COMPONENT MODELS IN OIL WEATHERING.

The over-all mass-transfer coefficient also utilizes H in a manner that takes into account the relative solubility of the species of interest in each phase. There is virtually no way to determine the relative mass transfer resistances without H (TREYBAL, 1955; LISS, 1974).

The technique originally described by MCAULIFFE (1966) to measure Henry's law coefficients using gas chromatography involves multiple equilibrations of equal volumes of aqueous and gaseous phases. A large glass syringe with a Luer-Lok fitting is filled 1:1 with liquid and clean nitrogen or air. The syringe is then capped off and agitated vigorously to create an equilibrium between phases. Most of the gas is then flowed through a gas sample loop which is an integral part of the analytical system (a gas chromatograph). At some point in this flow, a valve is turned and the gas in the loop (typically 0.1 to 10 ml) is introduced into the gas chromatograph. The rest of the gas is discharged from the syringe and fresh gas in introduced. The process is repeated a number of times.

The mathematical description of this procedure using equal volumes was given by McAullife and yields:

$$\log G_n = an + b \tag{4.54}$$

$$a = -\log (H + 1) \tag{4.55}$$

$$b = \log HX_o \tag{4.56}$$

where G_n is the amount of the compound of interest in the gas during the n-th equilibration, H is Henry's law coefficient, and X_o is the original amount of the compound in the system. Equation (4.54) shows that a plot of the log of compound concentration (or GC peak height) vs equibration number n gives a straight line. The negative slope of this line gives the log of (H + 1).

In measurements of Henry's law coefficients for petroleum components, it is not necessarily convenient to use equal volumes of liquid and gaseous phases. Some compounds have large distribution coefficients and some have relatively small values. Also, when the fresh oil/air system is measured, it has been found to not be desirable to deal with 25 ml of oil in the partitioning syringe. Therefore, a re-derivation of equations (4.54) through (4.56) for unequal volumes of gas/liquid has been done. Considering a measurement system with unequal liquid and gas volumes, V_l and V_g, respectively, G_i can be defined as the amount of a distributing component in the gas phase during the i-th equilibration. Similarly, L_i is the amount in the liquid phase during the i-th equilibration. The total amount of the substance is:

$$X_i = G_i + L_i \tag{4.57}$$

and the Henry's law coefficient becomes:

$$H = \frac{\text{concentration in gas}}{\text{concentration in liquid}} = \frac{G_i V_L}{V_g L_i} \tag{4.58}$$

r can be defined as:

$$r = \frac{V_L}{V_g} \tag{4.59}$$

and as a result the gas phase amount, G_i, can be re-expressed:

$$G_i = X_i - L_i = X_i - \frac{rG_i}{H} = \frac{Hx_i - rG_i}{H} \tag{4.60}$$

$$HG_i = Hx_i - rG_i \tag{4.61}$$

$$G_i = \frac{HX_i}{r + H} \tag{4.62}$$

$$G_i = \frac{(H/r)x_i}{1 + H/r} \tag{4.63}$$

Similarly, the liquid phase amount, L_i, can be written:

$$L_i = \frac{x_i}{1 + H/r} \tag{4.64}$$

The fractional amounts the component in the gas and liquid phases, f_g and f_L, respectively, can be expressed as:

$$f_g = \frac{G_i}{x_i} = \frac{(H/r)x_i}{x_i(1 + H/r)} = \frac{H/r}{(1 + H/r)} \tag{4.65}$$

$$f_L = \frac{L_i}{x_i} = \frac{x_i}{x_i(1 + H/r)} = \frac{1}{(1 + H/r)} \tag{4.66}$$

For subsequent equilibrations (i.e., i+1, i+2 .... i+n), equation (4.63) can be generalized to:

$$G_{i+1} = \frac{(H/r)}{1 + H/r}\left[x_i - \frac{H/r}{1 + H/r}\, x_i\right] \tag{4.67}$$

or redefining the subscripts finally yields:

$$G_m = \frac{(H/r)x_o}{(H/r + 1)^m} \qquad (4.68)$$

G_m can be experimentally obtained as component-specific gas chromatographic data, and if equation (4.68) is rearranged to logrithmic form it takes on a linear form ($y = mx + b$) - a plot of log G_m vs (m) has a slope equal to $-\log(H/r + 1)$. Only one phase of the system needs to be sampled, any ratio of volumes can be used, many compounds can be measured at one time, and standards do not have to be run since only relative amounts are used in the calculations.

Henry's law coefficients have been measured in this study using equation (4.68). A 50 ml glass Hamilton gas-tight syringe with a Luer fitting is used along with a sample loop (of varying sizes) installed into a six-port Valco valve which allows the loop gas to be initially purged to the atmosphere prior to introduction into the carrier gas of the gas chromatograph. The valve is enclosed in an insulated enclosure, heated, and temperature controlled. The gas is delivered to the valve by 1/16-inch tubing. In order to avoid inconsistencies and pressure differences which could effect equilibrium, the syringe is discharged with a Sage Instruments Syringe infusion pump set at a very slow rate. A Hewlett-Packard 5731A gas chromatograph with a flame ionization detector and 3385A Automatic Integration System has been employed. A 6-ft glass column packed with 1% SP-1000 on Carbopak B 60/80 is currently being used, and plans for future studies incorporate the use of a 30-m glass capillary column using SE-54 or SE-30 as the liquid phase.

In order to verify the ability of this experimental technique, a number of measurements have been made on hydrocarbons dissolved in distilled water. The extent of "known" Henry's law data is very limited, however a few literature values (MACKAY, 1975) have been found for comparison. Typically, the compound of interest is equilibrated with distilled water in a separatory

funnel for a number of hours. Then the water can be taken from the funnel stopcock directly into the syringe. Figure 4-12 presents a plot of resultant data for benzene and Table 4-6 presents some of the data obtained so far in this program which can be compared to previously measured values.

The technique is reproducible, with a scatter in the data of about 10 to 20 percent. All of the Henry's law values are in approximate agreement with the literature values except for iso-octane. This has not been explained, but it is suspected that the previously cited value is incorrect.

Currently, Henry's law measurements on the oil-air system are being completed. This is requiring the use of a capillary column for enhanced analytical resolution. The combination of the two columns will enable us to obtain Henry's law coefficients for all of the compounds that partition to a reasonable extent to the gaseous phase.

In order to get H values for compounds that have very low partial pressures in oil, a slightly different approach is being taken. Instead of sampling the gas, the liquid (oil) is sampled after every 5 or 10 equilibrations. The partitioning theory presented for water is applicable, however the measurement technique is the same except that the liquid sample involves the oil being dissolved in an appropriate amount of solvent (CS_2) and analyzed directly.

4.6.2 Diffusion Coefficients for Volatile Components Through Oil

To fully develop a model for oil weathering it is necessary to have diffusion coefficients for a variety of components in oil. Two problems pose obstacles to straight-forward application of the diffusion equations to describe the migration of components within an oil mass. First, the oil is usually in the form of a continually spreading slick and the continually altering thickness of the slick is a complicating factor. In addition, as lighter components are lost from the surface of the slick and skins begin to

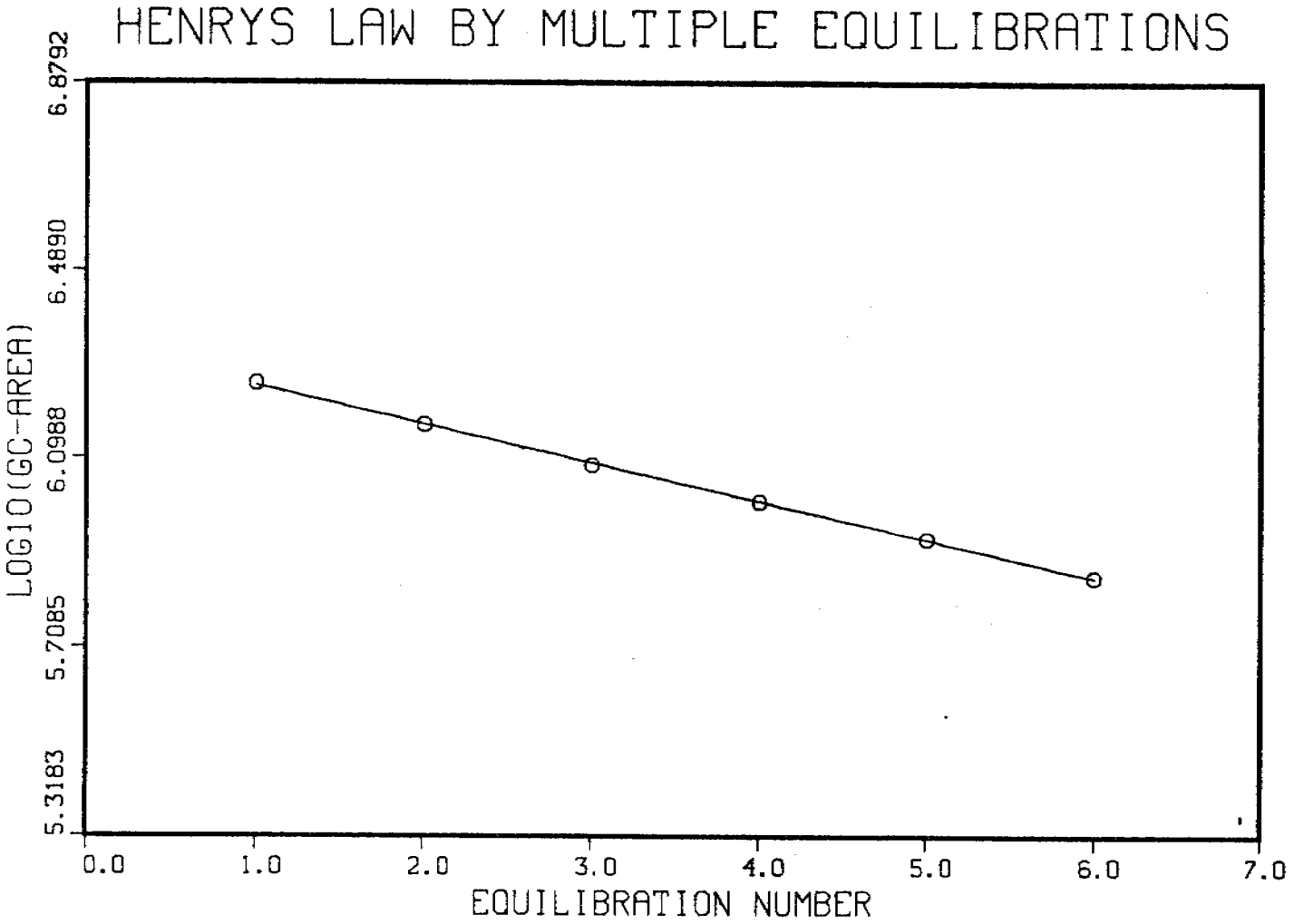

FIGURE 4-12. EXPERIMENTAL DATA FOR BENZENE.

TABLE 4-5. HENRY'S LAW RESULTS.

Compound	Ratio $\frac{V_\ell}{V_s}$ **	r*	H(atm m^3/mole)	H(literature)	$\frac{H}{H(lit.)} \times 100$
Benzene	25/25	-.9980	5.5×10^{-3}	5.5×10^{-3}	100
Benzene	14/36	-.9997	4.3×10^{-3}		78
Benzene	25/25	-.9998	5.0×10^{-3}		98
Benzene	25/25	-.9998	5.0×10^{-3}		91
Benzene	14/36	-.9998	4.9×10^{-3}		90
Benzene	14/36	-.9999	4.8×10^{-3}		87
Toluene	25/25	-.9999	5.3×10^{-3}	6.68×10^{-3}	79
Toluene	21/19	-.9890	5.6×10^{-3}		84
Iso-octane	31/19	-.990	~0.18	3.04	5.9
Iso-octane	31/19	-.997	0.098		3.2
n-Hexane	31/19	---	0.87	1.20	72.5
n-Hexane	36/14	---	1.04	1.20	87.1
Benzene/Toluene***	26/24	-.9985/-.9948	$5.04 \times 10^{-3}/5.07 \times 10^{-3}$	$5.5 \times 10^{-3}/6.68 \times 10^{-3}$	91/76

* correlation coefficient

** V_ℓ = volume of liquid, V_g = volume of gas

*** combined Benzene/Toluene

form, the impact on transfer of components across that interface is major. It is important, therefore, to be able to account for changing slick thickness and for slick skin permeability.

This section treats these points, beginning with multicomponent diffusion and commenting on the problems of developing a model that accounts for slick thinning. As an outgrowth of this, an approach is explained for treating laboratory experimental data in a way that will yield diffusion coefficients free from the effect of thinning. Problems associated with modeling skin formation are discussed, and an approach is presented.

4.6.2.1 Diffusion Through a Thinning Slick

This case can be thought of in terms of one-dimensional diffusion through a plane slab of thickness b. Assuming an impenetrable barrier at the plane boundary (y = 0). Also, at y = b, it is assumed that the ambient medium is sufficiently stirred that all volatiles are at zero concentration in that plane.

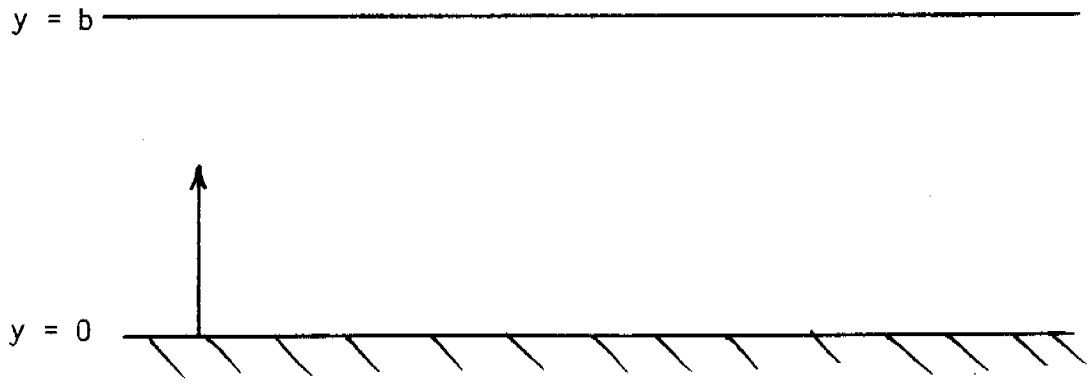

If $b = b_o$ = constant, and if diffusivity $\mathcal{D}$ is also constant, the (molar) concentration of any species is given by:

$$\frac{C}{C_o} = \frac{4}{\pi} \sum_{n=0}^{\infty} \frac{(-1)^n}{(2n+1)} \exp\left[\frac{-(2n+1)^2 \pi^2 \mathcal{D} t}{4b_o^2}\right] \cos\left[\frac{(2n+1)\pi y}{2b_o}\right] \tag{4.69}$$

where C_o is the (assumed uniform) concentration at $t = 0$. After some interval of time, t, the amount of the volatile species remaining in the slab is:

$$\int_o^b c\,dy = \frac{8C_o b}{\pi^2} \sum_{n=0}^{\infty} \frac{1}{(2n+1)^2} \exp\left[\frac{-(2n+1)^2 \pi^2 \mathcal{D} t}{4b^2}\right] \tag{4.70}$$

and the mass loss up to time t is:

$$MC_o b_o \left[1 - \int_o^{\phi} (C/C_o)\, dy/b_o\right] \tag{4.71}$$

where M = molecular weight and $\phi \equiv b/b_o$.

If an assumption is made that the volumes of all components are addictive, then the mass loss may be related to slab thickness as follows:

$$\rho_L(b_o - b) = \sum_i M_i C_{o_i} b_o \left[1 - \int_o^{\phi} (C/C_o)_i\, dy/b_o\right] \tag{4.72}$$

where ρ_L is the mass density of the slab, and the summation is over all volatile species.

If one makes a "quasi-steady state" assumption, stipulating that equation (4.70) is valid even for b varying with time, then an algebraic equation for b(t) is obtained:

$$1 - \phi = \sum_i m_i \left[1 - \frac{8\phi}{\pi^2} \sum_{n=0} \frac{1}{(2n+1)^2} \exp\left[\frac{-(2n+1)^2 \pi^2 \mathscr{D}_i t}{4b^2} \right] \right] \qquad (4.73)$$

or

$$1 - \phi = \sum_i m_i \left[1 - \frac{8\phi}{\pi^2} \sum_{n=0} \frac{1}{(2n+1)^2} \exp\left[\frac{-(2n+1)^2 \pi^2 \tau_i}{4\phi^2} \right] \right] \qquad (4.74)$$

where

$$\phi = b/b_o, \quad \tau_i = \mathscr{D}_i t/b_o^2, \quad m_i = \frac{M_i C_{o_i}}{\rho_L} \qquad (4.75)$$

One would expect this quasi-steady state assumption to be reasonably accurate for short time ($\phi \approx 1$).

In principle one could use equation (4.74) to calculate diffusion coefficients $\mathscr{D}_i$ from observations of $\phi(\tau)$. For a multicomponent system this would be impractical, since a multivariable fit of data on $\phi(\tau)$ would be required. Since the accuracy of equation (4.74) for large time periods is questionable, and since one would have to go to large time in order to have reasonable precision in data for $\phi(\tau)$, the use of equation (4.74) for determination of $\mathscr{D}_i$ is not suggested for multicomponent systems.

Having completed this analysis, it was concluded that the proper alterative approach should be to determine diffusion coefficients by monitoring the role of release of each species from the slab, at short time intervals

($\phi = 1$). This is done by measuring the appearance of each species in an inert stream that sweeps across the slab. If a sweep stream, initially free of every diffusing species, is provided at a flowrate q_o (volume/time), then the concentration of each species in that stream may be found, assuming constant pressure isothermal conditions in the sweep stream. If ρ_G is the density of the sweep gas, then the rate of flow of gas into the system is $\rho_G q_o$.

The mass rate of flow of diffusants into the system is $\sum AM_i N_i$, where A is the exposed area of the slab and N_i is the molar flux of species i from the slab. The mass fraction of species i in the exit stream is:

$$x_i = \frac{AM_i N_i}{\rho_G q_o + \sum AM_i N_i} \tag{4.76}$$

It is anticipated that $\sum AM_i N_i \ll \rho_G q_o$, therefore:

$$x_i = \frac{AM_i N_i}{\rho_G q_o} \tag{4.77}$$

Hence, from a measurement of each X_i, each N_i is found, to then be correlated to individual component diffusivities $\mathscr{D}$.

To avoid problems with the reduction in slab thickness, an expression for N_i that is accurate over small time interval is derived from the Leveque solution:

$$N_i = C_{oi}\sqrt{\mathscr{D}_i/\pi t} \tag{4.78}$$

Thus, $x_i(t)$ should be measured to determine $N_i(t)$, and from the slope of a plot of N_i vs $t^{-1/2}$, $\mathscr{D}$ can be found.

4.6.2.2 Rate of Slick Thinning

Although we have avoided treating the reduction in slab thickness as a variable in measuring diffusion coefficients, it is important to get some idea of the rate of thinning. From equation (4.74) for a single diffusing species, we must solve for ϕ:

$$\phi = \frac{1 - m}{1 - \frac{8m}{\pi^2} \sum_{n=0} \frac{1}{(2n+1)^2} \exp\left[\frac{-(2n+1)^2 \pi^2 \tau}{4\phi^2}\right]} \qquad (4.79)$$

Again for short time intervals, it is convenient to use the Leveque solution for N, and find ϕ from:

$$\phi = 1 - \frac{2m}{\sqrt{\pi}} \tau^{1/2} \qquad (4.80)$$

Another approach to this problem is to apply the perturbation solution as described by DUDA and VRENTAS (1969). Since only the first few terms are used, the available solution is restricted to small values of M. A comparison of solutions is:

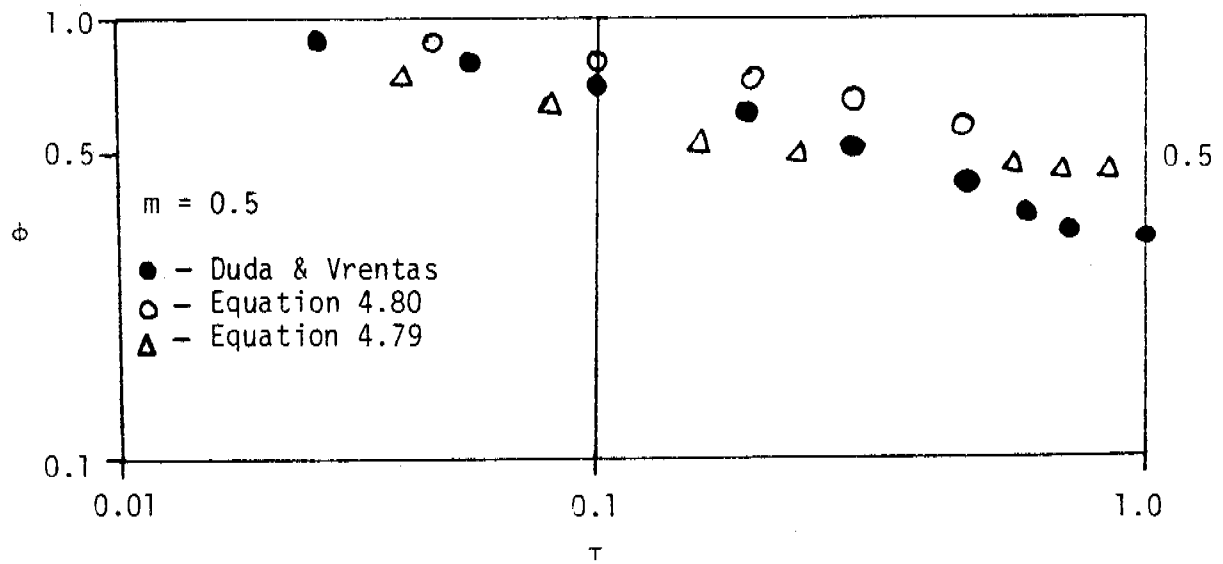

Equation (4.80) is expected to be valid only for small τ. Equation (4.79) shows (correctly) that ϕ approaches a value of 1-m at long τ. Also, the Duda and Vrentas solution is inaccurate over its mid-range, where it predicts that ϕ falls below $\phi = 0.5$. It does correctly give $\phi = 0.5$ as τ exceeds 3. The Duda and Vrentas solution is probably accurate at small τ. The value of $m = 0.5$ examined here ($m = -N_b$ in their notation) is a little large for their perturbation solution.

It is interesting to examine the fractional loss of a species from the slab, as a function of time. We expect that slab thinning will increase the rate of loss, but we do not know the degree of this increase. If the thickness remained uniform, the fraction of each species remaining would be found from:

$$f = 1 - \frac{8}{\pi^2} \sum_{n=0} \frac{1}{(2n+1)^2} \exp\left[\frac{-(2n+1)^2\pi^2\tau}{4}\right] \qquad (4.81)$$

or, for short times:

$$f \approx \frac{2}{\sqrt{\pi}} \tau^{1/2} \qquad (4.82)$$

The figure following shows f calculated using the above equations as well as f using the Duda and Vrentas solution. As expected, taking account of slab thinning leads to more rapid loss of diffusible species.

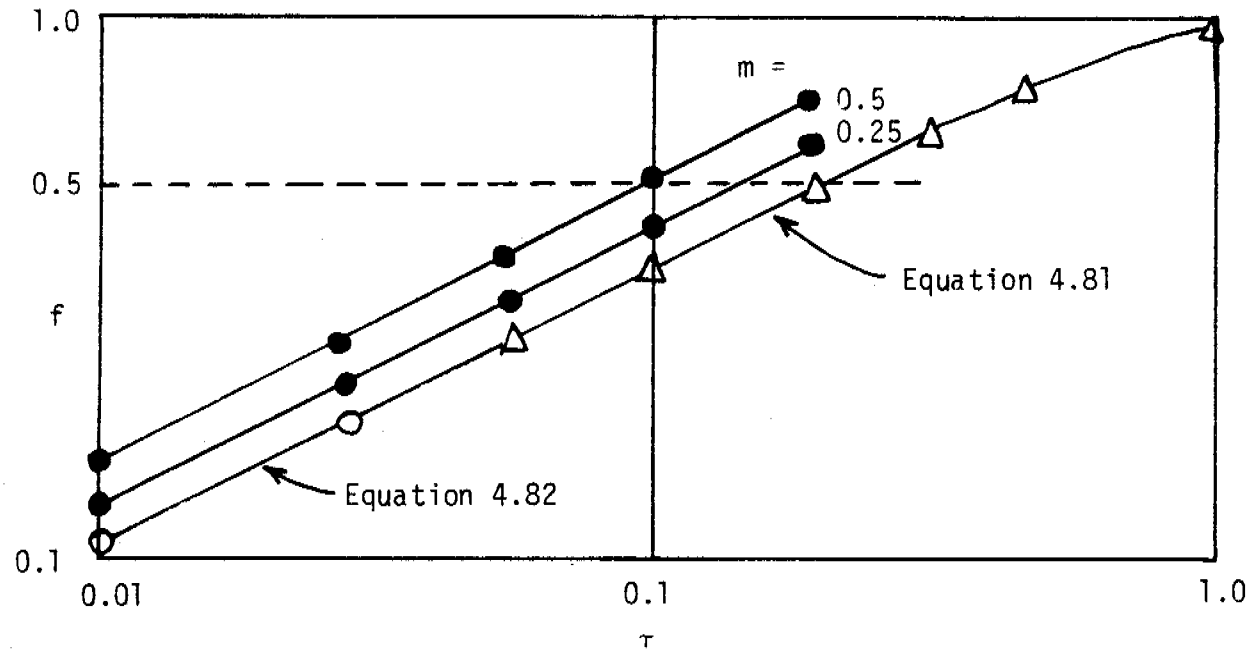

Even though the Duda and Vrentas solution is suspect in its mid-range for such large values of m, it is still useful to observe the effect of slab thinning on the half-time for release of a volatile component. For a slab of uniform thickness, the half-time is found to be $\tau_{1/2} = 0.2$. For $m = 0.25$ we find $\tau_{1/2} = 0.15$, and for $m = 0.5$, the value is reduced to $\tau_{1/2} = 0.1$.

4.6.3 The Role of Internal Circulation in the Weathering of a Thin Oil Slick

When a slick of oil floats upon a rough sea, its motion is determined by the local wind and wave action. These external forces could be strong enough to produce motion within the slick. Previous analyses of weathering have focussed on mass transfer by diffusion within the slick, and on convection across the slick/water and slick/air interfaces. Our efforts have attempted to produce a model that allows an estimate of the extent of internal motion, and the degree to which that motion enhances mass transfer of components to the environment.

The simplest model is derived from Figure 4-13 which shows an idealized oil slick. The slick is taken to be a slab of uniform thickness, H, and length, L, in the wind direction and we assume L>>H. Further, the width normal to the wind direction, W, also is assumed to satisfy W>>H. The wind generates a shear stress τ on the upper surface, which produces a velocity, V, in the wind direction, along the plane of the slick/air interface. We assume that the slick is stationary with respect to the water, or equivalently that V is measured relative to the mean velocity of the slick with respect to the water. Thus the physical model is as shown in Figure 4-14.

We are interested in the velocity profile v(y), and in then examining the effect of velocity on mass transfer at the slick/air interface. The velocity profile, under the approximations, satisfies:

$$0 = -\frac{\partial p}{\partial x} + \mu \frac{\partial^2 v}{\partial y^2} \qquad (4.83)$$

$$v = V \quad \text{at} \quad y = H$$

$$v = 0 \quad \text{at} \quad y = 0$$

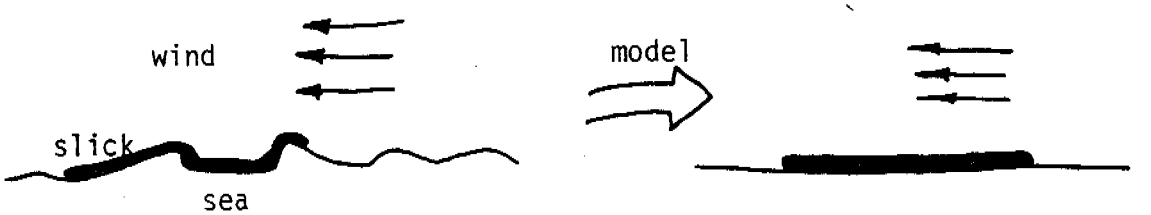

FIGURE 4-13. OIL SLICK ON THE SEA.

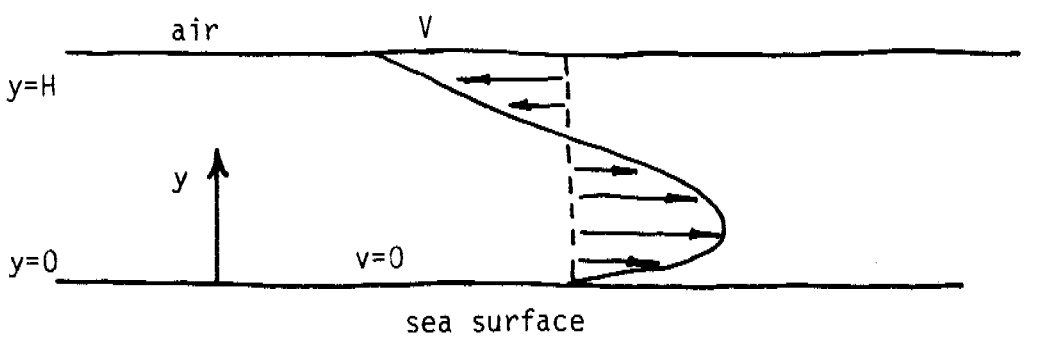

FIGURE 4-14. CIRCULATION WITHIN THE SLICK

and is found to be:

$$v = V\frac{y}{H} - \frac{1}{2\mu}\, y(H - y)\frac{\partial p}{\partial x} \tag{4.84}$$

We have assumed that $\partial p/\partial x$ is independent of y, equivalent to the assumption that the velocity is everywhere parallel to the planes (i.e., at both y = 0 and y = H). Of course this would not be true near the edges of the slick, where the flow reverses and returns across the lower region of the slick. We envision the flow induced in the slick by the wind to be like the motion of a tractor tread. The gradient $\partial p/\partial x$ is not known, but may be found by invoking the assumption that there is no net flow of oil in the x-direction:

$$\int_0^H v\, dy = 0 \tag{4.85}$$

Upon imposing this constraint we find:

$$\frac{\partial p}{\partial x} = \frac{6\mu V}{H^2} \tag{4.86}$$

and the velocity field is given as:

$$v = V\frac{y}{H}\left(2 - \frac{3y}{H}\right) \tag{4.87}$$

Next we examine the effect of this velocity field on mass transfer across the plane y = H. The basic case for comparison is the pure diffusion control situation, where there is no motion within the slab. From the classical solution to the pure diffusion problem we find:

$$\frac{C}{C_o} \approx \frac{8}{\pi^2} \exp\left(-\frac{\pi^2}{4}\frac{\mathcal{D}}{H^2}t\right) \quad \text{for} \quad \frac{\mathcal{D}t}{H^2} > 0.2 \tag{4.88}$$

where $\mathcal{D}$ is the diffusion coefficient of some species through the oil, and C/C_o is the fraction of the diffusible species remaining after time t. We may regard the term:

$$t_D \equiv \frac{4H^2}{\pi^2 \mathcal{D}} \tag{4.89}$$

to be a diffusion "time scale".

We can now impose a shear stress exerted by the wind which can set the slick liquid into circulation. Circulation aids diffusion by bringing regions of high concentration in the diffusible species into closer contact with the interface. In a sense this reduces the diffusion distance and should speed up the rate of removal by diffusion. We have investigated the magnitude of this enhanced removal, and how it might be correlated with slick and wind parameters.

A model can be formed along the physical bounds shown in Figure 4-15. Near the region y = H, we assume a classic Leveque-type diffusion problem. The circulating flow is mixed in the lower part of the slick and becomes the feed for the Leveque flow. Schematically, we separate the upper and lower regions into a diffusion region and a mixing region, connected by the circulating flow q. The magnitude of the circulating flow can be gotten from:

$$q/W = \int_{\frac{2}{3}H}^{H} v\,dy = \frac{4HV}{27} = \frac{H^2\tau}{27\mu} \tag{4.90}$$

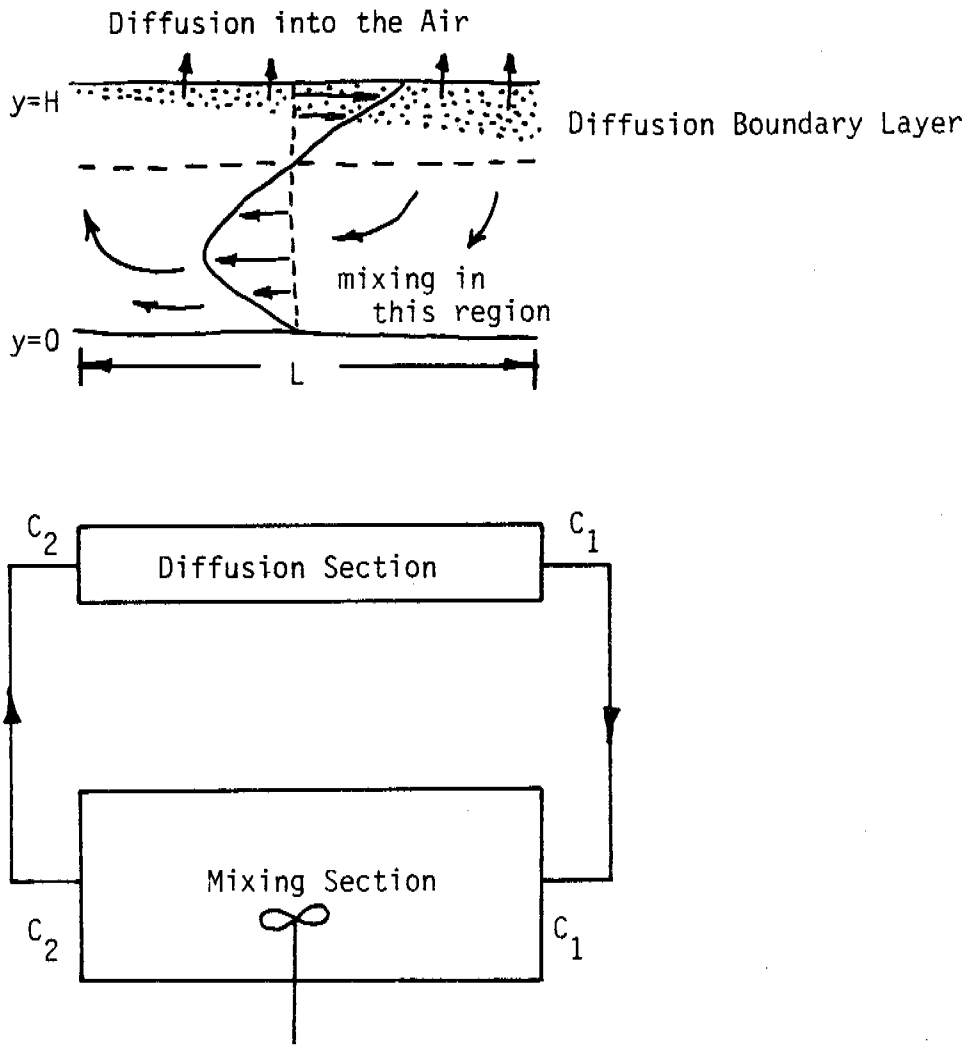

FIGURE 4-15. A MODEL FOR DIFFUSION WITH CIRCULATION

where W is the unit width in the z-direction. Along the slick/air interface the velocity is related to the shear stress τ by:

$$\tau = \mu \left.\frac{\partial v}{\partial y}\right|_{H} = 4\mu \frac{V}{H} \tag{4.91}$$

An average velocity of circulation as may be defined as:

$$\bar{V} = \frac{q/W}{H/3} = \frac{H\tau}{9\mu} \tag{4.92}$$

The Leveque solution gives:

$$\frac{C_2}{C_1} = 1 - 0.186(3)^{1/3}\left(\frac{9\,\delta\, L}{\bar{V}B^2}\right)^{2/3} \tag{4.93}$$

where C_1 and C_2 are defined as in Figure 4-15, $B = \frac{1}{3}H$ and $V = H\tau/9\mu$; more simply:

$$\frac{C_2}{C_1} = 1 - 21.7\left(\frac{\delta\, L\,\mu}{\tau H^3}\right)^{2/3} \tag{4.94}$$

For a simple stirred tank of volume v, a material balance can be stated as:

$$v\frac{dC_2}{dt} = q\left(C_2 - C_1\right) = -21.7\left(\frac{\delta\, L\mu}{\tau H^3}\right)^{2/3} q\, C_2 \tag{4.95}$$

and the solution for C_2 is expressed:

$$\frac{C_2}{C_{2_0}} = \exp\left(-t/t_c\right) \tag{4.96}$$

Thus we find, using Equations (4.90) and (4.95), that an appropriate time scale for circulation-enhanced loss is:

$$t_c = 0.8\left(\frac{L\mu H^3}{\ell^2 \tau}\right)^{1/3} \tag{4.97}$$

Of particular interest is the ratio t_D/t_c, which provides a measure of enhanced removal associated with circulation. We find:

$$E \equiv \frac{t_D}{t_c} = \frac{1}{2}\left(\frac{\tau H^3}{L\mu\ell}\right)^{1/3} \tag{4.98}$$

If we go back to Equation (4.91), we may write E as:

$$E = \frac{1}{2}\left(\frac{4\,VH^2}{L\ell}\right)^{1/3} = 0.79\left(\frac{VH}{\ell}\,\frac{H}{L}\right)^{1/3} \tag{4.99}$$

Even though we do not know V (it is related to the unknown τ) equation (4.99) is a useful form because it has the appearance of a Peclet number:

$$Pe = VH/\ell = \frac{\tau H^2}{4\mu\ell} \tag{4.100}$$

and:

$$E = 0.79(Pe/A)^{1/3} \tag{4.101}$$

where the aspect ratio A = L/H appears.

While this model has several assumptions and uncertainties, it provides the opportunity to assess the role of certain physical events that occur during the weathering process:

Slick Spreading

As H decreases and L increases, we see that E decreases. Thus, as spreading occurs, diffusion control dominates any effects of internal circulation.

Viscosity increase through loss of volatiles

Since a rough approximation for diffusion coefficients of volatiles in a viscous liquid suggests that $\mathcal{D} \approx 1/\mu$, we expect that the Peclet number will remain constant at fixed H. Thus the aging of the slick *per se* does not change the balance between diffusion and convection as the dominant mode of volatiles loss.

In order to assess the importance of internal circulation, in the context of this model, we must estimate the magnitude of E. This requires data from which the shear stress at the sea surface may be estimated. However, typical values of V, H, and $\mathcal{D}$ (e.g., V = 10 cm/s, H = 2 cm, $\mathcal{D} = 10^{-7}$ cm^2/s) and aspect ratio (L/H = 200) give an estimate for E of about 10^2, representing a significant enhancement in the rate of loss of volatiles. This circulation model assumes that the slick may spread across the sea surface, but that its motion is laminar. Another type of internal circulation is possible, driven by wave action which is shown in Figure 4-16.

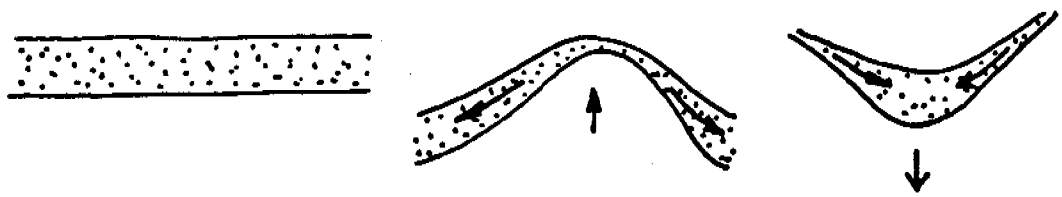

FIGURE 4-16. WAVE ACTION AS A MEANS OF PERIODIC MIXING ON A LOCAL SCALE.

A localized area within a large slick may alternately be thinned and thickened as the surface of the sea undergoes wave motion. We might regard this as a complete mixing process at that local level, and a model which accounts for this phenomenon might be taken along the following lines:

- o diffusion occurs from a uniform slab;
- o the slab is instantaneously mixed periodically;
- o diffusion occurs during intervals between mixing.

This is a relatively simple model to assess. Define t_M as the time interval between mixes (We expect that t_M is related to the temporal periodicity of the waves). If the slick has a mean concentration, C_o, of some species at time $t = 0$, then after an interval, t_M, the slick will be mixed and its mean concentration will be:

$$C_1 = C_o \left[1 - \left(4 \mathcal{D} t_M / \pi H^2\right)^{1/2}\right] \qquad (4.102)$$

$$= C_o(1 - F)$$

The slick will then continue to lose volatiles by diffusion, as before, except that the initial mean concentration is now C_1. In general, we would find, after n "mixes":

$$C_n = C_{n-1}(1 - F) \qquad (4.103)$$

and the solution of this difference equation, assuming F is constant, is:

$$C_n = C_o(1 - F)^n \qquad (4.104)$$

We may compare this solution to that for quiescent diffusion in the absence of mixing:

$$C/C_o = \frac{8}{\pi^2} \exp\left(-\frac{\pi^2}{4}\frac{\mathcal{D}}{H^2}t\right) + \frac{8}{9\pi^2}\exp\left(-\frac{9\pi^2}{4}\frac{\mathcal{D}t}{H^2}\right) + \cdots \quad (4.105)$$

and is we plot C/C_o vs $\mathcal{D}t/H^2$ (Figure 4-17) we see that:

$$t = n\,t_M \quad (4.106)$$

As expected, periodic mixing enhances the rate of loss of volatiles, the extent of enhancement depending upon the parameter F. From the half-times of these curves we may define a measure of the extent of enhancement by mixing, E_M, as:

$$E_M = \frac{\tau_{1/2}\,\text{(pure diffusion)}}{\tau_{1/2}\text{(periodic mixing)}} \quad (4.107)$$

Figure 4-18 shows E_m plotted as a function of F. Reasonable values of F can be estimated from:

$$F = \left(4\mathcal{D}t_M/\pi H^2\right)^{1/2} \quad (4.108)$$

We expect that H is of order 1 cm, with a range of perhaps 0.5 to 2 cm. The magnitude of $\mathcal{D}$ will depend strongly upon which volatile species is considered and might range from 10^{-8} to 10^{-6} cm^2/s. The wave interval, t_M, might take on values in the range 1 to 10 sec. F, then, would be in the range $10^{-4} \leq F \leq 10^{-2}$. If these estimates are reasonable, then it appears that this periodic mixing mechanism exerts a tremendous degree of enhancement of loss of volatiles on the slick in comparison to the pure, static diffusion model.

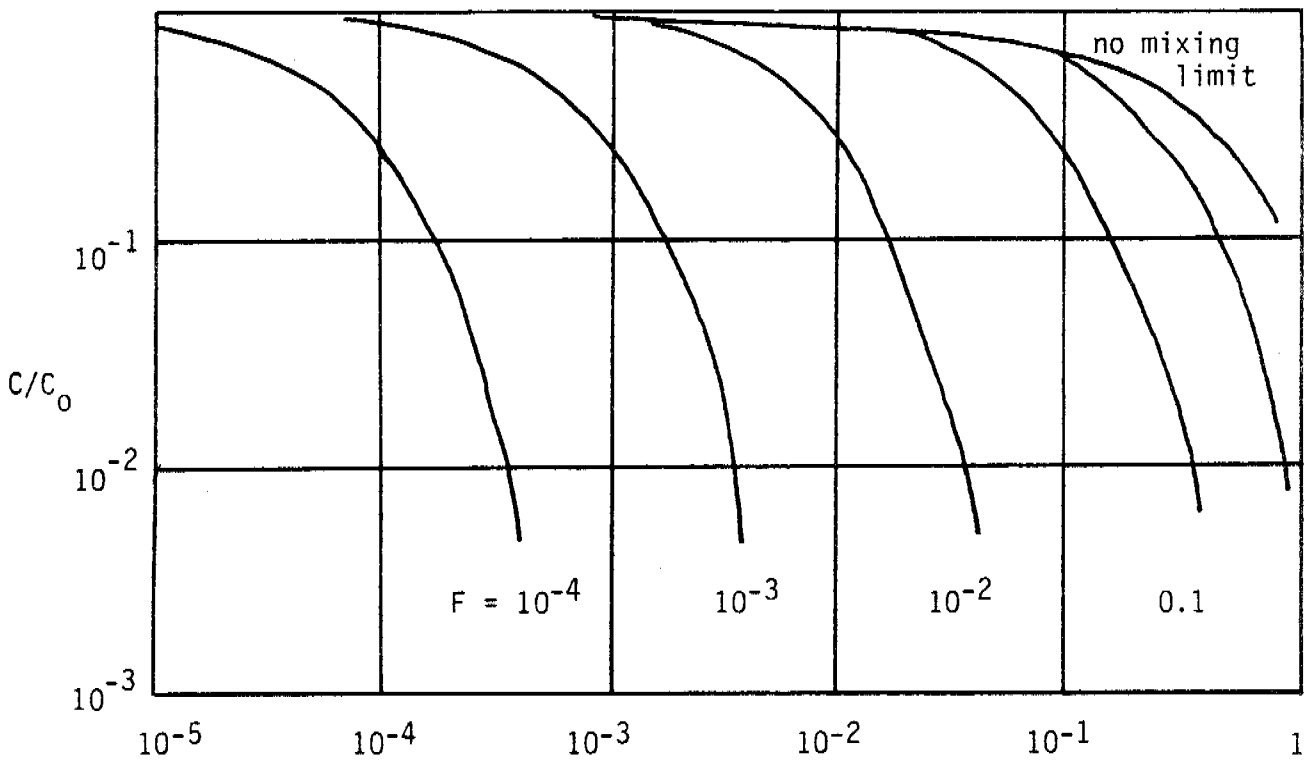

$$\mathscr{D}t/H^2 = \frac{\pi}{4} nF^2$$

FIGURE 4-17. EFFECT OF MIXING ON CONCENTRATION

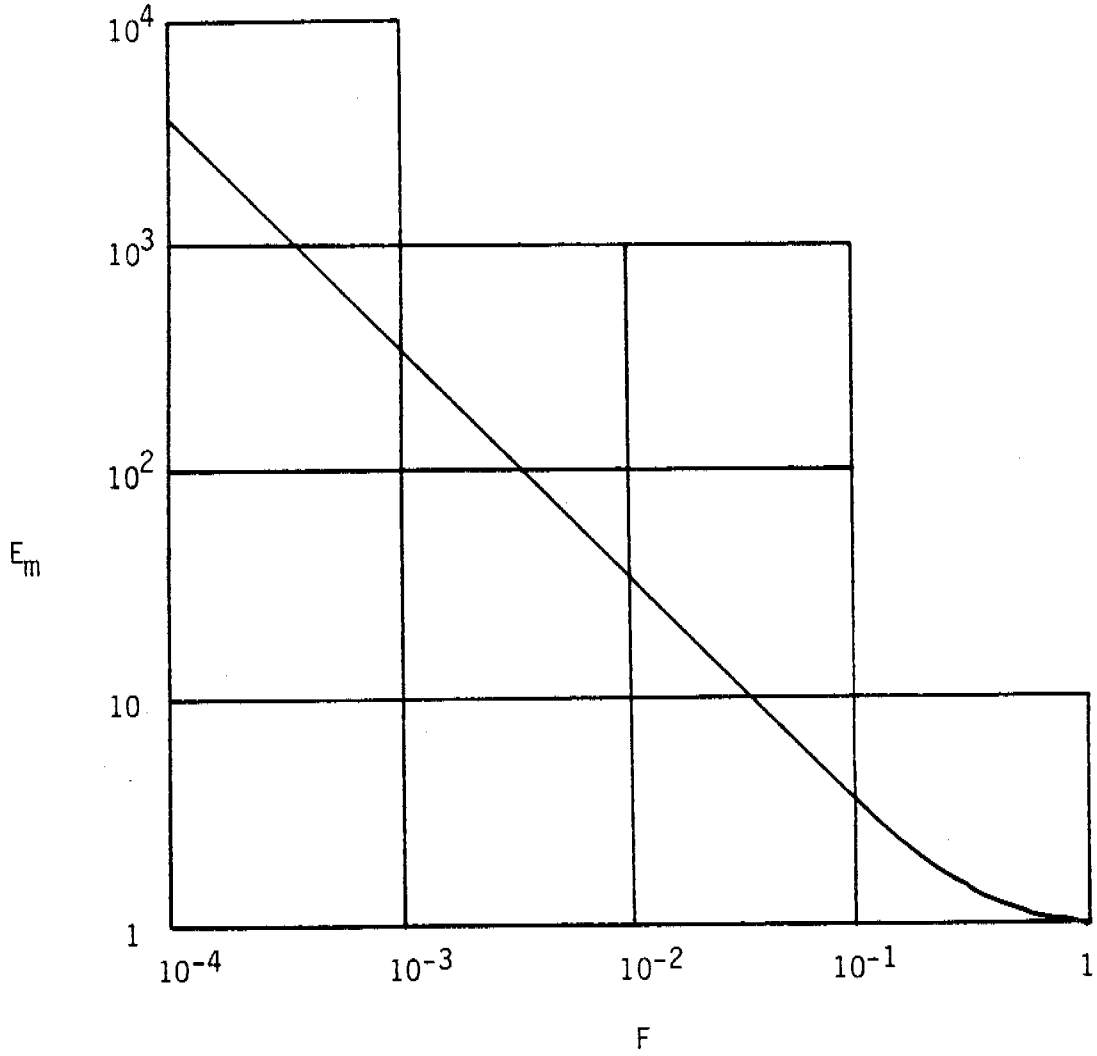

FIGURE 4-18. DEPENDENCE OF ENHANCEMENT FACTOR ON F

One difficulty with this approach is that it provides no connection between wave dynamics and the periodic mixing action, except through the time scale t_M. Nor does it address the question of whether the degree of mixing depends upon the viscosity of the oil. An "aged" slick will potentially be too viscous to be mixed by a wave. An expression to account for the ability of a wave to distort a slick, introducing slick viscosity and wave energy terms, is currently being contemplated.

5.0 EXPERIMENTAL PROGRAM RESULTS -- LA JOLLA, CALIFORNIA AND KASITSNA BAY, ALASKA

5.1 Evaporation/Dissolution Rate Determinations

Evaporation and dissolution are the two major weathering processes affecting oil after it is released into seawater; in some instances most of the volatile compounds may be lost by evaporative processes within 24 to 48 hours (JORDAN and PAYNE, 1980). The composition of an oil slick, its surface area and physical properties, the wind velocity, air and sea temperatures, sea state, and the intensity of solar radiation can all affect hydrocarbon evaporation rates (WHEELER, 1978).

Given sufficient time, evaporative processes can remove most of the volatile hydrocarbons with molecular weights less than nC-15, and in general pentadecane is the lightest normal alkane commonly found in weathered oils and tar balls (PAYNE, 1981). Further, it is rare to find hydrocarbons lighter than nC-12 in seawater extracts not associated with oil spill events. The volatile compounds encompassed below nC-15 make up anywhere from 20-50% of most crude oils, and the distillation curve data shown in Figure 3-12 illustrate that these components make up 50% of the overall mass of Murban crude, 46% of Cook Inlet crude, 31% of Prudhoe Bay crude and 25% of Wilmington crude oils. Hydrocarbon components with molecular weights less than nC-15 can make up as much as 75% or more in refined petroleum products and they constitute 10% or less of residual fuel oils such as Bunker C (CLARK and BROWN, 1977).

While other studies have been completed to determine the relative importance of evaporation vs dissolution for such compounds as benzene and cyclohexane (HARRISON et al., 1975; MCAULIFFE, 1977; SMITH and MCINTYRE, 1971), carefully controlled experiments were clearly required to examine the simultaneous affects of evaporation and dissolution on oil weathering. Acquisition of such data is critical for modification of algorithms and input components for the oil-weathering computer model and verification of predicted output where environmental parameters such as wind speed and air and water temperature could be controlled. To support this requirement, an evaporation/

dissolution chamber was constructed to allow simultaneous, compound-specific concentration determinations in air, oil and water phases such that evaporative and dissolution process rates could be determined as a function of time. Figure 5-1 presents three schematic diagrams of the evaporation/dissolution chamber showing its component parts and functional design, and Figure 5-2 shows the assembled evaporation/dissolution chamber. The circular design of the tank allows air to pass over the slick on a one time basis where an estimated 90% of the air flow is diverted up the exhaust vent showed in Figure 5-1A and out of the exhaust port into a vented duct. The velocity of the air stream is controlled by baffled systems on the blower shown in the foreground of Figure 5-2, and air velocities over the slick are measured using a Kurz air velocity meter installed 5 cm above the oil/seawater interface. To minimize sample contamination during experimental studies, the tank has been fabricated entirely of glass, stainless steel, anodized aluminum and teflon. The circular design was chosen over other shapes (e.g., rectangular) such that wind driven oil would not accumulate or pile up at one end of the chamber. In this manner a continuous oil slick can be maintained to simulate the conditions of airflow over a large surface oil slick.

For ambient temperature (19 to 23°C) studies, the chamber is assembled in a dedicated laboratory facility controlled by standard air conditioning. Lower temperature studies at 13 and 3°C have been conducted within a specially designed cold room where air and water temperatures can be carefully controlled and maintained. (In this enclosed chamber, lower molecular weight hydrocarbons lost due to evaporation processes are vented outside the laboratory.) Seawater for the system is obtained from the flow-through seawater aquarium supply source at Scripps Institution of Oceanography and filtered (0.45 m glass fiber filters) before use. During an experimental run, time series air samples are obtained by adsorbing volatile components onto Tenax® columns using a technique described in greater detail later (and in Appendix B), water column samples are obtained through the stopcocks in the sides of the chamber and "grab" oil samples are obtained through a specially designed sampling port in the top of the air-flow manifold. To ensure homogenity in

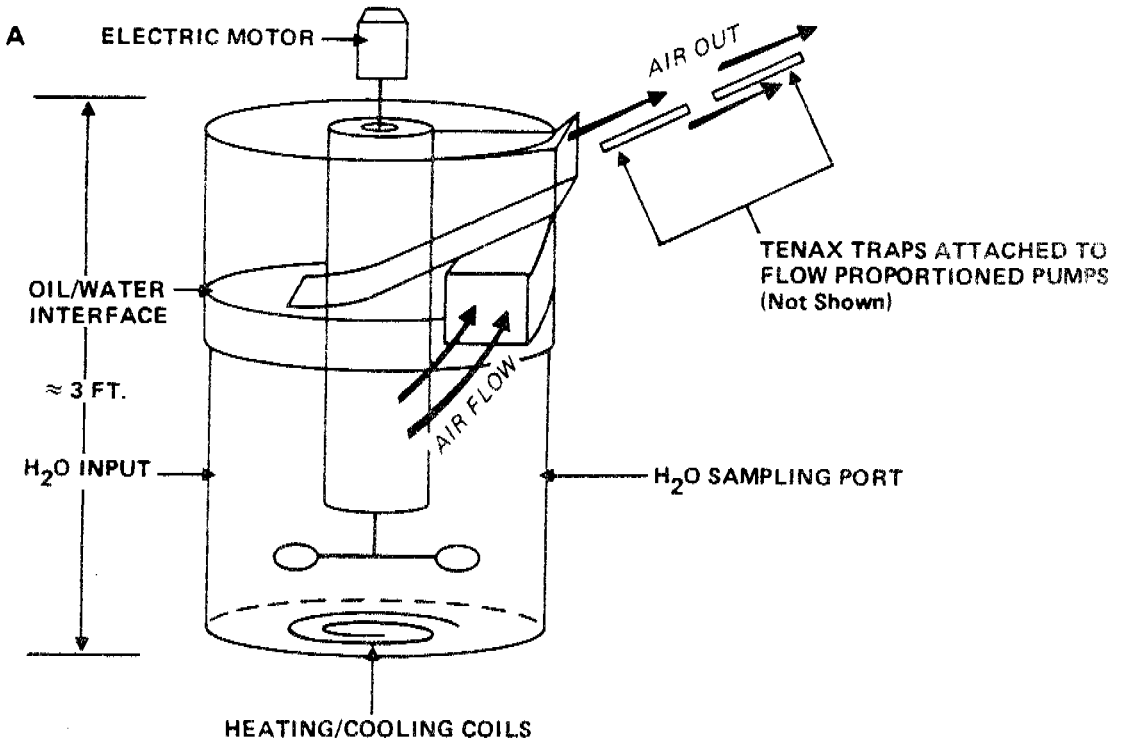

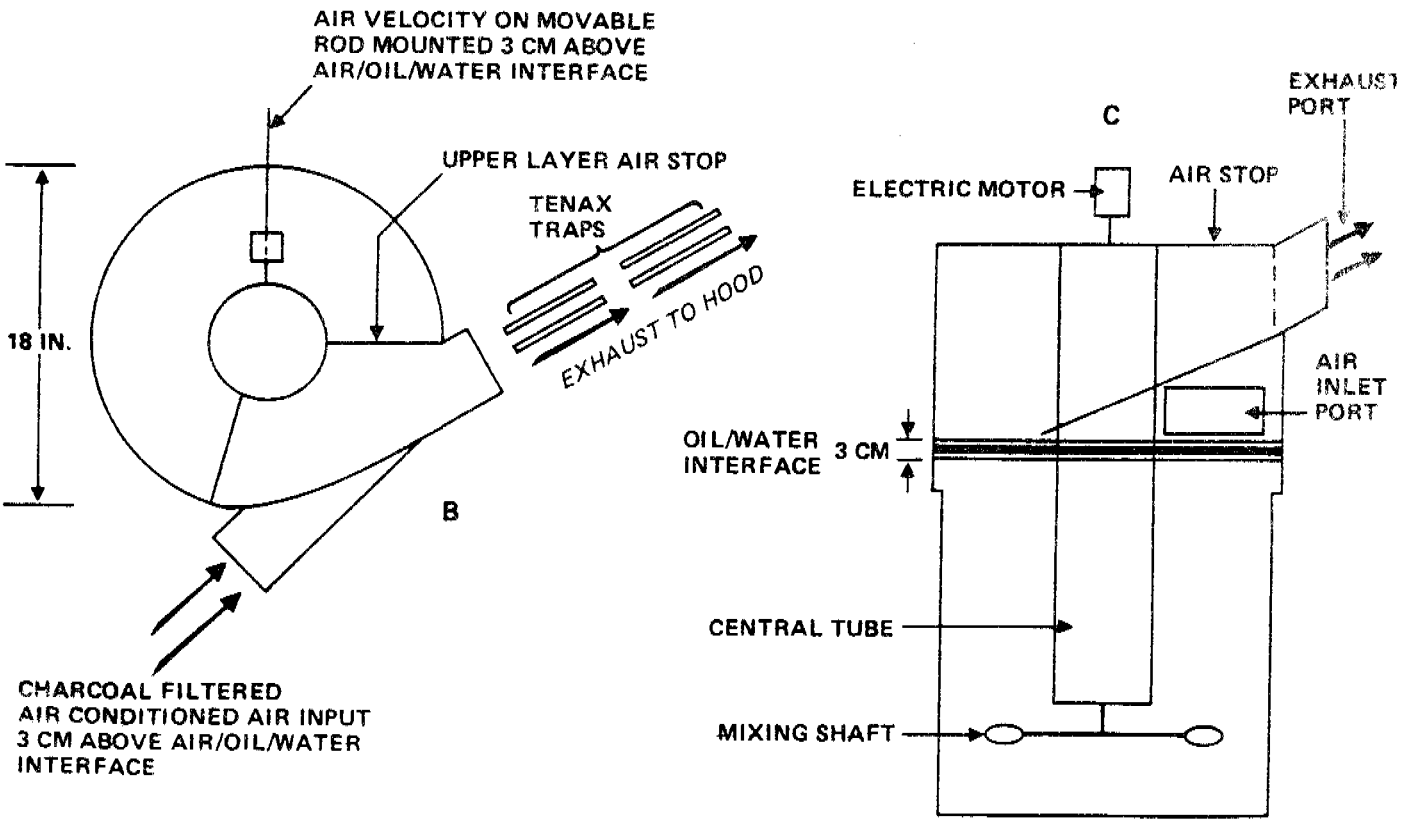

FIGURE 5-1. PROTOTYPE TANK DESIGN FOR EVAPORATION/DISSOLUTION EXPERIMENTS.

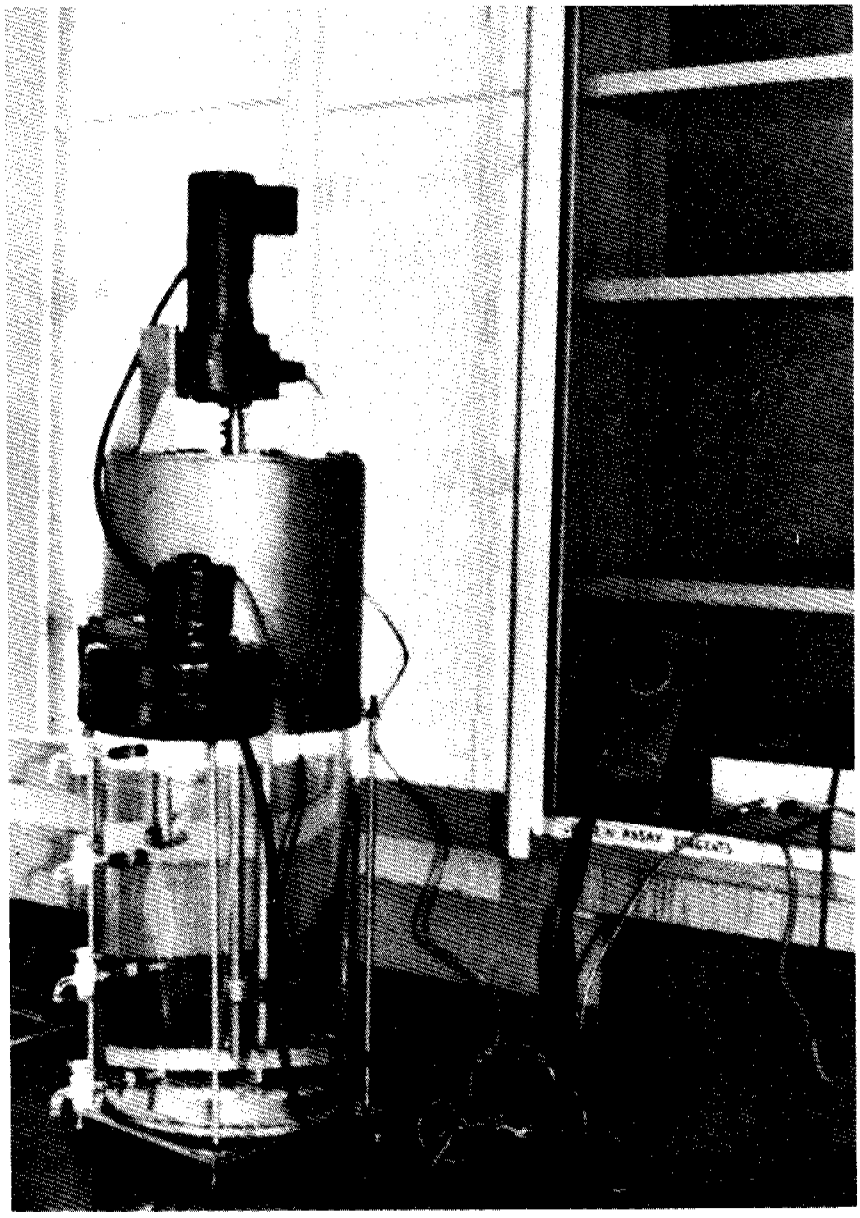

FIGURE 5-2. ASSEMBLED EVAPORATION/DISSOLUTION CHAMBER UTILIZED FOR COMPONENT SPECIFIC EVAPORATION/DISSOLUTION RATE DETERMINATIONS AS A FUNCTION OF TEMPERATURE AND WIND SPEED -- LA JOLLA, CALIFORNIA.

the water column, the water is agitated from below by means of a rotating paddle capable of generating eddy diffusion coefficients ranging from 10 to 100 cm^2/sec (September 1980 Quarterly Report).

5.1.1 Results of Evaporation/Dissolution Chamber Experiments - La Jolla

Before experimental studies on such a complex mixture as Prudhoe Bay crude oil were initiated, evaporation/dissolution experiments were completed using a simple, component mixture consisting of benzene, toluene, and cyclohexane at less than full saturation concentrations. The application of the results from these experiments toward the oil weathering model development was presented in detail in Sections 2.4.4 and 2.4.6, respectively, of our November 1980 Interim Quarterly Report.

After completing preliminary evaluation of the evaporation/dissolution chamber with the three component mixture mentioned above, a series of oil weathering experiments were undertaken with Prudhoe Bay crude oil at ambient (19 to 23°C) temperatures and at 3°C in the presence and absence of Corexit 9527. Table 5-1 presents computer listings of the time series oil and water samples collected in conjunction with these experiments. Each data entry in the table includes the chromatographic identifiers for the whole oil or aliphatic, aromatic and polar fractions of the representative samples as stored in the experiment (EXP) data base of the oil weathering model. From these sample-specific identifiers, individual compound concentrations can be retrieved from the computer data base for any desired fraction as a function of time and environmental conditions. At this time data for atmospheric volatile compound concentrations are still being obtained and reduced manually (Tenax® trap experiments); however, the reduced data output are then being entered into the computer for generation of time series decay curves for volatile compound losses.

Figure 5-3 presents time series packed column FID gas chromatograms obtained on the volatile components in the air above the spilled oil slick at

TABLE 5-1. COMPUTER LISTING OF SAMPLES FROM EVAPORATION/DISSOLUTION RUN #4 (19°C WITHOUT COREXIT).

LISTING OF HISTORY DATASET PAGE 1 OCT-28-1981

EXPERIMENT: EVAP 4 PRINCIPAL INVESTIGATOR: JRP
LOG PAGE: 9
PROJOB: PIN
START DATE: FEB-11-1981
END DATE: FEB-11-1981

THIS WAS THE FOURTH RUN OF THE EVAPORATION/DISSOLUTION TANK USING PRUDHOE BAY CRUDE AND SEAWATER AS THE TWO PHASES. MODERATE MIXING AND WIND CONDITIONS WERE EMPLOYED.

LISTING OF EXPERIMENT DATASET PAGE 1 OCT-28-1981

EXPERIMENT: EVAP 4
MEDIUM: OIL FRACTION TYPE: 1

	HP-LABEL	HRS	MINS	TEMPERATURES AIR	WATER	OIL	COREXIT PRESENT	WIND SPEED	MIXING	COMMENTS
52	1 FEB-20-1981	3	0	.00	17.30	17.30	NO	3.70	80.00	
53	1 FEB-24-1981	4	0	.00	18.10	18.10	NO	3.70	80.00	
76	3 FEB-26-1981	9	0	.00	18.40	18.40	NO	3.70	80.00	
67	13 FEB-25-1981	12	0	.00	18.30	18.30	NO	3.70	80.00	
64	15 FEB-26-1981	24	0	.00	17.10	17.10	NO	3.70	80.00	
5	7 MAR-06-1981	36	0	.00	17.70	17.70	NO	3.70	80.00	
62	11 FEB-27-1981	48	0	.00	17.70	17.70	NO	3.70	80.00	
63	13 FEB-27-1981	72	0	.00	17.90	17.90	NO	3.70	80.00	
84	15 FEB-27-1981	149	0	.00	.00	.00	NO	3.70	80.00	
87	17 FEB-27-1981	168	0	.00	.00	.00	NO	3.70	80.00	
88	88 FEB-27-1981	194	0	.00	.00	.00	NO	3.70	80.00	

LISTING OF EXPERIMENT DATASET PAGE 1 OCT-28-1981

EXPERIMENT: EVAP 4
MEDIUM: OIL FRACTION TYPE: 2

	HP-LABEL	HRS	MINS	TEMPERATURES AIR	WATER	OIL	COREXIT PRESENT	WIND SPEED	MIXING	COMMENTS
26	1 FEB-16-1981	0	0	.00	.00	15.50	NO	3.70	80.00	
27	3 FEB-16-1981	1	30	.00	.00	16.30	NO	3.70	80.00	
28	5 FEB-16-1981	3	0	.00	.00	17.30	NO	3.70	80.00	
29	7 FEB-16-1981	6	0	.00	18.10	18.10	NO	3.70	80.00	
31	9 FEB-16-1981	9	0	.00	18.40	.00	N	3.70	80.00	
32	32 FEB-17-1981	12	0	.00	18.30	18.30	NO	3.70	80.00	
33	13 FEB-17-1981	24	0	.00	17.10	17.10	NO	3.70	80.00	
34	15 FEB-17-1981	35	45	.00	.00	.00	NO	3.70	80.00	
35	17 FEB-17-1981	48	0	.00	17.70	17.70	NO	3.70	80.00	
46	11 FEB-18-1981	72	30	.00	17.90	17.90	NO	3.70	80.00	
47	13 FEB-18-1981	140	45	.00	.00	.00	NO	3.70	80.00	
48	15 FEB-18-1981	168	15	.00	18.60	18.60	NO	3.70	80.00	
49	17 FEB-18-1981	194	15	.00	18.80	18.80	NO	3.70	80.00	
52	1 FEB-18-1981	220	6	.00	17.90	17.90	NO	3.70	80.00	
53	5 FEB-18-1981	286	0	.00	18.80	18.80	NO	3.70	80.00	
15	5 FEB-20-1981	337	0	.00	18.60	18.60	NO	3.70	80.00	
16	7 FEB-20-1981	346	0	.00	15.90	15.90	NO	3.70	80.00	
17	9 FEB-20-1981	460	15	.00	18.30	18.30	NO	3.70	80.00	

LISTING OF EXPERIMENT DATASET PAGE 1 OCT-28-1981

EXPERIMENT: EVAP 4
MEDIUM: WATER FRACTION TYPE: 2

	HP-LABEL	HRS	MINS	TEMPERATURES AIR	WATER	OIL	COREXIT PRESENT	WIND SPEED	MIXING	COMMENTS
218	7 FEB-13-1981	1	30	.00	16.30	.00	NO	3.70	80.00	VOL WATER#1 L.
219	9 FEB-13-1981	3	0	.00	17.30	.00	NO	3.70	80.00	VOL WATER#1 L.
220	11 FEB-13-1981	6	0	.00	18.10	.00	NO	3.70	80.00	VOL WATER#1 L.
221	13 FEB-13-1981	9	0	.00	18.40	.00	NO	3.70	80.00	VOL WATER#1 L.
222	15 FEB-13-1981	12	0	.00	18.30	.00	NO	3.70	80.00	VOL WATER#1 L.
1	29 FEB-14-1981	24	0	.00	17.10	.00	NO	3.70	80.00	VOL WATER#1 L.
2	27 FEB-14-1981	36	0	.00	.00	.00	NO	3.70	80.00	VOL WATER#1 L.
3	29 FEB-14-1981	48	0	.00	17.70	.00	NO	3.70	80.00	VOL WATER#1 L.
4	5 FEB-15-1981	72	0	.00	17.90	.00	NO	3.70	80.00	VOL WATER#1 L.
6	35 FEB-16-1981	149	0	.00	.00	.00	NO	3.70	80.00	VOL WATER#1 L.
7	1 FEB-16-1981	168	0	.00	18.60	.00	NO	3.70	80.00	VOL WATER#1 L.
8	3 FEB-16-1981	194	0	.00	18.80	.00	NO	3.70	80.00	VOL WATER#1 L.

TABLE 5-1. COMPUTER LISTING OF SAMPLES FROM EVAPORATION/DISSOLUTION RUN #5 (19°C WITHOUT COREXIT). (Continued).

LISTING OF HISTORY DATASET PAGE 1 OCT-28-1981

EXPERIMENT: EVAP 5 PRINCIPAL INVESTIGATOR: JLL
LOG PAGE: 01
STATUS: FIN
START DATE: APR-24-1981
END DATE: JUN-04-1981

THIS WAS THE FIFTH RUN OF THE EVAPORATION DISSOLUTION TANK. PRUDHOE BAY CRUDE AND SEAWATER WERE THE TWO PHASES. TURBULENCE SETTING WAS #4 IN REVERSE, AND THE AIR FLOW GAUGE READS .99

LISTING OF EXPERIMENT DATASET PAGE 1 OCT-29-1981

EXPERIMENT: EVAP 5
MEDIUM: OIL FRACTION TYPE: 1

	HP-LABEL	HRS	MINS	TEMPERATURES AIR	WATER	OIL	COREXIT PRESENT	WIND SPEED	MIXING
49	3 JUN-26-1981	0	30	.00	21.20	21.20	NO	.99	44.00
53	5 JUN-17-1981	2	0	.00	21.40	21.40	NO	.99	44.00
64	7 JUN-18-1981	24	15	.00	21.00	21.00	NO	.99	44.00
65	9 JUN-18-1981	86	30	.00	21.00	21.00	NO	.99	44.00
51	7 JUN-27-1981	71	0	.00	20.90	20.90	NO	.99	44.00
54	1 JUN-27-1981	171	0	.00	22.50	22.50	NO	.99	44.00
56	5 JUN-27-1981	288	0	.00	20.30	20.30	NO	.99	44.00
58	9 JUN-27-1981	454	0	.00	21.50	21.50	NO	.99	44.00
60	13 JUN-28-1981	574	0	.00	22.20	22.20	NO	.99	44.00
64	19 JUN-28-1981	982	0	.00	.00	.00	NO	.99	44.00

LISTING OF EXPERIMENT DATASET PAGE 1 OCT-29-1981

EXPERIMENT: EVAP 5
MEDIUM: OIL FRACTION TYPE: 2

	HP-LABEL	HRS	MINS	TEMPERATURES AIR	WATER	OIL	COREXIT PRESENT	WIND SPEED	MIXING
50	5 JUN-26-1981	0	30	.00	21.20	21.20	NO	.99	44.00
66	11 JUN-18-1981	2	0	.00	21.40	21.40	NO	.99	44.00
72	13 JUN-18-1981	24	15	.00	21.00	21.00	NO	.99	44.00
52	9 JUN-27-1981	71	0	.00	20.90	20.90	NO	.99	44.00
55	3 JUN-27-1981	171	0	.00	22.50	22.50	NO	.99	44.00
57	7 JUN-27-1981	288	0	.00	20.30	20.30	NO	.99	44.00
59	11 JUN-27-1981	454	0	.00	21.50	21.50	NO	.99	44.00
61	15 JUN-28-1981	576	0	.00	22.20	22.20	NO	.99	44.00
65	21 JUN-28-1981	982	0	.00	.00	.00	NO	.99	44.00

LISTING OF EXPERIMENT DATASET PAGE 1 OCT-29-1981

EXPERIMENT: EVAP 5
MEDIUM: WATER FRACTION TYPE: 1

	HP-LABEL	HRS	MINS	TEMPERATURES AIR	WATER	OIL	COREXIT PRESENT	WIND SPEED	MIXING
18	23 JUN-30-1981	0	0	.00	21.20	21.20	NO	.99	44.00
19	25 JUN-30-1981	0	15	.00	21.20	21.20	NO	.99	44.00
20	27 JUN-30-1981	0	30	.00	21.20	21.20	NO	.99	44.00
21	29 JUN-30-1981	2	0	.00	21.40	21.40	NO	.99	44.00
67	3 JUL-07-1981	12	0	.00	21.00	21.00	NO	.99	44.00
68	5 JUL-07-1981	24	15	.00	21.00	21.00	NO	.99	44.00
69	7 JUL-07-1981	46	30	.00	21.00	21.00	NO	.99	44.00
71	11 JUL-07-1981	71	0	.00	20.90	20.90	NO	.99	44.00
58	19 JUL-15-1981	96	0	.00	20.40	20.40	NO	.99	44.00
78	3 JUL-08-1981	120	0	.00	21.60	21.60	NO	.99	44.00
80	5 JUL-08-1981	147	0	.00	22.30	22.30	NO	.99	44.00
82	7 JUL-08-1981	171	0	.00	22.50	22.50	NO	.99	44.00
83	9 JUL-08-1981	196	0	.00	21.90	21.90	NO	.99	44.00
84	11 JUL-08-1981	238	0	.00	21.60	21.60	NO	.99	44.00
92	5 JUL-09-1981	288	0	.00	20.30	20.30	NO	.99	44.00
93	7 JUL-09-1981	336	0	.00	.00	.00	NO	.99	44.00
59	21 JUL-15-1981	416	0	.00	23.40	23.40	NO	.99	44.00

LISTING OF EXPERIMENT DATASET PAGE 1 OCT-29-1981

EXPERIMENT: EVAP 5
MEDIUM: WATER FRACTION TYPE: 2

	HP-LABEL	HRS	MINS	TEMPERATURES AIR	WATER	OIL	COREXIT PRESENT	WIND SPEED	MIXING
8	5 JUN-29-1981	1	0	.00	21.20	21.20	NO	.99	44.00
9	7 JUN-29-1981	1	15	.00	21.20	21.20	NO	.99	44.00
10	9 JUN-30-1981	1	30	.00	21.20	21.20	NO	.99	44.00
11	11 JUN-30-1981	1	0	.00	21.20	21.20	NO	.99	44.00
12	13 JUN-30-1981	2	0	.00	21.40	21.40	NO	.99	44.00
13	15 JUN-30-1981	3	0	.00	21.50	21.50	NO	.99	44.00
7	3 JUN-29-1981	4	30	.00	22.10	22.10	NO	.99	44.00
24	5 JUL-01-1981	12	0	.00	21.00	21.00	NO	.99	44.00
25	7 JUL-01-1981	24	15	.00	21.00	21.00	NO	.99	44.00
27	11 JUL-01-1981	46	30	.00	21.00	21.00	NO	.99	44.00
39	3 JUL-02-1981	71	0	.00	20.90	20.90	NO	.99	44.00
40	5 JUL-02-1981	96	0	.00	22.50	22.50	NO	.99	44.00
41	7 JUL-02-1981	120	0	.00	21.60	21.60	NO	.99	44.00
42	9 JUL-03-1981	147	0	.00	22.30	22.30	NO	.99	44.00
43	11 JUL-03-1981	171	0	.00	22.50	22.50	NO	.99	44.00
44	13 JUL-03-1981	196	0	.00	21.90	21.90	NO	.99	44.00
45	15 JUL-03-1981	218	0	.00	21.60	21.60	NO	.99	44.00
47	19 JUL-03-1981	336	0	.00	.00	.00	NO	.99	44.00

TABLE 5-1. COMPUTER LISTING OF SAMPLES FROM EVAPORATION/DISSOLUTION RUN #6 (3°C WITHOUT COREXIT). (Continued).

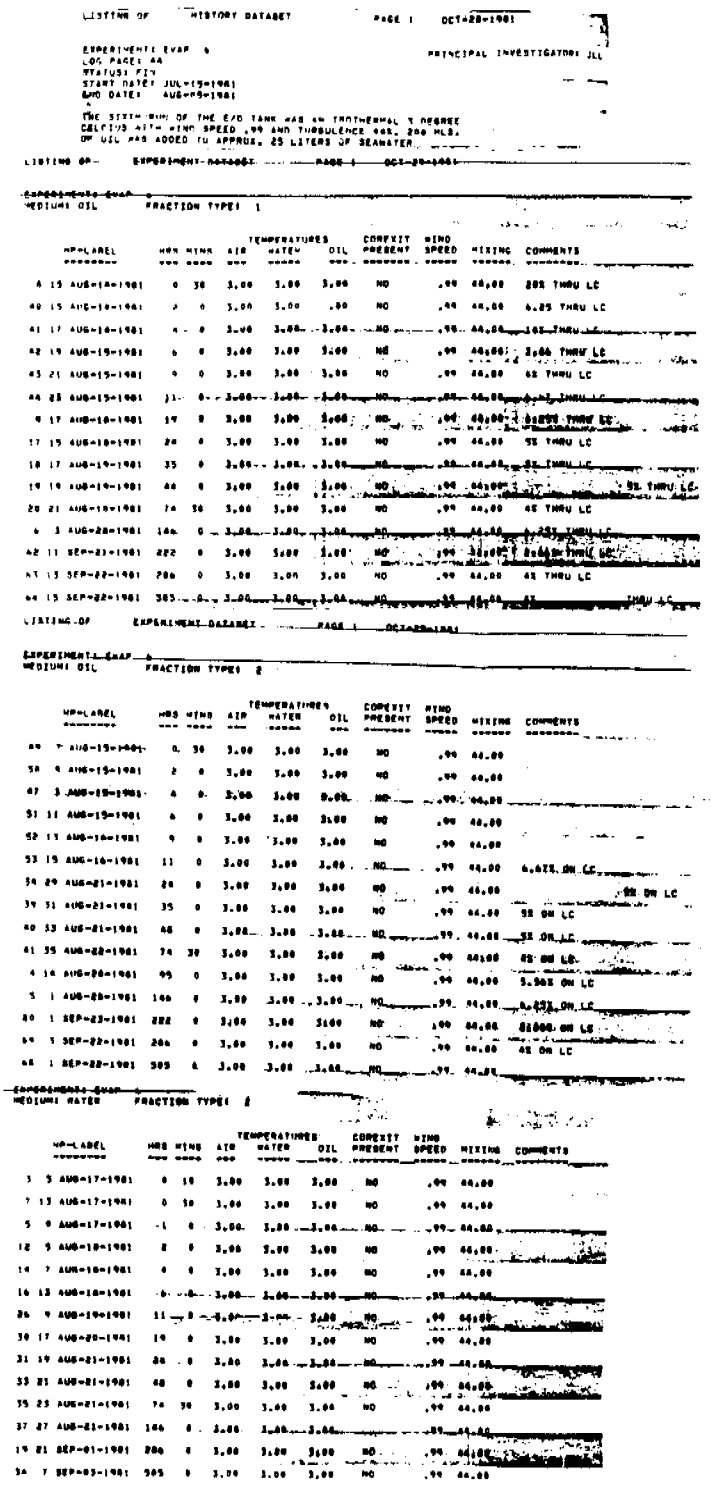

LISTING OF HISTORY DATASET PAGE 1 OCT-28-1981

EXPERIMENT: EVAP 6
LOG PAGE: 44
STATUS: FIN
START DATE: JUL-15-1981
END DATE: AUG-05-1981

THE SIXTH RUN OF THE E/D TANK WAS AN ISOTHERMAL 3 DEGREE CELCIUS WITH WIND SPEED .99 AND TURBULENCE 468, 280 MLS. OF OIL WAS ADDED TO APPROX. 25 LITERS OF SEAWATER.

LISTING OF EXPERIMENT DATASET PAGE 1 OCT-28-1981

EXPERIMENT: EVAP 6
MEDIUM: OIL FRACTION TYPE: 1

HR-LABEL	HRS	MINS	TEMPERATURES AIR	WATER	OIL	COREXIT PRESENT	WIND SPEED	MIXING	COMMENTS
4 15 AUG-14-1981	0	30	3.00	3.00	3.00	NO	.99	44.00	20% THRU LC
40 15 AUG-16-1981	2	0	3.00	3.00	.00	NO	.99	44.00	6.25 THRU LC
41 17 AUG-16-1981	4	0	3.00	3.00	3.00	NO	.99	44.00	10% THRU LC
42 19 AUG-19-1981	6	0	3.00	3.00	3.00	NO	.99	44.00	3.8% THRU LC
43 21 AUG-19-1981	9	0	3.00	3.00	3.00	NO	.99	44.00	6% THRU LC
44 23 AUG-19-1981	11	0	3.00	3.00	3.00	NO	.99	44.00	9.1% THRU LC
9 17 AUG-18-1981	19	0	3.00	3.00	3.00	NO	.99	44.00	3.125% THRU LC
17 15 AUG-18-1981	24	0	3.00	3.00	3.00	NO	.99	44.00	5% THRU LC
18 17 AUG-19-1981	35	0	3.00	3.00	3.00	NO	.99	44.00	5% THRU LC
19 19 AUG-19-1981	46	0	3.00	3.00	3.00	NO	.99	44.00	5% THRU LC
20 21 AUG-19-1981	74	30	3.00	3.00	3.00	NO	.99	44.00	4% THRU LC
6 3 AUG-20-1981	144	0	3.00	3.00	3.00	NO	.99	44.00	4.25% THRU LC
42 11 SEP-21-1981	222	0	3.00	3.00	3.00	NO	.99	44.00	2.44% THRU LC
43 13 SEP-22-1981	286	0	3.00	3.00	3.00	NO	.99	44.00	4% THRU LC
44 15 SEP-22-1981	385	0	3.00	3.00	3.00	NO	.99	44.00	4% THRU LC

LISTING OF EXPERIMENT DATASET PAGE 1 OCT-28-1981

EXPERIMENT: EVAP 6
MEDIUM: OIL FRACTION TYPE: 2

HR-LABEL	HRS	MINS	TEMPERATURES AIR	WATER	OIL	COREXIT PRESENT	WIND SPEED	MIXING	COMMENTS
49 7 AUG-15-1981	0	30	3.00	3.00	3.00	NO	.99	44.00	
50 9 AUG-15-1981	2	0	3.00	3.00	3.00	NO	.99	44.00	
47 3 AUG-15-1981	4	0	3.00	3.00	3.00	NO	.99	44.00	
51 11 AUG-15-1981	6	0	3.00	3.00	3.00	NO	.99	44.00	
52 13 AUG-16-1981	9	0	3.00	3.00	3.00	NO	.99	44.00	
53 15 AUG-16-1981	11	0	3.00	3.00	3.00	NO	.99	44.00	6.42% ON LC
36 29 AUG-21-1981	28	0	3.00	3.00	3.00	NO	.99	44.00	5% ON LC
39 31 AUG-21-1981	35	0	3.00	3.00	3.00	NO	.99	44.00	5% ON LC
40 33 AUG-21-1981	46	0	3.00	3.00	3.00	NO	.99	44.00	5% ON LC
41 35 AUG-22-1981	74	30	3.00	3.00	3.00	NO	.99	44.00	4% ON LC
4 14 AUG-20-1981	95	0	3.00	3.00	3.00	NO	.99	44.00	5.56% ON LC
5 1 AUG-20-1981	144	0	3.00	3.00	3.00	NO	.99	44.00	4.25% ON LC
30 1 SEP-23-1981	222	0	3.00	3.00	3.00	NO	.99	44.00	2.44% ON LC
69 3 SEP-22-1981	286	0	3.00	3.00	3.00	NO	.99	44.00	4% ON LC
68 1 SEP-22-1981	385	0	3.00	3.00	3.00	NO	.99	44.00	

EXPERIMENT: EVAP 6
MEDIUM: WATER FRACTION TYPE: 2

HR-LABEL	HRS	MINS	TEMPERATURES AIR	WATER	OIL	COREXIT PRESENT	WIND SPEED	MIXING	COMMENTS
3 5 AUG-17-1981	0	10	3.00	3.00	3.00	NO	.99	44.00	
7 13 AUG-17-1981	0	50	3.00	3.00	3.00	NO	.99	44.00	
5 9 AUG-17-1981	1	0	3.00	3.00	3.00	NO	.99	44.00	
12 5 AUG-18-1981	2	0	3.00	3.00	3.00	NO	.99	44.00	
14 7 AUG-18-1981	4	0	3.00	3.00	3.00	NO	.99	44.00	
16 13 AUG-18-1981	6	0	3.00	3.00	3.00	NO	.99	44.00	
26 9 AUG-19-1981	11	0	3.00	3.00	3.00	NO	.99	44.00	
30 17 AUG-20-1981	19	0	3.00	3.00	3.00	NO	.99	44.00	
31 19 AUG-21-1981	28	0	3.00	3.00	3.00	NO	.99	44.00	
33 21 AUG-21-1981	48	0	3.00	3.00	3.00	NO	.99	44.00	
35 23 AUG-21-1981	74	30	3.00	3.00	3.00	NO	.99	44.00	
37 27 AUG-21-1981	144	0	3.00	3.00	3.00	NO	.99	44.00	
19 21 SEP-01-1981	286	0	3.00	3.00	3.00	NO	.99	44.00	
5A 7 SEP-03-1981	385	0	3.00	3.00	3.00	NO	.99	44.00	

TABLE 5-1. COMPUTER LISTING OF SAMPLES FROM EVAPORATION/DISSOLUTION RUN #7 (3°C WITH COREXIT). (Continued).

LISTING OF HISTORY DATASET PAGE 1 OCT-29-1981

EXPERIMENT: EVAP 7 PRINCIPAL INVESTIGATOR: ILL
LOG PAGE: 46
STATUS: FI
START DATE: AUG-27-1981
END DATE: SEP-21-1981

THE CONDITIONS IN THIS E/D RUN WERE IDENTICAL TO
THOSE OF E/D 6 (3 DEGREE ISO.) EXCEPT THAT 10 GLS.
OF COREXIT WAS WELL MIXED IN THE OIL BEFORE IS WAS SPILLED.

LISTING OF EXPERIMENT DATASET PAGE 1 OCT-29-1981

EXPERIMENT: EVAP 7
MEDIUM: WATER FRACTION TYPE: 1

	HP-LABEL	HRS	MINS	TEMPERATURES AIR	WATER	OIL	COREXIT PRESENT	WIND SPEED	MIXING	COMMENTS	
93	0 SEP-09-1981	0	0	3.00	3.00	3.00	YES	.99	44.00	VOA ON 5 MLS.	VOL OIL/COR=20
91	0 SEP-08-1981	0	15	3.00	3.00	3.00	YES	.99	44.00	VOA ON 5 MLS.	VOL OIL/COR=20
90	0 SEP-08-1981	0	30	3.00	3.00	3.00	YES	.99	44.00	VOA ON 5 MLS.	VOL OIL/COR=20
89	0 SEP-08-1981	1	0	3.00	3.00	3.00	YES	.99	44.00	VOA ON 5 MLS.	VOL OIL/COR=20
88	0 SEP-08-1981	2	0	3.00	3.00	3.00	YES	.99	44.00	VOA ON 5 MLS.	VOL OIL/COR=20
87	0 SEP-08-1981	4	0	3.00	3.00	3.00	YES	.99	44.00	VOA ON 5 MLS.	VOL OIL/COR=20
86	0 SEP-08-1981	8	0	3.00	3.00	3.00	YES	.99	44.00	VOA ON 5 MLS.	OIL/COR=20
85	0 SEP-08-1981	12	0	3.00	3.00	3.00	YES	.99	44.00	VOA ON 5 MLS.	OIL/COR=20
80	0 SEP-04-1981	36	0	3.00	3.00	3.00	YES	.99	44.00	VOA ON 5 MLS.	VOL OIL/COR=20
79	0 SEP-04-1981	48	0	3.00	3.00	3.00	YES	.99	44.00	VOA ON 5 MLS.	VOL OIL/COR=20
78	0 SEP-04-1981	96	0	3.00	3.00	3.00	YES	.99	44.00	VOA ON 5 MLS.	VOL OIL/COR=20
96	0 SEP-09-1981	192	0	3.00	3.00	3.00	YES	.99	44.00	VOA ON 5 MLS.	VOL OIL/COR=20
95	0 SEP-09-1981	299	0	3.00	3.00	3.00	YES	.99	44.00	VOA ON 5 MLS.	VOL OIL/COR=20

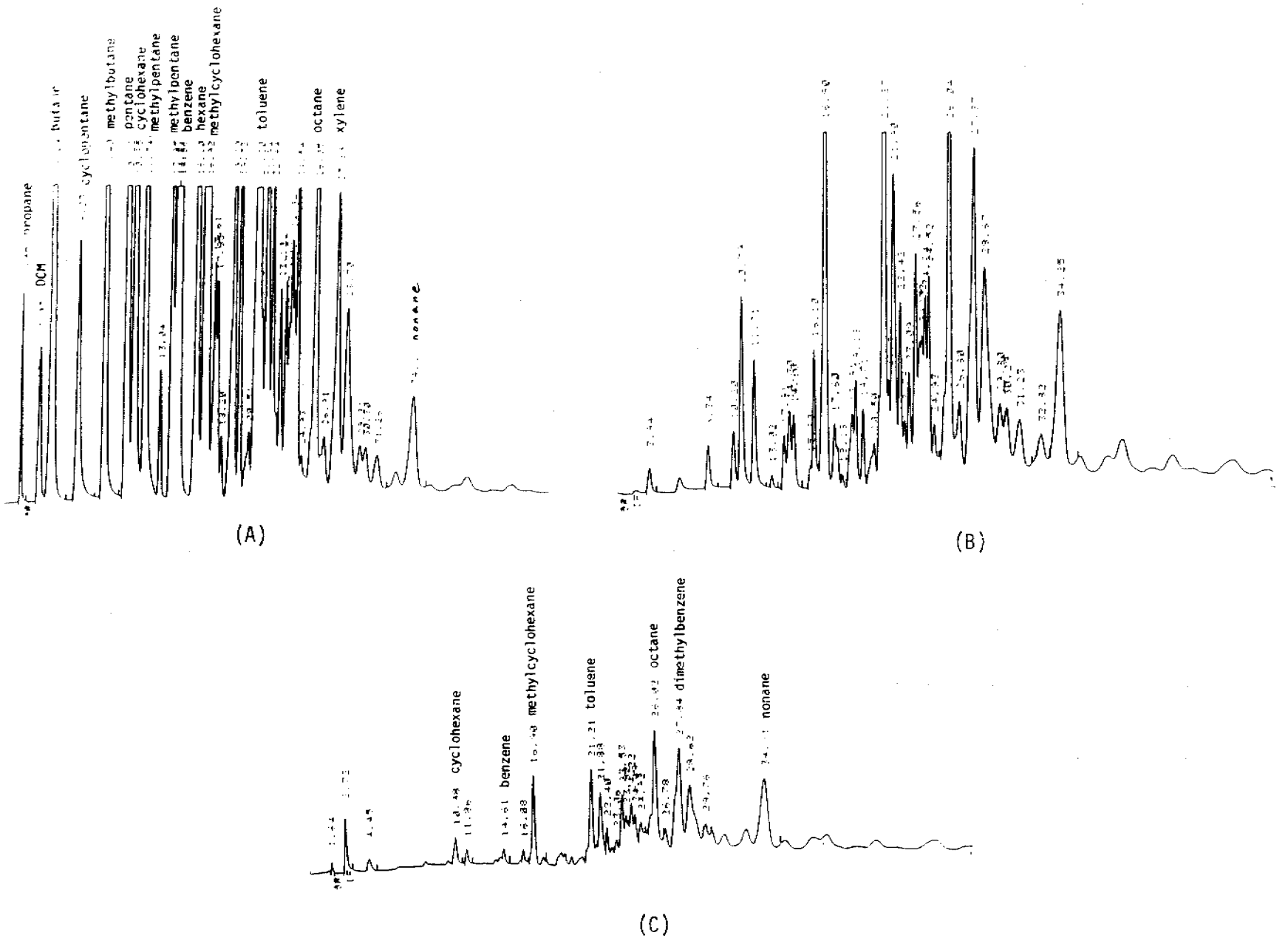

FIGURE 5-3. PACKED COLUMN FLAME IONIZATION DETECTOR GAS CHROMATOGRAMS OBTAINED ON HEAT-DESORBED VOLATILE COMPONENTS TRAPPED ON TENAX® FROM EVAPORATION/DISSOLUTION EXPERIMENT COMPLETED AT 19°C UNDER INFLUENCE OF A 7 KNOT WIND (E/D-4). (A) AIR SAMPLE 15 MINUTES AFTER THE SPILL (FRONT TRAP); (B) AIR SAMPLE 6 HOURS AFTER THE SPILL (FRONT TRAP); (C) AIR SAMPLE 12 HOURS AFTER THE SPILL (FRONT TRAP); (D) BACKUP IN-SERIES TRAP 15 MINUTES AFTER THE SPILL SHOWING LIMITED BREAKTHROUGH OF ONLY 4 INDIVIDUAL ALIPHATIC COMPONENTS; (E) BACKGROUND AIR SAMPLE (CONTROL) COLLECTED BEFORE SPILL INITIATED. ALL SAMPLES OBTAINED BY VACUUM TRAPPING EXHAUST AIR STREAM FROM EVAPORATION/DISSOLUTION CHAMBER AT A FLOW RATE OF 25 ML/MIN FOR 60 SECONDS.

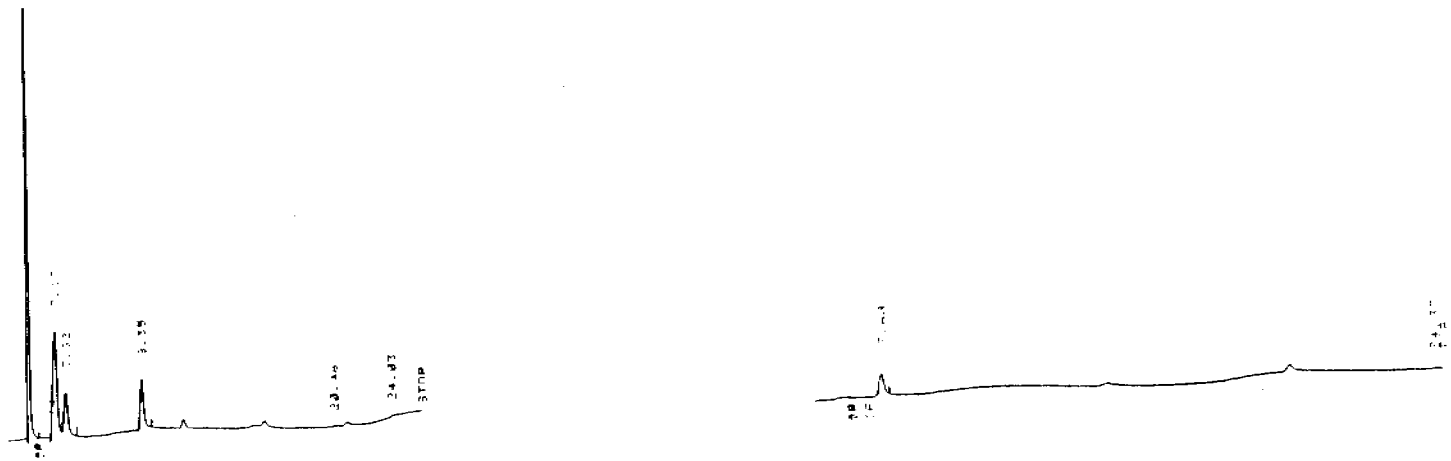

FIGURE 5-3. PACKED COLUMN FLAME IONIZATION DETECTOR GAS CHROMATOGRAMS OBTAINED ON HEAT-DESORBED VOLATILE COMPONENTS TRAPPED ON TENAX® FROM EVAPORATION/DISSOLUTION EXPERIMENT COMPLETED AT 19°C UNDER INFLUENCE OF A 7 KNOT WIND (E/D-4). (A) AIR SAMPLE 15 MINUTES AFTER THE SPILL (FRONT TRAP); (B) AIR SAMPLE 6 HOURS AFTER THE SPILL (FRONT TRAP); (C) AIR SAMPLE 12 HOURS AFTER THE SPILL (FRONT TRAP); (D) BACKUP IN-SERIES TRAP 15 MINUTES AFTER THE SPILL SHOWING LIMITED BREAKTHROUGH OF ONLY 4 INDIVIDUAL ALIPHATIC COMPONENTS; (E) BACKGROUND AIR SAMPLE (CONTROL) COLLECTED BEFORE SPILL INITIATED. ALL SAMPLES OBTAINED BY VACUUM TRAPPING EXHAUST AIR STREAM FROM EVAPORATION/ DISSOLUTION CHAMBER AT A FLOW RATE OF 25 ML/MIN FOR 60 SECONDS. (Continued).

19°C (Evaporation/Dissolution Run 4; denoted E/D-4). This technique allows quantitation of lower molecular weight compounds ranging from propane through nonane as a function of time. As the chromatograms in Figure 5-3, B and C illustrate very rapid losses of lower molecular weight components below octane are observed. The chromatogram in Figure 5-3D shows the in-series backup Tenax trap from the 15 minute sample, and only limited breakthrough of lower molecular weight compounds such as butane and methylbutane are noted. Figure 5-3E presents a time zero Tenax background air control sample showing no component contamination before the spill occurred. Additional details on the sampling procedure and methodology for analyses of volatiles using this Tenax trap procedure are presented in Appendix B - Methods.

From the type of data obtained and shown in Figure 5-3 it is possible to generate time series airborne concentrations of these volatile compounds as shown by the data in Table 5-2 and the graphs in Figure 5-4. Clearly, airborne concentrattions of monocyclic aromatics such as benzene and toluene are observed to fall off rapidly to non-detectable levels within 7 to 8 hours under these conditions. Similar exponential decay curves are observed for volatile aliphatic compounds such as pentane, methylpentane and octane (Figure 5-5).

Simultaneously collected water samples analyzed by a purge and trap technique similar to that developed by BELLAR and LICHTENBERG, (1974) allows determination of water column concentrations of these same volatile components as a function of time, Table 5-3 and Figure 5-6 present such time series data (from FID-4) for benzene, toluene, cyclohexane and xylene. In the water column data, an initial increase in aromatic hydrocarbon concentrations is noted with the concentration maximum occurring after 4-5 hours. Under these conditions, the absolute maximum of individual compounds are determined by the seawater solubility of the compound of interest and its mole fraction in the parent oil. After the maximum concentration buildup at 4-5 hours (controlled by compound specific mass transfer coefficients) exponential decreases in the water-borne concentrations are then noted due to the gradual seawater/air partitioning and evaporative loss of these compounds.

TABLE 5-2. TIME-SERIES AIR-BORN CONCENTRATIONS OF VOLATILE COMPONENTS ABOVE PRUDHOE BAY CRUDE OIL WEATHERING AT 19°C UNDER A 7 KNOT WIND. (Tenax samples from E/D-4).

Compound	time 0 0.0226 L	30 min .0255	45 min .0286	1 hour .0273 L	1 hour 15 min .028	1 hour 30 min .0245	1 hour 45 min .0176	2 hrs .028	2.5 hrs .022	3 hrs .031	4 hrs .025	5 hrs .0316	6 hrs .020	8 hrs .024
Butane	11.9	3.54	3.05	2.65	1.17	ND	ND	ND	ND	ND	ND	ND	ND	ND
Cyclopentane	2.46	0.761	0.689	0.382	ND	ND	ND	ND	ND	ND	ND	ND	ND	ND
Methylbutane	7.30	2.22	2.59	1.08	1.19	0.675	1727	0.439	0.592	0.241	ND	ND	ND	ND
Pentane	16.1	3.88	3.50	1.79	1.64	0.816	0.682	0.496	0.426	0.222	ND	ND	ND	ND
Cyclohexane	7.52	2.70	2.80	1.39	1.36	0.816	0.682	0.488	0.454	0.323	0.320	0.253	0.85	ND
Methylpentane	7.32	2.34	2.21	1.14	1.19	0.537	0.565	0.400	0.557	0.180	ND	ND	ND	ND
Benzene	3.8	1.17	1.18	0.670	0.670	0.653	1.08	0.748	0.636	0.355	0.160	0.443	0.003	ND
Hexane	12.0 µg/l	4.78	6.29	3.30	3.89	2.12	2.39	2.62	4.95	0.806	1.68	1.77	0.550	ND
Methylcyclohexane	15.6	5.64	5.63	3.11	3.14	1.48	1.47	1.25	1.23	0.717	0.247	0.222	ND	ND
Toluene	14.3 µg/l	4.98	5.17	2.97	2.79	1.55	1.42	0.975	0.864	0.484	0.20	0.253	ND	ND
Ethyl Benzene	1.47	0.576	0.555	0.318	0.306	ND	ND	ND	ND	ND	ND	ND	ND	ND
Cumene & n-octane	6.08µg/l	2.63	2.60	1.75	1.63	1.35	1.27	1.20	1.09	0.806	0.520	0.348	ND	ND

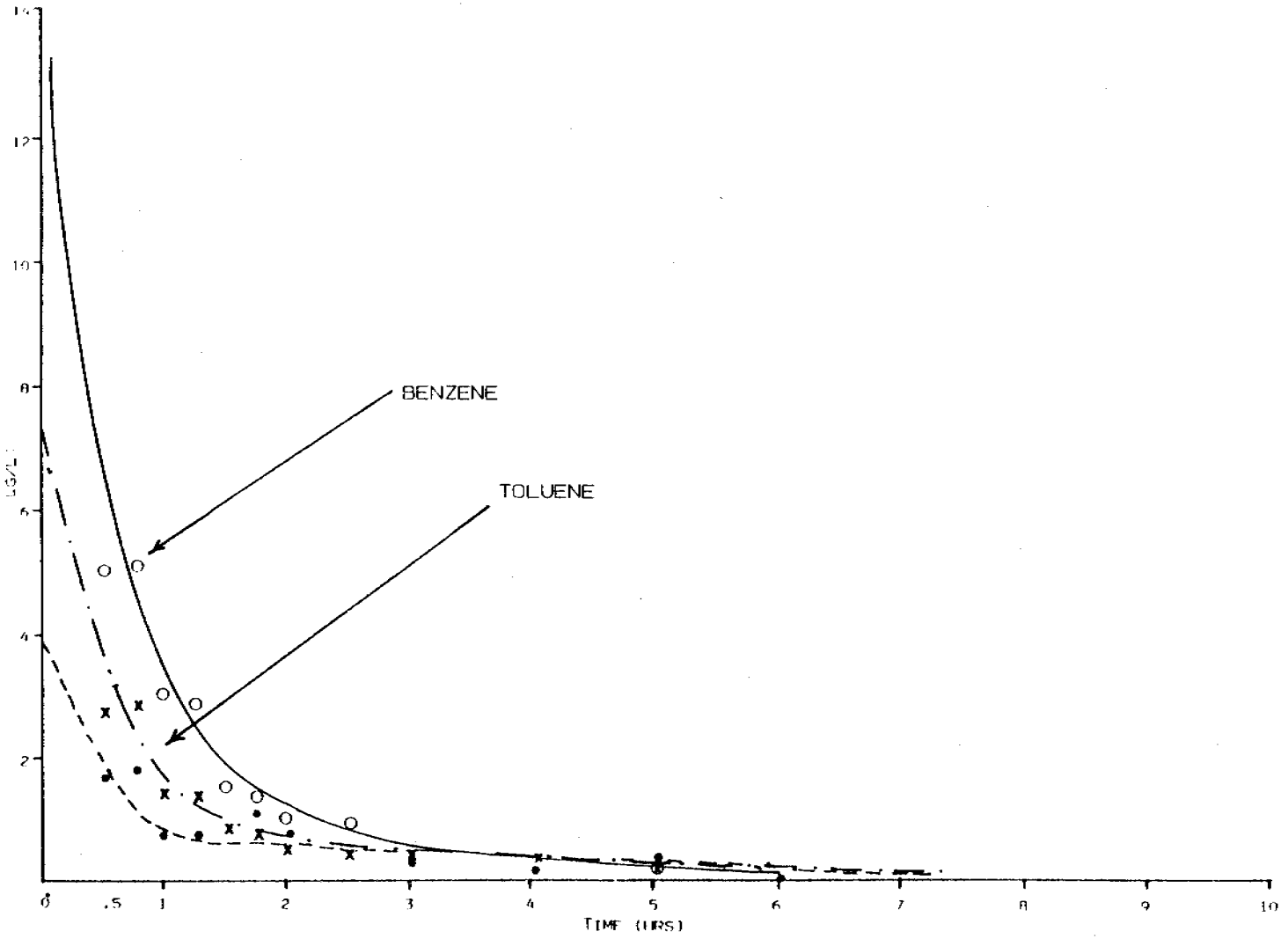

FIGURE 5-4. VOLATILE AROMATIC COMPONENT CONCENTRATIONS IN THE AIR STREAM ABOVE A 200 ml "SLICK" OF PRUDHOE BAY CRUDE OIL WEATHERING AT 19°C UNDER INFLUENCE OF A 7 KNOT WIND. (Evaporation/dissolution chamber run 4).

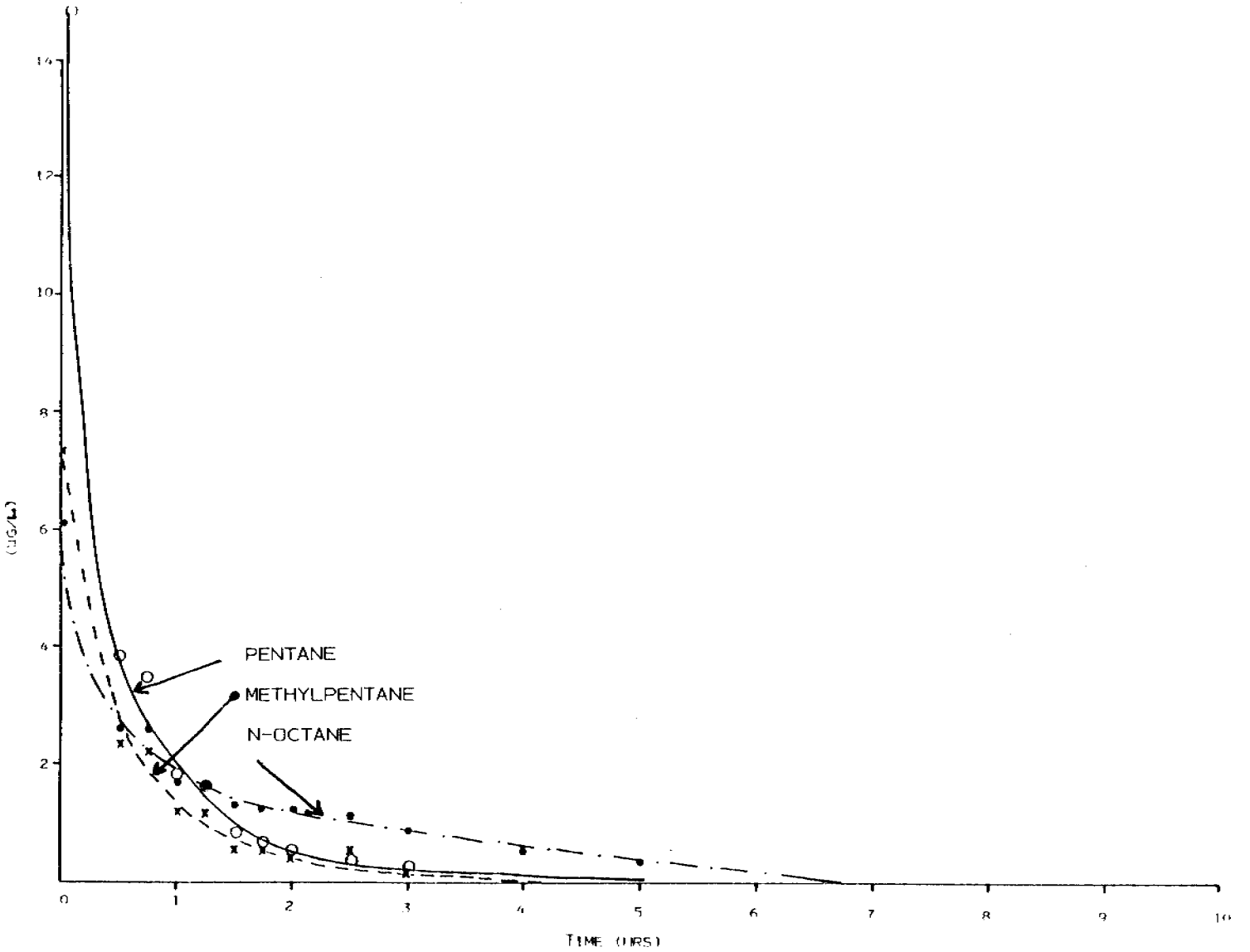

FIGURE 5-5. VOLATILE ALIPHATIC COMPONENT CONCENTRATIONS IN THE AIR STREAM ABOVE A 200 ml "SLICK" OF PRUDHOE BAY CRUDE OIL WEATHERING AT 19°C UNDER INFLUENCE OF A 7 KNOT WIND. (Evaporation/dissolution chamber run 4).

TABLE 5-3. TIME-SERIES WATER COLUMN CONCENTRATIONS OF LOWER MOLECULAR WEIGHT ALIPHATIC AND AROMATIC COMPONENTS FROM PRUDHOE BAY CRUDE OIL WEATHERING AT 19°C UNDER INFLUENCE OF A 7 KNOT WIND. (Evaporation/dissolution Exp-4; purge and trap analyses after Bellar & Lichtenberg, 1974).

Compound	15 min	30 min	45 min	1 hour	1.5 hours	2 hours	2.5 hours	6 hours	11 hours	20 hours	26 hours	32 hours	38 hours	44 hours	50 hours	56 hours	62 hours
Cyclopentane	43.7	48.7	54.6	54.6	48.7	63.9	61.7	64.0	48.0	31.0	25.2	19.4	13.0	8.21	3.59	ND	ND
Methylbutane	21.4	23.2	24.2	24.2	24.4	27.0	26.0	27.3	21.1	15.1	13.3	10.8	7.51	5.01	2.75	ND	ND
Pentane	96.2	90.1	98.4	98.0	58.6	108.0	105.0	67.4	58.6	42.0	30.4	40.6	25.6	17.8	6.2	2.6	ND
Cyclohexane	50.2	50.0	52.4	53.0	61.4	62.4	62.6	59.8	44.0	30.4	26.8	21.2	15.0	10.2	6.2	1.8	ND
Methylpentane	57.6	54.7	57.2	57.4	59.8	64.6	66.3	57.6	42.8	29.7	25.1	21.9	15.1	10.2	4.60	ND	ND
Benzene	424.0	494.0	588.0	647.0	661.0	669.0	688.0	482.0	309.0	136.0	1.21	69.0	21.6	0.800	ND	ND	ND
Methylcyclohexane	36.6	28.0	28.1	27.0	27.7	30.1	31.5	26.4	18.7	13.9	12.7	11.0	8.01	5.61	3.32	ND	ND
Toluene	377.0	354.0	492.0	650.0	604.0	608.0	680.0	406.0	231.0	77.0	ND	49.6	3.80	ND	ND	ND	ND
Ethyl Benzene	19.5	11.4	19.3	375.0	26.8	25.8	34.3										
n-Octane	6.40	4.20	4.6	6.6	5.2	4.2	5.41	3.40	3.20	2.80	1.60	1.80	1.60	1.20	1.20	1.20	ND

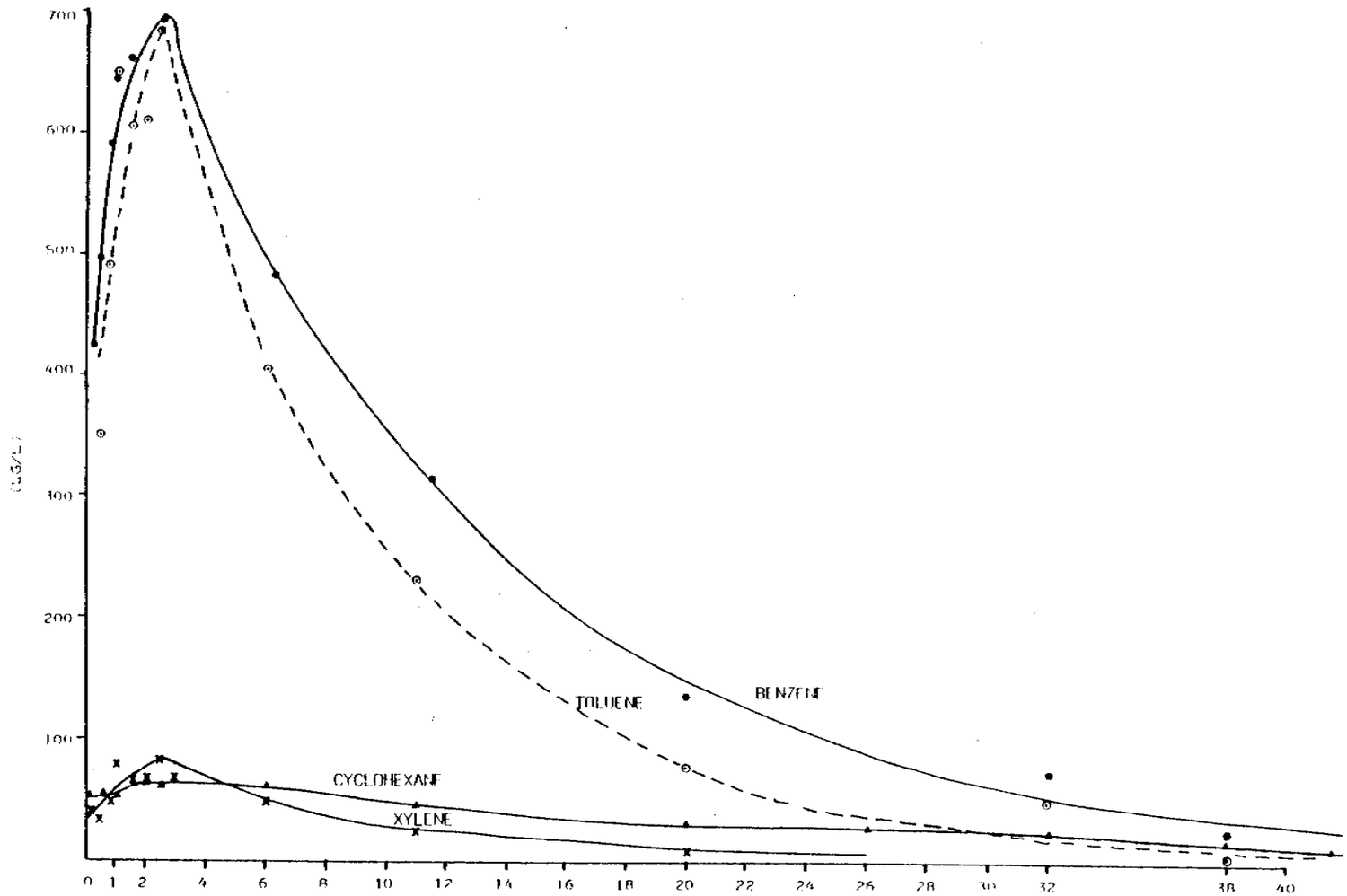

FIGURE 5-6. WATER COLUMN CONCENTRATIONS OF LOWER MOLECULAR WEIGHT AROMATIC COMPONENTS FROM PRUDHOE BAY CRUDE OIL WEATHERING AT 19°C UNDER INFLUENCE OF A 7 KNOT WIND. (Evaporation/dissolution Exp-4; purge and trap analyses after Bellar & Lichtenberg, 1974).

Intermediate and higher molecular weight component-specific data can only be generated by more detailed time-series sampling, methylene chloride extraction and fractionation of oil and water phases followed by capillary gas chromatographic analyses. Figure 5-7 presents the time-series FID capillary column gas chromatograms obtained on the aliphatic fractions of the oil samples from one such evaporation run (E/D-4) undertaken at 19°C under the influence of 7 knot winds. Sampling times for the chromatograms shown in Figure 5-7 are as follows: A, 0 hours; B, 2 hours; C, 1 day; D, 3 days; E, 7 days; F, 12 days; G, 24 days; and H, 41 days. Quite clearly, general evaporative trends can be observed from the chromatograms, Figure 5-7, and rapid loss of compounds below Kovat index 1000 are observed after as little as 2 hours. The time series concentration profiles for the intermediate and higher molecular weight compounds are somewhat more subtle with only limited additional losses occurring and Tables 5-4 and 5-5 present time series concentrations of selected aromatic hydrocarbons in the oil and sub-surface water column, respectively.

Examination of the myriad of peaks in the time series chromatograms and the data in Tables 5-4 and 5-5 clearly shows the efficacy of developing a sound data management system for handling the extensive array of compound-specific data in the oil and water phases during the weathering process. Specifically, for each sample phase (oil, water and air) at each sampling time, literally hundreds of component-specific concentrations are generated. While such data can be worked up manually and plotted as shown in Figures 5-8 through 5-13, comparisons of oil weathering behavior as a function of temperature (or the presence or absence of dispersants, etc.) can best be accomplished through computer manipulation of data. Further, comparison of predicted vs. observed compound-specific (or even pseudo-component or distillation unit) data for oil weathering behavior can only be handled with an advanced data system such as the one being utilized in this program. During development of this GC data base system, however, it was necessary to manually reduce and plot some of the initial individual compound time dependent concentrations as shown in Figures 5-8 through 5-13. Figures 5-14 and 5-15 present

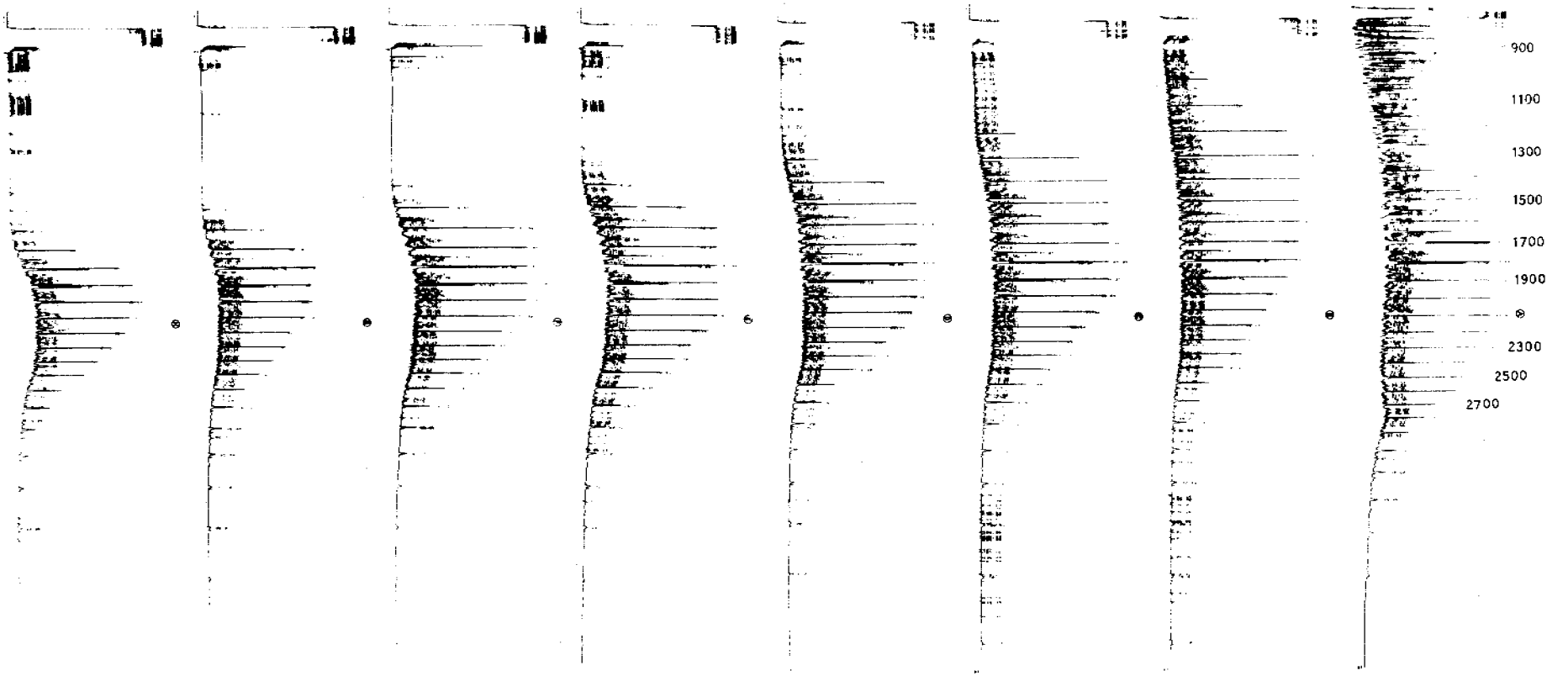

FIGURE 5-7. FLAME IONIZATION DETECTOR CAPILLARY GAS CHROMATOGRAMS OBTAINED ON PRUDHOE BAY CRUDE OIL WEATHERING AT 19°C UNDER INFLUENCE OF A 7 KNOT WIND (E/D-4). SAMPLING TIMES: (A) ZERO HOURS; (B) 2 HOURS; (C) 1 DAY; (D) 3 DAYS; (E) 7 DAYS; (F) 12 DAYS; (G) 24 DAYS; AND (H) 41 DAYS.

TABLE 5-4. TIME DEPENDENT AROMATIC COMPOUND CONCENTRATIONS IN OIL EXTRACTS FROM EVAPORATION/ DISSOLUTION WEATHERING AT 19°C UNDER A 7 KNOW WIND. (Concentrations in µg/g).

COMPOUND	RI (min)	Konat	0 hrs.	1.5 hr	3.0	6.0	8.75	12.0	24.0	35.75	48.0	72.5	140.75	< 168.25	126.25	270.	290.	337.	384.	460.25
Ethylbenzene	7.22	957	26.9		16.3	10.7														
1,4 & 1,3-dimethylbenzene	7.68	967	304.	124.	131.	99.1	78.5	76.6	76.9											
1,2-dimethylbenzene	8.59	991	114.	94.1	102.	69.6	61.3	21.0	17.2											
Propylbenzene	11.38	959	12.6	15.9	14.8	15.9														
1-ethyl-2-methylbenzene	11.81	959	130.	105.	101.	71.6	56.8	11.8												
1-methylethylbenzene	12.68	977	20.7	20.9	22.1	49.9	31.7													
1,2,4-trimethylbenzene	13.48	991	263.	329.	303.	200.	126.	40.3	18.1											
1,2,3-trimethylbenzene	14.86	1019	230	298	270.	186.	120.	56.5												
2,3-dihydro-1-methyl-1H-indene	15.98	1015		21.6	19.7	12.7														
2,3-dihydro-5-methyl-1H-indene	16.21	1002	820	122.	114.	95.3	66.7	29.2												
1,2,3,5-tetramethylbenzene	21.65	1008	83.8	127.	126.	97.0	69.1	56.8	23.7											
1,2,3,4-tetrahydronaphthalene	22.09	1056	83.2	148.	139.	120.	102.	55.8												
Naphthalene	23.26	1179	290.	521.	513.	424.	304.	227.	79.1		18.1	18.1								
1-methylnaphthalene	25.57	1.010	560.	948.	990.	905.	730.	697.	441.	120	366.	310.	94.1	45.1	33.3	23.1				
2-methylnaphthalene	26.17	1298	890.	1509.	1530.	1430.	1150.	1050.	661.	161.	517	419.	88.8	35.4	24.8	16.8				
1,1'-biphenyl	27.85	1375	182.	344.	360.	344.	122.	125.	161.	131.	80.8	35.8	12.0	22.1	15.4	16.6	8.82			
2-ethylnaphthalene	28.45	1302	124.	221.	234.	220.	196.	182.	130.	24.0	140.	144	89.1	53.9	50.7	38.1	25.3	22.8		
1,3-dimethylnaphthalene	28.94	1298	540.	820.	859.	812.	716.	708.	613.	241.	557.	576.	348.	284.	247.	185.	124.	120.	29.2	
2,3-dimethylnaphthalene	30.62	1403	208.	221.	223.	205.	167.	195.	160.	140.	142	123	77.1		123	93.9	65.5	72.7	58.2	45.9
1,8-methylene bis-benzene	37.64	1001	281.	459.	469.	425.	390.	391.	339.	298.	300	411.	128.	272	253	227.	133	140.	116	117.
Dibenzothiophene	40.12	1244	246.	316.	334.	318.	276.	285.	318.	267.	279.	316	121	197	137	114	152	177.	156	149.
Phenanthrene	49.30	1171	297.	247.	278.	264.	230.	238.	260.	246.	244.	280	270	248	221.	259	175.	111	281.	159.
4-methyldibenzothiophene	52.05	1045	176.	248.	249.	250.	223.	221.	253.	222	240	223	264	219	252.	241.	109	136	259.	160.
2-methylphenanthrene	53.58	1007	120.	161.	150.	149.	151.	150.	180.	157.	147.	162	150.	159.	158	148.	163.	139	179.	148.
3-methylphenanthrene	54.47	1011	169.	212.	215.	213.	178.	197.	216.	193.	200	207	139	201.	171.	70.	110	253.	224	222.
2,3-dimethylphenanthrene	58.16	2027	242.	264.	275.	264.	225.	243.	275.	250.	249.	229	255.	248.	252.	193.	119	187	302.	302.

TABLE 5-5. TIME DEPENDENT AROMATIC COMPOUND CONCENTRATIONS IN WATER EXTRACTS BENEATH A SLICK UNDERGOING EVAPORATION/DISSOLUTION WEATHERING AT 19°C UNDER A 7 KNOT WIND. (Concentration in µg/l).

Compound	RI (min)	Kovat	0 hr	1.5	3.0	6.0	8.75	12.0	24.0	35.75	48.0	72.5	140.75	668.25	194.25
Ethylbenzene	7.27	857		10.6	21.0	22.7	17.6	17.5	3.54	5.12	4.51		1.23		2.88
1,4 & 1,3-dimethylbenzene	7.64	867		55.2	71.7	98.7	44.5	64.4	18.6	29.7	16.1		9.15		6.78
1,2-dimethylbenzene	8.59	893		30.2	41.5	55.9	42.3	40.7	120..	17.4	8.42		2.61		1.87
Propylbenzene	11.38	951		3.19	128	88.6	170	61.0		59.4	2.92				
1-ethyl-2-methylbenzene	11.81	959		6.97	13.2	18.2	8.64	13.8		4.92	1.92				
1-methylethylbenzene	12.68	977		3.89	7.81	11.2	8.85	9.01	2.32	4.09	1.08				
1,2,4-trimethylbenzene	13.40	991		12.6	10.9	21.9	3.01	14.1	6.26	3.75	3.11				
1,2,x-trimethylbenzene	14.86	1019		8.16	10.6	18.6	2.40	13.9	8.30	9.48					
2,3-dihydro-1H-indane	15.49	1031			1.51	2.17	2.81	1.18		1.14	4.25				
2,3-dihydro-1-methyl-1H-indane	18.21	1082			1.61	2.92	3.81	2.05	1.17	2.17					
1,2,3,5-tetramethylbenzene	21.65	1148								1.77					
1,2,3,4-tetrahydronapthalene	22.09	1156				2.51	1.87	2.00	1.00	2.95	1.47				
Napthalene	23.26	1179		14.4	17.2	35.5	6.77	32.0	32.4	38.3	21.6				
1-Methylnapthalene	29.57	1304		4.43	1.40	7.52		2.32	24.6	24.4	22.4	9.32	4.89	1.67	
2-Methylnapthalene	28.77	1288		5.98	1.81	9.36		1.76	30.6	32.2	26.6	8.27	4.09	2.17	1.46
1,1-bi-phenyl	32.85	1375						1.98	4.06	5.59	3.90	2.05	1.31		
2-ethylnapthalene	33.45	1387								2.17					
1,5-dimethylnapthalene	33.94	1398							3.86	1.67		2.54	2.76	1.51	
2,3-dimethylnapthalene	34.62	1413							1.40		1.19		1.49		1.47
1,1-methylene-bisbenzene	37.64	1481									1.50				
1,6,7-trimethylnapthalene	39.52	1525													
Dibenzothiophene	48.32	1744													
Phenanthrene	49.34	1771													
4-methyldibenzothiophene	52.05	1845													
2-methylphenanthrene	53.58	1887													
x-methylphenanthrene	54.42	1911													
2,3-dimethylphenanthrene	58.36	2027													

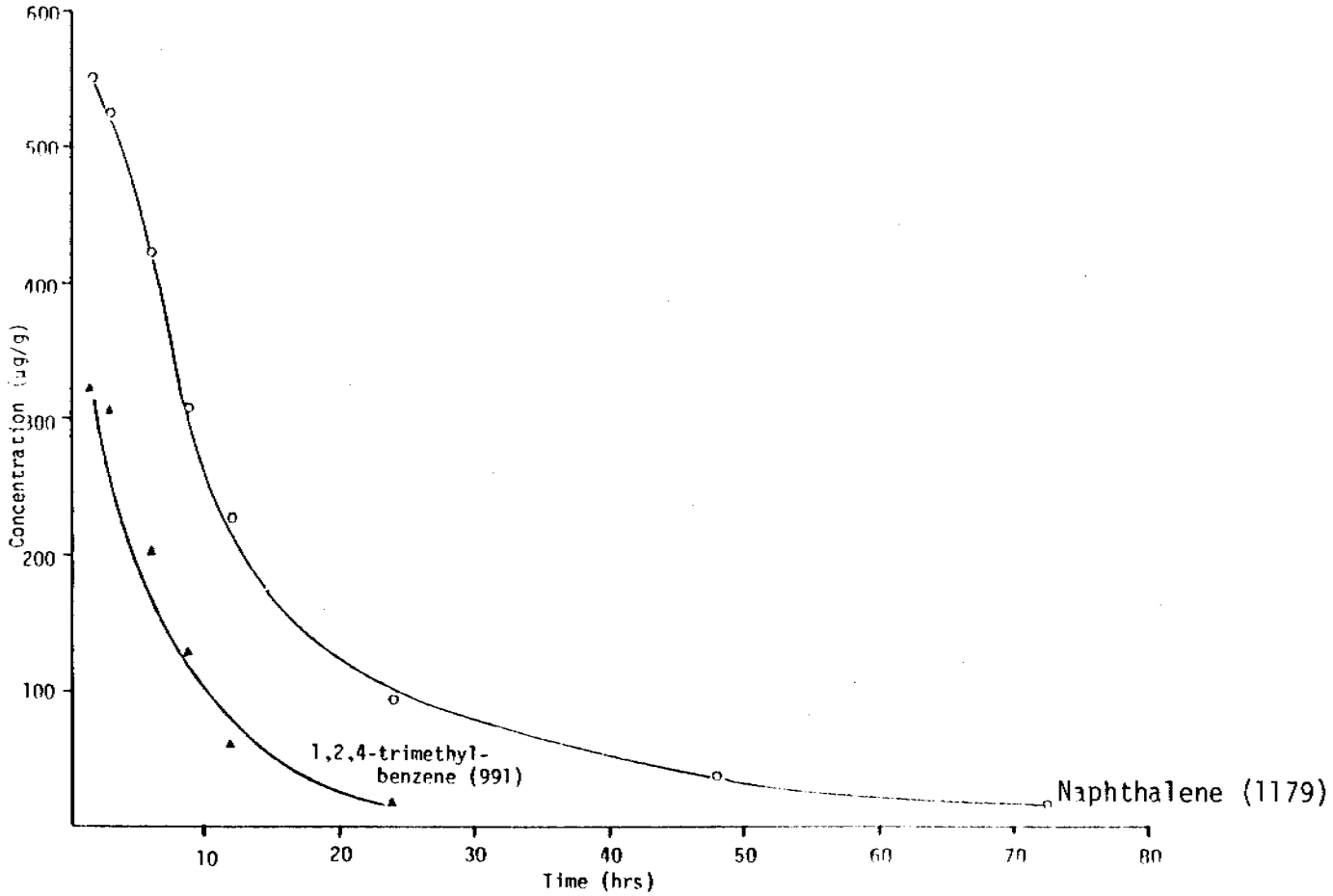

FIGURE 5-8. TIME-DEPENDENT CONCENTRATION IN OIL WEATHERING AT 19°C UNDER INFLUENCE OF A 7 KNOT WIND.

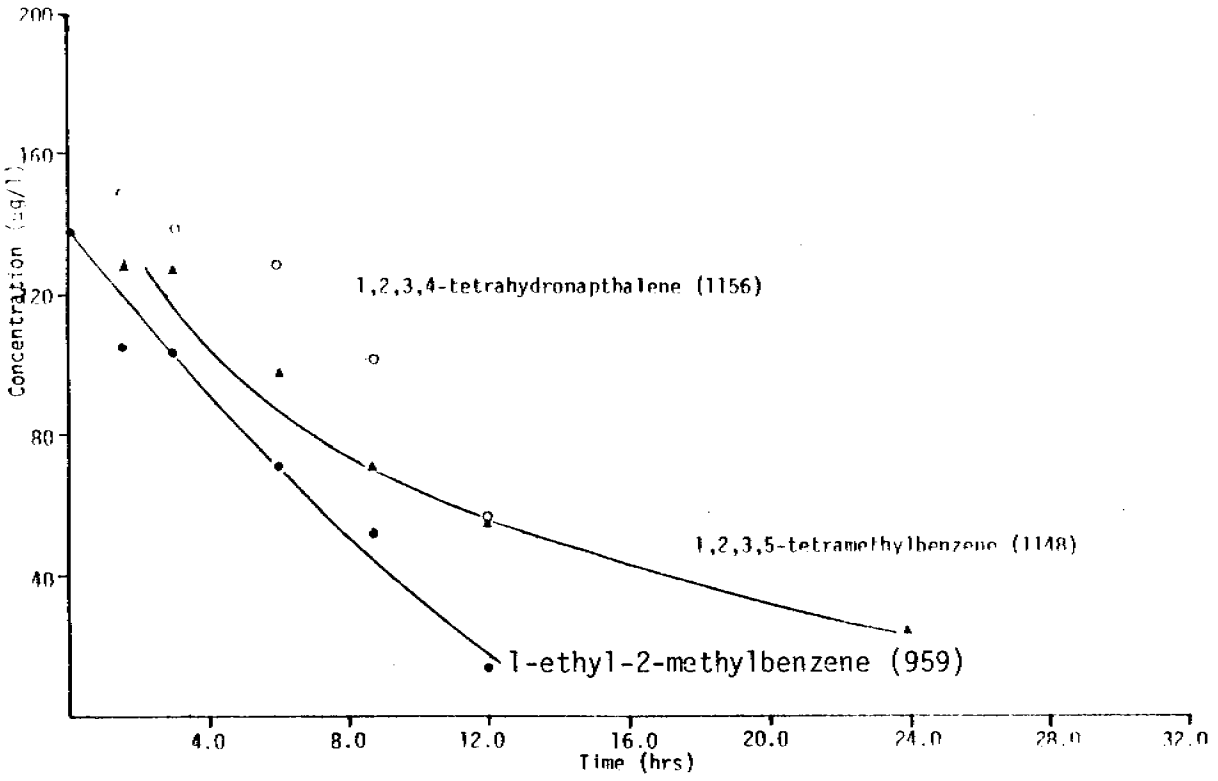

FIGURE 5-9. TIME-DEPENDENT CONCENTRATION IN OIL WEATHERING AT 19^{o}C UNDER INFLUENCE OF A 7 KNOT WIND.

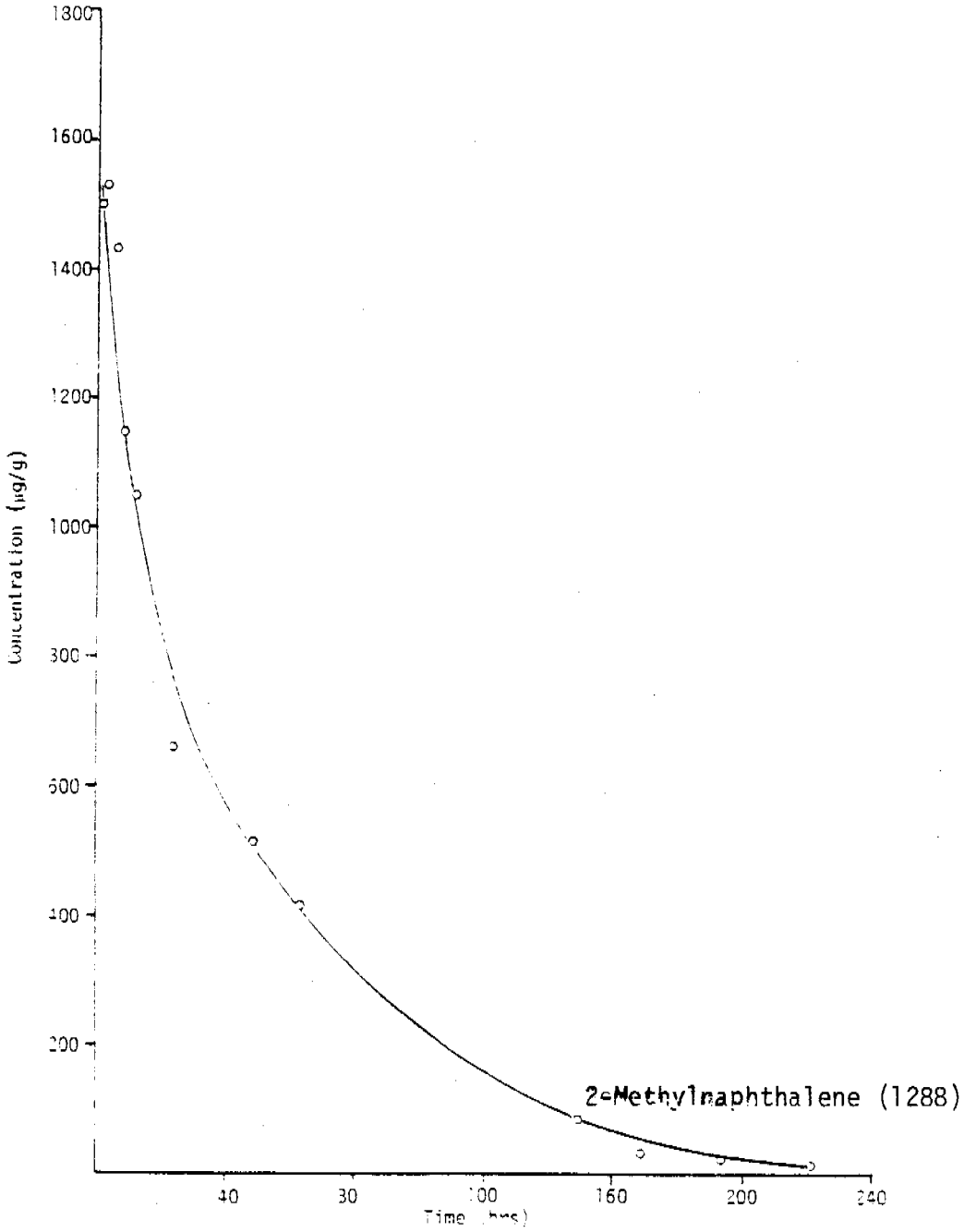

FIGURE 5-10. TIME-DEPENDENT CONCENTRATION IN OIL WEATHERING AT 19°C UNDER INFLUENCE OF A 7 KNOT WIND.

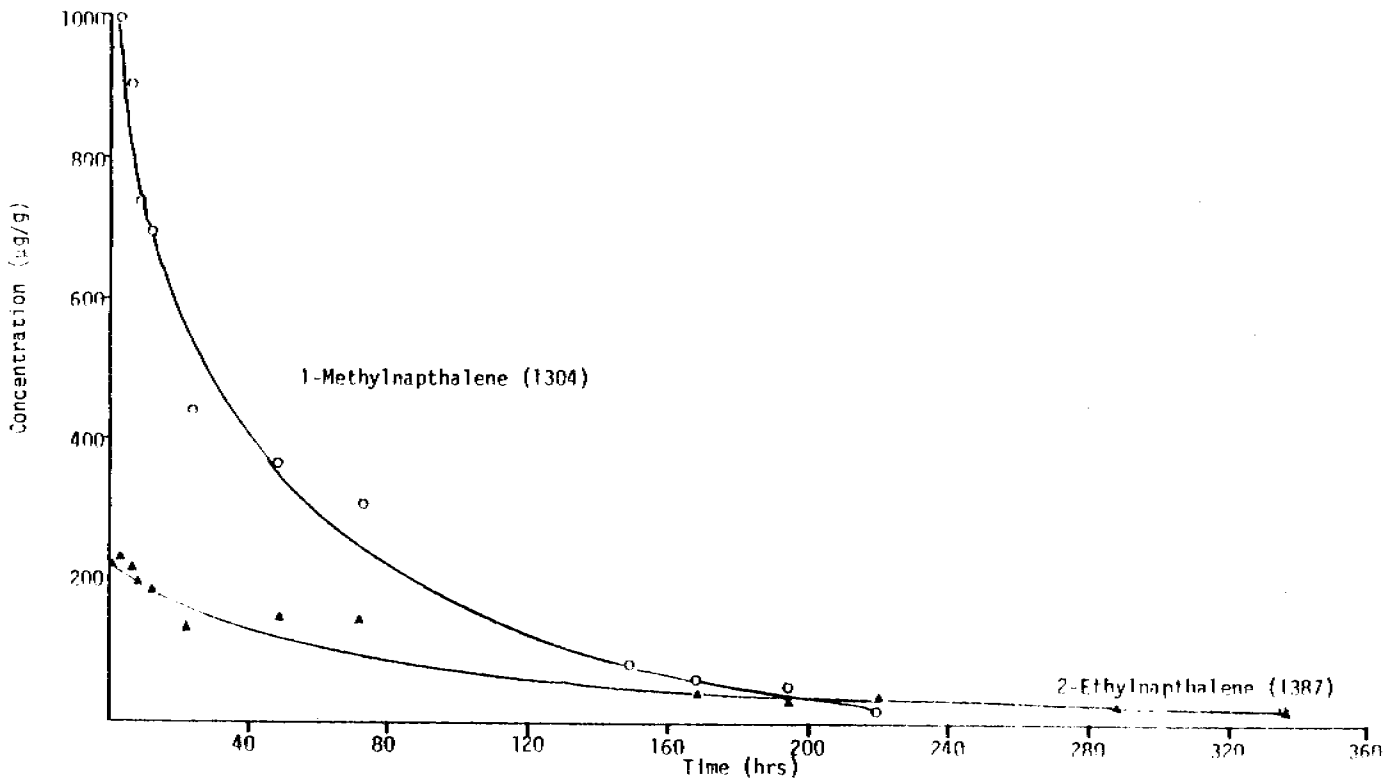

FIGURE 5-11. TIME-DEPENDENT CONCENTRATION IN OIL WEATHERING AT 19°C UNDER INFLUENCE OF A 7 KNOT WIND.

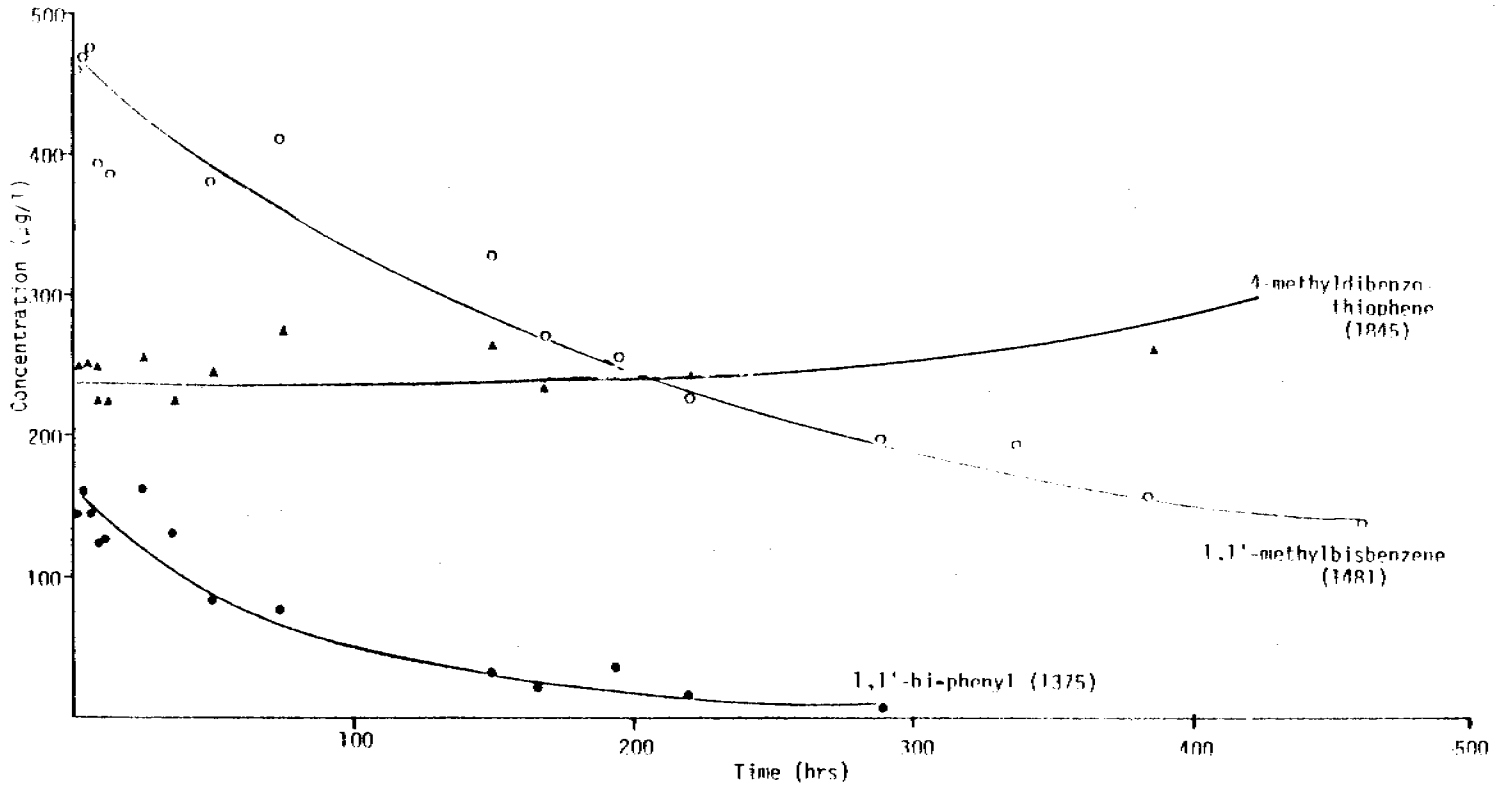

FIGURE 5-12. TIME-DEPENDENT CONCENTRATION IN OIL WEATHERING AT 19°C UNDER INFLUENCE OF A 7 KNOT WIND.

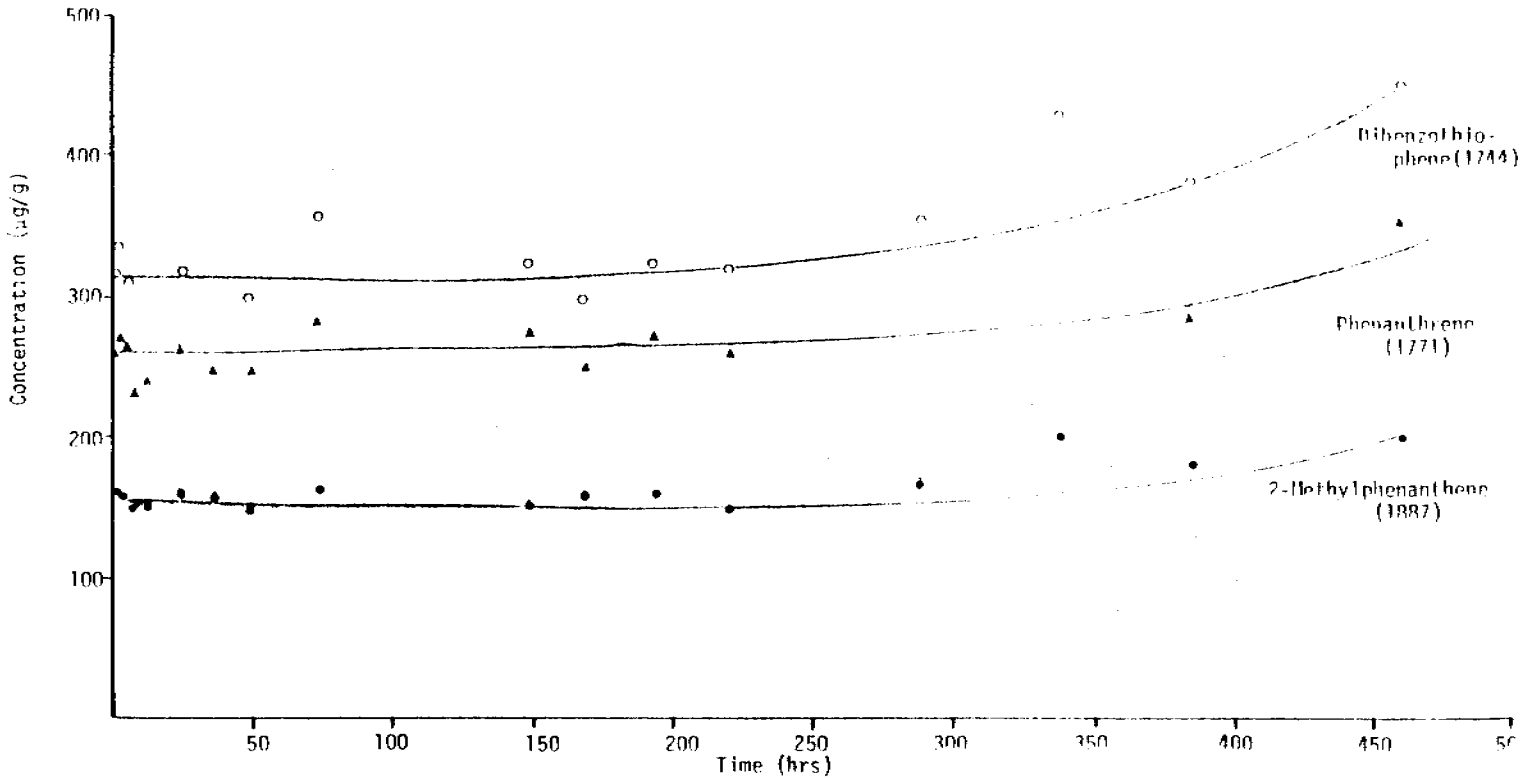

FIGURE 5-13. TIME-DEPENDENT CONCENTRATION IN OIL WEATHERING AT 19°C UNDER INFLUENCE OF A 7 KNOT WIND.

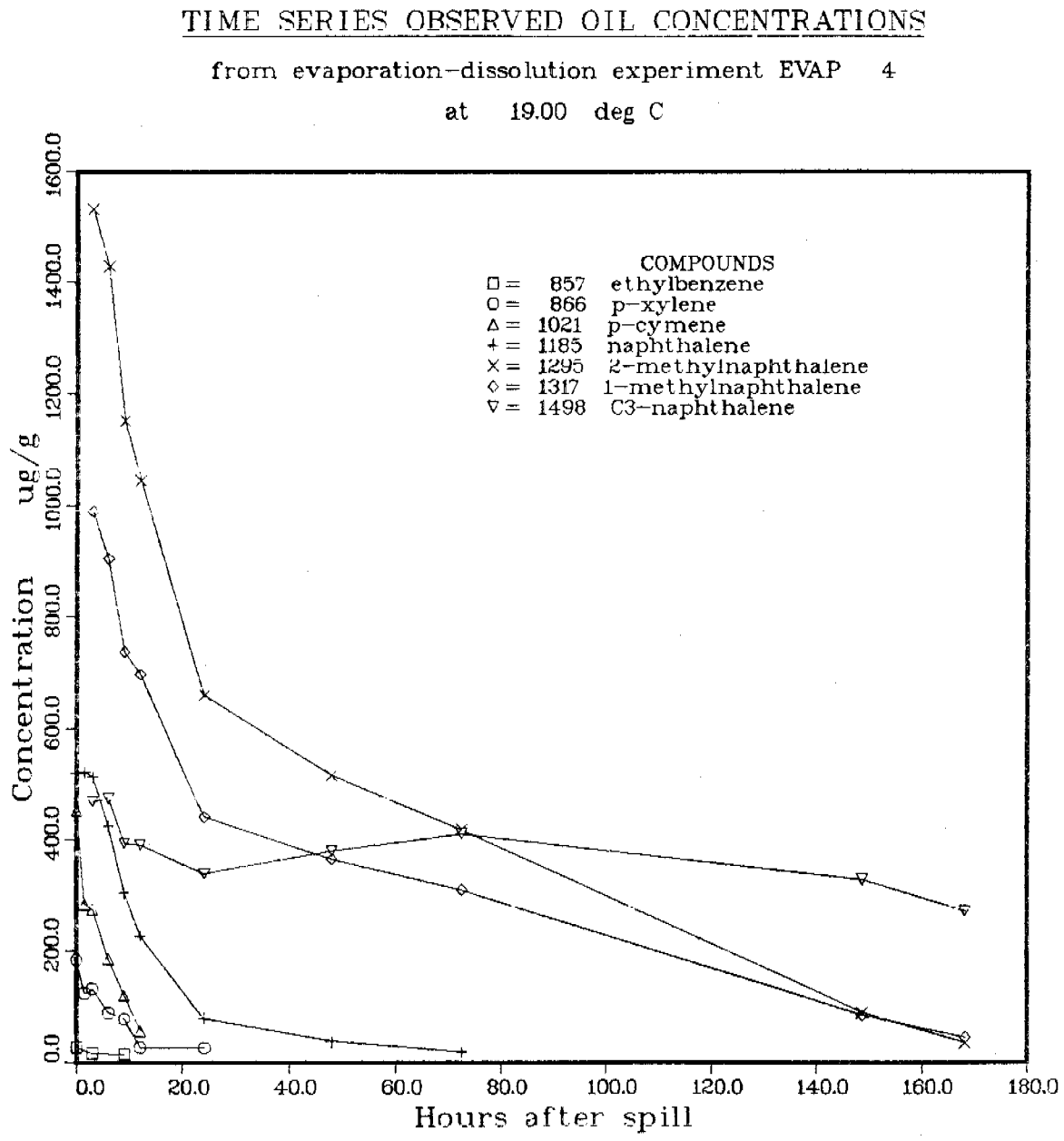

FIGURE 5-14. COMPUTER GENERATED TIME-SERIES PLOTS OF SPECIFIC COMPONENT CONCENTRATIONS REMAINING IN PRUDHOE BAY CRUDE OIL WEATHERING AT 19°C UNDER INFLUENCE OF A 7 KNOT WIND. (E/D-4 DATA FROM EXP DATA BASE OF OIL WEATHERING MODEL).

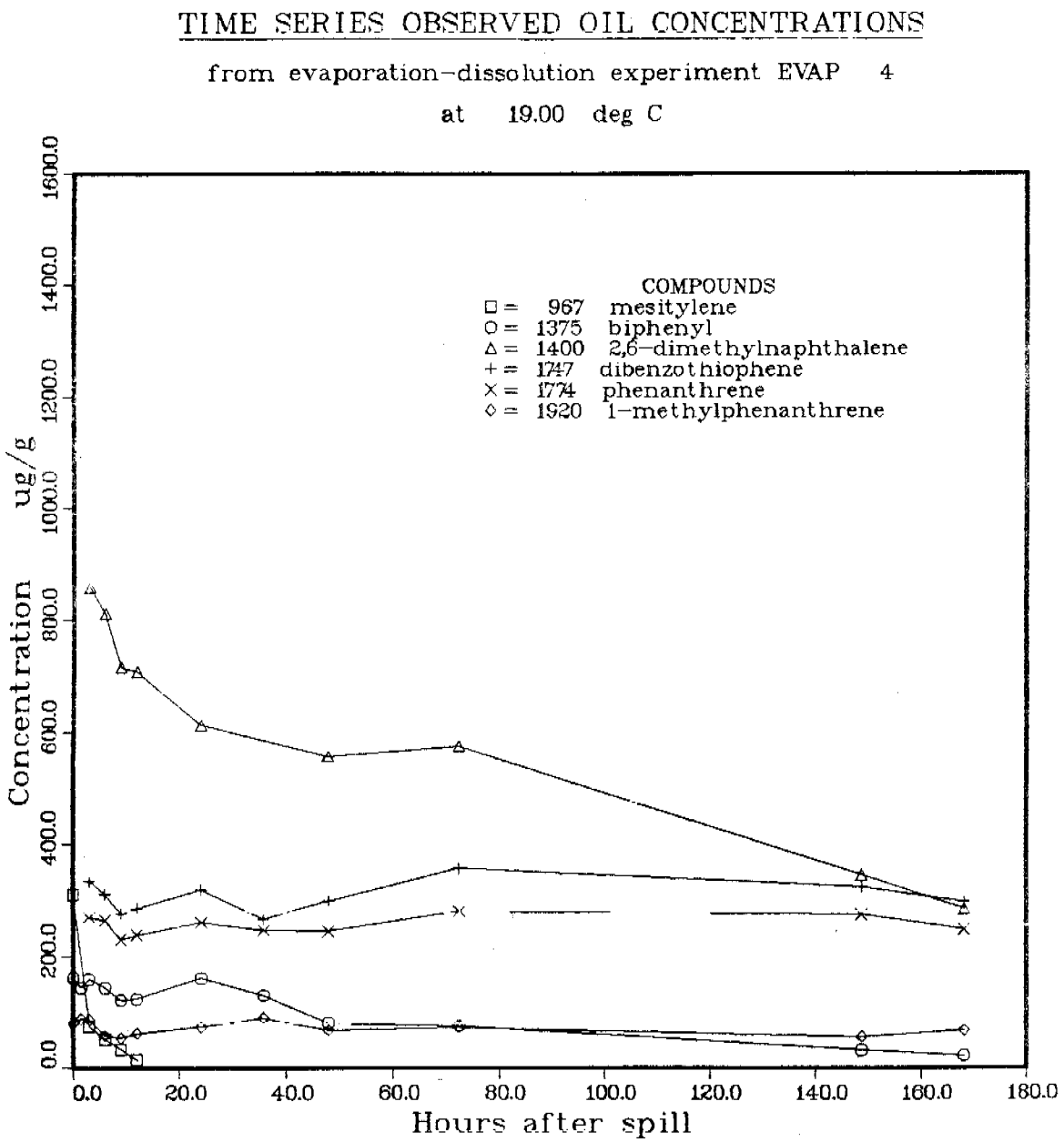

FIGURE 5-15. COMPUTER GENERATED TIME-SERIES PLOTS OF SPECIFIC HIGHER MOLECULAR WEIGHT COMPONENT CONCENTRATIONS REMAINING IN PRUDHOE BAY CRUDE OIL WEATHERING AT 19°C UNDER INFLUENCE OF A 7 KNOT WIND. (E/D-4 DATA FROM EXP DATA BASE OF OIL WEATHERING MODEL).

the more recently computer generated plots of the oil phase component concentrations from E/D-4.

The oil slick component concentration graphs (Figures 5-8 through 5-15 show the exponential decrease of the lower molecular weight components from the slick and the longer-term stability and residence of the higher molecular weight polynuclear aromatics, heterocyclic PNA's and their respective alkyl-substituted homologs.

The concentrations of lower molecular weight compounds such as ethylbenzene and 1,2-diethylbenzene were observed to decrease very rapidly in the first several hours, and after a period of 6 hours ethylbenzene (KOVAT 857) was no longer observed in the surface oil. Likewise, 1-ethyl-2-methylbenzene (KOVAT 959) showed a very rapid decrease in concentration with no detectable material present after 12 hours (Figure 5-9). Evaporation and dissolution of 1,2,4-trimethylbenzene (KOVAT 991) were somewhat slower (Figure 5-8), but its exponential decay resulted in no detectable material after approximately 24 hours, and the concentration of its isomer, 1,2,3-trimethylbenzene (KOVAT 1019) is seen to decrease rapidly in a 12-hour period. Tetramethylbenzene (KOVAT 1148) was observed to decrease exponentially over the first 24 hours to the point where it was no longer observed (Figure 5-9). Tetrahydronaphthalene (KOVAT 1156) was also lost before 12 hours occurred and naphthalene decreased in an exponential fashion over a 74 hour period to where it was no longer detectable (Figures 5-8 and 5-9). The alkyl-substituted polynuclear aromatics showed longer residence times in the oil, with 2-methylnaphthalene (KOVAT 1288) and 1-methylnaphthalene (KOVAT 1304) present for 220 hours (Figures 5-10 and 5-11). They too showed an exponential decrease in concentration in the oil, and 1,1-biphenyl (KOVAT 1375) and 2-ethylnaphthalene (KOVAT 1387) showed similar effects as their concentrations dropped off exponentially to the point where they were no longer observed after 250 hours (Figures 5-11 and 5-12). The compounds with molecular weights above alkyl-substituted naphthalenes showed longer residence times in the oil, as this is illustrated in Figure 5-12 for 1,1-methylene bis-benzene (KOVAT 1487) which was still present after

475 hours although its concentration had dropped by a factor of 4 in an exponential fashion during that period.

Dibenzothiophene, the major sulfur heterocyclic aromatic compound in Prudhoe Bay crude oil, did not show a significant decrease over a 500-hour period due to either evaporation or dissolution (Figure 5-13). In fact, the relative concentration of dibenzothiophene increased slightly in the weathered-oil-residue due to the loss of the lower molecular weight components. Phenanthrene (KOVAT 1771) also showed a slight increase in relative concentration as did the alkyl-substituted 4-methyldibenzothiophene (KOVAT 1845) and 2-methylphenanthrene (KOVAT 1887; Figure 5-13). Although these compounds do have limited water solubilities, as reported by CLARK and MACLEOD (1977), they are not readily dissolved from the oil into the water column and they are apparently not removed to any appreciable degree by evaporation after the slick becomes diffusion controlled.

Water column concentrations of these same aromatic compounds are presented in Table 5-5 and Figures 5-16 through 5-21 show the manually plotted time-dependent concentration changes for several selected compounds. Figure 5-22 presents the computer generated plots of many of the same compounds for comparison. As was noted in detail in our November, 1980 Interim Quarterly Report, initial increases of concentrations of the lower molecular weight aromatics in the water column occur within the first 5 to 10 hours while higher molecular weight component concentrations peak at after a slightly longer period. Interestingly, after approximately 10 hours, exponential decreases in the water column concentrations occurred due to evaporative loss through air/sea exchange. While the methylene chloride extraction technique does not allow evaluation of benzene and toluene (due to hexane and benzene solvent interference during capillary chromatography), these concentrations can be determined by the purge and trap results as shown in Table 5-3 and Figure 5-6. It is possible with the methylene chloride extraction and subsequent fractionation procedure to quantify the water column and oil slick concentrations for other aromatics, ranging from ortho-, meta- and para-xylenes (1-2, 1-3, and

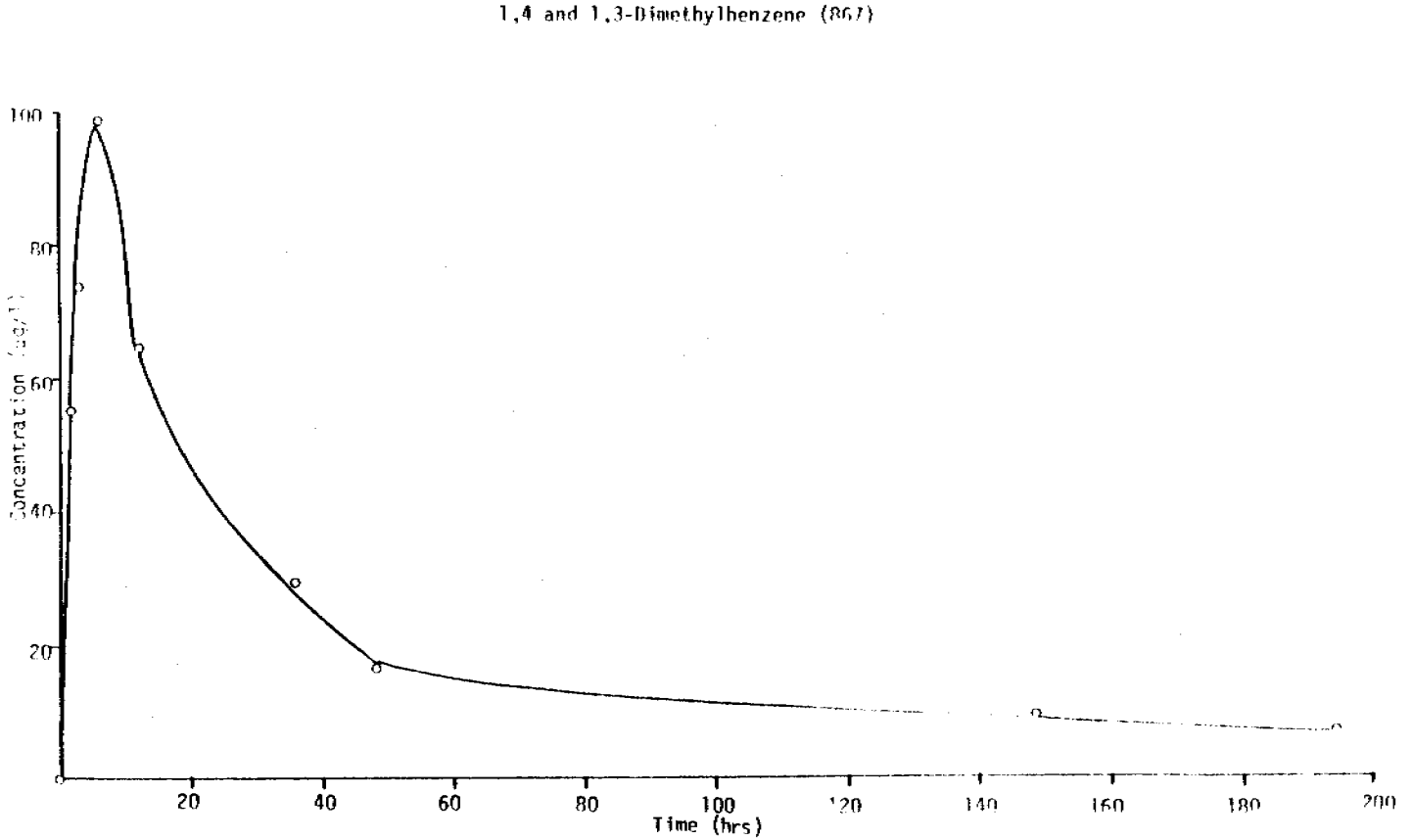

FIGURE 5-16. TIME-DEPENDENT CONCENTRATION IN THE WATER COLUMN WEATHERING AT 19°C UNDER INFLUENCE OF A 7 KNOT WIND.

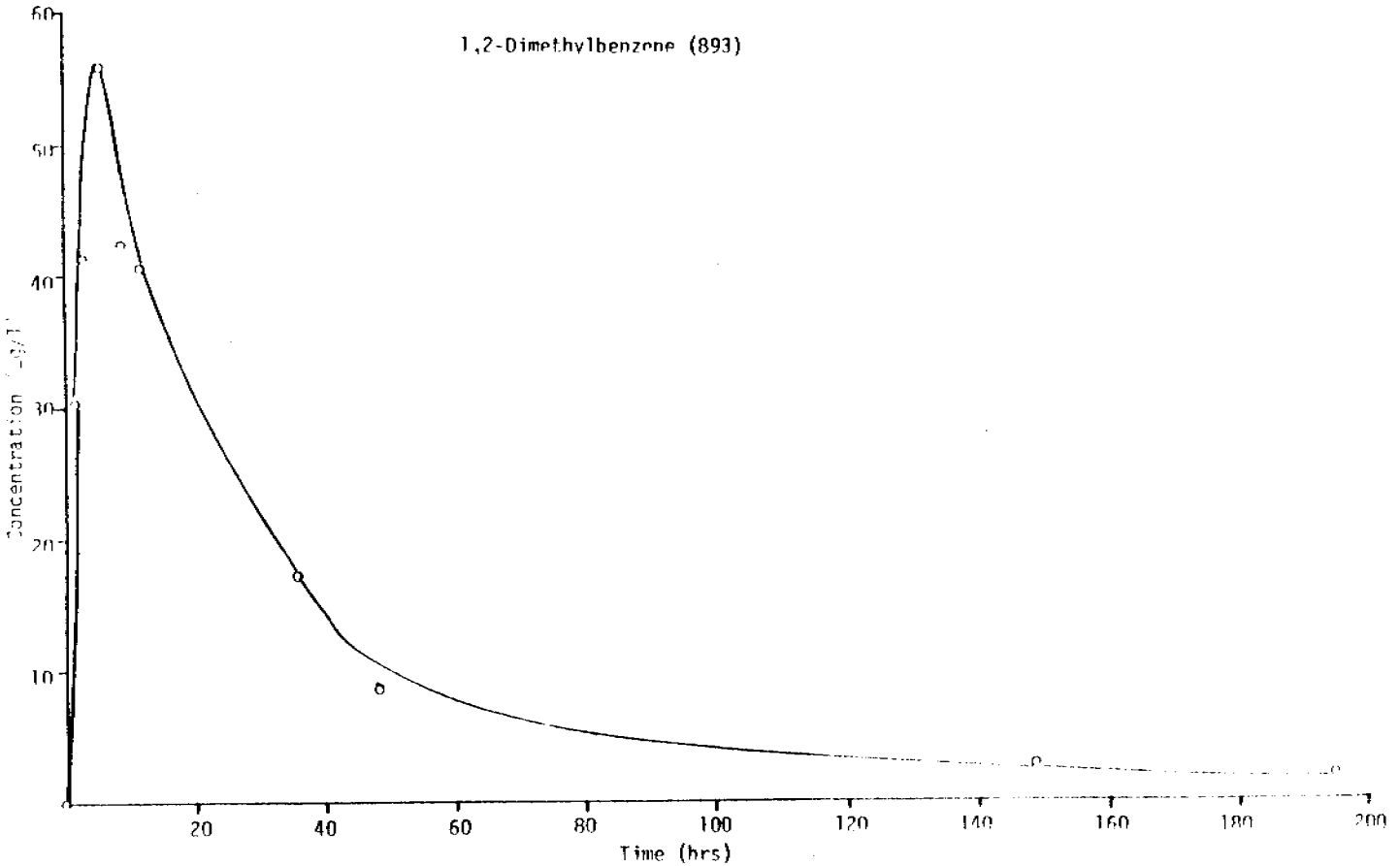

FIGURE 5-17. TIME-DEPENDENT CONCENTRATION IN THE WATER COLUMN WEATHERING AT 19°C UNDER INFLUENCE OF A 7 KNOT WIND.

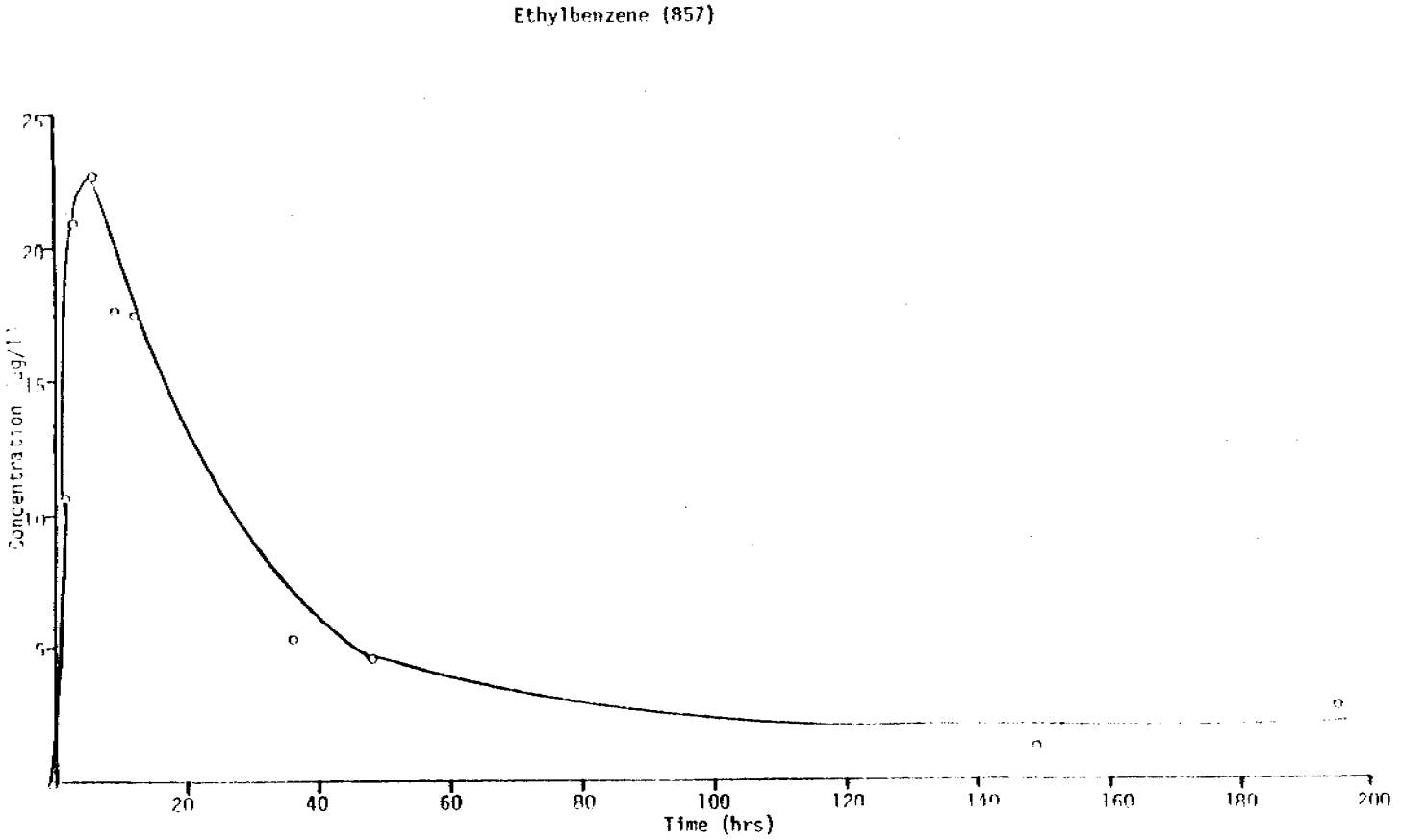

FIGURE 5-18. TIME-DEPENDENT CONCENTRATION IN THE WATER COLUMN WEATHERING AT 19°C UNDER INFLUENCE OF A 7 KNOT WIND.

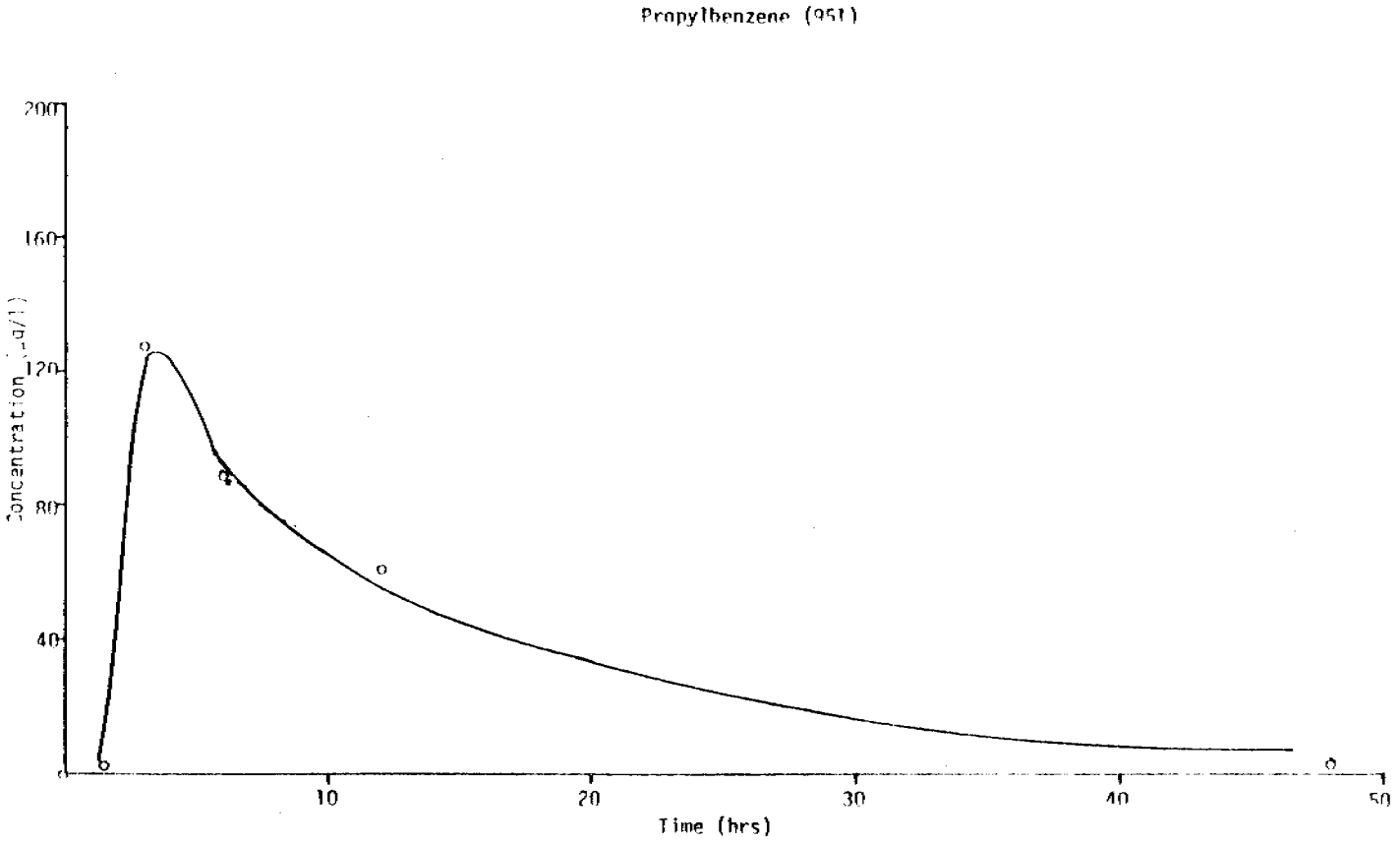

FIGURE 5-19. TIME-DEPENDENT CONCENTRATION IN THE WATER COLUMN WEATHERING AT 19^{o}C UNDER INFLUENCE OF A 7 KNOT WIND.

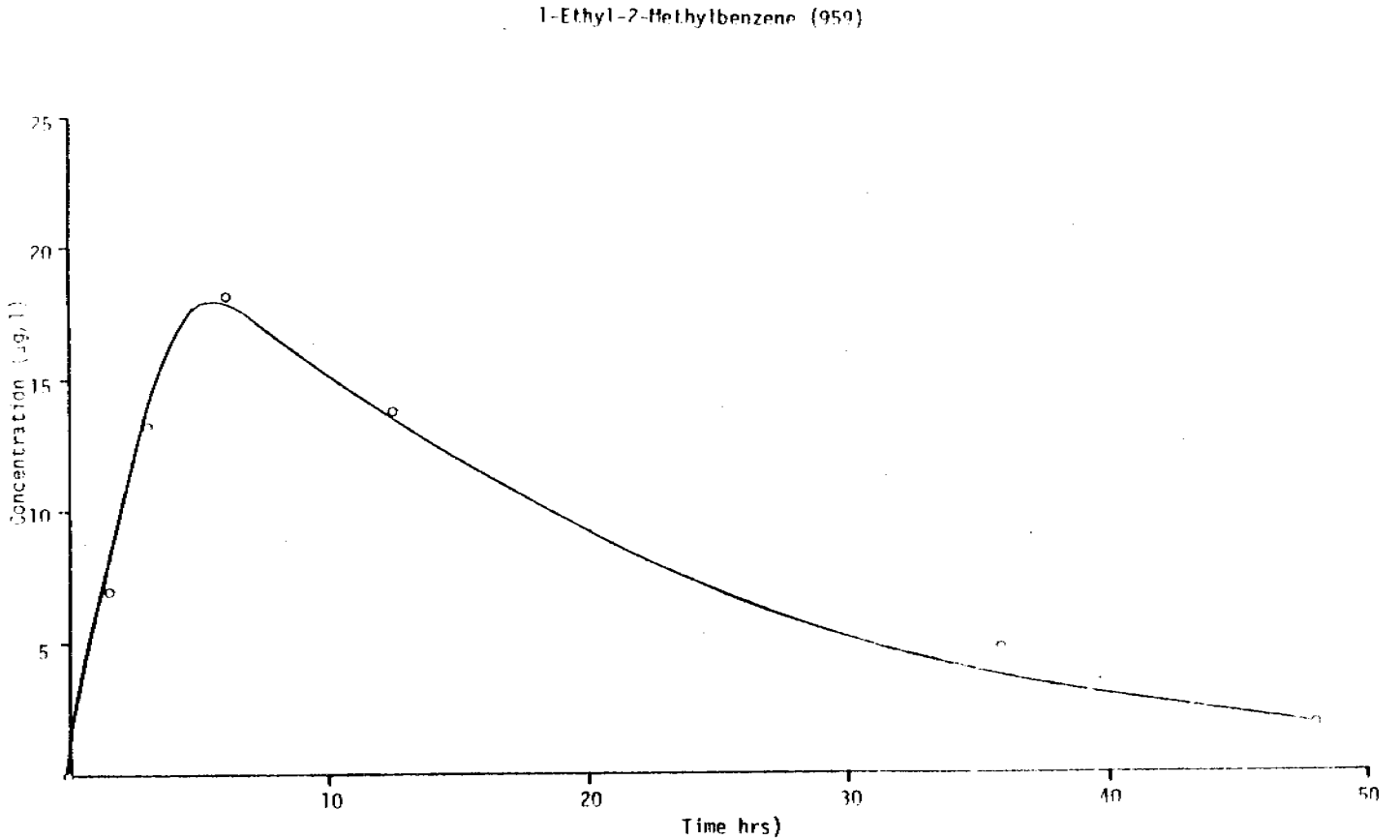

FIGURE 5-20. TIME-DEPENDENT CONCENTRATION IN THE WATER COLUMN WEATHERING AT 19°C UNDER INFLUENCE OF A 7 KNOT WIND.

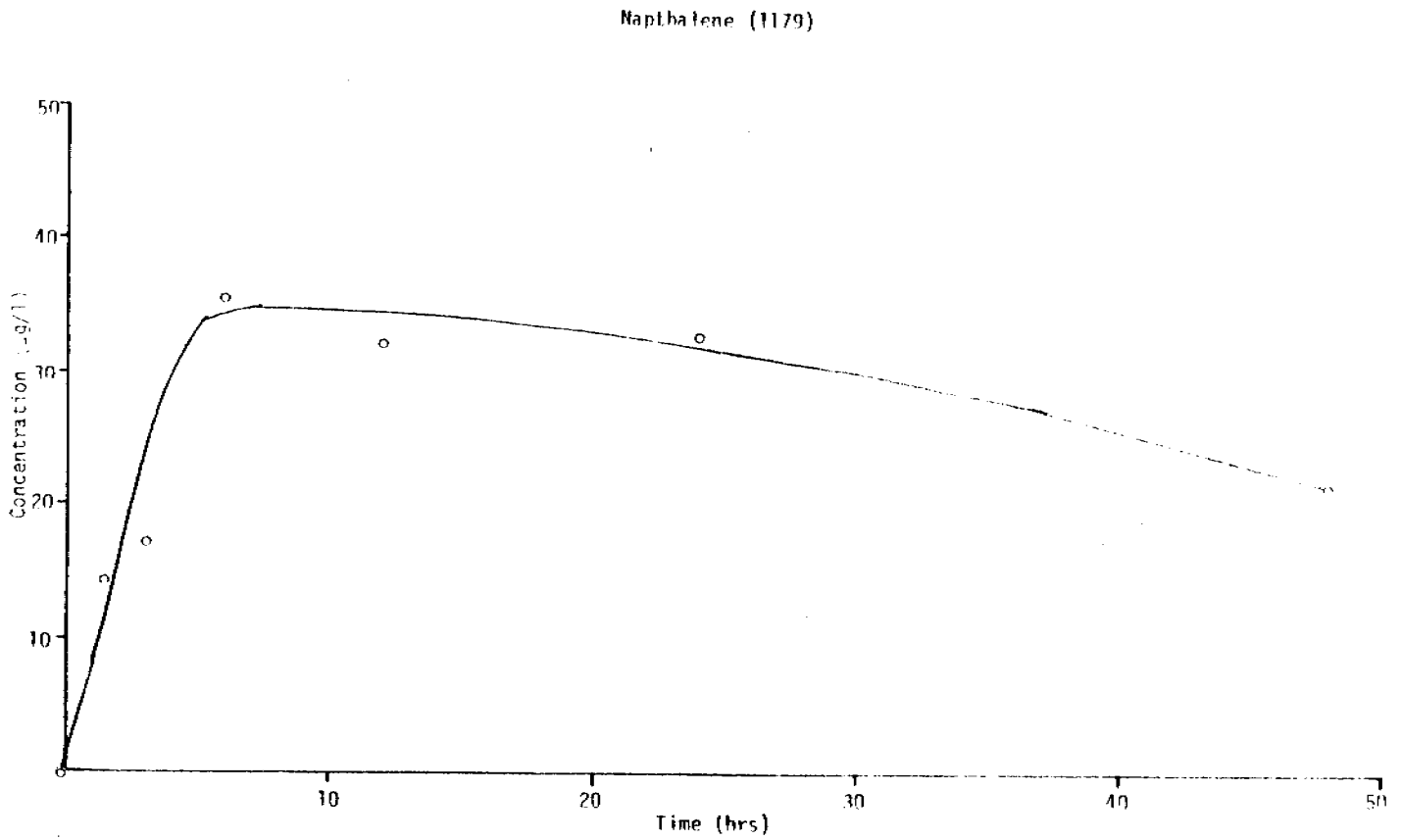

FIGURE 5-21. TIME-DEPENDENT CONCENTRATION IN THE WATER COLUMN WEATHERING AT 19°C UNDER INFLUENCE OF A 7 KNOT WIND.

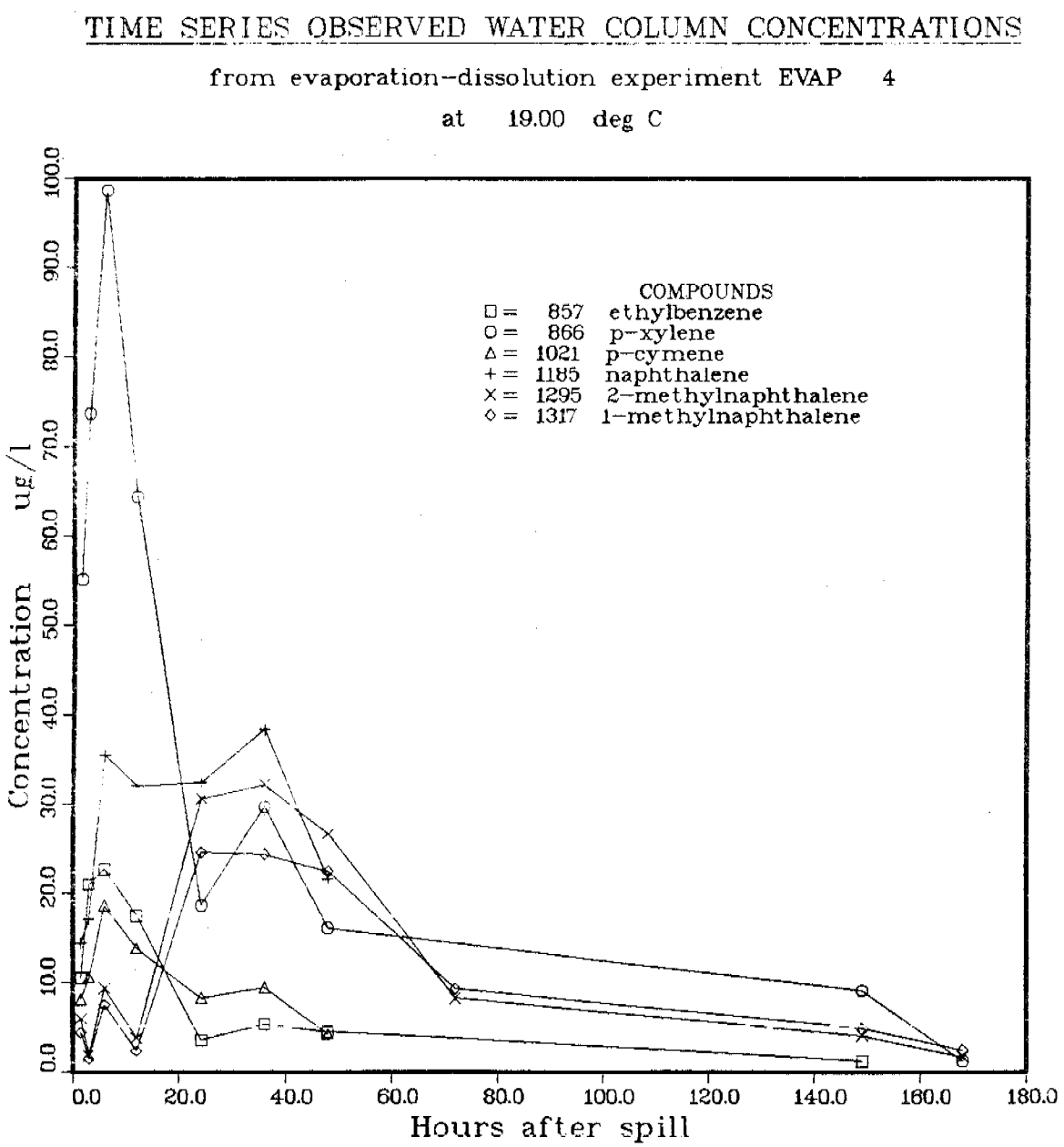

FIGURE 5-22. COMPUTER GENERATED TIME-SERIES PLOTS OF SPECIFIC COMPONENT CONCENTRATIONS REMAINING IN THE WATER BENEATH A PRUDHOE BAY CRUDE OIL SLICK WEATHERING AT 19°C UNDER INFLUENCE OF A 7 KNOT WIND. (E/D-4 DATA FROM EXP DATA BASE OF OIL WEATHERING MODEL).

1-4-dimethylbenzenes) through alkyl-substituted phenanthrenes. Figure 5-16 shows the time-dependent changes and concentrations of meta- and para-xylene with time. The initial buildup to 100 μm/l in the first 5 hours was very similar to that observed when the purge and trap technique was used for similar measurements as reported in Figure 5-6. Validation of the compatability of the measurement techniques is provided by the similar values and trends obtained by these two significantly different methods (purge and trap FID GC vs methylene chloride extraction, fractionation and FID chromatography). Likewise, concentration buildup and declines for ortho-xylene and ethylbenzene were similar when measured by both techniques. Figure 5-17 shows the time-dependent concentration changes in the water column for ortho-xylene, and these data also clearly parallel those observed for the other two isomers. Similar profiles are obtained for ethylbenzene, propylbenzene and 1-ethyl-2-methylbenzene in the subsequent Figures (5-18 through 5-20). Polynuclear aromatics starting with naphthalene show somewhat later concentration maxima and longer retention in the water column as shown by the data in Figures 5-21 and 5-22.

Each of the maximum concentrations reached during the initial stages of dissolution reflect the mole fraction of the component in the oil and the relative activity coefficients of the compound in the oil and the water. In almost all instances, however, the concentrations in the water column in the evaporation/dissolution chamber do not reach the higher values obtained during the closed system (separatory funnel) oil/seawater partition coefficient determinations described in the next section. This presumably reflects the rapid loss from the oil of the specific components due to evaporative processes and the concomitant decrease in overall mole fraction of these lower molecular weight materials in the oil. Finally, as these materials are ultimately removed from the oil slick reservoir itself, the water column concentrations undergo a decrease beneath the slick. In the case of the higher molecular weight naphthalenes and alkyl-substituted naphthalenes, this decrease does not occur until 10 to 20 hours after the spill incident (20 hours for 1-methylnaphthalene, 35 hours for 2-methylnaphthalene, 35 hours for biphenyl). This is

presumably due to the longer residence time of these higher molecular weight materials in the oil causing their longer residence time in the water column beneath the slick.

During the initial evaporation/dissolution experiment using Prudhoe Bay crude oil, the oil was added from a height of 6-8" above the water and significant plunging of oil droplets into the water column was noted. While such droplet formation no doubt occurs in a real-spill event, such behavior significantly complicates development of algorithms for evaporation and dissolution because of the greatly enhanced surface area of the oil droplets exposed to the water column. Development of dissolution algorithms to account for this droplet formation is much more complicated and is still undergoing evaluation at this time. Therefore, in subsequent evaporation/dissolution experiments, the oil was added via a horizontally placed transfer tube located 0.5 cm above the water surface. In this manner, the oil was observed to spread as a smooth slick over the water and significant 1 to 10-mm oil droplet dispersion was prevented. In that the algorithms for dissolution require input parameters such as the surface area of the oil slick exposed to the water, it was believed that this approach would provide much better experimental data to compare against computer predicted output for evaporation and dissolution weathering in the stirred tank experiments. Further, during the initial evaporation/ dissolution experiments using a 7 knot wind, 5 to 10-cm holes were "blown" in the surface slick. While such breakup of surface slicks in ocean systems is also known to occur, this behavior in the evaporation/ dissolution chamber complicates modeling of the observed results and generation of agorithms. For this reason, in subsequent evaporation/dissolution experiments, the wind speed was dropped to 1 knot such that buildup of volatile components would not occur in the air above the slick but that holes were not blown into the slick at the same time.

To evaluate these changes in the experimental procedure, a second 19°C evaporation/dissolution experiment was undertaken and Figures 5-23 and 5-24 present the computer plotted time-series observed oil concentrations from

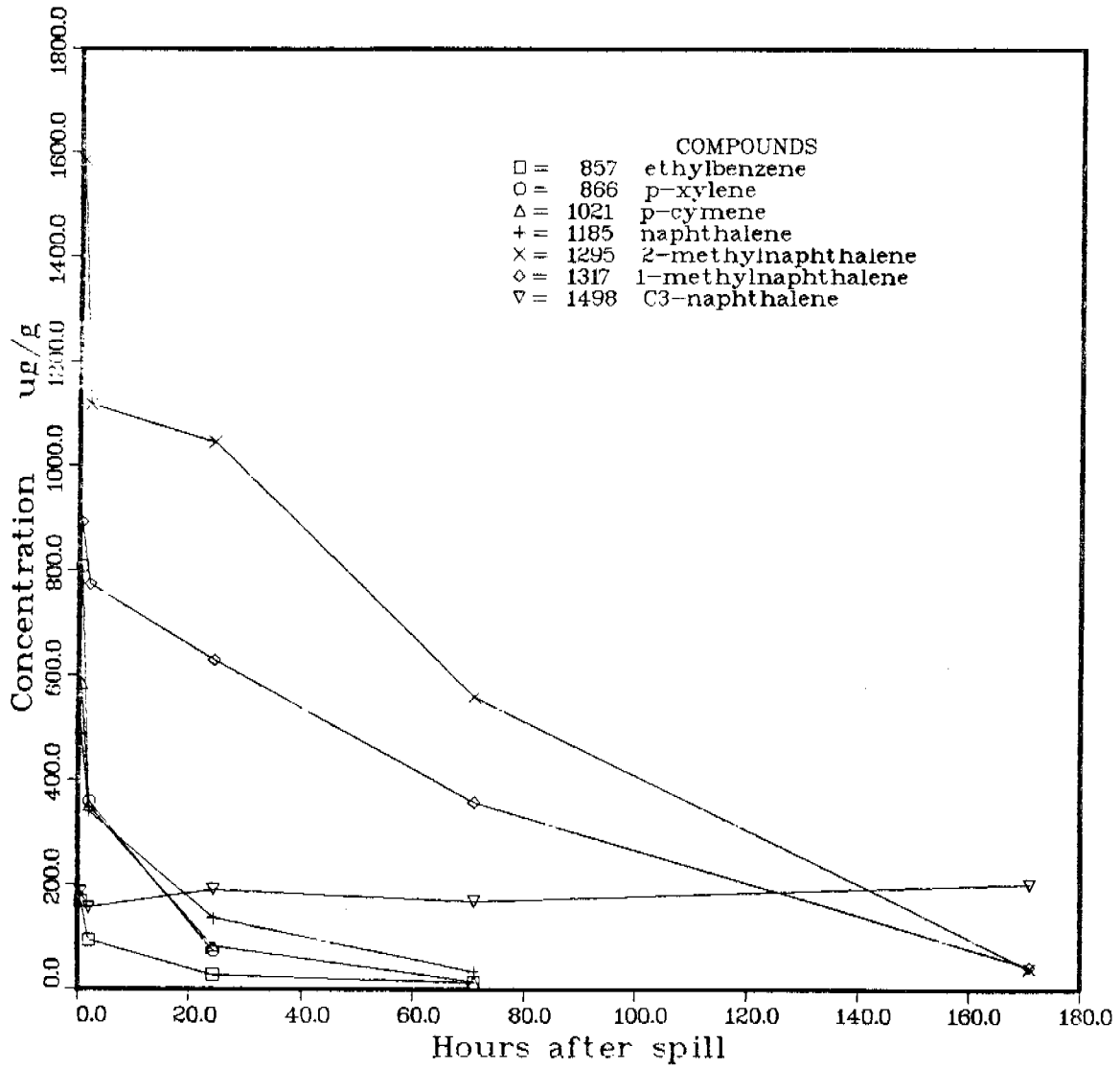

FIGURE 5-23. COMPUTER GENERATED TIME-SERIES PLOTS OF SPECIFIC COMPONENT CONCENTRATIONS REMAINING IN PRUDHOE BAY CRUDE OIL WEATHERING AT 19°C UNDER INFLUENCE OF A 1 KNOT WIND. (E/D-5 DATA FROM EXP DATA BASE OF OIL WEATHERING MODEL).

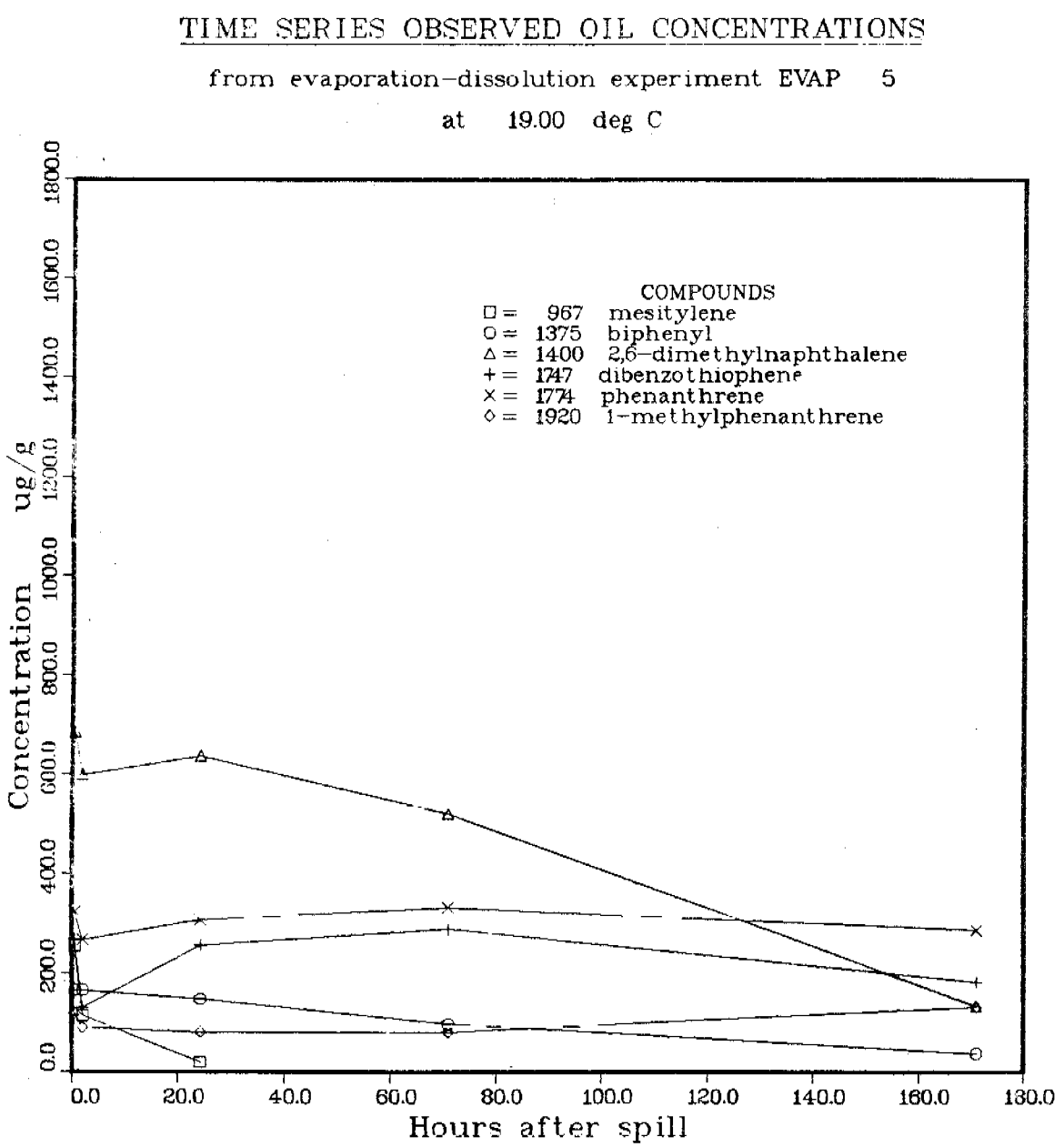

FIGURE 5-24. COMPUTER GENERATED TIME-SERIES PLOTS OF SPECIFIC COMPONENT CONCENTRATIONS REMAINING IN THE WATER BENEATH A PRUDHOE BAY OIL SLICK WEATHERING AT 19°C UNDER INFLUENCE OF A 1 KNOT WIND. (E/D-5 DATA FROM EXP DATA BASE OF OIL WEATHERING MODEL).

that experiment. Quite clearly, the reduction in wind speed affects the rate of loss of the lower molecular weight components as can be seen by comparing Figures 5-23 and 5-14. Longer residence times of compounds from ethylbenzene through naphthalene are observed in the slick under these conditions. The residence time of higher molecular weight components such as mesitylene (Kovat 967) through 1-methylphenanthrene are not drastically affected. That is, their residence time in the slick is significant over the 180 hours of experiment as would be anticipated. Reduction of the formation of oil in water dispersed droplets also significantly affects the amounts of hydrocarbons dissolved in the water column, as would be expected from the significantly decreased oil/water interfacial surface area. Figure 5-25 presents the computer generated plot of the water column concentrations from evaporation/dissolution exp 5 where the oil was added to the evaporation/dissolution chamber with the horizontally positioned addition tube. Comparison of the data in Figure 5-22 with 5-25 shows that a factor of 2 to 3 decrease is observed in the water column concentrations as a result of this more gentle oil-addition procedure. As noted above, these modifications to the experimental procedure were necessitated by the requirement to maintain as carefully a controlled oil/water surface area as possible for verification of algorithms derived to predict dissolution phenomena. Results of observed vs predicted water column concentrations are presented in Section 5.1.5.

Rate constants are being determined at this time for the specific hydrocarbon compound concentration decreases from the slick. As these data become available, they will be compared to computer modeled output for verification of predicted behavior versus observed laboratory results as illustrated in Section 5.1.5.

Figures 5-26 and 5-27 present the gas chromatograms on the aliphatic and aromatic fractions of time series oil samples collected from an evaporation/dissolution experiment conducted under a 1-2 knot wind at 3°C (E/D-6). In this instance, time series samples were collected 30 minutes after the spill and at times 2 hours, 1 day, 3 days, 6 days, 12 days and 21

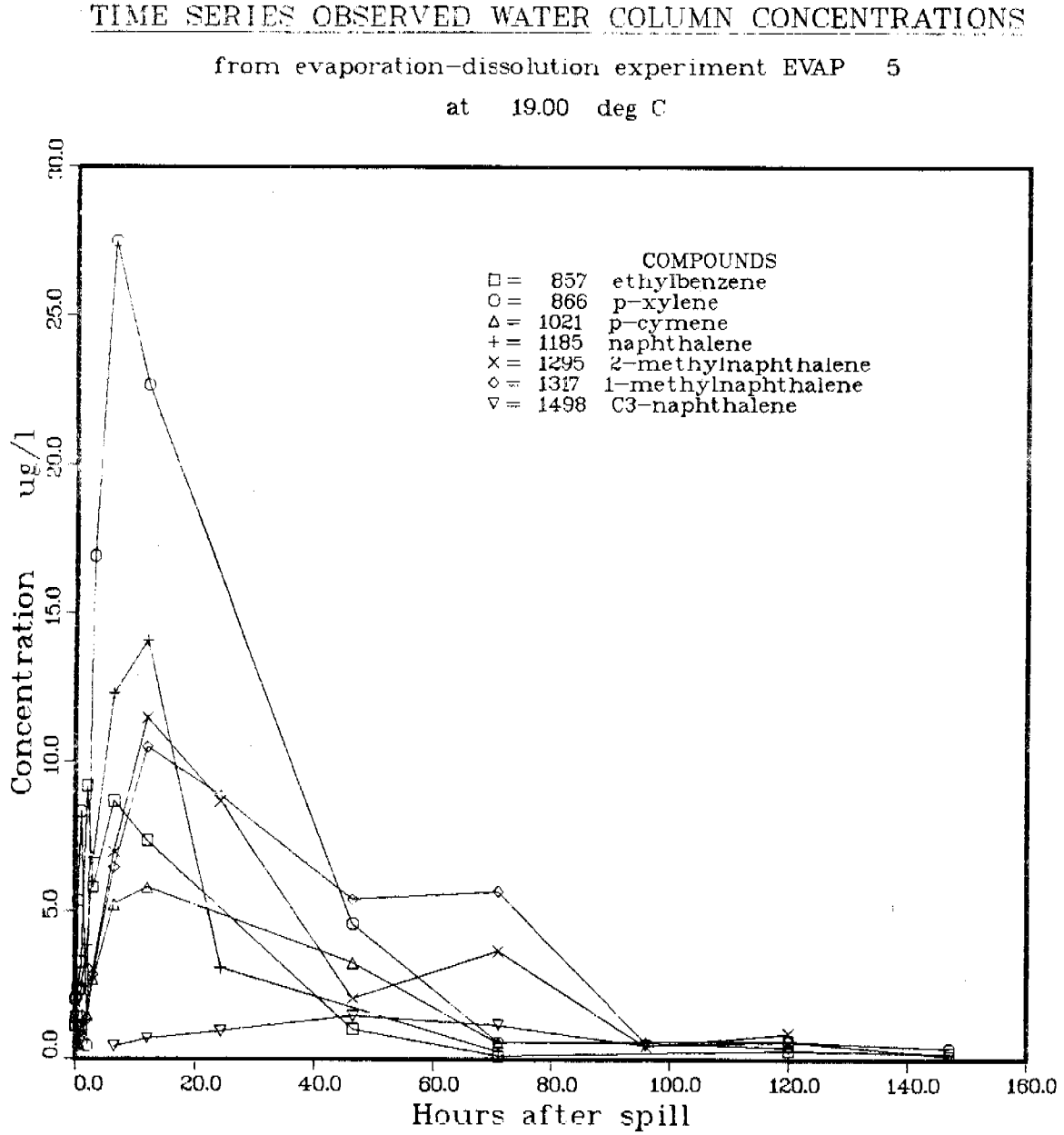

FIGURE 5-25. COMPUTER GENERATED TIME-SERIES PLOTS OF SPECIFIC COMPONENT CONCENTRATIONS REMAINING IN THE WATER BENEATH A PRUDHOE BAY CRUDE OIL SLICK WEATHERING AT 19°C UNDER INFLUENCE OF A 1 KNOT WIND. (E/D-5 DATA FROM EXP DATA BASE OF OIL WEATHERING MODEL).

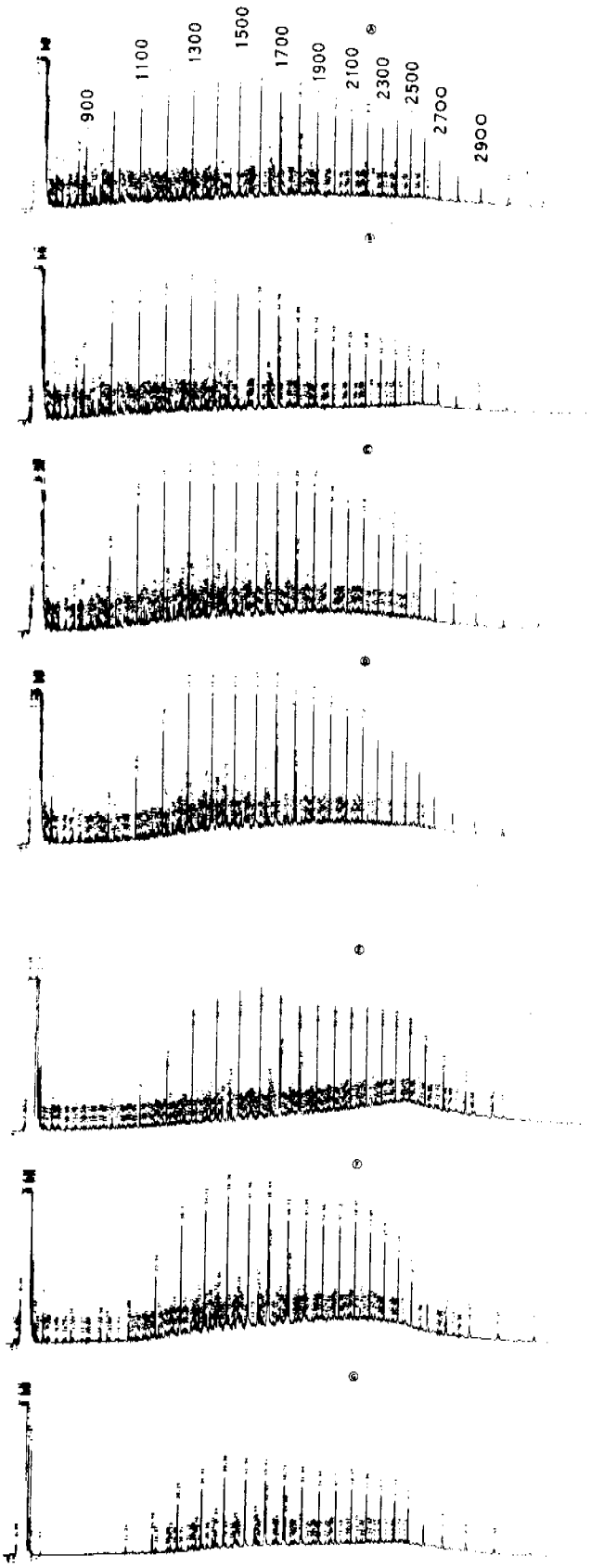

FIGURE 5-26. FLAME IONIZATION DETECTOR CAPILLARY GAS CHROMATOGRAMS OF ALIPHATIC COMPONENTS REMAINING IN PRUDHOE BAY CRUDE OIL WEATHERING AT 3°C UNDER INFLUENCE OF A 1 KNOT WIND (E/D-6). TIME-SERIES SAMPLING POINTS AFTER THE "SPILL": (A) 30 MINUTES; (B) 2 DAYS; (C) 1 DAY; (D) 3 DAYS; (E) 6 DAYS; (F) 12 DAYS; AND (G) 21 DAYS.

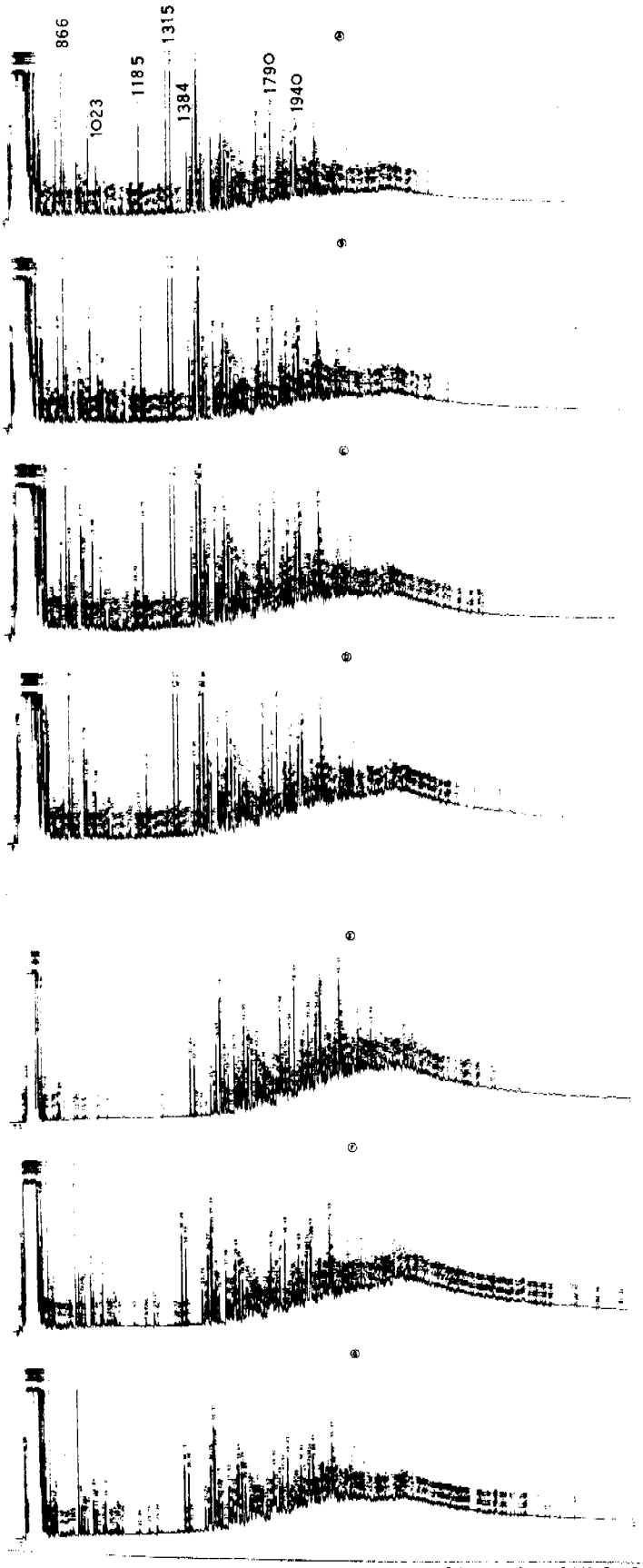

FIGURE 5-27. FLAME IONIZATION DETECTOR CAPILLARY GAS CHROMATOGRAMS OF AROMATIC COMPONENTS REMAINING IN PRUDHOE BAY CRUDE OIL WEATHERING AT 3°C UNDER INFLUENCE OF A 1 KNOT WIND (E/D-6). TIME-SERIES SAMPLING POINTS AFTER THE "SPILL": (A) 30 MINUTES; (B) 2 HOURS; (C) 1 DAY; (D) 3 DAYS; (E) 6 DAYS; (F) 12 DAYS; AND (G) 21 DAYS.

days following the initial spill event. On comparing these chromatograms to the chromatograms shown earlier in Figure 5-7, it can be seen that loss of lower molecular weight components due to volatilization is slightly inhibited at this lower temperature. This is perhaps best observed in examining the computer generated plots of specific compound concentrations in the oil vs time as shown in Figure 5-28 and 5-29.

Comparison of these latter figures to the computer plotted figures (5-23 and 5-24) for the 19°C experiment show significantly longer residence times of the intermediate molecular weight components compared to those lost at the higher temperature (note difference in time scales for Figures 5-28 and 5-29 vs 5-23 and 5-24). The lower molecular weight components (up to p-cymene) appear to be lost at approximately the same rates (after 60 hrs) in both experiments. The same relative increases in concentrations of higher molecular weight compounds such as dibenzothiophene, phenanthrene and methyl-phenanthrene can be observed in both experiments. Gas chromatograms for the time series water column samples obtained in the 3°C evaporation/dissolution experiment are presented in Figure 5-30. These chromatograms show the slow build-up of the relatively more water soluble lower and intermediate molecular weight alkyl-substituted aromatics in the water column. In this instance, however, the maximum water column concentrations are reached after approximately 50 hours and longer as shown by the computer plot of water column concentrations for this experiment (Figure 5-31). Obviously, many additional samples and chromatograms had to be obtained for generation of these plots but inclusion of additional chromatographic profiles in a report such as this is not practical. Clearly, however, the selected chromatograms and time-series concentration plots show the early water column buildup of the lower molecular weight compounds of interest such as toluene, ortho- and para-xylenes and alkyl-substituted benzenes. The higher molecular weight compounds such as naphthalenes and alkyl-substituted naphthalenes then reach maximum concentrations in the water column at 40-60 hours and then remain in the water column, not being lost through air/sea exchange and evaporation, for longer periods of time. It is quite interesting to compare the chromatographic profiles

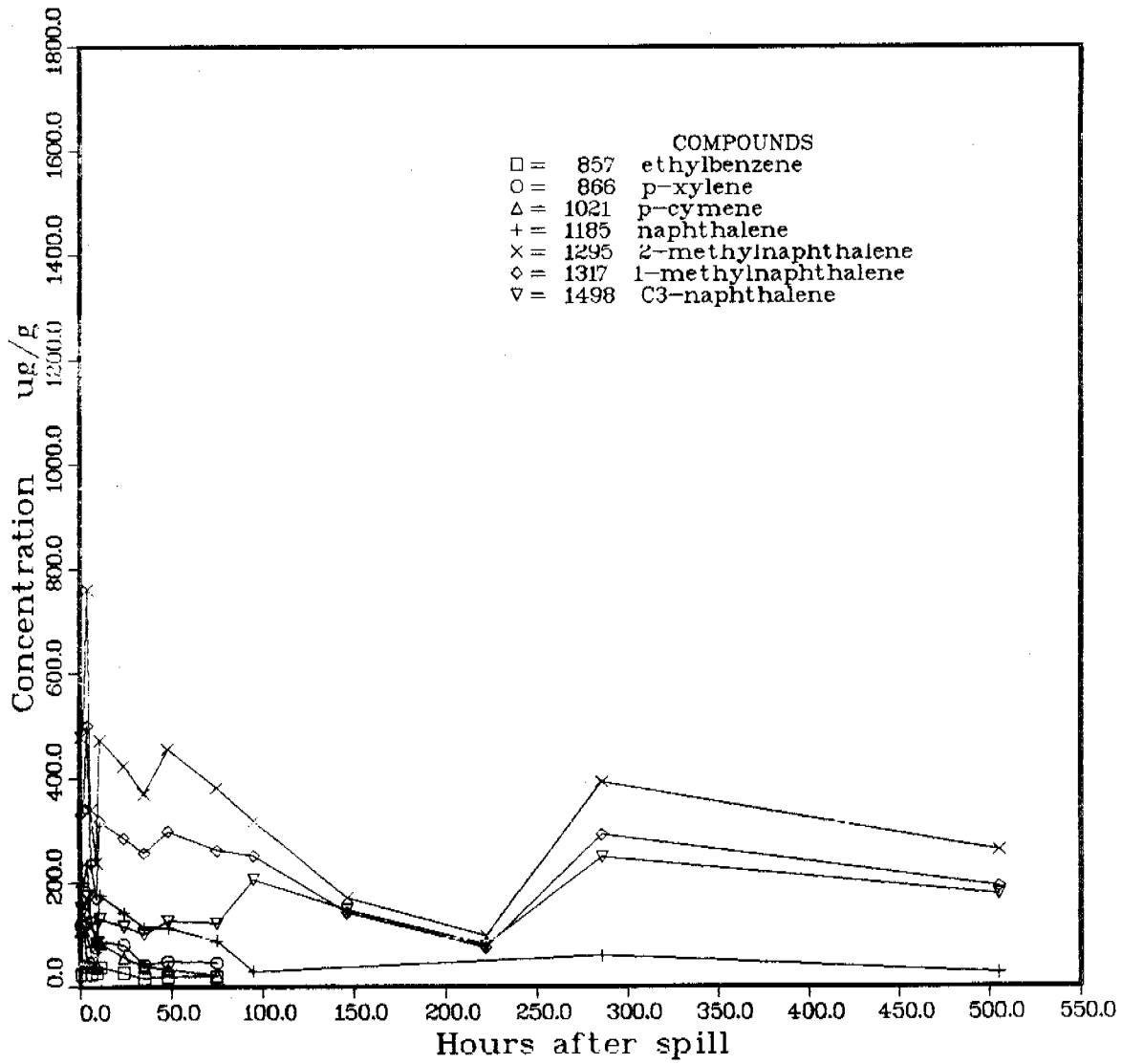

FIGURE 5-28. COMPUTER GENERATED TIME-SERIES PLOTS OF SPECIFIC COMPONENT CONCENTRATINS REMAINING IN PRUDHOE BAY CRUDE OIL WEATHERING AT 3°C UNDER INFLUENCE OF A 1 KNOT WIND. (E/D-6 DATA FROM EXP DATA BASE OF OIL WEATHERING MODEL).

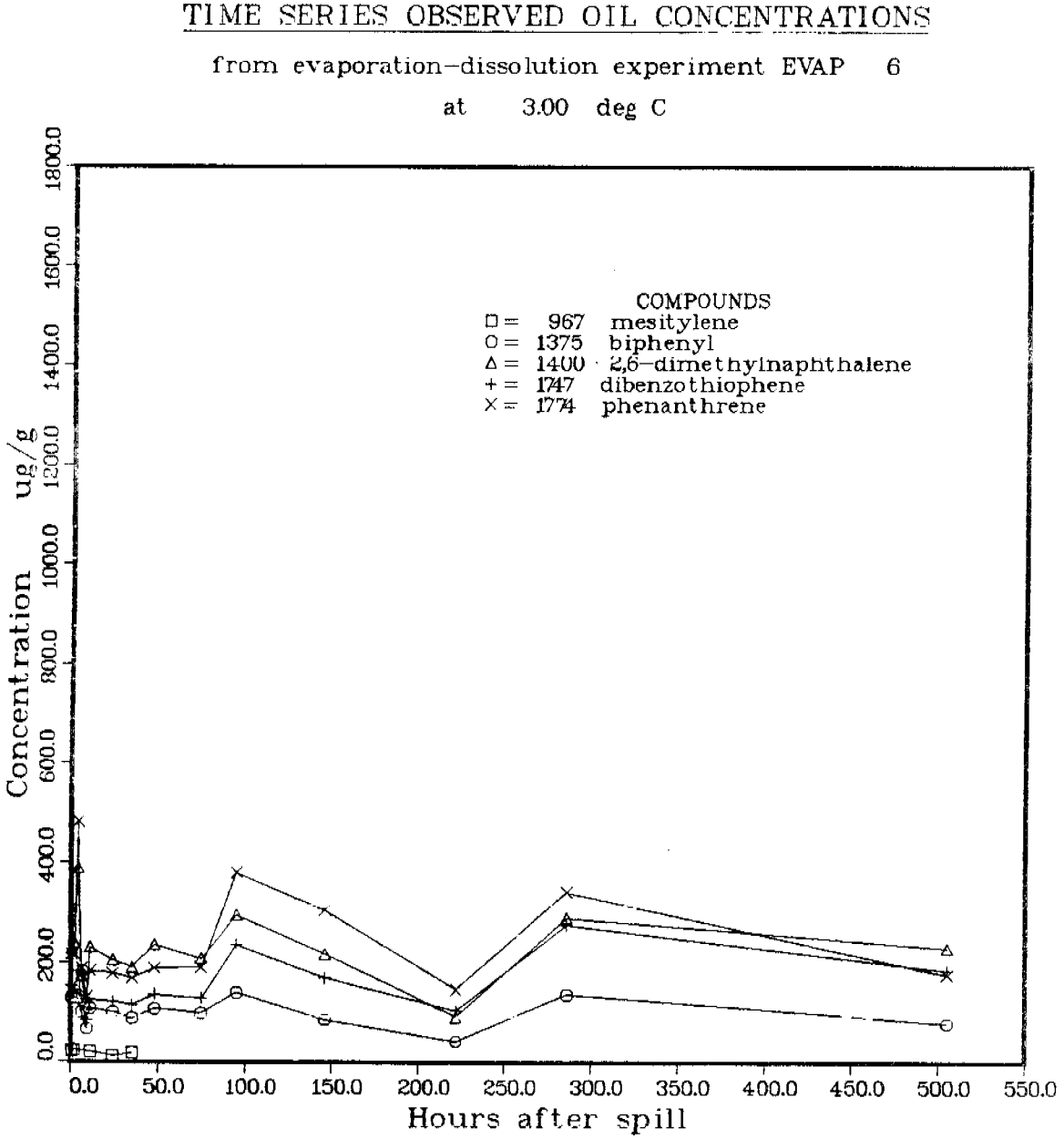

FIGURE 5-29. COMPUTER OPERATED TIME-SERIES PLOTS OF SPECIFIC HIGHER MOLECULAR WEIGHT COMPONENT CONCENTRATIONS REMAINING IN PRUDHOE BAY CRUDE OIL WEATHERING AT 3°C UNDER A INFLUENCE OF A 1 KNOT WIND. (E/D-6 DATA FROM EXP DATA BASE OF OIL WEATHERING MODEL).

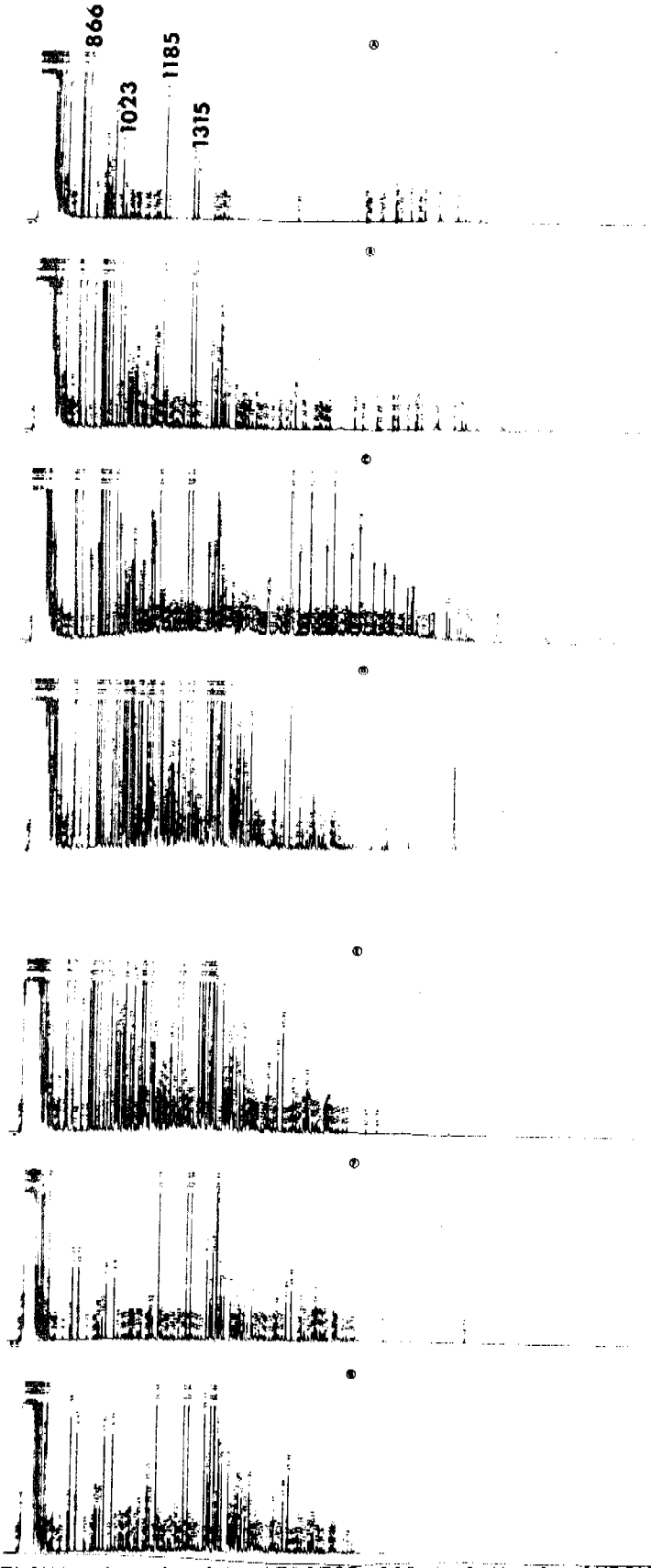

FIGURE 5-30. FLAME IONIZATION DETECTOR CAPILLARY GAS CHROMATOGRAMS OF THE AROMATIC COMPONENTS REMAINING IN THE WATER COLUMN BENEATH A PRUDHOE BAY CRUDE OIL SLICK WEATHERING AT 3°C UNDER INFLUENCE OF A 1 KNOT WIND (E/D-6). TIME-SERIES SAMPLING POINTS AFTER THE "SPILL": (A) 30 MINUTES; (B) 2 HOURS; (C) 1 DAY; (D) 3 DAYS (E).6 DAYS; (F) 12 DAYS; and (G) 21 DAYS.

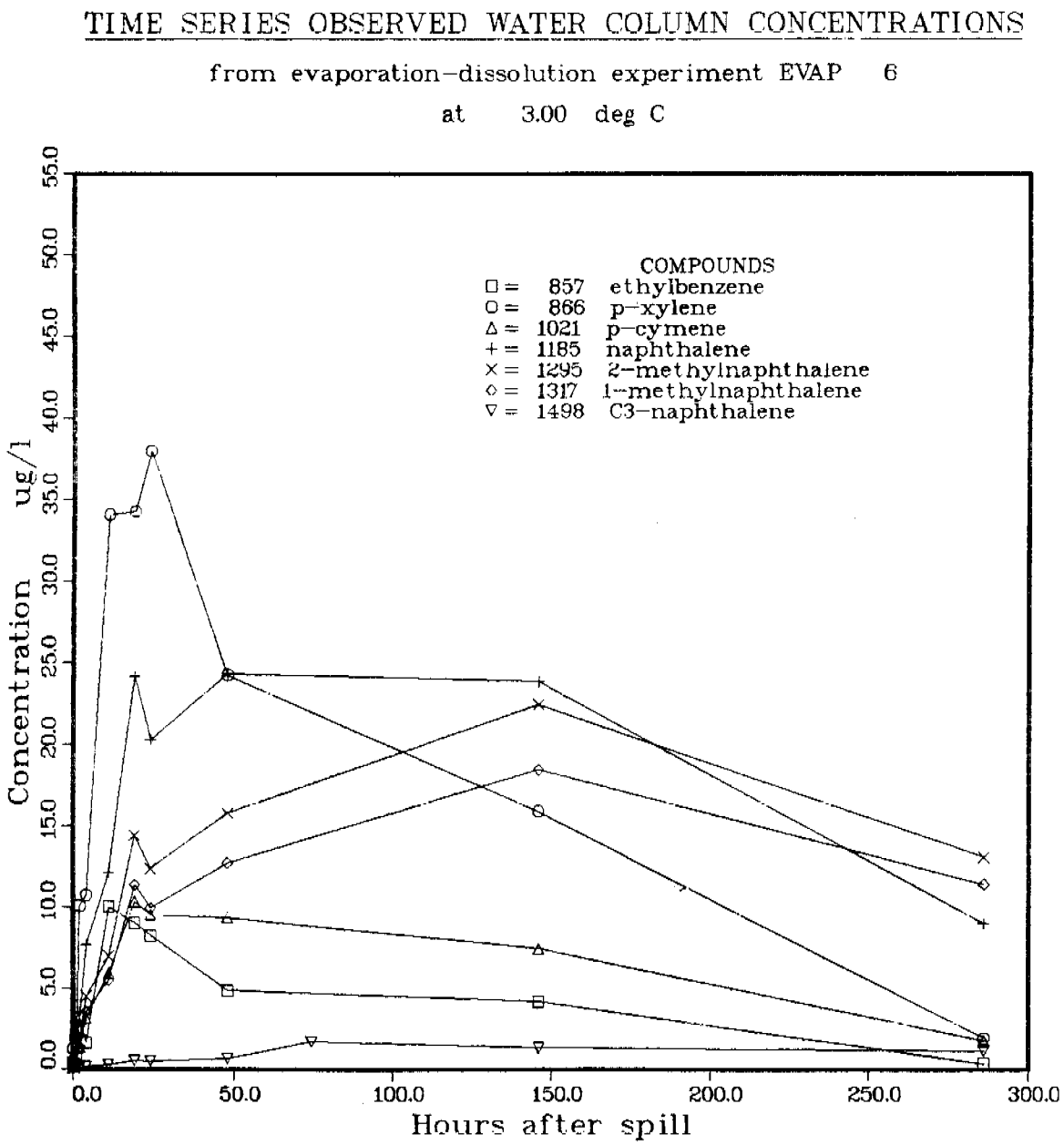

FIGURE 5-31. COMPUTER GENERATED TIME-SERIES PLOTS OF SPECIFIC AROMATIC COMPONENT CONCENTRATIONS REMAINING IN THE WATER COLUMN BENEATH A PRUDHOE BAY CRUDE OIL SLICK WEATHERING AT 3°C UNDER INFLUENCE OF A 1 KNOT WIND. (E/D-6 DATA FROM EXP DATA BASE OF OIL WEATHERING MODEL).

of the water column extracts (Figure 5-30) with the aromatic fractions of the oil sample extracts (Figure 5-27), in that the aromatics present in the water column are clearly skewed towards the lower molecular weight range. The lower molecular weight compounds in the oil are rapidly lost due to the combined effects of evaporation/dissolution such that, with time, only the higher molecular weight aromatic compounds remain in the slick up to the 21 days that this experiment was run.

5.1.2 Outdoor Evaporation/Dissolution Studies in Flow-Through Aquaria at Kasitsna Bay, Alaska

Part of the Summer 1980, Kasitsna Bay program involved construction of outdoor flow-through aquaria for long-term sub-arctic evaporation/dissolution and microbial degradation studies. Figure 5-32 presents a schematic diagram of the outdoor flow-through tank arrangement, and Figure 5-33 is a photograph of the outdoor flow-through tanks before installation of a cover to minimize fresh-water input from rain and snowfall. In September and October of 1980 four long-term microbial degradation experiments were begun: flow was maintained in two tanks where oil was allowed to weather in the presence and absence of Corexit 9527 (Tanks 3 and 7, respectively), and two tanks were maintained in a static condition where similarly treated oils were allowed to weather in the absence of continuous seawater flow (Tanks 5 and 2, respectively).

At the onset of the Spring, 1981 program, the four outdoor tanks were again examined and sampled, and two of the systems (Tanks 3 and 7) were left undisturbed to provide for continued longer term microbial degradation of the partially weathered oil over the summer months. Additional details on the results obtained from these and other long-term microbial degradation experiments are described in Section 5.2.

A more ambitious series of evaporation/dissolution experiments were then undertaken during the Spring 1981 program in these outdoor tanks using

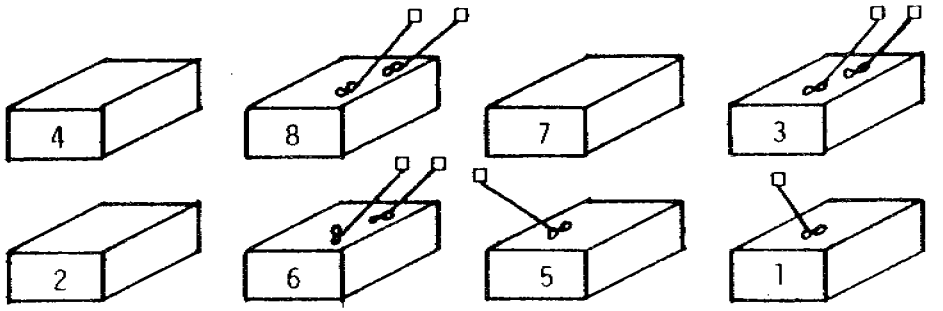

Kasitsna Bay Revised New Experimental Plan 5-1-81

Tank No.	Mousse	Oil	Turbulance	Corexit	Flow
6	+	-	+	+	+
4	+	-	-	-	+
8	+	-	+	-	+
2	+	-	-	+	+
5	-	+	+	+	+
3	-	7 month old weathered oil	+	+	—
1	-	+	+	-	+
7	-	7 month old weathered oil	-	-	+

FIGURE 5-32. SCHEMATIC DIAGRAM OF OUTDOOR FLOW-THROUGH TANK CONFIGURATION AT KASITSNA BAY, ALASKA. THE MATRIX PRESENTS THE EXPERIMENTAL DESIGN AND TANK CONFIGURATION AS USED DURING THE SPRING/SUMMER 1981 FIELD PROGRAM.

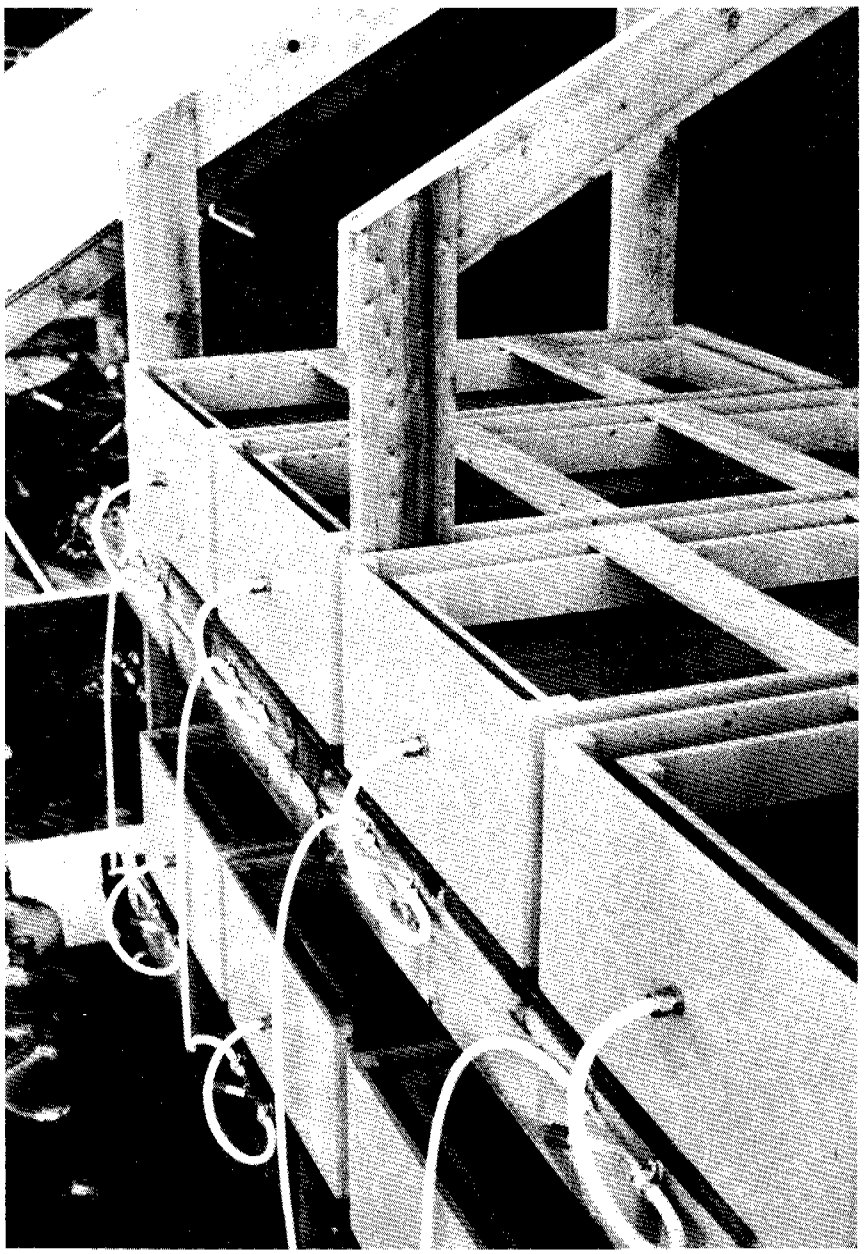

FIGURE 5-33. OUTDOOR FLOW-THROUGH OIL WEATHERING TANKS AT KASITSNA BAY, ALASKA BEFORE INSTALLATION OF A LEAN-TO COVER TO MINIMIZE FRESH WATER INPUT FROM RAIN AND SNOWFALL.

the matrix design as presented in Figure 5-32. That is, evaporation/dissolution phenomena were examined with fresh Prudhoe Bay crude oil and artificially generated mousse in the presence and absence of turbulence and in the presence and absence of the dispersant Corexit 9527 as shown by the matrix design (Figure 5-32). Time-series photographs and chemical composition data were obtained on all of the experimental systems, and Table 5-6 presents the sampling times, the sample type (oil or water) and the chromatographic identifiers associated with each sample as required for computer data reduction.

Time-series capillary column chromatographic profiles were obtained on the oil fractions during the experimental runs at Kasitsna Bay and digitized data were recorded on magnetic tape and returned to La Jolla for incorporation into the data base for the oil weathering model. As in the evaporation/dissolution experiments in La Jolla, two types of water samples were obtained, with the first being 25-ml whole water samples in Pierce septum-capped vials for analysis of volatile organics by the purge and trap technique. In addition, 20 to 40-L samples of the discharged water from each tank were obtained and extracted with methylene chloride for later laboratory fractionation and GC and GC/MS analyses.

As the data in Table 5-6 show, numerous samples were collected to provide quantitative data on evaporation/dissolution rates of oil under a wide variety of conditions; however, only three selected experiments are addressed in this report. Specifically, these include evaporation/dissolution results from: fresh oil in the presence of turbulence (Tank 1); artificially generated mousse in the presence of turbulence (Tank 8); and fresh crude oil plus Corexit in the presence of turbulence (Tank 5).

The importance of examining the evaporation/dissolution behavior of an artificially generated water-in-oil emulsion stemmed from the fact that significant increases in viscosity and specific gravity have been observed for many water-in-oil emulsions, and these increases have been shown to affect spreading, dispersion, interaction with suspended particulate material and

TABLE 5-5A OUTDOOR TANK #1 OIL, WATER AND AIR SAMPLING TIMES

Blank, 0 hr, 1 hr, 7.5 hrs, 26 hrs, 53 hrs, 93 hrs, 150 hrs,
4 months, 6 months

Computer listing of analyzed samples with reduced data in EXP data base of Oil Weathering Model

[illegible] OF EXPERIMENT DATASET PAGE 1 OCT-29-1981

EXPERIMENT: ALA 1
MEDIUM: [illegible] FRACTION TYPE: 1

	SP-LABEL	HRS	MINS	TEMPERATURES AIR	WATER	OIL	COREXIT PRESENT	WIND SPEED	MIXING	COMMENTS
A1	1 AUG-20-1981	2440	0	15.00	11.00	.00	NO	.00	10.00	TANK 1 FRESH OIL + TURB PH2 F1 WATER AFTER 4 MONTH

LISTING OF EXPERIMENT DATASET PAGE 1 OCT-29-1981

EXPERIMENT: ALA 1
MEDIUM: WATER FRACTION TYPE: 2

	SP-LABEL	HRS	MINS	TEMPERATURES AIR	WATER	OIL	COREXIT PRESENT	WIND SPEED	MIXING	COMMENTS
B7	9 AUG-21-1981	2880	0	15.00	11.00	.00	NO	.00	10.00	TANK 1 FRESH OIL + TURB PH2 F2 WATER AFTER 4 MONTH

LISTING OF EXPERIMENT DATASET PAGE 1 OCT-29-1981

EXPERIMENT: ALA 1
MEDIUM: WATER FRACTION TYPE: 3

	SP-LABEL	HRS	MINS	TEMPERATURES AIR	WATER	OIL	COREXIT PRESENT	WIND SPEED	MIXING	COMMENTS
15	1 AUG-23-1981	2880	0	15.00	11.00	.00	NO	.00	10.00	TANK 1 FRESH OIL + TURB PH2 F3 WATER AFTER 4 MONTH

LISTING OF EXPERIMENT DATASET PAGE 1 OCT-29-1981

EXPERIMENT: ALA 1
MEDIUM: OIL FRACTION TYPE: 0

	SP-LABEL	HRS	MINS	TEMPERATURES AIR	WATER	OIL	COREXIT PRESENT	WIND SPEED	MIXING	COMMENTS
34	13 MAY-03-1981	0	0	20.00	13.00	.00	NO	.00	10.00	TANK 1 TURB + FRESH OIL, TIMEZERO OIL SAMPLE
92	25 AUG-10-1981	2880	0	15.00	11.00	.00	NO	.00	10.00	TANK 1 TURB + FRESH OIL=BRN FLUID AFTER 4 MONTHS
135	15 SEP-21-1981	3600	0	15.00	11.00	.00	NO	.00	10.00	TANK 1 TURB + FRESH OIL=POOLED OIL SAMPLED AFTER 5 MONTH
135	5 SEP-11-1981	3600	0	15.00	11.00	.00	NO	.00	10.00	TANK 1 TURB + FRESH OIL = OIL SAMPLED AFTER 5 MONTH

LISTING OF EXPERIMENT DATASET PAGE 1 OCT-29-1981

EXPERIMENT: ALA 1
MEDIUM: FILM FRACTION TYPE: 0

	SP-LABEL	HRS	MINS	TEMPERATURES AIR	WATER	OIL	COREXIT PRESENT	WIND SPEED	MIXING	COMMENTS
5A	5 SEP-29-1981	3600	0	15.00	11.00	.00	NO	.00	10.00	TANK 1 TURB + FRESH OIL = SURFACE FILM AFTER 5 MONTH

TABLE 5-5 B OUTDOOR TANK #2 OIL, WATER AND AIR SAMPLING TIMES

Blank, 0 hr, 1 hr, 7.5 hrs, 26 hrs, 53 hrs, 93 hrs, 150 hrs,
4 months, 6 months

Computer listing of analyzed samples with reduced data in EXP data base of Oil Weathering Model

LISTING OF EXPERIMENT DATASET — PAGE 1 OCT-30-1981

EXPERIMENT: ALA 2
MEDIUM: OIL FRACTION TYPE: 0

	HR-LABEL	HRS	MINS	TEMPERATURES AIR	WATER	OIL	COREXIT PRESENT	WIND SPEED	MIXING	COMMENTS
15	20 MAY-09-1981	0	0	20.00	13.00	.00	YES	.00	.00	TANK 2 MOUSSE+ COREXIT+TIME ZERO OIL SAMPLE
93	24 MAY-04-1981	53	0	.00	13.00	.00	YES	.00	.00	TANK 2 MOUSSE +COREXIT+OIL SAMPLED AFTER 53 HOURS
18	3 AUG-09-1981	2880	0	15.00	11.00	.00	YES	.00	.00	TANK 2 MOUSSE +COREXIT+ OIL SAMPLE AFTER 4 MONTHS
103	3 SEP-08-1981	3600	0	15.00	11.00	.00	YES	.00	.00	TANK 2 MOUSSE +COREXIT = MOUSSE SAMPLED AFTER 5 MONTH
16	2 APR-24-1981	4320	0	20.00	13.00	.00	YES	.00	.00	TANK 2 MOUSSE PLUS COREXIT AFTER 6 MONTHS
77	15 OCT-02-1981	4320	0	15.00	11.00	.00	YES	.00	.00	TANK 2 MOUSSE +COREXIT=MOUSSE SAMPLED AFTER 6 MONTHS

LISTING OF EXPERIMENT DATASET PAGE 1 OCT-29-1981

EXPERIMENT: ALA 2
MEDIUM: FILM FRACTION TYPE: 0

	HR-LABEL	HRS	MINS	TEMPERATURES AIR	WATER	OIL	COREXIT PRESENT	WIND SPEED	MIXING	COMMENTS
19	5 AUG-09-1981	2880	0	15.00	11.00	.00	YES	.00	.00	TANK 2 MOUSSE +COREXIT+SURFACE FILM AFTER 4 MONTHS

LISTING OF EXPERIMENT DATASET PAGE 1 OCT-29-1981

EXPERIMENT: ALA 2
MEDIUM: WATER FRACTION TYPE: 1

	HR-LABEL	HRS	MINS	TEMPERATURES AIR	WATER	OIL	COREXIT PRESENT	WIND SPEED	MIXING	COMMENTS
75	23 AUG-30-1981	2880	0	15.00	11.00	.00	YES	.00	.00	TANK 2 MOUSSE +COREXIT+PH2 P1WATER AFTER 4 MONTHS

LISTING OF EXPERIMENT DATASET PAGE 1 OCT-29-1981

EXPERIMENT: ALA 2
MEDIUM: WATER FRACTION TYPE: 2

	HR-LABEL	HRS	MINS	TEMPERATURES AIR	WATER	OIL	COREXIT PRESENT	WIND SPEED	MIXING	COMMENTS
58	11 AUG-21-1981	2880	0	15.00	11.00	.00	YES	.00	.00	TANK 2 MOUSSE + COREXIT+PH2 P2 WATER AFTER 4 MONTHS

LISTING OF EXPERIMENT DATASET PAGE 1 OCT-29-1981

EXPERIMENT: ALA 2
MEDIUM: WATER FRACTION TYPE: 0

	HR-LABEL	HRS	MINS	TEMPERATURES AIR	WATER	OIL	COREXIT PRESENT	WIND SPEED	MIXING	COMMENTS
26	27 APR-27-1981	4320	0	20.00	13.00	.00	YES	.00	.00	TANK 2 MOUSSE PLUS COREXIT H2O SAMPLE 6 MONTHS

TABLE 5-6 C OUTDOOR TANK #3 OIL, WATER AND AIR SAMPLING TIMES

Blank, 0 hr, 1 hr, 6 hrs, 24 hrs, 93 hrs, 150 hrs,
4 months, 6 months

Computer listing of analyzed samples with reduced data in EXP data base of Oil Weathering Model

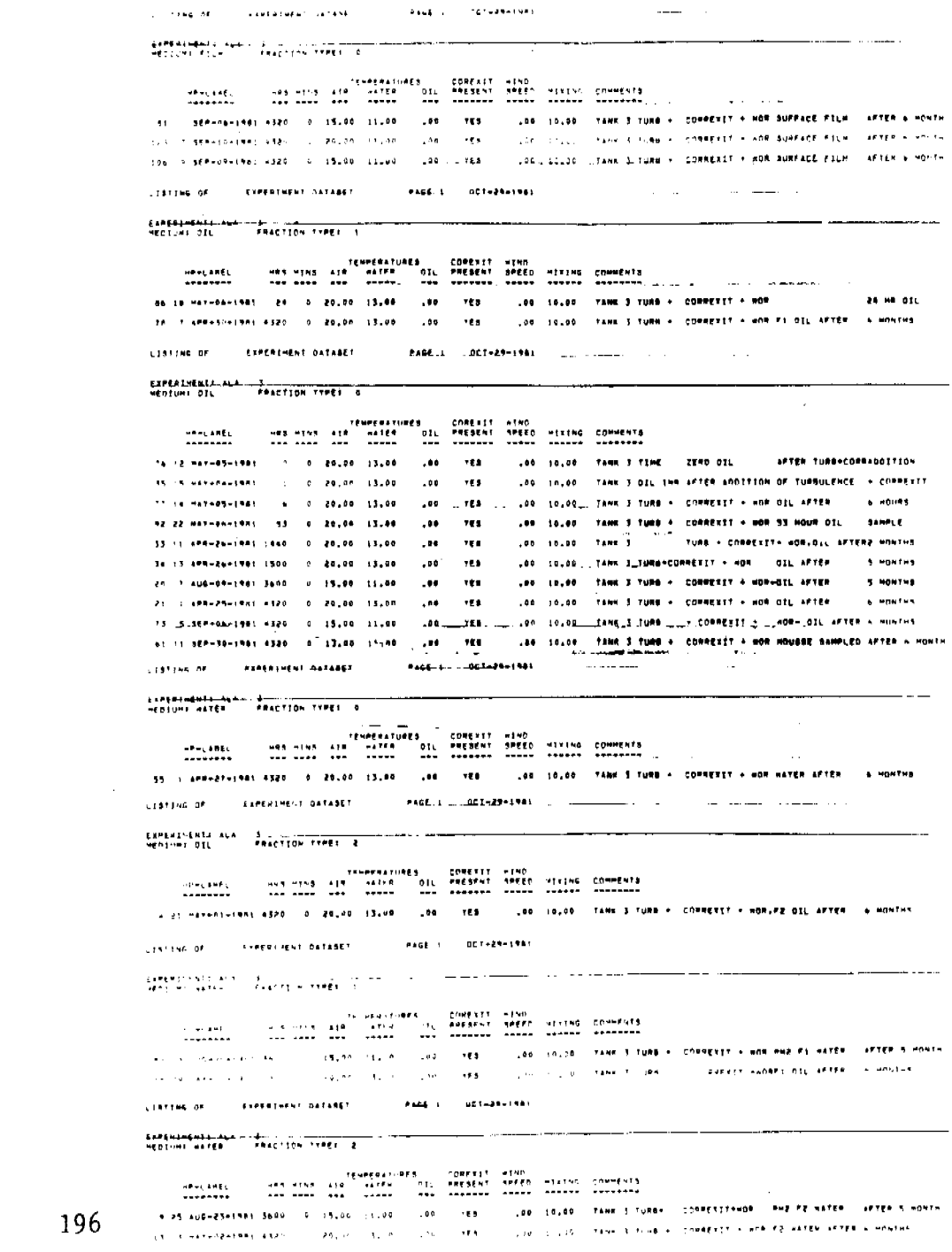

TABLE 5-6 D OUTDOOR TANK #4 OIL, WATER AND AIR SAMPLING TIMES

Blank, 0 hr, 1 hr, 7.5 hrs, 26 hrs, 53 hrs, 93 hrs, 150 hrs,
4 months, 6 months

Computer listing of analyzed samples with reduced data in EXP data base of Oil Weathering Model

LISTING OF EXPERIMENT DATASET PAGE 1 OCT-29-1981

EXPERIMENT ALA 4
MEDIUM: WATER FRACTION TYPE: 3

	HP-LABEL	HRS	MINS	TEMPERATURES AIR	WATER	OIL	COREXIT PRESENT	WIND SPEED	MIXING	COMMENTS			
47	9 AUG-31-1981	2880	0	15.00	11.00	.00	NO	.00	.00	TANK 4 MOUSSE	ONLY	PH2 F3 WATER	AFTER 4 MONTH

LISTING OF EXPERIMENT DATASET PAGE 1 OCT-29-1981

EXPERIMENT ALA 4
MEDIUM: WATER FRACTION TYPE: 1

	HP-LABEL	HRS	MINS	TEMPERATURES AIR	WATER	OIL	COREXIT PRESENT	WIND SPEED	MIXING	COMMENTS			
70	3 AUG-20-1981	2880	0	15.00	11.00	.00	NO	.00	.00	TANK 4 MOUSSE	ONLY-PH2 WATER,F1,AFTER		4 MONTHS

LISTING OF EXPERIMENT DATASET PAGE 1 OCT-29-1981

EXPERIMENT ALA 4
MEDIUM: OIL FRACTION TYPE: 0

	HP-LABEL	HRS	MINS	TEMPERATURES AIR	WATER	OIL	COREXIT PRESENT	WIND SPEED	MIXING	COMMENTS			
21	14 MAY-10-1981	0	0	20.00	13.00	.00	NO	.00	.00	TANK 4 MOUSSE	ONLY = TIME	ZERO OIL	SAMPLE
39	29 AUG-10-1981	2880	0	15.00	11.00	.00	NO	.00	.00	TANK 4 MOUSSE	ONLY=NORMAL	MOUSSE AFTER	4 MONTHS
21	9 AUG-09-1981	2880	0	15.00	11.00	.00	NO	.00	.00	TANK 4 MOUSSE	ONLY = CRUSTY	ZERO OIL	4 MONTHS
129	23 SEP-11-1981	3600	0	15.00	11.00	.00	NO	.00	.00	TANK 4 MOUSSE	ONLY = MOUSSE	UNDER CRUST	AFTER 5 MONTH
110	17 SEP-08-1981	3600	0	15.00	11.00	.00	NO	.00	.00	TANK 4 MOUSSE	ONLY=STRANDED	CRUST SAMPLED	AFTER 5 MONTH
109	15 SEP-09-1981	3600	0	15.00	11.00	.00	NO	.00	.00	TANK 4 MOUSSE	ONLY = MOUSSE	SAMPLED AFTER	5 MONTHS
74	7 SEP-06-1981	3600	0	15.00	11.00	.00	NO	.00	.00	TANK 4 MOUSSE	ONLY = FLAKES	SAMPLED AFTER	5 MONTHS
12A	21 SEP-11-1981	3600	0	15.00	11.00	.00	NO	.00	.00	TANK 4 MOUSSE	ONLY = MOUSSE	UNDERSIDE AFTER	5 MONTHS
111	17 SEP-09-1981	3600	0	15.00	11.00	.00	NO	.00	.00	TANK 4 MOUSSE	ONLY=STRANDED	OIL CRUST	AFTER 5 MONTH
107	11 SEP-09-1981	3600	0	15.00	11.00	.00	NO	.00	.00	TANK 4 MOUSSE	ONLY = CRUST	SAMPLED AFTER	5 MONTHS
108	13 SEP-09-1981	3600	0	15.00	11.00	.00	NO	.00	.00	TANK 4 MOUSSE	ONLY = UNDER	CRUST SAMPLED	AFTER 5 MONTH
63	15 SEP-30-1981	4320	0	15.00	11.00	.00	NO	.00	.00	TANK 4 MOUSSE	ONLY = MOUSSE	SAMPLED AFTER	6 MONTHS
64	17 SEP-30-1981	4320	0	15.00	11.00	.00	NO	.00	.00	TANK 4 MOUSSE	ONLY = CRUSTY	MOUSSE SAMPLED	AFTER 6 MONTH

TABLE 5-6E OUTDOOR TANK #5 OIL, WATER AND AIR SAMPLING TIMES

Blank, 0 hr, 1 hr, 8 hrs, 26 hrs, 53 hrs, 93 hrs, 150 hrs,
4 months

Computer listing of analyzed samples with reduced data in EXP data base of Oil Weathering Model

LISTING OF EXPERIMENT DATABASE PAGE 1 OCT-29-1981

EXPERIMENT: ALA 5
MEDIUM: H2O FRACTION TYPE: 0

	HP-LABEL	HRS	MINS	TEMPERATURES AIR	WATER	OIL	COREXIT PRESENT	WIND SPEED	MIXING	COMMENTS
47	29 APR-27-1931	4320	0	20.00	13.00	.00	YES	.00	10.00	TANK 5 TURB + CORREXIT + FRESH OIL; 6 MONTHS

LISTING OF EXPERIMENT DATABASE PAGE 1 OCT-29-1981

EXPERIMENT: ALA 5
MEDIUM: OIL FRACTION TYPE: 0

	HP-LABEL	HRS	MINS	TEMPERATURES AIR	WATER	OIL	COREXIT PRESENT	WIND SPEED	MIXING	COMMENTS
36	17 MAY-04-1981	0	0	20.00	13.00	.00	YES	.00	10.00	TANK 5 TURB + CORREXIT+FRESH OIL;TIME ZERO OIL SAMPLE
46	20 MAY-05-1981	8	0	20.00	13.00	.00	YES	.00	10.00	TANK 5 TURB + CORREXIT+FRESH OIL-8 HOUR OIL SAMPLE
97	32 MAY-07-1981	53	0	20.00	13.00	.00	YES	.00	10.00	TANK 5 TURB + CORREXIT+FRESH OIL-93 HOUR OIL SAMPLE

LISTING OF EXPERIMENT DATABASE PAGE 1 OCT-29-1981

EXPERIMENT: ALA 5
MEDIUM: WATER FRACTION TYPE: 1

	HP-LABEL	HRS	MINS	TEMPERATURES AIR	WATER	OIL	COREXIT PRESENT	WIND SPEED	MIXING	COMMENTS
79	3 AUG-20-1981	2880	0	15.00	11.00	.00	YES	.00	10.00	TANK 5 FRESH OIL+CORREXIT+ TURB+PH2 F1 H2OAFTER 4 MONTH

LISTING OF EXPERIMENT DATABASE PAGE 1 OCT-29-1981

EXPERIMENT: ALA 5
MEDIUM: WATER FRACTION TYPE: 3

	HP-LABEL	HRS	MINS	TEMPERATURES AIR	WATER	OIL	COREXIT PRESENT	WIND SPEED	MIXING	COMMENTS
53	5 AUG-31-1981	2880	0	15.00	11.00	.00	YES	.00	10.00	TANK 5 FRESH OIL + TURB + CORREXIT PH2 F3 H2O-4 MC

TABLE 5-6 F OUTDOOR TANK #6 OIL, WATER AND AIR SAMPLING TIMES

Blank, 0 hr, 1 hr, 6 hrs, 19 hrs, 30 hrs, 45 hrs, 100 hrs,
4 months

Computer listing of analyzed samples with reduced data in EXP data base of Oil Weathering Model

LISTING OF EXPERIMENT DATASET PAGE 1 OCT-29-1981

EXPERIMENT: ALA 6
MEDIUM: OIL FRACTION TYPE: 0

	HP-LABEL	HRS	MINS	TEMPERATURES AIR	WATER	OIL	COREXIT PRESENT	WIND SPEED	MIXING	COMMENTS
22	16 MAY-19-1981	0	0	20.00	13.00	.00	YES	.00	10.00	TANK 6 TURB + CORREXIT+MOUSSETIME ZERO OIL SAMPLE
58	9 AUG-12-1981	2880	0	15.00	11.00	.00	YES	.00	10.00	TANK 6 MOUSSE +CORREXIT+TURB OIL AFTER 4 MONTHS

LISTING OF EXPERIMENT DATASET PAGE 1 OCT-29-1981

EXPERIMENT: ALA 6
MEDIUM: WATER FRACTION TYPE: 1

	HP-LABEL	HRS	MINS	TEMPERATURES AIR	WATER	OIL	COREXIT PRESENT	WIND SPEED	MIXING	COMMENTS
11	29 AUG-23-1981	2880	0	15.00	11.00	.00	YES	.00	10.00	TANK 6 MOUSSE + CORREXIT + TURB;PH2 WATER F1 AFTER 4 MO

LISTING OF EXPERIMENT DATASET PAGE 1 OCT-29-1981

EXPERIMENT: ALA 6
MEDIUM: WATER FRACTION TYPE: 2

	HP-LABEL	HRS	MINS	TEMPERATURES AIR	WATER	OIL	COREXIT PRESENT	WIND SPEED	MIXING	COMMENTS
85	5 AUG-21-1981	2880	0	15.00	11.00	.00	YES	.00	10.00	TANK 6 MOUSSE+ CORREXIT+TURB PH2:F2 WATER AFTER 4 MONTH

LISTING OF EXPERIMENT DATASET PAGE 1 OCT-29-1981

EXPERIMENT: ALA 6
MEDIUM: WATER FRACTION TYPE: 3

	HP-LABEL	HRS	MINS	TEMPERATURES AIR	WATER	OIL	COREXIT PRESENT	WIND SPEED	MIXING	COMMENTS
2	25 AUG-22-1981	2880	0	15.00	11.00	.00	YES	.00	10.00	TANK 6 MOUSSE+ CORREXIT+TURB PH2 F3 WATER AFTER 4 MONTH

TABLE 5-6 G OUTDOOR TANK #7 OIL, WATER AND AIR SAMPLING TIMES

6 months, 11 months

Computer listing of analyzed samples with reduced data in EXP data base of Oil Weathering Model

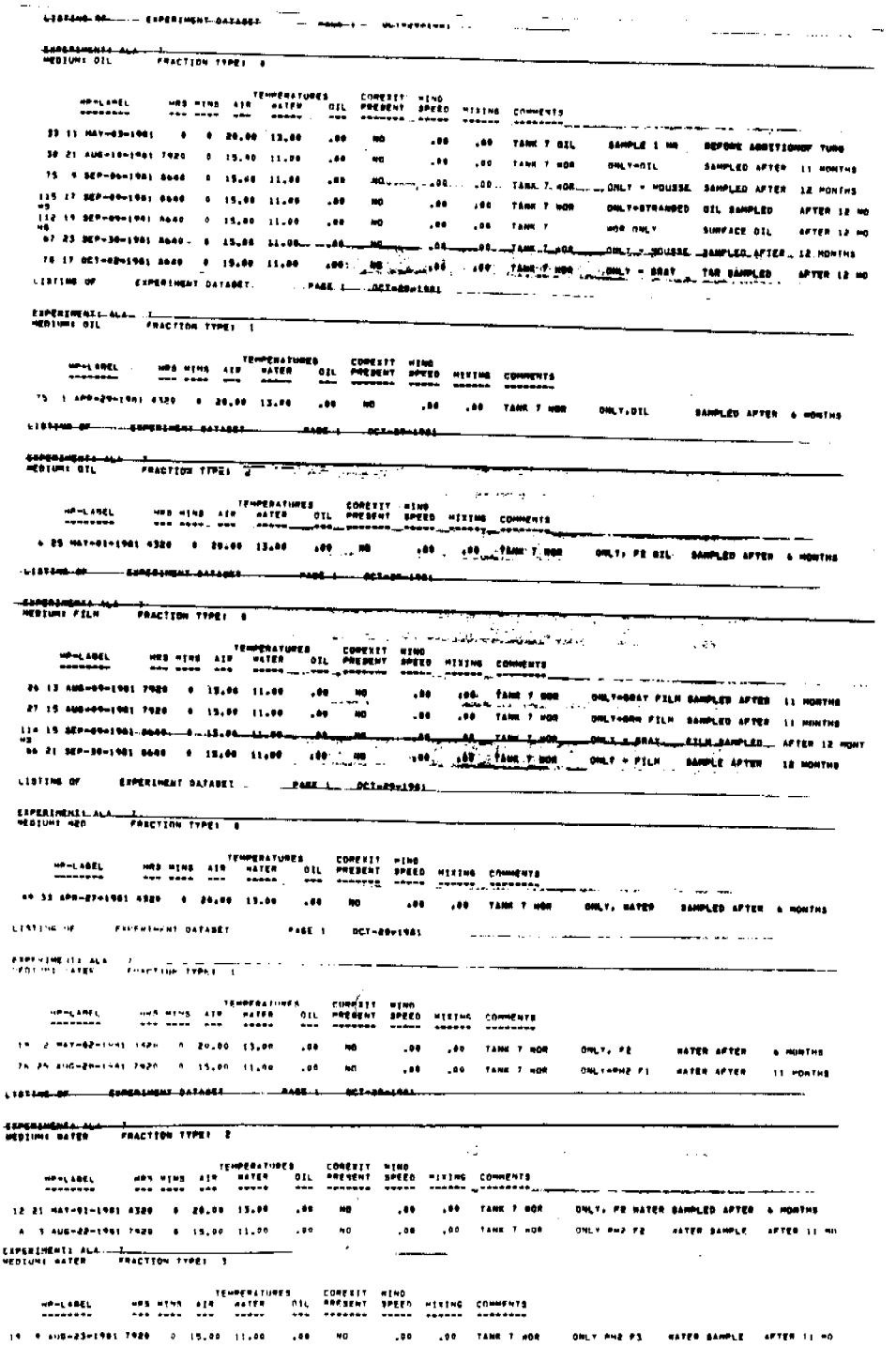

TABLE 5-6 H OUTDOOR TANK #8 OIL, WATER AND AIR SAMPLING TIMES

Blank, 0 hr, 1 hr, 6 hrs, 19 hrs, 30 hrs, 45 hrs, 100 hrs,
4 months

Computer listing of analyzed samples with reduced data in EXP data base of Oil Weathering Model

LISTING OF EXPERIMENT DATASET PAGE 1 OCT-29-1981

EXPERIMENT: ALA 0
MEDIUM: OIL FRACTION TYPE: 0

	MP-LABEL	HRS	MINS	TEMPERATURES AIR	WATER	OIL	COREXIT PRESENT	WIND SPEED	MIXING	COMMENTS
59	11 AUG-12-1981	2880	0	15.00	11.00	.00	NO	.00	10;00	TANK 8 MOUSSE +TURB=MOUSSE SAMPLED AFTER 4 MONTHS

LISTING OF EXPERIMENT DATASET PAGE 1 OCT-29-1981

EXPERIMENT: ALA 0
MEDIUM: WATER FRACTION TYPE: 1

	MP-LABEL	HRS	MINS	TEMPERATURES AIR	WATER	OIL	COREXIT PRESENT	WIND SPEED	MIXING	COMMENTS
60	29 AUG-29-1981	2880	0	15.00	11.00	.00	NO	.00	10;00	TANK 8 MOUSSE +TURB=PH2 F1 WATER AFTER 4 MONTHS

LISTING OF EXPERIMENT DATASET PAGE 1 OCT-29-1981

EXPERIMENT: ALA 0
MEDIUM: WATER FRACTION TYPE: 2

	MP-LABEL	HRS	MINS	TEMPERATURES AIR	WATER	OIL	COREXIT PRESENT	WIND SPEED	MIXING	COMMENTS
13	33 AUG-23-1981	2880	0	15.00	11.00	.00	NO	.00	10;00	TANK 8 MOUSSE +TURB PH2 F2 WATER SAMPLE AFTER 4 MONTH

LISTING OF EXPERIMENT DATASET PAGE 1 OCT-29-1981

EXPERIMENT: ALA 0
MEDIUM: WATER FRACTION TYPE: 3

	MP-LABEL	HRS	MINS	TEMPERATURES AIR	WATER	OIL	COREXIT PRESENT	WIND SPEED	MIXING	COMMENTS
20	11 AUG-24-1981	2880	0	.00	.00	.00	NO	.00	10;00	TANK 8 MOUSSE +TURB PH2 F3 WATER SAMPLE AFTER 4 MONTH

presumably evaporation/dissolution (PAYNE, 1981). TWARDUS (1980) indicated that no quantitative data existed on how mousse affects evaporation, but it was suspected that once mousse formation occurred, evaporation would occur at reduced rates. Similar predictions have been made by NOGATA and KONDO (1977), and, in our Spring 1981 experiments, attempts were made to quantify any differences in lower molecular weight volatile compound losses from fresh Prudhoe Bay crude oil and artificially (shaker table) generated mousse where evaporation was prevented during mousse formation in a sealed teflon container. Specifically, in this experiment, a water-in-oil emulsion (or artificial mousse) was generated with fresh Prudhoe Bay crude oil by mixing 80 parts filtered seawater with 20 parts fresh oil in sealed teflon containers on a shaker table for 48 hours.

This fresh mousse was then poured onto the water surface in Outdoor Tank #8 and propeller driven turbulence was introduced to determine if differential rates of lower molecular weight hydrocarbon losses occurred in the more viscious water-in-oil emulsion compared to fresh Prudhoe Bay crude (Tank No. 1). As in the corresponding evaporation/dissolution chamber experiments in La Jolla, volatile compound concentrations were measured in the air 1 to 2 inches above the slick by pumping measured volumes of air through stainless steel columns packed with Tenax® at different time intervals following the spills. In both Tanks 1 and 8, turbulence was induced by propeller mixing. The water and air temperatures at the time of sampling were 6° and 6 to 12°C, respectively. After sampling, the Tenax® traps were capped with stainless Swagelok® fittings and stored at room temperature until FID GC analyses, using the procedures described in Appendix B. Backup columns in series with the front columns showed no breakthrough of lower molecular weight material 95+% recovery on the front traps. Interestingly, the qualitative appearance of the temperature programmed components of the volatiles from both systems were remarkedly similar (PAYNE, 1981), and the time-series data presented graphically in Figures 5-34A and 5-34B illustrate that essentially identical losses of lower molecular weight compounds ranging from butane to xylene were obtained for both the fresh oil and fresh mousse. The data in Figure 5-34C; however, show

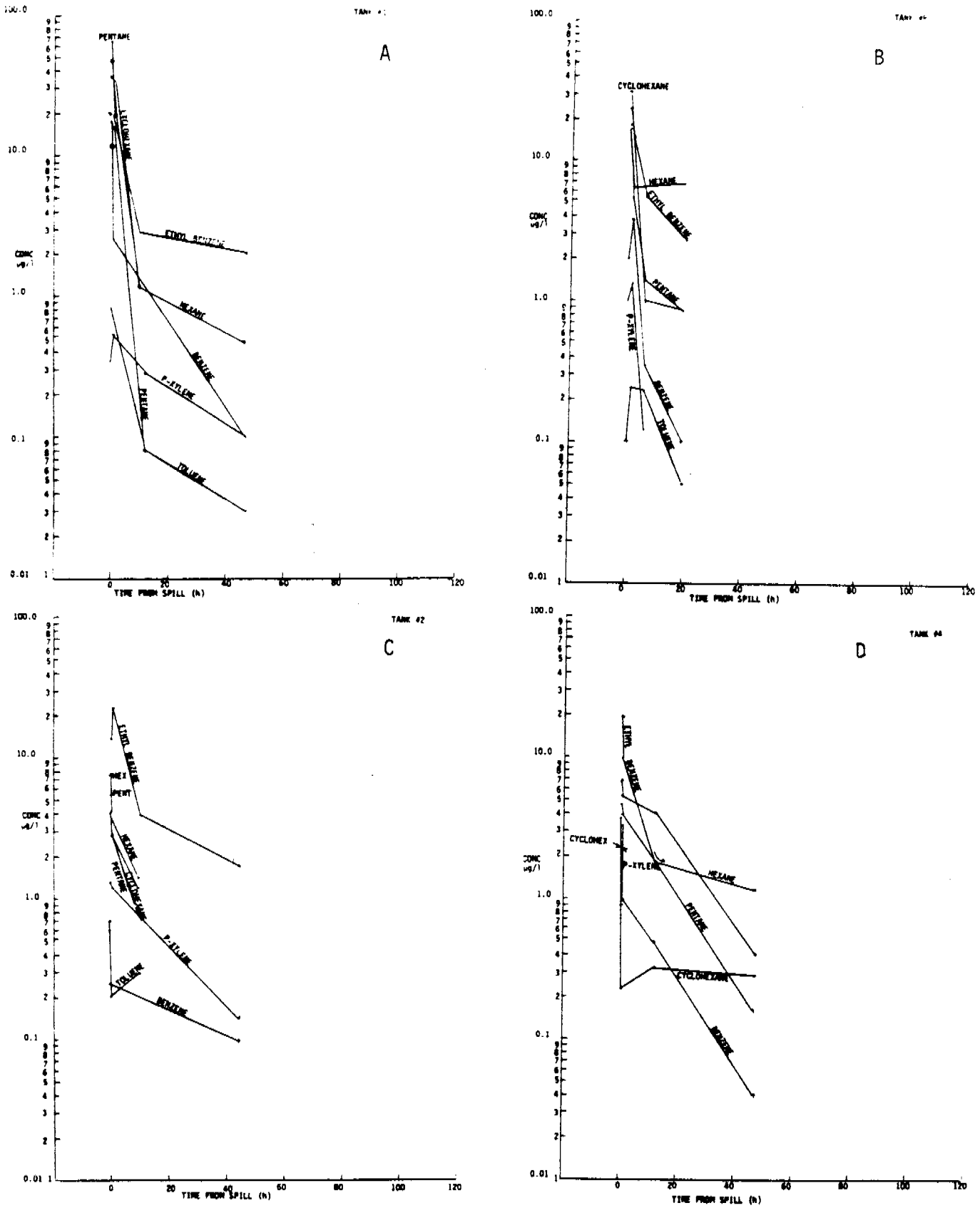

FIGURE 5-34. TENAX TRAP/FID GC DATA ON SUB-ARCTIC VOLATILE COMPONENT LOSS FROM PRUDHOE BAY CRUDE OIL AND MOUSSE ON FLOW-THROUGH SEAWATER ENCLOSURES IN KASITSNA BAY, ALASKA. A) FRESH OIL AND TURBULANCE; B) FRESH MOUSSE AND TURBULANCE; C) FRESH MOUSSE (NO TURBULANCE); D) FRESH MOUSSE AND COREXIT 9527 (NO TURBULANCE). WATER TEMP 6°C, AIR TEMP 6-13°C.

slightly longer retention of these compounds in mousse spread on seawater in the absence of turbulence. One of the static (non-propeller mixed) mousse systems (Tank 2) was also treated with Corexit 9527 immediately after the spill (Figure 5-34D), but this apparently did not affect evaporation loss compared to the non-dispersant treated control (Figure 5-34C).

Figure 5-35 presents selected time-series glass capillary gas chromatographic profiles obtained on the fresh oil samples in the flow-through tank in the presence of turbulence (Tank 1). The sampling points in Figure 5-35 are for times of: 1 hour, 26 hours, 4 months and 6 months. Figure 5-36 presents the time-series gas chromatographic profiles obtained on the artificially generated mousse in the presence of turbulence at sampling times 0, 30 hours and 4 months (Tank 8). Very similar losses of the lower molecular weight components below nC-9 appeared to have occurred in both the fresh oil and artificial mousse experiments however, slightly longer retention of lower molecular weight components is suggested in the artificial mousse case when examining the four month data (Figure 5-36C). Also, while only limited or no microbial degradation is suggested during the first 24 to 30-hour period, more significant microbial utilization of the aliphatics as opposed to the branched chain isoprenoids can be observed in the four month old samples from both the fresh crude and artificially generated mousse. In the fresh oil plus turbulence experiment, the nC-17/pristane and nC-18/phytane ratios dropped to 0.38 and 0.51, respectively after four months, and in the chromatogram of the four month old weathered mousse (Figure 5-36C) the nC-17/pristane and nC-18/phytane ratios dropped to 0.75 and 0.92, respectively. The values for these ratios in fresh Prudhoe Bay crude oil are 1.7 and 1.6, respectively. It should also be noted that after four months of weathering in both systems, the unresolved complex mixture had increased significantly. The effects of microbial degradation are even more striking in Figure 5-35D which presents the weathered sample from the fresh oil plus turbulence tank after 6 months of weathering during the sub-arctic summer months from June through October, 1981. In the 6 months old sample (Figure 5-35D) the isoprenoid compounds, pristane (Kovat 1710) and phytane (Kovat 1815) dominate all of the other resolved components.

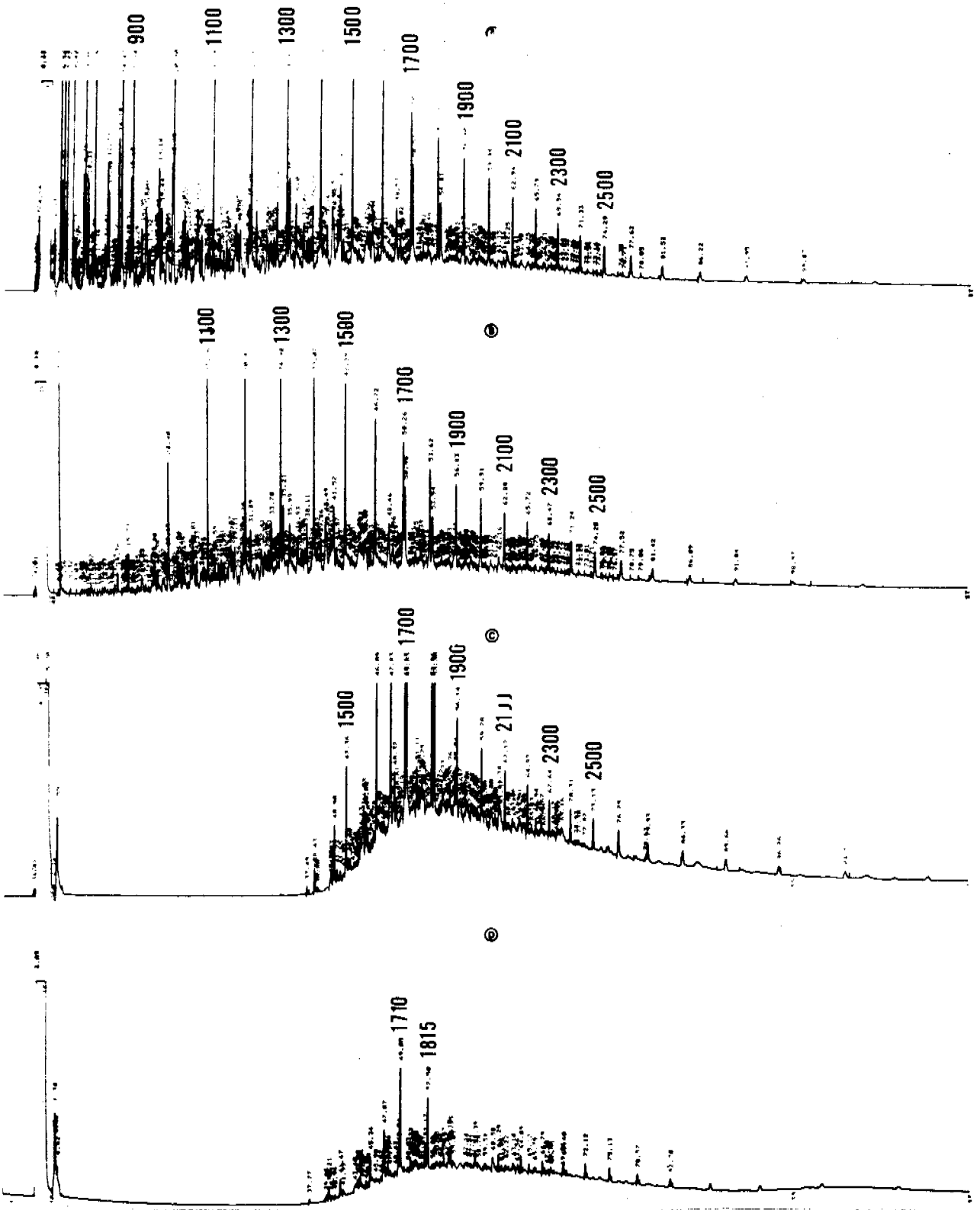

FIGURE 5-35. FLAME IONIZATION DETECTOR CAPILLARY GAS CHROMATOGRAMS OBTAINED ON PRUDHOE BAY CRUDE OIL WEATHERING IN THE PRESENCE OF PROPELLER DRIVEN TURBULANCE IN THE OUTDOOR FLOW-THROUGH AQUARIA (TANK #1) AT KASITSNA BAY, ALASKA. TIME-SERIES SAMPLING POINTS AFTER THE "SPILL": (A) 1 HOUR; (B) 26 HOURS, (C) 4 MONTHS; AND (D) 6 MONTHS.

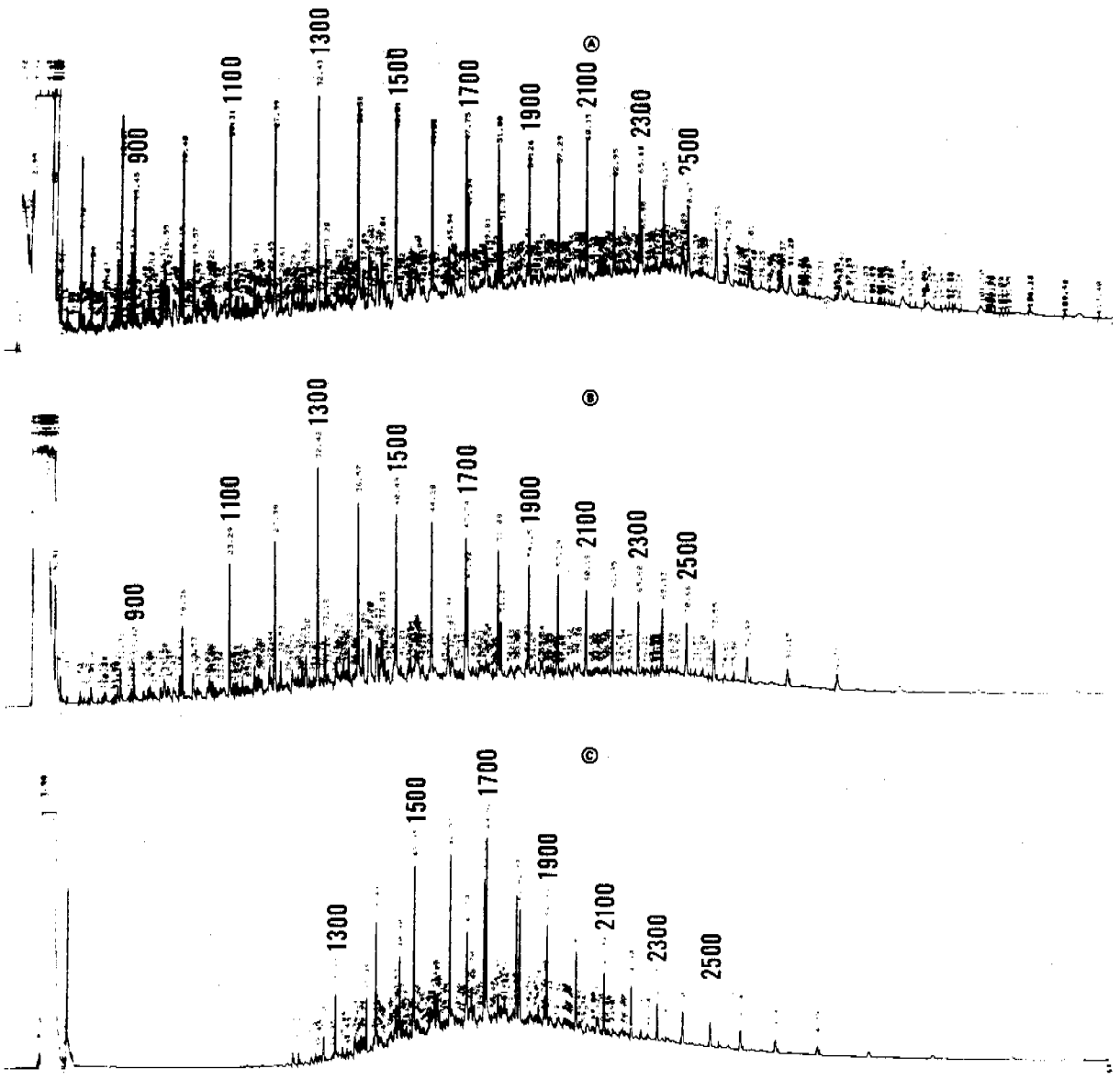

FIGURE 5-36. FLAME IONIZATION DETECTOR CAPILLARY GAS CHROMATOGRAMS OBTAINED ON ARTIFICALLY GENERATED MOUSSE (USING PRUDHOE BAY CRUDE OIL) WEATHERING IN THE PRESENCE OF PROPELLER DRIVEN TURBULANCE IN THE OUTDOOR FLOW-THROUGH AQUARIA (TANK #8) AT KASITSNA BAY, ALASKA. TIME-SERIES SAMPLING POINTS AFTER THE "SPILL" (A) 5 MIN; (B) 30 HOURS; AND (C) 4 MONTHS.

Easier comparisons of the relative retention of the higher molecular weight components can be made by examination of the computer generated time-series concentration profiles obtained from capillary FID gas chromatographic analyses of the oil and mousse from the well-stirred tanks as shown in Figure 5-37. Kovat indices for the compounds in each plot are identified in the figures, and these data confirm that compounds in the range of nC-9 through nC-11 are preferentially retained in the mousse sample for longer periods of time (Figures 5-37A and C). Figures 5-38A and 5-38B show the time-series concentrations of components with Kovat indices ranging from 1300 to 2000 for the oil and artificially generated mousse samples, respectively. A similar relative increase in these higher molecular weight compound concentrations (in μg/g oil) is noted for both the oil and mousse after approximately 25 hours, and this is due to the removal of significant mass of the oil by evaporation of the lower molecular weight components (compounds with molecular weights above nC-15 are not lost during this time frame). Absolute concentrations of the individual components in each of the mousse sample plots (on a μg/g of mousse basis) are lower than those of the fresh oil because of the additional mass of seawater (80% by weight) in the water-in-oil emulsions.

Thus, in the presence of turbulence in these studies, the higher viscosity of the 80% water-in-oil mousse did not significantly affect evaporative loss of the lower molecular weight components boiling below xylene, but some reduction in evaporation was noted for intermediate molecular weight compounds (Kovat indices 800 to 1100) in the mousse. More significant differences were noted in the amounts of oil and fresh mousse that were dissolved and dispersed into the water column due to the turbulent regimes, and Table 5-7 presents selected time series water column concentrations for the two systems. The three orders of magnitude difference between the fresh oil and fresh mousse systems clearly reflects the latter's resistance towards dissolution and dispersion to droplets.

Figure 5-39 presents the glass capillary gas chromatograms on the time series oil samples from outdoor tank #5 from the Spring 1981 experiments

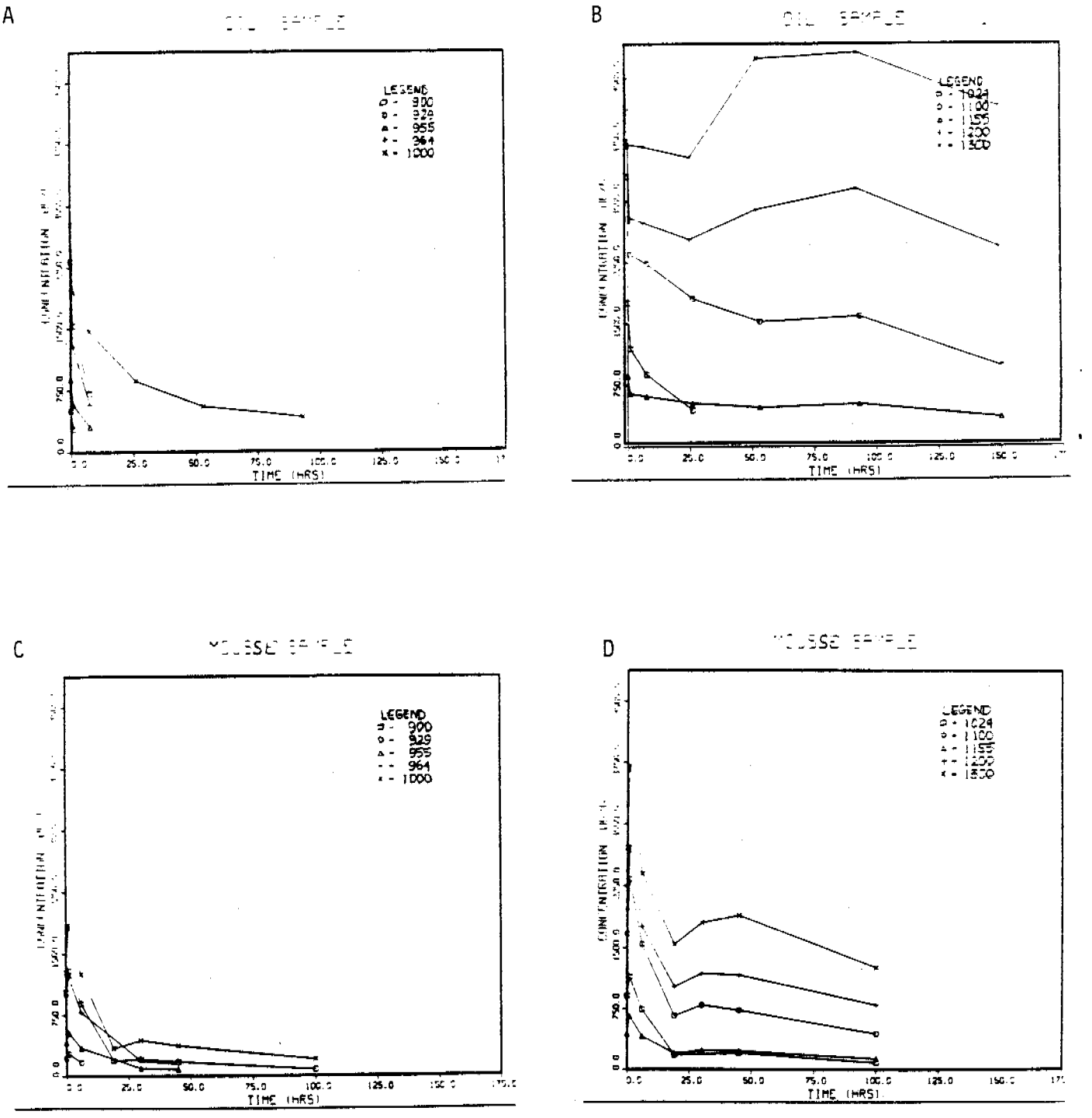

FIGURE 5-37. COMPUTER GENERATED PLOTS OF CAPILLARY FID-GC INTERMEDIATE MOLECULAR WEIGHT COMPONENTS REMAINING IN PRUDHOE BAY CRUDE OIL AND MOUSSE WEATHERING UNDER SUB-ARCTIC CONDITIONS ON FLOW-THROUGH SEAWATER ENCLOSURES AT KASITSNA BAY, ALASKA. KOVAT INDICES ARE IDENTIFIED ON EACH PLOT. A AND B-FRESH PRUDHOE BAY CRUDE AND TURBULANCE; C AND D-FRESH PRUDHOE BAY MOUSSE AND TURBULANCE. TEMPERATURE AS IN FIGURE 5-34.

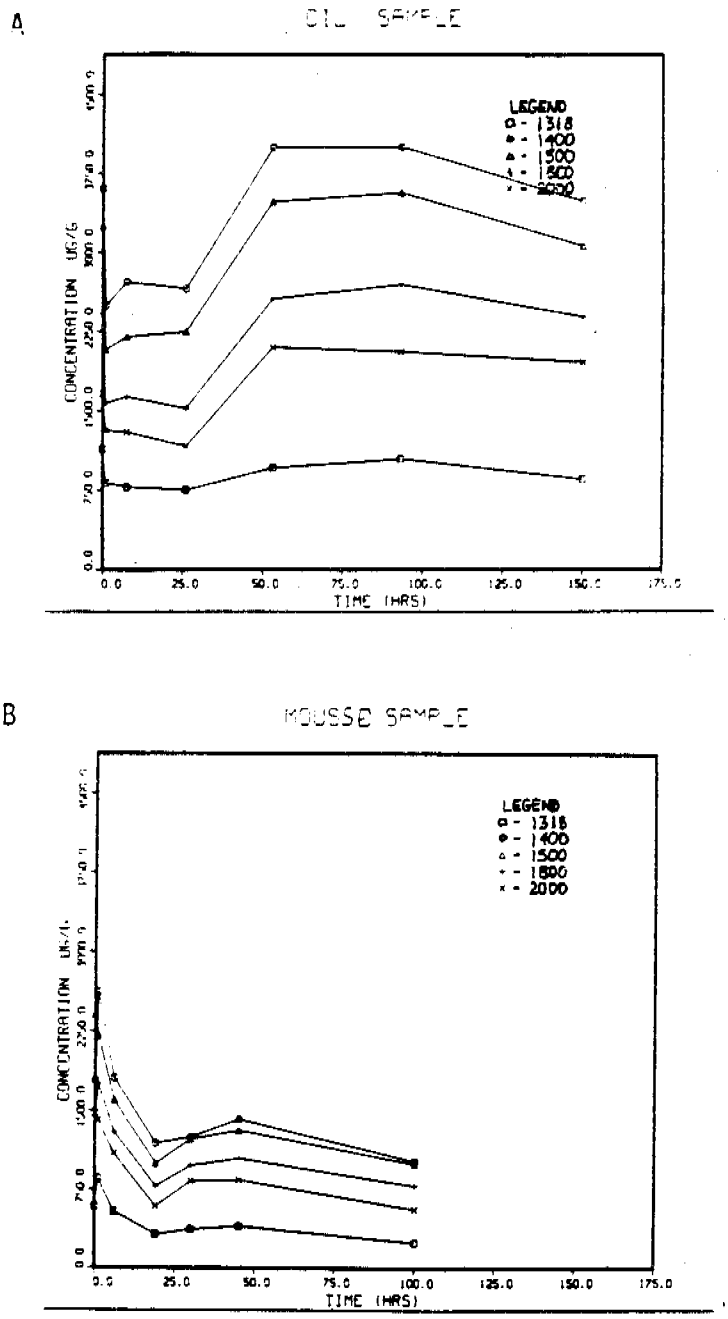

FIGURE 5-38. COMPUTER GENERATED PLOTS OF CAPILLARY FID-GC DATA ON HIGHER MOLECULAR WEIGHT COMPONENTS REMAINING IN PRUDHOE BAY CRUDE OIL AND MOUSSE WEATHERING UNDER SUB-ARCTIC CONDITIONS ON FLOW-THROUGH SEAWATER ENCLOSURES AT KASITSNA BAY, ALASKA. KOVAT INDICES ARE IDENTIFIED ON EACH PLOT AND ENVIRONMENTAL CONDITIONS ARE AS IN FIGURE 5-34.

TABLE 5-7. TIME-SERIES WATER COLUMN CONCENTRATIONS (μg/l) OF DISSOLVED AND DISPERSED HYDROCARBONS FROM FRESH PRUDHOE BAY CRUDE OIL AND MOUSSE WEATHERING ON FLOW-THROUGH SEAWATER ENCLOSURES (TURBULENT REGIME) AT KASITSNA BAY, ALASKA. (WATER TEMPERATURE 6°C, AIR TEMPERATURE 6-13°C). CONCENTRATIONS DETERMINED BY CAPILLARY TEMPERATURE-PROGRAMMED FID GAS CHROMATOGRAPHY.

Fresh Oil	0 hrs	1 hrs	7.5 hrs	26 hrs	53 hrs
Resolved Components	7200	4740	1400	10110+	659
Unresolved Complex Mixture	3140	1460	420	447	114

Fresh Mousse*	0 hrs	1 hrs	6 hrs	19 hrs	30 hrs	45 hrs	100 hrs
Resolved Components	23	7	29	18	10	24	34
Unresolved Complex Mixture	ND	ND	12	45	37	69	59

*Water column concentrations corrected for total oil volume added as "mousse."

ND = none detected

+Possibly due to excessive oil droplet entrainment

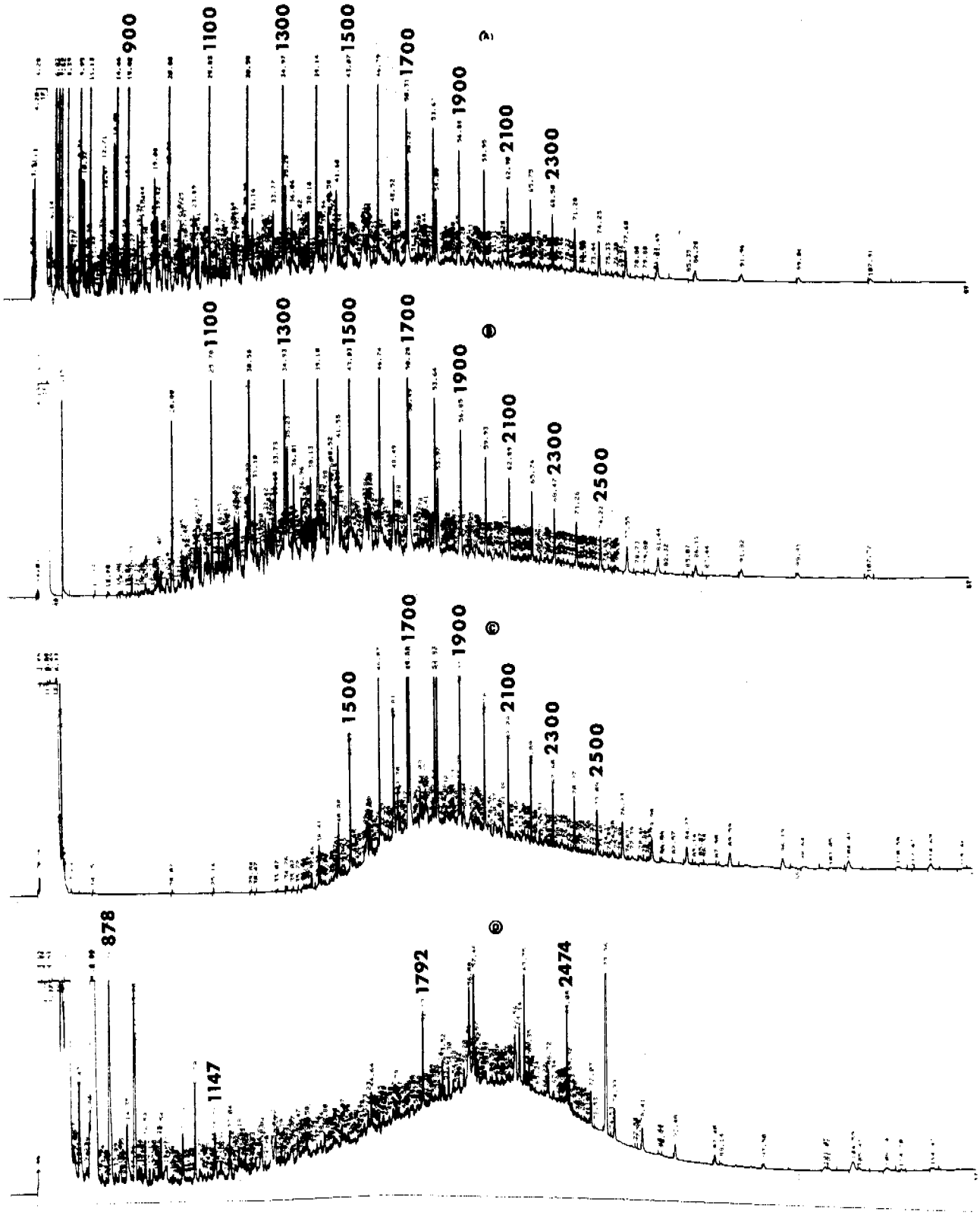

FIGURE 5-39. FLAME IONIZATION DETECTOR CAPILLARY GAS CHROMATOGRAMS OBTAINED ON PRUDHOE BAY CRUDE OIL PLUS COREXIT (OIL:COREXIT = 20:1) WEATHERING IN THE PRESENCE OF PROPELLER DRIVEN TURBULANCE IN THE OUTDOOR FLOW-THROUGH AQUARIA (TANK #5) AT KASITSNA BAY, ALASKA. TIME-SERIES SAMPLING POINTS AFTER THE "SPILL": (A) 1 HOURS; (B) 23 HOURS: (C) 4 MONTHS. CHROMATOGRAM D WAS OBTAINED ON THE POLAR (F3) FRACTION OBTAINED FROM AN ACIDIFIED WATER COLUMN SAMPLE AFTER 4 MONTHS OF IN SITU WEATHERING.

(fresh oil plus Corexit, 20:1, in the presence of turbulence). These data included to allow direct comparison to the fresh oil plus turbulence experiment in tank #1 over the same time frame as shown in Figure 5-35. As in the non Corexit fresh oil experiment, the most effective initial weathering mechanism was due to evaporation as compounds below Kovat indices 1000 were clearly lost during the first 24 hours. Visual observation of the water column extracts from this tank, however, also indicated that enhanced removal of oil into the water column occurred as a result of the dispersant. Water column extracts are undergoing analyses at this time.

As noted above, the tanks were maintained in a flow-through condition during the period of April to October 1981 to allow indigenous microbial populations to be fully operative, and Figure 5-39C shows the chromatographic profiles obtained on the Corexit treated oil after 4 months of weathering. Interestingly, the chromatogram is nearly identical to the chromatogram in Figure 5-36C, the patchy mousse from stirred Tank 1 which was not treated with Corexit in April. As in the other case, most of the components below nC-14 have been removed by evaporation and dissolution processes during the warmer summer months, and the change in the nC-17/pristane and nC-18/phytane ratios to values of 1.1 and 1.0, respectively, illustrates the effects of microbial degradation. Surprisingly, the decrease in these ratios is not as great as that observed for Tank 1, although this is quite possibly due to the fact that the oil sample from Tank 5 was scraped from the side of the tank and not taken from the water surface. Unfortunately, some time during the four month weathering period between April and July, the water level in Tank 5 increased and overflowed and much of the oil was lost. After the water level was returned to the appropriate height in the outdoor tank, the stranded oil was then not subject to additional degradation from water-borne micro-organisms.

This observation is in line with similar findings by BLUMER et al. (1973) where they studied stranded oil on intertidal rocks from the beaches of Bermuda. In their studies, oil which was stranded in the upper intertidal zones away from the water showed only limited degradation due to bacterial processes, and weathering was limited to evaporation and photo-oxidation.

The chromatogram in Figure 5-39D shows the water column extract of the aromatic fraction under the oil after 4 months weathering during the spring and summer months. In that the tank overflowed sometime during that period, it might a priori be expected that more of the water soluble components would be lost due to air-sea exchange. Furthermore, since the tanks were maintained in a flow-through condition during this period, removal of water soluble components by advection might be anticipated. There are still significant levels of aromatic components remaining in the water column over this time period, although the lower molecular weight aromatics from benzene through naphthalene have been removed.

As noted in Table 5-6, additional time series (up to 150 hours) samples and chromatograms were obtained on the other outside tank experiments shown schematically in Figure 5-32. Some of these tank experiments are considered in Section 5.2.5 which deals with longer term microbial degradation results, and others are in various stages of analyses and computer data reduction. As such, they will not be discussed further here.

5.1.3 Outdoor Wave-Tank Experiments -- Kasitsna Bay

As noted above, the outdoor microbial degradation tanks were utilized for evaporation/dissolution experiments during the Spring 1981 program where turbulence was induced from propeller mixing. Even with this approach however, the turbulence regime was not entirely satisfactory and did not closely approximate that which would be observed in open ocean oil spill situations. Therefore, during the Summer 1981 program, a 2,500-L wave tank was designed and constructed on the outdoor platform supporting the trace organic geochemistry laboratory at Kasitsna Bay (Figure 5-40). The wave tank was equipped with a 7-foot diameter paddle-wheel at one end, with eight blades driven by a one horsepower electric motor via a chain/sprocket drive mechanism. To minimize contamination of water or oil samples from the construction materials of the tank itself, several precautions were taken. First, the tank was constructed of marine plywood and then coated with two coats of 2-part epoxy. After the

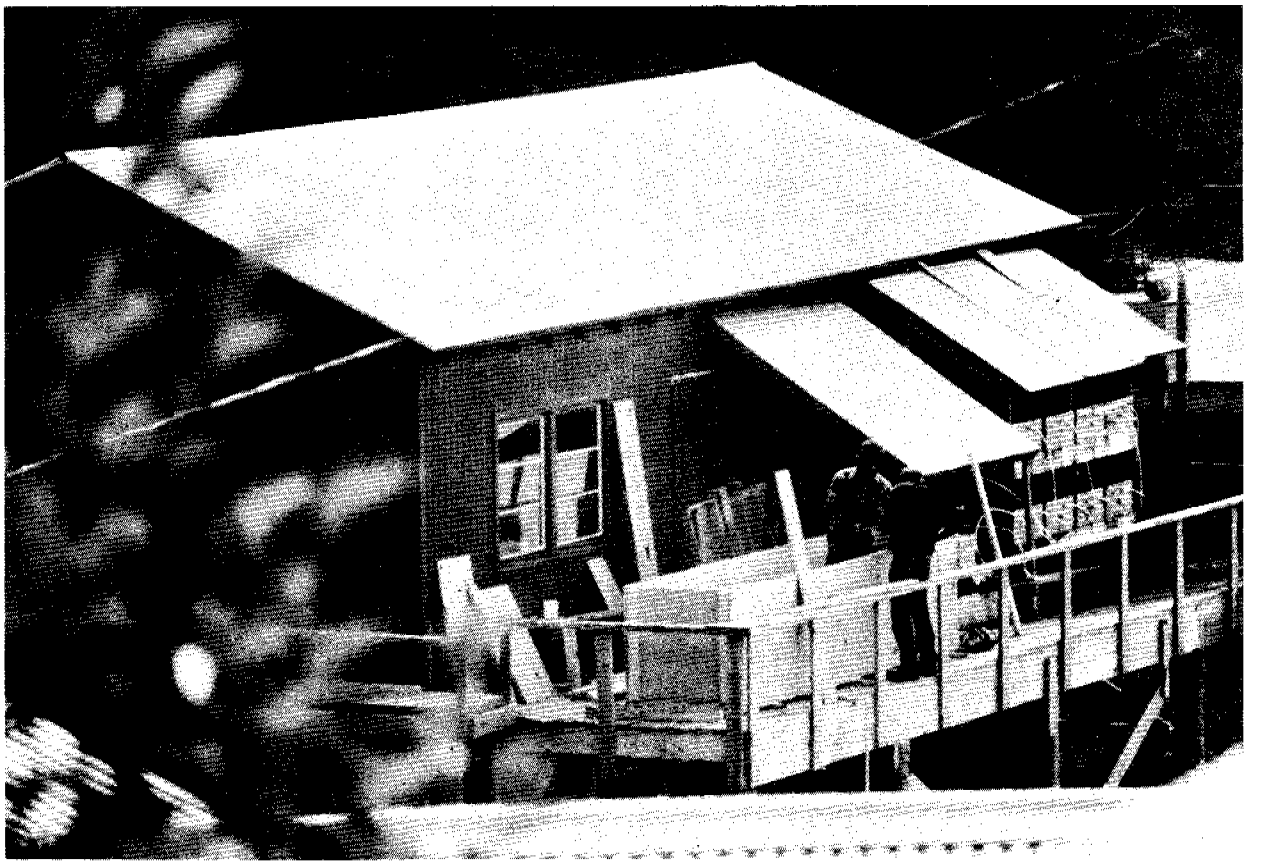

FIGURE 5-40. CONSTRUCTION OF THE 2,500 L WAVE TANK ON THE OUTDOOR PLATFORM ADJACENT TO THE ORGANIC GEOCHEMISTRY LABORATORY FACILITY AT KASITSNA BAY, ALASKA.

epoxy had cured for five days the tank was filled with seawater and the paddle wheel wave generation apparatus was actuated and allowed to run for 48 hours. At a reduced paddle-wheel speed of 12 rpm, 4 to 8 inch standing waves could be generated, and when progressing waves, slightly out of phase with the standing wave pattern randomly occurred, simulated wave breaking turbulence was obtained. With a seawater flow-through rate of 15 L/min and a tank turnover of one tank volume per 3 hours, this then assured that any organics which would be leached from the cured 2-part epoxy would be flushed from the tank during this initial rinse process. Furthermore, before any actual oil weathering experiments were undertaken the tank was completely drained and then refilled with fresh seawater and allowed to run again for a period of 12 hours before initiation of the actual oil weathering studies in September 1981.

After the initial curing and check out of the tank system, 15 L of Prudhoe Bay crude oil (Figure 5-41), were spilled into the tank and extended weathering was then allowed to occur with samples being collected over a 21-day period as shown in Table 5-8. At each sampling point, Tenax® trapped air samples were obtained to monitor volatile hydrocarbon concentrations in the atmosphere at a distance of 3 to 4 inches above the slick, and 20-L water samples were obtained to measure the time dependent dissolution of lower molecular weight aromatic compounds under these more realistic open ocean conditions. Oil samples were also obtained for compound-specific concentration determinations in the resultant slick and mousse (Figure 5-42).

When the oil was initially spilled, significant quantities of 1 to 10-mm sized droplets of dispersed oil were noted in the water column (through a window installed in the side of the tank) and estimates of these dispersed oil concentrations are being obtained from examination of whole seawater extracts obtained at the time series intervals shown in Table 5-8. After approximately 12 hours the significant dispersion phenomena ceased and the oil accumulated at the far end of the wave tank away from the turbulence introduced by the paddles.

FIGURE 5-41. INITIATION OF 16.5 L "OIL SPILL" IN THE 2,500 L WAVE TANK AT KASITSNA BAY, ALASKA. SEA-WATER FLOW-THROUGH RATE OF 15 L/MIN PROVIDING A TANK TURNOVER RATE OF 1 TANK VOLUME PER 3 HOURS HAS BEEN MAINTAINED DURING THIS LONG-TERM EXPERIMENT. STANDING WAVES ARE GENERATED WITH THE PADDLE-WHEEL SHOWN AT THE FAR END OF THE FIGURE.

TABLE 5-8. COMPUTER LISTING OF SAMPLES FROM WAVE TANK, KASITSNA BAY, ALASKA

LISTING OF HISTORY DATASET PAGE 1 OCT-28-1981

EXPERIMENT# WAVE 1
LOC PAGE: 70
STATUS: (1)
START DATE: SEP-09-1981
END DATE: OCT-04-1981

PRINCIPAL INVESTIGATOR: DR

OIL WAS SPILLED IN A WAVE TANK THAT WAS CONSTRUCTED AT KASITSNA BAY, ALASKA TO DETERMINE LONG TERM EFFECTS OF TURBULENCE ON WEATHERED KAY CRUDE.

LISTING OF EXPERIMENT DATASET PAGE 1 OCT-28-1981

EXPERIMENT# WAVE 1
MEDIUM: OIL FRACTION TYPE: 1

HR-LABEL	HRS	MINS	TEMPERATURES AIR	TEMPERATURES WATER	TEMPERATURES OIL	CORexIT PRESENT	WIND SPEED	MIXING	COMMENTS			
11A 1 SEP-09-1981	0	0	15.00	11.00	.00	NO	.00	10.00	WAVE TANK	TIME ZERO	OIL	SAMPLE
117 3 SEP-10-1981	1	0	15.00	11.00	.00	NO	.00	10.00	WAVE TANK	1 HOUR	OIL	SAMPLE
118 5 SEP-10-1981	3	0	15.00	11.00	.00	NO	.00	10.00	WAVE TANK	3 HOUR	OIL	SAMPLE
119 7 SEP-10-1981	6	0	15.00	11.00	.00	NO	.00	10.00	WAVE TANK	6 HOUR	OIL	SAMPLE
121 9 SEP-10-1981	12	0	15.00	11.00	.00	NO	.00	10.00	WAVE TANK	12 HOUR	OIL	SAMPLE
123 13 SEP-10-1981	24	0	15.00	11.00	.00	NO	.00	10.00	WAVE TANK	24 HOUR	OIL	SAMPLE
131 27 SEP-11-1981	36	0	15.00	11.00	.00	NO	.00	10.00	WAVE TANK	36 HOUR	OIL	SAMPLE
134 1 SEP-11-1981	48	0	15.00	11.00	.00	NO	.00	10.00	WAVE TANK	48 HOUR	OIL	SAMPLE
147 54 SEP-12-1981	72	0	15.00	11.00	.00	NO	.00	10.00	WAVE TANK	3 DAY	OIL	SAMPLE
161 9 SEP-15-1981	120	0	15.00	11.00	.00	NO	.00	10.00	WAVE TANK	5 DAY	OIL	SAMPLE
166 15 SEP-16-1981	132	0	15.00	11.00	.00	NO	.00	10.00	WAVE TANK	7 DAY	OIL	SAMPLE
19 21 SEP-20-1981	240	0	15.00	11.00	.00	NO	.00	10.00	WAVE TANK	10 DAY	OIL	SAMPLE
39 57 SEP-24-1981	336	0	15.00	11.00	.00	NO	.00	10.00	WAVE TANK	14 DAY	OIL	SAMPLE
85 11 OCT-02-1981	504	0	15.00	11.00	.00	NO	.00	10.00	WAVE TANK	21 DAY	OIL	SAMPLE

LISTING OF EXPERIMENT DATASET PAGE 1 OCT-28-1981

EXPERIMENT# WAVE 1
MEDIUM: AIR FRACTION TYPE: 0

HR-LABEL	HRS	MINS	TEMPERATURES AIR	TEMPERATURES WATER	TEMPERATURES OIL	CORexIT PRESENT	WIND SPEED	MIXING	COMMENTS			
0 0 SEP-09-1981	0	0	15.00	11.00	.00	NO	.00	10.00	WAVE TANK	TIME ZERO	AIR	SAMPLE
0 0 SEP-10-1981	1	0	15.00	11.00	.00	NO	.00	10.00	WAVE TANK	1 HOUR	AIR	SAMPLE
0 0 SEP-10-1981	3	0	15.00	11.00	.00	NO	.00	10.00	WAVE TANK	3 HOUR	AIR	SAMPLE
0 0 SEP-10-1981	6	0	15.00	11.00	.00	NO	.00	10.00	WAVE TANK	6 HOUR	AIR	SAMPLE
0 0 SEP-10-1981	12	0	15.00	11.00	.00	NO	.00	10.00	WAVE TANK	12 HOUR	AIR	SAMPLE
0 0 SEP-10-1981	24	0	15.00	11.00	.00	NO	.00	10.00	WAVE TANK	24 HOUR	AIR	SAMPLE
0 0 SEP-11-1981	36	0	15.00	11.00	.00	NO	.00	10.00	WAVE TANK	36 HOUR	AIR	SAMPLE
0 0 SEP-11-1981	48	0	15.00	11.00	.00	NO	.00	10.00	WAVE TANK	48 HOUR	AIR	SAMPLE
0 0 SEP-12-1981	72	0	15.00	11.00	.00	NO	.00	10.00	WAVE TANK	3 DAY	AIR	SAMPLE
0 0 SEP-15-1981	120	0	15.00	11.00	.00	NO	.00	10.00	WAVE TANK	5 DAY	AIR	SAMPLE
0 0 SEP-17-1981	172	0	15.00	11.00	.00	NO	.00	10.00	WAVE TANK	7 DAY	AIR	SAMPLE
0 0 SEP-20-1981	240	0	15.00	11.00	.00	NO	.00	10.00	WAVE TANK	10 DAY	AIR	SAMPLE
0 0 SEP-24-1981	336	0	15.00	11.00	.00	NO	.00	10.00	WAVE TANK	14 DAY	AIR	SAMPLE
0 0 OCT-02-1981	504	0	15.00	11.00	.00	NO	.00	10.00	WAVE TANK	21 DAY	AIR	SAMPLE

LISTING OF EXPERIMENT DATASET PAGE 1 OCT-28-1981

EXPERIMENT# WAVE 1
MEDIUM: WATER FRACTION TYPE: 0

HR-LABEL	HRS	MINS	TEMPERATURES AIR	TEMPERATURES WATER	TEMPERATURES OIL	CORexIT PRESENT	WIND SPEED	MIXING	COMMENTS			
0 0 SEP-09-1981	0	0	15.00	11.00	.00	NO	.00	10.00	WAVE TANK	TIME ZERO	WATER	SAMPLE
0 0 SEP-10-1981	1	0	15.00	11.00	.00	NO	.00	10.00	WAVE TANK	1 HOUR	WATER	SAMPLE
0 0 SEP-10-1981	3	0	15.00	11.00	.00	NO	.00	10.00	WAVE TANK	3 HOUR	WATER	SAMPLE
0 0 SEP-10-1981	6	0	15.00	11.00	.00	NO	.00	10.00	WAVE TANK	6 HOUR	WATER	SAMPLE
0 0 SEP-10-1981	12	0	15.00	11.00	.00	NO	.00	10.00	WAVE TANK	12 HOUR	WATER	SAMPLE
0 0 SEP-10-1981	24	0	15.00	11.00	.00	NO	.00	10.00	WAVE TANK	24 HOUR	WATER	SAMPLE
0 0 SEP-11-1981	36	0	15.00	11.00	.00	NO	.00	10.00	WAVE TANK	36 HOUR	WATER	SAMPLE
0 0 SEP-11-1981	48	0	15.00	11.00	.00	NO	.00	10.00	WAVE TANK	48 HOUR	WATER	SAMPLE
0 0 SEP-12-1981	72	0	15.00	11.00	.00	NO	.00	10.00	WAVE TANK	3 DAY	WATER	SAMPLE
0 0 SEP-15-1981	120	0	15.00	11.00	.00	NO	.00	10.00	WAVE TANK	5 DAY	WATER	SAMPLE
0 0 SEP-17-1981	172	0	15.00	11.00	.00	NO	.00	10.00	WAVE TANK	7 DAY	WATER	SAMPLE
0 0 SEP-20-1981	240	0	15.00	11.00	.00	NO	.00	10.00	WAVE TANK	10 DAY	WATER	SAMPLE
0 0 SEP-24-1981	336	0	15.00	11.00	.00	NO	.00	10.00	WAVE TANK	14 DAY	WATER	SAMPLE
0 0 OCT-02-1981	504	0	15.00	11.00	.00	NO	.00	10.00	WAVE TANK	21 DAY	WATER	SAMPLE

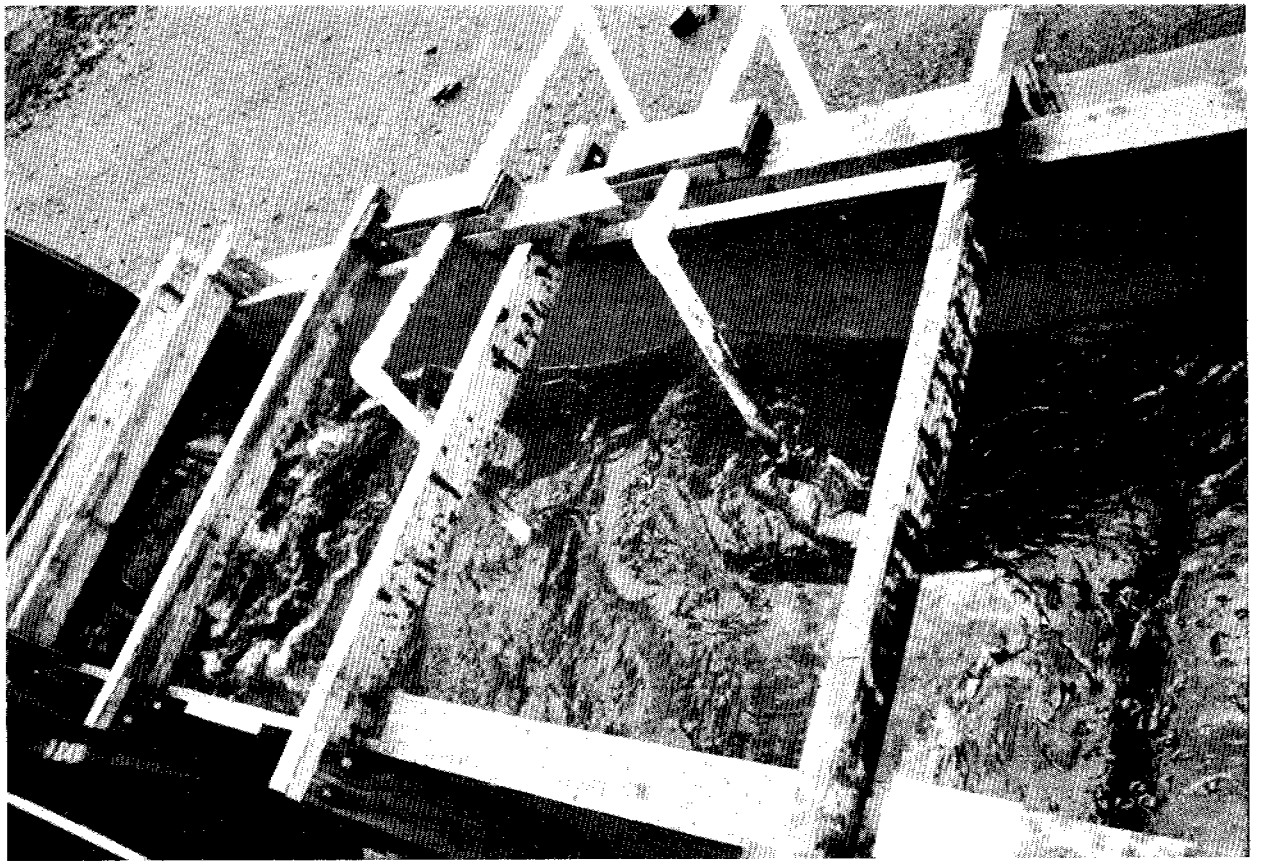

FIGURE 5-42. ACCUMULATED PRUDHOE BAY MOUSSE AT THE QUAISANT END OF THE WAVE TANK AFTER APPROXIMATELY 48 HOURS OF SUB-ARCTIC AMBIENT WEATHERING DURING SEPTEMBER 1981.

Figure 5-43 presents the flame ionization detector capillary gas chromatograms obtained on selected oil samples as a function of time. Clearly the removal of lower molecular weight aliphatics and aromatics due to evaporation/dissolution processes can be noted. While clear loss of the lower molecular weight components is evident from these chromatograms, adequate tracking of the individual compound concentrations can only be effectively completed with the utilization of the computer system. Each of the oil samples was analyzed at the Kasitsna Bay facility on the HP 5840 gas chromatograph which had been modified to allow fused silica capillary column analyses, and the digital output data were stored on magnetic tape. Upon return to the laboratory in La Jolla, CA, these tapes were then loaded into the DEC-10 computer system, and Figures 5-44 and 5-45 present computer generated compound concentrations (relative to nC-20) for selected aliphatic compounds in the whole crude oil samples. From these curves, quantitative rates for the losses of the lower molecular weight components are being obtained, and in the Section 5.1.5, pedicted losses vs. observed behavior are discussed in detail. The approach of normalizing the compound speciffic data to nC-20 individual comppound concentrations on a μg/g oil sample basis become difficult to interpret because of the factor of four increase in oil-in-water mass due to entrainment of water droplets during the formation of the stable emulsion. Evaporation and dissolution losses of n-C20 itself have been shown to be negligible during this time frame, and as such this compound can be used as an "internal standard" against which other component concentrations can be compared.

In conjunction with the oil and seawater sampling, larger volume samples of oil/mousse were obtained for density and viscosity determinations and Table 5-9 presents the kinematic viscosity data for a limited number of samples which have been worked up to date. Density and percent incorporated water data are being obtained at this time.

Although these data are still in the preliminary stages of development we anticipate that the results generated from the wave tank experiments will go further towards contributing to our overall understanding of combined

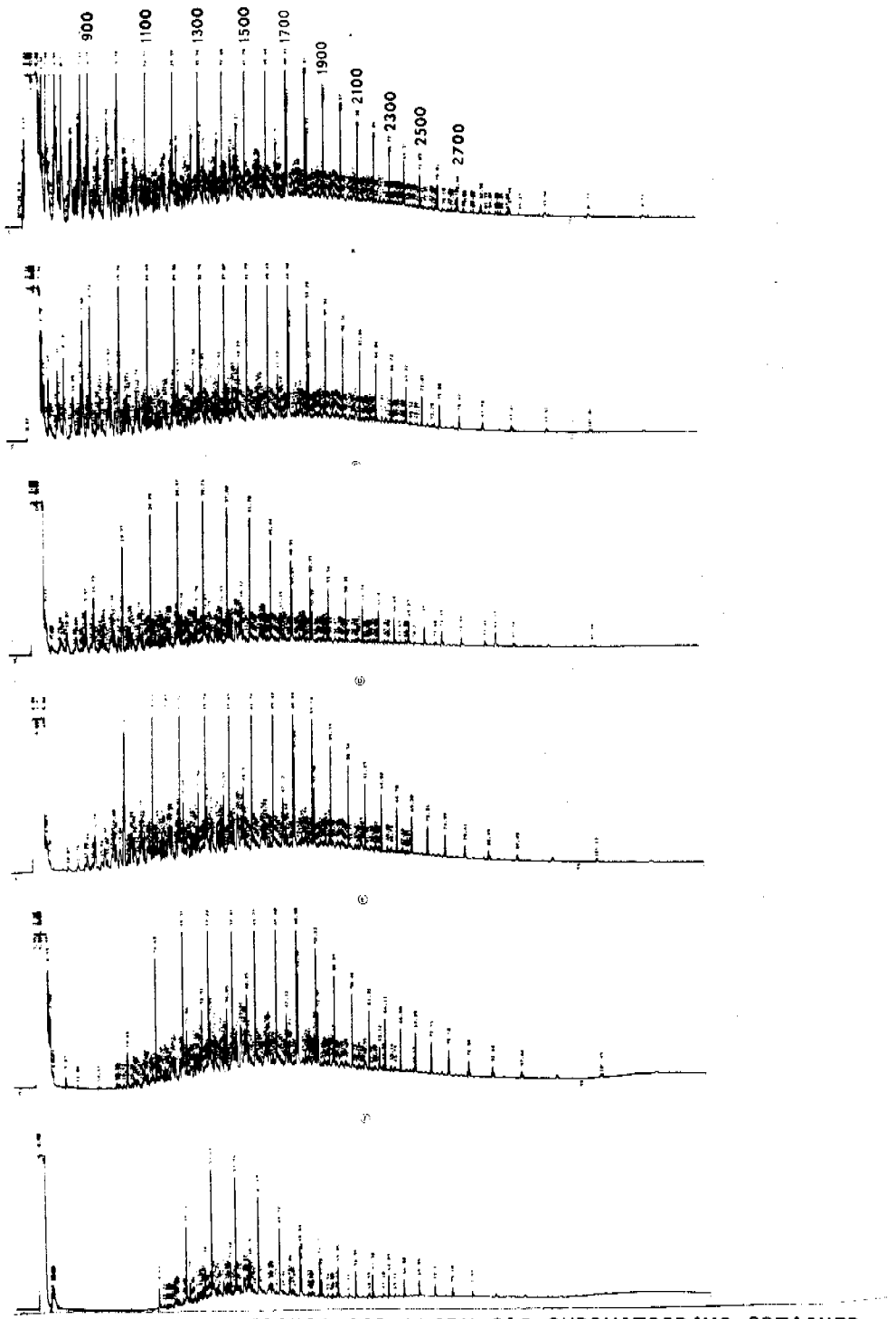

FIGURE 5-43. FLAME IONIZATION DETECTOR CAPILLARY GAS CHROMATOGRAMS OBTAINED ON PRUDHOE BAY CRUDE OIL WEATHERING UNDER SUB-ARCTIC AMBIENT CONDITIONS IN THE 2,500 L WAVE TANK AT KASITSNA BAY. TIME-SERIES SAMPLING POINTS AFTER THE "SPILL": (A) 0 HOURS; (B) 6 HOURS; (C) 12 HOURS; (D) 48 HOURS; (E) 10 DAYS; AND (F) 23 DAYS.

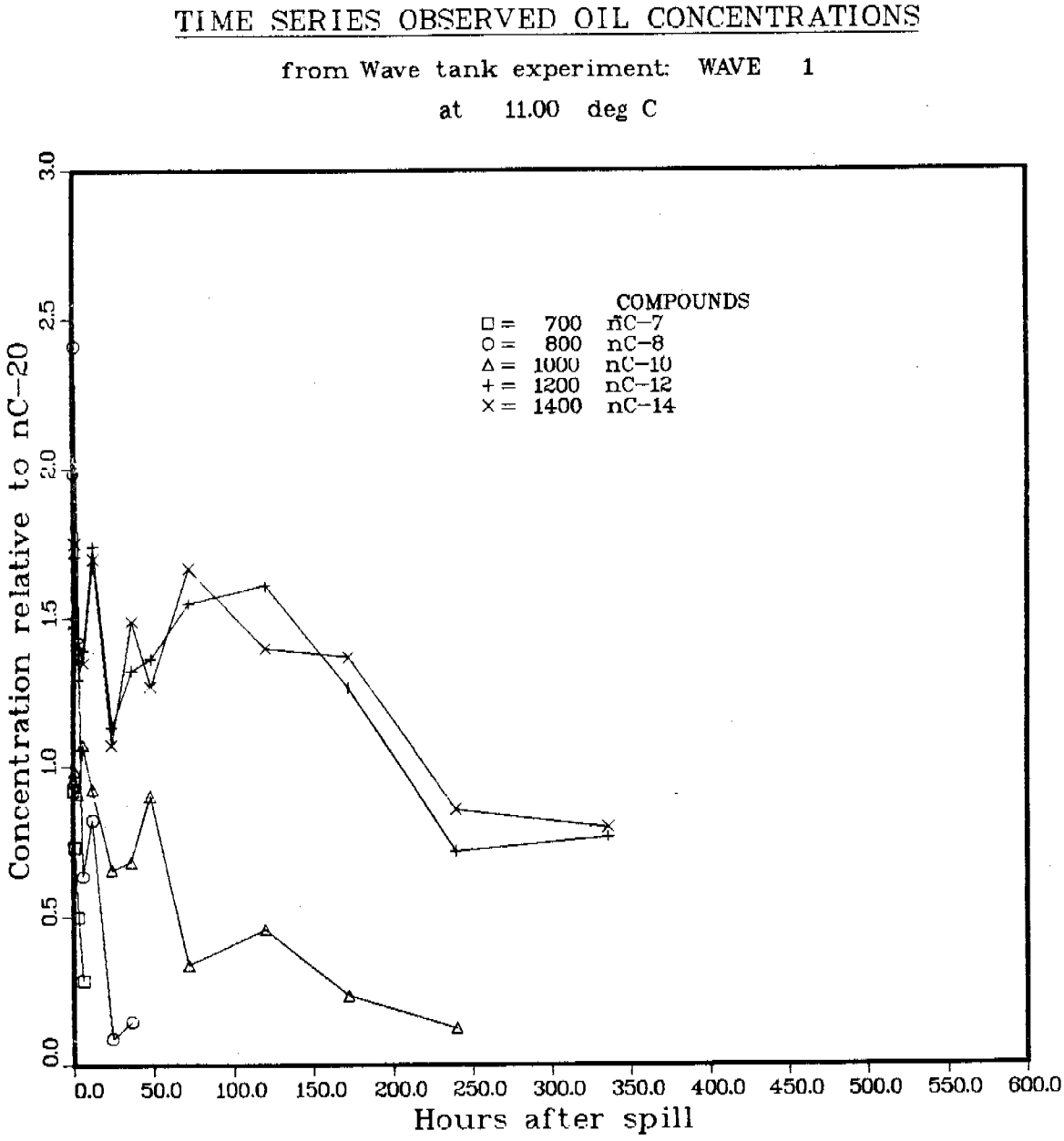

FIGURE 5-44. COMPUTER GENERATED TIME-SERIES PLOTS OF SPECIFIC COMPONENT CONCENTRATIONS REMAINING IN THE PRUDHOE BAY CRUDE OIL SLICK WEATHERING UNDER AMBIENT SUB-ARCTIC CONDITIONS IN THE 2,500 L WAVE TANK AT KASITSNA BAY. ALL CONCENTRATIONS HAVE BEEN NORMALIZED TO THE CONCENTRATION OF nC-20 AT EACH SAMPLING POINT.

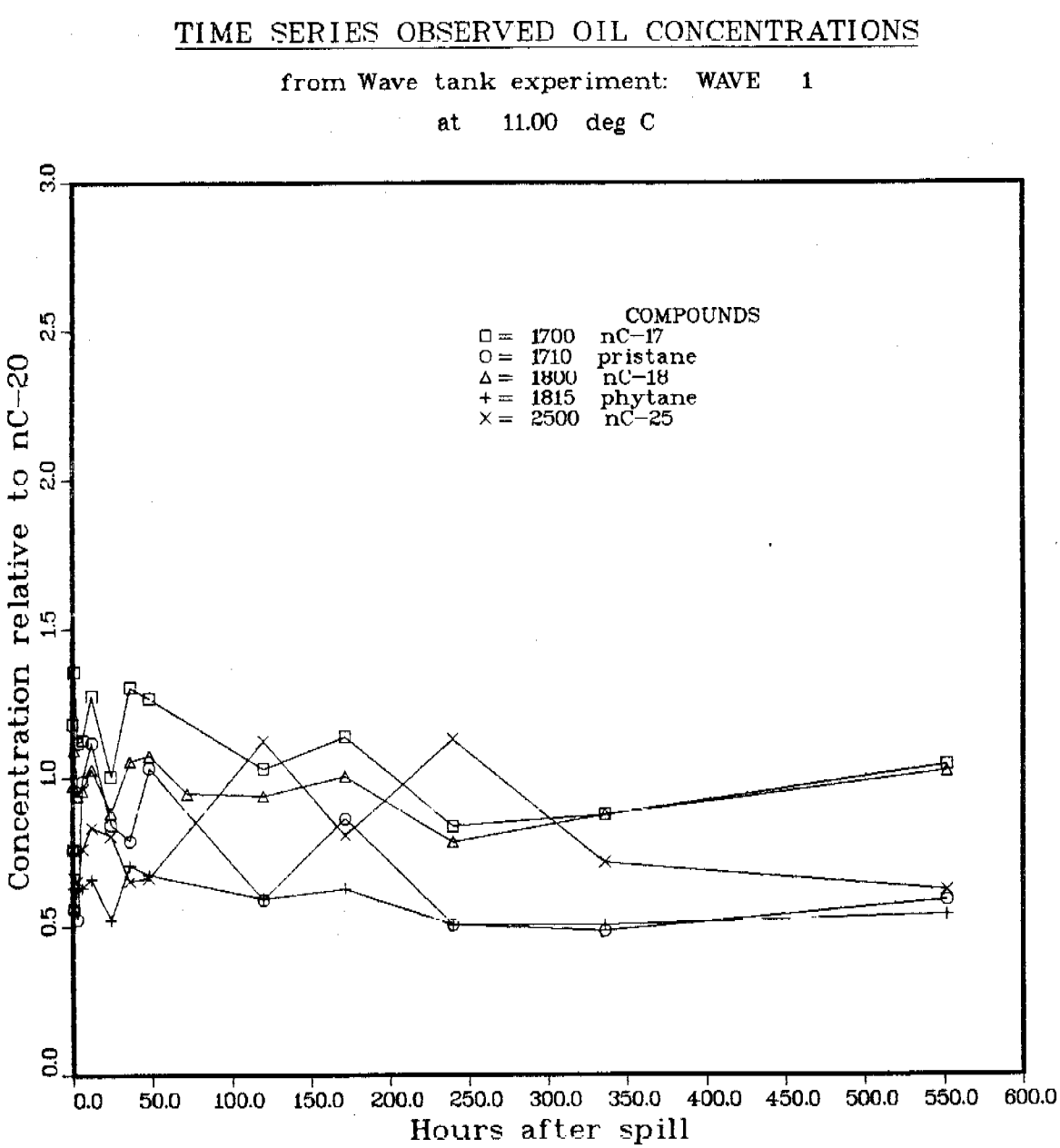

FIGURE 5-45. COMPUTER GENERATED TIME-SERIES PLOTS OF HIGHER MOLECULAR WEIGHT COMPONENT CONCENTRATIONS REMAINING IN THE PRUDHOE BAY CRUDE OIL SLICK WEATHERING UNDER AMBIENT SUB-ARCTIC CONDITIONS IN THE 2,500 L WAVE TANK AT KASITSNA BAY. ALL CONCENTRATIONS HAVE BEEN NORMALIZED TO THE CONCENTRATION OF nC-20 AT EACH SAMPLING POINT.

TABLE 5-9. KINEMATIC VISCOSITIES OF WAVE TANK MOUSSE*.

Sampling Time	Viscosity @ 38°C (cSt)
Day 0 (fresh oil)	21.2
Day 2	432
Day 5	709
Day 13	2400
Day 18	2615
Day 27	2300

* in accordance with ASTM method D445

sub-arctic open ocean oil weathering processes than any other field experiment undertaken to date. That is, in this tank all of the interactive processes which affect the chemical changes which occur to spilled petroleum can be allowed to act under as nearly natural conditions as possible. Specifically, the high water turn-over rate in the tank will facilitate microbial population changes from tidal cycling within Kasitsna Bay (GRIFFITH and MORIETA, 1980) to be reflected in microbial degradation processes. The position of the tank away from the protective walls of the geochemistry laboratory allows adequate sunlight exposure, and fresh water input from rain and snowfall are not affected.

During the first three weeks of the wave tank experiment, daily weather and integrated solar intensity measurements were taken (Table 5-10), and during our upcoming scheduled sampling trips to Kasitsna Bay in November and January, 1982, these measurement will be repeated. Biweekly air and water temperatures are being collected in the interim by NOAA resident laboratory manager. Because of the high turbulence in the tank and the relatively high watr turn-over rates, it is anticipated that the system will remain unfrozen during the winter months, therefore long-term weathering "open-ocean" effects during sub-arctic winter can also be evaluated. Longer term degradation of Prudhoe Bay mousse will also be possible and, as was noted above, time series samples for physical chemistry studies (viscosity, density, etc.) were collected along with samples for compositional analysis.

The edge effects from the tank walls serve to corral the test oil at one end of the tank. As a result, the oil slick appeared to behave very similarly at the oil water boundary to the edge of large open ocean oil spills such as the IXTOC-I blowout in the Gulf of Mexico (PAYNE et al., 1980). For example, at the edges of the continuous oil slick from the IXTOC spill, waves were observed to break over the oil, creating a significant dampening affect on the water surface. This wave action then either displaced the surface oil "mat" downward 4 to 5 inches, after which it resurfaced or it forced its way under the oil toward the center of the slick, where it folded over itself

TABLE 5-10. WEATHER OBSERVATIONS DURING WAVE TANK EXPERIMENTS -- KASITSNA BAY, ALASKA, SUMMER/FALL 1981.

Date	Max. T	Min. T	Obsn. Temp.	Precip.	Radiation	Comments
9/9/81	--	--	57°F		(quantax 10^{20})	Clear
9/10	60°F	39°F	45°F		8.0	Clear
9/11	56°F	41°F	45°F		7.29	Clear
9/12	53°F	40°F	45°F	0.05 in.	5.5	Overcast
9/13	51°F	40°F	46°F	0.06	5.0	Overcast
9/14	53°F	44°F	48°F	0.09	3.43	Overcast
9/15	56°F	45°F	46°F	0.45	7.68	Overcast
9/16	56°F	45°F	47°F	0.42	5.36	Overcast
9/17	55°F	45°F	46°F	0.53	5.05	Overcast
9/18	57°F	46°F	47°F	0.31	4.96	Overcast
9/19	55°F	45°F	47°F	0.62	5.63	Overcast
9/20	55°F	46°F	47°F		6.57	Partly Cloudy
9/21	55°F	42°F	45°F		6.95	Partly Cloudy
9/22	49°F	36°F	40°F		8.08	Clear
9/23	53°F	45°F	37°F		7.25	Partly Cloud
9/24	48°F	38°F	45°F		6.05	Partly Cloudy
9/25	48°F	38°F	35°F		Missed	Snow Pellets
9/26	Missed					Rain
9/27	50°F	42°F	45°F	0.06	5.50	Rain
9/28	48°F	36°F	42°F		6.3	Rain
9/29	45°F	35°F	38°F		6.27	Snow-No accumulation
9/30	44°F	35°F	37°F		7.05	Snow-No accumulation

Observations made at 5:00 PM Local time

enhancing incorporation of water droplets (PAYNE, 1981). Similar behavior was observed in the wave tank.

As additional samples are obtained during the November and January, 1981 experiments, longer term weathering phenomena (combined microbial, photochemical, dispersion and emulsification processes) will be elucidated. Further, as the water samples obtained during the first 24 days are examined, estimates on the percent of the slick lost due to the initial dispersive action of the wave turbulence may be obtained. Ultimately, these data will be used in conjunction with predicted behavior from the oil weathering model for incorporation of dispersive phenomena into the overall oil mass-balance considerations. Examples of preliminary matches of predicted vs observed losses due to evaporation/dissolution are presented in Section 5.1.5.

5.1.4 Determination of Liquid/Liquid Partition Coefficients and Water Solubilities of Component Petroleum Hydrocarbons as a Function of Temperature

In order to adequately predict evaporation/dissolution phenomena with the oil weathering model, thermodynamic data in the form of equilibrium distribution coefficients are required to describe interphase mass transfer. These data are typically referred to as Henry's Law coefficients for evaporation or liquid-liquid partition coefficients (M-values) for dissolution. These data are used to describe how far from equilibrium the three phases are in terms of concentrations, and the departure from equilibrium measured on an arbitrary scale multiplied by the appropriate mass transfer coefficients yield the mass flux across the phase boundary from oil into the water and atmosphere.

To determine the liquid-liquid partition coefficients (M-values) for all of the components of interest in Prudhoe Bay crude oil, a series of equilibrium experiments were undertaken at 3, 13 and 23°C. In these experiments known volumes of oil and water were equilibrated in separatory funnels for 48 hours, with their phases being vigorously shaken at time zero and then allowed

to settle with occasional swirling over the first 24-hour period. Additional mixing (swirling) was done 13 hours before sampling and the phases were allowed to separate without further agitation. Water and oil phase samples were then removed and the samples were extracted with equal volumes of methylene chloride (800 ml).

During initial attempts at M-value determinations, a number of problems were encountered due to the formation of 1 to 5 μm micelles of dispersed oil in the water column phase, and this problem was discussed in depth in Appendix A. Incorporation of micelles into the aqueous phase led to anomalously high levels of "dissolved" petroleum hydrocarbons (exceeding solubility limits in some cases) in the aqueous phase. This micelle phenomenon yielded M-value partition coefficients which were anomalously low, and with these M-values initially predicted rates of dissolution of higher molecular weight components were too high. In addition to the microscopic examinations of the aqueous phases from these M-value experiments which confirmed the presence of micelles, indirect evidence of micelle formation was obtained by the presence of higher molecular weight n-alkanes in the aqueous phase. These compounds have extremely limited water solubilities (less than 0.8 μg/L for compounds with molecular weight greater than nC-18; SUTTON AND CALDER, 1974) and their presence in water column extracts were as evidence of micelle formation.

Because of these initial difficulties due to the oil-in-water dispersions, a number of additional M-value experiments were then undertaken where the oil and water phases were not as vigorously agitated. Figure 5-46 presents FID capillary gas chromatograms of (A) the whole unfractionated oil, (B) the aliphatic fraction of the surface oil, (C) the aromatic fraction of the surface oil, and (D) the unfractionated water column extract from under the slick. Initially, M-value determinations were attempted using L/C fractionated water column samples; however, only trace levels of aliphatic components were detected in the fractionated samples, and some breakthrough of the lower molecular weight aromatics (benzene, toluene, xylenes, and ethylbenzene)

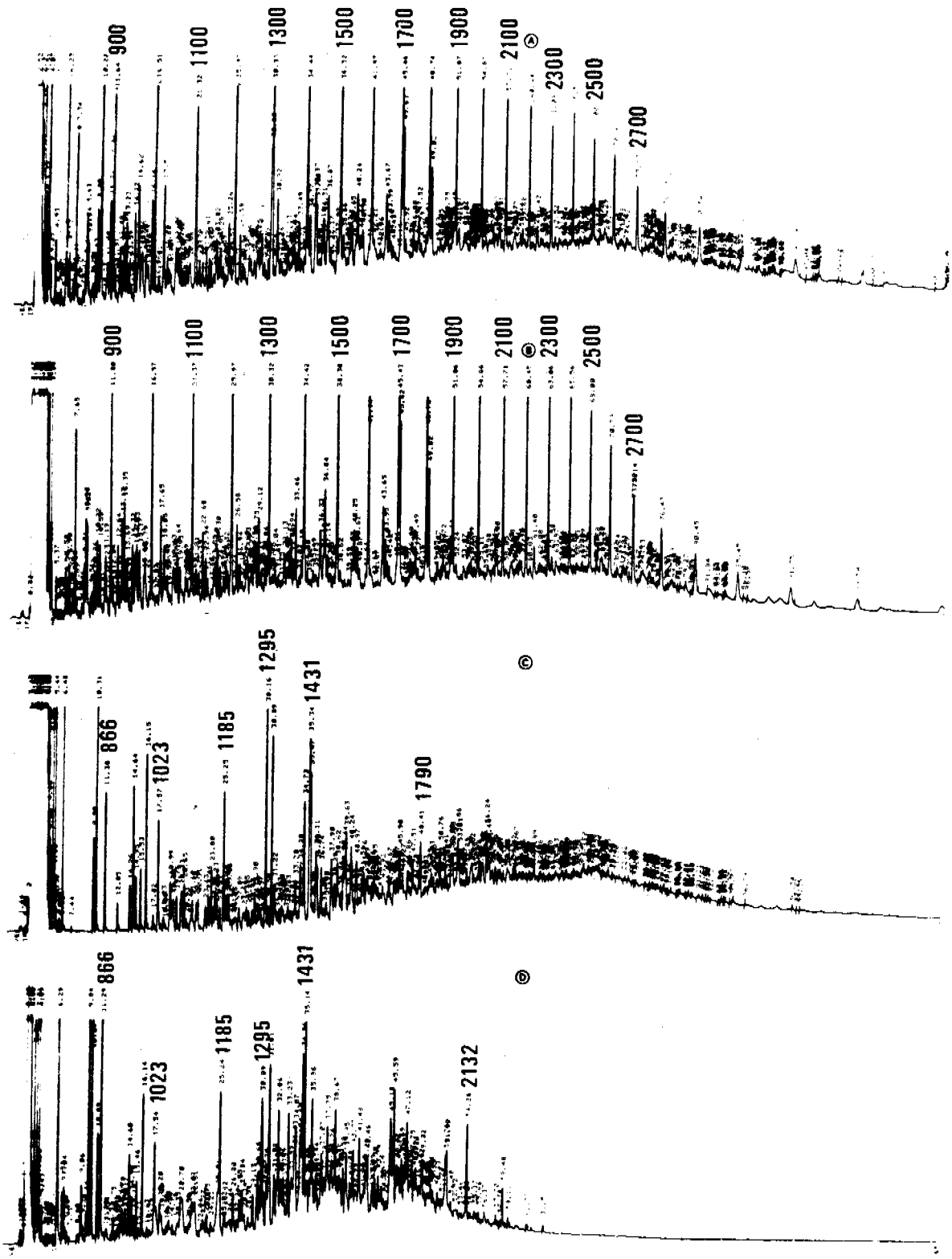

FIGURE 5-46. FLAME IONIZATION DETECTOR CAPILLARY GAS CHROMATOGRAMS OBTAINED ON SPECIFIC SAMPLES USED FOR COMPOUND SPECIFIC OIL/SEAWATER PARTITION COEFFICIENT (M VALUE) DETERMINATIONS. (A) UNFRACTIONED OIL; (B) ALIPHATIC FRACTION OF THE SURFACE OIL; (C) AROMATIC FRACTION OF THE SURFACE OIL AND (D) THE UNFRACTIONATED WATER COLUMN EXTRACT BENEATH THE SLICK. (KOVAT INDICES ARE SHOWN ABOVE MAJOR PEAKS).

during the liquid column chromatography was noted. This phenomenon complicated ratio determinations for oil phase and water phase concentrations, so later M-value determinations were completed using unfractionated water column samples. In that the majority of components which are subject to dissolution are aromatic hydrocarbons, this procedure does not limit the data obtained. Figure 5-47 presents the reconstructed ion gas chromatogram of the water column extract, and Table 5-11 lists the identifications of the aromatic compounds of interest.

From this latest series of partition coefficient experiments, M-values for individual compounds at various temperatures were obtained, Table 5-12 presenting the calculated values for oil/seawater partitioning at 3 and 23°C. These values were obtained using a sub-program in the overall oil weathering model called M-VAL, which matches the oil phase and water phase specific compound concentrations by Kovat retention indices. Also shown in Table 5-12 are the identifications of selected compounds as determined by the GC/MS analysis of the water column and fractionated (F2) oil sample extracts.

These values are then used in the evaporation/dissolution oil weathering model as described in Section 4.0 of this report. The following Section 5.1.5 presents the results of predicted vs observed evaporation and dissolution behavior for specific compounds as measured in the evaporation/dissolution chamber at 23 and 3°C and in the wave tank experiments completed at Kasitsna Bay.

5.1.5 Predicted vs Observed Evaporation/Dissolution Results

As described in detail in the modeling section (4.0), two distinctly different modeling approaches are being taken in our efforts to predict oil weathering behavior. The component-specific model predicts individual compound concentrations in the slick as a function of time and the pseudo-compound (or fractional-distillation cut) approach allows predictions of overall oil mass balance. Output data from the component-specific approach predicts time series concentrations in the slick, air and water column based on

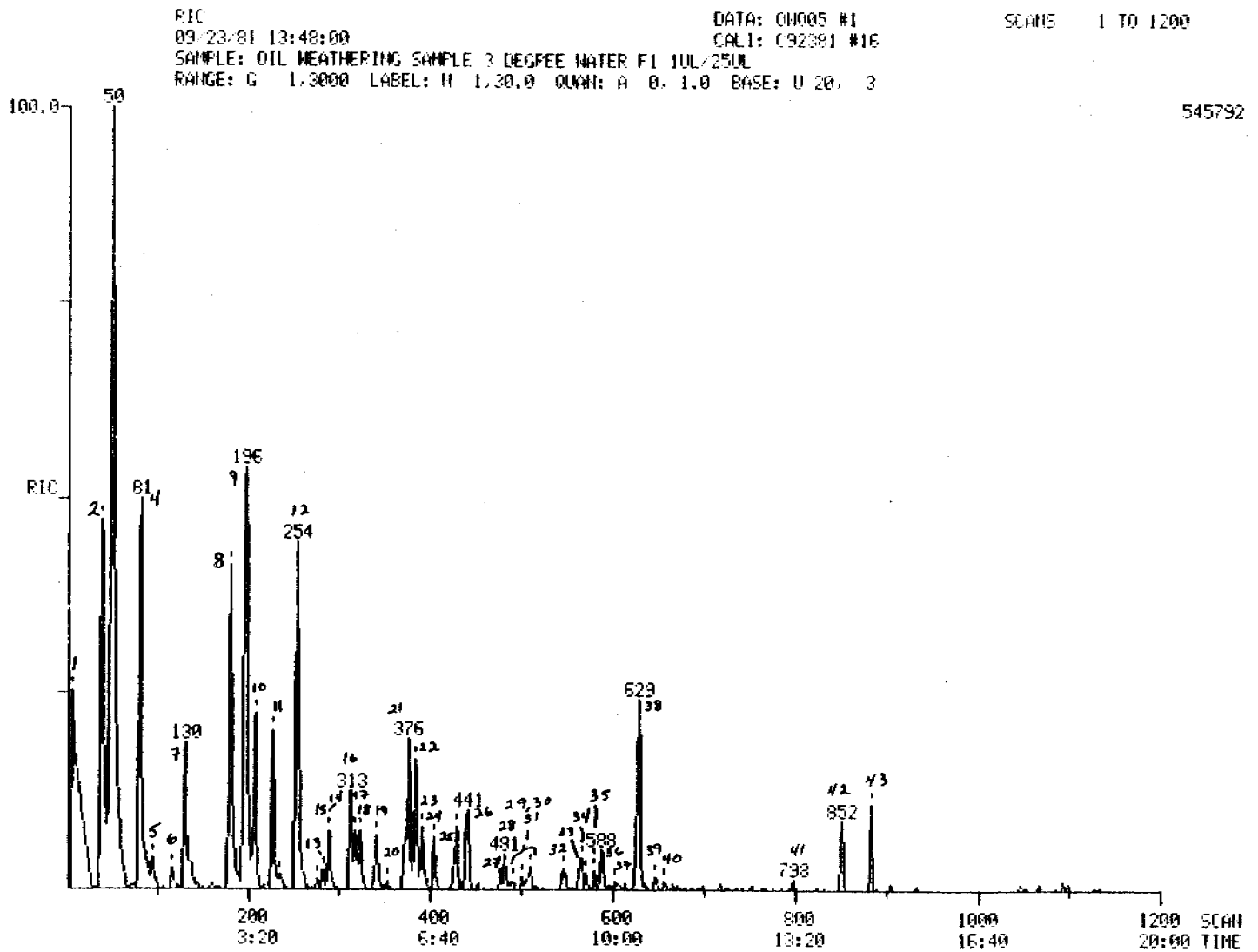

FIGURE 5-47. RECONSTRUCTED ION CHROMATOGRAM (RIC) FROM CAPILLARY GC/MS ANALYSES OF WATER COLUMN EXTRACTS FROM OIL/SEAWATER PARTITION COEFFICIENT EXPERIMENTS. IDENTIFICATIONS OF THE NUMBERED PEAKS IN THE CHROMATOGRAM ARE PRESENTED IN TABLE 5-11.

TABLE 5-11. COMPOUNDS IDENTIFIED BY GC/MS ANALYSES OF WATER COLUMN EXTRACTS FROM OIL/SEAWATER PARTITION COEFFICIENT (M-VALUE) EXPERIMENTS.

1	methyl chloride (solvent)
2	ethylbenzene
3	p-xylene
4-	o-xylene
5	nonane
6	C_9H_{16}
7	cumene
8	n-propylbenzene
9	ethylmethylbenzene
10	trimethylbenzene
11,12	C_3 benzenes
13	decane
14,15	C_4 benzenes
16-18	C_3 benzenes
19	unsaturated C_3 benzene
20	methylisopropylbenzene
21	methylpropylbenzene
22	C_4 benzene
23	ethyldimethylbenzene
24-28	C_4 benzenes
29	t-amylbenzene
30	C_4 benzene
31	tetramethylbenzene
32,33	unsaturated C_4 benzenes
34	C_4 benzene
35	C_5 benzene
36	tetralin
37	C_5 benzene
38	naphthalene
39	C_2 indane
40	unsaturated C_5 benzene (possibly a methyltetralin or a C_2 indane)
41	methyltetralin
42	2-methylnaphthalene
43	3-methylnaphthalene

TABLE 5-12. OIL/SEAWATER LIQUID-LIQUID PARTITION COEFFICIENTS (M-VALUES) DETERMINED AT 3 AND 23°C.

M - Values Determined at 3^{o} and 23^{o}

Kovats	M - Values			Compounds
	3^{o}oil/3^{o}-wat	23^{o2}-oil/23^{o1}-wat	23^{o2}-oil/23^{o2}-wat	
765	652	688	583	toluene
859	2,660	2,690	2,250	ethylbenzene
867	3,030	3,060	2,550	p-xylene
892	2,730	2,260	1,900	o-xylene
923	8,840	8,520	7,310	cumene
953	13,400	14,645	14,800	n-propylbenzene
961	12,100	10,800	9,370	ethylmethylbenzene
967	14,900	13,600	11,800	mesitylene
979	10,800	9,350	7,840	C_3 benzene
992	------	11,200	9,080	C_3 benzene
1021	14,800	5,830	9,660	p-cymene
1035	3,530	1,990	2,450	naphthalene
1066	68,800	------	38,800	C_4 benzene
1086	10,740	4,290	2,530	ethyldimethylbenzene
1121	57,300	6,530	12,600	tetramethylbenzene
1163	------	26,300	22,000	naphthalene
1185	5,570	6,720	6,900	naphthalene
1199	------	19,900	15,500	C_5 benzene unsaturated
1237	------	5,180	5,240	2-methylnaphthalene
1284	3,900	1,110	1,070	C_6 benzene
1296	35,800	14,900	11,000	2-methylnaphthalene
1316	30,400	5,320	4,830	1-methylnaphthalene
1338	------	4,690	4,060	
1343	10,100	951	951	
1371	3,210	466	424	C_7 benzene
1425	128,000	------	93,400	dimethylnaphthalene
1428	67,000	------	23,200	dimethylnaphthalene
1461	------	44,500	53,900	
1469	5,670	889	1,000	n-octylbenzene
1476	58,300	9,030	6,920	C_3 naphthalene
1499	------	6,910	6,590	
1510	23,300	7,130	6,460	2-isopropylnaphthalene
1523	47,300	6,120	6,610	
1528	------	10,000	10,600	1-isopropyl naphthalene
1537	47,400	7,930	6,660	trimethyl naphthalene
1546	4,600	925	714	

TABLE 5-12. OIL/SEAWATER LIQUID-LIQUID PARTITION COEFFICIENTS (M-VALUES) DETERMINED AT 3 AND 23°C. (Continued).

M - Values Determined at 3^{o} and 23^{o} (continued)

Kovats	M - Values			Compounds
	3^{o}oil/3^{o}-wat	23^{o2}-oil/23^{o1}-wat	23^{o2}-oil/23^{o2}-wat	
1589	7,880	1,730	1,440	
1642	13,400	2,150	2,160	
1715	71,800	------	9,460	methyl fluorene
1743	------	8,030	6,950	
1841	9,760	5,270	4,080	
1867	30,100	11,900	10,800	methyldibenzothiophene
2154	------	5,280	3,920	

thermodynamic properties such as Henry's Law of constants, liquid-liquid partitioning coefficients and mass transfer coefficients.

Predicted vs observed water column concentrations for benzene, cyclohexane and toluene were generated in the evaporation/dissolution chamber and preliminary results from these studies were described in our November 1980 Interim Quarterly Report. A much more sophisticated evaporation-dissolution model has since been generated, allowing prediction of specific compound concentrations in the water column beneath an oil slick.

A significant improvement in the model has come from the utilization of Henry's law coefficients in the calculation of the mass-transfer coefficient at the oil-air interface. Previously, only benzene, toluene and cyclohexane were modeled, and since these compounds all have similar volatilities, they behave in a similar manner. However, when considering compounds which are much less volatile (e.g., naphthalane), water column concentrations will peak much later than the concentrations of benezene, toluene, and cyclohexane. This is due to the fact that the less volatile compounds leave the oil-water phases much more slowly, allowing more time to transfer from the oil to the water phase. The equations being used to predict water and oil column concentrations are those presented in the November Quarterly (PAYNE et al., 1980), with changes being made only to the over-all mass transfer coefficient at the oil-air interface. Tables 5-13 through 5-24 present specific numerical output for six selected compounds examined in the evaporation and dissolution experiments at 3 and 21°C. The output presented in these tables is all the information needed to calculate the water and oil concentrations. The KW, KA, and KO values are individual-phase mass transfer coefficients; the M-value and Henry's law coefficient was derived from the Antoine vapor pressure equation and the constants, ANTA, ANTB, and ANTC are from REID et al. (1977). The quantities A through Z2 on the output are intermediate results used to calculate the final concentrations. For the water column concentrations:

$$y = Z1*EXP(D1*TIME) + Z2*EXP(D2*TIME)$$

TABLE 5-13. STIRRED TANK MODEL COMPUTER PREDICTED WATER COLUMN CONCENTRATIONS FROM EVAPORATION/DISSOLUTION EXPERIMENTS: KOVAT 854 ETHYLBENZENE.

STIRRED TANK MODEL FOR KOVAT 857, ETHYLBENZENE
FROM THE KEYBOARD, KW = 3.000E+00, KA = 1.500E+03, KO = 1.000E+00 CM/HR
M (OIL/WATER) = 2.660E+03, HENRYS LAW (AIR/OIL) = 4.040E-05 DIMENSIONLESS, AT 3.000E+00 DEG C
ANTA = 1.602E+01, ANTB = 3.290E+03, ANTC = -5.993E+01
MOLE WT OF OIL = 2.000E+02, DENSITY = 8.000E-01 GM/CC
VO = 2.000E+02 ML, VW = 3.000E+04 ML
XZERO = 4.740E+02 MICROGRAMS/GRAM OF OIL, AREA = 6.170E+02 CM*CM
OVER-ALL KW AT WATER-OIL = 2.997E+00 CM/HR
OVER-ALL KO AT OIL-AIR = 5.725E-02 CM/HR
A = -6.163E-02, B = 2.317E-05
C = 9.245E+00, D = -1.801E-01
H = 1.220E-01
D1 = -5.985E-02, D2 = -1.819E-01
C1 = 6.920E+00, C2 = 4.671E+02
Z1 = 9.001E-02, Z2 = -9.001E-02
WATER CONCENTRATION PEAKS AT 9.109E+00 HOURS
WHERE THE WATER CONCENTRATION = 3.501E-02, AND THE OIL CONCENTRATION = 9.312E+01
AND THE CONCENTRATION RATIO (OIL/WATER) = 2.660E+03

HOUR	H2O	OIL
0.20	2.144E-03	4.572E+02
0.40	4.106E-03	4.411E+02
0.60	6.130E-03	4.255E+02
0.80	7.979E-03	4.104E+02
1.00	9.730E-03	3.959E+02
1.20	1.141E-02	3.819E+02
1.40	1.300E-02	3.685E+02
1.60	1.451E-02	3.554E+02
1.80	1.594E-02	3.429E+02
2.00	1.729E-02	3.308E+02
2.25	1.889E-02	3.163E+02
2.50	2.037E-02	3.024E+02
2.75	2.176E-02	2.891E+02
3.00	2.306E-02	2.765E+02
3.25	2.426E-02	2.643E+02
3.50	2.537E-02	2.528E+02
3.75	2.640E-02	2.417E+02
4.00	2.736E-02	2.311E+02
4.25	2.824E-02	2.210E+02
4.50	2.905E-02	2.113E+02
6.00	3.263E-02	1.617E+02
8.00	3.473E-02	1.133E+02
10.00	3.487E-02	7.950E+01
12.00	3.374E-02	5.605E+01
14.00	3.188E-02	3.961E+01
16.00	2.964E-02	2.810E+01
18.00	2.724E-02	2.004E+01
20.00	2.482E-02	1.439E+01
22.00	2.248E-02	1.040E+01
24.00	2.026E-02	7.505E+00
26.00	1.819E-02	5.409E+00
28.00	1.629E-02	4.165E+00
30.00	1.456E-02	3.144E+00
32.00	1.299E-02	2.406E+00
34.00	1.158E-02	1.860E+00
36.00	1.031E-02	1.472E+00
38.00	9.169E-03	1.177E+00
40.00	8.152E-03	9.552E-01
42.00	7.244E-03	7.853E-01
44.00	6.436E-03	6.535E-01

TABLE 5-14. STIRRED TANK MODEL COMPUTER PREDICTED WATER COLUMN CONCENTRATIONS FROM EVAPORATION/DISSOLUTION EXPERIMENTS: KOVAT 867, P-XYLENE.

STIRRED TANK MODEL FOR KOVAT 867, P-XYLENE
FROM THE KEYBOARD, KW = 3.000E+00, KA = 1.500E+03, KO = 1.000E+00 CM/HR
N (OIL/WATER) = 3.030E+03, HENRYS LAW (AIR/OIL) = 4.032E-05 DIMENSIONLESS, AT 3.000E+00 DEG C
ANTA = 1.609E+01, ANTB = 3.347E+03, ANTC = -5.780E+01
MOLE WT OF OIL = 2.000E+02, DENSITY = 8.800E-01 GM/CC
VO = 2.000E+02 ML, VW = 3.000E+04 ML
XZERO = 1.794E+03 MICROGRAMS/GRAM OF OIL, AREA = 6.170E+02 CM*CM
OVER-ALL KW AT WATER-OIL = 2.997E+00 CM/HR
OVER-ALL KO AT OIL-AIR = 5.702E-02 CM/HR
A = -6.164E-02, B = 2.034E-05
C = 9.246E+00, D = -1.790E-01
R = 1.205E-01
D1 = -6.006E-02, D2 = -1.806E-01
C1 = 2.355E+01, C2 = 1.770E+03
Z1 = 3.029E-01, Z2 = -3.029E-01
WATER CONCENTRATION PEAKS AT 9.135E+00 HOURS
WHERE THE WATER CONCENTRATION = 1.168E-01, AND THE OIL CONCENTRATION = 3.538E+02
AND THE CONCENTRATION RATIO (OIL/WATER) = 3.030E+03

HOUR	H20	OIL
0.20	7.126E-03	1.731E+03
0.40	1.391E-02	1.670E+03
0.60	2.038E-02	1.611E+03
0.80	2.653E-02	1.555E+03
1.00	3.238E-02	1.500E+03
1.20	3.794E-02	1.447E+03
1.40	4.322E-02	1.397E+03
1.60	4.824E-02	1.348E+03
1.80	5.300E-02	1.300E+03
2.00	5.752E-02	1.255E+03
2.25	6.283E-02	1.200E+03
2.50	6.779E-02	1.148E+03
2.75	7.242E-02	1.098E+03
3.00	7.673E-02	1.050E+03
3.25	8.074E-02	1.004E+03
3.50	8.446E-02	9.602E+02
3.75	8.791E-02	9.184E+02
4.00	9.110E-02	8.784E+02
4.25	9.404E-02	8.402E+02
4.50	9.675E-02	8.036E+02
6.00	1.087E-01	6.157E+02
8.00	1.159E-01	4.322E+02
10.00	1.163E-01	3.040E+02
12.00	1.126E-01	2.143E+02
14.00	1.065E-01	1.515E+02
16.00	9.901E-02	1.075E+02
18.00	9.100E-02	7.664E+01
20.00	8.294E-02	5.493E+01
22.00	7.510E-02	3.962E+01
24.00	6.769E-02	2.881E+01
26.00	6.078E-02	2.113E+01
28.00	5.443E-02	1.567E+01
30.00	4.863E-02	1.175E+01
32.00	4.338E-02	8.927E+00
34.00	3.865E-02	6.876E+00
36.00	3.440E-02	5.372E+00
38.00	3.059E-02	4.259E+00
40.00	2.719E-02	3.424E+00
42.00	2.416E-02	2.791E+00
44.00	2.145E-02	2.304E+00

TABLE 5-15. STIRRED TANK MODEL COMPUTER PREDICTED WATER COLUMN CONCENTRATIONS FROM EVAPORATION/DISSOLUTION EXPERIMENTS: KOVAT 1021, 1-METHYL-4-ISOPROPYLBENZENE.

```
STIRRED TANK MODEL FOR KOVAT 1021, 1-METHYL-4-ISOPROPYLB
FROM THE KEYBOARD, KW =  3.000E+00, KA =  1.500E+03, KO =  1.000E+00 CM/HR
M (OIL/WATER) =  1.480E+04, HENRYS LAW (AIR/OIL) =  5.463E-06 DIMENSIONLESS, AT  3.000E+00 DEG C
ANTA =  1.594E+01, ANTB =  3.539E+03, ANTC = -7.010E+01
MOLE WT OF OIL =  2.000E+02, DENSITY =  8.000E-01 GM/CC
VO =  2.000E+02 ML, VW =  3.000E+04 ML
XZERO =  4.530E+02 MICROGRAMS/GRAM OF OIL, AREA =  6.170E+02 CM*CM
OVER-ALL KW AT WATER-OIL =  2.999E+00 CM/HR
OVER-ALL KO AT OIL-AIR =  8.127E-03 CM/HR
A = -6.169E-02, B =  4.168E-06
C =  9.253E+00, D = -2.570E-02
H =  3.807E-02
D1 = -2.466E-02, D2 = -6.273E-02
C1 =  4.406E+02, C2 =  1.239E+01
Z1 =  4.959E-02, Z2 = -4.959E-02
WATER CONCENTRATION PEAKS AT  2.453E+01 HOURS
WHERE THE WATER CONCENTRATION =  1.644E-02, AND THE OIL CONCENTRATION =  2.433E+02
AND THE CONCENTRATION RATIO (OIL/WATER) =  1.480E+04
```

HOUR	H2O	OIL
0.20	3.743E-04	4.507E+02
0.40	7.422E-04	4.484E+02
0.60	1.104E-03	4.461E+02
0.80	1.459E-03	4.438E+02
1.00	1.808E-03	4.415E+02
1.20	2.150E-03	4.393E+02
1.40	2.487E-03	4.370E+02
1.60	2.817E-03	4.348E+02
1.80	3.142E-03	4.325E+02
2.00	3.461E-03	4.303E+02
2.25	3.852E-03	4.276E+02
2.50	4.233E-03	4.249E+02
2.75	4.607E-03	4.222E+02
3.00	4.971E-03	4.195E+02
3.25	5.328E-03	4.168E+02
3.50	5.676E-03	4.141E+02
3.75	6.016E-03	4.115E+02
4.00	6.348E-03	4.089E+02
4.25	6.672E-03	4.063E+02
4.50	6.989E-03	4.037E+02
6.00	8.735E-03	3.885E+02
8.00	1.069E-02	3.692E+02
10.00	1.227E-02	3.509E+02
12.00	1.353E-02	3.336E+02
14.00	1.451E-02	3.171E+02
16.00	1.525E-02	3.015E+02
18.00	1.578E-02	2.867E+02
20.00	1.614E-02	2.726E+02
22.00	1.635E-02	2.593E+02
24.00	1.644E-02	2.466E+02
26.00	1.641E-02	2.345E+02
28.00	1.630E-02	2.231E+02
30.00	1.612E-02	2.122E+02
32.00	1.587E-02	2.018E+02
34.00	1.557E-02	1.920E+02
36.00	1.523E-02	1.827E+02
38.00	1.486E-02	1.738E+02
40.00	1.446E-02	1.653E+02
42.00	1.405E-02	1.573E+02
44.00	1.362E-02	1.497E+02

TABLE 5-16. STIRRED TANK MODEL COMPUTER PREDICTED WATER COLUMN CONCENTRATIONS FROM EVAPORATION/DISSOLUTION EXPERIMENTS: KOVAT 1185, NAPHTHALENE.

STIRRED TANK MODEL FOR KOVAT 1185, NAPHTHALENE
FROM THE KEYBOARD, KW = 3.000E+00, KA = 1.500E+03, KO = 1.000E+00 CM/HR
M (OIL/WATER) = 5.570E+03, HENRYS LAW (AIR/OIL) = 6.590E-07 DIMENSIONLESS, AT 3.000E+00 DEG C
ANTA = 1.614E+01, ANTB = 3.992E+03, ANTC = -7.130E+01
MOLE WT OF OIL = 2.880E+02, DENSITY = 8.800E-01 GM/CC
VO = 2.000E+02 ML, VW = 3.000E+04 ML
XZERO = 5.200E+02 MICROGRAMS/GRAM OF OIL, AREA = 6.170E+02 CM*CM
OVER-ALL KW AT WATER-OIL = 2.990E+00 CM/HR
OVER-ALL KO AT OIL-AIR = 9.807E-04 CM/HR
A = -6.167E-02, B = 1.107E-05
C = 9.250E+00, D = -4.711E-03
H = 6.045E-02
D1 = -2.966E-03, D2 = -6.341E-02
C1 = 5.050E+02, C2 = 1.501E+01
Z1 = 9.524E-02, Z2 = -9.524E-02
WATER CONCENTRATION PEAKS AT 5.066E+01 HOURS
WHERE THE WATER CONCENTRATION = 7.812E-02, AND THE OIL CONCENTRATION = 4.351E+02
AND THE CONCENTRATION RATIO (OIL/WATER) = 5.570E+03

HOUR	H2O	OIL
0.20	1.144E-03	5.195E+02
0.40	2.273E-03	5.190E+02
0.60	3.386E-03	5.185E+02
0.80	4.485E-03	5.181E+02
1.00	5.570E-03	5.176E+02
1.20	6.640E-03	5.171E+02
1.40	7.696E-03	5.166E+02
1.60	8.738E-03	5.162E+02
1.80	9.767E-03	5.157E+02
2.00	1.078E-02	5.152E+02
2.25	1.203E-02	5.146E+02
2.50	1.326E-02	5.141E+02
2.75	1.447E-02	5.135E+02
3.00	1.566E-02	5.129E+02
3.25	1.682E-02	5.124E+02
3.50	1.797E-02	5.118E+02
3.75	1.910E-02	5.112E+02
4.00	2.021E-02	5.107E+02
4.25	2.131E-02	5.101E+02
4.50	2.238E-02	5.096E+02
6.00	2.846E-02	5.063E+02
8.00	3.566E-02	5.022E+02
10.00	4.194E-02	4.982E+02
12.00	4.741E-02	4.943E+02
14.00	5.217E-02	4.906E+02
16.00	5.630E-02	4.870E+02
18.00	5.987E-02	4.835E+02
20.00	6.296E-02	4.801E+02
22.00	6.562E-02	4.768E+02
24.00	6.791E-02	4.736E+02
26.00	6.986E-02	4.704E+02
28.00	7.152E-02	4.673E+02
30.00	7.292E-02	4.642E+02
32.00	7.410E-02	4.612E+02
34.00	7.508E-02	4.583E+02
36.00	7.588E-02	4.554E+02
38.00	7.653E-02	4.525E+02
40.00	7.705E-02	4.497E+02
42.00	7.745E-02	4.469E+02
44.00	7.774E-02	4.441E+02

TABLE 5-17. STIRRED TANK MODEL COMPUTER PREDICTED WATER COLUMN CONCENTRATIONS FROM EVAPORATION/DISSOLUTION EXPERIMENTS: KOVAT 1295, 2-METHYLNAPHTHALENE.

STIRRED TANK MODEL FOR KOVAT 1295, 2-METHYLNAPHTHALENE
FROM THE KEYBOARD, KW = 3.000E+00, KA = 1.500E+03, KO = 1.000E+00 CM/HR
M (OIL/WATER) = 3.580E+04, HENRYS LAW (AIR/OIL) = 1.592E-07 DIMENSIONLESS, AT 3.000E+00 DEG C
ANTA = 1.627E+01, ANTB = 4.237E+03, ANTC = -7.475E+01
MOLE WT OF OIL = 2.000E+02, DENSITY = 8.000E-01 GM/CC
VO = 2.000E+02 ML, VW = 3.000E+04 ML
XZERO = 1.260E+03 MICROGRAMS/GRAM OF OIL, AREA = 6.170E+02 CM*CM
OVER-ALL KW AT WATER-OIL = 3.000E+00 CM/HR
OVER-ALL KO AT OIL-AIR = 2.380E-04 CM/HR
A = -6.169E-02, B = 1.723E-06
C = 9.254E+00, D = -9.951E-04
E = 6.122E-02
B1 = -7.334E-04, B2 = -6.196E-02
C1 = 1.255E+03, C2 = 5.384E+00
Z1 = 8.547E-02, Z2 = -8.547E-02
WATER CONCENTRATION PEAKS AT 7.246E+01 HOURS
WHERE THE WATER CONCENTRATION = 3.323E-02, AND THE OIL CONCENTRATION = 1.190E+03
AND THE CONCENTRATION RATIO (OIL/WATER) = 3.580E+04

HOUR	H20	OIL
0.20	4.316E-04	1.260E+03
0.40	8.578E-04	1.259E+03
0.60	1.279E-03	1.259E+03
0.80	1.694E-03	1.259E+03
1.00	2.105E-03	1.259E+03
1.20	2.510E-03	1.259E+03
1.40	2.910E-03	1.258E+03
1.60	3.306E-03	1.258E+03
1.80	3.696E-03	1.258E+03
2.00	4.081E-03	1.258E+03
2.25	4.557E-03	1.257E+03
2.50	5.024E-03	1.257E+03
2.75	5.485E-03	1.257E+03
3.00	5.938E-03	1.256E+03
3.25	6.384E-03	1.256E+03
3.50	6.823E-03	1.256E+03
3.75	7.256E-03	1.255E+03
4.00	7.681E-03	1.255E+03
4.25	8.100E-03	1.255E+03
4.50	8.513E-03	1.255E+03
6.00	1.006E-02	1.253E+03
8.00	1.365E-02	1.251E+03
10.00	1.612E-02	1.248E+03
12.00	1.829E-02	1.246E+03
14.00	2.021E-02	1.244E+03
16.00	2.189E-02	1.242E+03
18.00	2.337E-02	1.240E+03
20.00	2.468E-02	1.238E+03
22.00	2.582E-02	1.236E+03
24.00	2.683E-02	1.234E+03
26.00	2.771E-02	1.232E+03
28.00	2.849E-02	1.230E+03
30.00	2.917E-02	1.228E+03
32.00	2.976E-02	1.226E+03
34.00	3.028E-02	1.224E+03
36.00	3.073E-02	1.223E+03
38.00	3.112E-02	1.221E+03
40.00	3.147E-02	1.219E+03
42.00	3.176E-02	1.217E+03
44.00	3.202E-02	1.215E+03

TABLE 5-18. STIRRED TANK MODEL COMPUTER PREDICTED WATER COLUMN CONCENTRATIONS FROM EVAPORATION/DISSOLUTION EXPERIMENTS: KOVAT 1317, 1-METHYLNAPHTHALENE.

STIRRED TANK MODEL FOR KOVAT 1317, 1-METHYLNAPHTHALENE
FROM THE KEYBOARD, KW = 3.000E+00, KA = 1.500E+03, KO = 1.000E+00 CM/HR
N (OIL/WATER) = 3.040E+04, HENRYS LAW (AIR/OIL) = 1.204E-07 DIMENSIONLESS, AT 3.000E+00 DEG C
ANTA = 1.620E+01, ANTB = 4.267E+03, ANTC = -7.014E+01
MOLE WT OF OIL = 2.000E+02, DENSITY = 8.000E-01 GM/CC
VO = 2.000E+02 ML, VW = 3.000E+04 ML
XZERO = 7.370E+02 MICROGRAMS/GRAM OF OIL, AREA = 6.170E+02 CM*CM
OVER-ALL KW AT WATER-OIL = 3.000E+00 CM/HR
OVER-ALL KO AT OIL-AIR = 1.000E-04 CM/HR
A = -6.169E-02, B = 2.029E-06
C = 9.254E+00, D = -8.616E-04
H = 6.145E-02
D1 = -5.545E-04, D2 = -6.200E-02
C1 = 7.333E+02, C2 = 3.684E+00
Z1 = 2.434E-02, Z2 = -2.434E-02
WATER CONCENTRATION PEAKS AT 7.676E+01 HOURS
WHERE THE WATER CONCENTRATION = 2.312E-02, AND THE OIL CONCENTRATION = 7.028E+02
AND THE CONCENTRATION RATIO (OIL/WATER) = 3.040E+04

HOUR	H2O	OIL
0.20	2.973E-04	7.369E+02
0.40	5.909E-04	7.367E+02
0.60	8.808E-04	7.366E+02
0.80	1.167E-03	7.365E+02
1.00	1.450E-03	7.364E+02
1.20	1.729E-03	7.362E+02
1.40	2.003E-03	7.361E+02
1.60	2.277E-03	7.360E+02
1.80	2.546E-03	7.359E+02
2.00	2.812E-03	7.358E+02
2.25	3.139E-03	7.356E+02
2.50	3.461E-03	7.355E+02
2.75	3.779E-03	7.353E+02
3.00	4.091E-03	7.352E+02
3.25	4.398E-03	7.350E+02
3.50	4.701E-03	7.349E+02
3.75	4.999E-03	7.347E+02
4.00	5.292E-03	7.346E+02
4.25	5.581E-03	7.344E+02
4.50	5.866E-03	7.343E+02
6.00	7.481E-03	7.334E+02
8.00	9.411E-03	7.323E+02
10.00	1.111E-02	7.312E+02
12.00	1.261E-02	7.302E+02
14.00	1.393E-02	7.292E+02
16.00	1.510E-02	7.282E+02
18.00	1.613E-02	7.272E+02
20.00	1.703E-02	7.263E+02
22.00	1.782E-02	7.254E+02
24.00	1.852E-02	7.245E+02
26.00	1.914E-02	7.236E+02
28.00	1.968E-02	7.227E+02
30.00	2.015E-02	7.218E+02
32.00	2.057E-02	7.209E+02
34.00	2.093E-02	7.201E+02
36.00	2.125E-02	7.192E+02
38.00	2.153E-02	7.184E+02
40.00	2.177E-02	7.175E+02
42.00	2.198E-02	7.167E+02
44.00	2.216E-02	7.159E+02

TABLE 5-19. STIRRED TANK MODEL COMPUTER PREDICTED WATER COLUMN CONCENTRATIONS FROM EVAPORATION/DISSOLUTION EXPERIMENTS: KOVAT 857, ETHYLBENZENE.

STIRRED TANK MODEL FOR KOVAT 857, ETHYLBENZENE
FROM THE KEYBOARD, KW = 3.000E+00, KA = 1.500E+03, KO = 1.000E+00 CM/HR
H (OIL/WATER) = 2.400E+03, HENRYS LAW (AIR/OIL) = 1.232E-04 DIMENSIONLESS, AT 2.100E+01 DEG C
ANTA = 1.602E+01, ANTB = 3.290E+03, ANTC = -5.995E+01
MOLE WT OF OIL = 2.000E+02, DENSITY = 8.000E-01 GM/CC
VO = 2.000E+02 ML, VW = 3.000E+04 ML
X/ZERO = 4.740E+02 MICROGRAMS/GRAM OF OIL, AREA = 6.170E+02 CM*CM
OVER-ALL KW AT WATER-OIL = 2.996E+00 CM/HR
OVER-ALL KO AT OIL-AIR = 1.560E-01 CM/HR
A = -6.162E-02, B = 2.568E-05
C = 9.243E+00, D = -4.050E-01
R = 4.245E-01
B1 = -6.106E-02, B2 = -4.056E-01
C1 = 6.250E-01, C2 = 4.734E+02
Z1 = 2.067E-02, Z2 = -2.067E-02
WATER CONCENTRATION PEAKS AT 4.884E+00 HOURS
WHERE THE WATER CONCENTRATION = 1.860E-02, AND THE OIL CONCENTRATION = 4.464E+01
AND THE CONCENTRATION RATIO (OIL/WATER) = 2.400E+03

HOUR	H2O	OIL
0.20	2.305E-03	4.302E+02
0.40	4.369E-03	3.904E+02
0.60	6.215E-03	3.543E+02
0.80	7.862E-03	3.216E+02
1.00	9.329E-03	2.919E+02
1.20	1.063E-02	2.649E+02
1.40	1.179E-02	2.404E+02
1.60	1.282E-02	2.182E+02
1.80	1.372E-02	1.981E+02
2.00	1.452E-02	1.798E+02
2.25	1.537E-02	1.593E+02
2.50	1.609E-02	1.411E+02
2.75	1.670E-02	1.251E+02
3.00	1.719E-02	1.108E+02
3.25	1.759E-02	9.819E+01
3.50	1.791E-02	8.702E+01
3.75	1.816E-02	7.712E+01
4.00	1.835E-02	6.835E+01
4.25	1.848E-02	6.059E+01
4.50	1.856E-02	5.371E+01
6.00	1.832E-02	2.613E+01
8.00	1.700E-02	1.011E+01
10.00	1.534E-02	4.023E+00
12.00	1.369E-02	1.695E+00
14.00	1.216E-02	7.939E-01
16.00	1.078E-02	4.352E-01
18.00	9.546E-03	2.839E-01
20.00	8.451E-03	2.130E-01
22.00	7.480E-03	1.740E-01
24.00	6.621E-03	1.485E-01
26.00	5.860E-03	1.293E-01
28.00	5.186E-03	1.137E-01
30.00	4.590E-03	1.003E-01
32.00	4.062E-03	8.865E-02
34.00	3.595E-03	7.842E-02
36.00	3.182E-03	6.938E-02
38.00	2.816E-03	6.140E-02
40.00	2.492E-03	5.434E-02
42.00	2.206E-03	4.809E-02
44.00	1.952E-03	4.256E-02

TABLE 5-20. STIRRED TANK MODEL COMPUTER PREDICTED WATER COLUMN CONCENTRATIONS FROM EVAPORATION/DISSOLUTION EXPERIMENTS: KOVAT 867, P-XYLENE.

STIRRED TANK MODEL FOR KOVAT 867, P-XYLENE
FROM THE KEYBOARD, KW = 3.000E+00, KA = 1.500E+03, KO = 1.000E+00 CM/HR
M (OIL/WATER) = 2.800E+03, HENRYS LAW (AIR/OIL) = 1.220E-04 DIMENSIONLESS, AT 2.100E+01 DEG C
ANTA = 1.609E+01, ANTB = 3.347E+03, ANTC = -5.780E+01
MOLE WT OF OIL = 2.880E+02, DENSITY = 8.000E-01 GM/CC
VO = 2.000E+02 ML, VW = 3.000E+04 ML
XZERO = 1.794E+03 MICROGRAMS/GRAM OF OIL, AREA = 6.170E+02 CM*CM
OVER-ALL KW AT WATER-OIL = 2.997E+00 CM/HR
OVER-ALL KO AT OIL-AIR = 1.547E-01 CM/HR
A = -6.163E-02, B = 2.201E-05
C = 9.245E+00, D = -4.806E-01
R = 4.199E-01
D1 = -6.115E-02, D2 = -4.811E-01
C1 = 2.073E+00, C2 = 1.792E+03
Z1 = 9.404E-02, Z2 = -9.404E-02
WATER CONCENTRATION PEAKS AT 4.912E+00 HOURS
WHERE THE WATER CONCENTRATION = 6.079E-02, AND THE OIL CONCENTRATION = 1.702E+02
AND THE CONCENTRATION RATIO (OIL/WATER) = 2.800E+03

HOUR	H2O	OIL
0.20	7.403E-03	1.680E+03
0.40	1.419E-02	1.488E+03
0.60	2.019E-02	1.345E+03
0.80	2.555E-02	1.221E+03
1.00	3.033E-02	1.110E+03
1.20	3.459E-02	1.008E+03
1.40	3.837E-02	9.156E+02
1.60	4.172E-02	8.310E+02
1.80	4.468E-02	7.556E+02
2.00	4.728E-02	6.865E+02
2.25	5.009E-02	6.009E+02
2.50	5.246E-02	5.400E+02
2.75	5.444E-02	4.790E+02
3.00	5.607E-02	4.249E+02
3.25	5.740E-02	3.769E+02
3.50	5.846E-02	3.344E+02
3.75	5.929E-02	2.967E+02
4.00	5.991E-02	2.632E+02
4.25	6.035E-02	2.335E+02
4.50	6.062E-02	2.072E+02
6.00	5.991E-02	1.014E+02
8.00	5.565E-02	3.946E+01
10.00	5.025E-02	1.371E+01
12.00	4.485E-02	6.569E+00
14.00	3.984E-02	3.910E+00
16.00	3.531E-02	1.593E+00
18.00	3.127E-02	1.000E+00
20.00	2.767E-02	7.209E-01
22.00	2.449E-02	5.853E-01
24.00	2.167E-02	4.951E-01
26.00	1.918E-02	4.294E-01
28.00	1.697E-02	3.766E-01
30.00	1.502E-02	3.320E-01
32.00	1.329E-02	2.933E-01
34.00	1.176E-02	2.593E-01
36.00	1.041E-02	2.294E-01
38.00	9.208E-03	2.030E-01
40.00	8.148E-03	1.796E-01
42.00	7.210E-03	1.589E-01
44.00	6.380E-03	1.406E-01

TABLE 5-21. STIRRED TANK MODEL COMPUTER PREDICTED WATER COLUMN CONCENTRATIONS FROM EVAPORATION/DISSOLUTION EXPERIMENTS. KOVAT 1021, 1-METHYL-4-ISOPROPYLBENZENE.

```
STIRRED TANK MODEL FOR KOVAT 1021, 1-METHYL-4-ISOPROPYLB
FROM THE KEYBOARD, KW =  3.000E+00, KA =  1.500E+03, KO =  1.000E+00 CM/HR
M (OIL/WATER) =  7.500E+03, HENRYS LAW (ATM/OIL) =  2.040E-03 DIMENSIONLESS, AT  2.100E+01 DEG C
ANTA =  1.594E+01, ANTB =  3.599E+03, ANTC = -7.010E+01
MOLE WT OF OIL =  2.880E+02, DENSITY =  8.000E-01 GM/CC
VO =  2.000E+02 ML, VW =  3.000E+04 ML
XZERO =  4.530E+02 MICROGRAMS/GRAM OF OIL, AREA =  6.170E+02 CM*CM
OVER-ALL KW AT WATER-OIL =  2.999E+00 CM/HR
OVER-ALL KO AT OIL-AIR =  2.969E-02 CM/HR
A = -6.160E-02, B =  8.223E-06
C =  9.251E+00, D = -9.284E-02
R =  3.571E-02
D1 = -5.940E-02, D2 = -9.512E-02
C1 =  2.886E+01, C2 =  4.241E+02
Z1 =  1.043E-01, Z2 = -1.043E-01
WATER CONCENTRATION PEAKS AT  1.318E+01 HOURS
WHERE THE WATER CONCENTRATION =  1.790E-02, AND THE OIL CONCENTRATION =  1.342E+02
AND THE CONCENTRATION RATIO (OIL/WATER) =  7.500E+03
```

HOUR	H20	OIL
0.20	7.336E-04	4.447E+02
0.40	1.445E-03	4.365E+02
0.60	2.134E-03	4.285E+02
0.80	2.802E-03	4.206E+02
1.00	3.448E-03	4.129E+02
1.20	4.075E-03	4.053E+02
1.40	4.681E-03	3.978E+02
1.60	5.268E-03	3.905E+02
1.80	5.836E-03	3.833E+02
2.00	6.385E-03	3.763E+02
2.25	7.046E-03	3.677E+02
2.50	7.680E-03	3.593E+02
2.75	8.287E-03	3.510E+02
3.00	8.868E-03	3.430E+02
3.25	9.424E-03	3.351E+02
3.50	9.956E-03	3.275E+02
3.75	1.046E-02	3.200E+02
4.00	1.095E-02	3.127E+02
4.25	1.141E-02	3.055E+02
4.50	1.185E-02	2.985E+02
6.00	1.409E-02	2.599E+02
8.00	1.612E-02	2.161E+02
10.00	1.730E-02	1.798E+02
12.00	1.782E-02	1.496E+02
14.00	1.787E-02	1.246E+02
16.00	1.755E-02	1.037E+02
18.00	1.698E-02	8.646E+01
20.00	1.623E-02	7.209E+01
22.00	1.536E-02	6.014E+01
24.00	1.443E-02	5.020E+01
26.00	1.347E-02	4.193E+01
28.00	1.250E-02	3.504E+01
30.00	1.154E-02	2.931E+01
32.00	1.062E-02	2.453E+01
34.00	9.732E-03	2.054E+01
36.00	8.893E-03	1.722E+01
38.00	8.105E-03	1.444E+01
40.00	7.369E-03	1.213E+01
42.00	6.686E-03	1.019E+01
44.00	6.055E-03	8.570E+00

TABLE 5-22. STIRRED TANK MODEL COMPUTER PREDICTED WATER COLUMN CONCENTRATIONS FROM EVAPORATION/DISSOLUTION EXPERIMENTS: KOVAT 1185, NAPHTHALENE.

STIRRED TANK MODEL FOR KOVAT 1185, NAPHTHALENE
FROM THE KEYBOARD, KW = 3.000E+00, KA = 1.500E+03, KO = 1.000E+00 CM/HR
M (OIL/WATER) = 6.800E+03, HENRYS LAW (AIR/OIL) = 2.996E-06 DIMENSIONLESS, AT 2.100E+01 DEG C
ANTA = 1.614E+01, ANTB = 3.992E+03, ANTC = -7.130E+01
MOLE WT OF OIL = 2.880E+02, DENSITY = 8.800E-01 GM/CC
VO = 2.000E+02 ML, VW = 3.000E+04 ML
XZERO = 5.200E+02 MICROGRAMS/GRAM OF OIL, AREA = 6.170E+02 CM*CM
OVER-ALL KW AT WATER-OIL = 2.999E+00 CM/HR
OVER-ALL KO AT OIL-AIR = 4.474E-03 CM/HR
A = -6.167E-02, B = 9.070E-06
C = 9.251E+00, D = -1.516E-02
R = 4.999E-02
B1 = -1.342E-02, B2 = -6.341E-02
C1 = 5.019E+02, C2 = 1.809E+01
Z1 = 9.434E-02, Z2 = -9.434E-02
WATER CONCENTRATION PEAKS AT 3.106E+01 HOURS
WHERE THE WATER CONCENTRATION = 4.902E-02, AND THE OIL CONCENTRATION = 3.333E+02
AND THE CONCENTRATION RATIO (OIL/WATER) = 6.800E+03

HOUR	H2O	OIL
0.20	9.360E-04	5.184E+02
0.40	1.858E-03	5.169E+02
0.60	2.765E-03	5.153E+02
0.80	3.659E-03	5.137E+02
1.00	4.539E-03	5.122E+02
1.20	5.405E-03	5.107E+02
1.40	6.258E-03	5.091E+02
1.60	7.098E-03	5.076E+02
1.80	7.925E-03	5.061E+02
2.00	8.738E-03	5.046E+02
2.25	9.738E-03	5.027E+02
2.50	1.072E-02	5.008E+02
2.75	1.168E-02	4.989E+02
3.00	1.262E-02	4.971E+02
3.25	1.354E-02	4.952E+02
3.50	1.445E-02	4.934E+02
3.75	1.534E-02	4.915E+02
4.00	1.620E-02	4.897E+02
4.25	1.706E-02	4.879E+02
4.50	1.789E-02	4.861E+02
6.00	2.256E-02	4.754E+02
8.00	2.793E-02	4.617E+02
10.00	3.245E-02	4.485E+02
12.00	3.623E-02	4.357E+02
14.00	3.935E-02	4.234E+02
16.00	4.191E-02	4.115E+02
18.00	4.396E-02	4.000E+02
20.00	4.559E-02	3.888E+02
22.00	4.684E-02	3.781E+02
24.00	4.777E-02	3.676E+02
26.00	4.841E-02	3.575E+02
28.00	4.881E-02	3.477E+02
30.00	4.899E-02	3.382E+02
32.00	4.900E-02	3.290E+02
34.00	4.885E-02	3.201E+02
36.00	4.857E-02	3.114E+02
38.00	4.817E-02	3.030E+02
40.00	4.768E-02	2.948E+02
42.00	4.711E-02	2.869E+02
44.00	4.647E-02	2.792E+02

TABLE 5-23. STIRRED TANK MODEL COMPUTER PREDICTED WATER COLUMN CONCENTRATIONS FROM EVAPORATION/DISSOLUTION EXPERIMENTS. KOVAT 1295. 2-METHYLNAPHTHALENE.

STIRRED TANK MODEL FOR KOVAT 1295, 2-METHYLNAPHTHALENE
FROM THE KEYBOARD, KW = 3.000E+00, KA = 1.500E+03, KO = 1.000E+00 CM/HR
M (OIL/WATER) = 1.300E+04, HENRYS LAW (AIR/OIL) = 8.402E-07 DIMENSIONLESS, AT 2.100E+01 DEC C
ANTA = 1.627E+01, ANTB = 4.237E+03, ANTC = -7.475E+01
MOLE WT OF OIL = 2.000E+02, DENSITY = 8.000E-01 GM/CC
VO = 2.000E+02 ML, VW = 3.000E+04 ML
XZERO = 1.260E+03 MICROGRAMS/GRAM OF OIL, AREA = 6.170E+02 CM*CM
OVER-ALL KW AT WATER-OIL = 2.999E+00 CM/HR
OVER-ALL KO AT OIL-AIR = 1.259E-03 CM/HR
A = -6.169E-02, B = 4.745E-06
C = 9.253E+00, D = -4.595E-03
R = 5.861E-02
D1 = -3.836E-03, D2 = -6.244E-02
C1 = 1.244E+03, C2 = 1.632E+01
Z1 = 1.020E-01, Z2 = -1.020E-01
WATER CONCENTRATION PEAKS AT 4.760E+01 HOURS
WHERE THE WATER CONCENTRATION = 7.977E-02, AND THE OIL CONCENTRATION = 1.037E+03
AND THE CONCENTRATION RATIO (OIL/WATER) = 1.300E+04

HOUR	H2O	OIL
0.20	1.180E-03	1.259E+03
0.40	2.360E-03	1.258E+03
0.60	3.517E-03	1.257E+03
0.80	4.658E-03	1.255E+03
1.00	5.785E-03	1.254E+03
1.20	6.896E-03	1.253E+03
1.40	7.993E-03	1.252E+03
1.60	9.075E-03	1.251E+03
1.80	1.014E-02	1.250E+03
2.00	1.120E-02	1.249E+03
2.25	1.249E-02	1.247E+03
2.50	1.377E-02	1.246E+03
2.75	1.503E-02	1.244E+03
3.00	1.626E-02	1.243E+03
3.25	1.747E-02	1.242E+03
3.50	1.867E-02	1.240E+03
3.75	1.984E-02	1.239E+03
4.00	2.099E-02	1.237E+03
4.25	2.213E-02	1.236E+03
4.50	2.324E-02	1.235E+03
6.00	2.956E-02	1.227E+03
8.00	3.703E-02	1.216E+03
10.00	4.354E-02	1.206E+03
12.00	4.920E-02	1.195E+03
14.00	5.412E-02	1.185E+03
16.00	5.838E-02	1.176E+03
18.00	6.205E-02	1.166E+03
20.00	6.522E-02	1.157E+03
22.00	6.793E-02	1.147E+03
24.00	7.025E-02	1.138E+03
26.00	7.221E-02	1.129E+03
28.00	7.387E-02	1.120E+03
30.00	7.525E-02	1.111E+03
32.00	7.640E-02	1.102E+03
34.00	7.733E-02	1.094E+03
36.00	7.808E-02	1.085E+03
38.00	7.867E-02	1.077E+03
40.00	7.911E-02	1.068E+03
42.00	7.943E-02	1.060E+03
44.00	7.963E-02	1.052E+03

TABLE 5-24. STIRRED TANK MODEL COMPUTER PREDICTED WATER COLUMN CONCENTRATIONS FROM EVAPORATION/DISSOLUTION EXPERIMENTS: KOVAT 1317, 1-METHYLNAPHTHALENE.

STIRRED TANK MODEL FOR KOVAT 1317, 1-METHYLNAPHTHALENE
FROM THE KEYBOARD, KW = 3.000E+00, KA = 1.500E+03, KO = 1.000E+00 CM/HR
M (OIL/WATER) = 5.000E+03, HENRYS LAW (AIR/OIL) = 6.661E-07 DIMENSIONLESS, AT 2.100E+01 DEG C
ANTA = 1.620E+01, ANTB = 4.267E+03, ANTC = -7.815E+01
MOLE WT OF OIL = 2.180E+02, DENSITY = 0.800E-01 GM/CC
VO = 2.000E+02 ML, VW = 3.000E+04 ML
XZERO = 7.370E+02 MICROGRAMS/GRAM OF OIL, AREA = 6.170E+02 CM*CM
OVER-ALL KW AT WATER-OIL = 2.990E+00 CM/HR
OVER-ALL KO AT OIL-AIR = 9.982E-04 CM/HR
A = -6.166E-02, B = 1.233E-05
C = 9.249E+00, D = -4.929E-03
H = 6.062E-02
D1 = -2.985E-03, D2 = -6.361E-02
C1 = 7.134E+02, C2 = 2.363E+01
Z1 = 1.499E-01, Z2 = -1.499E-01
WATER CONCENTRATION PEAKS AT 5.046E+01 HOURS
WHERE THE WATER CONCENTRATION = 1.229E-01, AND THE OIL CONCENTRATION = 6.146E+02
AND THE CONCENTRATION RATIO (OIL/WATER) = 5.000E+03

HOUR	H2O	OIL
0.20	1.806E-03	7.363E+02
0.40	3.588E-03	7.356E+02
0.60	5.346E-03	7.348E+02
0.80	7.081E-03	7.341E+02
1.00	8.793E-03	7.334E+02
1.20	1.048E-02	7.327E+02
1.40	1.215E-02	7.320E+02
1.60	1.379E-02	7.313E+02
1.80	1.542E-02	7.306E+02
2.00	1.702E-02	7.299E+02
2.25	1.899E-02	7.291E+02
2.50	2.093E-02	7.282E+02
2.75	2.283E-02	7.274E+02
3.00	2.471E-02	7.265E+02
3.25	2.655E-02	7.257E+02
3.50	2.837E-02	7.249E+02
3.75	3.015E-02	7.240E+02
4.00	3.190E-02	7.232E+02
4.25	3.362E-02	7.224E+02
4.50	3.532E-02	7.216E+02
6.00	4.491E-02	7.168E+02
8.00	5.626E-02	7.107E+02
10.00	6.615E-02	7.049E+02
12.00	7.477E-02	6.993E+02
14.00	8.226E-02	6.939E+02
16.00	8.875E-02	6.886E+02
18.00	9.437E-02	6.836E+02
20.00	9.923E-02	6.786E+02
22.00	1.034E-01	6.739E+02
24.00	1.070E-01	6.692E+02
26.00	1.100E-01	6.646E+02
28.00	1.126E-01	6.601E+02
30.00	1.148E-01	6.558E+02
32.00	1.167E-01	6.515E+02
34.00	1.182E-01	6.472E+02
36.00	1.195E-01	6.431E+02
38.00	1.205E-01	6.390E+02
40.00	1.213E-01	6.349E+02
42.00	1.219E-01	6.309E+02
44.00	1.223E-01	6.270E+02

Figures 5-48 and 5-49 present the predicted water column concentrations at 21 and 3°C for the compounds presented in Tables 5-13 through 5-24. These figures clearly show the less volatile compounds persisting in the water column. This is what has been recently observed experimentally as shown in plots of observed component concentration (Figures 5-25 and 5-31). The experimental observations indicate that the naphthalenes tail-off much faster than predicted. This rapid tail-off could be due to some other degradation mechanism such as biological weathering (discussed in Section 5.2).

In general, the predicted time of occurrence of the peak water concentrations is quite good, but the peak concentrations do not always agree well. The prediction of the peak concentration is directly dependent on the initial concentration and the M-value. While our M-value data represent first-of-a-kind measurements, future determinations will no doubt yield improvements.

When utilizing the pseudo-component approach, characterization output from the oil weathering model is in the form of distillation cuts (pseudo-compounds) which remain in the oil slick as a function of time. Figure 5-50 presents time series plots of the predicted "distillation curves" from oil weathering at 13°C under natural environmental conditions, and Figure 5-51 presents normalized distillation curves for the "distillable components". Figures 5-52 and 5-53 present the observed hydrocarbon concentration distillation curves (real and normalized to total "distillable") generated from the wave tank gas chromatographic data discussed in the previous sections.

The observed distillation fraction curves were generated by summing all of the total resolved components in each chromatogram (as shown in Figure 5-43 in the previous section) by Kovat indices and then correlating these cumulative sums with the recorded boiling point for each n-alkane throughout the range of nC-7 through nC-28. These figures were generated using the program PBDIST which is an integral portion of the overall oil weathering model.

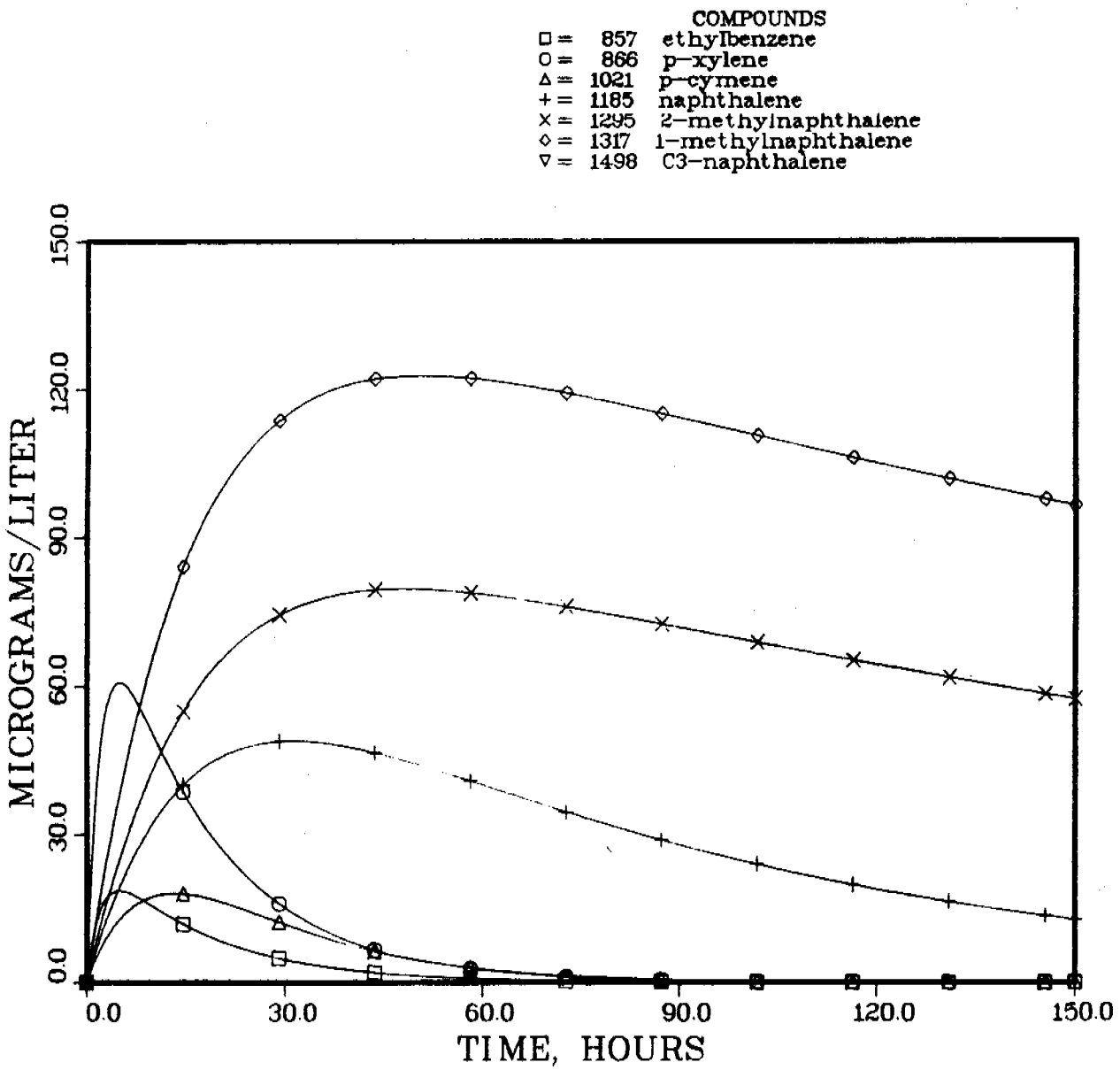

FIGURE 5-48. PREDICTED WATER COLUMN CONCENTRATIONS, STIRRED TANK MODEL AT 19°C.

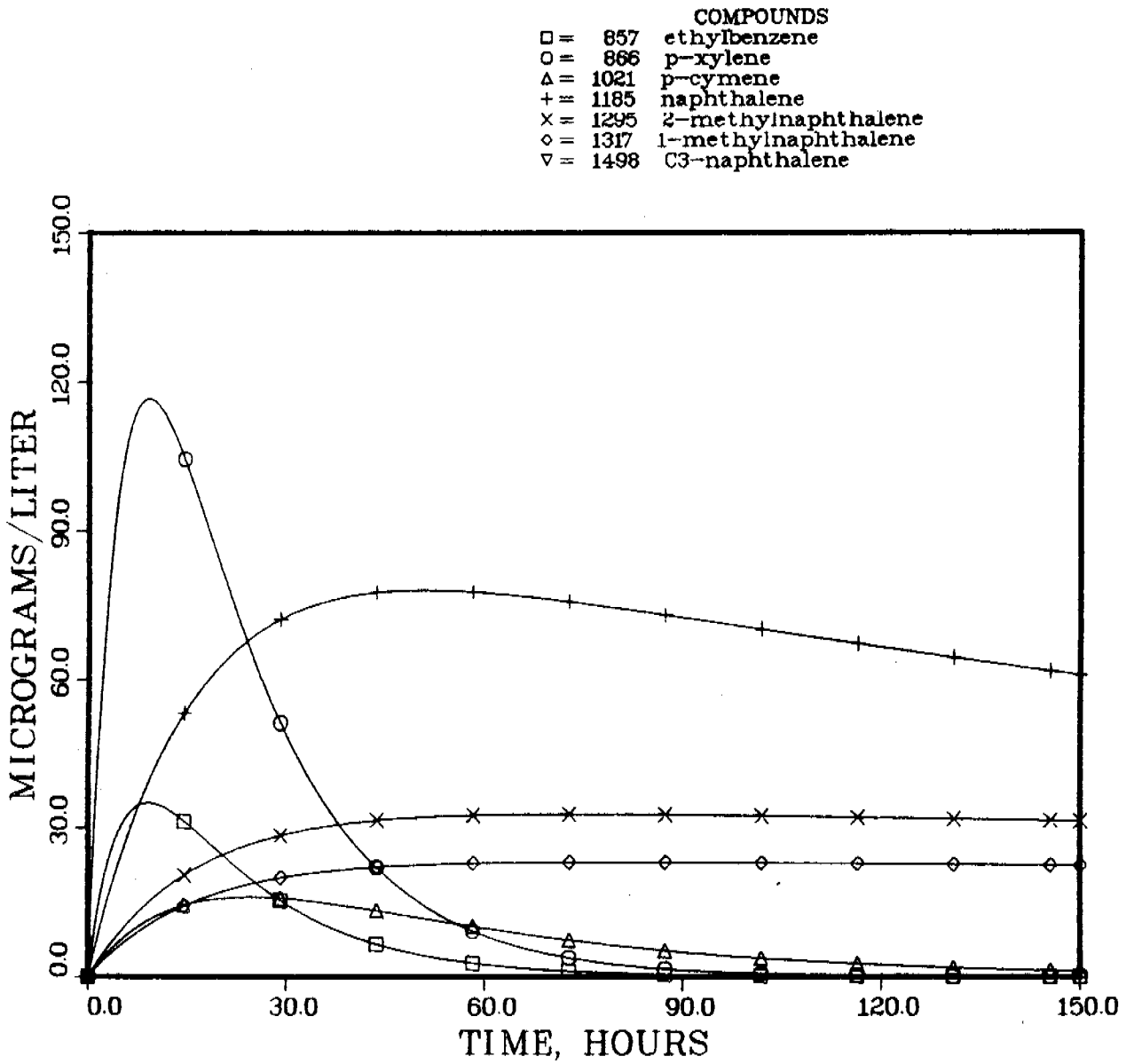

FIGURE 5-49. PREDICATED WATER COLUMN CONCENTRATIONS, STIRRED TANK MODEL AT 3°C.

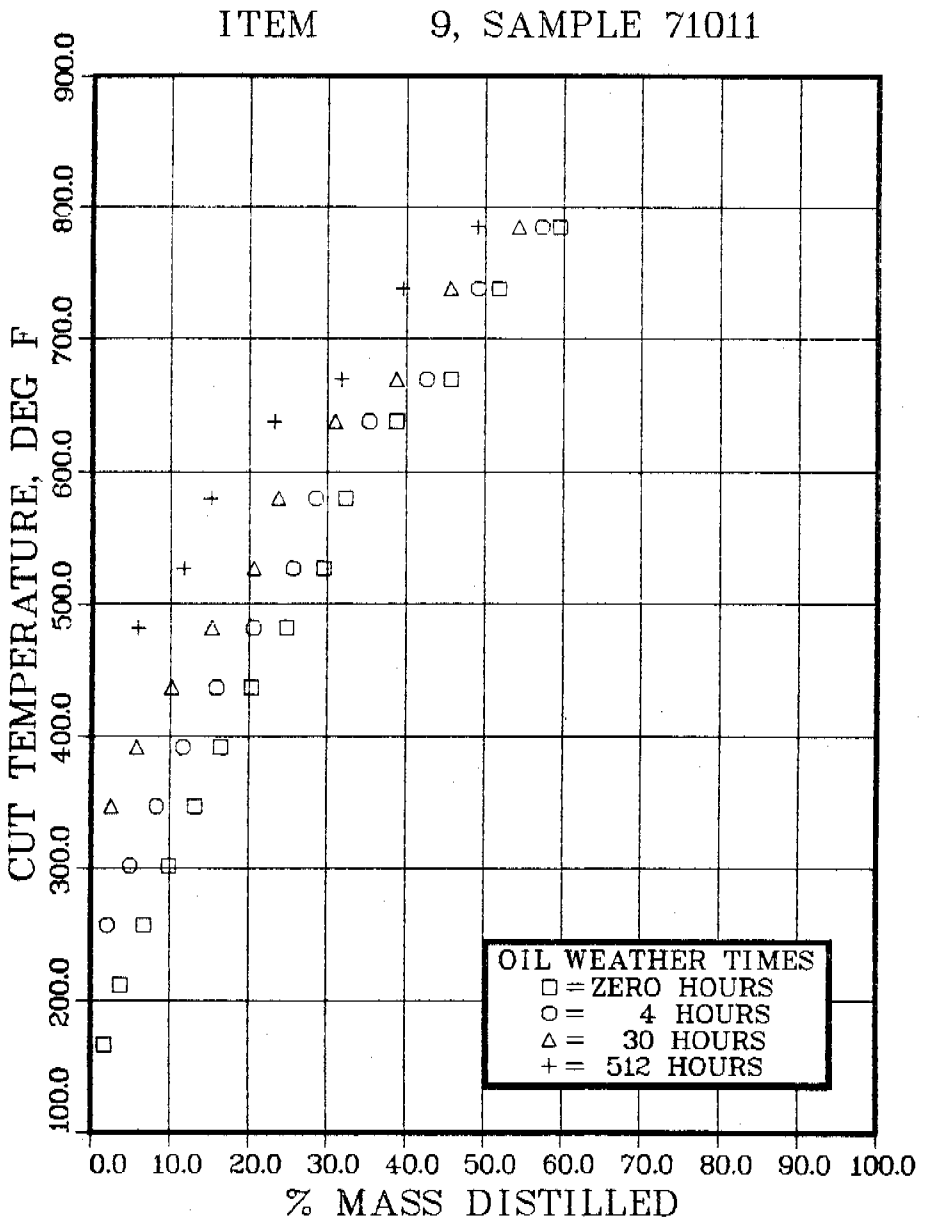

FIGURE 5-50. COMPUTER PREDICTED MASS BALANCE DISTILLATION CURVES FOR OIL WEATHERING IN THE WAVE TANK EXPERIMENT AT 55°F.

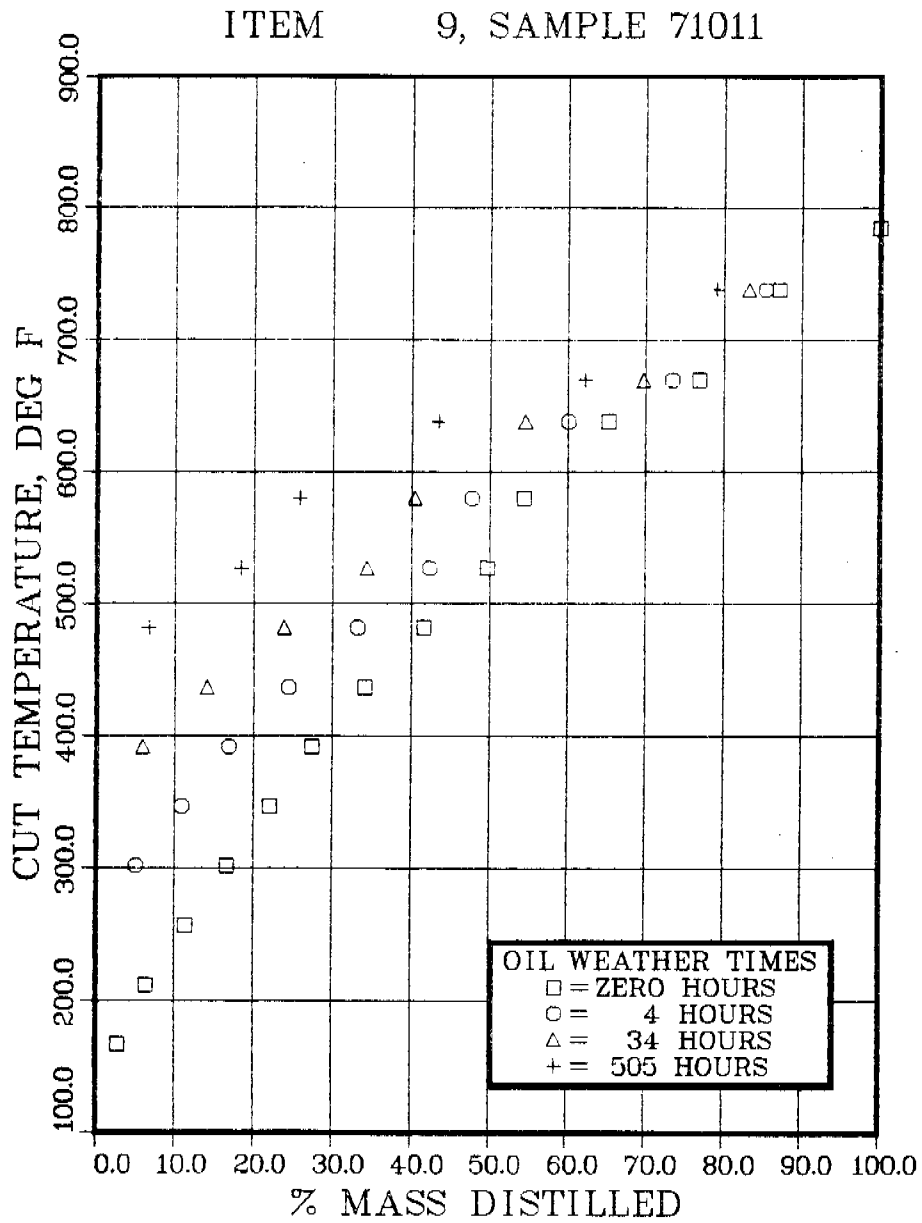

FIGURE 5-51. COMPUTER PREDICTED TOTAL DISTILLABLE BOILING POINT DISTRIBUTION CURVES FOR OIL WEATHERING IN THE WAVE TANK EXPERIMENT AT 55°F.

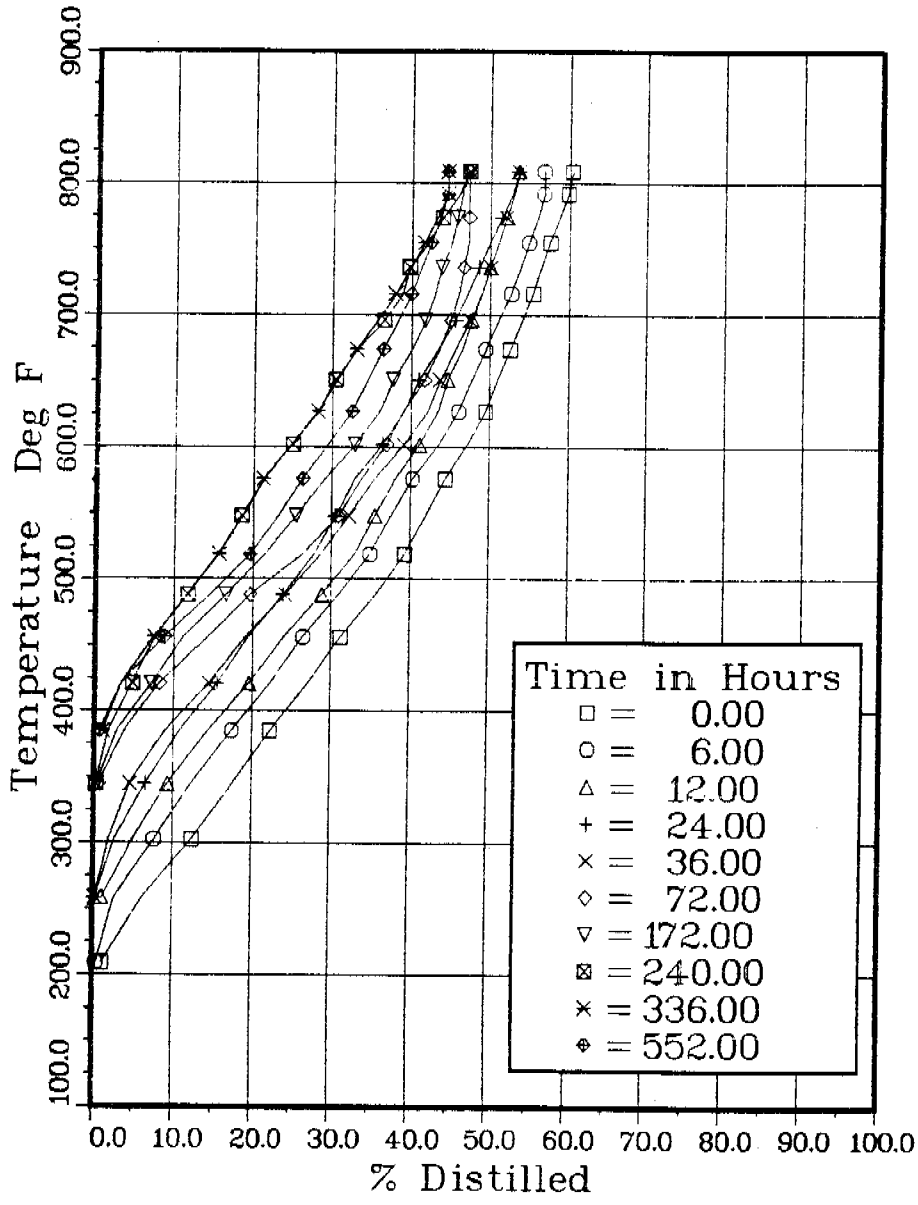

FIGURE 5-52. OBSERVED MASS BALANCE DISTILLATION CURVES GENERATED FROM GAS CHROMATOGRAPHIC DATA IN EXP DATA BASE FOR PRUDHOE BAY CRUDE OIL WEATHERING IN THE WAVE TANK EXPERIMENT AT KASITSNA BAY, ALASKA.

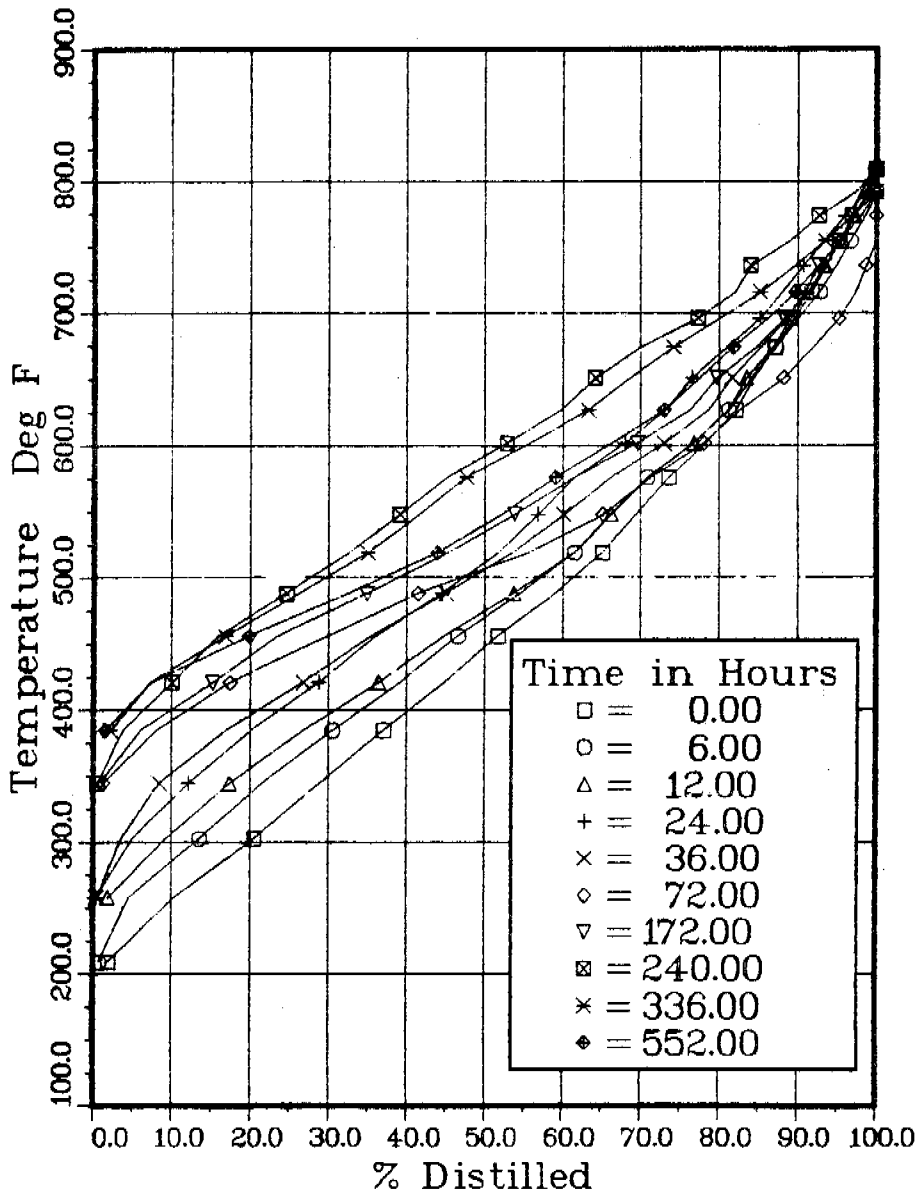

FIGURE 5-53. OBSERVED TOTAL DISTILLABLE BOILING POINT DISTRIBUTION CURVES GENERATED FROM GAS CHROMATOGRAPHIC DATA IN EXP DATA BASE FOR PRUDHOE BAY CRUDE OIL WEATHERING IN THE WAVE TANK EXPERIMENT AT KASITSNA BAY, ALASKA.

5.2 Microbial Degradation Studies

5.2.1 Summary of Year I Activities

The major themes of the microbial degradation studies being conducted in this program have been: (1) examination of the degradation of petroleum components in terms of specific compound susceptibility, (2) isolation and characterization of stable oxidized products arising from catabolic processes, and (3) quantification of the degree and rates of partitioning of these products into the air, oil and seawater phases (i.e., away from the slick-seawater interface).

To determine the extent of petroleum component partitioning attributable to the purely physical/chemical (i.e., abiotic) dissolution and evaporation processes occurring simultaneously with microbial degradation, it was our initial approach to create and maintain a biotic/abiotic contrast in flow-through seawater aquarium systems in order to limit microbial metabolic influence on slick disposition. As indicated in our November 1980 Interim Report, considerable difficulty was encountered in maintenance of such a contrast within the continuously flowing experimental systems. Continued efforts demonstrated that a significant microbial/abiotic contrast could not be maintained for longer than 6 to 8 days, and results suggested that the main problem in maintenance of such a contrast is one of the residence time for bacteria within the experimental systems. If the fraction of the indigenous marine bacteria which survive the sterilization attempts (by UV irradiation and $HgCl_2$ poisoning) cannot be flushed from the system at a rate substantially faster than the microbial population recovery dynamics (doubling times), repopulation and subsequential bacterial contamination of the "abiotic" experimental system is apparently inevitable.

Since the elevated flow rates utilized for the most recent sterilization attempts cannot be exceeded due to the analytically detrimental influence

on petroleum compound and oxidation product recoveries, such attempts to create and maintain this type of contrast were re-evaluated. A new experimental approach was developed, to facilitate continuation of the study of microbial degradation of crude petroleum. This new approach is quite viable with respect to the empirical needs of the overall modeling efforts, while at the same time alleviating the necessity for maintaining a biotic/abiotic contrast within the experimental system.

During the winter season of 1980-81, definitive microbial degradation studies were initiated with the continuous-flow experimental systems at Scripps Institution of Oceanography. The operational parameters for the aquaria included presence/absence of Corexit 9527, flow rates which provided approximately one tank volume change per 24 hours, and Prudhoe Bay crude petroleum at a volume ratio (oil-to-seawater) of about 1:200. Samples of the seawater effluent (20-40 liters) were taken at 0.5, 1, 2, 5, 10, 17, 24, 31, 38, 45 and 66 days, acidified (to pH 2.0) and CH_2Cl_2 extracted. The bulk extracts were fractionated by liquid/solid silica gel chromatography into aliphatic, aromatic and polar fractions. The polar fractions are expected to contain the majority of anticipated oxygenated products, and capillary GC-FID and GC/MS analyses of selected samples lend support to this hypothesis.

Seawater effluent extracts from weathered (Day 17) Prudhoe Bay crude and extracts of fresh crude were analyzed by capillary GC/MS. The aromatic fractions of the fresh crude and the weathered extracts (from two experimental systems) demonstrated strong qualitative resemblance; however, the polar fractions of fresh and weathered crude extracts were significantly different. Several tentatively identified compounds from the experimentally weathered crude extracts, which were absent in the corresponding fraction of fresh Prudhoe Bay crude, strongly suggest microbial degradation processes. These tentatively include benzenemethanol, 4-methylbenzenemethanol, 3-methylbenzoic acid, and a variety of phenols. Although the proposed mechanisms of microbial metabolism of petroleum hydrocarbons and the associated products are diverse, certain pathways have been delineated as being reasonably common with respect

to catabolism of aromatic compounds to hydroxylated and carboxylated moeities (JORDAN and PAYNE, 1980). Additional GC/MS characterization of both aromatic and polar fractions from Day 45 seawater effluent extracts were undertaken, and the results are discussed below (see Oxidized Product Characterizations).

5.2.2 Continued Studies - Year II

Two areas of experimental effort have been undertaken: (1) the continuous-flow experiments were continued at Scripps Institution of Oceanography and at NOAA's Kasitsna Bay facility; and (2) the static tank experiments were conducted at SAI's La Jolla facility. Results to date will be presented below with major emphasis placed on the continuous-flow studies.

Continuous-Flow Studies

The continuous-flow experimental approach was designed with the intent of providing a dynamic characterization of marine microbial populations and their inherent metabolic capacity for degrading petroleum components as a function of interaction with petroleum. This can be described as the time-dependent response within the indigenous heterotrophic population towards a greater relative abundance of hydrocarbonoclastic (hydrocarbon-degrading) microbes, as indicated by a concomitant increase in degradation potential of the system as measured by increased ^{14}C-labeled compound degradation. This has been empirically demonstrated by increases in the rates of mineralization to $^{14}CO_2$ of selected ^{14}C-labeled hydrocarbons as a function of continued exposure to crude oil within the experimental aquariums. Additional components of the "response time" include (2) determinations of heterotrophic bacterioplankton growth rates from incorporation of tritium-labeled thymidine into deoxyribonucleic acid (DNA) and enumeration of bacterial cells by epifluorescence microscopy; and (3) determinations of overall metabolic activity by uptake of tritium-labeled leucine and glucose, and assays of relative metabolic activity by microautoradiography.

An EPA approved bacterial strain mixture (Petrobac®) was incorporated into the experimental scheme (as well as in the static tank study). This mixture was developed by Polybac Corporation (Allentown, PA, U.S.A.) for certain oil degradation applications and is composed of individual strains originating from conventional selective adaptation and mutation techniques to utilize specific compound types (e.g., hydrocarbons, phenols, etc.). The blend also contains "background" microbes which are capable of degrading major metabolites from the specialized strains. It is of importance to note that this product was developed for degradation of oil in contact with a solid substrate (e.g., beach-stranded petroleum) and that Polyboc Corporation does not recommend its application to open water petroleum spills. However, their interest in the metabolic products arising from the interaction of the Petrobac®mixture with Prudhoe Bay crude petroleum under the given experimental conditions resulted in a high degree of cooperation between SAI and Polybac Corporation during the project.

It was also of interest to examine the influence of concentration levels of available dissolved inorganic nutrients (PO_4^{-3}, NO^-_2, NO^-_3, and NH_3) and dissolved oxygen upon microbial metabolic activities. To facilitate this, a nutrient solution was introduced (via a peristaltic pump system) into two of the experimental aquariums to maintain elevated levels (with respect to incoming seawater) and aeration of the seawater supplying these two tanks was provided. The experimental matrix presented below delineates the combinations of nutrient and dissolved O_2 supplementation, as well as innoculation with the Petrobac® strains for each experimental system. A schematic of the overall system is presented in Figure 5-54 and the Figure 5-55 shows the completed flow-through system as utilized at SIO and Kasitsna Bay.

Tank	Prudhoe Bay	Flow	Petrobac®	Nutrients/O_2
2	+	+	+	+
3	+	+	-	+
5	+	+	+	-
6	+	+	-	-

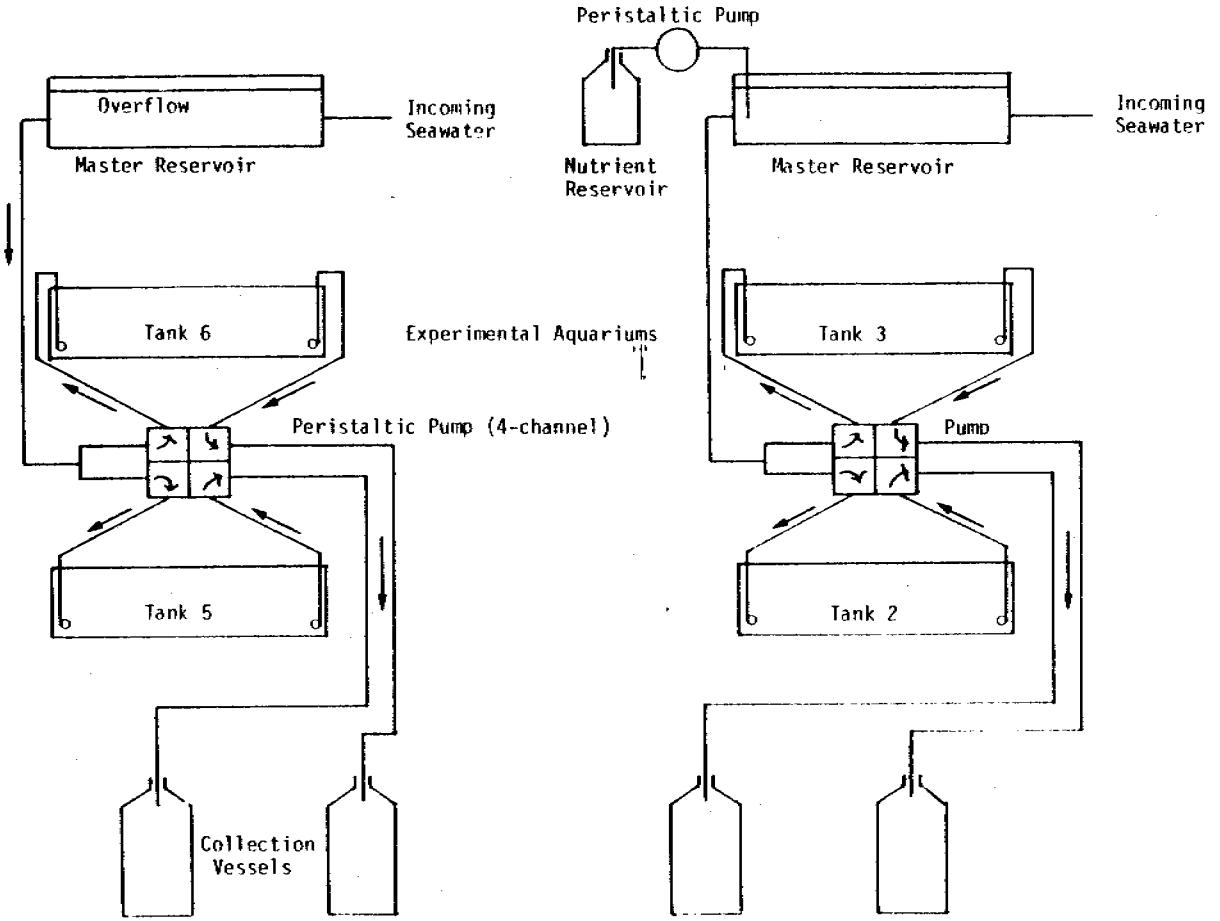

FIGURE 5-54. DIAGRAM AND PHOTOGRAPH OF THE CONTINUOUS-FLOW SEAWATER EXPERIMENTAL SYSTEMS AT SCRIPPS INSTITUTE OF OCEANOGRAPHY AND THE NOAA KASITSNA BAY FACILITY.

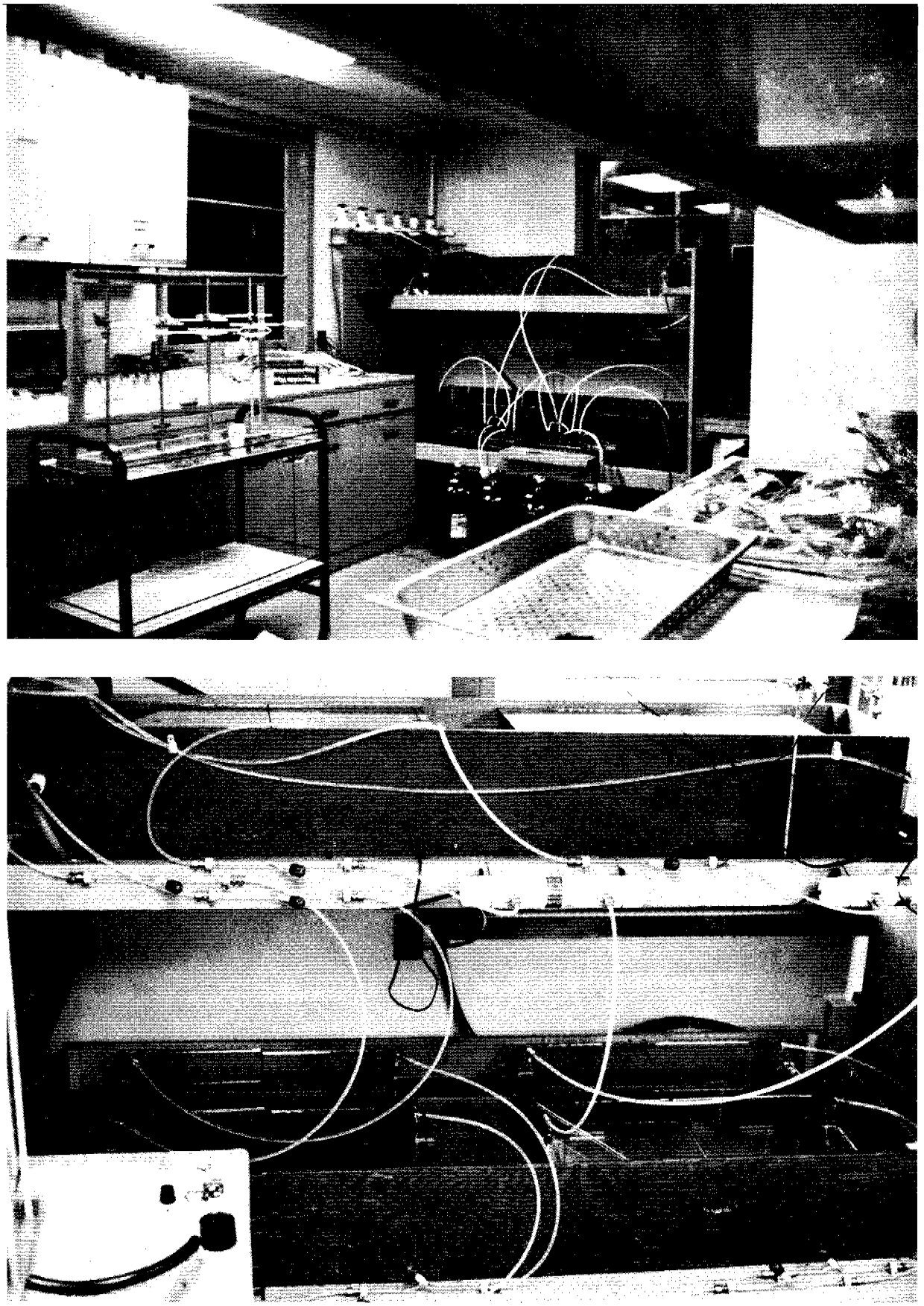

FIGURE 5-55. GENERAL VIEW OF CONTINUOUS-FLOW EXPERIMENTAL SYSTEM AT KASITSNA BAY, ALASKA FACILITY (TOP) AND CLOSEUP OF SYSTEM (BOTTOM) WITH ORIGINAL UV STERILIZATION UNITS.

Static-Tank Study

The main purpose of the static tank experiment performed at SAI's La Jolla facility was to provide samples (seawater extracts and weathered oil) containing metabolic products arising from microbial degradation of Prudhoe Bay crude oil. Due to the inherent difficulty in recovering such oxidized products from continuously-flowing aquaria, small static seawater aquaria (30 liter) were set up with the following combinations of indigenous microbes, Petrobac® strains, fresh oil, artificially generated (shaker table) mousse, dissolved oxygen and nutrient supplementation (at two levels of nitrogen and phosphorous):

Tank	Indigenous Microbes	Petrobac®	Fresh Crude	Mousse	Aeration (O_2)	Nutrients
1	+	+	+	-	+	+ (1)
2	+	-	+	-	+	+ (1)
3	+	+	+	-	+	+ (2)
4	+	-	+	-	+	+ (2)
5	+	+	-	+	+	+ (1)
6	+	-	-	+	+	+ (1)
7	+	+	-	+	+	+ (2)
8	+	-	-	+	+	+ (2)
9	+	-	+	-	+	-
10	+	-	-	-	+	-

Nutrient levels were initiated at approximately (1) 10 μM nitrogen (NH_4NO_3-N) and 1 μM phosphorous (KH_2PO_4-P); and (2) 100 μM nitrogen (NH_4NO_3-N) and 10 μM phosphorous (KH_2PO_4-P). Seawater samples for nutrient and pH determinations were taken weekly although the data are not available at the time of this writing. After approximately 50 days the seawater was removed from each

tank (30 liters), acidified to pH 2.0 and CH_2Cl_2 extracted. The remaining oil was also sampled and stored frozen for analysis. The samples from this experiment are being utilized for the portion of this program dealing with development of analytical methods for polar oxidized petroleum compounds.

5.2.3 Oxidized Product Characterizations

The objective of this phase of the oil weathering modeling study is the identification of some of the major oxygenated petroleum compounds which can be found in the polar (F3) fraction in extracts of seawater with considerable exposure time to microbial weathering of surface slicks of Prudhoe Bay crude oil. This section presents the results of the GC/MS analyses of two such fractions. Figure 5-56 presents the reconstructed ion chromatogram (RIC) of the sample obtained from an outside aquarium oil weathering experiment from Kasitsna Bay and could thus include some photo-oxidation products; and Figure 5-57 presents the RIC from the same (polar) fraction from an indoor aquarium experiment conducted at SIO, and thus exposed only to a minimum of artificial light. Tables 5-25 and 5-26 present the tentative compound and functional group identities of the numbered peaks in Figures 5-56 and 5-57, respectively. The peak identifications on peaks of significant size were obtained by computer matching to the 30,000 compounds in the EPA/NIH library of our Finnigan 4021 GC/MS system. The search program selects five compounds which show the best mass spectra data fit with the unknown compound spectrum and gives an estimate of both fit and purity. The suggested compounds were screened to eliminate those compounds whose molecular weights or volatilities were not consistent with the relative GC retention time. In many cases the program produced several possible homologs of a suggested class of compounds, and we plan to use selected standards of various compound classes to pinpoint the assignment of such peaks. Table 5-27 presents lists of standards (by functional group class) which are being obtained for GC/MS retention time verification and expansion of the spectral library data base. At this time, most of the peaks existing from GC/MS analyses of selected fractions can be labelled

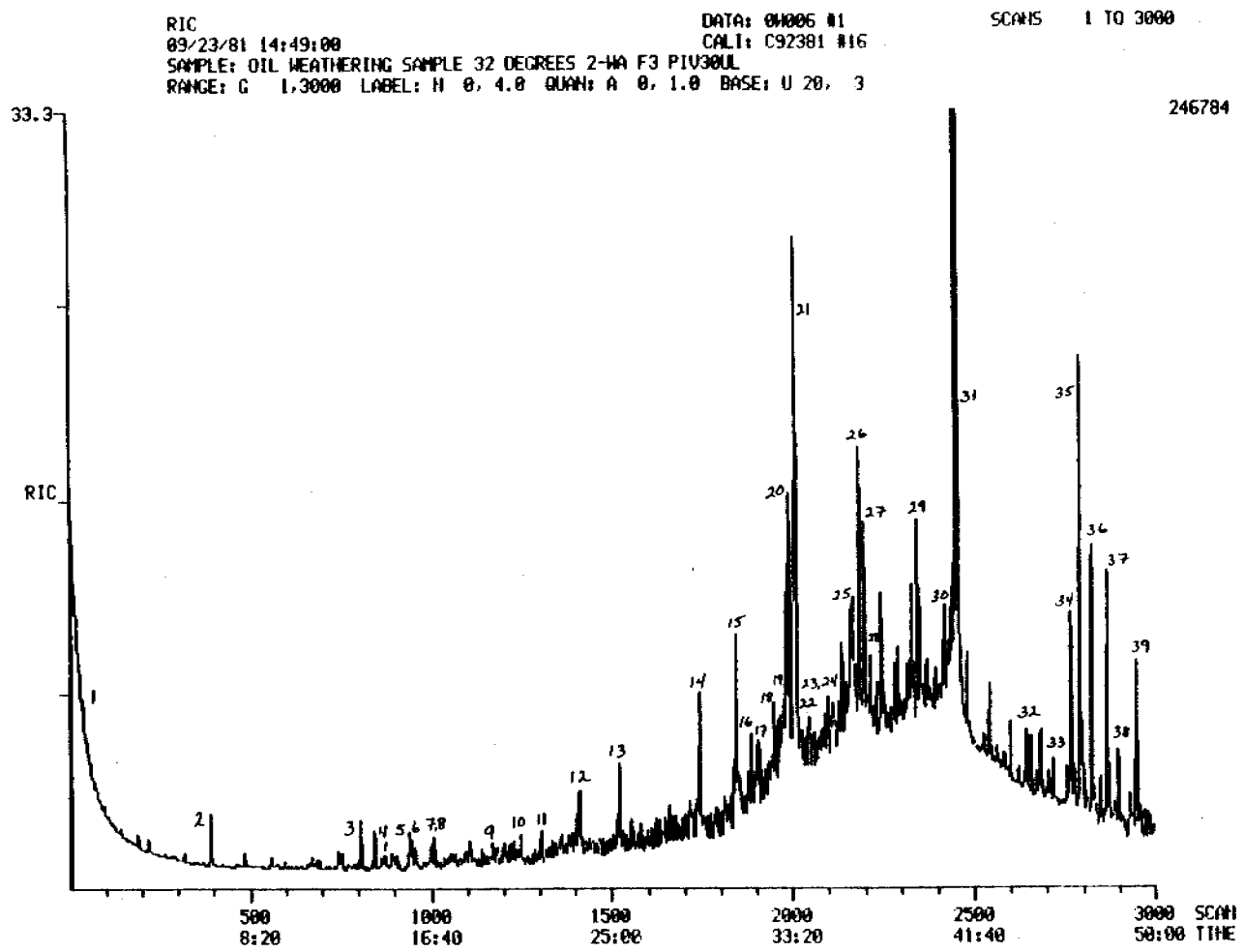

FIGURE 5-56. RECONSTRUCTED ION CHROMATOGRAM (RIC) FROM GC/MS ANALYSES OF THE POLAR (F3) WATER COLUMN EXTRACT OBTAINED FROM OUTDOOR FLOW-THROUGH TANK #2 FROM KASITSNA BAY, ALASKA. IDENTIFICATION OF THE NUMBERED PEAKS IN THE RIC ARE SHOWN IN TABLE 5-25.

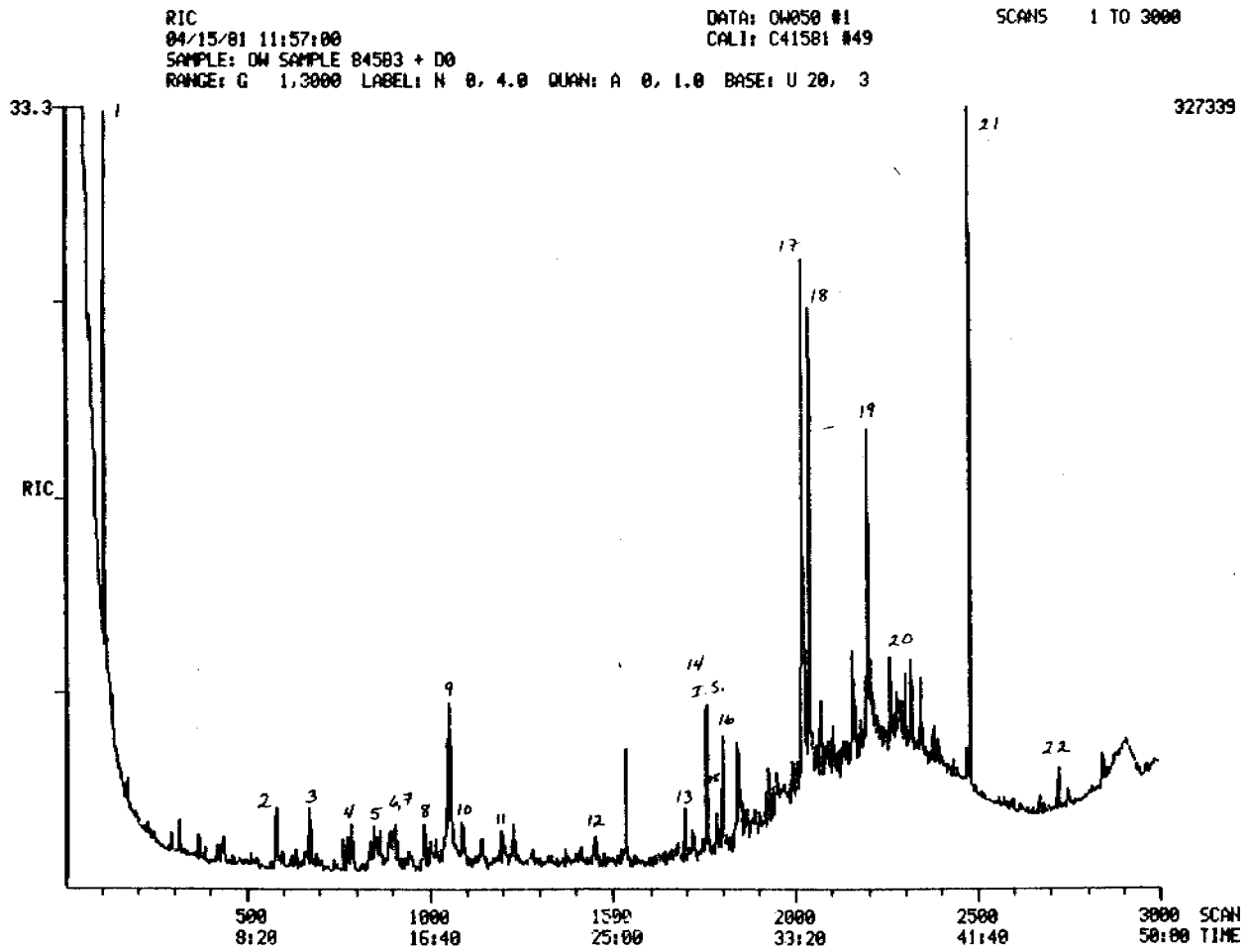

FIGURE 5-57. RECONSTRUCTED ION CHROMATOGRAM (RIC) FROM GC/MS ANALYSES OF POLAR (F3) WATER COLUMN EXTRACT OBTAINED FROM INDOOR FLOW-THROUGH TANK #3 AT SCRIPPS INSTITUTE OF OCEANOGRAPHY. IDENTIFICATIONS OF THE NUMBERED PEAKS IN THE RIC ARE SHOWN IN TABLE 5-25.

TABLE 5-25. TENTATIVE COMPOUND IDENTIFICATIONS FOR THE KASITSNA BAY POLAR (F3) FRACTION (see Figure 5-56).

Peak No.	Scan No.	Tentative Identification
1	38	Low molecular weight ketone
2	391	C_7 - C_8 aldehyde
3	807	C_9 - C_{10} aldehyde or alcohol
4	846	C_3 benzyl alcohol or C_4 phenol
5	945	C_3 benzyl alcohol or C_2 benzoic acid
6	959	o-(hydroxymethyl) benzoic acid
7	1003	C_3 benzyl alcohol or C_2 benzoic acid
8	1011	C_{10} - C_{11} aldehyde or alcohol
9,10	1250(4)	C_3 benzoic acids
11	1305	C_3 tetrahydrobenzofuranone
12	1415	Fatty acid
13	1523	Dibenzylether
14	1746	Fatty acid
15	1845	Long chain aldehyde
16	1888	Fatty acid
17	1902	Long chain aldehyde
18	1949	Long chain alcohol
19	1957	Fatty acid, methyl ester
20	----	Unsaturated fatty acid
21	1994	Phthalate ester
22-24	2006-2100	Fatty acids
25	----	Long chain aldehyde/alcohol
26,27	2187,2201	Fatty acids
28	2219	Long chain alcohol
29	2348	Fatty acid
30,31	2445,2456	Phthalate esters
32-39	2645-2951	Steroids

TABLE 5-26. TENTATIVE COMPOUND IDENTIFICATIONS FOR THE SIO POLAR (F3) FRACTION (see Figure 5-57).

Peak No.	Scan No.	Tentative Identification
1	42	Cyclohexanone
2	110	p-Methylbenzyl alcohol
3	680	Methylacetophenone
4	788	2,5-Dimethylbenzyl alcohol
5	850	o-Toluic acid
6	909	m-Toluic acid
7	915	p-Toluic acid
8	----	C_2 benzoic acid
9	----	Acrylate or crotonate ester
10	1092	3,4-dimethylbenzoic acid
11	----	Acrylate or crotonate ester
12	----	Long chain fatty acid
13	1698	Fluorenone
14	----	D-10 phenanthrene (internal std.)
15	----	Long chain fatty acid
16	----	Acrylate or crotonate ester
17	----	Long chain unsaturated fatty acid
18	----	Long chain unsaturated fatty acid
19	----	Long chain saturated aldehyde or alcohol
20	----	Phthalate ester
21	----	C_8 phthalate ester (d.)
22	----	Steroid

TABLE 5-27. STANDARDS CURRENTLY BEING OBTAINED AND ANALYZED TO PROVIDE RELATIVE RETENTION TIME AND QUADRUPOLE MASS SPECTRAL DATA FOR INCORPORATION INTO THE FINNIGAN MASS SPECTRAL LIBRARY AND VERIFICATION OF OXIDIZED PRODUCT COMPOUND IDENTIFICATIONS.

Acids

normal acids: C_3 to C_{12}, C_{14}, C_{16}, and C_{18}
benzoic acid
2-ethylhexanoic acid
2-naphthoic acid
terephthalic acid
undecylenic acid

Alcohols

normal 1-alkanols: C_1 to C_{12}, C_{14}, C_{16}, C_{18}, C_{20}, and C_{22}
straight chain, 2-alkanols: C_3 to C_5
2,3-butanediol
cyclohexanol
2-ethyl-1-butanol
2-methyl-1-butanol
3-methyl-1-butanol
2-methyl-2-butanol
3-methyl-3-pentanol
4-methyl-2-pentanol
2-methyl-1-propanol
2-methyl-2-propanol
3-pentanol

Aldehydes

n-alkanals: C_3 - C_{14}
acrolein
benzaldehyde
glutaric dialdehyde
2-methylpropanal
3-methylbutanal

Esters

methyl esters of normal acids: C_{10} - C_{22}
ethyl esters of normal acids: C_2 - C_6
propyl esters of normal acids: C_2 - C_6
methyl eicosenoate
methyl eicosadienoate
methyl eicosatrienoate
methyl erucate
methyl 2-hydroxydecanoate
methyl 2-hydroxydodecanoate
methyl 3-hydroxydodecanoate
methyl 2-hydroxyhexadecanoate
methyl 2-hydroxytetradecanoate

TABLE 5-27. STANDARDS CURRENTLY BEING OBTAINED AND ANALYZED TO PROVIDE RELATIVE RETENTION TIME AND QUADRUPOLE MASS SPECTRAL DATA FOR INCORPORATION INTO THE FINNIGAN MASS SPECTRAL LIBRARY AND VERIFICTION OF OXIDIZED PRODUCT COMPOUND IDENTIFICATIONS. (Continued).

methyl 3-hydroxytetradecanoate
methyl methacrylate
methyl 4-methylhexadecanoate
methyl linolenate
methyl nervonate
methyl oleate
methyl palmitoleate

Ketones

normal 2-alkanones C_3 to C_{13}, C_{15}, C_{17}, and C_{19}
2,6-dimethyl-4-heptanone
2-heptanone
4-heptanone
isophorone
5-methyl-3-heptanone
5-methyl-2-hexanone
4-methyl-2-pentanone
3-pentanone

Phenols

4-t-butylcatechol
m-cresol
2,3-dihydroxynaphthalene
1,4-dihydroxynaphthalene
2,3-dimethylphenol
2,4-dimethylphenol
4,6-dinitro-2-methylphenol
2,4-dinitrophenol
o-ethylphenol
p-ethylphenol
1-naphthol
2-naphthol
2-nitrophenol
4-nitrophenol
phenol
2,4,6-trimethylphenol

Phthalate Esters

di-n-alkyl: C_1 to C_{12}
butyl benzyl
di-(2-ethylhexyl)
di-isobutyl
di-isopropyl

only by possible compound class with a rather broad range of possible molecular weights. All GC/MS data from analyses of experimental samples are stored on 9-track magnetic tape, so additional compound searches and data manipulation can and will be completed as data on selected standards are obtained.

Both samples, from our flow-through tanks at Scripps Institution of Oceanography and at Kasitsna Bay showed an expected assortment of aldehydes, alcohols and acids. The reconstructed ion chromatogram from Kasitsna Bay showed almost twice as many significant peaks as that from SIO, including a number of higher molecular weight compounds with GC/MS data consistent with several steroidal compounds. In this instance, however, none of the specific steroids selected from the library showed very close fit with the GC/MS data. With few exceptions there were no specific assignments to the peaks of the Kasitsna Bay extract. Only the compound class is assigned and several isomers and/or homologs must be considered.

In particular, the Scripps sample does not show the diverse selection of steroidal possibilities in the high molecular weight region, although there is a small broad peak in that region of the chromatogram which could possibly be attributed to steroidal components. In this sample, several peaks show a reasonably good fit with specific compound assignments: p-methylbenzyl alcohol, the three toluic acids, and fluorenone, although the retention times of these peaks need to be checked against standards. In comparison, the polar extracts isolated from fresh oil samples show nothing in this region. (See Figures 3-1 through 3-4 in Section 3.0.)

It must be stressed that all of the compound and compound class assignments presented here must be considered as tentative only. In many cases, the GC/MS data are not highly convincing, and for many peaks the purity is not very high. The GC/MS data were obtained from a quadrupole mass spectrometer, and thus, are not completely consistent with the GC/MS data of the library which were generated on magnetic sector instruments.

The glass capillary/gas chromatographic (GC^2) data have been compared with our set of existing standards which for the most part give only a rough guide to the expected retention times for the oxygenated compounds of interest. As noted above, additional standards have been selected (based on these initial compound identifications) and ordered to facilitate these analyses.

Additional work is continuing on the following projects: (1) analyses of additional polar fractions isolated from seawater extracts from the static tank experiments plus other flow-through experiments from both SIO and Alaska; (2) derivativization (methylation and/or trimethylsilylation) of the samples for clarification of assignment of alcohols, phenols, and acids; (3) selection and accumulation of suitable polar standards for GC^2 retention time calibration and for more precise GC/MS data comparison (generation of GC/MS data sets from known standards run on our quadrupole instrument); and (4) acquisition of additional MS library data (Wiley Interscience and in-house laboratory standards).

5.2.4 Results to Date - Continuous Flow Studies (SIO and Kasitsna Bay)

Sampling Design

The continuous-flow experimental aquarium systems at Scripps Institution of Oceanography (SIO) and NOAA's Kasitsna Bay facility were set up (Summer 1981) and run for at least one week prior to initiation of each experiment to allow sufficient time for bacterial fouling, population buildup and stabilization of the microbial community within the aquariums. The tanks receiving the Petrobac® strains were innoculated with the bacterial slurry (prepared as needed from the dry spore-containing mix supplied by Polybac Corp.) each day until Day 7 after initiation of the experiments. After Day 7, the tanks were innoculated every other day for the remainder of the experimental time schedule.

The experimental aquaria and the incoming seawater were sampled for the radiolabeled substrate assays (^{14}C-hexadecane, ^{14}C-methylnaphthalene, ^{14}C-naphthalene; ^{3}H-glucose, ^{3}H-leucine, ^{3}H-thymidine) on Days 0, 1, 2, 4, 5, 6, 7, 9, 12, 14, 16, 19, 21, 23, 26, 28, 30, 35, 42, 49, and 56 at SIO and on the same schedule up to Day 30 at Kasitsna Bay. Samples for nutrients, epifluorescence and autoradiography assays were taken on Days 0, 1, 2, 4, 7, 14,, 21, and 28 for both experiments. Seawater samples (20 to 30 liters) for petroleum hydrocarbon and metabolic product analyses were taken on Days 1, 2, 5, 9, 16, 23, 30, 43 and 58 at SIO and up to Day 30 at Kasitsna Bay. To initiate each experiment, approximately 200 ml of Prudhoe Bay crude was added to each experimental aquarium shortly after sampling for the Day 0 assays listed above. Flow rates through the tanks were maintained by peristaltic pumps (Masterflex, Cole-Parmer Corp.) to provide a seawater throughput of about one tank volume (20 liters) per day.

^{14}C-Hydrocarbon Degradation

One of the important "components" of the overall microbial response to input of crude oil into the marine environment relates to the ability of the naturally occurring heterotrophic microbes to utilize the petroleum as a food (organic carbon) source. This capacity is referred to as "degradation potential", and can be inferred from the relative degree of mineralization (metabolism to CO_2) of representative petroleum hydrocarbons. Should selection within the heterotrophic fraction of the indigenous population favor an increase in relative abundance of hydrocarbon degraders, this should be reflected by a concomitant increase in degradation potential. One approach to empirically define this potential, which is sensitive and reproducible, involves exposing the microbes to a ^{14}C-labeled petroleum hydrocarbon substrate, allowing sufficient time for degradation to occur with subsequent trapping of evolved $^{14}CO_2$ and quantification by liquid scintillation spectrometry. This approach has been taken in various forms in past studies (HARRISON et al. (1971); CAPARELLO and LA ROCK (1975); WALKER and COLWELL (1976); HODSON et al. (1977)), however experimental conditions in most cases have made it difficult

or totally infeasible to extrapolate results to a real spill situation. We have attempted to utilize the degradation potential approach with the continuously flowing seawater aquaria systems at SIO and Kasitsna Bay with the intention of providing empirical information that would be useful in modeling the impact of microbial degradation of spilled petroleum. Although caution must be taken in extrapolating results from a study utilizing such "controlled ecosystems" to open ocean spills, it is felt that our approach optimizes the ability to empirically describe the impact of oil upon various microbiological metabolic processes.

The degradation potential assay involves addition of a ^{14}C-labeled hydrocarbon substrate to seawater samples from the experimental aquaria and incoming seawater, incubation in stoppered vials for 24 hrs. at in situ temperatures, trapping of $^{14}CO_2$ and quantification by liquid scintillation spectrometry (details presented in Appendix B). The labeled substrates selected were ^{14}C-hexadecane, ^{14}C-methylnaphthalene, and ^{14}C-naphthalene. The selection was based upon both availability and representation within the compounds and class types found in Prudhoe Bay crude, as well as other crude petroleums.

As indicated previously, the sampling points were concentrated at the beginning of each experiment to best detect and describe any degradation potential increase following input of Prudhoe Bay crude into the four experimental aquariums. The incoming seawater (from the master reservoirs) was also sampled at each time point and assayed to check for "background" hydrocarbon degradation potential.

The data for the ^{14}C-hydrocarbon degradation studies have been converted to g/liter-day and are presented graphically in Figures 5-58 for SIO results and Figure 5-59 for Kasitsna Bay, Alaska. The assumption made for data conversion is that trapping and detection of the ^{14}C carbon indicates loss of parent compound molecular structure even though total mineralization (to CO_2) cannot be deduced. The results from the SIO experiment demonstrate a dramatic increase in the amount of labeled substrate mineralized to $^{14}CO_2$

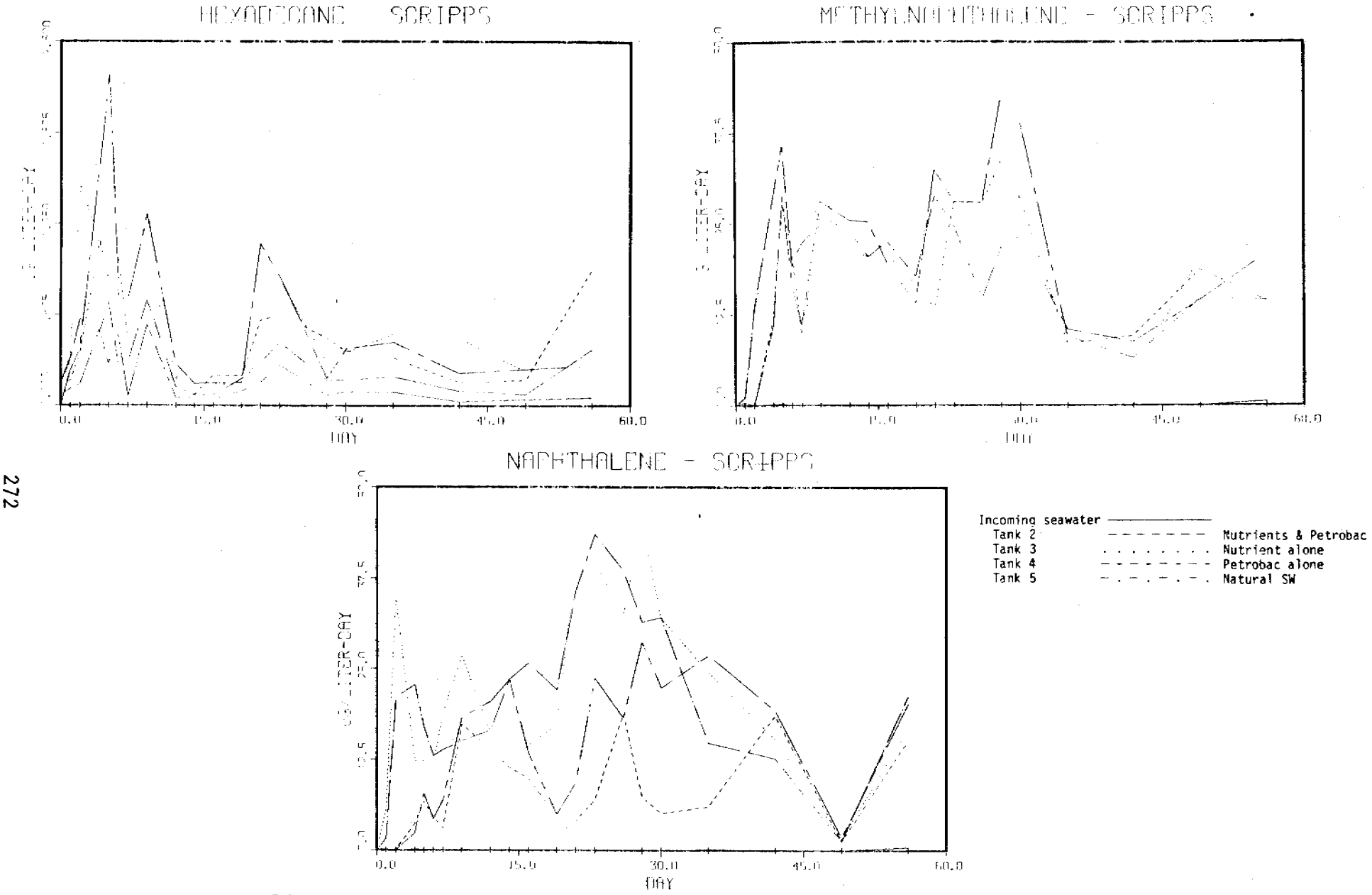

FIGURE 5-58. ^{14}C-HYDROCARBON DEGRADATION DATA, SCRIPPS INSITUTION OF OCEANOGRAPHY, SUMMER 1981. DATA FOR EACH SUBSTRATE ARE DEPICTED FOR ALL EXPERIMENTAL AQUARIA AND INCOMING SEAWATER. VERTICAL LINES ON ABSCISSA INDICATE SAMPLING POINTS.

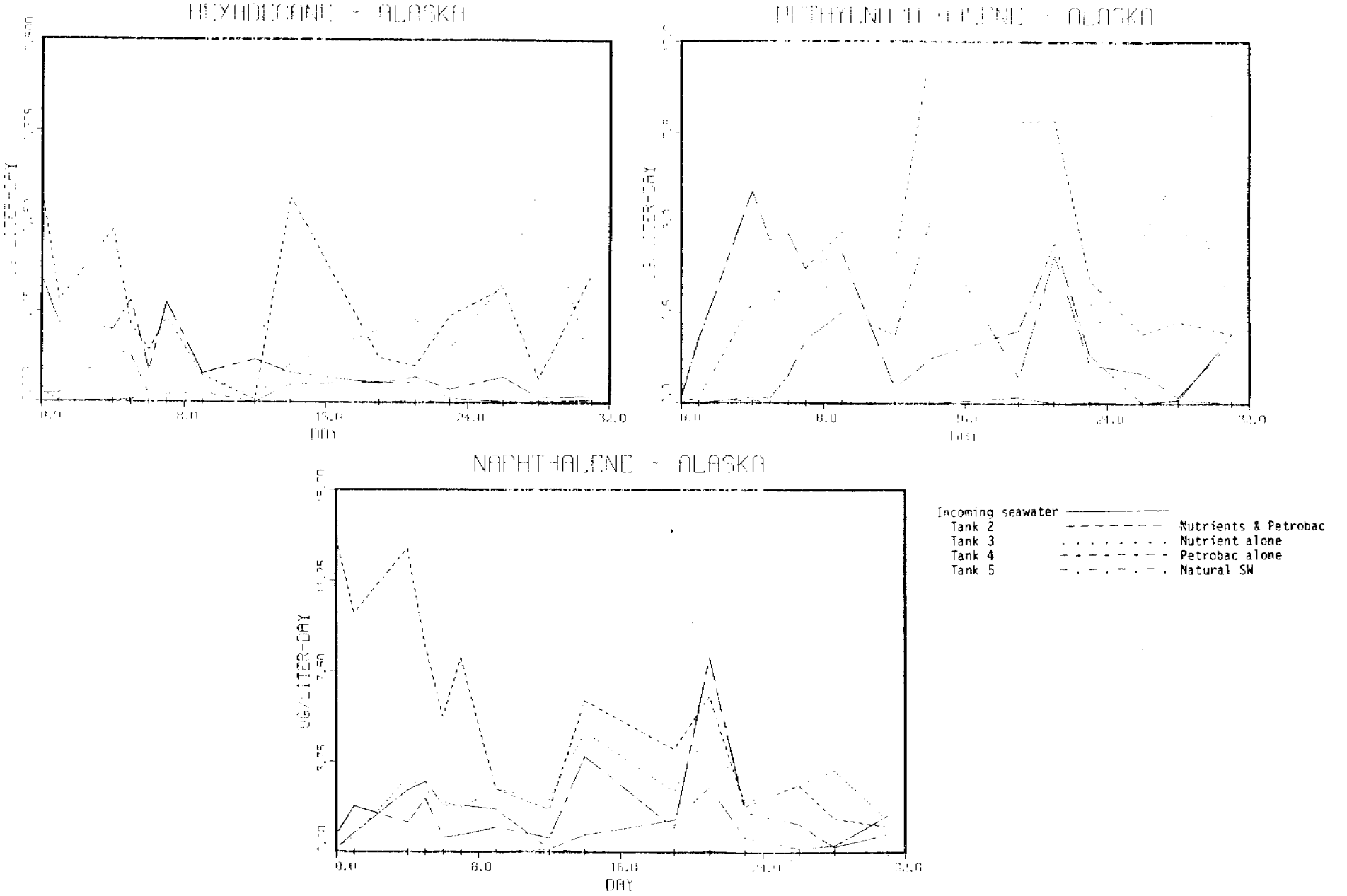

FIGURE 5-59. ^{14}C-HYDROCARBON DEGRADATION DATA, KASITSNA BAY, ALASKA, SUMMER 1981. DATA FOR EACH SUBSTRATE ARE DEPICTED FOR ALL EXPERIMENTAL AQUARIA AND INCOMING SEAWATER. VERTICAL LINES ON ABSCISSA INDICATE SAMPLING POINTS.

within 48 hrs after introduction of oil for all three hydrocarbons. At Day 0, hexadecane was slightly degraded although no capacity was apparent for degrading the methylnaphthalene and naphthalene substrates for any of the samples. The incoming seawater never demonstrated any degradation capacity for the aromatic compounds until Day 56, although the hexadecane was degraded to some extent with the pattern (note Figure) being similar to the four experimental systems. Tanks 3 and 5 (both with indigenous microbes only) demonstrated slightly greater utilization of hexadecane over the course of the experiment, with a peak utilization of approximately 5% of the added labeled substrate (again note that percent degradation is based upon the label itself and not the entire compound). All experimental systems followed similar trends (incoming seawater included) with time with an overall degradation rate of roughly 1.5% of the added substrate during any given 24 hr incubation period.

In comparing the relative rates of degradation for radiolabeled hydrocarbon substrates, it must be emphasized that the loss of label (^{14}C) from the parent molecule does not necessarily imply an "upper limit" on the amount of substrate which has been oxidized by microbes. In other words, certain metabolic conversions of the parent compound to other stable forms may occur <u>without</u> loss of the label. In this case, the degradation rate, as based upon detection and quantification of the last ^{14}C label, would be an underestimation of the actual amount of the original parent substrate "attached" by the microbial enzymatic systems. As will be noted below, the degradation data suggest that the hexadecane substrate was degraded at much lower rates than for either of the aromatic compounds. However, it is entirely possible that the mode of metabolic conversion for the aliphatic substrate renders the parent compound into stable forms (e.g., carboxylic acids, acetates) which may or may not undergo further mineralization during the 24-hr period of incubation.

Both of the labeled aromatic hydrocarbon substrates were degraded at substantially higher rates (based on $^{14}CO_2$ production) compared to hexadecane for the SIO experiment. All four experimental aquaria seawater exhibited quite similar patterns for methylnaphthalene, with dramatic increases in the

amounts of substrate mineralization within 48 to 72 hrs to approximately 11%, with an average rate of roughly 6% per day over the 56 days of monitoring. Less consistency between experimental systems is apparent for the naphthalene data, although average degradation rates are comparable to those for methylnaphthalene. Two trends in the aromatic hydrocarbon substrates are worth noting: (1) the tanks innoculated with the Petrobac® mixture (tanks 2 and 5) responded more slowly than tanks with indigenous microbes alone, particularly noticable for the naphthalene data; and (2) in the case of naphthalene, the tanks with and without added Petrobac® exhibited similar trends, although the indigenous or "natural" tanks exhibited higher overall rates of substrate degradation.

The ^{14}C-hydrocarbon data for the Kasitsna Bay experiment (Figure 5-59) demonstrated several similarities to the results from SIO: (1) hexadecane was apparently utilized to a lesser extent than either methylnaphthalene or naphthalene; (2) the incoming seawater demonstrated very little capacity for degrading any of the substrates; and (3) some similarities exist between experimental tanks for the two aromatic hydrocarbons, although to a lesser extent than with the SIO systems. Only in the case of methylnaphthalene was a definite increase apparent in rate of mineralization for all four tanks after introduction of Prudhoe Bay crude. Capacity to degrade hexadecane prior to oil introduction was demonstrated by samples from tanks 2 and 5 (which received Petrobac® innoculation) and for naphthalene in tank 2 only. Two additional trends which contrast the results from the SIO experiment are: (1) greater methylnaphthalene utilization for nutrient supplemented tanks (2 and 3) where nutrient supplementation had no apparent effect in SIO mineralization rate data; and (2) rates of substrate degradation were substantially lower in the Kasitsna Bay systems for all three hydrocarbons relative to the SIO experiment. This could be attributable to generally lower metabolic activities due to colder water temperatures, as they averaged 19 to 21°C during the course of the SIO study and 9 to 11°C for the Alaska study. The epifluorescence and autoradiography assays will provide an indication of relative mocrobial abundance and metabolic activity, respectively, between the SIO and Kasitsna Bay systems. However, these analyses are still underway at the time of this writing such that no definitive data are yet available.

^{3}H-Labelled Substrate Uptake/Incorporation

To further assess the impact of spilled petroleum upon microbial heterotrophic activity, it is necessary to determine influences on heterotrophic production (growth rates), microbial biomass, general metabolic activity and relative metabolic activity (e.g., % metabolically active microbes within the heterotrophic population). The utilization of radiolabeled organic substrates at near ambient concentrations for determining rates of uptake and/or incorporation into cell biomass is a viable and sensitive empirical approach and has been pursued in past studies (AZAM and HOLM-HANSEN, 1973; HODSON et al., 1977; FUHRMAN et al., 1980; FUHRMAN and AZAM, 1980; GRIFFITHS and MORITA, 1981). The use of tritium-labelled organic compounds (sugars, amino acids, etc.) of high specific activities allows for direct measurement of uptake at near ambient concentrations (10^{-8} to 10^{-9} M) and precludes the necessity of extrapolation using the Michaelis-Menten equation (as is needed when substrate concentrations are utilized which are greater than those normally found in the marine environment).

The incorporation of ^{3}H-thymidine into bacterial DNA serves as a reasonable measure of DNA synthesis and cell production, although several assumptions and measurements are required for conversion of thymidine incorporation data into production estimates (FUHRMAN and AZAM, 1980). The level or rate of uptake (nmoles/liter-day) is converted to bacterial cell production rates (cells/liter-day) with an estimation of the DNA content of natural marine bacteria. This conversion has been recently refined by FUHRMAN and AZAM (in press, 1981), into separate coefficients for the nearshore and offshore (> 10 km) waters studied (Southern California Bight). Estimations of average cell biomass by epifluorescence photomicroscopy allow for further data conversion from production rates (cells/liter-day) to organic carbon production (μg/C/liter-day). This is accomplished by determining cell size (volume) distributions and correlating the data to the amount of carbon per cell with a conversion factor developed by WATSON et al. (1977).

General metabolic activities have been determined by the ^{3}H-glucose and ^{3}H-leucine. The specific techniques utilized do not differentiate between substrate respired from that incorporated (assimilated) into cell biomass, and therefore the overall uptake cannot be used to estimate cellular production. However, FUHRMAN et al. (1980) found significant rank correlations between thymidine incorporation (mol/liter-day), thymidine turnover rates (%/hr), bacterial abundance or biomass (from epifluorescence microscopy) and glucose turnover rates (%/hr) in the euphotic zone of the Southern California Bight. Their results suggest that these methods may be comparable for assaying relative total bacterial activity between water samples.

An additional component of overall metabolic activity, in relation to the presence of crude petroleum, is that of relative or percent metabolic activity within the heterotrophic microbial population at any point in time. Although the epifluorescence microscopy yields information on bacterial abundance and biomass, it gives no indication of the metabolic state or relative activity. The latter type of information can be useful in the interpretation of the ^{3}H-glucose, ^{3}H-leucine, and ^{3}H-thymidine assay data and is provided by microautoradiography. This approach gives indication of the percent metabolically active heterotrophs as determined from the fraction of cells which have taken up a radiolabelled organic substrate during a short period of incubation.

As details for the techniques mentioned above are presented in Appendix B, it will suffice here to briefly describe the procedures. The ^{3}H-thymidine incorporation assay involves incubation of a seawater sample at in situ temperatures for uptake and subsequent incorporation into DNA of added labelled thymidine. The sample is filtered and the retained cells are extracted to remove non-incorporated label, and the amount of incorporated thymidine is determined by liquid scintillation spectrometry (LSC). The ^{3}H-glucose and ^{3}H-leucine uptake assays are very similar to the thymidine procedure except that no extraction step is performed to remove intracellular pools prior to quantification of retained label by LSC. In the epifluorescence techniques the cellular DNA is stained with a fluorescing dye, the sample is filtered and

the retained cells are counted and photographed under a phase contrast microscope fitted with an epifluorescent illuminator. The microautoragiography procedure is actually a combined autoradiography/epifluorescence technique in that cells are both radioactively and fluorescently labelled resulting from uptake of ^{3}H-leucine and DNA staining with the fluorescent dye, respectively. The sample is filtered and the filter is treated with a photographic emulsion and developed. The cells having sufficient radioactivity from substrate uptake have silver grains associated with them, and comparison of total cells from epifluorescence examination to cells with associated silver grains indicates the percentage of active cells present at the time of sampling.

The ^{3}H-thymidine incorporation, ^{3}H-leucine uptake, and ^{3}H-glucose uptake data for the SIO and Kasitsna Bay experiments are presented graphically in Figures 5-60 and 5-61, respectively. All data have been converted to uptake rates in nmoles/liter-day and are being normalized to uptake on a per bacterial cell basis at the time of this writing.

In the SIO thymidine incorporation experiments, all four experimental aquaria demonstrated similar patterns in terms of an initial increase in incorporation rates after introduction of oil, followed by a general decline and periodic fluctuations during the 56 days of monitoring. Higher rates of incorporation were apparent in the Petrobac® innoculated tanks (2, 5), which may be attributable to higher overall numbers of cells. The incoming seawater remained relatively inactive during the course of the experiment, and this may also be attributable to the relative abundance of bacteria (abundance data will be discussed below).

The leucine uptake data from the SIO experiment appear difficult to interpret due to the large fluctuations with time and between experimental systems. However, there is a significant difference between Petrobac® innoculated tanks (2, 5) and the tanks with "natural" microbes only (3, 6) in that the Petrobac® tanks demonstrated a slight decrease in leucine uptake after oil introduction whereas tanks 3 and 6 exhibited a sharp rise in uptake rates

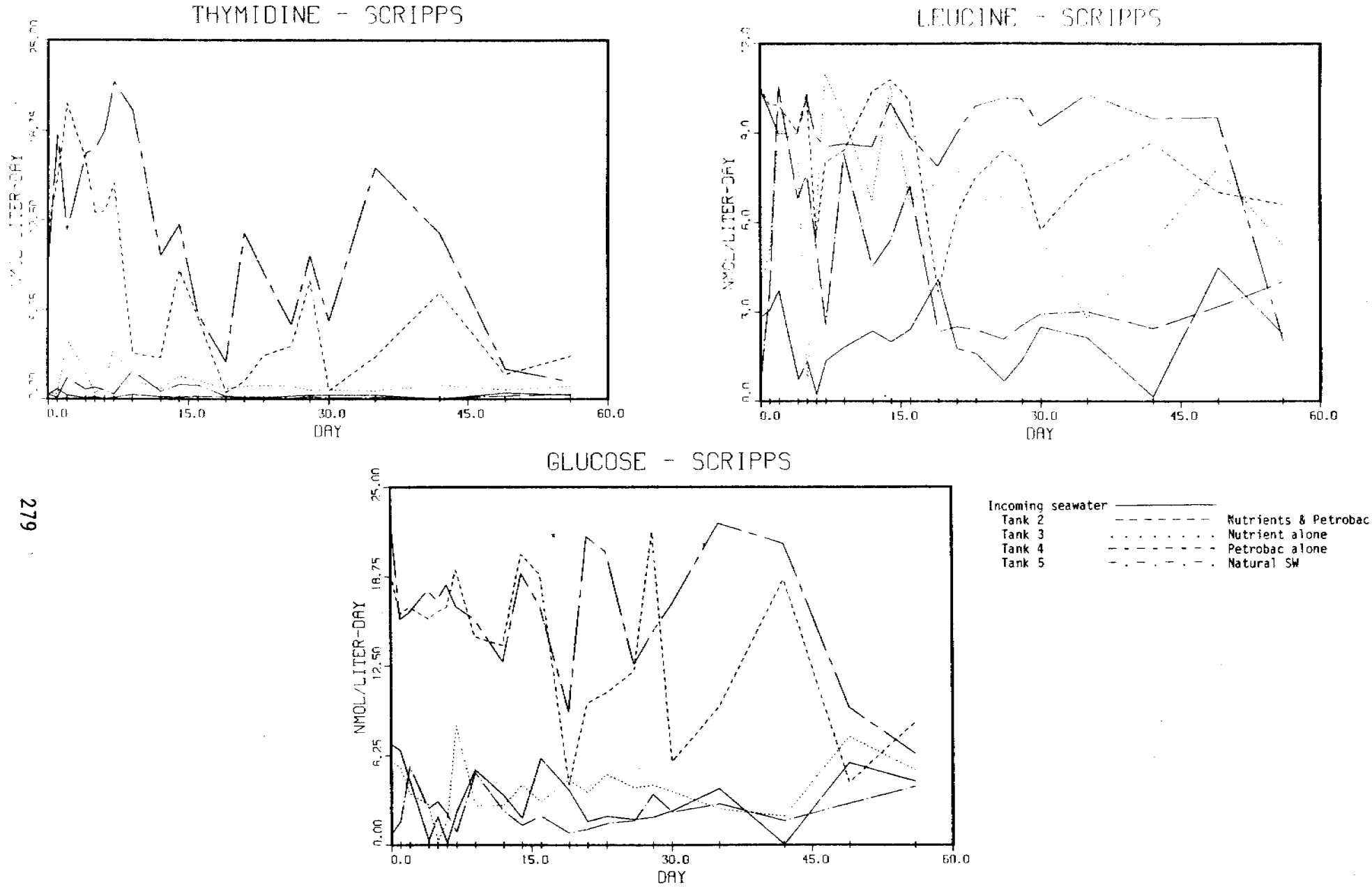

FIGURE 5-60. ^{3}H-THYMIDINE INCORPORATION, ^{3}H-LEUCINE AND ^{3}H-GLUCOSE UPTAKE DATA, SCRIPPS INSTITUTE OF OCEANOGRAPHY, SUMMER, 1981. DATA FOR EACH SUBSTRATE IS DEPICTED FOR ALL EXPERIMENTAL AQUARIUMS AND INCOMING SEAWATER. VERTICAL LINES ON ABSCISSA INDICATE SAMPLING POINTS.

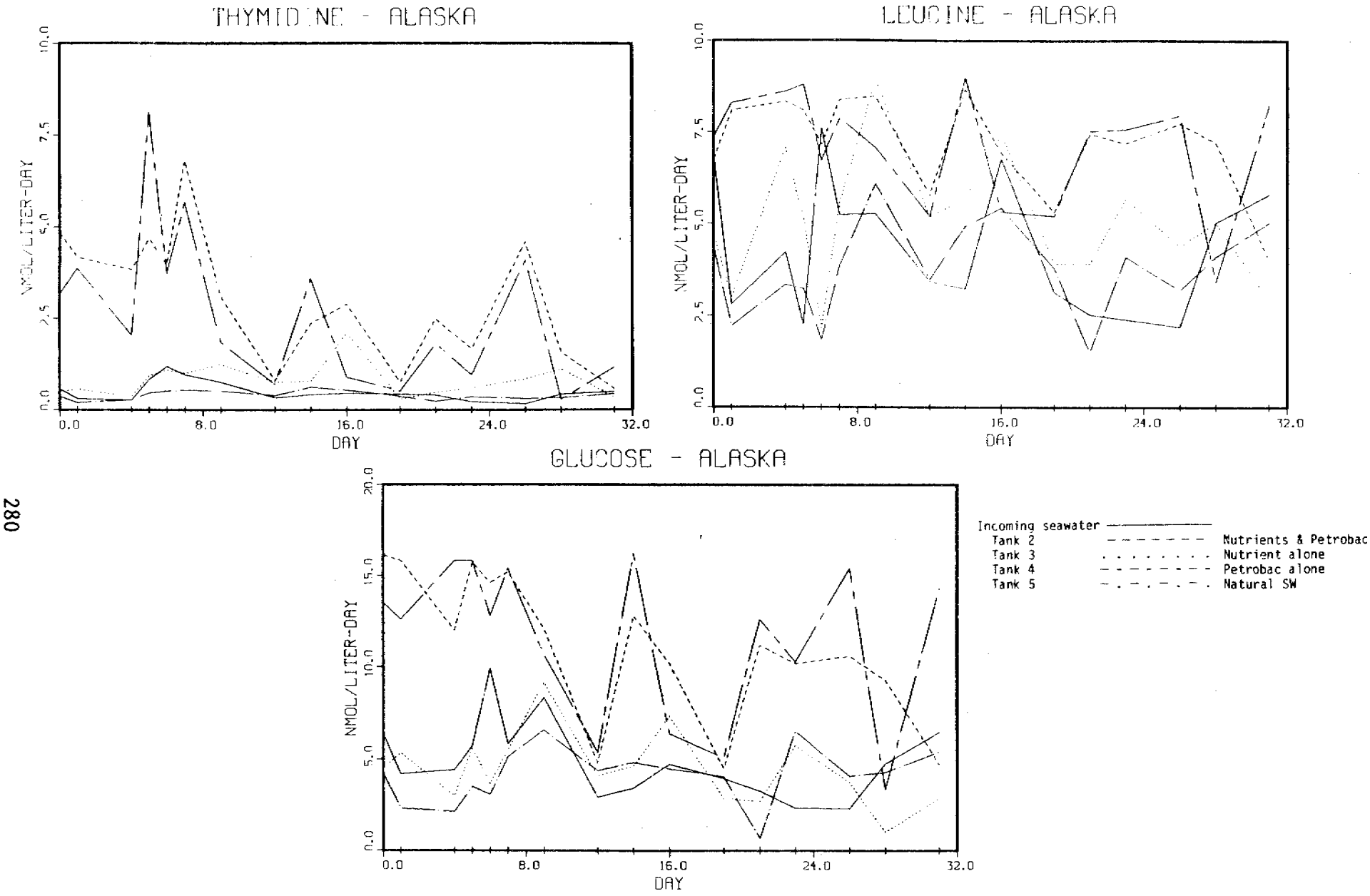

FIGURE 5-61. ^{3}H-THYMIDINE INCORPORATION, ^{3}H-LEUCINE AND ^{3}H-GLUCOSE UPTAKE DATA, KASITSNA BAY, ALASKA, SUMMER, 1981. DATA FOR EACH SUBSTRATE IS DEPICTED FOR ALL EXPERIMENTAL AQUARIUMS AND INCOMING SEAWATER. VERTICAL LINES ON ABSCISSA INDICATE SAMPLING POINTS.

followed by declines. Some stability in trends among the systems is apparent after two weeks which in some cases paralleled trends of the incoming seawater.

The SIO glucose uptake data demonstrate a general decline in rates after oil introduction with exception to tank 6. The Petrobac® innoculated tanks (2, 5) exhibited higher rates of uptake over the course of the experiment and this may be attributable to higher bacterial abundance. Tanks 3 and 5 behaved very similarly to the incoming seawater for this particular substrate.

The thymidine incorporation data for the Kasitsna Bay experiment bear resemblances to the SIO results in that (1) a general increase in thymidine incorporation is apparent after oil introduction with roughly the same period of response, and (2) the Petrobac® innoculated aquaria demonstrated generally higher rates of incorporation. Epifluorescence data for the Kasitsna Bay experiment are not available at this time, so references to relative microbe abundance cannot be made.

The leucine uptake data for Kasitsna Bay are difficult to interpret, as was the corresponding SIO data, due to variance between systems. The Petrobac® innoculated tanks (2, 5) demonstrated no real impact from oil introduction and had generally higher levels of uptake. The tanks with "natural" microbes only exhibited a drop in uptake after oil introduction, however this drop was also apparent for the incoming seawater which supposedly had never been exposed to spilled petroleum.

The glucose uptake data from Kasitsna Bay bear resemblance to that from SIO in that (1) most systems demonstrated some decline in uptake and (2) the Petrobac® innoculated systems showed generally higher uptake rates, where the other experimental tanks (3, 5) more closely followed trends of the incoming seawater.

As indicated previously, bacterial abundance data from epifluorescence microscopy is available only from the SIO experiment at this time. Samples were taken for epifluorescence counts from each experimental aquarium and the incoming seawater every day for the first week and then on a weekly basis. The incoming seawater contained approximately 10^6 cells/ml throughout the study and this was stable.

The tanks receiving Petrobac® innoculations (2, 3) averaged roughly 5 x 10^6 cells/ml with tank 2 demonstrating the greatest variations including a large increase on Day 7 to 32 x 10^6 cells/ml, followed by a decline to previous levels. The tanks with "natural" microbe populations (3, 6) contained approximately 2 x 10^6 cells/ml and were relatively stable.

The epifluorescence photomicroscopy for counts and biomass determinations, as well as the microautoradiography for all remaining samples from the SIO and Kasitsna Bay are being completed at the time of this writing.

Relations Between ^{14}C and ^{3}H Substrate Assay

To determine if any relationships exist between the degradation of the ^{14}C-labelled hydrocarbons and uptake/incorporation of the ^{3}H-labelled organic substrates, the data for each experimental system were plotted individually to include all substrates for the given experiment. The results from the SIO study are depicted in Figures 5-62 to 5-65, and for the Kasitsna Bay study in Figures 5-66 to 5-70.

As noted previously, a dramatic difference in degradation rates of hexadecane vs methylnaphthalene and naphthalene appears to exist for all experimental systems for both the SIO and Kasitsna Bay studies. The aromatic hydrocarbon substrates were degraded at significantly higher levels than the aliphatic compound, which seems to be in contrast to trends arising in many past studies (JORDAN and PAYNE, 1980). Both aromatic hydrocarbon substrates were degraded at comparable rates for all systems in each experiment, and the

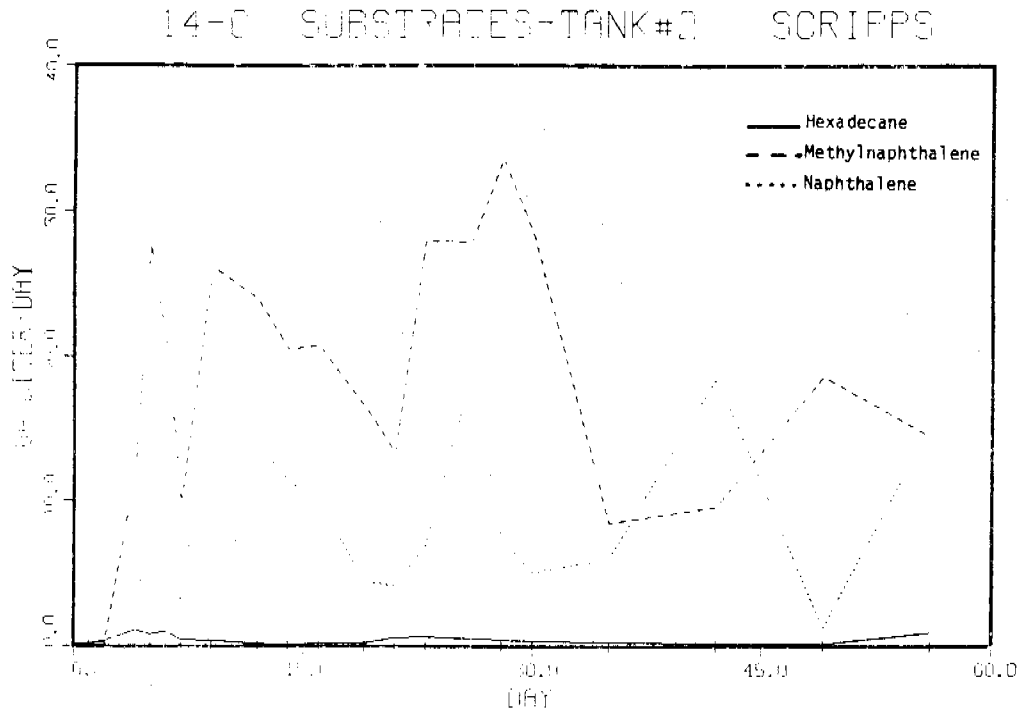

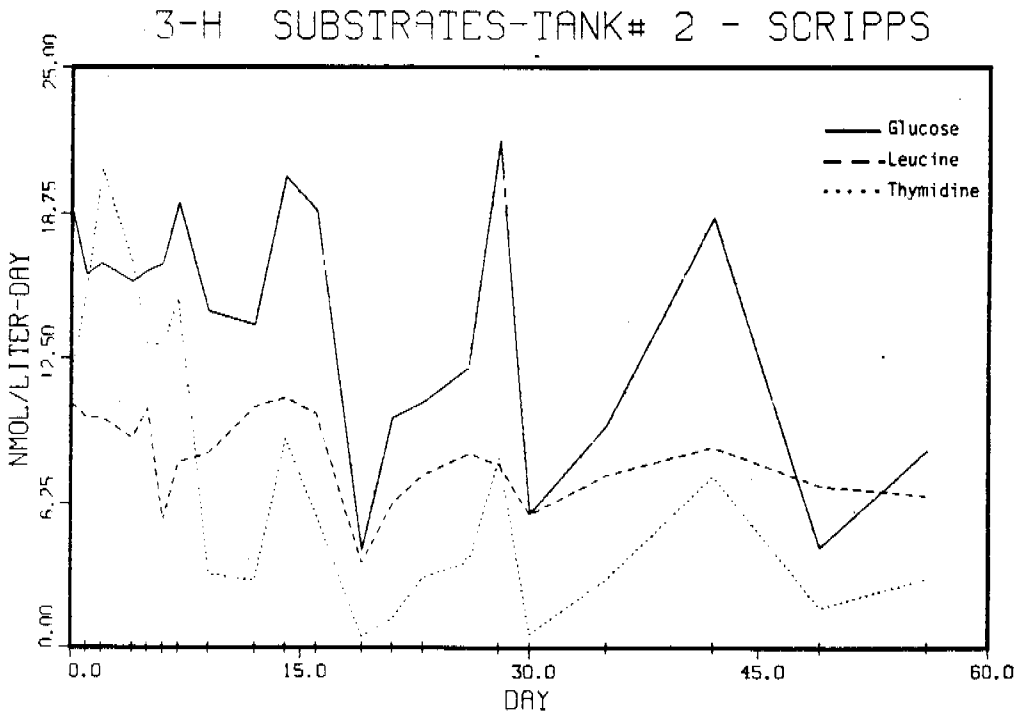

FIGURE 5-62. ^{14}C-HYDROCARBON DEGRADATION AND ^{3}H-SUBSTRATE INCORPORATION/ UPTAKE DATA FOR EXPERIMENTAL TANK 2 (PETROBAC AND NUTRIENTS), SCRIPPS INSTITUTE OF OCEANOGRAPHY, SUMMER 1981. VERTICAL LINES ON ABSCISSA INDICATE SAMPLING POINT.

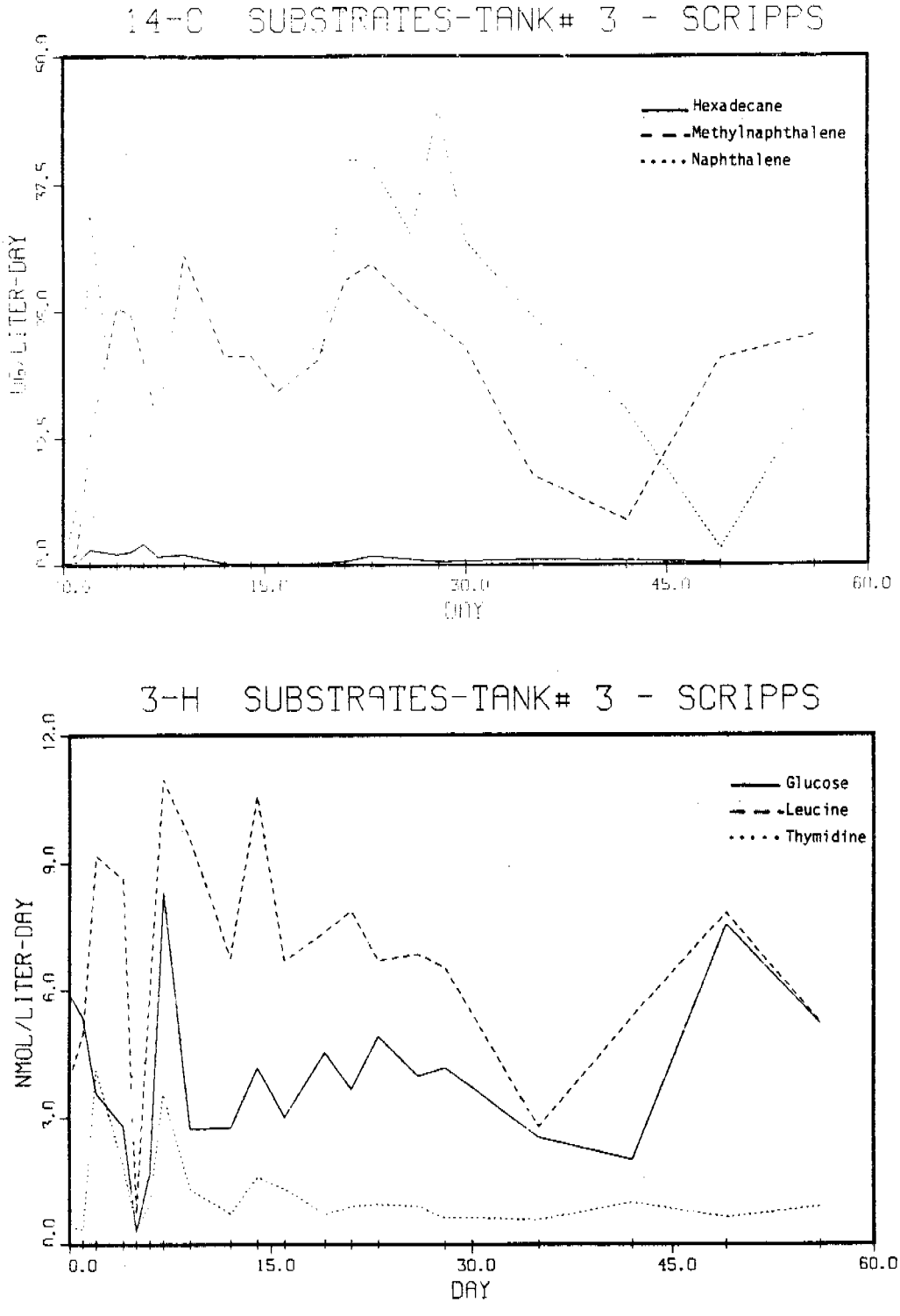

FIGU FIGURE 5-63. ^{14}C-HYDROCARBON DEGRADATION AND ^{3}H-SUBSTRATE INCORPORATION/ UPTAKE DATA FOR EXPERIMENTAL TANK 3 (NUTRIENTS ALONE), SCRIPPS INSTITUTE OF OCEANOGRAPHY, SUMMER 1981. VERTICAL LINES ON ABSCISSA INDICATE SAMPLING POINTS.

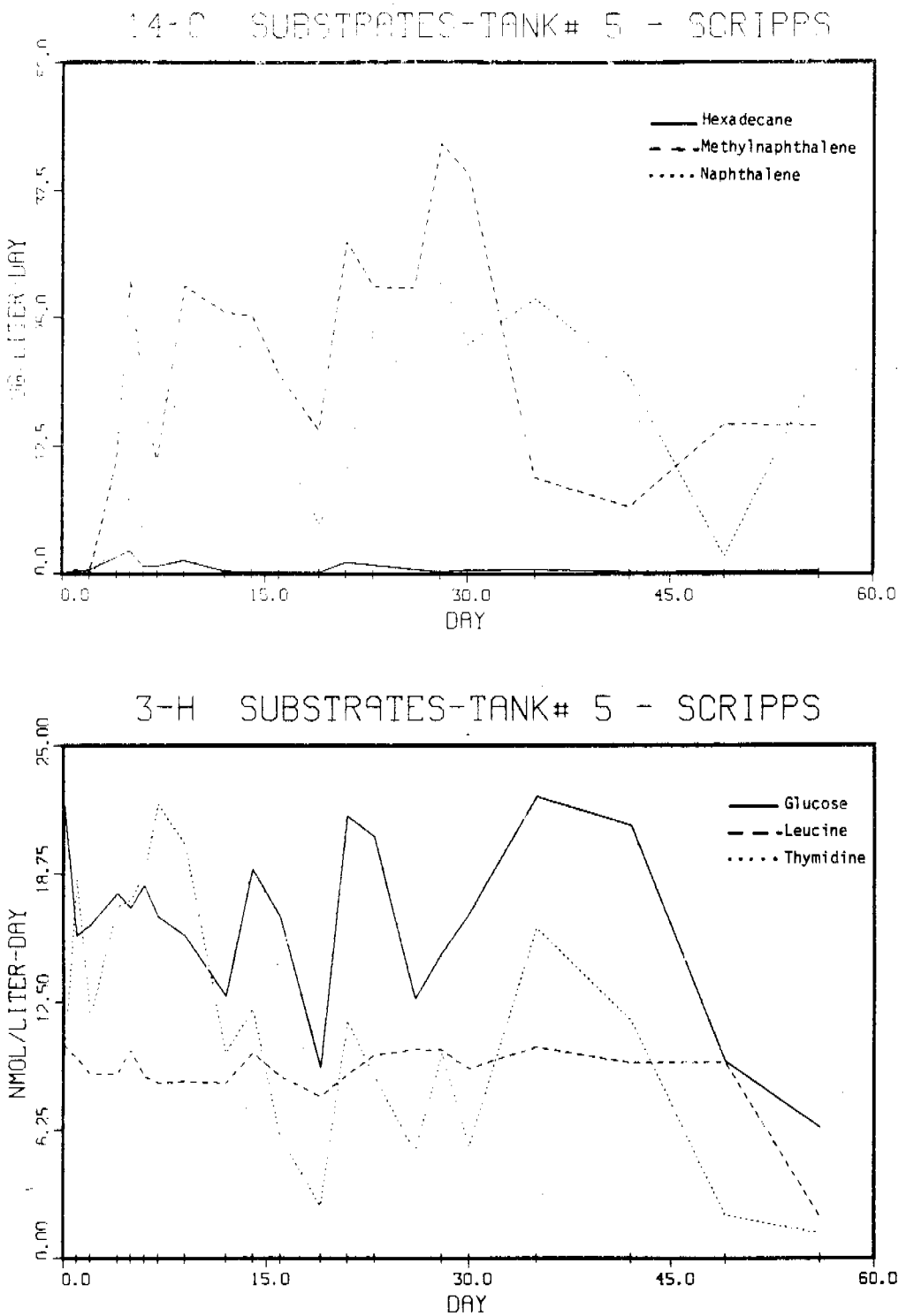

FIGURE 5-64. ^{14}C-HYDROCARBON DEGRADATION AND ^{3}H-SUBSTRATE INCORPORATION/ UPTAKE DATA FOR EXPERIMENTAL TANK 5 (PETROBAC ALONE), SCRIPPS INSTITUTE OF OCEANOGRAPHY, SUMMER 1981. VERTICAL LINES ON ABSCISSA INDICATE SAMPLING POINTS.

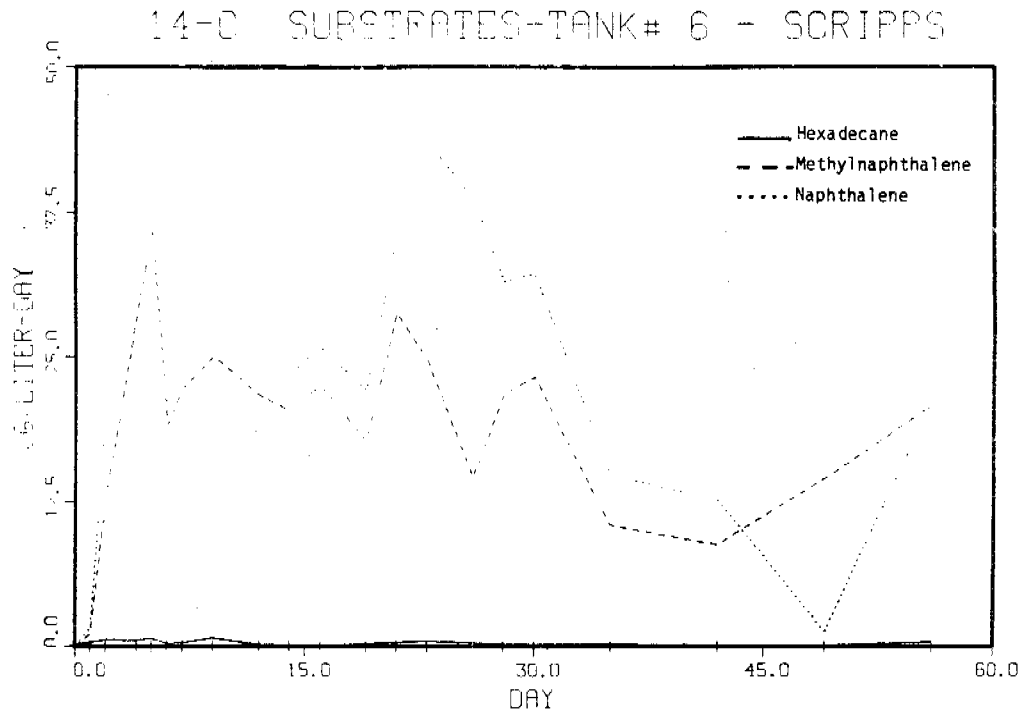

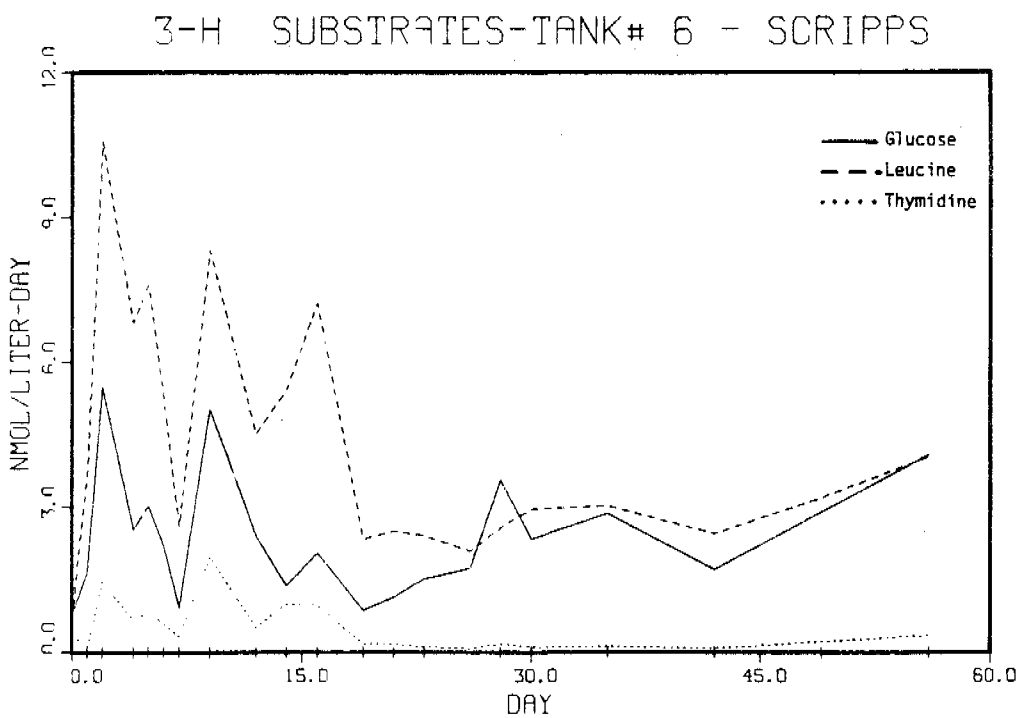

FIGURE 5-65. ^{14}C-HYDROCARBON DEGRADATION AND ^{3}H-SUBSTRATE INCORPORATION/UPTAKE DATA FOR EXPERIMENTAL TANK 6 (NATURAL SEAWATER), SCRIPPS INSTITUTE OF OCEANOGRAPHY, SUMMER 1981. VERTICAL LINES ON ABSCISSA INDICATE SAMPLING POINTS.

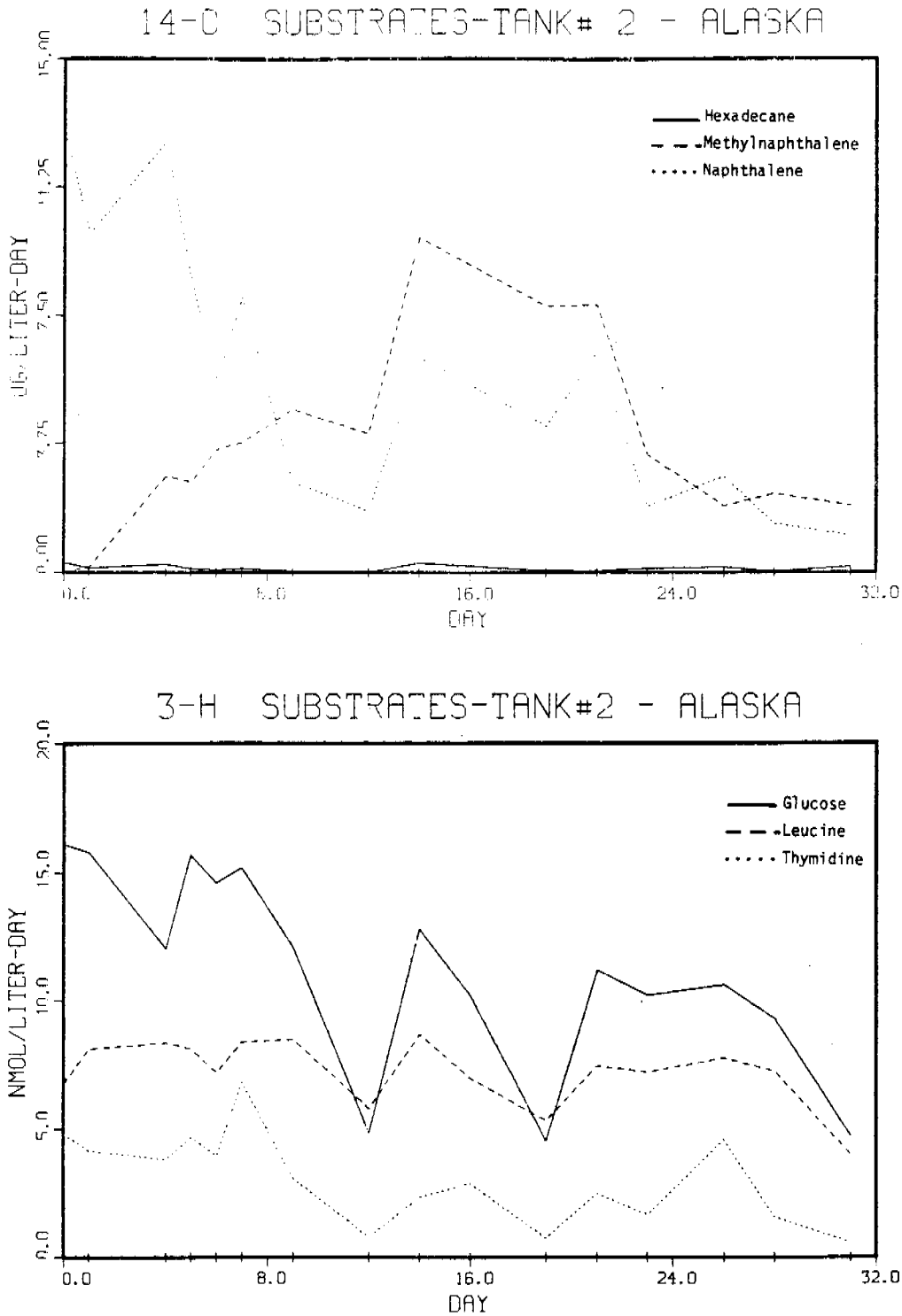

FIGURE 5-66. ^{14}C-HYDROCARBON DEGRADATION AND ^{3}H-SUBSTRATE INCORPORATION/ UPTAKE DATA FOR EXPERIMENTAL TANK #2 (PETROBAC AND NUTRIENTS), KASITSNA BAY, ALASKA, SUMMER, 1981. VERTICAL LINES ON ABSCISSA INDICATE SAMPLING POINTS.

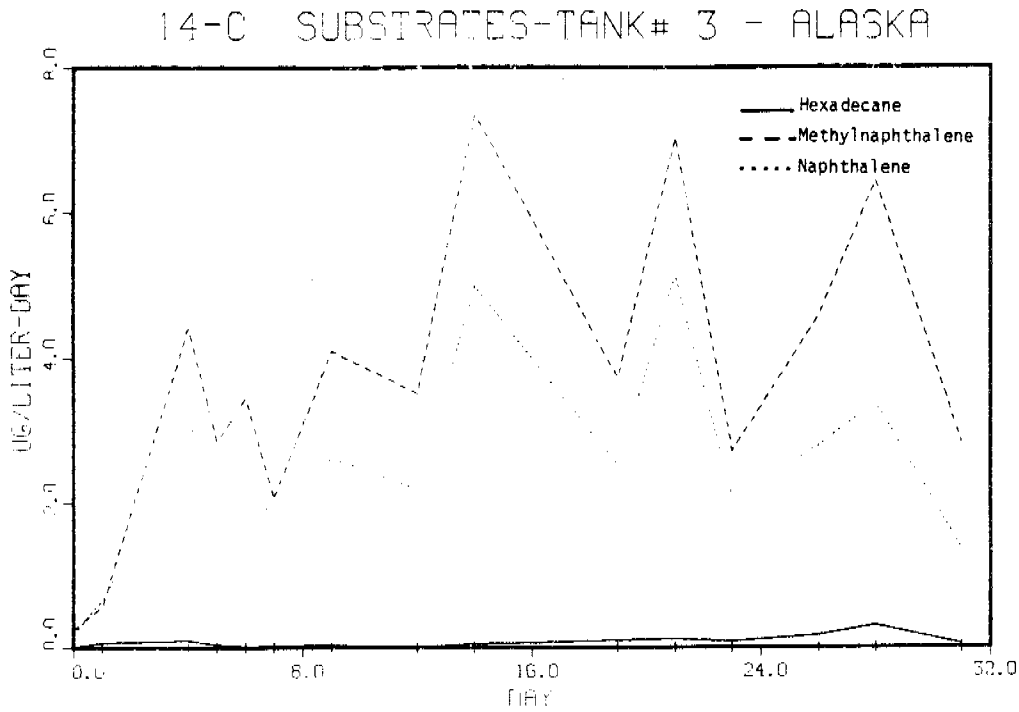

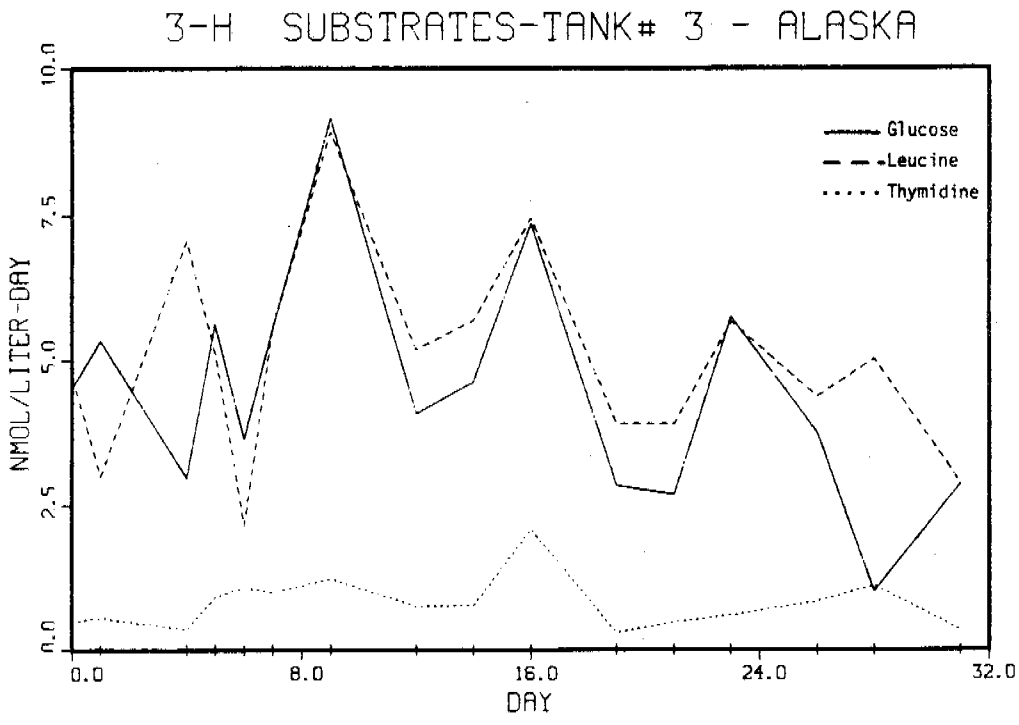

FIGURE 5-67. ^{14}C-HYDROCARBON DEGRADATION AND ^{3}H-SATURATE INCORPORATION/ UPTAKE DATA FOR EXPERIMENTAL TANK #3 (NUTRIENTS ALONE), KASITSNA BAY, ALASKA, SUMMER, 1981. VERTICAL LINES ON ABSCISSA INDICATE SAMPLING POINTS.

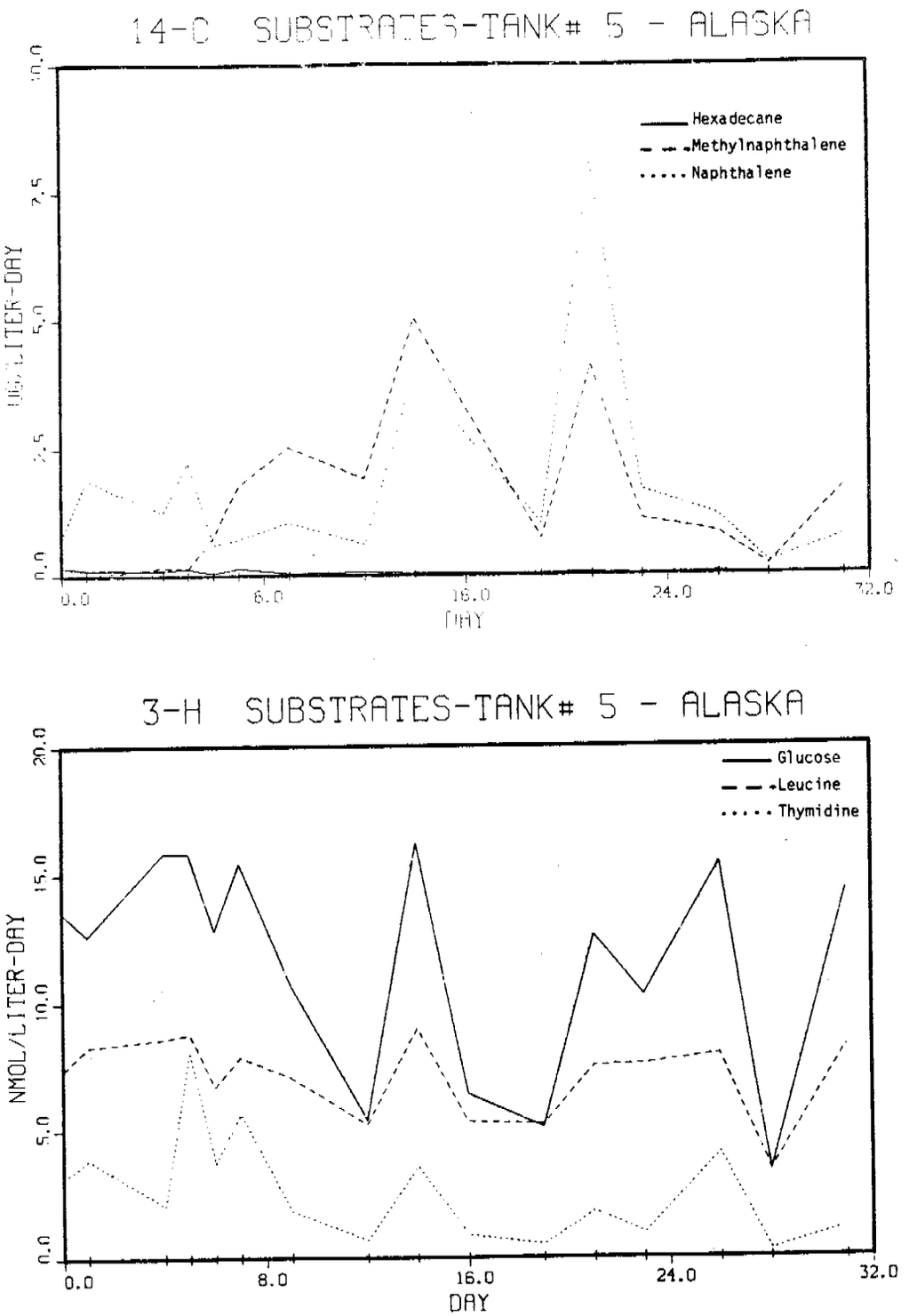

FIGURE 5-68. ^{14}C-HYDROCARBON DEGRADATION AND ^{3}H-SUBSTRATE INCORPORATION/ UPTAKE DATA FOR EXPERIMENTAL TANK #5 (PETROBAC ALONE), KASITSNA BAY, ALASKA, SUMMER, 1981. VERTICAL LINES ON ABSCISSA INDICATE SAMPLING POINTS.

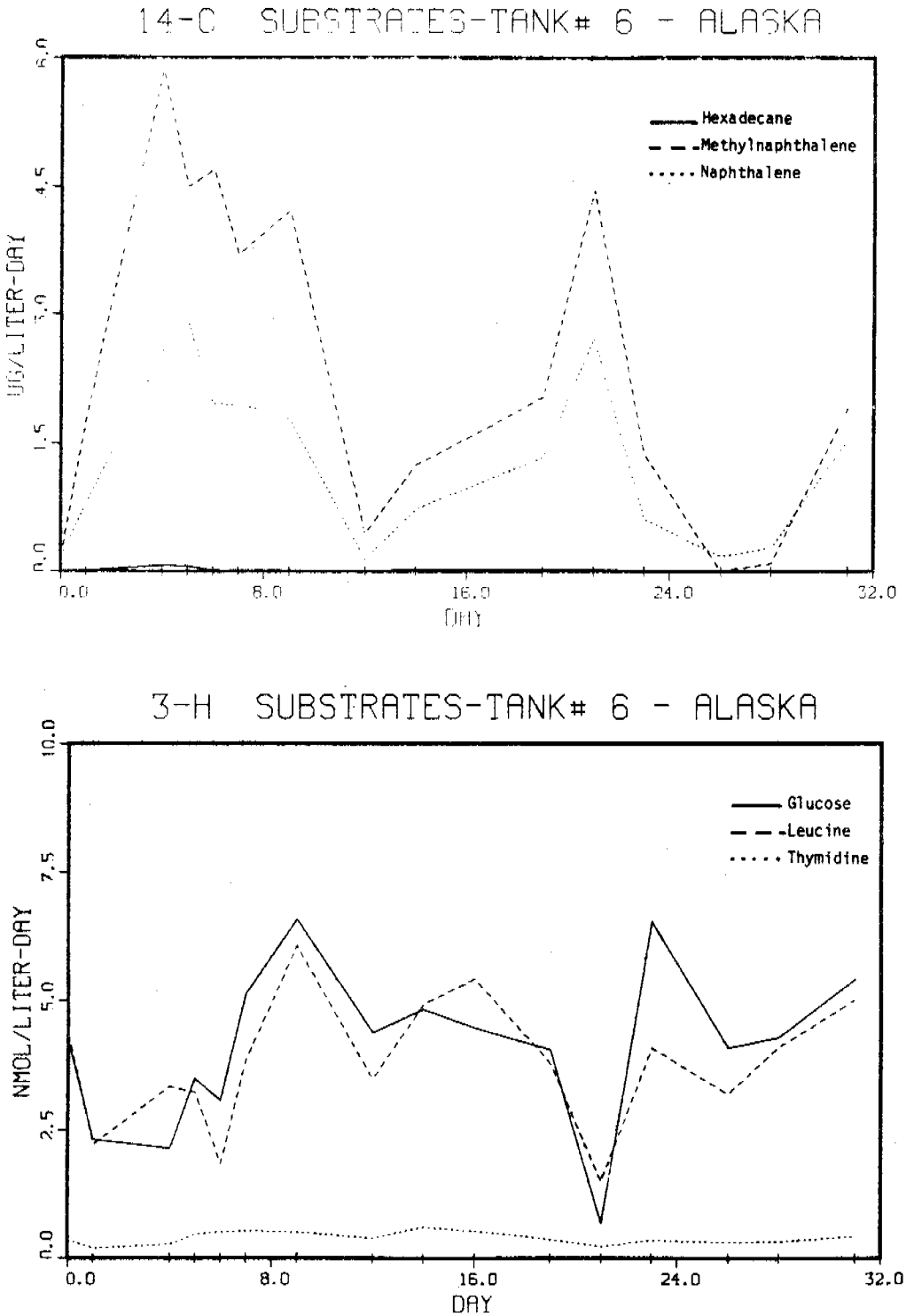

FIGURE 5-69. ^{14}C-HYDROCARBON DEGRADATION AND ^{3}H-SUBSTRATE INCORPORATION/ UPTAKE DATA FOR EXPERIMENTAL TANK #6 (NATURAL SEAWATER), KASITSNA BAY, ALASKA, SUMMER, 1981. VERTICAL LINES ON ABSCISSA INDICATE SAMPLING POINTS.

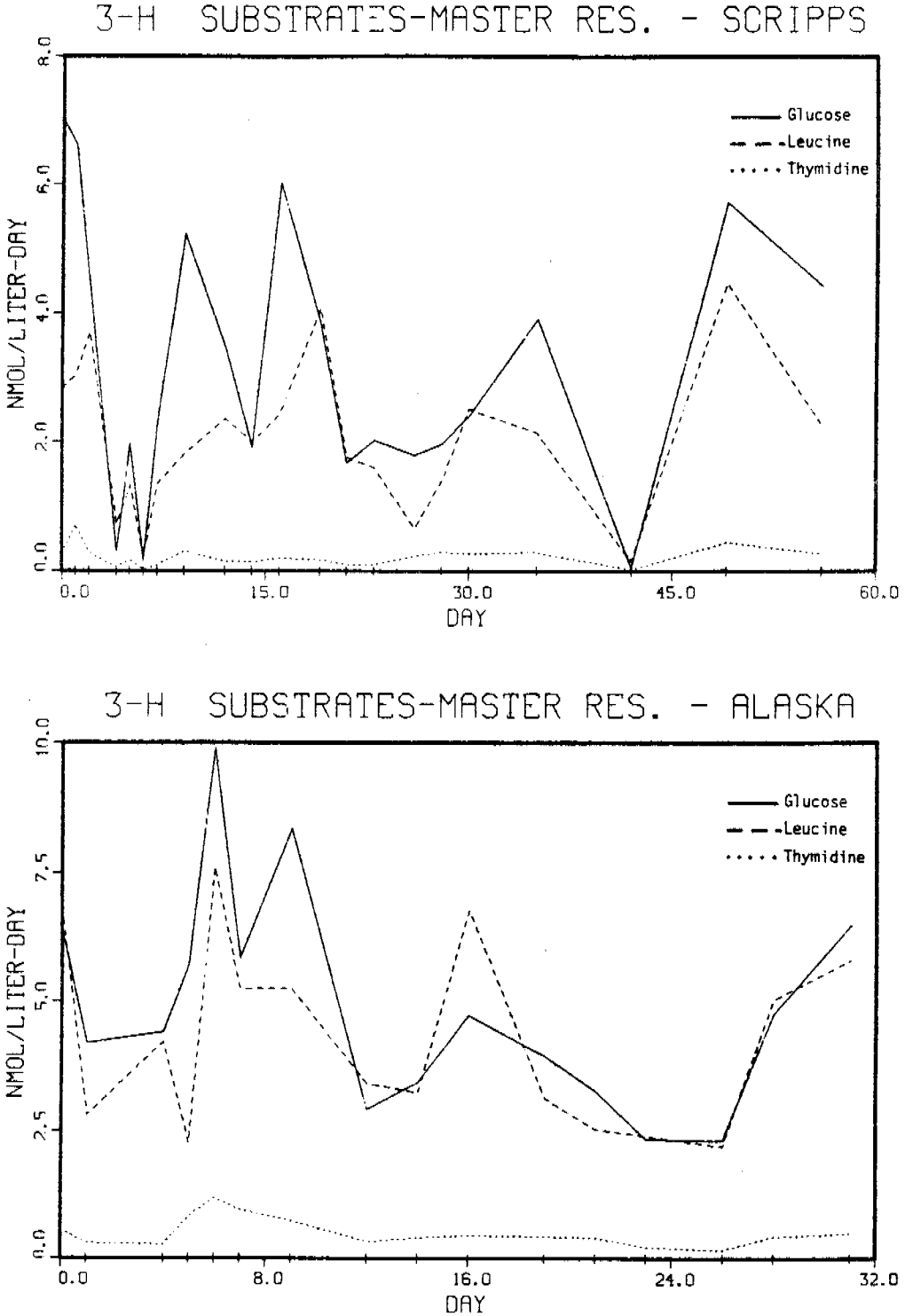

FIGURE 5-70. ^{3}H-THYMIDINE INCORPORATION, ^{3}H-GLUCOSE AND ^{3}H-LEUCINE UPTAKE DATA FOR INCOMING SEAWATER (SCRIPPS INST. OF OCEANOGRAPHY AND KASITSNA BAY, ALASKA, SUMMER 1981). VERTICAL LINES ON ABSCISSA INDICATE SAMPLING POINTS.

patterns (relative rates) were also very similar between the two substrates in most cases. However, it must again be emphasized that the relative rates of degradation between labelled substrates, as based upon loss of the ^{14}C label, does not imply an upper limit on the actual amount of parent substrate undergoing metabolic conversion during the given period of incubation. This consideration could most certainly negate the apparent contrast in rates of degradation between the aliphatic and aromatic substances.

To further assess the soundness of utilizing data from this empirical approach for generating rates of degradation, it would be valuable to examine the partitioning of the parent labeled hydrocarbon substrate and associated metabolic products into the bacterial cell material and surrounding water column. This would be helpful in evaluating the apparent rate data for any given labelled substrate in that the approach would not rely solely upon loss of the ^{14}C label (to $^{14}CO_2$), and evidence of metabolic conversion of the parent compound without loss of label can be obtained. To facilitate this evaluation in future experiments, we will determine the relative concentrations of labelled hydrocarbon substrate in the polar and nonpolar fractions of both cellular extracts and surrounding seawater (filtrate) for samples incubated with a given ^{14}C-labelled hydrocarbon. The bacterial cells will be isolated by filtration and then the filter and filtrate will be extracted with the appropriate organic solvent. The polar and nonpolar fractionation can be accomplished with liquid solid (silica gel), column chromatography procedure, and the radioactivity for the fractions can be determined by liquid scintillation spectrometry. The polar fractions for both the cellular and water (filtrate) extracts should contain metabolized components and the nonpolar fractions should contain parent substrate. Since only the ^{14}C label will be detected, interference from other components (e.g., polar lipid material) is not a problem. The activity of all fractions together with the trapped $^{14}CO_2$ should provide for a mass balance determination for the amount of labelled hydrocarbon substrate originally added to the seawater sample.

In terms of relations between the ^{14}C and ^{3}H-labelled substrate trends, only in tanks 2 and 3 for the SIO study was a definite increase in hydrocarbon substrate degradation present which paralled increases in rates of thymidine incorporation and glucose and leucine uptake after introduction of oil (Figures 5-62, 5-63). In most cases, no apparent impacts on the ^{3}H-labelled substrate incorporation/uptake rates following oil introduction are obvious from the data. This is particularly true for the systems receiving the Petrobac® innoculations. It should be noted however, that the experimental aquaria in the Kasitsna Bay study demonstrated generally lower rates of ^{14}C- and ^{3}H-labelled substrate utilization (relative to the SIO study), and that "experimental noise" from variance inherent in the techniques may tend to obscure general trends unless they are highly prominant.

In summary, the trends which are most apparent in the data for the continuously-flowing experiments conducted at SIO and Kasitsna Bay are the following:

- o the ^{14}C-hexadecane appeared to be degraded at much slower rates than either ^{14}C-methylnaphthalene or ^{14}C-naphthalene (note previous statements on interpretation of relative rates).
- o both aromatic hydrocarbon substrates were utilized at comparable rates with patterns (relative rates over time) following closely in most systems.
- o generally lower rates of degradation were apparent for the Kasitsna Bay study relative to the SIO experiment.
- o in most cases, dramatic increases in degradation rates for the ^{14}C-hydrocarbon substrates occurred within 48 hrs. of oil introduction.
- o nutrient supplementation had no apparent influence on degradation rates except for some slight evidence in the Kasitsna Bay study (note Figures 5-66 vs 5-68, and 5-67 vs 5-69).
- o Increases in ^{3}H-thymidine incorporation into cell DNA were apparent after oil introduction for the SIO data and to a much lesser extent for the Kasitsna Bay study.

- high variance in the ^{3}H-glucose and ^{3}H-leucine data exists for most experimental systems in both studies with no apparent impact from oil introduction except for some initial trends.

- only in two of the experimental aquaria (SIO) was there a concomittant increase in both ^{14}C-labelled and ^{3}H-labelled substrate utilization after introduction of Prudhoe Bay crude.

Further Data Development - Relationships to Modeling Efforts

To evaluate the removal of petroleum components from the slick-seawater interface due to microbial degradation, certain extrapolations may be made from ^{14}C-hydrocarbon degradation rate data. This approach will give an approximation of microbially-induced compound removal to help in development of the proper algorithms. The question to be answered by such approximations is one of relative significance (e.g., compared to dissolution, do microbes help to remove substantial amounts of organic carbon?). The existing rate data for the ^{14}C-hydrocarbon substrates will be converted to total petroleum hydrocarbon compound rates by utilizing the relative abundance of hexadecane to aliphatic content and the relative abundance of methylnaphthalene and naphthalene to overall aromatic hydrocarbon content of Prudhoe Bay crude. This type of extrapolation is forced to assume that hexadecane is a "typical" aliphatic and that methylnaphthalene and naphthalene are "typical" aromatics in terms of biodegradability. This approach also says nothing for residual components; however, it will serve as a first-estimate of microbial impact upon overall dissolution. The ^{14}C-substrate data will also be normalized to a "per cell" basis for estimation of uptake of organic carbon into the bacterial biomass. Completion of the epifluorescence analyses will be required for this, so estimates (e.g., mass of C/liter-day uptake) cannot be made at this time.

As previously indicated, the rates of degradation for a particular ^{14}C-labelled hydrocarbon substrate are based upon the loss and subsequent detection of the label (^{14}C in $^{14}CO_2$), and this may lead to an underestimation of the actual amount of parent material metabolized during the incubation period. Efforts are being undertaken to provide a basis for evaluating each

of the three substratus in terms of a mass balance approach. As described in Section 5.2.4, the approach can provide evidence of metabolic conversions without loss of the ^{14}C label and this would then infer an underestimation of the metabolism rate as based upon detection of $^{14}CO_2$. If a mass balance can de derived, then corrections can be made on existing $^{14}CO_2$ data for better estimations of degradation rates (with "degradation" defined as loss of parent compound molecular structure).

The ^{3}H-thymidine data are being utilized to estimate bacterial secondary production by taking into account the average DNA content of cells and the average organic carbon content (related to cell volumes). These production estimates will be compared to organic carbon uptake estimates from the ^{14}C-substrate data to see if organic carbon flux information can be derived.

5.2.5 Petroleum Hydrocarbon Analyses from Selected Flow-Through Microbial Degradation Experiments

Limited-Term Hydrocarbon Analyses -- SIO

Attention will be limited in this section to selected seawater extracts from the SIO study, as all petroleum hydrocarbon analyses by capillary gas chromatography for the SIO continuous-flow experiments have not been completed at this time. The chromatograms depicted in Figures 5-71 to 5-73 represent the aromatic (F2) and polar (F3) fractions (silica gel liquid-solid chromatographic fractionation) analyzed by fused-silica capillary gas chromatography with flame ionization (FID) detection. The fractions are from the CH_2Cl_2 seawater extracts for tanks 5 (Petrobac® innoculated) and 6 ("natural" microbes only) for several sampling points (Day 2, 5, 9, and 23 days).

The aliphatic (F1) fractions from all seawater samples analyzed to date for the SIO study contained only trace amounts of aliphatic hydrocarbons, which is to be expected since the less volatile higher molecular weight aliphatic compounds, which would have a longer retention in the oil slick, also

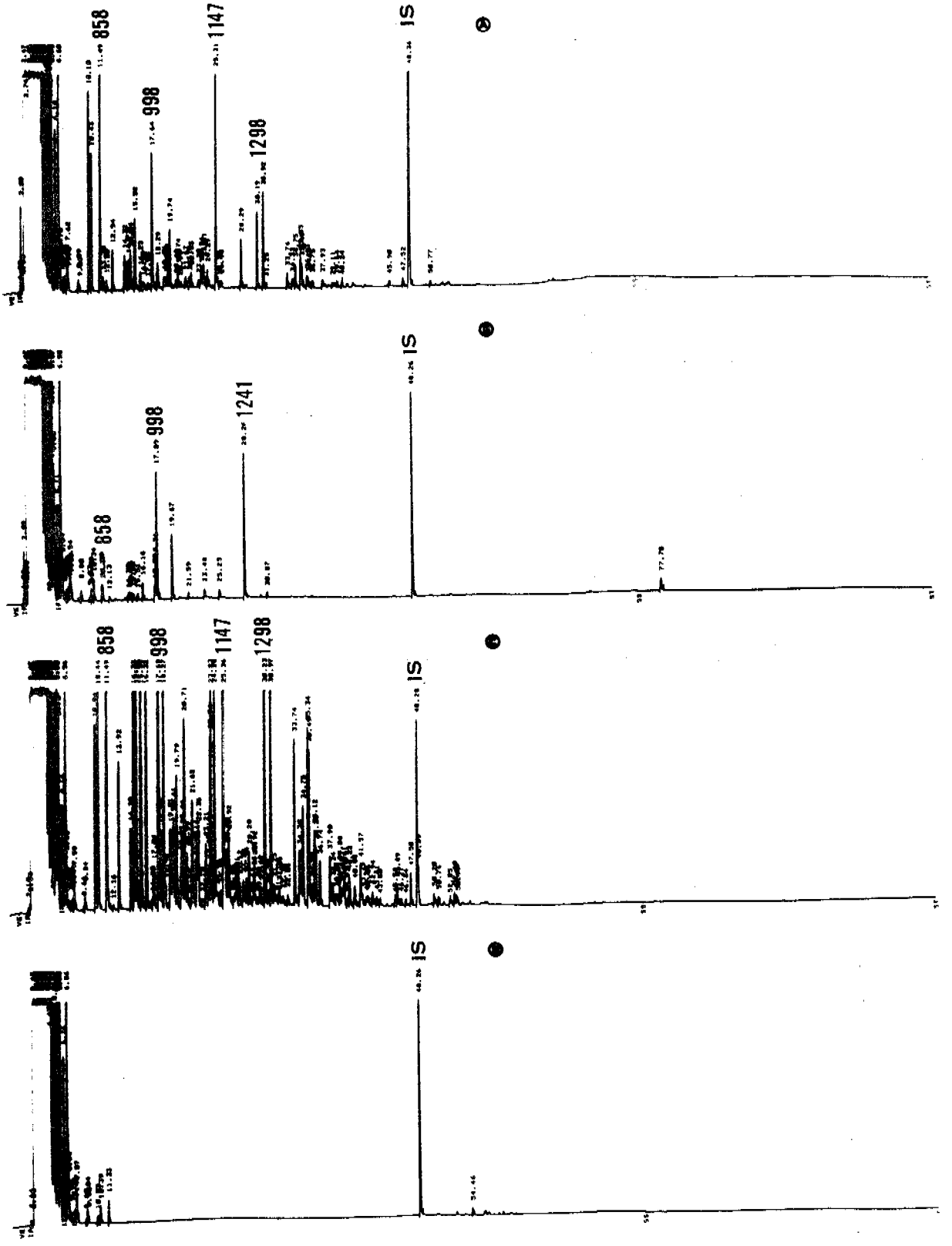

FIGURE 5-71. FLAME IONIZATION DETECTOR CAPILLARY GAS CHROMATOGRAMS FROM SCRIPPS INSTITUTE OF OCEANOGRAPHY WATER COLUMN AROMATIC FRACTIONS FROM TANKS 5 AND 6: (A) TANK 5, DAY 2; (B) TANK 5, DAY 5; (C) TANK 6, DAY 2; AND (D) TANK 6, DAY 5. (IS = INTERNAL STANDARD).

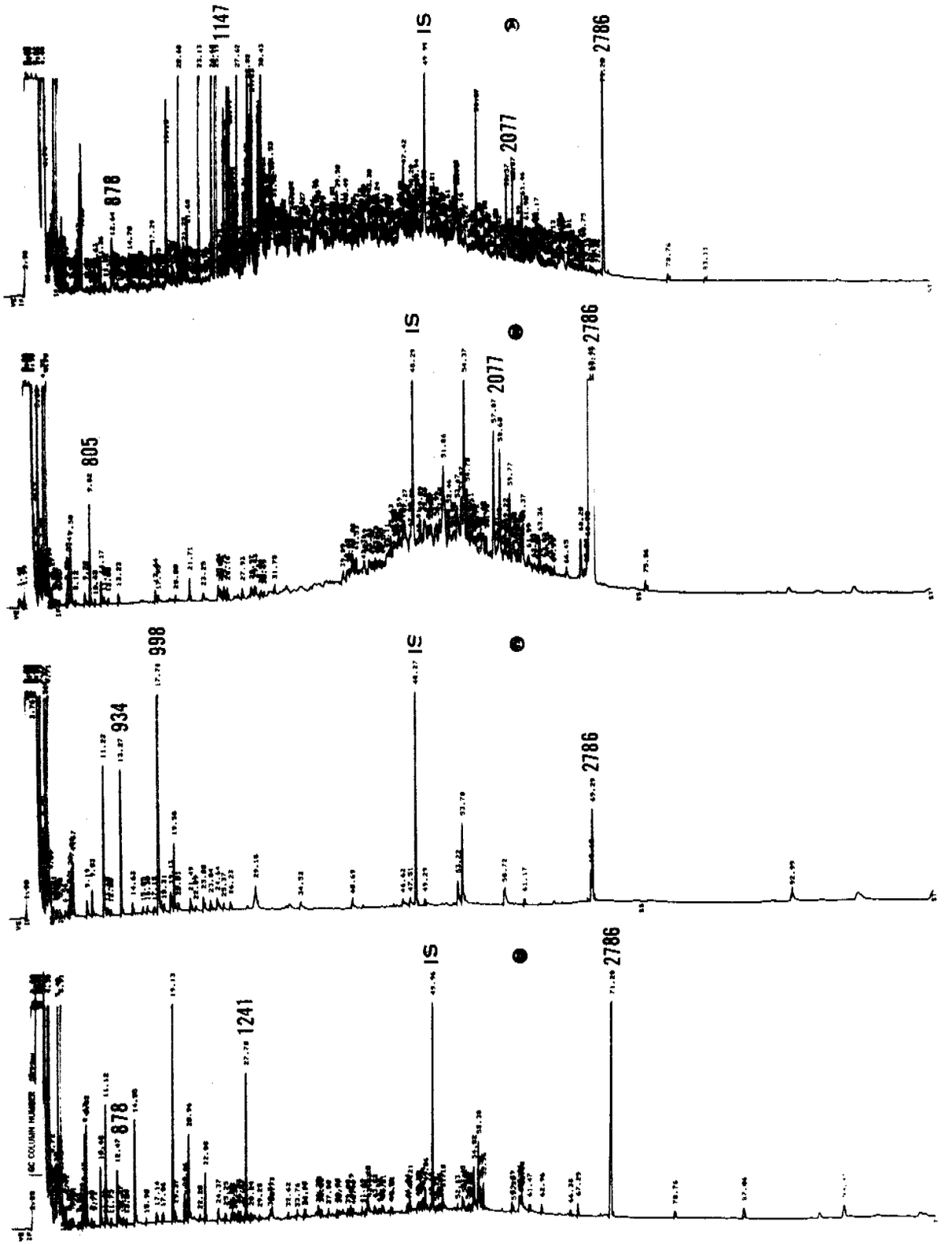

FIGURE 5-72. FLAME IONIZATION DETECTOR CAPILLARY GAS CHROMATOGRAMS FROM SCRIPPS INSTITUTE OF OCEANOGRAPHY WATER COLUMN POLAR FRACTIONS FROM TANKS 5 AND 6: (A) TANK 6, DAY 2; (B) TANK 6, DAY 5; (C) TANK 5, DAY 2; AND (D) TANK 5, DAY 5. (IS = INTERNAL STANDARD).

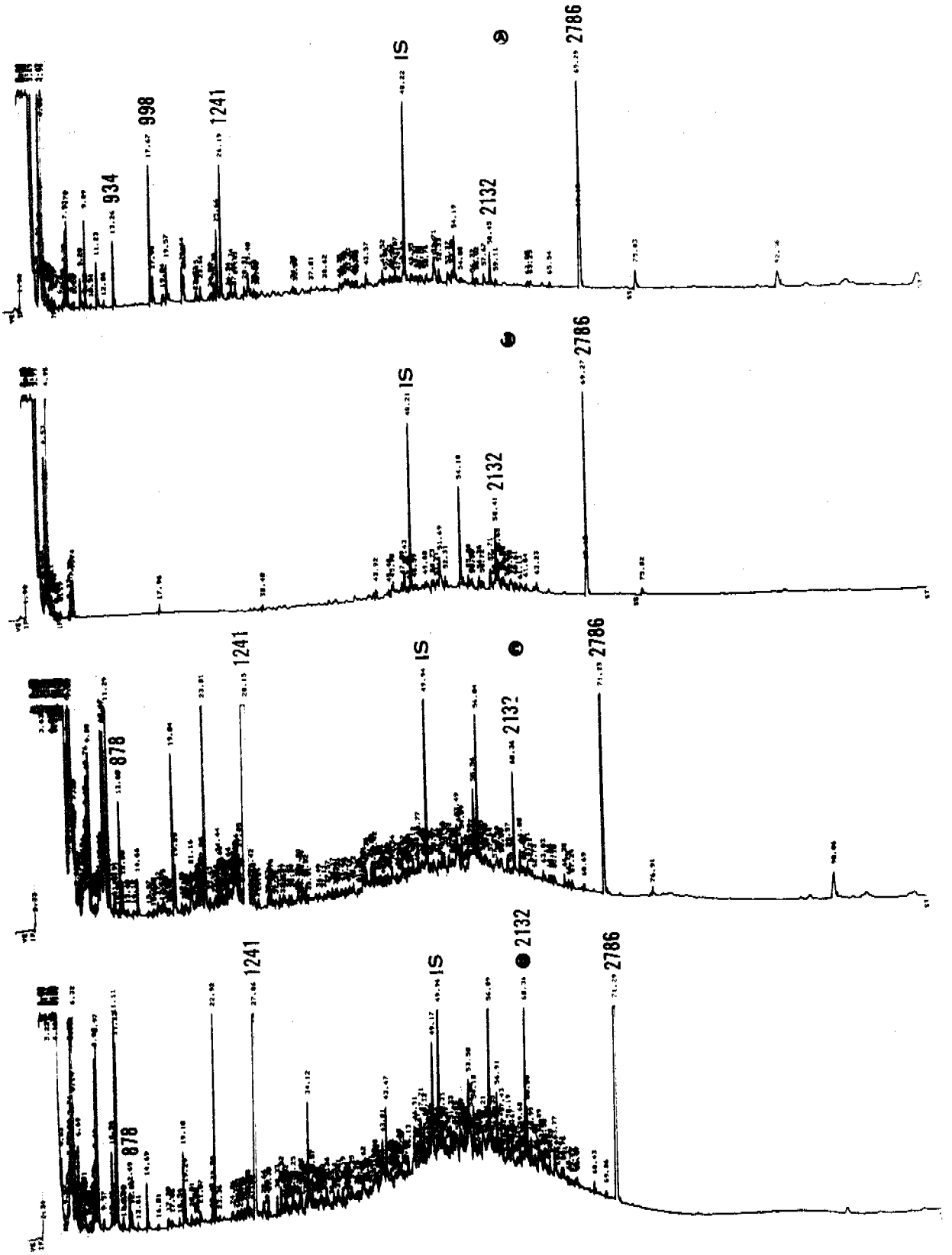

FIGURE 5-73. FLAME IONIZATION DETECTOR CAPILLARY GAS CHROMATOGRAMS FROM SCRIPPS INSTITUTE OF OCEANOGRAPHY WATER COLUMN POLAR FRACTIONS FROM TANKS 5 AND 6: (A) TANK 5, DAY 9; (B) TANK 6, DAY 9; (C) TANK 5, DAY 23; AND (D) TANK 6, DAY 23. (IS = INTERNAL STANDARD).

have low solubilities relative to the more volatile (e.g., CH_4 to nC5) aliphatic components.

The chromatograms in Figure 5-71 demonstrate a time dependence of aromatic compounds passing into the water column. This can be noted by contrasting chromatograms from tank 5 for (A) Day 2 to (B) Day 5, and from tank 6 for (C) Day 2 to (D) Day 5. Chromatograms for corresponding fractions for sampling points prior to and after Days 2 and 5 are devoid of aromatic compounds. This quick "passage" of lighter molecular weight aromatics is most dramatic for the tank 6 fractions (chromatograms C and D) and the compounds present are most likely xylenes, alkyl benzenes, and alkyl naphthalenes.

Figures 5-72 and 5-73 depict chromatograms for polar (F3) fractions from tanks 5 and 6. It is of interest to note the differences between those for tank 6 (Figure 5-72) between (A) Day 2 and (B) Day 5, whereas the corresponding samples from tank 5 (chromatograms C and D) are quite similar. As was demonstrated by the ^{14}C-labelled hydrocarbon degradation data (Figures 5-64 and 5-65), tank 6 degradation activity increased sharply during this time period (Days 2 to 5) whereas tank 5 had a more delayed response to oil introduction. However, more complete identification of the compounds present in the tank 6 samples for these two sampling points is required to help substantiate or reject the potential correlation between the ^{14}C-hydrocarbon degradation activities and the appearance of polar compounds in the extracts from these experimental systems.

After this time period, relatively few compounds were apparent in the polar fractions for these two aquaria until several weeks had passed since oil introduction. This is evidenced in the chromatograms in Figure 5-73 for Days 9 and 23. Although it should be noted that twice the volume of seawater was sampled and extracted for Day 23 as for Day 9, obvious differences exist between tank 5 and 6 Day-9 fractions (chromatograms A and B) and the corresponding fractions from Day 23 (chromatograms C and D). It is also of interest to note the fairly strong qualitative resemblance between the Day-23 samples for (C) tank 5 and (D) tank 6.

This particular experiment was run for 56 days and analyses of remaining fractions from the SIO experimental aquaria are being completed at the time of this writing. Selected samples will be screened by GC/MS for oxidized products arising from microbial degradation of parent petroleum components.

Longer-term Hydrocarbon Analyses -- Kasitsna Bay

As noted in Section 5.1.2 of the evaporation/dissolution chapter, several long-term (6 months to 1 year) sub-arctic microbial degradation experiments were initiated in the outdoor tanks at the Kasitsna Bay laboratory in October, 1980. At that time, the tank configurations were set-up as shown below:

Tank 7	Flow-through condition	Fresh oil
Tank 3	Flow-through condition	Fresh oil + Corexit (20:1)
Tank 2	Static condition	Fresh oil
Tank 5	Static condition	Fresh oil + Corexit (20:1)

During the Spring, 1981 program, after six months of weathering, oil and water column samples were obtained from the four tanks and the flow-through tanks 3 and 7 were maintained to continue longer term weathering studies. All of the remaining oil from the static tanks (2 and 5) was then removed and frozen for future analysis (if desired), and 40-L seawater samples were obtained, acidified, (to pH 2.0), extracted with CH_2Cl_2 and analyzed.

This section describes results of chemical analyses of the oil and water samples from these longer-term studies and presents additional results obtained from the 6 month to 1 year sampling period in the flow-through tanks 3 and 7. In addition, results are presented on summer (May through October) microbial degradation studies undertaken on fresh crude and artificially generated mousse in the presence and absence of turbulence and Corexit (as shown by the matrix diagram presented earlier in Section 5.1.2, Figure 5-32).

Two of the more significant findings of these longer term microbial degradation studies relate to the appearance of (1) clear seasonal trends in bacterial utilization and (2) differential microbial degradation with dependence on the status of the oil slick itself (e.g., stranded oil, mousse patches, surface slicks, oil droplets). As will be noted below, the chromatograms of samples collected after six months of ambient static tank weathering during the winter period from October 1980 through April 1981 showed only limited microbial degradation.

The significance of chromatographic analyses depicted in Figures 5-74 and 5-75 relates to a demonstration of the type of overall weathering which may occur during the subarctic winter season for oil stranded in an aquatic environment which experiences little flushing. This may be the case for an estuarine situation, where the water column beneath the slick is relatively stagnant. Limited evaporation would be expected due to the cold temperatures, and a "buildup" of the more water-soluble petroleum components in the underlying water column may occur. Microbial degradation of the oil slick and solubilized petroleum components in the water might also be limited due to cold water temperatures, as well as limitations in nutrient supplies from lack of water column flushing and subsequent nutrient replenishment.

Figure 5-74 depicts the aliphatic and aromatic fraction chromatograms obtained from oil samples which had weathered over the six months winter period. In this experiment, both the oil and water (in tank 2) were maintained in a static condition from October of 1980 to April 1981. In the aliphatic fraction (Figure 5-74A) n-alkanes are present down to nC-12, and the 17/pristane and 18/phytane ratios are approximately 1.79 and 1.85, respectively. These values are nearly identical to the corresponding ratios obtained from analysis of the starting oil and suggest limited microbial degradation during that time interval, in that isoprenoids are generally thought to be less biodegradable than their straight-chain counterparts (BLUMER et al., 1973). Furthermore, during the winter months, it is clear that loss of lower molecular weight components by evaporation processes was inhibited due to the colder subarctic

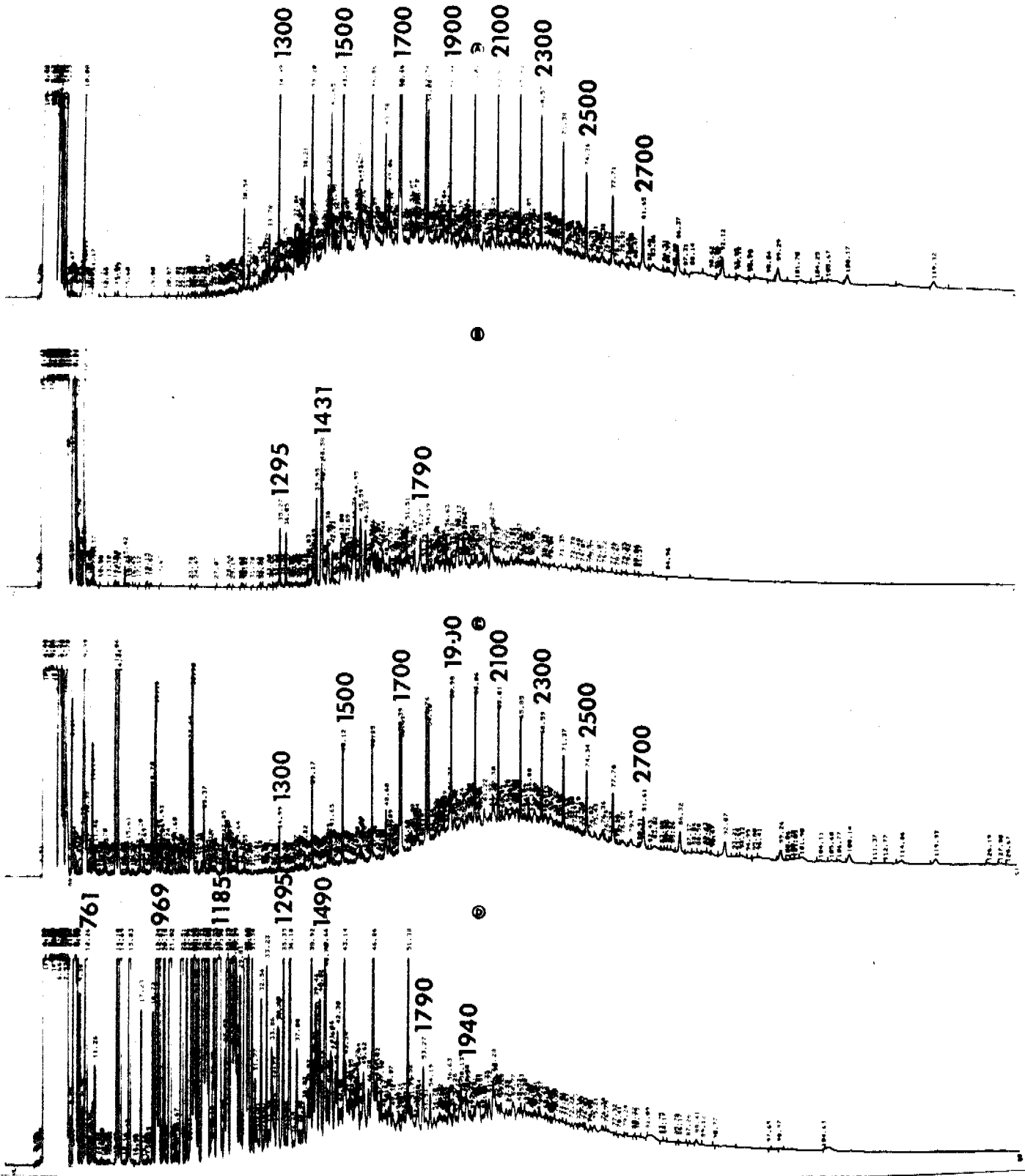

FIGURE 5-74. FLAME IONIZATION DETECTOR CAPILLARY GAS CHROMATOGRAMS OF PRUDHOE BAY CRUDE OIL AND SEAWATER SAMPLES OBTAINED AFTER 6 MONTHS OF SUB-AMBIENT WEATHERING FROM OCTOBER TO APRIL 1981 UNDER STATIC (NO-FLOW) CONDITIONS (TANK 2). A AND B REPRESENT THE ALIPHATIC AND AROMATIC FRACTIONS OF THE OIL, RESPECTIVELY, AND C AND D REPRESENT THE ALIPHATIC AND AROMATIC FRACTIONS OF THE WATER COLUMN, RESPECTIVELY.

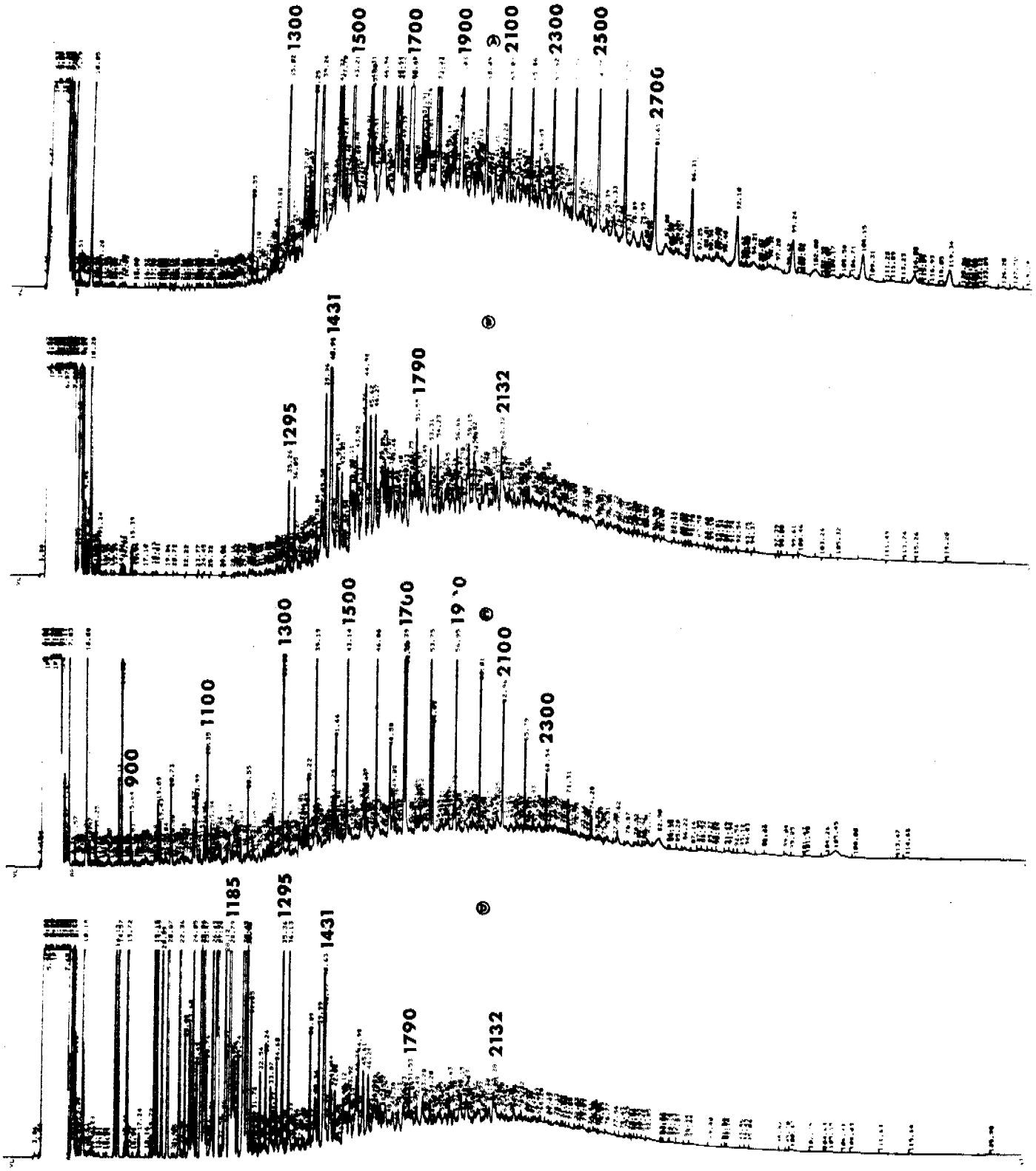

FIGURE 5-75. FLAME IONIZATION DETECTOR CAPILLARY GAS CHROMATOGRAMS OF PRUDHOE BAY CRUDE OIL PLUS COREXIT AND SEAWATER SAMPLES OBTAINED AFTER 6 MONTHS OF SUB-AMBIENT WEATHERING FROM OCTOBER TO APRIL 1981 UNDER STATUS (NO-FLOW) CONDITIONS (TANK 5). A AND B REPRESENT THE ALIPHATIC AND AROMATIC FRACTIONS OF THE OIL, RESPECTIVELY, AND C AND D REPRESENT THE ALIPHATIC AND AROMATIC FRACTIONS OF THE WATER COLUMN, RESPECTIVELY.

temperature regimes. (Water temperatures were near 4°C when the experiments were initiated, and periodic freezing and thawing occurred during January and February, 1981.) Figure 5-74B shows the aromatic fraction of the oil, and this also shows that evaporation, and dissolution of compounds with Kovat indices less than 1200 has occurred from the surface oil slick. These more water soluble components are clearly evident in the acidified water extracts obtained from the water beneath the slick; Figure 5-74C and 5-74D depict the aliphatic and aromatic fractions, respectively, of the acidified water column extract from the outdoor tank 2. While the capillary column is clearly overloaded, the presence of exceedingly high levels of aromatic compounds in the water can be observed. Aromatic compounds present include benzene, toluene, xylenes, alkyl substituted naphthalenes, and phenanthrenes. The exceedingly high levels in the aromatic fraction also help to explain the limited breakthrough of some of these components into the aliphatic fraction (Figure 5-74C) during the liquid column chromatography.

In that the outdoor tank was stagnant during the six month period between October to April of 1981, these lower molecular components would not be readily removed by advection. However, they might a priori be expected to be lost due to the evaporative processes. One hypotheses to explain the lack of this anticipated loss is that the oil on the surface of the water formed a skin or cap which then prevented additional loss of these more water soluble aromatic compounds from the water column via evaporative processes. Similar observations were made by PAYNE, et al. (1980) during the sub-surface IXTOC-I blowout in the Gulf of Mexico in 1979, where elevated levels of benzene, toulene, and xylenes were found in the water column. In that instance, it was also believed that the oil coating on the water acted as a cap to inhibit efficient air-sea exchange and that removal of the compounds by evaporation would only occur after advection of the water away from the slick (or wind driven movement of the slick itself).

Figure 5-75 presents the chromatograms of oil samples from the static tank experiment of oil plus Corexit (tank 5) after the same period of weathering. Qualitatively the chromatograms appear very similar to those in Figure

5-74, and it can be seen that during the winter months, most of the volatile components with molecular weights less than nC-12 (Kovat Index 1200) were lost (Figure 5-75). Figure 5-75b shows that the aromatic compounds with molecular weights less than the methylnaphthalenes were lost by evaporative and dissolution processes.

The aliphatic fraction of the acidified water column extract (Figure 5-75C) has higher levels of aliphatic compounds compared to the aliphatic fraction for the tank 2 water (Figure 5-74C), and this is presumably due to the influence of the dispersant.

Figure 5-75D shows the chromatogram obtained on the aromatic fraction of the water column extract from this tank, and as in the other case from the winter experiments, high levels of aromatic hydrocarbons are observed to remain in the water after six months of subarctic weathering. As noted before, this presumably reflects diffusion controlled processes limiting loss of these components through the viscous oil slick cover.

As noted above, outdoor tanks 3 and 7 were maintained in the flowing condition during the period of April through October 1981, and during this period, significant increases in microbial degradation of the oil in the tanks were noted. Further, in examining the oil from the different tanks, longer term oil weathering processes were observed to be clearly dependent on the status of the stranded or floating oil. Specifically, microbial degradation appeared to be primarily a surface phenomenon, and evidence of extensive microbial processes was limited to surface films emanating from larger oil/mousse patches.

Evidence of the differential weathering patterns observed in oil droplets versus surface film are presented in Figure 5-76. Figure 5-76A presents the capillary column gas chromatogram (non-fractionated) obtained on oil droplets observed in outside tank 3 after eleven months of continuous weathering in the flow through system. Interestingly, compounds are present down to

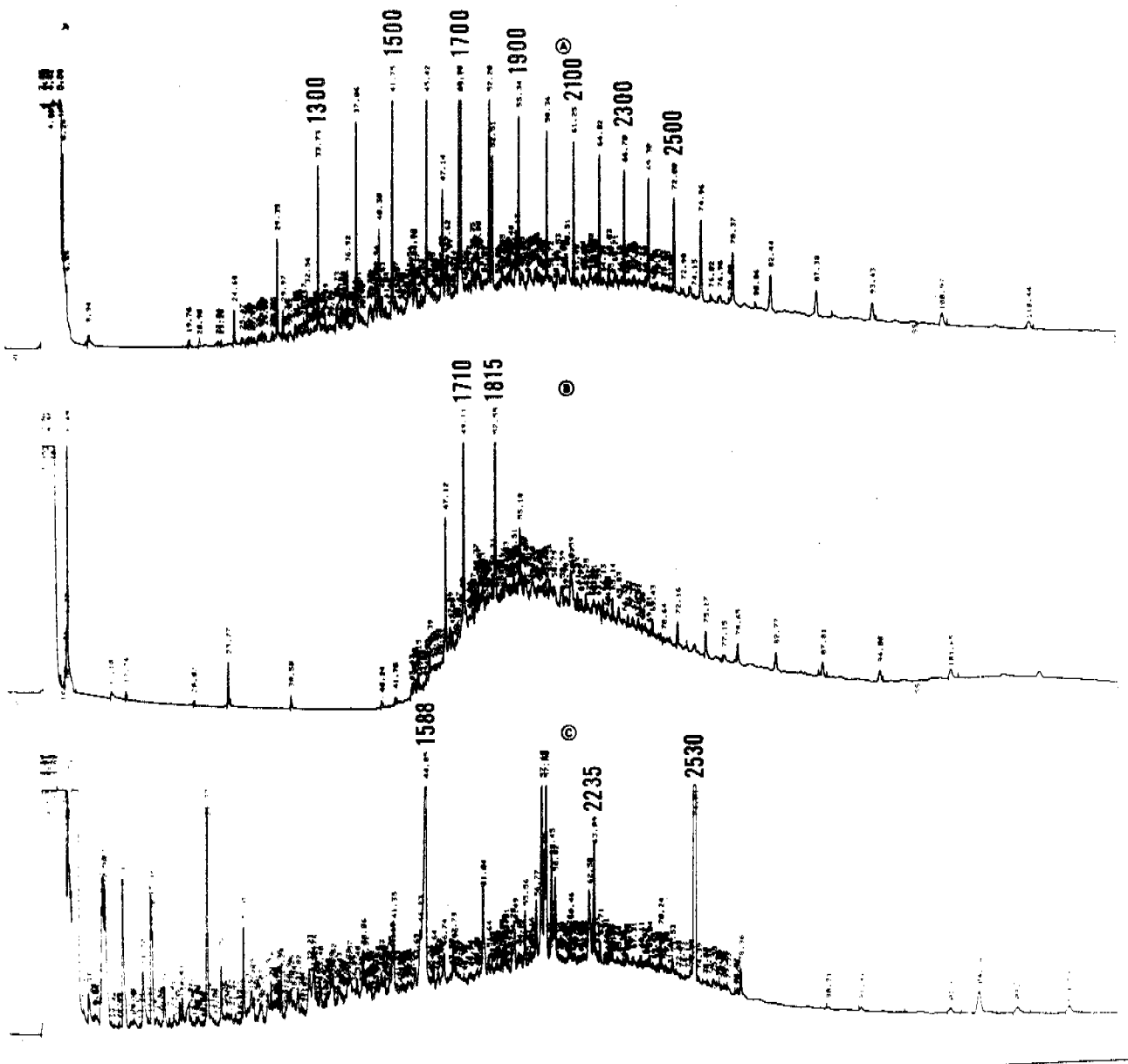

FIGURE 5-76. FLAME IONIZATION DETECTOR CAPILLARY GAS CHROMATOGRAMS OF WEATHERED OIL AND WATER COLUMN SAMPLES AFTER 11 MONTHS OF CONTINUOUS SUB-ARCTIC WEATHERING (OCTOBER 1980 TO SEPTEMBER 1981) IN THE OUTDOOR FLOW-THROUGH AQUARIA (TANK 3): (A) OIL DROPLETS (ENTIRE EXTRACT); (B) SURFACE FILM EMINENTING FROM OIL PATCHES (ENTIRE EXTRACT); AND (C) ACIDIFIED SEAWATER EXTRACT.

Kovat indices 1100 showing limited evaporation from the interior of the droplet. In this instance, formation of a surface crust on the oil during the winter months, presumably limited further evaporation/dissolution losses and microbial activity over the summer.

Figure 5-76B, however, shows extensive evaporative and microbial degradation losses in the translucent film emanating from the larger patches of the oil in the outdoor tank. In this instance the only major resolved components remaining in the chromatogram are those of pristane and phytane and other possible isoprenoids. The chromatogram is also characterized by a relatively large unresolved complex mixture and higher molecular weight n-alkanes ranging from nC_{23} through nC_{29}.

Figure 5-76C presents the chromatogram obtained from the acidified water extract after eleven months of natural weathering under the subarctic conditions. Clearly there are a number of polar compounds present in the sample extract and GC/MS analyses before and after derivitizations with diazomethane are underway at this time.

Figure 5-77A presents the FID capillary gas chromatogram for a large patch of floating mousse from tank 2 (artificial mousse and Corexit) after five months of weathering (May to September). Essentially complete loss of compounds below nC-13 due to evaporation and dissolution can be observed. From the appearance of the chromatogram, however microbial degradation is not readily apparent in this sample. This is believed to be due to the fact that the higher concentrations of relatively unweathered components making up the interior of the patch mask any selective microbial utilization of specific alkanes which might have occurred on the lower surface, which was exposed to the water column.

Figure 5-77B presents the chromatogram obtained on a sample of stranded mousse collected in September from the sides of tank 2, and this also shows

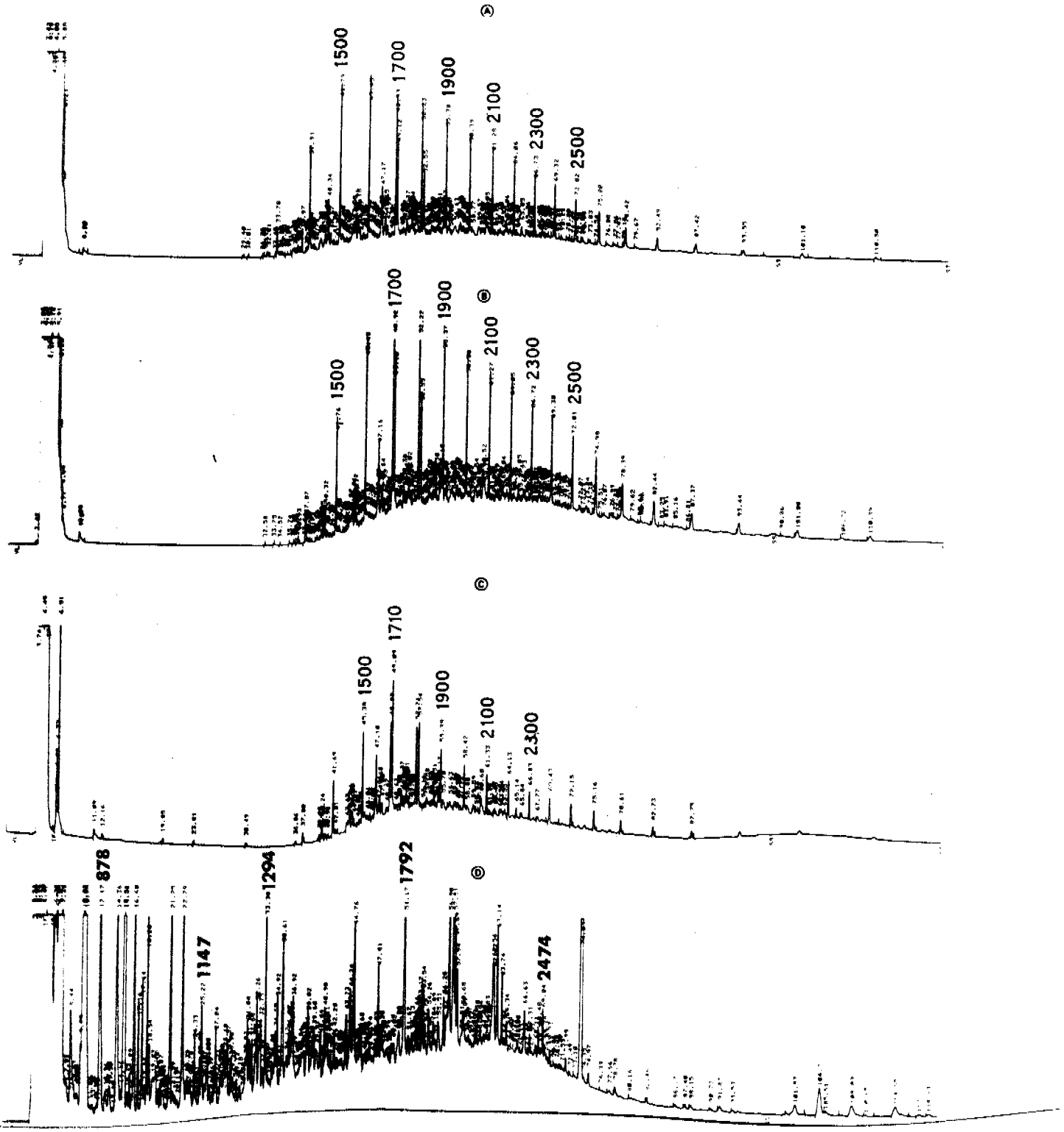

FIGURE 5-77. FLAME IONIZATION DETECTOR CAPILLARY GAS CHROMATOGRAMS OF ARTIFICALLY GENERATED PRUDHOE BAY MOUSSE PLUS COREXIT AFTER 5 MONTHS OF WEATHERING (MAY TO SEPTEMBER 1981) IN THE OUTDOOR FLOW-THROUGH AQUARIA (TANK 2) AT KASITSNA BAY, ALASKA: (A) ARTIFICIAL MOUSSE FLOATING ON THE WATER COLUMN; (B) STRANDED MOUSSE FROM THE SIDE OF THE CORRAL; (C) SURFACE FILM EMINENTING FROM MOUSSE PATCHES; AND (D) ACIDIFIED SEAWATER EXTRACTS.

only limited microbial degradation although a slight increase in loss of compounds below Kovat index 1400 is noted. This presumably reflects elevated temperatures encountered during atmospheric exposure.

Figure 5-77C shows the chromatogram obtained from a translucent film extending from the bulk of the mousse patch from tank 2. In this instance a loss of aliphatic and aromatic compounds below 1500 is evident and enhanced microbial degradation is suggested by the nC-17/pristane and nC-18/phytane ratios of 0.61 and 0.73, respectively.

Figure 5-77D shows the acidified water extract obtained from a 31.7 liter water sample obtained four months after the mousse was initially spilled in the flow through water system. This extract has been submitted to GC/MS analysis and Figure 5-56 (in Section 5.2.3) presents the reconstructed ion chromatogram obtained on that sample. The disparity in the appearance of the chromatogram in Figure 5-56 compared to Figure 5-77D can be attributed to inadvertent loss of lower molecular components before GC/MS analysis during transport to our La Jolla facility. An additional sea water extract of this tank was obtained after seven months of weathering and is undergoing extraction and fractionation at this time. Hopefully, this sample will provide sufficient material in this lower molecular weight range to facilitate GC/MS analysis. As noted earlier, the numbered peaks in Figure 5-56 have been tentatively identified by GC/MS. (Table 5-25 presents those compound identifications).

5.3 Oil/Suspended Particulate Material Interactions

5.3.1 Effects of Oil on SPM Settling Rates - La Jolla Studies

During the first half of this program, oil/suspended particulate material interactions were studied to determine adsorption/desorption rates at different temperatures and to determine the affects of these processes on sedimentation rates with various types of particulate material. These studies were undertaken with fresh Prudhoe Bay crude oil and Prudhoe Bay crude which

had undergone evaporation/dissolution weathering for 48 hours. The presence and absence of the dispersant Corexit 9527 (10 parts oil to 1 part dispersant) were also incorporated as experimental variables, and three types of relatively pure sediments were utilized (carbonate, silica and deep basin clay; Table 5-28). Sedimentation rate determinations were made using a Cahn 2000 series sediment balance, and a particle size range of 4.0 ϕ to 9.0 ϕ (62 μm to 2 μm) was used.

The sediment material being analyzed was added to the stirred chamber shown in Figure 5-78, and aliquots were taken at times 0, 3 hours, 24 hours and 48 hours for analyses on the sediment balance. The data were then analyzed to yield final wet and dry weights of (settled) particulates and according to the Waddell settling equations to yield mean, median, skewness and kurtosis data on the grain size distribution.

Waddell Settling formula

$$T = \frac{K}{D^2}$$

T = time (minutes
D = diameter (microns)

$$K = \frac{0.3\ h\ v\ 10^8}{(d_s - d_l)\ g}$$

h = height of column of water
v = viscosity (poises)
d_s = density (solid) g/ml
d_l = density (liquid) g/ml
g = gravity in cm/sec

TABLE 5-28. GRAIN SIZE AND MAJOR METALLIC CATION ABUNDANCES FOR INITIAL OIL/SUSPENDED PARTICULATE MATERIAL EXPERIMENTS.

Dispersive X-ray Analysis (SEM)

Sample	Relative Atom % Mg	Al	Si	K	Ca	Fe
Commercial Diatomite	-	-	93	-	6	1
Milled Foram Sand	2	2	12	-	85	1
San Nicolas Basin Clay	2	6	48	3	35	6

Grain Size Information

Sample	Median	Mean	Skewness	Kurtosis
Commercial Diatomite	5.5	5.5	+ .03	1.0
Milled Foram Sand	5.4	5.9	+ .25	.8
San Nicolas Basin Clay	5.5	5.8	+ .19	0.8

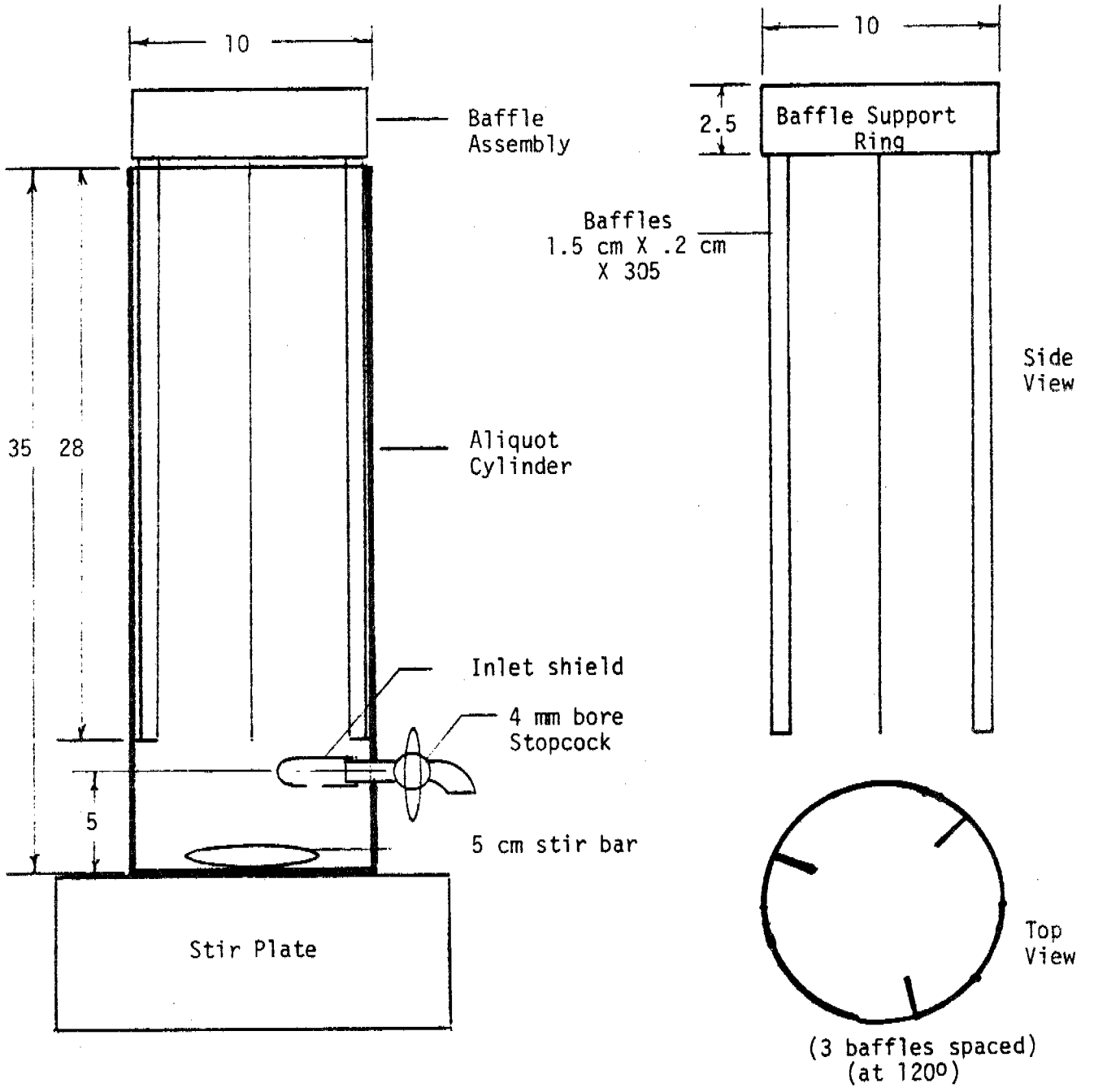

Note: All dimensions in cm.

FIGURE 5-78. ALIQUOT CYLINDER ASSEMBLY FOR OIL/SPM INTERACTION STUDIES.

Graphical Statistics

$$\text{Skewness} = \frac{\phi 16 + \phi 84 - 2\phi 50}{2(\phi 84 - \phi 16)} + \frac{\phi 5 + \phi 95 - 2\phi 50}{2(\phi 95 - \phi 5)}$$

$$\text{Kurtosis} = \frac{\phi 95 - \phi 5}{2.44(\phi 75 - \phi 75)}$$

$$\text{Mean} = \frac{\phi 84 + \phi 16}{2}$$

Median = ϕ size at 50% cumulative weight

Results from these initial studies were presented in detail in the September 1980 Interim Report, and therefore, will not be discussed in detail here. Essentially only very slight perturbations in SPM settling characteristics were observed as a result of oil, oil plus Corexit, and mousse interactions. Tables 5-29 and 5-30 present results from initial interaction studies completed with diatomite powder and deep basin clay (San Nicolas), respectively. From these results some subtle changes in the median and mean sediment size characteristics with both substrate types were observed for the oil-Corexit mixtures; however, oil alone did not have as significant an effect on these parameters. Table 5-31 presents a summary of the settling experiments using San Nicolas Basin sediment and oil and oil plus Corexit. Results of the first two runs with oil and the Corexit-oil mixture indicated minor interactions which can be detected in the settling rate data. The small increase in phi size (decrease in grain size) for both the median and mean and the decrease in settled weight percent are indicative of some buoyant force at work and/or of adsorption of oil, decreasing the effective density of the particles below a critical size (FEELY et al., 1978; BASSIN and ICHIYE, 1977). The largest settled weight differences occur in the oil/Corexit sediment experiments; however, the median, mean, skewness and kurtosis were not as drastically affected by the oil or oil plus Corexit interaction. Time-series changes in the phi size, skewness and final weight settled as a result of oil exposure are shown in Figure 5-79, and while the affect of exposure on all

TABLE 5-29. INITIAL INTERACTION, STATISTICAL EFFECTS OF DENSITY, DISPERSANT, AND SAMPLE WEIGHT ON DIATOMITE POWDER AT 23°C.

Sample	Addition	ρ	Method of Injection	Dry Weight	Wet wt.* Dry wt.	Median	Mean	Shewness	Kurtosis
A	.01N Calgon	.997	30cc in cent. tube	200 mg	.57	5.50	5.49	+.03	1.04
Run #4	---	1.025	30cc in cent. tube	200 mg	.51	5.37	5.41	+.11	1.13
Run #5	---	.997	40cc in cent. tube	300 mg	.56	5.57	5.49	-.38	1.06
Run #6	---	1.025	6cc in 10cc syringe	160 mg	.50	5.47	5.50	+.13	1.27
Run #7	Oil only	1.025	30cc in cent. tube	205 mg	.51	5.42	5.50	+.98	1.11
Run #8	Oil-Corexit	1.024	30cc in cent. tube	200.2 mg	.35	5.59	5.84	+.16	.78
Run #9	Oil-Corexit	.997	30cc in cent. tube	204 mg	.52	5.50	5.50	+.03	1.05
Run #10	Oil-Corexit	.997	30cc in cent. tube	208 mg	.56	5.70	5.70	+.03	.98
Run #11	Oil-Corexit	.997	separate addition of sediment and oil	211 mg	.54	5.69	5.73	+.08	1.05

* Ratio of sedimentation balance weight (weight of sediment in water)/dry weight of added sediment.

TABLE 5-30. STATISTICAL SUMMARY OF DEEP BASIN CLAY (SAN NICOLAS) AMBIENT TEMP (23°C), SEAWATER, MIXING TIME = 15 min.

Date	Oil	10:1 Corexit	(0-4) Run Rating	Median	Mean	Skewness	Kurtosis	Final Wt.	% Settle
7/22/80	---	---	4.0	5.53	5.80	+.19	.75	108.9	100%
7/23/80	---	---	4.0	5.32	5.51	+.21	.89	105.5	100%
7/21/80	X	X	2.5	4.89	5.31	+.37	.98	72.5	68%
7/28/80	X	X	3.5	4.92	5.35	+.35	.95	71.9	67%
7/24/80	X	---	4.0	5.36	5.75	+.26	.87	91.7	86%

Run Reproducibility

	Mean	Skewness	Kurtosis	Final Wt.
Sediment	5.66± 0.2	.21 ± .01	.82 ± .1	107 ± 2.4
Sediment-oil-Corexit	5.33± 0.03	.36 ± 0.1	.97 ± .02	72.2 ± 0.4

TABLE 5-31. SUMMARY OF SAN NICOLAS BASIN SUSPENDED PARTICULATE MATERIAL AND FRESH PRUDHOE BAY CRUDE OIL INTERACTIONS.

	CONDITIONS			STATISTICS				final weight recovered (wet)
	Additive	temp.	time	median	mean	skewness	kurtosis	
1.	none	23°C	0	5.25	5.47	+ .21	.91	78.4
2.	oil	"	3 hrs.	5.50	5.69	+ .17	.87	77.5
3.	oil	"	24 hrs	5.79	5.91	+ .11	.94	74.3
4.	oil	"	48 hrs.	6.03	6.02	+ .005	.90	71.5
5.	oil & corexit	"	0	5.25	5.28	+ .90	.75	44.70
6.	" "	"	3 hrs.	5.13	5.39	+ .28	1.05	26.32
7.	" "	"	24 hrs.	5.30	5.30	+ .08	.85	34.05
8.	" "	"	48 hrs.	5.91	6.13	+ .12	.81	31.15

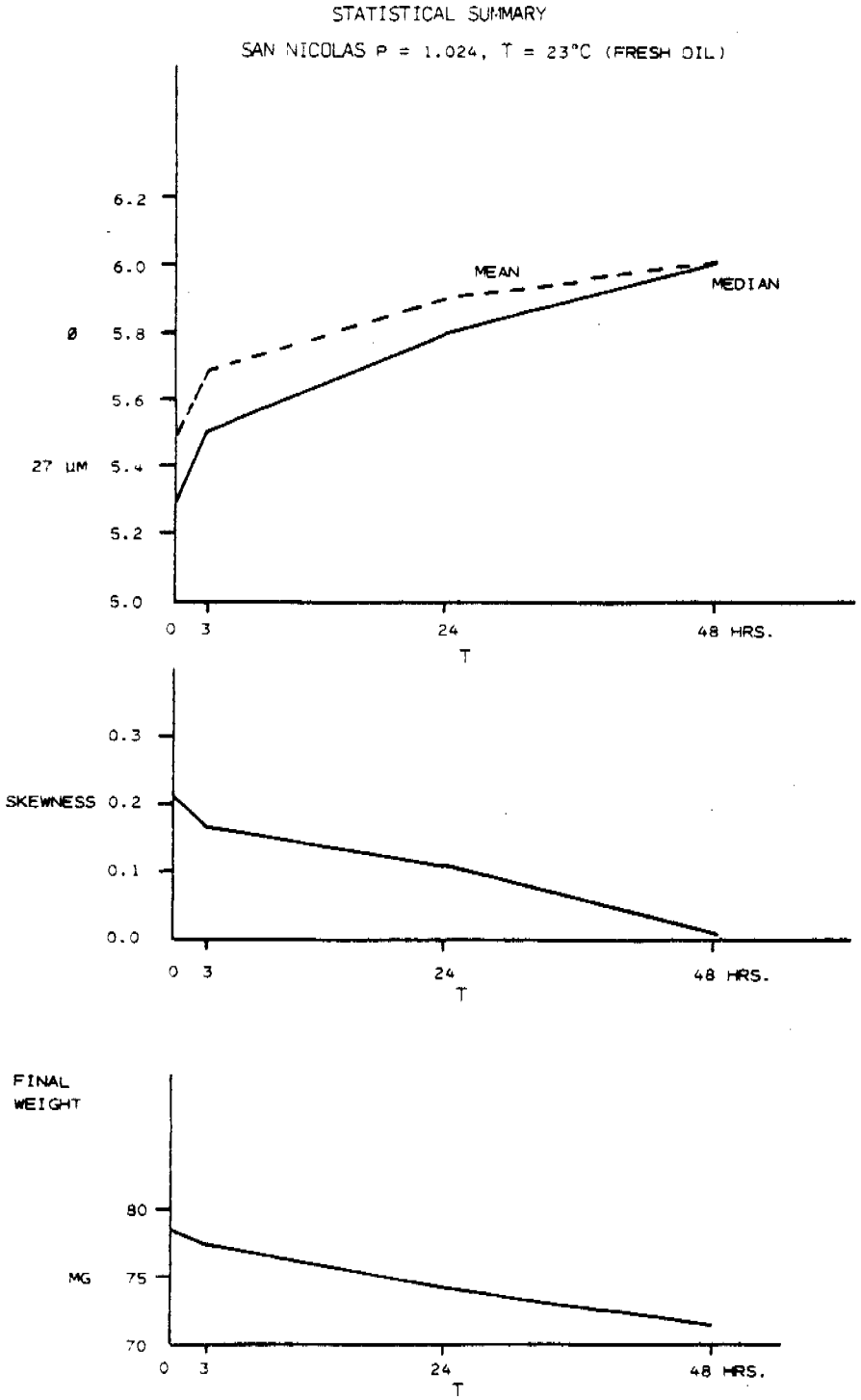

FIGURE 5-79. GRAPHICAL DISPLAY OF THE AFFECTS OF THE INTERACTION TIME FOR SAN NICOLAS BASIN SEDIMENT AND FRESH PRUDHOE BAY CRUDE OIL ON MAJOR STATISTICAL PARAMETERS (SEE TABLE 5-31). THE EFFECT OF TIME ON ALL THREE PARAMETERS IS STATISTICALLY SIGNIFICANT BUT NOT CONSIDERED TO BE MINOR.

three parameters is statistically significant, their overall perturbation to SPM characteristics were considered to be minor.

5.3.2 Detailed Analyses of Suspended Particulate Materials Characteristic of Lower Cook Inlet Alaskan Waters

As a result of the above findings, examinations of phi size and settling characteristics of oil/SPM mixtures were discontinued, and attention was instead directed towards the compound specific nature of the oil suspended particulate material interactions. Further, in an effort to satisfy environmental manager's needs with regard to oil/SPM interactions in Alaskan waters, attention was focused on the compound specific adsoprtion of petroleum hydrocarbon components onto sediments and fines representative of Lower Cook Inlet suspended particulate material.

Thus, during the Spring 1981 Kasitsna Bay program, studies were initiated to locate intertidal sites having significant deposits of sediment fines representative of Lower Cook Inlet suspended particulate material, and samples of these sediments were characterized as to their physical and compound specific oil retention properties. From the results of these initial investigations, two intertidal sites were selected as sources of divergent but representative samples of Lower Cook Inlet SPM. These sediments were then used for outdoor flow-through oil/SPM interaction experiments during the summer 1981 program at Kasitsna Bay.

Figure 5-80 presents a navigational chart for the Lower Cook Inlet/Shelikof Strait area, and Figure 5-81 shows expanded detail of the Kachemak Bay region. Sampling sites for initial SPM characterizations were selected using "Cook Inlet-southern part, navigational chart (1:200,000)-NOAA, C&GS 8554"; and, the unpublished Environmental Sensitivity Index (ESI) for Lower Cook Inlet (RUBY and MAIERO, 1979).

Suspended particulate material in Kachemak Bay was considered to have four primary sources:

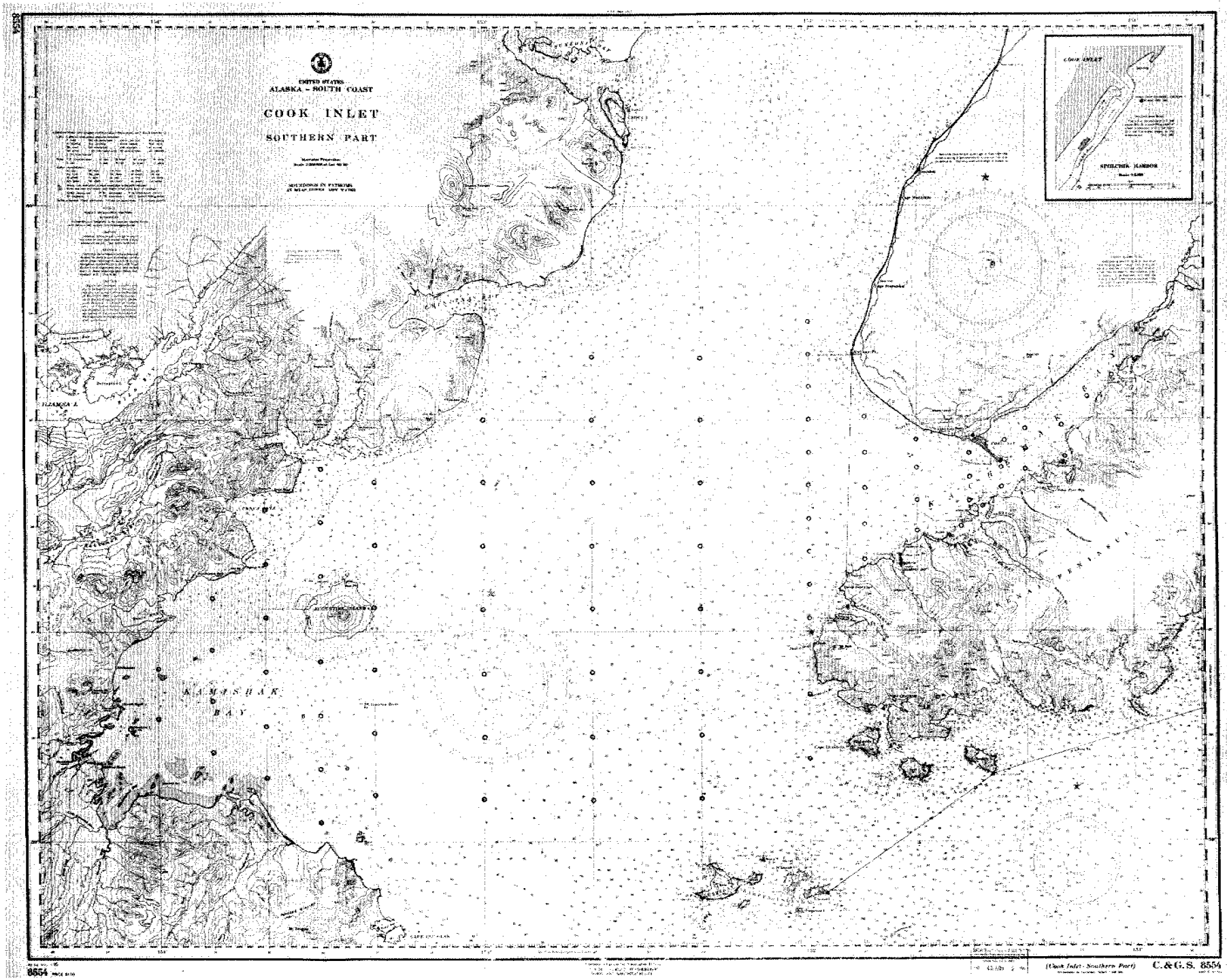

FIGURE 5-80. US DEPARTMENT OF COMMERCE COAST AND GEODETIC SURVEY. CHART #8554 OF THE LOWER COOK INLET REGION.

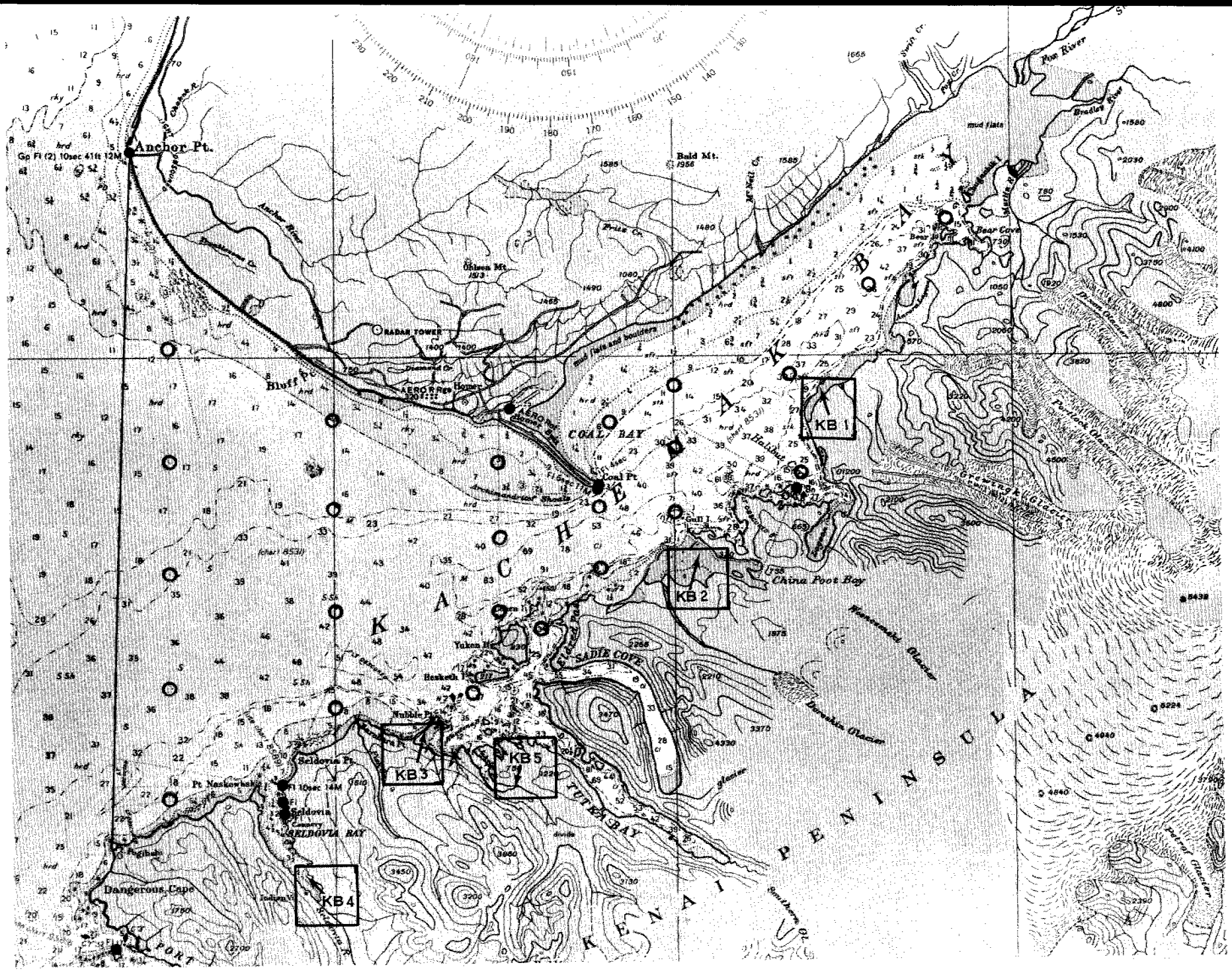

FIGURE 5-81. EXPANDED VIEW OF THE KACHEMAK BAY, KASITSNA BAY REGION (FROM C.&G.S. CHART 8554). SAMPLING SITES FOR OIL/SPM INTERACTION STUDIES AND INTERTIDAL OILED-CORRAL EXPERIMENTS ARE DENOTED AS: KB-1 GREWINGK GLACIER DELTA; KB-2 CHINA POOT BAY MUD FLATS KB-3 COMPOSITE SEDIMENT; KB-4 SELDOVIA RIVER SALT MARSH DETRITAL SEDIMENTS; KB-5 [illegible] OF INTERTIDAL MUD FLATS.

- o Marine waters introduced to Kachemak Bay by tides and currents from Lower Cook Inlet (Gulf of Alaska and Shelikof Straits)
- o Glacial melt waters
- o Terrestrial sources-runoff
- o Marsh detritus

A secondary source to any site was also considered to be resuspension of sediment through wind and wave scour and transport of sediments by tidal actions and long-shore and bottom currents.

The Spring 1981 sampling program was designed such that 3 sediment types which were representative of Lower Cook Inlet suspended particulate material could be obtained, and these included: pure glacial till, tidal flats supported primarily by marine deposits and tidal flats supported by marsh detritus and terrestrial runoff. To represent these sediment types, four primary sites were selected for sampling and these are shown on Figure 5-81 as KB-1, KB-2, KB-3 and KB-4. At each site, fine particulates and sediment floc were obtained from the upper 1 to 2 cm of deposits exposed during lower tidal excursions. Detailed descriptions of each site follow.

KB-1: Grewingk Glacier Delta and Melt Stream

This site is characterized as a large, protected, delta subject to tidal marine flushing and fresh water input from the Grewingk Glacier melt stream. The glacier is central and 3 to 4 miles southeast of the tidal flat which is bounded on the west by a wide gravel spit oriented southwest to northeast as formed by northeasterly moving tides and longshore currents in Kachemak Bay (Figure 5-81). Glacial sediments were found directly behind the tip of the gravel spit at the point that the glacial waters met the marine waters which were draining from the southern section of the flat. These deposits of glacial silt (2-5 mm thick) formed a mat which could be removed from underlying sediment, and samples of this material were obtained for oil/SPM characterization studies. The exposed surfaces of small to medium cobble in

the area were also covered with a similar mat of glacial silt, but quantitative sampling of this material was not possible. The richest glacial deposits were restricted to an area of approximately 800 meters^2 out of approximately 20,000 meters^2 inspected.

The influence of glacial melt waters served to increase biological productivity as evidenced by large stands of Ulva sp. accompanied by significant numbers of amphipods. Filamentous brown algae were ubiquitous to the flat. Bird use of the area appeared moderate - evidence of bird tracks was lower than expected.

The glacial melt water was "milky" (bluish white) and had a fresh-bitter taste. The mouth of the delta (interface of drainage and receiving waters) was subject to erosion due to the meandering of the delta channel, and as such, the site at which samples were taken is considered to be geologically active. Little perburbation of the area was noted on re-occupying the station during the Summer 1981 field program; however, it was apparent that the sampling site may not remain in its present state for extended periods of time. Overall energy is low; however, localized disturbances may affect the subject sediment when incoming or outgoing tidal waters covering the flat are a few centimeters to a 1/3 meter deep (or depth equaling fetch height) so that wind driven waves can scour the bottom. This type of activity could make the placement of study plots difficult, and as a result of this instability and because of logistical considerations, extended oil/SPM interaction studies in the flow-through tanks at Kasitsna Bay facilities were not undertaken with this site as a source of SPM. Further discussions of the results of oil/SPM interaction studies using the substrate from KB-1 are presented in Section 5.3.4.

KB-2/China Poot Bay - Mud Flats

The area at which samples were taken is common to protected tidal flats in Lower Cook Inlet and Prince William Sound (RUBY and MAIERO, 1979). The sampling site is located on the southwest section of the flats, and this

site is protected from wave energy by a long, curved gravel spit forming the boundary between China Poot and Kachemak Bay (Figure 5-81). There is no source of fresh water immediately adjacent to the sampling site. The sources of sediment at this site are expected to be primarily of marine (i.e., outer bay) origin. The flat is very high in biological productivity - clams, polycheates and amphipods were abundant. It is apparent that benthic organisms are constantly reworking these sediments - fecal pellets and burrows were in profusion, and for the most part, the sediments appeared to be well oxidized with little or no evidence of H_2S.

The sampling area included "random" surficial samples taken from the sloping face of the flat (slope of 12:1 on the lower face to 23:1 on the upper face) and the flat itself (average slope along transect of 75:1). The sediments on the slope face (to a depth of approximately 10 cm) consisted of a thin veneer of brown organic sediments in a consolidated mat having a thickness of 2 - 5 mm overlying black silt/sand homogeneous, well oxidized sediments. These sediments were well packed and did not yield to any degree to foot pressure. In comparison, the sediment composition on the flat proper was visually alike the sediments of the slope; however, the underlying black sediments were in a moderately reduced state (moderate H_2S noted). Sample KB-2B was obtained from these reduced sediments while KB-2 was obtained on the 0-1 cm subsection from the slope face. Biological activity was higher on the flats compared to the slope face (evidence of siphon holes, etc.) and interstitial water was observed in each cross-section of sediment. The upper flat sediments were not as firm as those of the slope so that foot pressure could easily cause a depression. The reduced state (notable H_2S present) may be a function of the ability of the flats to: drain quickly, increasing retention of organics (as opposed to wave action gently scouring the somewhat steeper slope with each tidal cycle), heating of the flats by solar energy (slope would be subject to direct sunlight during a limited portion of the sun's arc), and increased bacterial activity.

KB-3, Kasitsna Bay - Composite Shell Fragments, Sand and Mud

The Kasitsna Bay sediment sample was taken from the interior of the bay along a tidal flat adjacent to Nubble Pt. (see Figure 5-81). The mud flats are located on the east side of a small spit located in the western interior of the Bay. Wave energy is minimized in this portion of the bay because of the short distance between spits; however, tidally generated currents appear significant. The sampling station lies at the foot of a sand/gravel beach having a moderate slope (1:17) to the high tide wrach and a steep slope (1:9) from the high tide to the maximum storm tide wrach on Nubble Pt.

The sediments on the protected flats consist of an unsorted matrix of sand, gravel and shell fragments bound tightly together with silts and organic materials. The nature of the components in the sediments indicate that material is transported to this area as a result of bottom scour (tidal) and longshore transport. Biological productivity is high. The flats were populated with vegetation stands of Ulva, Fucus and Enteromorpha accompanied by Mytilus, Balanus and numerous polycheates and amphipods. The holdfasts of the plants and byssal threads of the mussels appear to play a significant role in trapping sediments on the flats.

The sediments at this station were unique to the sediment samples collected during the spring season. Sediments sampled at other sites were fairly well sorted and somewhat homogeneous. Bottom scour did not seem to contribute to the sediment at the other stations and shell fragments were not as abundant. This station appears to contain representative composite of the components of the other stations sampled.

KB-4, Seldovia Bay - Salt Marsh in Upper Bay

The sample from this station was taken in a submerged tidal channel in the Spartina sp. marsh at the head of Seldovia Bay. The marsh lies to the north of Seldovia River (Figure 5-81).

The sediments of the marsh are composed primarily of organic, decomposing detritus originating from the Spartina marsh. The normal cycle of the marsh is to die back in early winter and regrow in spring of the following year. When the marsh plants die back, the dead vegetative material is matted down, by wind and snow to form a thick vegetative cover over the flat. New shoots sprout from the rhizome mat in the spring pushing through the decomposing vegetative mat. In spring, the old vegetative mat decomposes introducing a significant amount of organic material to the marsh channels and flats in the vicinity of the marsh. Our sampling effort occurred during the stage of regrowth/decomposition.

The sampling station is adjacent to the mouth of Seldovia River. Incoming tides transport the fresh water runoff (overlying the denser marine wedge) onto the marsh so that terrestrial sediments may be deposited with marsh detritus. The transport of fresh water onto the marsh was confirmed during sampling as incoming tidal waters tasted totally fresh.

The marsh was rich in invertebrates and showed signs of heavy bird use (tracks).

Table 5-32 presents an overall description of the sediment/SPM samples collected at each site, and Table 5-33 presents size-compositional data derived from visual and microscopic observations of the samples collected from the four sites. From these examinations a pure form compositional diagram for the samples was prepared and is presented in Figure 5-82A. Figure 5-82B characterizes the sediments as far as suspected sediment source.

Immediately after these samples were collected, they were extracted and analyzed at the Kasitsna Bay facility for background biological and potential petroleum hydrocarbon content (from previous spill events). These analyses were completed at that time such that if the results had then indicated previous petroleum hydrocarbon contamination, alternative sampling sites could have been selected and sampled during the spring program before returning to

TABLE 5-32. OBSERVED CHARACTERISTICS AND OVERALL DESCRIPTIONS OF SEDIMENT/SPM SAMPLES COLLECTED DURING THE SPRING 1981 KASITSNA BAY FIELD PROGRAM.

	1	2	2B	3	4
Sediment Component	Glacial Silts Fine sand Gravel	Silt Fine sand	Silt Fine sand	Organics, Silt Fine-medium sand Gravel, shell frag.	Organics, Silt
Sediment Classification	Sandy Silt	Sandy Silt	Silty Sand	Conglomerate	Detritus/Silt
°/oo	0-5	15-30	15-30	15-30	0-5
	Wet: Gray brown color. Very fine sediments, easy to suspend - remain in suspension easily. Silts gray when in suspension-settle portion brown. Dry: Blue gray color - Sample cements together when dry. Sufficient pressure needed to break sample apart.	Wet: Green brown color. Muddy-suspended easily, heavier fraction forms a "clay" on the bottom of the trap - Remains in suspension easily. Dry: Green gray color fragments easily but needs sufficient pressure to reduce it all the way to powdered form.	Wet: Brown black color. Silt suspended easily and sand (black) settles quickly. Sand forms the majority of the sample, silts remain in suspension easily. Dry: Gray black color. Very fine sand is black in color. Drying causes clumping rather than laying powder easily.	Wet: Brown color. Silt and organics suspend easily. Organics appear to be a flock or mucoid sand, gravel and shell fragments settle easily. Organics approx. 50% of sample. Dry: Brown gray color. Sample cements together-difficult to break apart. Silt and organics act as a strong bonding agent.	Wet: Brown color. Silt and plant fiber suspend easily. Fibers settle first followed by the very small sandy silt-a small fraction of the silt remains in suspension over 8 hours. Dry: Brown color. Drys as silt/fiber matrix. Flakes when broken. Easy to powder.

TABLE 5-33. SIZE COMPOSITIONAL DATA DERIVED FROM VISUAL AND MICROSCOPIC OBSERVATIONS OF SPM SAMPLES COLLECTED FROM INTERTIDAL SAMPLING SITES KB-1, KB-2, KB-2B, KB-3 AND KB-4 (SPRING 1981 KASITSNA BAY PROGRAM).

	1	2	2B	3	4
Cobble				X	
Heavy Gravel				X	
Medium Gravel	X			X	
Heavy Sand				X	
Medium Sand			X	X	
Light Sand	X	X	X	X	
Silt	X	X	X	X	X
Glacial Silt	X	?	?	?	
Organics		X	X	X	X

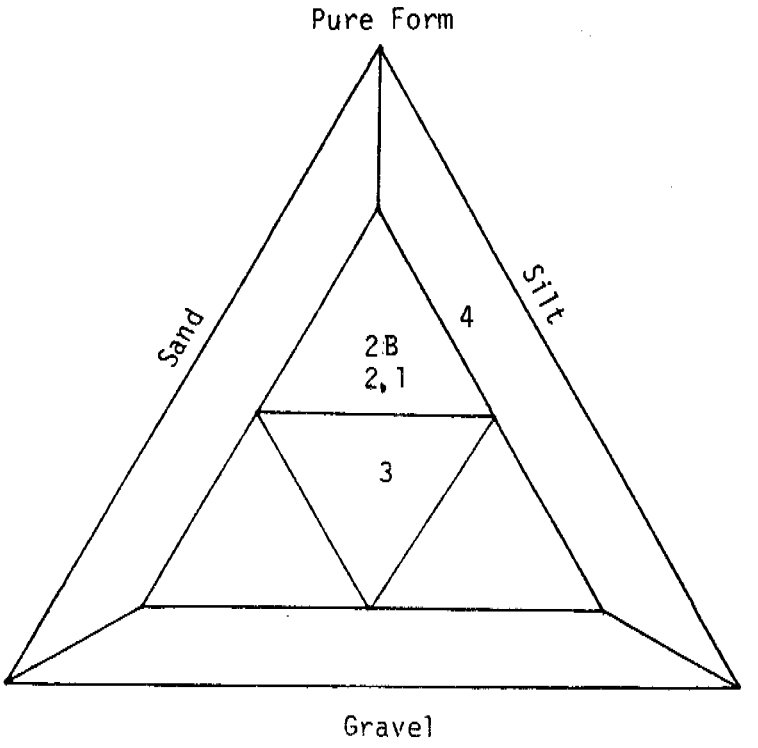

1 - silts, sand - sandy silt (glacial)
2 - sand, silts - sandy silt (marine)
2B - silts, sand - silty sand (marine)
3 - organics, silt, sand, gravel - conglomerate (marine)
4 - organics, silt - silt (organic)

	Glacial	Marine	Terrest.	Marsh
Glacial	1	1		
Marine		2,2B,3	4	
Terrest.			4	
Marsh				

FIGURE 5-82. (A) FIELD ESTIMATED SIZE COMPOSITIONAL DIAGRAM FOR SEDIMENT/SPM SAMPLES COLLECTED DURING THE SPRING PROGRAM; (B) SEDIMENTARY SOURCE DIAGRAM DERIVED FROM FIELD OBSERVATION DATA.

La Jolla. Particular attention was paid to the sediments from KB-4, the Seldovia River salt marsh, because of a Bunker C spill which occurred in Seldovia Bay (down stream) during 1978. Observations were completed during that spill event from vessels, aircraft and through the use of drift cards (MAIERO and MAYNARD, November 1978), and the results of those studies had indicated that the oil did not enter the upper end of the Bay. Fortunately, the capillary column gas chromatographic data confirmed that no prior contamination of that area (or any of the other sites) had occurred, and only trace levels of biogenic compounds were detected in any of the analyses. As a result, no additional field sampling was required during the spring program, and the frozen sediment samples were then shipped to La Jolla for additional characterization and initial oil/SPM interaction studies.

5.3.3 Additional Suspended Particulate Material Sample Characterization by Scanning Electron Microscopy

Upon returning to our laboratories in La Jolla, CA additional characterizations of the sediment/SPM samples were undertaken and these included: specific surface area determinations, scanning electron microscopy (SEM), dispersive X-ray compositional analyses and diffractive X-ray mineralogical analyses. The results of the SEM analyses are presented below; however, the X-ray diffraction studies have not been completed at this time so these data will be included in subsequent reports.

Each sample for SEM analyses was prepared by transferring a 55 to 57-mg sediment sample into 35 ml of deionized water. The sample was then shaken for 15 min on a wrist action shaker; this water was then transferred to a 50-cc plastic polyethylene centrifuge tube with a side arm to withdraw subsamples using a 3-cc syringe.

After bubbling with N_2 to insure SPM suspension, the sediment/water mixture was diluted twice and filtered through a 0.2 μm pore size nuclepore filter to yield 135 to 139 μg per filter. This filter was then sputter coated with gold for scanning electron microscopy analyses on a model ISI Super IIIA

SEM. Figures 5-83 through 5-92 present two selected fields from each SPM sample as shown below.

Figure 5-83 - KB-1 Grewingk Glacial Till
Upper 0-5 mm of deposits removed from Glacier Delta

Figure 5-85 - KB-2A China Poot Bay
Upper 0-1 cm of deposits from intertidal mud flats

Figure 5-87 - KB-2B China Poot Bay
Lower 1-B cm composite from intertidal mud flats

Figure 5-89 - KB-3 Kasitsna Bay
Upper 0-1 cm composite of sediment floc from protected mud flats

Figure 5-91 - KB-4 Seldovia River Estuary
Upper 0-1 cm composite of sediment/detrital floc from channel in Spartina sp. salt marsh

Following each set of SEM photomicrographs, a schematic diagram is presented which identifies the major components present.

Because the μg loading on each filter represents the same overall mass/filter area, direct compositional comparisons can be made for all the SPM samples. Thus, in Figure 5-83 it can be seen that diatoms and several larger clay fragments make up the majority of the sample by weight, while the majority of the surface is covered by less than 5- m clay fragments.

In Figure 5-85 of the surface 0 to 1-cm sample from China Poot Bay, the upper photographs show several plant fragments, and large clay fragments while a significantly reduced level of less than 5 μm clay fragments compared

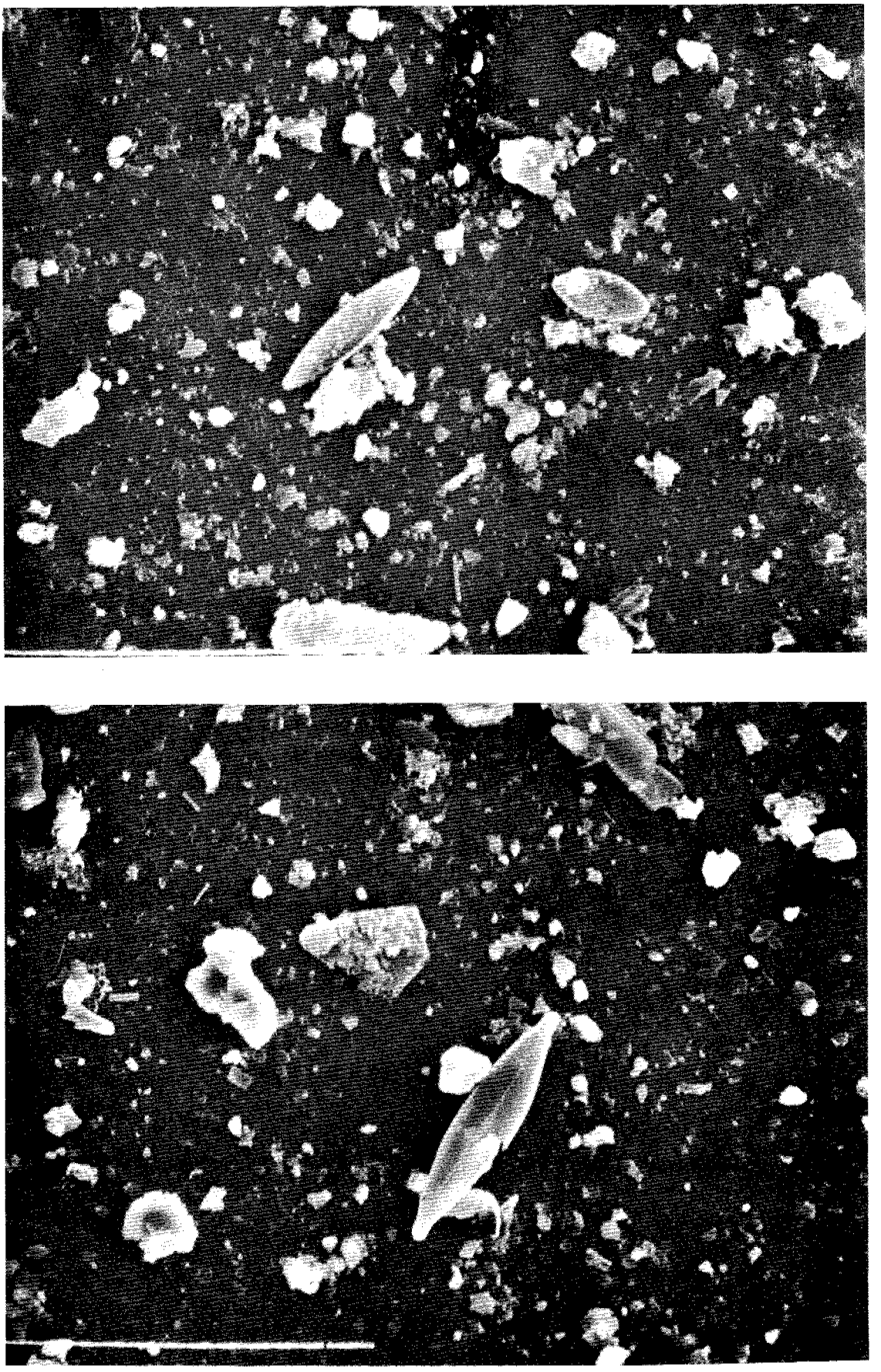

FIGURE 5-83 SCANNING ELECTRON MICROGRAPHS (1400X) OF KB-1-81 (Grewingh Glacier).

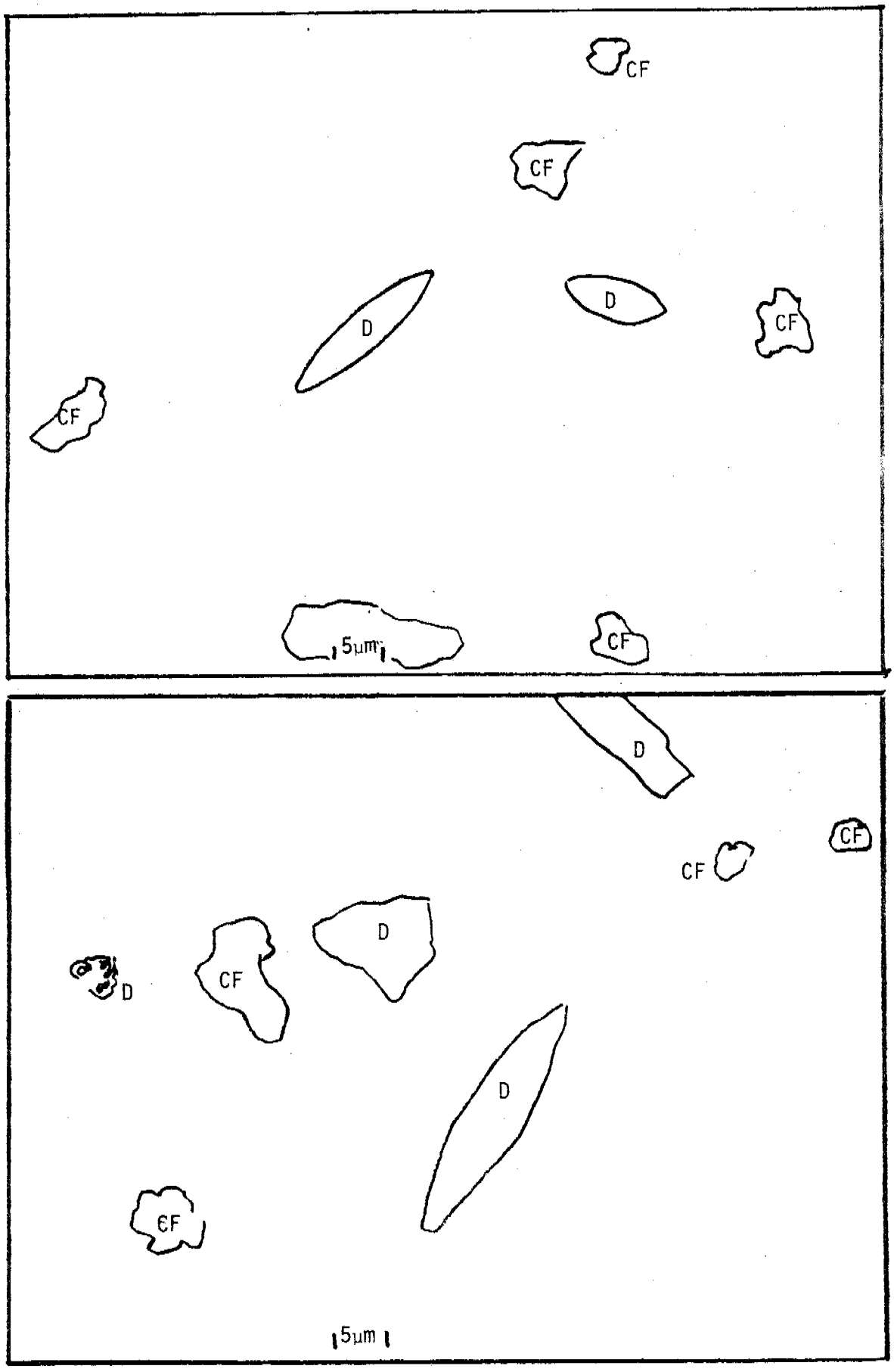

FIGURE 5-84 . IDENTIFICATION OF MAJOR COMPONENTS IN SEM PHOTO-MICROGRAPH OF KB-1-81 (Grewingh Glacier).

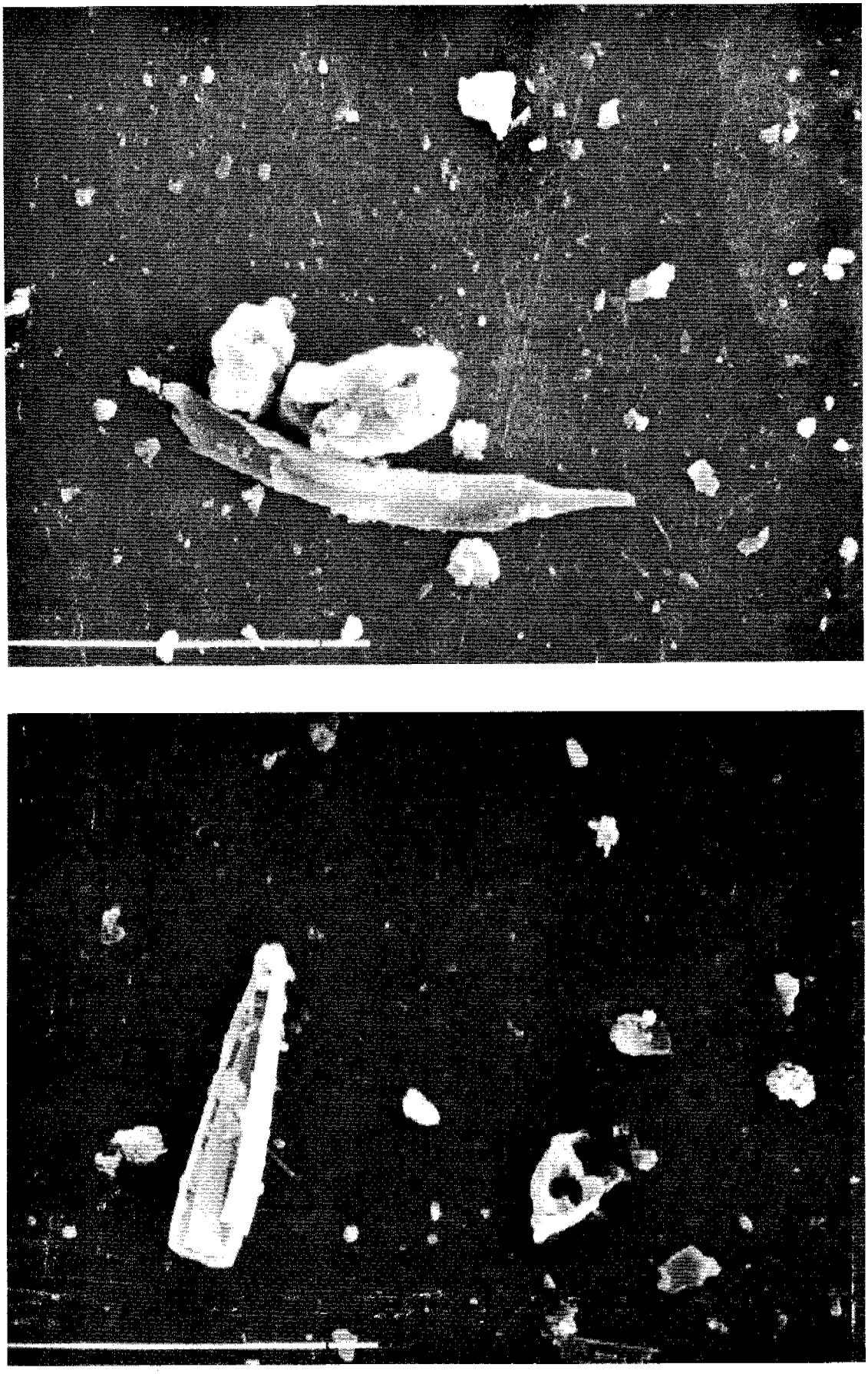

FIGURE 5-85 . SCANNING ELECTRON MICROGRAPHS (1400X) OF KB-2-81A (China Poot Bay 0-1 cm).

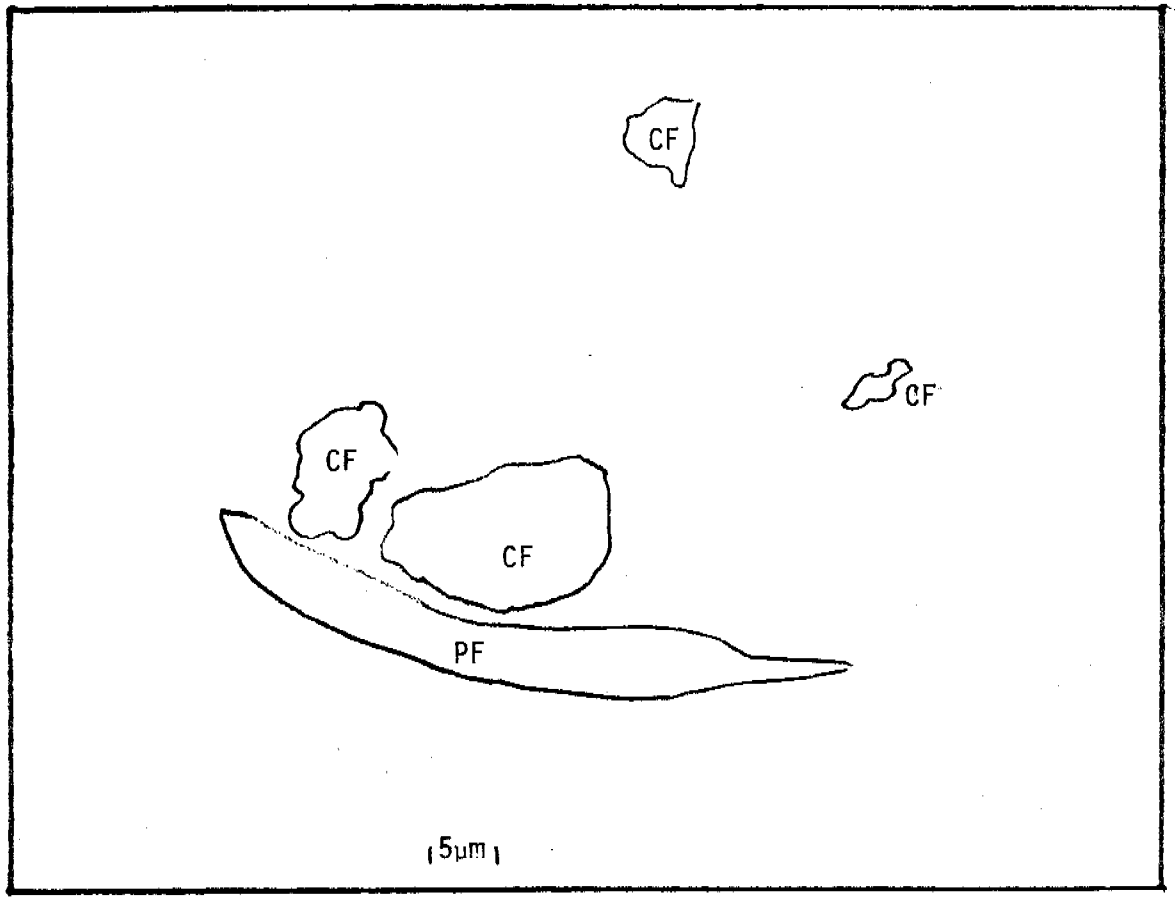

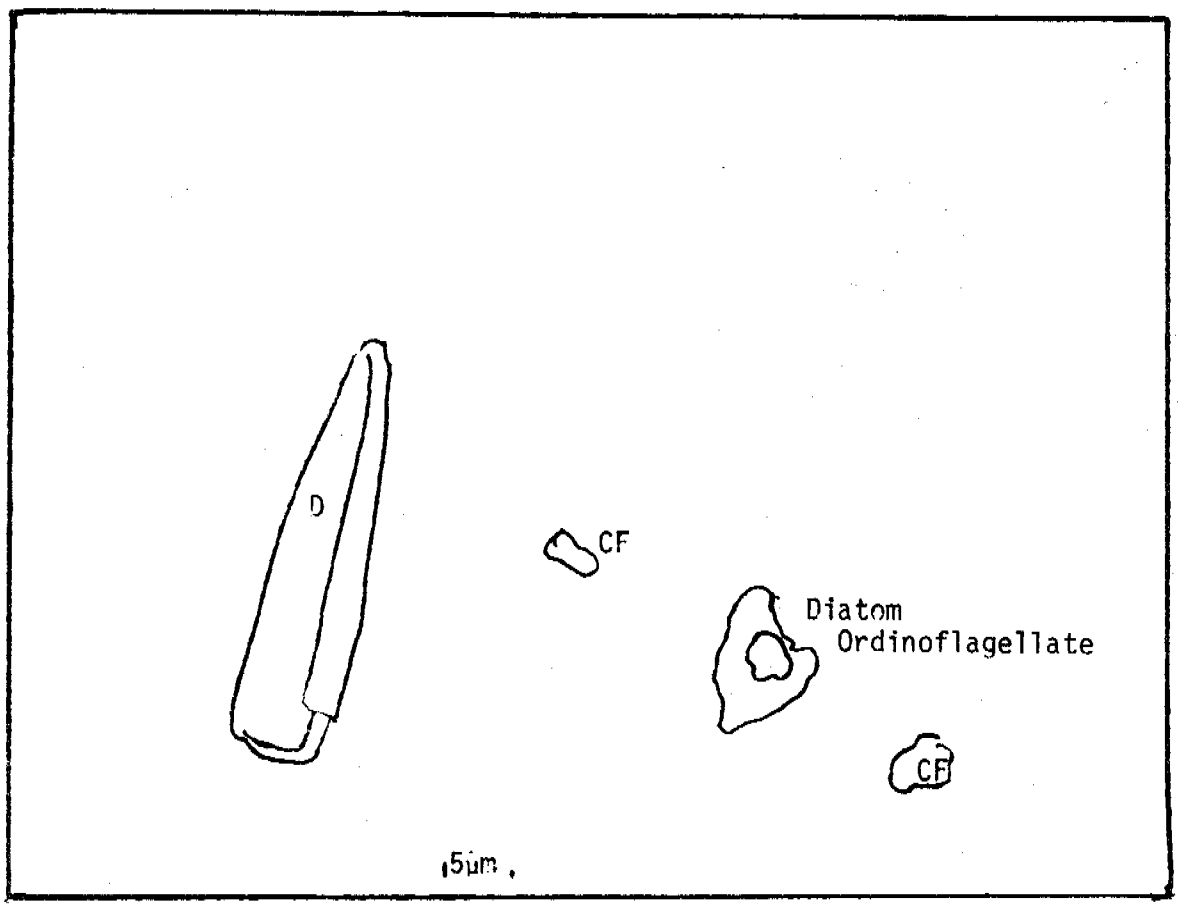

FIGURE 5-86. IDENTIFICATION OF MAJOR COMPONENTS IN SEM PHOTO-MICROGRAM OF KB-2-81A (China Poot Bay 0-1 cm).

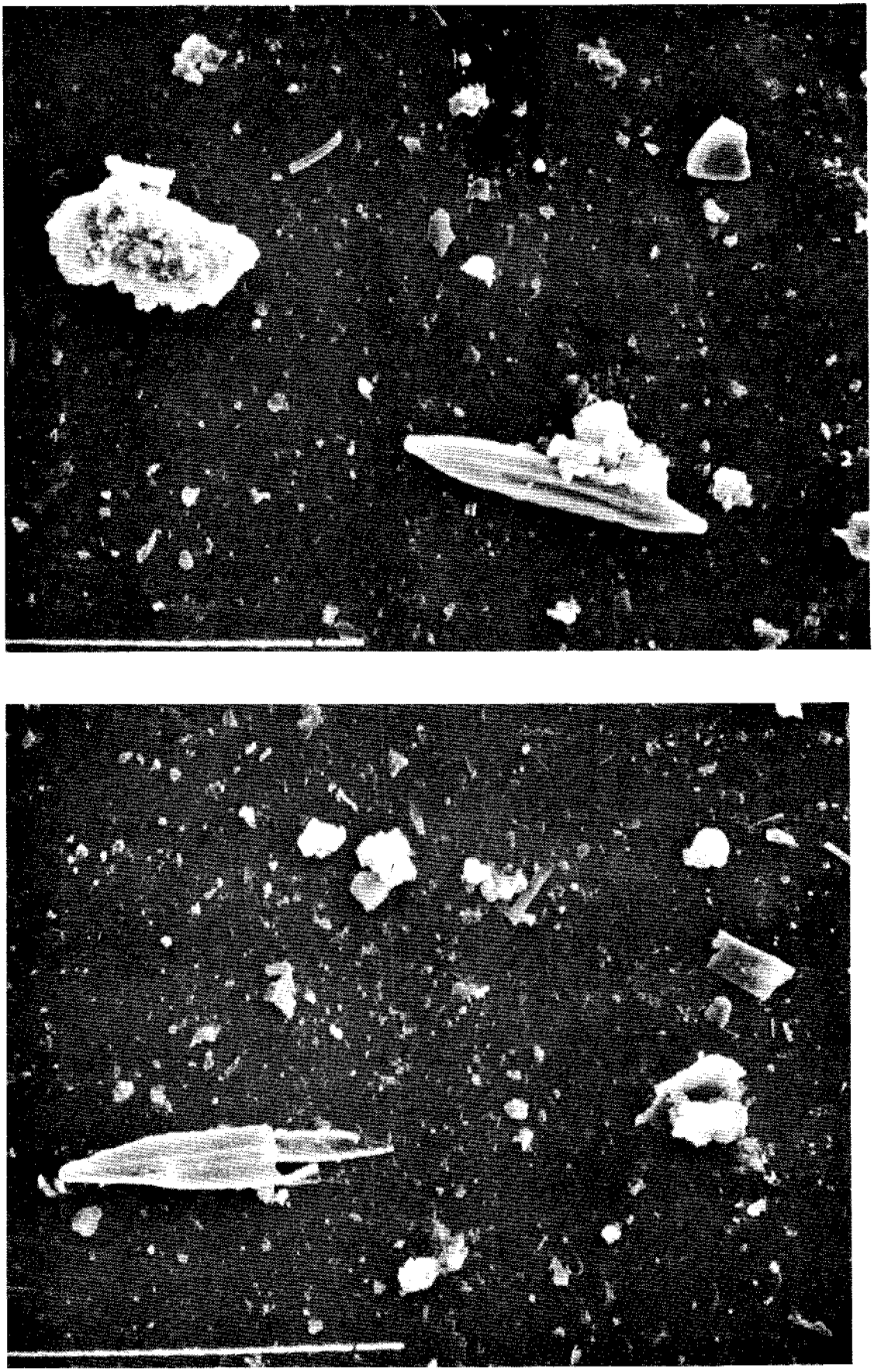

FIGURE 5-87. SCANNING ELECTRON MICROGRAPHS (1400X) OF KB-2-81B (China Poot Bay 1-8 cm).

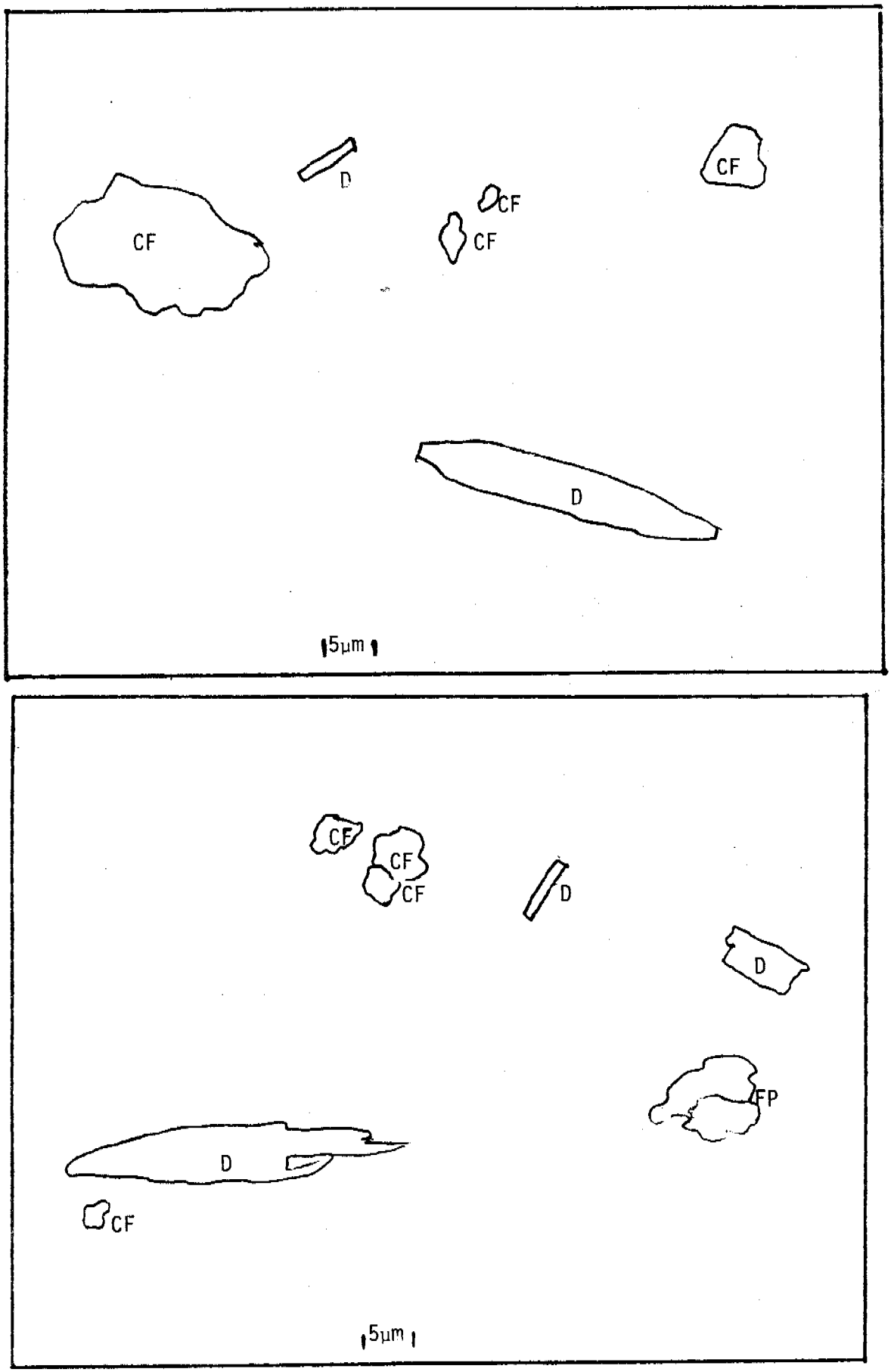

FIGURE 5-88 . IDENTIFICATION OF MAJOR COMPONENTS IN SEM PHOTO-MICROGRAM OF KB-2-81B (China Poot Bay 1-8 cm).

FIGURE 5-89. SCANNING ELECTRON MICROGRAPHS (1400X) OF KB-3-81 (Kasitsna Bay).

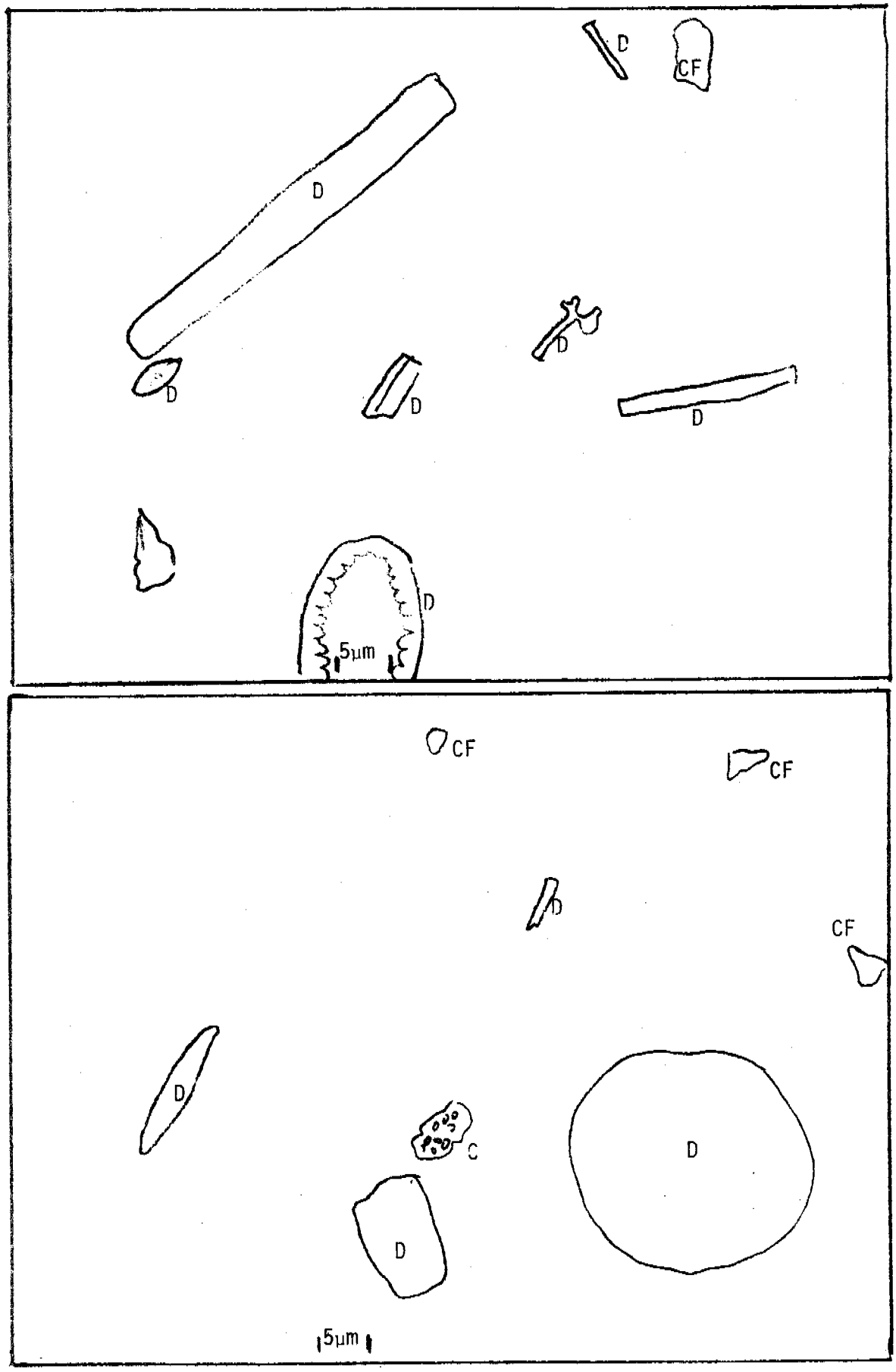

FIGURE 5-90. IDENTIFICATION OF MAJOR COMPONENTS IN SEM PHOTO-MICROGRAM OF KB-3-81 (Kasitsna Bay).

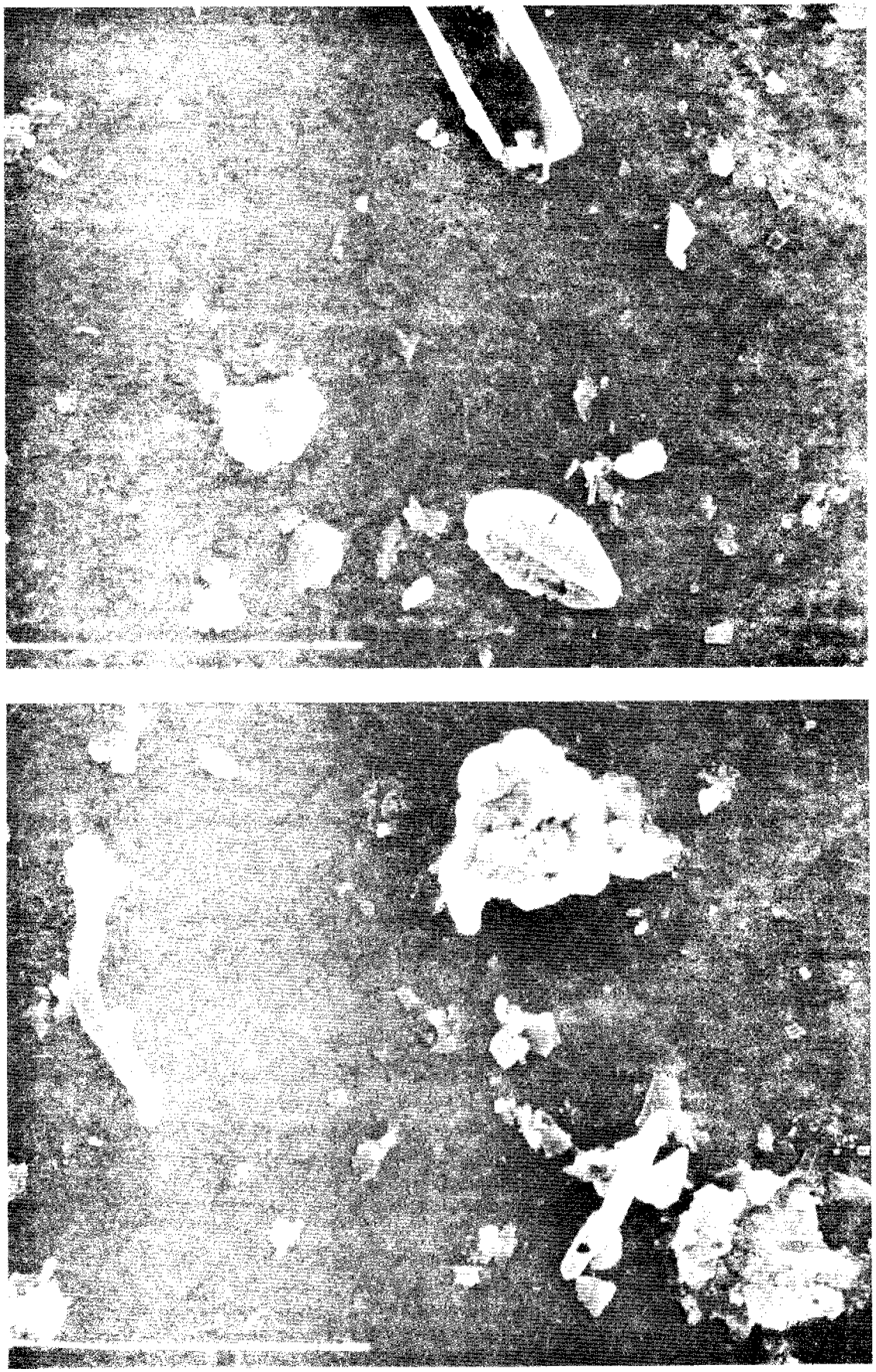

FIGURE 5-91. [illegible] ELECTRON MICROGRAPHS (1400X) OF KB-4-81 (Satilla River Estuary).

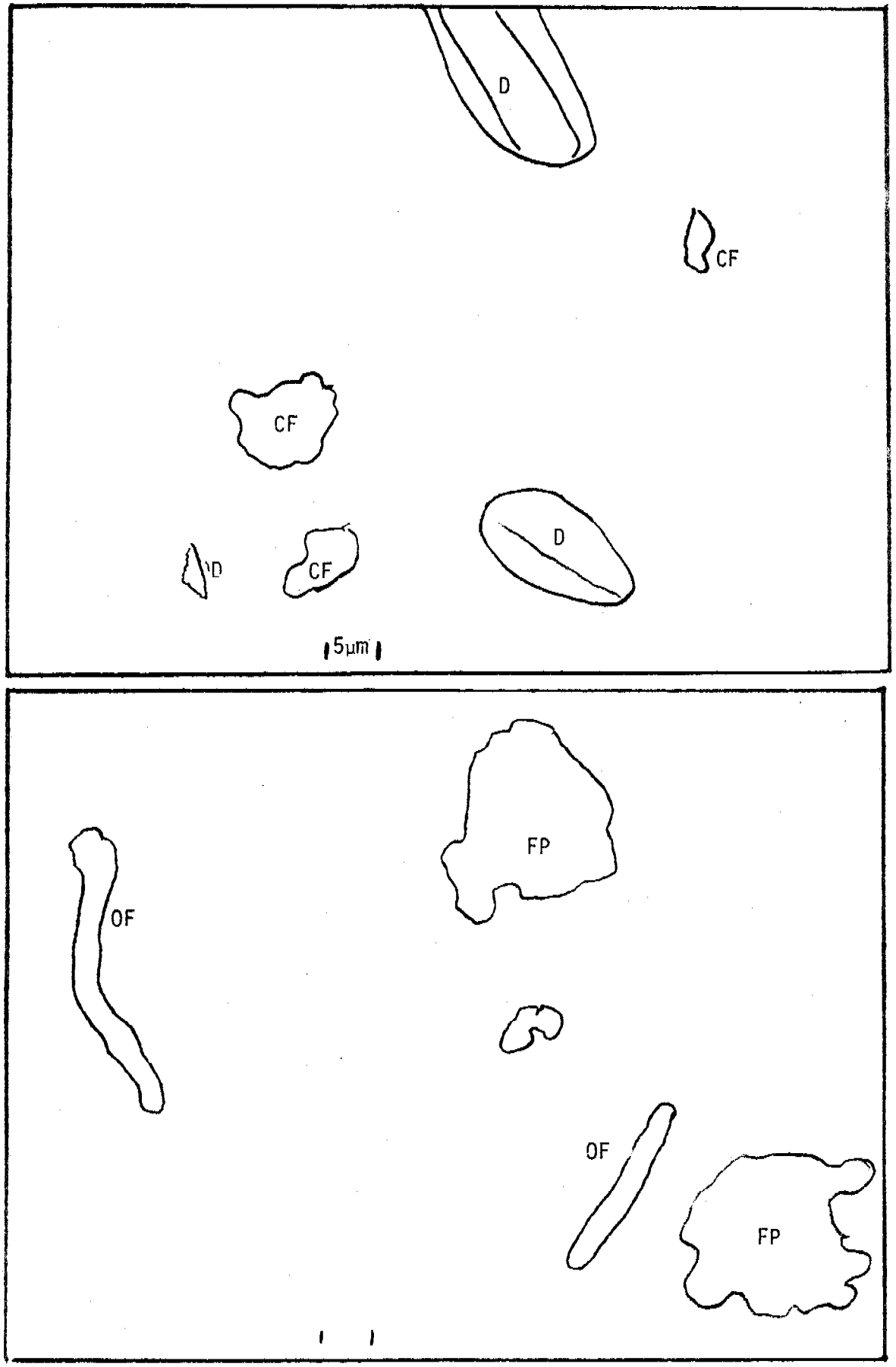

FIGURE 5-92. IDENTIFICATION OF MAJOR COMPONENTS IN SEM PHOTO-MICROGRAM OF KB-4-81 (Seldovia River Estuary).

to the sample from the Grewingk Glacier delta is observed. In the lower photograph for the 0 to 1-cm sample (Figure 5-85), a large diatom and a smaller fragment of what appears to be a diatom are present in addition to two larger clay flake fragments as shown in the schematics in Figure 5-86. The 1 to 8-cm depth sample from China Poot (Figure 5-87) shows a higher relative composition of clay <5 m fragments compared to the surface 0 to 1-cm sample, although the 1 to 8-cm sample is also characterized by several diatoms and clay fragments. In the second field from the 1 to 8-mm sample, another large diatom can be observed along with several fecal pellets and smaller diatom fragments mixed in with the less than 5- m clay fragments.

In Figure 5-89 for KB-3 (Kasitsna Bay) the photographs show exceedingly high levels of diatom fragments and several clay fragments. In comparison to other sites sampled, there are significantly more diatom fragments at KB-3, however, here too several clay fragments in the 5 micron range can be observed.

The SEM photographs from KB-4 (Seldovia River Estuary) show very few clay fragments (Figures 5-91 and 5-92), and in general the samples are characterized by several large organic fragments, fecal pellets and a few diatoms.

Additional discussions of how the SEM characterizations correlate with hydrocarbon adsorption potential follow the next section on oil/SPM interactions (5.3.4), however, from the initial examination it is apparent that from a minerological standpoint, all five SPM types are basically from the same source which is believed to be terrestrial rock flour generated by glacial action, melting snow and river runoff. This is best represented by the SEM characterications of the rock flour from the Grewingk Glacier (KB-1). The other sites selected then show various degrees of dilution of this rock flour material with other components. KB-3 (Kasitsna Bay) SPM was primarily diluted by silica tests from diatoms. KB-4 (Seldovia River Estuary) exhibited evidence of some of the same basic mineralogical material and was diluted by decaying organic plant material which was primarily derived from the Spartina

salt marsh. The two sediment samples from China Poot Bay (KB-2 and KB-2B) exhibited intermediate results in that the lower (1 to 8-cm subsection) showed extensive concentrations of terrestrial clay flakes with dilution by plant fragments and diatom skeletons. Interestingly, in this instance, the upper 0 to 1-cm sample contained fewer less than 5 μm sized clay flakes by weight and larger contributions from plant fragments and diatoms compared to the 1 to 8-cm samples.

5.3.4 Compound Specific Oil/SPM Partitioning Experiments

After the various sediment samples were characterized with regard to compositional makeup, a series of static equilibrium partitioning experiments were undertaken to evaluate their relative adsorption potential for individual components in Prudhoe Bay crude oil. From these results, two representative sediment samples showing the greatest and least affinity for crude oil adsorption were then to be selected for extended flow-through outdoor tank experiments in Kasitsna Bay during the Summer, 1981 program. Specifically, these Summer, 1981 experiments were designed to examine partitioning of oil components onto suspended particulate material as a function of the degree of subarctic evaporation and dissolution weathering.

For these initial oil/SPM characterization experiments, 20 grams of each sediment type were added to filtered seawater and the mixtures were agitated at 23° with magnetic stir bars. Care was taken in adjusting the stirring motors to insure that vortexing in the samples did not occur, and 3.5 ml of fresh Prudhoe Bay crude oil were added to each beaker. The beakers were covered (watch glass) and the mixtures were allowed to stir for 4 days and then allowed to settle over an additional 12-hr period. At that time the sedimentary material from the bottom of each beaker was carefully siphoned under vacuum taking care to ensure that none of the sediment came into direct contact with the oil during removal. Similarly, 300-ml aliquots of the water beneath the oil slicks were removed for determination of water column burdens. The respective sediment and water column samples from each experiment were

then extracted and analyzed for petroleum hydrocarbon contamination along with unexposed sediment samples to determine background level hydrocarbon components present at each site.

Table 5-34 presents the total resolved component and UCM concentrations for the aliphatic and aromatic fractions from the sediment and water column extracts. Specific aromatic compound concentration burdens are also listed for the two phases examined in each experiment. From the data in the Table 5-34, it is possible to rank the sediments according to their overall adsorption efficiency for total and specific petroleum hydrocarbon components, and in the order of decreasing adsorption potential they are: KB-4 (Seldovia River salt marsh detritus); KB-1 (Grewingk Glacial till); KB-2A (China Poot Bay surface sediment); KB-2B (China Poot Bay 1 to 8-cm sediment) and KB-3 (Kasitsna Bay composite sediments). These rankings were generated by examining the cumulative sum of the n-alkanes and total resolved and UCM component concentrations in the aliphatic fractions and the total resolved and UCM component concentrations observed in the aromatic fractions for each sediment type. Numerical rankings in the order of 1 through 5 were given to each sediment for each parameter described above, and these rankings were then summed to arrive at an overall total to reflect each sediment type's affinity for oil. Specific compound concentrations were also considered in this ranking, as were the relative water column concentrations above each sediment. That is, an inverse relationship was observed between particulate adsorption potential and the levels of hydrocarbons observed in the water above each sediment type, and this relationship was also used in the overall rankings.

Figures 5-93 and 5-94 present the capillary gas chromatograms obtained on the sediment and water samples from the most adsorptive (Bay-4, Seldovia River salt marsh) and least adsorptive (Bay-3, Kasitsna Bay composite sediment) samples, respectively. Each figure is arranged as follows: Chromatogram "A" represents the aliphatic hydrocarbons in the oil-exposed sediments; Chromatogram "B" represents the background level of aliphatic hydrocarbons measured in the unexposed sample; Chromatogram "C" represents the aliphatic hydrocarbons in the water column extract; Chromatogram "D" represents

TABLE 5-34. RESULTS OF EQUILIBRIUM PARTITIONING OIL/SPM INTERACTION STUDIES (STATIC SYSTEM, 19°C).

	ALIPHATIC FRACTION**				AROMATIC FRACTION***											
							Benzenes	Naphthalenes						Phenanthrenes	
Sample*	Total Res	Total UCM	Σn-alk	Σn-alk Branched	Total Res	Total UCM	1,4&1,3-dimethyl (884)	ethyl (874)	naphthalene (1196)	2-methyl (1305)	1-methyl (1322)	2-ethyl (1404)	2,3-dimethyl (1430)	1,6,7-trimethyl (1542)	phenanthrene (1788)	2-methyl (1904)
K. Bay-1 Sediment	340,000	73,000	26,000	0.08	46,000	42,000	15	62	40	630	400	103	440	290	570	390
Aqueous Phase	4,760	0	33	0.007	601	75	2.9	0.56	1.3	7.4	7.4	9.8	3.1	1.0	0.23	-
K. Bay-2A Sediment	795,000	18,000	16,000	0.02	385,000	7,100	46	270	90	550	310	96	240	143	200	83
Aqueous Phase	3,380	0	11	0.003	1,907	0	3.4	1.4	3.3	7.2	6.8	0.7	2.2	1.0	-	-
K. Bay-2B Sediment	647,000	51,000	14,000	0.02	9,600	22,000										
Aqueous Phase	170	0	17	0.1	2,720	0										
K. Bay-3 Sediment	85,000	10,000	5,000	0.06	12,000	10,000	33	130	4	91	83	25	89	35	44	-
Aqueous Phase	5,840	0	8	0.001	512	0	2.0	0.74	-	0.63	4.4	0.28	2.3	0.28	0.53	-
K. Bay-4 Sediment	253,000	262,000	60,000	0.3	44,000	75,000	12	200	29	48	370	125	337	210	71	-
Aqueous Phase	Not reduced very low		-	-	2,180	0	2.9	0.46	0.16	0.49	1.3	0.12	2.2	0.34	-	-

*K. Bay-1--Grewingh Glacier Till - fine grained terrestrial plus diatoms, many flakes 5 μm and less - Specific Surface Area 9.1
K. Bay-2A-China Poot Bay surface 1 cm - mostly > 5 μm terr plus some plant " 8.2
K. Bay-2B-China Poot Bay depth 1-8 cm - most material < 5 μm " 15.2
K. Bay-3--Kasitsna Bay consolidated sediment - 90% diatoms > 5 μm, some terr. ≤ 5 μm " 9.1
K. Bay-4--Seldovia River salt marsh - organic plus fecal pellets " 11.1

**Sediment concentration in μg/kg, water concentration in μg/l

***Sediment concentration in ug/kg, water concentration in μg/l; numbers in parentheses are compound Kovat indices.

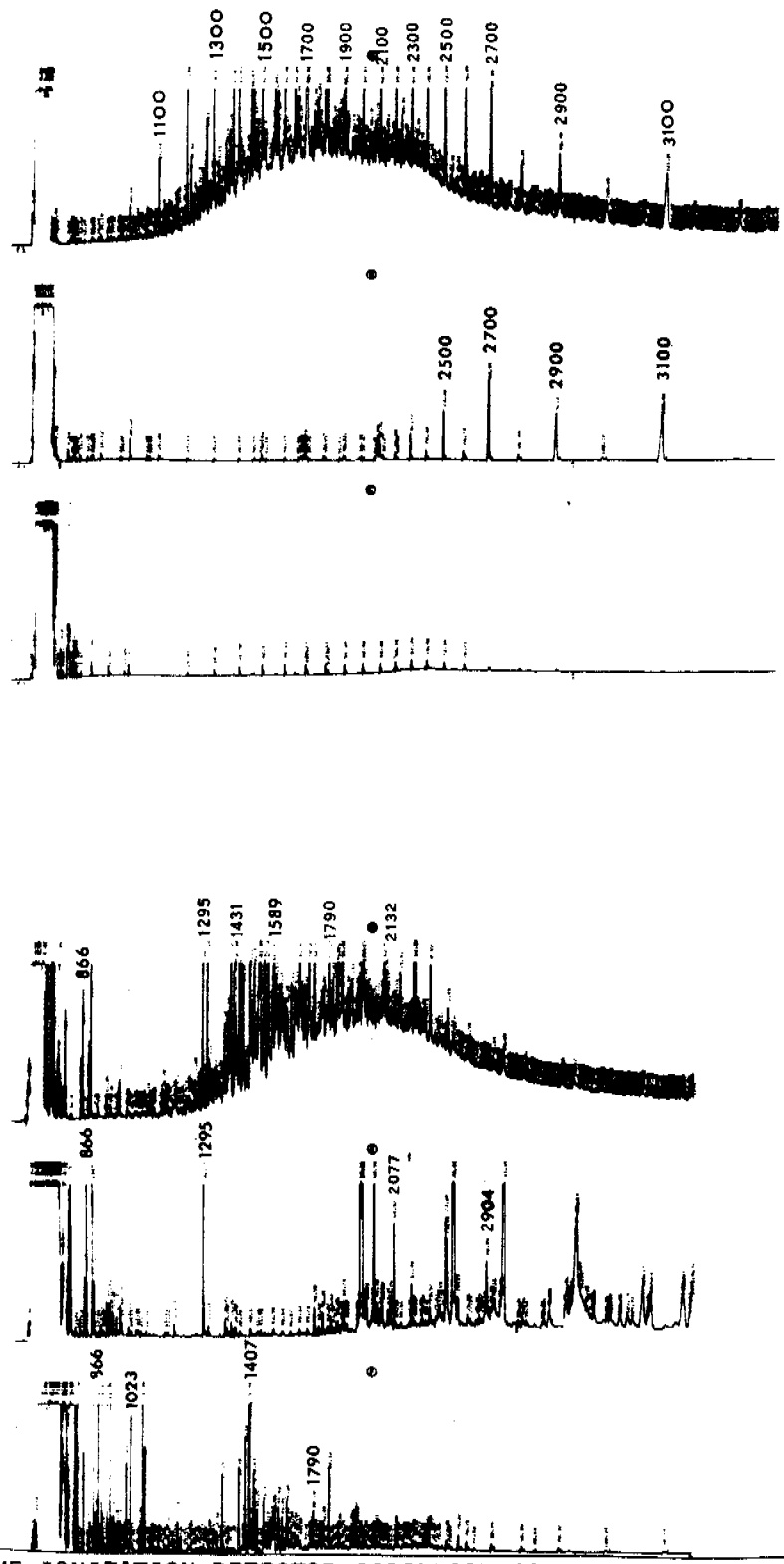

FIGURE 5-93. FLAME IONIZATION DETECTOR CAPILLARY GAS CHROMATOGRAMS FROM KB-4 (SELDOVIA RIVER SALT MARSH) OIL/SPM INTERACTION STUDIES: (A) ALIPHATIC HYDROCARBONS IN THE OIL EXPOSED SEDIMENTS; (B) BACKGROUND LEVEL ALIPHATIC HYDROCARBONS MEASURED IN UN-EXPOSED SEDIMENT; (C) ALIPHATIC HYDROCARBONS IN THE WATER COLUMN EXTRACT; (D) AROMATIC HYDROCARBONS IN THE OIL EXPOSED SEDIMENTS; (E) BACKGROUND LEVEL AROMATIC HYDROCARBON COMPONENTS MEASURED IN THE UNEXPOSED SAMPLE; AND (G) AROMATIC HYDROCARBONS IN THE WATER COLUMN EXTRACT.

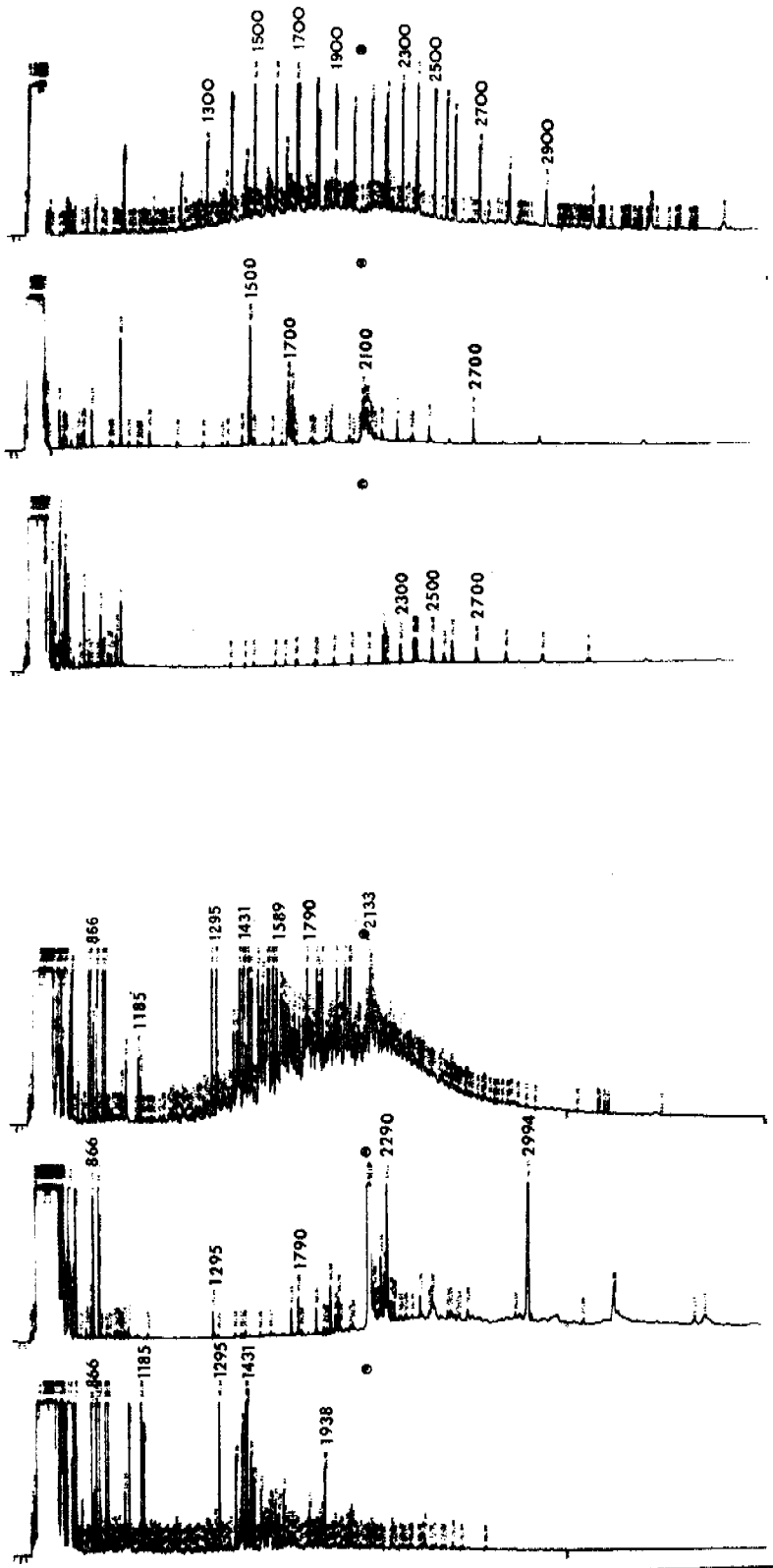

FIGURE 5-94. FLAME IONIZATION DETECTOR CAPILLARY GAS CHROMATOGRAMS FROM KB-3 (KASITSNA BAY COMPOSITE SEDIMENT) OIL/SPM INTERACTION STUDIES: (A) ALIPHATIC HYDROCARBONS IN THE OIL EXPOSED SEDIMENTS; (B) BACKGROUND LEVEL ALIPHATIC HYDROCARBONS MEASURED IN UN-EXPOSED SEDIMENT; (C) ALIPHATIC HYDROCARBONS IN THE WATER COLUMN EXTRACT; (D) AROMATIC HYDROCARBONS IN THE OIL EXPOSED SEDIMENTS; (E) BACKGROUND LEVEL AROMATIC HYDROCARBON COMPONENTS MEASURED IN THE UNEXPOSED SAMPLE; AND (G) AROMATIC HYDROCARBONS IN THE WATER COLUMN EXTRACT.

the aromatic hydrocarbons in the oil-exposed sediments; Chromatogram "E" represents the background level aromatic hydrocarbon components measured in the unexposed sample; and Chromatogram "G" represents aromatic hydrocarbons in the water column extract. Clearly, the most significant differences appear in considering the aliphatic fractions for the oil-exposed sediments, (Chromatograms A in Figures 5-93 and 5-94). The Seldovia River salt marsh sample shows a significant unresolved complex mixture and a suite of normal and branched hydrocarbons extending from nC-10 through nC-31. While this same suite of compounds is observed in the Kasitsna Bay sediments, the unresolved complex mixture is significantly smaller as is reflected in the reduced UCM data in Table 5-34. The aliphatic fraction chromatograms on the unexposed sediments showed some differences, with higher molecular weight odd numbered n-alkanes clearly predominating in the Seldovia River salt marsh sample. Specifically, nC-23, nC-25, nC-27 and nC-29 from plant wax components are clearly the most predominant feature in Figure 5-93B. Slightly higher aliphatic water column concentrations are observed in the samples from KB-3 compared to KB-4, and this reflects the inverse relationship noted above for SPM adsorption potential and water column hydrocarbon burdens.

The aromatic fractions of the contaminated sediments appear to be very similar, however, here again the unresolved complex mixture in the Seldovia River salt marsh sample is significantly larger, and higher levels of individual aromatic components with Kovat indices extending from 1400 to 1788 are noted with the organic-rich Seldovia River salt marsh SPM. The data in Table 5-34 also illustrate that a factor of 7 increase in total aromatic unresolved component concentrations is noted in comparing the Seldovia River and Kasitsna Bay sediment samples. The aromatic fractions of the uncontaminated sediments (Chromatograms E in Figures 5-93 and 5-94) show several significant differences, and in particular more higher molecular weight components can be observed in the sediment sample from the salt marsh. The large peaks near Kovat index 1900 to 2200 in the middle of both chromatograms are believed to be due to polyunsaturated components of biogenic origin; however, additional identifications of components in the aromatic fractions of the unexposed samples will not be available until additional GCMS analyses are undertaken.

Interestingly, the aromatic fraction of the water column components appear very similar for both samples. This largely reflects the higher compound-specific seawater solubilities for the lower molecular weight alkyl-substituted benzenes in the Kovat indices range of 700 to 874 and the limited solubilities of the alkyl-substituted naphthalenes in the Kovat index range of 1305 through 1542. It should be noted, in general, that the lower molecular weight aromatics do not specifically adsorbe onto the particulate material, but that they instead reside in the water column beneath the slick. Several lower molecular weight aromatics are suggested by the chromatogram in Figure 5-94D of the aromatic fraction of the sediment sample from KB-3; however, their presence may simply reflect inclusion of slightly greater volumes of water collected during siphoning off the sediment sample.

In terms of the overall oil affinity of the five selected SPM samples, several interesting correlations can be made between the composition data of the SPM as determined by scanning electron microscopy and the results from the glass capillary/gas chromatographic analyses. Specifically, the Seldovia Bay estuary SPM had the highest overall affinity for oil, and the SEM photos illustrate that this material was primarily composed of diatoms and larger (greater than 30 μm) organic fragments and fecal pellets. It also contains a few clay fragments which, as will be shown below, also have a very high affinity for oil.

The fine glacial rock flower or till from the Grewingk Glacial delta exhibited the next highest affinity for hydrocarbons, and in many instances, showed an equal or greater affinity for specific aromatic compounds compared to the organic rich detrital sediments from the Seldovia Bay estuary. The SEM photographs of this material show that the sample is primarily very small clay fragments plus a relatively limited number of diatoms, which no doubt came from the marine input and flushing of the intertidal zone. The high affinity for oil in this instance, is believed to be due to the high surface area (on a surface area per weight basis) due to the profusion of fine clay fragments.

Because of this material's high affinity for oil and the fact that the near-shore waters in many areas in Alaska receive significant contributions of SPM from glacial till, this sample was considered to be ideal for extended long-term studies. Ironically, only small amounts of this relatively pure material could be obtained from intertidal sources near Kasitsna Bay, and where it was found, only limited amounts could be obtained by scrapping very thin belts or deposits from standing pools at the glacier delta. Because of the active geological nature of this site, however, a continued source of this material could not be depended upon. Further, the site was only accessible by whaler and as such, logistical and weather constraints were considered to be major obstacles which would prevent obtaining the necessary kilogram quantities of this material for inclusion in the flow-through oil/SPM interaction studies.

The SPM sample with the next highest affinity for oil was the surface 0 to 1-cm mat from China Poot Bay (K Bay-2A). The SEM photographs of this sample showed it to be primarily made up of clay and plant fragments with an occasional diatom skeleton. The 1 to 8-cm depth sample from this site also showed high affinities for aliphatic and aromatic components; and the SEM photographs in this case showed a higher concentration of the less than 5 μm sized clay fragments with additional input and/or dilution from diatoms. The SPM sample from K Bay-3 (Kasitsna Bay) which showed the lowest affinity for adsorption, consisted almost exclusively of diatom fragments (by weight) with a few clay fragments in the less than 5 micrometer size range appearing in the background of the SEM photos.

The results of these initial oil/SPM interaction studies are in good agreement with the work of several other authors who have investigated oil/sediment interactions. Several of these similarities and one striking difference (dealing with a previous study on Glacial till) are considered in the following discussion.

With regard to similarities, GERRING et al. (1979) also reported the fractionation or partitioning of lower molecular weight aromatic compounds

(including up to 3-ring aromatics) into the dissolved phase before adsorption of the oil onto suspended particulate material and subsequent sinking. In test tank studies completed at the Marine Ecosystem Research Laboratory at the University of Rhode Island, they found that the aromatic/aliphatic ratio in the sediment was much lower than that in the parent oil suggesting that preferential dissolution of lower molecular weight compounds may be occurring. Specifically, 2-34% of the higher molecular weight aliphatic, acyclic and greater than 3-ring hydrocarbons were absorbed onto the suspended particulates and sediments in contrast to 0.1% of the more water soluble naphthalene and methylnaphthalene components which were the predominant aromatic materials in the No. 2 fuel oils used in their studies.

WINTER (1978) also observed similar partitioning in studying two simulated oil spills and one mixture of aromatic compounds added to a test tank. The petroleum derived alkanes were approximately 10 times greater in the particulate fraction, and the lower molecular weight aromatics were at least 5 times more concentrated in the dissolved phase.

In samples of suspended particulate material collected along transects perpendicular to the South Texas OCS near Corpus Christi, PARKER and MACKO (1978) noted that the concentrations of higher molecular weight (nC-28 through nC-30) compounds remained relatively constant with distance from the shore while the total particulate hydrocarbon burdens decreased with increasing distance. These authors attributed this to the introduction and sorption of the hydrocarbons near the shore with subsequent movement of particulate bound oil with preferential retention of the higher molecular weight compounds during weathering. Several higher molecular weight polynuclear aromatic hydrocarbons were also identified on the particulate material, and these included alkyl-substituted naphthalenes, phenanthrenes, dibenzothiophenes, fluoranthrene and pyrene. Concentrations of these materials were too low for quantitation; however, they could be detected by selected ion monitoring GC/MS. Similar partitioning of lower and higher molecular weight compounds have been

observed by DELAPPE et al. (1978) in a study designed to measure the partitioning of petroleum hydrocarbons among seawater particulates and the filter feeting Mytilus californianus.

PAYNE et al. (1980) and BOEHM and FIEST (1980) also observed a similar partitioning between lower and higher molecular weight compounds in the dissolved phase and suspended particulate material samples removed by filtration of large volume water samples obtained in the vicinity of the IXTOC-I blowout in the Gulf of Mexico.

In a laboratory study, MEYERS and QUINN (1973) found that the hydrocarbon adsorption efficiency (for the less than 44 μm particle sized fractions) decreased in the order of bentonite > kaolinite > illite > monmorillinite. Interestingly, when Meyers and Quinn treated sediment samples from Narragansette Bay with 30% peroxide to remove indigenous organic material, an increase in absorption potential was noted. These authors concluded that the organic material (which was presumably humic substances) presumably masked the sorption sites on the sediment thereby reducing the available surface area for adsorption of the organic compounds. SEUSS (1968), on the other hand, has suggested that a 3 to 4% organic material coating on clay will enhance sorption processes by providing, in effect, a lipophillic layer to enhance non-polar hydrophobic binding. These results would be more in line with the results of our most recent studies in comparing the adsorption potential of the organic rich materials from the Seldovia River estuary (KB-4) to the composite diatom rich sediment samples from Kasitsna Bay (KB-3).

In a laboratory study ZURCHER et al. (1978) considered the dissolution, suspension, aglomeration and adsorption of fuel oil onto pure kaolinite. In their studies, as in ours, the dissolved water column samples showed significant levels of lower molecular aromatics in the benzene to methylnaphthalene range, and the adsorbed fraction contained n-alkanes and aromatics from Kovat indices 1400 through 3200. The clay minerals in this experiment were shown to adsorb about 200 mg of hydrocarbons per kilogram of dry material.

MEYERS and QUINN (1973) reported a similar value of 162 mg/kilogram for dry kaolinite. Our data, in Table 5-34, suggest values in line with these earlier determinations with a low of 122 mg/kilogram (total resolved and UCM from both the aliphatic and aromatic fractions) from the SPM samples from Kasitsna Bay (KB-3) to a high of 1.2 g/kilogram for the 0 to 1-cm subsample from the tidal mud flats from China Poot Bay (KB-2A).

While the results of these most recent oil/SPM interaction studies using representative samples from the lower Cook Inlet parallel the findings reported by previous investigators, they are somewhat contradictory to recent results reported by MALINKY and SHAW (1979). These authors examined the association of two lower molecular weight petroleum components and suspended sediments (primarily gracially derived sediments from the south central Alaska region) and concluded that sedimentation of oil by the adsorption to suspended mineral particles may not be a major pathway for the dispersion of petroleum in the marine environment. In that study, however, they used ^{14}C-labelled decane and biphenyl at near saturation levels. In these experiments, the concentrations of the two hydrocarbons associated with the sediments was approximately 30% of the original aqueous concentration in parts per million. From loadings of permitted discharges in Port Valdez and measured sediments loads, the authors calculated that less than 3% of the oil released into the harbor could be associated with the sediment. Thus, the authors concluded that adsorption of hydrocarbons to suspended particulate material was not that significant, and that the role of suspended mineral particulate material may be far less significant in adsorption of polynuclear aromatic hydrocarbons in natural waters than is the role of total suspended matter. The applicability of their findings to real oil spills situations in natural environments may be limited, however, in light of the fact that they did not use a natural oil or even a water accommodated fraction of a natural oil, and by the fact that the compounds which were utilized have significantly higher water solubilities that the more toxic polynuclear aromatic hydrocarbons of interest. Clearly, the results of our studies on the glacially derived till from the Grewingk

Glacier show that it does have a high affinity for polynuclear aromatic hydrocarbons (see Table 5-34) and that the high surface area of the glacial till can provide an active site for oil adsorption and ultimate sedimentation.

5.3.5 Extension of Oil/SPM Interaction Studies During the Summer 1981 Program at Kasitsna Bay

After the initial characterization of the component specific affinity of the five representative SPM types, extended oil/SPM interaction studies were undertaken at Kasitsna Bay, Alaska during the Summer 1981 program. Unlike the previously completed experiment where oil was allowed to interact with suspended particulate material in a closed system, the more recent Alaska experiments were designed to look at the time-dependent partitioning of selected hydrocarbons onto SPM as other evaporative and dissolution processes were simultaneously occurring. That is, an overall SPM load was established in the flow-through seawater system in two of the outdoor tanks, and oil was then added to the tanks with turbulence induced by propeller mixing. The sediments chosen for these experiments were from KB-4, (Seldovia River Estuary) and KB-3 (Kasitsna Bay). As described previously these had the greatest and least affinity for specific components in the static equilibration experiments completed before the onset of the Summer 1981 Alaska field program.

For the Kasitsna Bay field experiments, a separate input water reservoir was constructed for tanks 5 and 6 in the outdoor flow-through system (Figure 5-95). Aliquots of sediment were then added directly to the water in each side of the biforcated reservoir (which was fed natural seawater) and a continuous supply of SPM burdened water was then fed into the outdoor tanks. One stirring motor was mounted on each side of the sediment/seawater reservoir to keep the finer grained sediment in suspension, and a peristaltic pump was used to feed the sediment laden water at a flow rate of 100 ml/minute to tanks 5 and 6, respectively. The sediment master reservoir contained 77 liters on each side, and weighed amounts of additional sediment was added periodically (every 3 to 10 hours) to maintain an overall sediment load in the master reservoir of 8.7 grams/l. When delivered to the 187 L experimental tanks at a

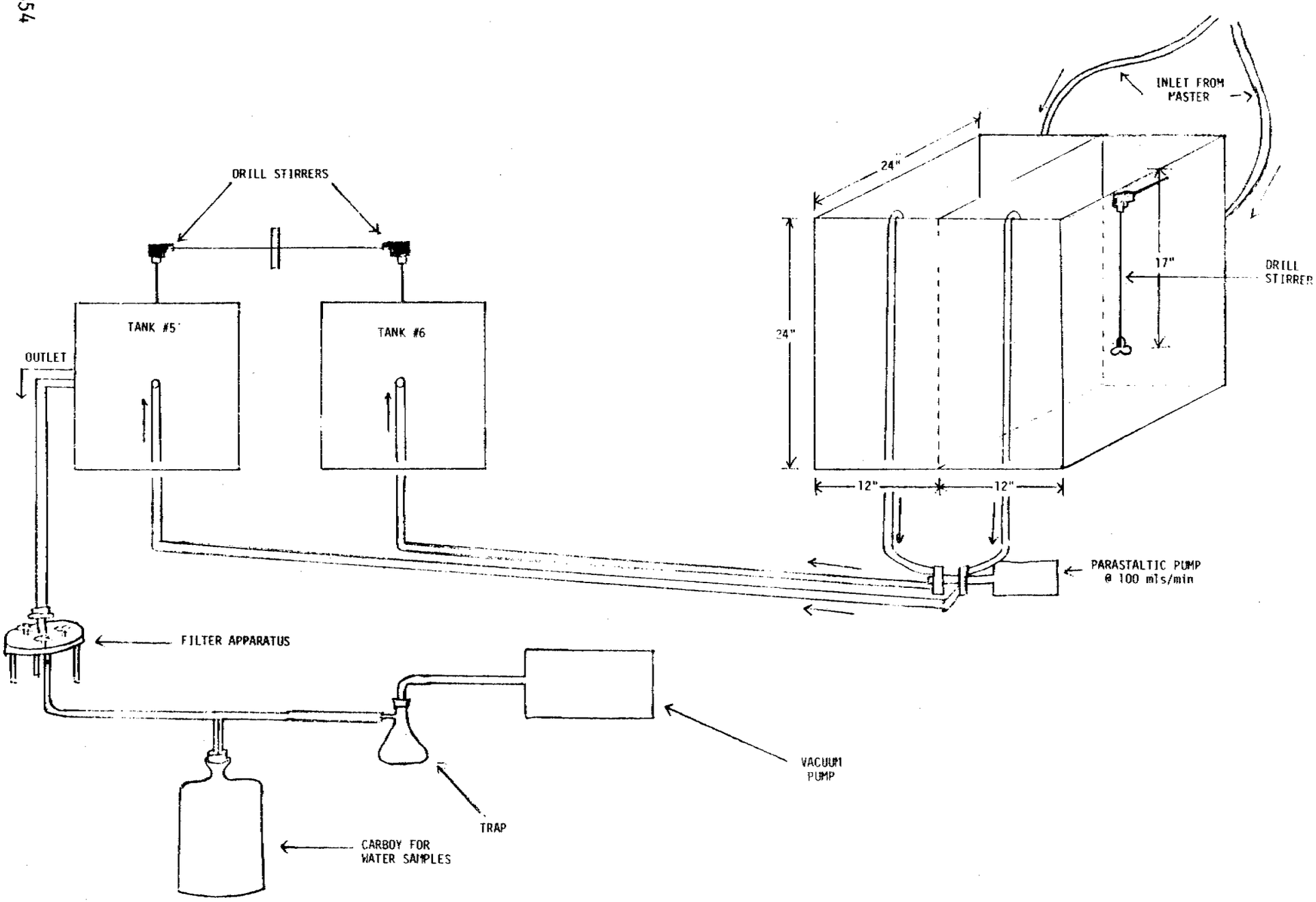

FIGURE 5-95. FLOW DIAGRAM FOR SPM STUDIES IN ALASKA.

flow rate of 100 ml/min, ultimate SPM loads of 40 mg/L for Kasitsna Bay and 20 mg/L for the Seldovia sediments were maintained in the experimental chambers. Tank 6 received sediments from Kasitsna Bay, and tank 5 received sediments from the Seldovia River salt marsh. Oil was then spilled as before onto the experimental tanks, and agitation was maintained within the experimental tanks with two additional stirring motors.

During the experiment, water samples from the exhaust ports of the respective tanks were filtered through a 293-mm diameter, 0.45-micron kiln-fired glass fiber filter to remove the suspended particulate material, and the filtered water column samples were contained in a glass carboy for methylene chloride extraction and analysis of the dissolved phase (Figure 5-96).

Prior to each large volume (20 L) sample for chemical analysis, a smaller 50-ml aliquot was filtered through tared 2.5 cm, 0.45 micron millipore filter for determinations of SPM loading. After each chemistry sample was obtained, the 293 mm diameter glass fiber filter was removed and folded into kiln-fired aluminum foil (Figure 5-97) and frozen awaiting shipment to La Jolla for later extraction and analyses. Water column samples, were extracted with methylene chloride (3 x 250 ml) at the Kasitsna Bay facility (PAYNE et al., 1980) and the methylene chloride extracts were then reduced in volume using Kurderna-Danish concentrators and dried (water removal) by passage through Na_2SO_4 columns. The concentrates were then sealed in scintillation vials with foil-lined caps and shipped to La Jolla for analysis.

Tables 5-35 and 5-36 present the time series sampling points, sample matrix and sediment loading as measured gravimetrically from tanks 5 and 6 during the running of the oil/SPM interaction studies. The methylene chloride extracts from each of the time-series steps shown in the table and the frozen filters are currently in storage at 3°C and -20°C, respectively, awaiting further extraction and analyses.

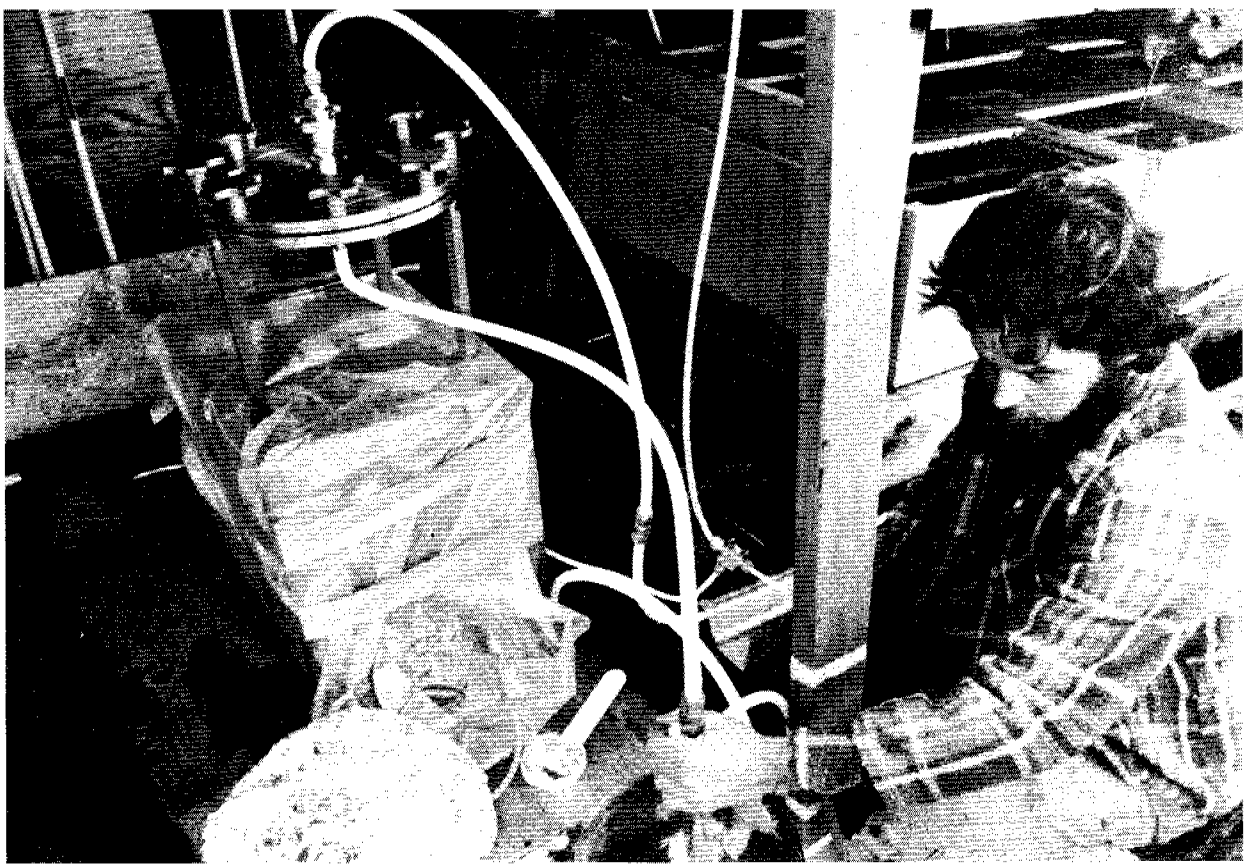

FIGURE 5-96. OUTDOOR TANKS AND FILTRATION SYSTEM USED FOR CONTINUOUS FLOW OIL/SPM INTERACTION STUDIES AT KASITSNA BAY, ALASKA. SUSPENDED PARTICULATE MATERIAL IS TRAPPED ON 293 mm DIAMETER KILN FIRED GLASS FIBER FILTERS MAINTAINED IN THE STAINLESS STEEL FILTER ASSEMBLY AND DISSOLVED HYDROCARBON COMPONENTS ARE EXTRACTED FROM THE WATER SAMPLES TRAPPED IN THE GLASS CARBOYS.

FIGURE 5-97. AFTER FILTRATION, FILTER SAMPLES WERE FOLDED INTO KILN-FIRED ALUMINUM FOIL AND FROZEN. WATER COLUMN SAMPLES WERE EXTRACTED WITH METHYLENECHLORIDE, DRIED OVER Na_2SO_4 CONCENTRATED (KD APPARATUS) AND SEALED IN FOIL CAPPED SCINTILLATION VIALS AND STORED AT 3°C. AT THE CONCLUSION OF THE SUMMER/FALL 1981 PROGRAM ALL SAMPLES WERE SHIPPED TO LA JOLLA FOR ADDITIONAL FRACTIONATION AND ANALYSES.

TABLE 5-35. SAMPLING TIMES AND SEDIMENT LOAD FOR FLOW-THROUGH OUTDOOR TANK SPM STUDIES USING SELDOVIA SALT MARSH SEDIMENT -- TANK 5 PARTICULATE MATERIAL, FILTERED SEAWATER AND OIL SAMPLES COLLECTED AT EACH TIME INDICATED.

Date	Time	Cumulative Time	Sediment Load (mg/ℓ)
9/20	1230	0 hrs	19
9/20	1530	3 hrs	--
9/20	1830	6 hrs	15
9/21	0030	12 hrs	18
9/21	1230	24 hrs	20
9/22	1230	2 days	23
9/24	1230	4 days	19
9/28	1230	8 days	36

TABLE 5-36. SAMPLING TIMES AND SEDIMENT LOAD FOR FLOW-THROUGH OUTDOOR TANK SPM STUDIES USING KASITSNA BAY SEDIMENT -- TANK 6 PARTICULATE MATERIAL, FILTERED SEAWATER AND OIL SAMPLES COLLECED AT EACH TIME INDICATED.

Date	Time	Cumulative Time	Sediment Load (mg/ℓ)
9/20	1200	0 hrs	36
9/20	1500	3 hrs	40
9/20	1800	6 hrs	39
9/21	0000	12 hrs	37
9/21	1200	24 hrs	39
9/22	1200	2 days	39
9/24	1200	4 days	32
9/28	1200	8 days	30

From these experiments we hope to derive time-series oil/SPM partition coefficients for specific compounds as a function of the overall degree of oil weathering. While the results of the initial oil/SPM interaction studies may appear to duplicate some aspects of previously published work, it should be pointed out that the purpose of completing the static experiments in La Jolla was not to repeat the earlier studies, but to determine which two of the five representative Lower Cook Inlet sediment types should be utilized for the extended oil/particulate material interaction studies where evaporation and dissolution weathering perturbations to the process were included as part of the experimental design. Furthermore, several features of our approach are unique, and these factors are important to our understanding of longer term sub-arctic oil/SPM interactions. First, no other study has examined a cross section of suspended particulate material types from the Lower Cook Inlet area and looked at the compound specific partitioning to the material as a function of its source. Secondly, the time series oil weathering experiments conducted during the Summer 1981 program were designed to evaluate the affects of changes in oil viscosity on oil/particulate material interactions. Specifically, oils which have undergone evaporation and dissolution weathering do not tend to form micells and dispersions of oil-in-water to the same degree that fresh oils do. This was observed in our wave tank experiment where 1 to 10 mm diameter droplets were clearly present for the first 12 hours of weathering but not thereafter and in the flow-through outdoor tanks where turbulence was introduced by propeller mixing. In both cases, oil/micell formation and dispersions were shown to fall off rapidly after the first 12 to 24 hours. As a result of this behavior, availability of oil micells in the water column will change with time, and this will significantly affect the degree to which oil is available for particulate interactions and the rates of these processes.

Our experiments were designed to evaluate these factors such that a better understanding of their influence on oil-SPM interactions could be focused toward developing more accurate predictive capabilities on the effects of suspended particulate material on actively weathering oil.

5.3.6 Long Term Fate of Stranded Oil in Selected Intertidal Regimes in the Lower Cook Inlet Kachemak Bay/Shelikof Strait Area

As another but related aspect of the oil weathering program, SAI scientists participated in a collaborative effort with Drs. Griffiths and Morita (RU 190) to evaluate long-term weathering trends in sub-tidal sediments which had been contaminated with fresh and artificially weathered Cook Inlet crude oil. In that the results of those analyses detailed the long-term (up to 1 year) chemical weathering of sedimented oil, and are therefore relevant to the overall goals of this program, a copy of our report on the chemical analyses of the subtidal sediments has been included as Appendix C of this report.

In the Griffiths and Morita program, fresh and artificially weathered* Cook Inlet crude oil samples were spiked into subtidal sediment quadrants, and these quadrants were then placed back into the subtidal regime in Kasitsna Bay and Sadie Cove. Three levels of spiking were utilized: 50 parts per thousand (ppt), 1 ppt and 0.1 ppt (using both fresh and artificially weathered crude), and samples from these experiments were chemically analyzed at time 0 and after 1 year of natural weathering in the subtidal regime.

After one year, essentially no measurable hydrocarbon biodegradation took place in the sediments which had been spiked at the 50 ppt level with either fresh or previously weathered Cook Inlet crude oil. Additionally, GRIFFITHS and MORITA (1980) reported that from time-coarse experiments using sediments treated at the 50 part per thousand level with fresh crude oil, that affects of the crude oil on glucose uptake would continue for 3 to 5 years and the effects on nitrogen fixation would continue for an estimated 2 to 8 years.

At 1 ppt extensive degradation of the lower molecular weight aliphatic fraction was noted, but many of the aromatic components were not degraded.

---

*Oil allowed to stand on seawater in static tanks for one week.

Statistically significant reductions in glucose uptake rates, nitrogen fixation rates, and redox potentials and a significant increase in respiration percentages were also noted. Interestingly, the effects on nitrogen fixation in the 1 to 50 ppt oil range were limited to fresh Cook Inlet crude. The weathered crude oil did not produce the same effects at these concentrations.

In the sediments treated with 0.1 ppt crude oil there was essentially 100% degradation of both the aliphatic and aromatic components after one year. No significant changes in glucose uptake or respiration rates were noted, and methane concentrations, CO_2 production rates, nitrogen fixation and denitrification rates were not significantly affected. There was, however, an 89% reduction in redox potential in the quadrants at this level and this finding was deemed to be important since redox potential is depressed after the crude oil has been degraded. It was suggested that the added carbon source plus the toxic effects of the oil itself caused in increased BOD in the system, and that this then further altered the sediment chemistry after the crude oil degraded.

Thus, while considerable data have been generated on the long-term fate and chemical weathering of oil in subtidal regimes in the Alaskan sub-arctic, no parallel set of data as yet exist on the rates and extents of the chemical weathering processes on stranded oil in sub-arctic intertidal zones. As part of this program then, a series of controlled intertidal oil-degradation experiments were initiated during the summer 1981 field study. The previously characterized sites, KB-1 through KB-4, plus an additional site (KB-5) at the head of Jakolof Bay (Figure 5-81), were thus revisited and a series of "controlled" intertidal sediment "oilings" were initiated.

At each of the sites a series of three 1 m^2 vented corrals were buried (Figure 5-98) in the intertidal sediments as the tide receded, and then each corral was "oiled" with 1.5 liters of fresh Prudhoe Bay crude oil (Figure 5-99). At each site a corral was placed in the upper intertidal zone at an elevation such that tidal flooding would occur only every 10 to 16 days during

FIGURE 5-98. INSTALLATION OF LOWER INTERTIDAL CORRAL FOR LONG-TERM STRANDED OIL STUDIES AT GREWINGK GLACIER (KB-1). DURING ALL CORRAL INSTALLATIONS, CARE WAS TAKEN TO ENSURE THAT THE SURFACE OF THE INTERIOR 1 m^2 PORTION OF THE TEST SITE WAS NOT DISTURBED.

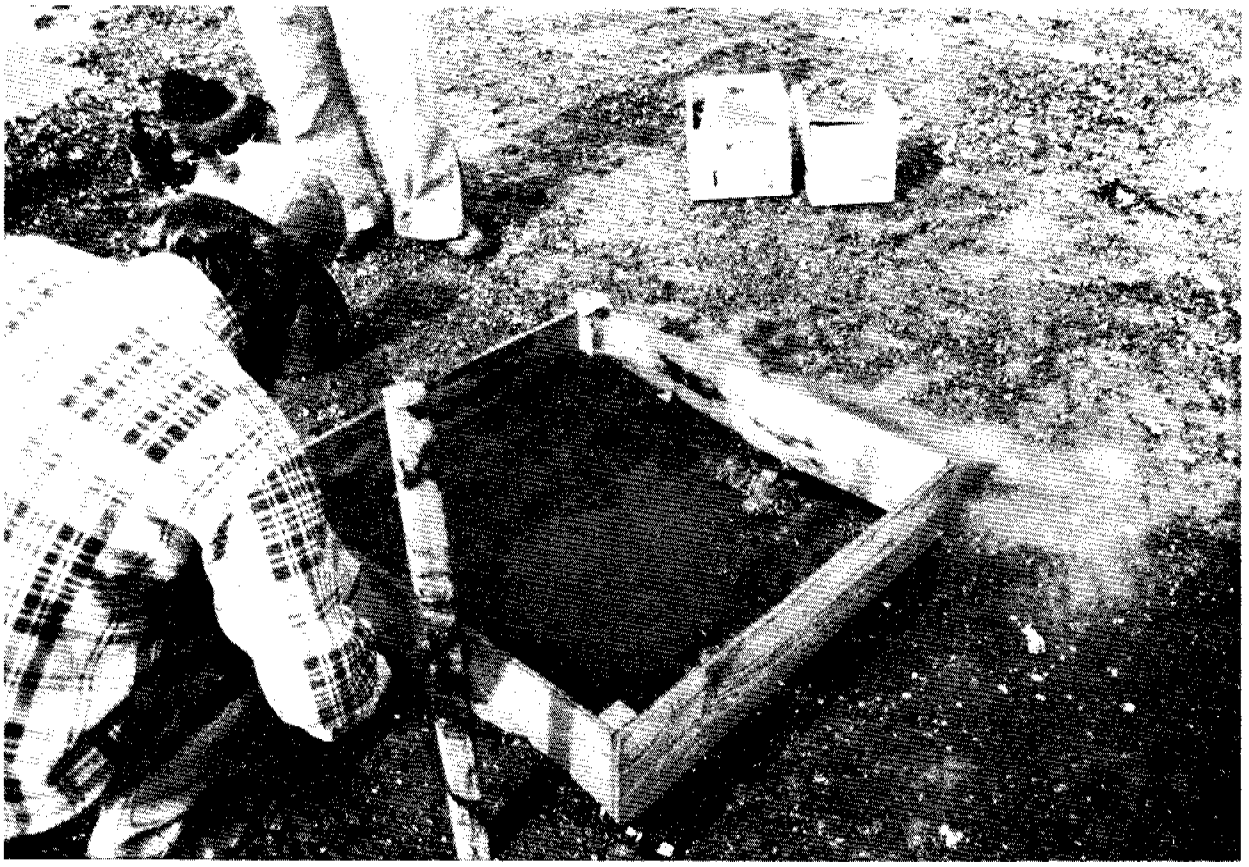

FIGURE 5-99. INTERTIDAL CORRAL AT CHINA POOT BAY (KB-2) 2 MINUTES AFTER 1.5 L ADDITION OF FRESH PRUDHOE BAY CRUDE OIL.

maximum tidal excursions (Figure 5-100). A second corral was then placed in the middle intertidal zone such that tidal action would be encountered daily, and finally, a third corral was buried in the lower intertidal zone such that during neep tides, the sediments would be continuously covered by seawater for several days. At three of the intertidal sites (specifically, KB-3, Kasitsna Bay; KB-4, Seldovia salt marsh; and KB-5, Jakolof Bay) additional quadrants were staked out adjacent to the intertidal corrals, and these sediments were "oiled" with 1.5 l of 10 day old weathered mousse from the wave tank experiments being run concurrently at the Kasitsna Bay facility.

By including naturally weathered mousse along with the fresh oil utilized in the experiments, the importance of open ocean weathering (specifically removal of lower molecular weight aromatic components due to evaporation and dissolution processes) on intertidal sediment impact and recovery could also be evaluated. Further, in that mousse and weathered crude oils have higher viscoscities and pour points than fresh crudes, the studies were intended to provide data on the difference in oil weathering as a function of the degree of penetration into the intertidal sediments.

No attempt was made to artificially mix the oil into the intertidal sediment, as the experiments were intended to simulate, as closely as possible, the effects of oil stranding after contamination during maximum tidal periods. Jakolof Bay was added to the other previously characterized sites, in that it is a location which experinces permanent shore-fast ice during several of the winter months. In this manner, it was hoped that the effects of this ice cover on intertidal oil weathering behavior could be examined. As shown by the scanning electron microscope data and oil adsorption potential results from these sites, significantly different intertidal substrates representative several low energy intertidal regimes are encompassed in this study.

Table 5-36 presents the time series sediment samples which were obtained following the oiling at each site. Additional samplings are planned

FIGURE 5-110. INSTALLATION OF UPPER INTERTIDAL CORRAL AT JACKOLOF BAY (KB-5). THIS SITE IS TYPICAL OF ONE WHICH WOULD BE EXPOSED ONLY DURING SPRING TIDES, APPROXIMATELY EVERY 2 WEEKS.

during our upcoming winter 1981/1982 field efforts. Immediately after sampling, the sediment samples from each site were frozen, and they are currently awaiting extraction and analyses which will be undertaken during the next several months. During the installation of the quadrants extreme care was taken to avoid disturbing the center of the quadrant such that oil penetration would not be artificially enhanced. Also, at each site, vertical transect and detailed photographic data were obtained such that the degree of tidal exposure can be quantitated over the anticipated 6-12 month duration of these experiments.

Initially we had intended to select three intertidal areas which would be representative of three environments of significantly different long-range oil vulnerability as indicated by the associated Hayes/Gundlach Environmental Susceptability Index (ESI) (GUNDLACH and HAYES, 1978; HAYES et al., 1976). This approach was modified, however, to examine the long-term weathering rates of oil in selectively different low-energy intertidal regimes as a function of sediment type, detrital input, fresh water availability and tidal exposure. Thus, while each of the intertidal sites selected could be classified with ESI indices values of 9 and 10 (sheltered tidal flats and/or marshes) subtle differences due to the topography at the selected sites (including fresh water input, extensive Spartina covering, possibility of wave scour, etc.) were included in the experimental design.

The purpose behind evaluation of differential hydrocarbon removal and oxygenated product formation is to determine if impact profiles can be generated as a function of the sub-arctic intertidal environment. These data will be useful to managers in oil spill predictions to assess long-term affects on different sub-arctic intertidal zones as a function of the energy regime and the sediment matrix. Correlation of these degradation rates with further refinement of numerical values (such as the Hayes/Gundlach index) will then be helpful in prediction and mapping ultimate long-term impacts for different intertidal zones. If oiled sediments from a particulate intertidal regime

were removed by storm activities and then redeposited in the nearshore subtidal region, potential rerelease of lower molecular weight aromatic compounds to the water column and/or inhibition of biotic activity as demonstrated by GRIFFITHS and MORITA (1980) in many of these sediments can take place. Knowledge of this potential behavior is felt to be important for long-term environmental impact assessment.

As noted above, data on longer term intertidal weathering of stranded oil can be obtained by reoccupying the field sites during the winter programs. In this regard, the corrals and marker stakes (assuming that they have not been removed or damaged by prior storm activities) will be critical in relocating the specific oiled sites. Logistics for the winter and spring field sampling efforts are being coordinated with NOAA's Kasitsna Bay resident manager to ensure that our actual arrival dates most closely coincide with the appropriate winter weather and ice conditions.

5.4 Recent Inter-Laboratory Inter-Calibration Programs

SAI's laboratory has routinely participated in inter-calibration programs: (1) an inter-calibration program among the participating hydrocarbon laboratories in the Southern California OCS BLM program (PAYNE et al., 1979a); (2) the first NOAA/OCSEAP sediment inter-calibration program using Duwamish River samples (PAYNE et al., 1979b); and (3) a water column extract and mousse inter-calibration among the major laboratories involved in the NOAA RESEARCHER cruise to study the IXTOC-I blowout (PAYNE et al., 1980a). As part of the Multivariant Analysis of Petroleum Weathering Program, a more recent Duwamish II sediment inter-calibration program was completed in January 1981. In the BLM inter-calibration program, several different methods were utilized by the participating laboratories, but excellent inter-laboratory accuracy and precision were obtained. In the first OCSEAP inter-calibration program, our own laboratory evaluated three separate methods: Soxhlet extraction; shaker table extraction; and Soxhlet extraction using solvents recommended by Dr. William MacLeod of NOAA/NMFS-Seattle. As in the previous inter-calibration

exercises, very good inter-method precision was obtained, and examination of our data and MacLeod's showed that essentially identical results were obtained in both laboratories.

In the most recent inter-calibration program, Duwamish II, a shaker table procedure for sediment extraction was used; however, the solvent systems were those which are typically utilized in our laboratory for hydrocarbon analyses. The results of our Duwamish II inter-calibration analysis are presented in Table 5-37. As the data indicate, fairly good precision was obtained, with coefficients of variations generally less than 20 percent for both the aliphatic and aromatic fractions. Figure 5-101 presents the relative concentrations of the polynuclear hydrocarbons obtained by our laboratory and by the NOAA/NMFS-Seattle laboratory. The profiles are nearly identical over a wide dynamic range, and the overall concentrations of amterials are well within one standard deviation. As the data suggest, very good agreement between our laboratory and the National Marine Fisheries Quality Control Laboratory is obtained. In general, when we conduct replicate analyses to evaluate laboratory precision, our results show that coefficients of variations for specific compounds at nanogram levels are near 20 percent or better.

TABLE 5-37. NOAA/NMFS INTERCALIBRATION RESULTS - DUWAMISH II, SCIENCE APPLICATIONS, INC.

Concentration of areas (µg/g dry wt)
Replicate No.

Sample #:	1	2	3	$\bar{X}$	CV*
Naphthalene	57.5	37.4	49.8	48.2	21
Benzothiophene	0	0	0	0	--
2-Methylnapthalene	41.2	45.2	60.9	49.1	21
1-Methylnaphthalene	16.6	15.8	19.5	17.3	11
Biphenyl	7.14	4.3	6.7	6.0	25
2,6-Dimethylnaphthalene	46.0	59.2	76.7	60.6	25
2,3,5-Trimethylnaphthalene	10.2	8.0	16.6	11.6	39
Fluorene	93.2	105.	115.	104.	10
Dibenzothiophene	93.0	85.6	91.2	89.9	4
Phenanthrene	536.	572.	471.	526.	10
Anthracene	168.	251.	310.	243.	29
1-Methylphenanthrene	29.8	29.9	29.1	29.6	1
Fluoranthene	1159.	1127.	1255.	1180.	6
Pyrene	731.	771.	941.	814.	14
Benz (a) anthracene	395.	467.	648	503.	26
Chrysene	722.	791.	1076.	863.	22
Benz (e) pyrene	320.	349.	574.	417.	33
Benz (a) pyrene	311.	412.	566.	430.	30
Perylene	263.	284.	355.	300.	16
Aliquot Weight	119.7	122.8	113.9	118.8	3.8
Percent Dry Weight	48.0	47.7	48.4	48.0	.73

Concentration of n-alkanes (µg/g dry wt)
Replicate No.

	1	2	3	$\bar{X}$	CV*
C_{14}	152	138	242	177	32
C_{15}	143	157	221	174	24
C_{16}	146	147	213	167	23
C_{17}	465	439	476	460	4
Pristane	433	438	466	446	4
C_{18}	141	149	214	168	24
Phytane	191	189	264	215	20
C_{19}	142	193	213	183	20
C_{20}	131	133	200	155	25
C_{21}	289	318	335	314	7
C_{22}	183	161	189	178	8
C_{23}	234	178	257	223	18
C_{24}	242	302	297	280	12
C_{25}	440	513	472	475	8
C_{26}	340	371	393	368	7
C_{27}	1159	1140	840	1046	17
C_{28}	345	366	421	377	10
C_{29}	857	834	768	820	6
C_{30}	827	736	815	793	6
C_{31}	1159	1349	1017	1175	14
C_{32}	310	309	265	295	9

*Coefficient of variation - Standard Deviation/Mean

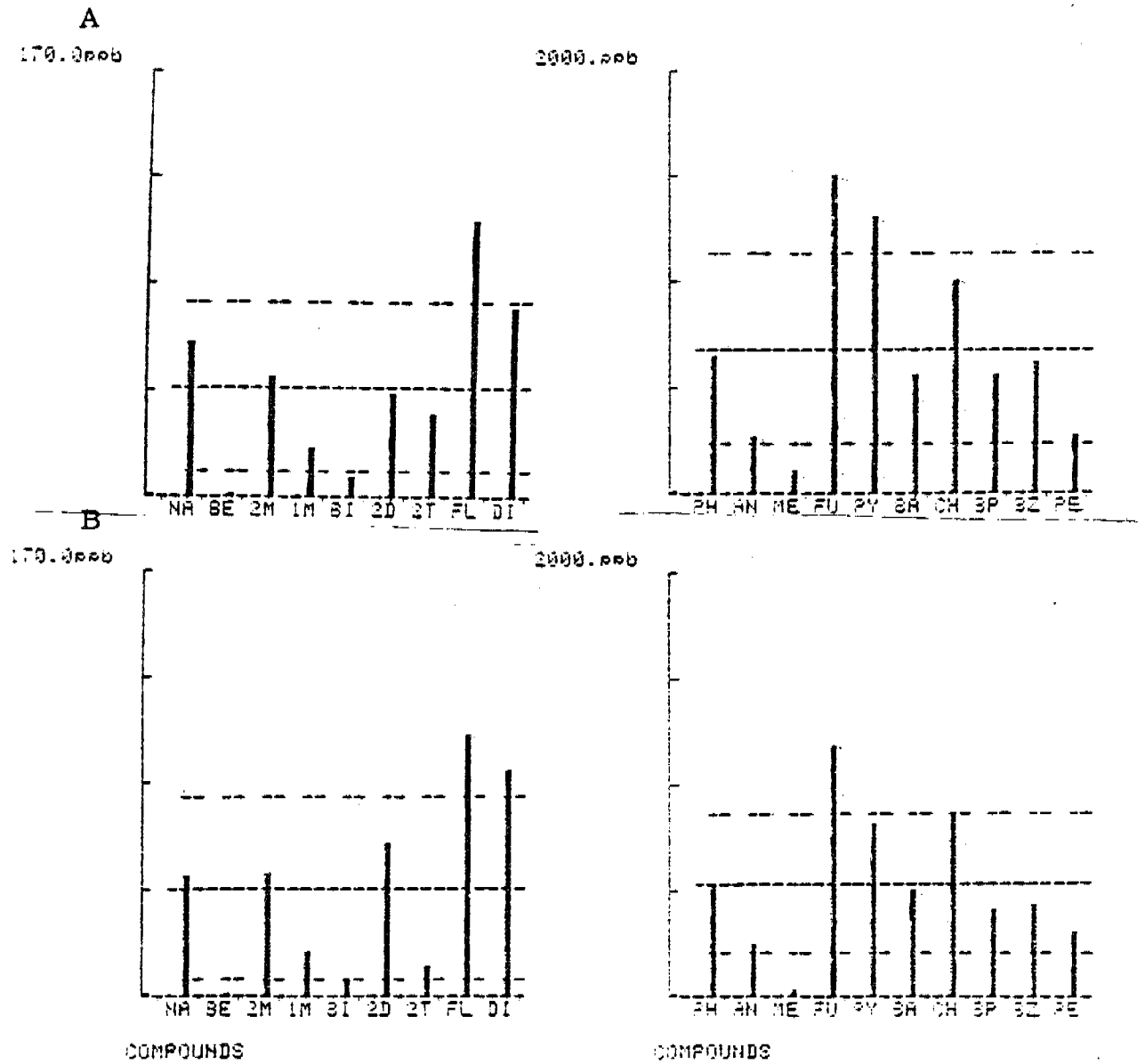

FIGURE 5-111. RELATIVE ABUNDANCE PLOTS FOR POLYNUCLEAR AROMATIC HYDROCARBONS DETECTED IN THE DUWAMISH II INTERCALIBRATION SAMPLES. (A) NOAA NATIONAL MARINE FISHERIES RESULTS AND (B) SCIENCE APPLICATIONS, INC. RESULTS. NOTE CHANGE IN CONCENTRATION SCALES BETWEEN DIBENZOTHIOPHENE (DI) AND PHENANTHRENE (PH); COMPOUND IDENTIFICATIONS FOR OTHER COMPONENTS ARE GIVEN IN TABLE 5-37.

6.0 CONCLUDING REMARKS AND RECOMMENDATIONS FOR UTILIZATION OF EXISTING AND FUTURE EXPERIMENTAL RESULTS FOR OIL WEATHERING MODEL DEVELOPMENT

Significant progress has been made in developing algorithms for evaporation and dissolution phenomena for both stirred tank and open ocean spill situations. With regard to the latter, both point source oil spills such as those resulting from tanker incidents and continuous source spill situations resulting from open ocean blowouts have been considered.

Our mathematical description of oil weathering in its present form considers evaporation using a pseudocomponent oil characterization, and evaporation and dissolution using a component-specific approach. This description will predict the mass of oil remaining in the slick as well as specific component concentrations in the oil and air and water columns. The major portions of these mathematical descriptions have been computerized, and the remainder are in the process of being coded and tested.

At this time, simulated oil spill mass balance and compound specific programs can be run for a variety of environmental situations. Further, the numerous experimental studies which have been completed provide a basis for comparing predicted and observed evaporation/dissolution behavior. In this regard the development of the GC data base system was critical in allowing compound-specific predicted vs observed concentrations. Predicted and observed results have been generated: (1) for stirred tank studies where water column and oil phase compound-specific data could be compared with computer predicted results, and (2) for oil distillation curves in order to compare predicted and observed mass balance for oil after varying stages of weathering. Specifically, predicted and observed mass balance distillation curves from the Kasitsna Bay wave tank experiments have been presented to illustrate the strength and application of the model and approach. Since a tremendous amount of information has been obtained from Kasitsna Bay field observations and measurements, it has been vital to properly design and implement the computer data base system for gas chromatographic data. Only by having this system developed and available could such field data be used directly for

verification and modification of the oil weathering model predictions. Specifically, from the combined results of La Jolla and Kasitsna Bay experiments, compound-specific data are now accessible (organized by Kovat retention indices) for generation of time-series observed concentration profiles for both the oil phase and water and air columns under a variety of environmental conditions.

Expansion and coupling of the existing dissolution algorithms to transport and dispersion models remains to be done; however, this is one of the topics which will be addressed in detail in upcoming NOAA-sponsored workshops on Oil Weathering Modeling and Transport which are scheduled to take place in Seattle in January 1982. Coupling of the dissolution algorithms with dispersion process algorithms will then allow time-dependent hydrocarbon concentration predications in the water column for simulated spill situations. This information will be important to environmental managers in making more accurate biological impact assessments. Additional algorithm development is clearly needed to incorporate dispersion processes, particularly when dealing with fresh oils. As noted in the discussions of the wave tank experiments from Kasitsna Bay, information on the percent oil dispersed by wave action is being derived from whole-water sample extracts which were obtained during the first 12 to 24 hours of those experimental studies.

With regard to the status of the oil weathering model development, the following activities are scheduled for completion by January 1982:

1) Incorporation of modifications such that evaporation/dissolution behavior can be predicted for any of 800 crude oils on which composition data are currently available through the Bartlesville Energy Technology Center (BETC).

2) Additional model testing will be carried out after all pertinent mathematics have been programmed. The pseudo-component oil-weathering model will be applicable to any crude or oil cut, such as heavy naphtha or a gas oil, for which data are available. Component-specific predictions for any given oil or distillation product require only that the sample be fractionated into aliphatic, aromatic and polar constituents and analyzed by

capillary gas chromatography. With this analysis the initial oil-component concentrations can be entered into the GC database of the model and thereby used for time-series component concentration calculations.

3) Other pertinent testing of the model includes the prediction of concentrations of specific compounds in the water column. The toxicity of these compounds to marine life is directly related to exposure time and to concentration. Thus, the model will be tested to predict water and air column concentrations for which appropriate component specific data are available. Coupling of this predicted dissolution behavior with transport and dispersion models will then be undertaken.

4) Two other observable features of weathered oil - viscosity and mousse formation - are considered to be important because of the effects they have on mass transport from the slick. Therefore, existing information on these topics along with the results of experiments reported here will be used to develop viscosity and mousse formation predictions.

Dispersion, microbial degradation, suspended particulate material/oil interactions, photo-oxidation and auto-oxidation are other oil weathering processes known to occur. However, these are only now beginning to be understood in a mechanistic sense and their mathematical descriptions are still relatively primitive. Each of these processes is somewhat more complicated than bulk transport processes, since often complex chemical reactions affecting many compounds are involved, and there are very few accurate descriptions of chemical reactions to be used for pseudo-component models in the manner of the evaporation process model developed to date. The resulting mathematical models involve many variables and will require thorough experimentation, derivation, programming and testing.

As a result of our initial experimental activities and algorithm development, it has become clear that additional physical properties data are required, and compound-specific Henry's law constant and diffusivity determinations are being completed in our laboratories at this time. As noted above, additional modeling program needs include development of algorithms for modeling dispersion phenomena and expansion of viscosity correlations on water-in-oil emulsions beyond the current Mackay formulations, which predict water-in-oil emulsion viscosity as a function of water content (MACKAY, 1980).

While compound-specific oil characterizations have been completed on the four crude oils examined in this program, it is now believed that additional work on the asphalts and residual (non-distillable) fractions is required. This is particularly important with regard to mousse formation where the presence of asphalts, higher molecular weight waxes, and metallo-porphyrin compounds have been implicated in the stabilization and formation of water-in-oil emulsions (PAYNE, 1981).

The microbial degradation experiments which have been conducted to date have produced data which allow calculation of total carbon flux into the water column as a result of bacterial processes; however, several additional experimental requirements have been defined as outlined below. Experiments conducted to evaluate the effects of nutrient supplementation on bacterial degradation rates have shown that only minimal effects are observed as a result of inorganic nutrient concentrations. An understanding of such information is necessary for development of algorithms for modeling microbial degradation behavior. Specifically, progress has been made in delineating which variables are important for development of algorithms for these processes and subsequent investigations are outlined at the end of this section.

The results of our oil/suspended particulate material interaction studies, which are being analyzed at this time, will better define the differences in adsorption and sedimentation of oil as a function of the degree of evaporation/dissolution weathering. With such information, it should be possible to develop algorithms for more accurate predictions of weathered oil/sedimentation behavior. In this regard, longer-term (two month and six month) data obtained from the flow-through wave tank experiments at Kasitsna Bay will be used to determine the density increases in open ocean mousse as a result of time dependent accommodation of suspended particulate material.

While initial photo-oxidation experiments were undertaken during the early phases of this program, detailed examinations of this complex phenomena have by design been postponed. Additional experiments need to be undertaken

to examine the increased flux of oil components to the water column as a result of photochemical oxidation processes.

The following synopses detail additional specific program areas and experimental requirements which need to be expanded upon in subsequent stages of this program.

Oil/Suspended Particulate Material Interactions

Experiments currently in progress are addressing the effects of time-dependent evaporation and dissolution "weathering" (viscosity change) on oil/SPM interactions. Additional collection and analyses of mousse and filtered water samples from the wave tank experiments currently in progress at Kasitsna Bay will yield data on the following:

- ambient SPM loads from Kasitsna Bay,
- density increases in 4 and 6 month old mousse due to accommodation and adsorption of SPM.

Parameters being considered for algorithm development for oil/SPM interactions include particulate load, particulate type, turbulence (as it affects dispersion of oil micelles), oil composition and viscosity (degree of weathering as it affects dispersion of micelles), and water temperature.

Water-in-Oil Emulsification (mousse formation)

Considerable progress has been made in developing correlations of percent water uptake and mousse viscosity (MACKAY, 1980). Wave tank experiments are underway to evaluate mousse formation from Prudhoe Bay crude oil as a function of chemical weathering (evaporation/dissolution, photo-oxidation, particulate adsorption and microbial degradation) and additional analyses are planned to further characterize the nondistillable residuum for percent asphalts, waxes and metallo-porphyrins. Using this experimental approach as a

starting point, other parameters for modeling mousse formation include: oil composition (asphalt, wax and metallo-porphyrin content in addition to standard compositional data), turbulence regeim, water temperature, oil viscosity, presence of microbial and photo-oxidation products, SPM accrection and density variations.

Microbial Degradation Studies

The utility of the ^{14}C-labelled hydrocarbon substrate data for estimations of overall parent petroleum hydrocarbon removal from an oil slick due to microbial degradation is based upon two assumptions: (1) the degradation potential assay, which relies upon detection of $^{14}CO_2$, serves as an accurate indicator of total degradation (defined as loss of parent compound molecular structure); and (2) the hydrocarbon substrates utilized are "typical" in terms of the biodegradability of other compounds in their class (e.g., hexadecane is a typical aliphatic, naphthalene is a typical aromatic). To further assess the soundness of this approach, the following activities are being pursued:

- determination of a mass balance for the ^{14}C-labeled substrates (i.e., how the parent compound and associated metabolites partition into the bacterial cell material and surrounding water column). This should provide an estimation of how accurate the detection of $^{14}CO_2$ is for defining total degradation.
- incorporation of additional ^{14}C-labeled hydrocarbon substrates into the degradation potential assay. Emphasis will be made on aromatics, potentially including such compounds as the PNAs benz(a)anthracene, benzo(a)pyrene, dibenz(a,h)anthracene, and dimethylbenz(a)anthracene.

Parameters which are currently being evaluated for final development of algorithms for modeling microbial processes include microbial biomass, oil slick surface area, inorganic and organic nutrient concentrations, dissolved oxygen concentrations, water temperature, and inhibition of bacterial activity as a result of the toxicity of dissolved lower molecular weight aromatics.

7.0 BIBLIOGRAPHY

API (1976). Technical Data Book - Petroleum Refining. American Petroleum Institute, Washington, D.C.

Azam, F., and O. Holm-Hansen (1973). Use of Tritiated Substrates in the Study of Heterotrophy in Seawater. Marine Biology. 23:191-196.

Ball, J. S., and H. T. Rall (1962). Nonhydrocarbon Components of a California Petroleum. Division of Refining, 42(3):128-145.

Bassin, J. J., and T. Ichiye (1977). Flocculation Behavior of Suspended Sediments and Oil Emulsions. Journal of Sedimentary Petrology, 47(2):671-677.

Bellar, T. A., and J. J. Lichtenberg (1974). Journal of American Water Works, 66:703.

Blumer, M., M. Ehrhardt, and J. H. Jones (1973). The Environmental Fate of Stranded Crude Oil. Deep Sea Research, 20:239-259.

Boehm, P. D., and D. L. Fiest (1980). Aspects of the Transport of Petroleum Hydrocarbons to the Offshore Benthos During the IXTOC-I Blowout in the Bay of Campeche. Proceedings of a Symposium on Preliminary Results from the Sept. 1979 Researcher/Pierce IXTOC-I Cruise. Key Biscayne, Florida, (June 9-10). NOAA Off. Mar. Poll. Assessment.

Butler, J. N. (1975). Evaporative Weathering of Petroleum Residues: The Age of Pelagic Tar. Marine Chemistry, Vol. 3, p. 9.

Caparello, D. M., and P. A. La Rock (1975). A Ratioisotope Assay for the Quantification of Hydrocarbon Biodegradation Potential in Environmental Samples. Microbial Ecology. 2:28-42.

Carslaw, H. S., and J. C. Jaeger (1959). Conduction of Heat in Solids, Oxford University Press.

Coleman, H. J., E. M. Shelton, D. T. Nichols, and C. J. Thompson (1978). Analyses of 800 Crude Oils from United States Oil Fields. BETC/RI-78/14, Bartlesville Energy Technology Center, Bartlesville, Oklahoma.

Clark, R. C., and D. W. Brown (1977). Petroleum: Properties and Analysis in Biota and Abiotic Systems. p. 1-89. In: D. C. Malins (ed.), Effects of Petroleum on Arctic and Subarctic Marine Environments and Organisms. Academic Press, New York.

Clark, R. C., and W. D. MacLeod, Jr. (1977). Inputs, Transport Mechanisms and Observed Concentrations of Petroleum in the Marine Environment, p. 91-223. In: D. C. Malins (ed.), Effects of Petroleum on Arctic and Subarctic Marine Environments and Organisms. Academic Press, New York.

de Lappe, B. W., R. W. Riseborough, J. C. Shropshire, W. R. Sisteck, E. F. Letterman, D. R. DeLappe, and J. R. Payne (1979). The Partitioning of Petroleum Related Compounds Between the Mussel Mytilus californianus and Seawater in the Southern California Bight. Draft Final Report II-15.0, Intertidal study of the Southern California Bight, submitted to Bureau of Land Management, D.C. by the Bodega Marine Laboratory, University of California, and Science Applications, Inc.

Evaluations of World's Import Crudes (1973). The Oil and Gas Journal, The Petroleum Publishing Co., Tulsa, Oklahoma, U.S.A.

Fallon, J. F., and K. M. Watson (1944). Thermal Properties of Hydrocarbons. National Petroleum News, June 7, p. 372.

Feely, R. A., J. D. Cline, and G. J. Massoth (1978). Transport Mechanisms and Hydrocarbon Adsorption Properties of Suspended Matter in Lower Cook Inlet. Quarterly Report, Pacific Marine Environmental Laboratory, NOAA, Seattle, Wash.

Fuhrman, J. A., Ammerman, J. W., and F. Azam (1980). Bacterioplankton in the Coastal Euphotic Zone: Distribution, Activity and Possible Relationships with Phytoplankton. Marine Biology, 60, 20:201-207.

Fuhrman, J. A., and F. Azam (1980). Bacterioplankton Secondary Production Estimates for Coastal Waters of British Columbia, Antarctica, and California. Applied and Environmental Microbiology. 39(6):1085-1095.

Fuhrman, J. A., and F. Azam (1980). Thymidine Incorporation as a Measure of Heterotrophic Bacterioplankton Production in Marine Surface Waters: Evaluation and Field Results. Marine Biology (in press).

Gamson, B. W., and K. M. Watson (1944). Vapor Pressures and Critical Properties of Organic Compounds. National Petroleum News, May 3, p. 259.

Gearing, J. N., P. J. Gearing, T. Wade, J. G. Quinn, H. B. McCarty, J. Farrington, and R. F. Lee (1979). The Rates of Transport and Fates of Petroleum Hydrocarbons in a Controlled Marine Ecosystem and a Note on Analytical Variability, p. 555-564, In: Proceedings, 1979 Oil Spill Conference (Prevention, Behavior, Control, Cleanup) 19-22 March, Los Angeles, Calif.

Gold, P. I. (1969). Estimating Thermophysical Properties of Liquid, Part 10; Viscosity. Chemical Engineering, July 14.

Gordon, D. C., P. D. Keizer, W. R. Hardstaff, and D. G. Aldous (1976). Fate of Crude Oil Spilled on Seawater Contained in Outdoor Tanks. Environmental Science and Technology, 10(6):580-585.

Griffiths, R. P., and R. Y. Morita (1980). Study of Microbial Activity and Crude Oil-Microbial Interactions in the Waters and Sediments of Cook Inlet and the Beaufort Sea. Final Report to the NOAA OCSEAP Office, Juneau, Alaska.

Gundlach, E. R., and M. O. Hayes (1978). Investigations of beach Processes. In: The Amoco Cadiz Oil Spill. A Preliminary Scientific Report, W. N. Hess (ed.), NOAA/EPA Special Report, pp. 85-196.

Harrison, M. J., Wright, R. T., and R. Y. Morita (1971). Method for Measuring Mineralization in Lake Sediments. Applied Microbiology. 21:698-702.

Harrison, W., M. A. Winnik, P. T. Y. Kwong, and D. Mackay (1975). Crude Oil Spills. Disappearance of Aromatic and Aliphatic Components from Small Sea-surface Slicks. Environmental Science and Technology, 9:231-234.

Hayes, M. O., P. J. Brown, and J. Michel (1976). Coastal Morphology and Sedimentation, Lower Cook Inlet, Alaska: With Emphasis on Potential Oil Spill Imports: Tech. Rept. No. 12-CRD, Coastal Research Division, Dept. of Geology, Univ. of South Carolina, 107 pp.

Hobbie, J. E., Daley, R. J., and S. Jasper (1977). Use of Nucleopore Filters for Counting Bacteria by Fluorescence Microscopy. Applied and Environmental Microbiology. 33(5):1225-1228.

Hodson, R. E., Azam, F., and R. F. Lee (1977). Effects of Four Oils on Marine Bacterial Populations: Controlled Ecosystem Pollution Experiment. Bulletin of Marine Science. 27(1):119-126.

Hougen, O. A., K. M. Watson, and R. A. Ragatz (1965). Chemical Process Principles, Part I. John Wiley & Sons, Inc., New York.

Jaeger, J. C. (1945). Conduction of Heat in a Slab in Contact with a Well-Stirred Fluid. Cambridge Philosophical Society, Proceedings, Vol. 41, p. 43.

John, P., and I. Souter (1976). Anal. Chem. 48:520.

Jordan, R. E., and J. R. Payne (1980). Fate and Weathering of Petroleum Spills in the Marine Environment: A Literature Review and Synopsis. Ann Arbor Science Publishers, Inc., Ann Arbor, Michigan.

Kovats, E. (1958). Helv. Chim. Acta, 41:1915.

Liss, P. G., and P. G. Slater (1974). Flux of Gases Across the Air-Sea Interface. Nature, Vol. 247, January 25, p. 181.

Lloyd, J. B. F. (1971). Nature, 231(64).

Lloyd, J. B. F. (1971). J. Forensic Sci. Soc., 11(83).

Mackay, D., J. Buist, R. Mascarenhas, and S. Paterson (1980). Oil Spill Processes and Models, report submitted to Research and Development Division, Environmental Emergency Branch, Environmental Impact Control Directorate, Environmental Protection Service, Environment Canada, Ottawa, Ontario, K1A 1C8.

Mackay, D., and R. S. Matsugu (1973). Evaporation Rates of Liquid Hydrocarbon Spills on Land and Water. The Canadian Journal of Chemical Engineering, Vol. 51, p. 434.

Mackay, D., and W. Y. Shiu (1977). Aqueous Solubility of Polynuclear Aromatic Hydrocarbons, Journal of Chemical Engineering Data, Vol. 22, #4, p. 399.

Maiero, D. J., and A. Ruby (1979). Environmental Sensitivity Index (ESI) for Lower Cook Inlet (unpublished manuscript).

Malinky, G. and D. G. Shaw (1979). Modeling the Association of Petroleum Hydrocarbons and Sub-Arctic Sediments, p. 621-624, In: Proceedings, 1979 Oil Spill Conference (Prevention, Behavior, Control, Cleanup), 19-22 March, Los Angeles, Calif.

McAuliffe, C. (1977). Evaporation and Solution of C_2 to C_{10} Hydrocarbons from Crude Oils on the Sea Surface. In: D. A. Wolfe (ed.), Fate and Effects of Petroleum Hydrocarbons in Marine Organisms and Ecosystems, Pergamon Press.

Meyer-Reil, L. A. (1978). Autoradiography and Epifluorescencce Microscopy Combined for the Determination of Number and Spectrum of Actively Metabolizing Bacteria in Natural Waters. Applied and Environmental Microbiology. 36(3):506-512.

Meyers, P. A., and J. G. Quinn (1973). Association of Hydrocarbons and Mineral Particles in Saline Solutions. Nature, 244:23-24.

Nagata, S., and G. Kondo (1977). Photo-Oxidation of Crude Oils, p. 617-620. In: Proceedings, 1977 Oil Spill Conference (March 8-10, New Orleans, LA) American Petroleum Inst. Pub. No. 4284.

Parker, P. L. and S. Macko (1978). An Intensive Study of the Heavy Hydrocarbons in the Suspended Particulate Matter of Seawater, Ch. 11 of South Texas Outer-Continental BLM Study.

Payne, J. R., P. J. Mankiewicz, J. R. Nemmers, R. E. Jordan, I. R. Kaplan, M. I. Venkatesan, S. Brenner, J. Bonilla, D. Meredith, B. Meyers, B. Haddad, A. L. Burlingame, A. Ensminger, G. Gould, and M. L. Moberg (1978a). High molecular weight petroleum hydrocarbon analytical procedures. Southern California Baseline Study, Benthic Year II. Volume III, Report 5.0. Final report submitted to the Bureau of Land Management, Department of Interior, Washington, D.C. by Science Applications, Inc.

Payne, J. R., J. R. Clayton, Jr., B. W. deLappe, P. L. Millikin, J. S. Parkin, R. K. Okazaki, E. F. Letterman, and R. W. Risebrough (1978b). Hydrocarbons in the Water Column. Southern California Baseline Study, Vol. II, Report 3.2.3., p. 1-207. Final Report, submitted to the Bureau of Land Management, Washington, D.C. by the University of California Bodega Marine Laboratory, Bodega Bay, California, and Science Applications, Inc., La Jolla, California.

Payne, J. R., P. J. Mankiewicz, J. E. Nemmers, R. E. Jordan, S. Brenner, M. I. Venkatesan, B. W. de Lappe, R. W. Risebrough, G. F. Gould, and M. L. Moberg (1979a). Southern California Outer Continental Shelf Baseline Studies: Intercalibration of participating hydrocarbon laboratories. Manuscript submitted in Oceans '79 conference proceedings for Oceans Conference, San Diego, California, 16-19 September, 1979.

Payne, J. R., J. E. Nemmers, R. E. Jordan, P. J. Mankiewicz, A. D. Oesterle, S. Laughon, and G. Smith (1979b). Measurement of petroleum hydrocarbon burdens in marine sediments by three commonly accepted procedures: results of a NOAA inter-laboratory calibration exercise, Fall, 1978. Submitted to Dr. John A. Calder, Staff Chemist, OCSEAP, U.S. Department of Commerce, National Oceanic and Atmospheric Administration, Environmental Research Laboratory, Boulder, CO, January 1979. pp. 1-34, plus appendix.

Payne, J. R., G. S. Smith, P. J. Mankiewicz, R. F. Shokes, N. W. Flynn, V. Moreno, and J. Altamirano (1980a). Horizontal and Vertical Transport of Dissolved and Particulate-Bound Higher-Molecular-Weight Hydrocarbons from the IXTOC-I Blowout, p. 119-167. In: Proceedings of a Symposium, Preliminary Results from the Sept. 1979 Researcher/Pierce IXTOC-I Cruise (June 9-10, Key Biscayne, Fla.) NOAA, Off. Mar. Poll. Assess.

Payne, J. R., N. W. Flynn, P. J. Mankiewicz, and G. S. Smith (1980b). Surface Evaporation/Dissolution Partitioning of Lower-Molecular-Weight Aromatic Hydrocarbons in a Down-Plume Transect from the IXTOC-I Wellhead, p. 239-265. In: Proceedings of a Symposium, Preliminary Results from the Sept. 1979 Researcher/Pierce IXTOC-I Cruise (June 9-10, Key Biscayne, Fla.) NOAA, Off. Mar. Poll. Assess.

Payne, J. R. (1981). A Review of the Formation and Behavior of Water-in-Oil Emulsions (Mousse) from Spilled Petroleum and Tar Ball Distributions, Chemistries and Fates in the World's Oceans. Background Information for Ocean Sciences Board on "Inputs, Fates and Effects of Petroleum in the Marine Environment," National Academy of Sciences.

Reid, R. C., J. M. Prausnitz, and T. K. Sherwood (1977). The Properties of Gases and Liquids, McGraw-Hill Book Company, New York.

Rohsenow, W. M., and J. P. Hartnett (1973). Handbook of Heat Transfer, McGraw-Hill Book Company, New York.

Smith, C. L., and W. G. MacIntyre (1971). Initial Aging of Fuel Oil Films of Seawater. In: Proceedings of the 1971 Joint Conference on Prevention and Control of Oil Spills, p. 457-461. American Petroleum Institute, Washington, D.C.

Suess, E. (1968). Calcium Carbonate Interactions with Organic Compounds. Ph.D. Thesis, Lehigh University, Bethlehem, PA.

Sutton, C. and J. A. Calder (1974). Solubility of Higher-Molecular-Weight n-paraffins in Distilled Water and Seawater. Environmental Science and Technology, 8:654-657.

Sutton, W. G. L (1943). On the Equation of Diffusion in a Turbulent Medium, Proceedings of the Royal Society (London), A182, p. 48.

Treybal, R. E. (1955). Mass-Transfer Operations, McGraw-Hill Book Company, New York.

Twardus, E. M. (1980). A Study to Evaluate the Combustibility and Other Physical and Chemical Properties of Aged oils and Emulsions. R and D Div., Environmental Emergency Branch, Environmental Protection Service, Ottawa, Ontario, Canada.

Vo-Dinh, T., R. B. Gammage, A. R. Hawthorne, and J. H. Thorngate (1978). Synchronous Spectroscopy for Analysis of Polynuclear Compounds. Environmental Science and Technology, 12(12):1297-1302.

Wakeham, S. G. (1977). Synchronous Fluorescence Spectroscopy and Its Application to Indigenous and Petroleum-Derived Hydrocarbons in Lacustrine Sediments. Environmental Science and Technology, 11(3):272-276.

Walker, J. D., and R. R. Colwell (1976). Measuring the Potential Activity of Hydrocarbon-Degrading Bacteria. Applied and Environmental Microbiology. 31(2):189-197.

Watson, K. M., E. F. Nelson, and G. B. Murphy (1935). Characterization of Petroleum Fractions. Industrial and Engineering Chemistry, Vol. 27, No. 12, p. 1460.

Watson, S. W., Novitsky, T. J., Quinby, H. L., and F. W. Valois (1977). Determination of Bacterial Number and Biomass in the Marine Environment. Applied and Environmental Microbiology. 33(4):940-946.

Weast, R. C., (ed.) (1972). Handbook of Chemistry and Physics, 53rd edition, Chemical Rubber Company.

Wheeler, R. B. (1978). The Fate of Petroleum in the Marine Environment. Exxon Production Research Co. Special Report.

Winters, J. K. (1978). Fate of Petroleum Derived Aromatic Compounds in Seawater Held in Outdoor Tanks, Ch. 12, South Texas Outer-Continental Shelf BLM Study.

Yang, W. C., and H. Yang. (1977). Modeling of Oil Evaporation in Aqueous Environment. Water Research, Vol. 11, p. 879.

Zurcher, F. and M. Thuer (1978). Rapid Weathering Processes of Fuel Oil in Natural Waters. Analysis and Interpretations. Environmental Science and Technology, 12(7):838-843.

APPENDIX A

COMPUTER PREDICTED WEATHERING RESULTS, COMPUTER CODE LISTINGS AND COMPUTER CODE FLOW CHART

The results presented in this appendix are examples of calculated results (pages A-2 through A-30), the current code listing (pages A-31 through A-43), and code flow chart (pages A-44 through A-74). The code presented here is still in a state of development with work remaining to be completed on the mass-transfer coefficient section.

The example calculation is for Prudhoe Bay crude oil, item 9, sample 71011 (COLEMAN, 1978) with temperatures of 32 and 42°F at wind speeds of 30 and 40 knots. The mass-transfer coefficient used is that due to Mackay (MACKAY, 1973). The output from the calculation is self explanatory and details the weathering of 15 cuts of this particular crude through 500 hours. These results are summarized in Table A-1 and show the effects of wind and temperatures over 500 hours.

Table A-1

SUMMARY OF OIL-WEATHERING CALCULATIONS FOR PRUDHOE BAY CRUDE OIL AFTER 500 HOURS

Temperature, °F	32	42	32	42
Wind, Knots	10	10	40	40
Mass Fraction Remaining for Cut #				
1	0	0	0	0
2	0	0	0	0
3	0	0	0	0
4	0	0	0	0
5	0	0	0	0
6	0.14	0.03	0	0
7	0.73	0.55	0.36	0.16
8	0.95	0.91	0.86	0.75
9	0.99	0.98	0.98	0.95
10	1	1	1	0.99
12	1	1	1	1
13	1	1	1	1
14	1	1	1	1

SUMMARY OF TBP CUTS CHARACTERIZATION FOR: PRUDHOE BAY, ITEM 9, SAMPLE 71011

	TB	API	VOL	MW	TC	PC	VC	A	B	T10	VIS	NC	NS
1	1.670E+02	7.270E+01	2.123E+00	8.921E+01	9.310E+02	3.430E+01	3.802E+02	3.227E+00	1.976E-01	4.604E+02	4.144E-01	3	1
2	2.120E+02	6.420E+01	2.629E+00	1.015E+02	9.852E+02	3.654E+01	4.370E+02	3.311E+00	2.111E-01	4.959E+02	4.919E-01	3	1
3	2.570E+02	5.670E+01	3.539E+00	1.139E+02	1.040E+03	3.514E+01	4.860E+02	3.391E+00	2.220E-01	5.315E+02	6.006E-01	3	1
4	3.020E+02	5.160E+01	3.640E+00	1.270E+02	1.091E+03	3.365E+01	5.410E+02	3.493E+00	2.341E-01	5.677E+02	7.474E-01	3	1
5	3.470E+02	4.760E+01	3.741E+00	1.431E+02	1.139E+03	3.218E+01	6.015E+02	3.613E+00	2.448E-01	6.044E+02	9.433E-01	3	1
6	3.920E+02	4.520E+01	3.539E+00	1.607E+02	1.184E+03	3.062E+01	6.713E+02	3.767E+00	2.554E-01	6.420E+02	1.200E+00	3	1
7	4.370E+02	4.150E+01	4.348E+00	1.779E+02	1.230E+03	2.942E+01	7.396E+02	3.969E+00	2.643E-01	6.796E+02	1.555E+00	3	1
8	4.830E+02	3.780E+01	4.853E+00	1.960E+02	1.275E+03	2.834E+01	8.111E+02	4.059E+00	2.724E-01	7.176E+02	2.046E+00	3	1
9	5.270E+02	3.480E+01	5.056E+00	2.125E+02	1.323E+03	2.760E+01	8.765E+02	4.178E+00	2.789E-01	7.551E+02	2.003E+00	3	1
10	5.800E+02	3.060E+01	2.831E+00	2.365E+02	1.375E+03	2.649E+01	9.715E+02	4.366E+00	2.879E-01	8.006E+02	3.043E+00	3	1
11	6.380E+02	2.910E+01	6.572E+00	2.721E+02	1.422E+03	2.487E+01	1.113E+03	4.676E+00	2.971E-01	8.530E+02	5.262E+00	3	1
12	6.700E+02	2.620E+01	6.876E+00	2.872E+02	1.454E+03	2.443E+01	1.172E+03	4.787E+00	3.007E-01	8.807E+02	7.034E+00	3	1
13	7.300E+02	2.400E+01	6.067E+00	3.346E+02	1.508E+03	2.288E+01	1.360E+03	5.202E+00	3.102E-01	9.441E+02	1.080E+01	3	1
14	7.850E+02	2.250E+01	7.402E+00	3.709E+02	1.544E+03	2.192E+01	1.504E+03	5.534E+00	3.168E-01	9.892E+02	1.768E+01	3	1
15	8.500E+02	1.140E+01	3.670E+01	6.000E+02	0.000E+00	0.000E+00	0.000E+00	0.000E+00	0.000E+00	0.000E+00	1.810E+02	0	0

TB = NORMAL BOILING TEMPERATURE, DEG F
API = API GRAVITY
VOL = VOLUME PER CENT OF TOTAL CRUDE
MW = MOLECULAR WEIGHT
TC = CRITICAL TEMPERATURE, DEG RANKINE
PC = CRITICAL PRESSURE, ATMOSPHERES
VC = CRITICAL VOLUME, CC/MOLE
A AND B ARE PARAMETERS IN THE VAPOR PRESSURE EQUATION
T10 IS THE TEMPERATURE IN DEG R WHERE THE VAPOR PRESSURE IS 10 MM HG
VIS IS THE KINEMATIC VISCOSITY IN CENTISTOKES AT 122 DEG F
NC = ERROR CODE, SHOULD BE LESS THAN 20
NS = ERROR CODE, SHOULD BE EQUAL TO 1
IGNORE THE ERROR CODES FOR COMPONENT NUMBER 15

CRUDE OIL CHARACTERIZATION AND PSEUDOCOMPONENT EVAPORATION MODEL
IDENTIFICATION: PRUDHOE BAY, ITEM 9, SAMPLE 71011

VAPOR PRESSURE IN ATMOSPHERES AT 3.200E+01 DEG F

	VP
1	3.784E-02
2	1.006E-02
3	2.584E-03
4	5.643E-04
5	1.123E-04
6	1.955E-05
7	3.176E-06
8	4.635E-07
9	6.603E-08
10	5.303E-09
11	2.092E-10
12	3.826E-11
13	4.512E-13
14	1.364E-14

MEAN MOLECULAR WEIGHT OF THE CRUDE = 2.730E+02

OVER-ALL MASS-TRANSFER COEFFICIENTS

WIND SPEED = 1.000E+01 KNOTS, OR 1.853E+04 M/HR
INITIAL SLICK DIAMETER = 7.116E+02 M, OR AREA = 3.975E+05 M**2

OVER-ALL MASS-TRANSFER COEFFICIENT FOR CUMENE = 1.553E+01 M/HR

CUT	M/HR	G-MOLES/(HR)(ATM)(M**2)	SPGR OF CUT
1	1.663E+01	7.428E+02	6.929E-01
2	1.638E+01	7.317E+02	7.230E-01
3	1.618E+01	7.228E+02	7.519E-01
4	1.600E+01	7.148E+02	7.728E-01
5	1.584E+01	7.077E+02	7.901E-01
6	1.570E+01	7.011E+02	8.008E-01
7	1.558E+01	6.959E+02	8.179E-01
8	1.548E+01	6.914E+02	8.338E-01
9	1.540E+01	6.879E+02	8.509E-01
10	1.531E+01	6.837E+02	8.729E-01
11	1.520E+01	6.788E+02	8.811E-01
12	1.516E+01	6.771E+02	8.973E-01
13	1.506E+01	6.727E+02	9.100E-01
14	1.500E+01	6.701E+02	9.188E-01

FOR THIS SPILL OF 5.000E+04 BARRELS, THE MASS IS 7.062E+03 METRIC TONNES

VOLUME FROM SUMMING THE CUTS = 7.9E+03 M**3, OR 5.000E+04 BARRELS

KINEMATIC VISCOSITY OF THE BULK CRUDE FROM THE CUTS = 4.8E+00 CENTISTOKES AT 122 DEG F

KINEMATIC VISCOSITY OF THE BULK CRUDE FROM THE CUTS = 8.8E+00 AT T = 32.0 DEG F

COUNT THE CUTS IN THE FOLLOWING OUTPUT FROM LEFT TO RIGHT

THE INITIAL MOLES IN THE SLICK ARE:
1.305E+06 1.401E+06 1.040E+06 1.741E+06 1.634E+06 1.395E+06 1.581E+06 1.637E+06 1.601E+06 8.267E+05 1.683E+06
1.699E+06 1.305E+06 1.466E+06 4.791E+06

THE INITIAL MASSES IN THE SLICK ARE:
1.164E+08 1.504E+08 2.105E+08 2.225E+08 2.338E+08 2.242E+08 2.813E+08 3.209E+08 3.403E+08 1.955E+08 4.588E+08
4.088E+08 4.367E+08 5.438E+08 2.875E+09

STEP SIZE OF 1.163E-01 IS BASED ON CUT 1

TIME = 1.0E+00 HOURS, MASS FRACTION OF EACH CUT REMAINING:
5.7E-01 8.5E-01 9.6E-01 9.9E-01 1.0E+00 1.0E+00 1.0E+00 1.0E+00 1.0E+00 1.0E+00 1.0E+00 1.0E+00 1.0E+00 1.0E+00
1.0E+00
FRACTION (BASED ON MASS) REMAINING IN THE SLICK = 9.9E-01, AREA = 5.7E+05 M**2

TIME = 2.1E+00 HOURS, MASS FRACTION OF EACH CUT REMAINING:
2.7E-01 6.9E-01 9.2E-01 9.8E-01 1.0E+00 1.0E+00 1.0E+00 1.0E+00 1.0E+00 1.0E+00 1.0E+00 1.0E+00 1.0E+00 1.0E+00
1.0E+00
FRACTION (BASED ON MASS) REMAINING IN THE SLICK = 9.8E-01, AREA = 7.1E+05 M**2

TIME = 3.1E+00 HOURS, MASS FRACTION OF EACH CUT REMAINING:
1.1E-01 5.4E-01 8.6E-01 9.7E-01 9.9E-01 1.0E+00 1.0E+00 1.0E+00 1.0E+00 1.0E+00 1.0E+00 1.0E+00 1.0E+00 1.0E+00
1.0E+00
FRACTION (BASED ON MASS) REMAINING IN THE SLICK = 9.7E-01, AREA = 8.2E+05 M**2

TIME = 4.2E+00 HOURS, MASS FRACTION OF EACH CUT REMAINING:
3.9E-02 4.0E-01 8.1E-01 9.5E-01 9.9E-01 1.0E+00 1.0E+00 1.0E+00 1.0E+00 1.0E+00 1.0E+00 1.0E+00 1.0E+00 1.0E+00

```
1.0E+00
FRACTION (BASED ON MASS) REMAINING IN THE SLICK =  9.6E-01, AREA =  9.1E+05 M**2


TIME =  5.2E+00 HOURS, MASS FRACTION OF EACH CUT REMAINING:
1.2E-02  2.9E-01  7.5E-01  9.4E-01  9.9E-01  1.0E+00  1.0E+00  1.0E+00  1.0E+00  1.0E+00  1.0E+00  1.0E+00  1.0E+00  1.0E+00
1.0E+00
FRACTION (BASED ON MASS) REMAINING IN THE SLICK =  9.6E-01, AREA =  1.0E+06 M**2


STEP SIZE OF  1.500E-01 IS BASED ON CUT   2

TIME =  6.4E+00 HOURS, MASS FRACTION OF EACH CUT REMAINING:
3.1E-03  2.0E-01  6.8E-01  9.2E-01  9.8E-01  1.0E+00  1.0E+00  1.0E+00  1.0E+00  1.0E+00  1.0E+00  1.0E+00  1.0E+00  1.0E+00
1.0E+00
FRACTION (BASED ON MASS) REMAINING IN THE SLICK =  9.5E-01, AREA =  1.1E+06 M**2


TIME =  7.4E+00 HOURS, MASS FRACTION OF EACH CUT REMAINING:
7.9E-04  1.3E-01  6.2E-01  9.0E-01  9.8E-01  1.0E+00  1.0E+00  1.0E+00  1.0E+00  1.0E+00  1.0E+00  1.0E+00  1.0E+00  1.0E+00
1.0E+00
FRACTION (BASED ON MASS) REMAINING IN THE SLICK =  9.5E-01, AREA =  1.2E+06 M**2


TIME =  8.5E+00 HOURS, MASS FRACTION OF EACH CUT REMAINING:
1.8E-04  8.7E-02  5.6E-01  8.8E-01  9.8E-01  1.0E+00  1.0E+00  1.0E+00  1.0E+00  1.0E+00  1.0E+00  1.0E+00  1.0E+00  1.0E+00
1.0E+00
FRACTION (BASED ON MASS) REMAINING IN THE SLICK =  9.5E-01, AREA =  1.2E+06 M**2


TIME =  9.5E+00 HOURS, MASS FRACTION OF EACH CUT REMAINING:
3.8E-05  5.6E-02  5.1E-01  8.6E-01  9.7E-01  1.0E+00  1.0E+00  1.0E+00  1.0E+00  1.0E+00  1.0E+00  1.0E+00  1.0E+00  1.0E+00
1.0E+00
FRACTION (BASED ON MASS) REMAINING IN THE SLICK =  9.4E-01, AREA =  1.3E+06 M**2


TIME =  1.1E+01 HOURS, MASS FRACTION OF EACH CUT REMAINING:
7.3E-06  3.5E-02  4.6E-01  8.4E-01  9.7E-01  9.9E-01  1.0E+00  1.0E+00  1.0E+00  1.0E+00  1.0E+00  1.0E+00  1.0E+00  1.0E+00
1.0E+00
FRACTION (BASED ON MASS) REMAINING IN THE SLICK =  9.4E-01, AREA =  1.3E+06 M**2


TIME =  1.2E+01 HOURS, MASS FRACTION OF EACH CUT REMAINING:
1.3E-06  2.2E-02  4.1E-01  8.2E-01  9.6E-01  9.9E-01  1.0E+00  1.0E+00  1.0E+00  1.0E+00  1.0E+00  1.0E+00  1.0E+00  1.0E+00
1.0E+00
FRACTION (BASED ON MASS) REMAINING IN THE SLICK =  9.4E-01, AREA =  1.4E+06 M**2


TIME =  1.3E+01 HOURS, MASS FRACTION OF EACH CUT REMAINING:
2.1E-07  1.3E-02  3.6E-01  8.0E-01  9.6E-01  9.9E-01  1.0E+00  1.0E+00  1.0E+00  1.0E+00  1.0E+00  1.0E+00  1.0E+00  1.0E+00
1.0E+00
FRACTION (BASED ON MASS) REMAINING IN THE SLICK =  9.4E-01, AREA =  1.5E+06 M**2


TIME =  1.4E+01 HOURS, MASS FRACTION OF EACH CUT REMAINING:
3.2E-08  7.6E-03  3.2E-01  7.8E-01  9.5E-01  9.9E-01  1.0E+00  1.0E+00  1.0E+00  1.0E+00  1.0E+00  1.0E+00  1.0E+00  1.0E+00
1.0E+00
FRACTION (BASED ON MASS) REMAINING IN THE SLICK =  9.3E-01, AREA =  1.5E+06 M**2


TIME =  1.5E+01 HOURS, MASS FRACTION OF EACH CUT REMAINING:
4.4E-09  4.3E-03  2.8E-01  7.6E-01  9.5E-01  9.9E-01  1.0E+00  1.0E+00  1.0E+00  1.0E+00  1.0E+00  1.0E+00  1.0E+00  1.0E+00
1.0E+00
FRACTION (BASED ON MASS) REMAINING IN THE SLICK =  9.3E-01, AREA =  1.6E+06 M**2
```

```
STEP SIZE OF  3.835E-01 IS BASED ON CUT   3

TIME =  1.6E+01 HOURS, MASS FRACTION OF EACH CUT REMAINING:
0.0E+00  2.1E-03  2.4E-01  7.3E-01  9.4E-01  9.9E-01  1.0E+00  1.0E+00  1.0E+00  1.0E+00  1.0E+00  1.0E+00  1.0E+00  1.0E+00
1.0E+00
FRACTION (BASED ON MASS) REMAINING IN THE SLICK =  9.3E-01, AREA =  1.6E+06 M**2


TIME =  1.7E+01 HOURS, MASS FRACTION OF EACH CUT REMAINING:
0.0E+00  1.1E-03  2.0E-01  7.1E-01  9.3E-01  9.9E-01  1.0E+00  1.0E+00  1.0E+00  1.0E+00  1.0E+00  1.0E+00  1.0E+00  1.0E+00
1.0E+00
FRACTION (BASED ON MASS) REMAINING IN THE SLICK =  9.3E-01, AREA =  1.7E+06 M**2


TIME =  1.8E+01 HOURS, MASS FRACTION OF EACH CUT REMAINING:
0.0E+00  5.6E-04  1.7E-01  6.8E-01  9.3E-01  9.9E-01  1.0E+00  1.0E+00  1.0E+00  1.0E+00  1.0E+00  1.0E+00  1.0E+00  1.0E+00
1.0E+00
FRACTION (BASED ON MASS) REMAINING IN THE SLICK =  9.3E-01, AREA =  1.7E+06 M**2


TIME =  2.0E+01 HOURS, MASS FRACTION OF EACH CUT REMAINING:
0.0E+00  2.8E-04  1.5E-01  6.6E-01  9.2E-01  9.9E-01  1.0E+00  1.0E+00  1.0E+00  1.0E+00  1.0E+00  1.0E+00  1.0E+00  1.0E+00
1.0E+00
FRACTION (BASED ON MASS) REMAINING IN THE SLICK =  9.2E-01, AREA =  1.8E+06 M**2


TIME =  2.1E+01 HOURS, MASS FRACTION OF EACH CUT REMAINING:
0.0E+00  1.3E-04  1.2E-01  6.4E-01  9.1E-01  9.8E-01  1.0E+00  1.0E+00  1.0E+00  1.0E+00  1.0E+00  1.0E+00  1.0E+00  1.0E+00
1.0E+00
FRACTION (BASED ON MASS) REMAINING IN THE SLICK =  9.2E-01, AREA =  1.8E+06 M**2


TIME =  2.2E+01 HOURS, MASS FRACTION OF EACH CUT REMAINING:
0.0E+00  6.4E-05  1.0E-01  6.1E-01  9.1E-01  9.8E-01  1.0E+00  1.0E+00  1.0E+00  1.0E+00  1.0E+00  1.0E+00  1.0E+00  1.0E+00
1.0E+00
FRACTION (BASED ON MASS) REMAINING IN THE SLICK =  9.2E-01, AREA =  1.9E+06 M**2


TIME =  2.3E+01 HOURS, MASS FRACTION OF EACH CUT REMAINING:
0.0E+00  3.0E-05  8.6E-02  5.9E-01  9.0E-01  9.8E-01  1.0E+00  1.0E+00  1.0E+00  1.0E+00  1.0E+00  1.0E+00  1.0E+00  1.0E+00
1.0E+00
FRACTION (BASED ON MASS) REMAINING IN THE SLICK =  9.2E-01, AREA =  1.9E+06 M**2


TIME =  2.4E+01 HOURS, MASS FRACTION OF EACH CUT REMAINING:
0.0E+00  1.4E-05  7.2E-02  5.7E-01  8.9E-01  9.8E-01  1.0E+00  1.0E+00  1.0E+00  1.0E+00  1.0E+00  1.0E+00  1.0E+00  1.0E+00
1.0E+00
FRACTION (BASED ON MASS) REMAINING IN THE SLICK =  9.2E-01, AREA =  1.9E+06 M**2


TIME =  2.5E+01 HOURS, MASS FRACTION OF EACH CUT REMAINING:
0.0E+00  6.1E-06  5.9E-02  5.4E-01  8.9E-01  9.8E-01  1.0E+00  1.0E+00  1.0E+00  1.0E+00  1.0E+00  1.0E+00  1.0E+00  1.0E+00
1.0E+00
FRACTION (BASED ON MASS) REMAINING IN THE SLICK =  9.2E-01, AREA =  2.0E+06 M**2


TIME =  2.6E+01 HOURS, MASS FRACTION OF EACH CUT REMAINING:
0.0E+00  2.7E-06  4.9E-02  5.2E-01  8.8E-01  9.8E-01  1.0E+00  1.0E+00  1.0E+00  1.0E+00  1.0E+00  1.0E+00  1.0E+00  1.0E+00
1.0E+00
FRACTION (BASED ON MASS) REMAINING IN THE SLICK =  9.1E-01, AREA =  2.0E+06 M**2


TIME =  2.6E+01 HOURS, MASS FRACTION OF EACH CUT REMAINING:
0.0E+00  1.1E-06  4.0E-02  5.0E-01  8.7E-01  9.8E-01  1.0E+00  1.0E+00  1.0E+00  1.0E+00  1.0E+00  1.0E+00  1.0E+00  1.0E+00
```

1.0E+00
FRACTION (BASED ON MASS) REMAINING IN THE SLICK = 9.1E-01, AREA = 2.1E+06 M**2

TIME = 2.9E+01 HOURS, MASS FRACTION OF EACH CUT REMAINING:
0.0E+00 4.9E-07 3.3E-02 4.0E-01 8.6E-01 9.8E-01 1.0E+00 1.0E+00 1.0E+00 1.0E+00 1.0E+00 1.0E+00 1.0E+00 1.0E+00
1.0E+00
FRACTION (BASED ON MASS) REMAINING IN THE SLICK = 9.1E-01, AREA = 2.1E+06 M**2

TIME = 3.0E+01 HOURS, MASS FRACTION OF EACH CUT REMAINING:
0.0E+00 2.0E-07 2.7E-02 4.6E-01 8.6E-01 9.7E-01 1.0E+00 1.0E+00 1.0E+00 1.0E+00 1.0E+00 1.0E+00 1.0E+00 1.0E+00
1.0E+00
FRACTION (BASED ON MASS) REMAINING IN THE SLICK = 9.1E-01, AREA = 2.2E+06 M**2

TIME = 3.1E+01 HOURS, MASS FRACTION OF EACH CUT REMAINING:
0.0E+00 8.2E-08 2.2E-02 4.4E-01 8.5E-01 9.7E-01 1.0E+00 1.0E+00 1.0E+00 1.0E+00 1.0E+00 1.0E+00 1.0E+00 1.0E+00
1.0E+00
FRACTION (BASED ON MASS) REMAINING IN THE SLICK = 9.1E-01, AREA = 2.2E+06 M**2

TIME = 3.2E+01 HOURS, MASS FRACTION OF EACH CUT REMAINING:
0.0E+00 3.3E-08 1.7E-02 4.2E-01 8.4E-01 9.7E-01 1.0E+00 1.0E+00 1.0E+00 1.0E+00 1.0E+00 1.0E+00 1.0E+00 1.0E+00
1.0E+00
FRACTION (BASED ON MASS) REMAINING IN THE SLICK = 9.1E-01, AREA = 2.2E+06 M**2

TIME = 3.3E+01 HOURS, MASS FRACTION OF EACH CUT REMAINING:
0.0E+00 1.3E-08 1.4E-02 4.0E-01 8.3E-01 9.7E-01 9.9E-01 1.0E+00 1.0E+00 1.0E+00 1.0E+00 1.0E+00 1.0E+00 1.0E+00
1.0E+00
FRACTION (BASED ON MASS) REMAINING IN THE SLICK = 9.1E-01, AREA = 2.3E+06 M**2

TIME = 3.4E+01 HOURS, MASS FRACTION OF EACH CUT REMAINING:
0.0E+00 5.0E-09 1.1E-02 3.8E-01 8.3E-01 9.7E-01 9.9E-01 1.0E+00 1.0E+00 1.0E+00 1.0E+00 1.0E+00 1.0E+00 1.0E+00
1.0E+00
FRACTION (BASED ON MASS) REMAINING IN THE SLICK = 9.1E-01, AREA = 2.3E+06 M**2

TIME = 3.6E+01 HOURS, MASS FRACTION OF EACH CUT REMAINING:
0.0E+00 0.0E+00 8.9E-03 3.6E-01 8.2E-01 9.7E-01 9.9E-01 1.0E+00 1.0E+00 1.0E+00 1.0E+00 1.0E+00 1.0E+00 1.0E+00
1.0E+00
FRACTION (BASED ON MASS) REMAINING IN THE SLICK = 9.1E-01, AREA = 2.3E+06 M**2

TIME = 3.7E+01 HOURS, MASS FRACTION OF EACH CUT REMAINING:
0.0E+00 0.0E+00 7.1E-03 3.4E-01 8.1E-01 9.6E-01 9.9E-01 1.0E+00 1.0E+00 1.0E+00 1.0E+00 1.0E+00 1.0E+00 1.0E+00
1.0E+00
FRACTION (BASED ON MASS) REMAINING IN THE SLICK = 9.0E-01, AREA = 2.4E+06 M**2

TIME = 3.8E+01 HOURS, MASS FRACTION OF EACH CUT REMAINING:
0.0E+00 0.0E+00 5.6E-03 3.3E-01 8.0E-01 9.6E-01 9.9E-01 1.0E+00 1.0E+00 1.0E+00 1.0E+00 1.0E+00 1.0E+00 1.0E+00
1.0E+00
FRACTION (BASED ON MASS) REMAINING IN THE SLICK = 9.0E-01, AREA = 2.4E+06 M**2

TIME = 3.9E+01 HOURS, MASS FRACTION OF EACH CUT REMAINING:
0.0E+00 0.0E+00 4.4E-03 3.1E-01 7.9E-01 9.6E-01 9.9E-01 1.0E+00 1.0E+00 1.0E+00 1.0E+00 1.0E+00 1.0E+00 1.0E+00
1.0E+00
FRACTION (BASED ON MASS) REMAINING IN THE SLICK = 9.0E-01, AREA = 2.4E+06 M**2

TIME = 4.0E+01 HOURS, MASS FRACTION OF EACH CUT REMAINING:
0.0E+00 0.0E+00 3.5E-03 2.9E-01 7.9E-01 9.6E-01 9.9E-01 1.0E+00 1.0E+00 1.0E+00 1.0E+00 1.0E+00 1.0E+00 1.0E+00

```
TIME =  1.0E+02 HOURS, MASS FRACTION OF EACH CUT REMAINING:
0.0E+00  0.0E+00  9.4E-11  6.8E-03  3.7E-01  8.1E-01  9.7E-01  1.0E+00  1.0E+00  1.0E+00  1.0E+00  1.0E+00  1.0E+00  1.0E+00
1.0E+00
FRACTION (BASED ON MASS) REMAINING IN THE SLICK =  8.7E-01, AREA =  3.8E+06 M**2


STEP SIZE OF  3.222E+00 IS BASED ON CUT   5

TIME =  1.5E+02 HOURS, MASS FRACTION OF EACH CUT REMAINING:
0.0E+00  0.0E+00  0.0E+00  9.4E-05  1.6E-01  7.3E-01  9.5E-01  9.9E-01  1.0E+00  1.0E+00  1.0E+00  1.0E+00  1.0E+00  1.0E+00
1.0E+00
FRACTION (BASED ON MASS) REMAINING IN THE SLICK =  8.6E-01, AREA =  4.6E+06 M**2


TIME =  2.1E+02 HOURS, MASS FRACTION OF EACH CUT REMAINING:
0.0E+00  0.0E+00  0.0E+00  5.6E-07  5.9E-02  6.1E-01  9.2E-01  9.9E-01  1.0E+00  1.0E+00  1.0E+00  1.0E+00  1.0E+00  1.0E+00
1.0E+00
FRACTION (BASED ON MASS) REMAINING IN THE SLICK =  8.5E-01, AREA =  5.3E+06 M**2


TIME =  2.6E+02 HOURS, MASS FRACTION OF EACH CUT REMAINING:
0.0E+00  0.0E+00  0.0E+00  1.6E-09  1.9E-02  5.6E-01  9.0E-01  9.8E-01  1.0E+00  1.0E+00  1.0E+00  1.0E+00  1.0E+00  1.0E+00
1.0E+00
FRACTION (BASED ON MASS) REMAINING IN THE SLICK =  8.5E-01, AREA =  5.9E+06 M**2


TIME =  3.1E+02 HOURS, MASS FRACTION OF EACH CUT REMAINING:
0.0E+00  0.0E+00  0.0E+00  0.0E+00  5.2E-03  4.0E-01  8.6E-01  9.8E-01  1.0E+00  1.0E+00  1.0E+00  1.0E+00  1.0E+00  1.0E+00
1.0E+00
FRACTION (BASED ON MASS) REMAINING IN THE SLICK =  8.4E-01, AREA =  6.4E+06 M**2


STEP SIZE OF  1.078E+01 IS BASED ON CUT   6

TIME =  3.6E+02 HOURS, MASS FRACTION OF EACH CUT REMAINING:
0.0E+00  0.0E+00  0.0E+00  0.0E+00  1.2E-03  3.1E-01  8.3E-01  9.7E-01  1.0E+00  1.0E+00  1.0E+00  1.0E+00  1.0E+00  1.0E+00
1.0E+00
FRACTION (BASED ON MASS) REMAINING IN THE SLICK =  8.4E-01, AREA =  6.9E+06 M**2


TIME =  4.2E+02 HOURS, MASS FRACTION OF EACH CUT REMAINING:
0.0E+00  0.0E+00  0.0E+00  0.0E+00  2.4E-04  2.4E-01  7.9E-01  9.7E-01  1.0E+00  1.0E+00  1.0E+00  1.0E+00  1.0E+00  1.0E+00
1.0E+00
FRACTION (BASED ON MASS) REMAINING IN THE SLICK =  8.3E-01, AREA =  7.4E+06 M**2


TIME =  4.7E+02 HOURS, MASS FRACTION OF EACH CUT REMAINING:
0.0E+00  0.0E+00  0.0E+00  0.0E+00  4.5E-05  1.0E-01  7.6E-01  9.6E-01  9.9E-01  1.0E+00  1.0E+00  1.0E+00  1.0E+00  1.0E+00
1.0E+00
FRACTION (BASED ON MASS) REMAINING IN THE SLICK =  8.3E-01, AREA =  7.9E+06 M**2


THE FINAL MASS FRACTIONS FOR THE SLICK AT  5.0E+02 HOURS ARE:
 0.000E+00  0.000E+00  0.000E+00  0.000E+00  1.071E-05  1.308E-01  7.274E-01  9.549E-01  9.935E-01  9.995E-01  1.000E+00
 1.000E+00  1.000E+00  1.000E+00  1.000E+00
 FRACTION (BASED ON MASS) REMAINING IN THE SLICK =  8.3E-01, AREA =  8.2E+06 M**2

*****************************************************************
```

CRUDE OIL CHARACTERIZATION AND PSEUDOCOMPONENT EVAPORATION MODEL
IDENTIFICATION: PRUDHOE BAY, ITEM 9, SAMPLE 71011

VAPOR PRESSURE IN ATMOSPHERES AT 4.200E+01 DEG F

	VP
1	5.192E-02
2	1.655E-02
3	3.968E-03
4	9.029E-04
5	1.878E-04
6	3.495E-05
7	5.868E-06
8	9.034E-07
9	1.356E-07
10	1.160E-08
11	5.655E-10
12	9.681E-11
13	1.297E-12
14	4.340E-14

MEAN MOLECULAR WEIGHT OF THE CRUDE = 2.730E+02

OVER-ALL MASS-TRANSFER COEFFICIENTS

WIND SPEED = 4.000E+01 KNOTS, OR 7.412E+04 M/HR
INITIAL SLICK DIAMETER = 7.116E+02 M, OR AREA = 3.976E+05 M**2

OVER-ALL MASS-TRANSFER COEFFICIENT FOR CUMENE = 4.380E+01 M/HR

CUT	M/HR	G-MOLES/(HR)(ATM)(M**2)	SPGR OF CUT
1	4.903E+01	2.147E+03	6.929E-01
2	4.830E+01	2.114E+03	7.230E-01
3	4.771E+01	2.089E+03	7.519E-01
4	4.718E+01	2.066E+03	7.728E-01
5	4.671E+01	2.045E+03	7.901E-01
6	4.628E+01	2.026E+03	8.008E-01
7	4.594E+01	2.011E+03	8.179E-01
8	4.564E+01	1.998E+03	8.358E-01
9	4.541E+01	1.988E+03	8.509E-01
10	4.513E+01	1.976E+03	8.729E-01
11	4.481E+01	1.962E+03	8.811E-01
12	4.469E+01	1.957E+03	8.973E-01
13	4.440E+01	1.944E+03	9.100E-01
14	4.423E+01	1.936E+03	9.188E-01

FOR THIS SPILL OF 5.000E+04 BARRELS, THE MASS IS 7.062E+03 METRIC TONNES

VOLUME FROM SUMMING THE CUTS = 7.9E+03 M**3, OR 5.000E+04 BARRELS

KINEMATIC VISCOSITY OF THE BULK CRUDE FROM THE CUTS = 4.0E+00 CENTISTOKES AT 122 DEG F

KINEMATIC VISCOSITY OF THE BULK CRUDE FROM THE CUTS = 8.1E+00 AT T = 42.0 DEG F

COUNT THE CUTS IN THE FOLLOWING OUTPUT FROM LEFT TO RIGHT

THE INITIAL MOLES IN THE SLICK ARE:
1.305E+06 1.401E+06 1.840E+06 1.741E+06 1.634E+06 1.395E+06 1.581E+06 1.637E+06 1.601E+06 8.267E+05 1.683E+06
1.699E+06 1.305E+06 1.466E+06 4.791E+06

THE INITIAL MASSES IN THE SLICK ARE:
1.164E+08 1.504E+08 2.185E+08 2.225E+08 2.338E+08 2.242E+08 2.813E+08 3.209E+08 3.403E+08 1.955E+08 4.580E+08
4.880E+08 4.367E+08 5.430E+08 2.875E+09

CUT 1 GOES AWAY IN MINUTES, THEREFORE IT WAS DELETED AND THE CUTS RENUMBERED

STEP SIZE OF 9.445E-02 IS BASED ON CUT 1

TIME = 1.0E+00 HOURS, MASS FRACTION OF EACH CUT REMAINING:
5.1E-01 8.4E-01 9.6E-01 9.9E-01 1.0E+00 1.0E+00 1.0E+00 1.0E+00 1.0E+00 1.0E+00 1.0E+00 1.0E+00 1.0E+00
FRACTION (BASED ON MASS) REMAINING IN THE SLICK = 9.7E-01, AREA = 5.6E+05 M**2

TIME = 2.1E+00 HOURS, MASS FRACTION OF EACH CUT REMAINING:
2.1E-01 6.7E-01 9.1E-01 9.8E-01 1.0E+00 1.0E+00 1.0E+00 1.0E+00 1.0E+00 1.0E+00 1.0E+00 1.0E+00 1.0E+00
FRACTION (BASED ON MASS) REMAINING IN THE SLICK = 9.5E-01, AREA = 6.9E+05 M**2

TIME = 3.1E+00 HOURS, MASS FRACTION OF EACH CUT REMAINING:
6.0E-02 5.1E-01 8.6E-01 9.7E-01 9.9E-01 1.0E+00 1.0E+00 1.0E+00 1.0E+00 1.0E+00 1.0E+00 1.0E+00 1.0E+00
FRACTION (BASED ON MASS) REMAINING IN THE SLICK = 9.4E-01, AREA = 8.0E+05 M**2

TIME = 4.2E+00 HOURS, MASS FRACTION OF EACH CUT REMAINING:
1.9E-02 3.7E-01 8.0E-01 9.5E-01 9.9E-01 1.0E+00 1.0E+00 1.0E+00 1.0E+00 1.0E+00 1.0E+00 1.0E+00 1.0E+00
FRACTION (BASED ON MASS) REMAINING IN THE SLICK = 9.4E-01, AREA = 8.9E+05 M**2

STEP SIZE OF 1.447E-01 IS BASED ON CUT 2

TIME = 5.2E+00 HOURS, MASS FRACTION OF EACH CUT REMAINING:
4.9E-03 2.6E-01 7.4E-01 9.4E-01 9.9E-01 1.0E+00 1.0E+00 1.0E+00 1.0E+00 1.0E+00 1.0E+00 1.0E+00 1.0E+00
FRACTION (BASED ON MASS) REMAINING IN THE SLICK = 9.3E-01, AREA = 9.7E+05 M**2

TIME = 6.2E+00 HOURS, MASS FRACTION OF EACH CUT REMAINING:
1.1E-03 1.8E-01 6.8E-01 9.2E-01 9.9E-01 1.0E+00 1.0E+00 1.0E+00 1.0E+00 1.0E+00 1.0E+00 1.0E+00 1.0E+00
FRACTION (BASED ON MASS) REMAINING IN THE SLICK = 9.2E-01, AREA = 1.0E+06 M**2

TIME = 7.2E+00 HOURS, MASS FRACTION OF EACH CUT REMAINING:
2.1E-04 1.2E-01 6.2E-01 9.1E-01 9.8E-01 1.0E+00 1.0E+00 1.0E+00 1.0E+00 1.0E+00 1.0E+00 1.0E+00 1.0E+00
FRACTION (BASED ON MASS) REMAINING IN THE SLICK = 9.2E-01, AREA = 1.1E+06 M**2

TIME = 8.2E+00 HOURS, MASS FRACTION OF EACH CUT REMAINING:
3.7E-05 7.6E-02 5.6E-01 8.9E-01 9.8E-01 1.0E+00 1.0E+00 1.0E+00 1.0E+00 1.0E+00 1.0E+00 1.0E+00 1.0E+00
FRACTION (BASED ON MASS) REMAINING IN THE SLICK = 9.2E-01, AREA = 1.2E+06 M**2

TIME = 9.2E+00 HOURS, MASS FRACTION OF EACH CUT REMAINING:
5.0E-06 4.8E-02 5.0E-01 8.7E-01 9.7E-01 1.0E+00 1.0E+00 1.0E+00 1.0E+00 1.0E+00 1.0E+00 1.0E+00 1.0E+00
FRACTION (BASED ON MASS) REMAINING IN THE SLICK = 9.1E-01, AREA = 1.2E+06 M**2

TIME = 1.0E+01 HOURS, MASS FRACTION OF EACH CUT REMAINING:
8.3E-07 2.9E-02 4.5E-01 8.5E-01 9.7E-01 9.9E-01 1.0E+00 1.0E+00 1.0E+00 1.0E+00 1.0E+00 1.0E+00 1.0E+00
FRACTION (BASED ON MASS) REMAINING IN THE SLICK = 9.1E-01, AREA = 1.3E+06 M**2

TIME = 1.1E+01 HOURS, MASS FRACTION OF EACH CUT REMAINING:
1.1E-07 1.7E-02 4.0E-01 8.3E-01 9.7E-01 9.9E-01 1.0E+00 1.0E+00 1.0E+00 1.0E+00 1.0E+00 1.0E+00 1.0E+00
FRACTION (BASED ON MASS) REMAINING IN THE SLICK = 9.1E-01, AREA = 1.3E+06 M**2

TIME = 1.2E+01 HOURS, MASS FRACTION OF EACH CUT REMAINING:
1.2E-08 1.0E-02 3.6E-01 8.1E-01 9.6E-01 9.9E-01 1.0E+00 1.0E+00 1.0E+00 1.0E+00 1.0E+00 1.0E+00 1.0E+00
FRACTION (BASED ON MASS) REMAINING IN THE SLICK = 9.1E-01, AREA = 1.4E+06 M**2

TIME = 1.3E+01 HOURS, MASS FRACTION OF EACH CUT REMAINING:
1.3E-09 5.8E-03 3.1E-01 7.9E-01 9.6E-01 9.9E-01 1.0E+00 1.0E+00 1.0E+00 1.0E+00 1.0E+00 1.0E+00 1.0E+00
FRACTION (BASED ON MASS) REMAINING IN THE SLICK = 9.0E-01, AREA = 1.5E+06 M**2

TIME = 1.4E+01 HOURS, MASS FRACTION OF EACH CUT REMAINING:
0.0E+00 3.2E-03 2.7E-01 7.7E-01 9.5E-01 9.9E-01 1.0E+00 1.0E+00 1.0E+00 1.0E+00 1.0E+00 1.0E+00 1.0E+00
FRACTION (BASED ON MASS) REMAINING IN THE SLICK = 9.0E-01, AREA = 1.5E+06 M**2

STEP SIZE OF 3.759E-01 IS BASED ON CUT 3

TIME = 1.6E+01 HOURS, MASS FRACTION OF EACH CUT REMAINING:
0.0E+00 1.5E-03 2.3E-01 7.4E-01 9.5E-01 9.9E-01 1.0E+00 1.0E+00 1.0E+00 1.0E+00 1.0E+00 1.0E+00 1.0E+00
FRACTION (BASED ON MASS) REMAINING IN THE SLICK = 9.0E-01, AREA = 1.6E+06 M**2

TIME = 1.7E+01 HOURS, MASS FRACTION OF EACH CUT REMAINING:
0.0E+00 7.4E-04 2.0E-01 7.2E-01 9.4E-01 9.9E-01 1.0E+00 1.0E+00 1.0E+00 1.0E+00 1.0E+00 1.0E+00 1.0E+00
FRACTION (BASED ON MASS) REMAINING IN THE SLICK = 9.0E-01, AREA = 1.6E+06 M**2

TIME = 1.8E+01 HOURS, MASS FRACTION OF EACH CUT REMAINING:
0.0E+00 3.6E-04 1.7E-01 6.9E-01 9.4E-01 9.9E-01 1.0E+00 1.0E+00 1.0E+00 1.0E+00 1.0E+00 1.0E+00 1.0E+00 1.0E+00
FRACTION (BASED ON MASS) REMAINING IN THE SLICK = 8.9E-01, AREA = 1.7E+06 M**2

TIME = 1.9E+01 HOURS, MASS FRACTION OF EACH CUT REMAINING:
0.0E+00 1.7E-04 1.4E-01 6.7E-01 9.3E-01 9.9E-01 1.0E+00 1.0E+00 1.0E+00 1.0E+00 1.0E+00 1.0E+00 1.0E+00 1.0E+00
FRACTION (BASED ON MASS) REMAINING IN THE SLICK = 8.9E-01, AREA = 1.7E+06 M**2

TIME = 2.0E+01 HOURS, MASS FRACTION OF EACH CUT REMAINING:
0.0E+00 7.8E-05 1.2E-01 6.4E-01 9.2E-01 9.9E-01 1.0E+00 1.0E+00 1.0E+00 1.0E+00 1.0E+00 1.0E+00 1.0E+00 1.0E+00
FRACTION (BASED ON MASS) REMAINING IN THE SLICK = 8.9E-01, AREA = 1.7E+06 M**2

TIME = 2.1E+01 HOURS, MASS FRACTION OF EACH CUT REMAINING:
0.0E+00 3.5E-05 9.9E-02 6.2E-01 9.2E-01 9.9E-01 1.0E+00 1.0E+00 1.0E+00 1.0E+00 1.0E+00 1.0E+00 1.0E+00 1.0E+00
FRACTION (BASED ON MASS) REMAINING IN THE SLICK = 8.9E-01, AREA = 1.8E+06 M**2

TIME = 2.2E+01 HOURS, MASS FRACTION OF EACH CUT REMAINING:
0.0E+00 1.5E-05 8.3E-02 6.0E-01 9.1E-01 9.9E-01 1.0E+00 1.0E+00 1.0E+00 1.0E+00 1.0E+00 1.0E+00 1.0E+00 1.0E+00
FRACTION (BASED ON MASS) REMAINING IN THE SLICK = 8.9E-01, AREA = 1.8E+06 M**2

TIME = 2.3E+01 HOURS, MASS FRACTION OF EACH CUT REMAINING:
0.0E+00 6.6E-06 6.8E-02 5.8E-01 9.0E-01 9.8E-01 1.0E+00 1.0E+00 1.0E+00 1.0E+00 1.0E+00 1.0E+00 1.0E+00 1.0E+00
FRACTION (BASED ON MASS) REMAINING IN THE SLICK = 8.9E-01, AREA = 1.9E+06 M**2

TIME = 2.5E+01 HOURS, MASS FRACTION OF EACH CUT REMAINING:
0.0E+00 2.8E-06 5.6E-02 5.5E-01 9.0E-01 9.8E-01 1.0E+00 1.0E+00 1.0E+00 1.0E+00 1.0E+00 1.0E+00 1.0E+00 1.0E+00
FRACTION (BASED ON MASS) REMAINING IN THE SLICK = 8.8E-01, AREA = 1.9E+06 M**2

TIME = 2.6E+01 HOURS, MASS FRACTION OF EACH CUT REMAINING:
0.0E+00 1.2E-06 4.6E-02 5.3E-01 8.9E-01 9.8E-01 1.0E+00 1.0E+00 1.0E+00 1.0E+00 1.0E+00 1.0E+00 1.0E+00 1.0E+00
FRACTION (BASED ON MASS) REMAINING IN THE SLICK = 8.8E-01, AREA = 2.0E+06 M**2

TIME = 2.7E+01 HOURS, MASS FRACTION OF EACH CUT REMAINING:
0.0E+00 4.7E-07 3.8E-02 5.1E-01 8.8E-01 9.8E-01 1.0E+00 1.0E+00 1.0E+00 1.0E+00 1.0E+00 1.0E+00 1.0E+00 1.0E+00
FRACTION (BASED ON MASS) REMAINING IN THE SLICK = 8.8E-01, AREA = 2.0E+06 M**2

TIME = 2.8E+01 HOURS, MASS FRACTION OF EACH CUT REMAINING:
0.0E+00 1.9E-07 3.1E-02 4.9E-01 8.8E-01 9.8E-01 1.0E+00 1.0E+00 1.0E+00 1.0E+00 1.0E+00 1.0E+00 1.0E+00 1.0E+00
FRACTION (BASED ON MASS) REMAINING IN THE SLICK = 8.8E-01, AREA = 2.0E+06 M**2

TIME = 2.9E+01 HOURS, MASS FRACTION OF EACH CUT REMAINING:
0.0E+00 7.2E-08 2.5E-02 4.7E-01 8.7E-01 9.8E-01 1.0E+00 1.0E+00 1.0E+00 1.0E+00 1.0E+00 1.0E+00 1.0E+00 1.0E+00
FRACTION (BASED ON MASS) REMAINING IN THE SLICK = 8.8E-01, AREA = 2.1E+06 M**2

TIME = 3.0E+01 HOURS, MASS FRACTION OF EACH CUT REMAINING:
0.0E+00 2.8E-08 2.0E-02 4.5E-01 8.6E-01 9.8E-01 1.0E+00 1.0E+00 1.0E+00 1.0E+00 1.0E+00 1.0E+00 1.0E+00 1.0E+00
FRACTION (BASED ON MASS) REMAINING IN THE SLICK = 8.8E-01, AREA = 2.1E+06 M**2

TIME = 3.1E+01 HOURS, MASS FRACTION OF EACH CUT REMAINING:
0.0E+00 1.0E-08 1.6E-02 4.3E-01 8.6E-01 9.7E-01 1.0E+00 1.0E+00 1.0E+00 1.0E+00 1.0E+00 1.0E+00 1.0E+00 1.0E+00
FRACTION (BASED ON MASS) REMAINING IN THE SLICK = 8.8E-01, AREA = 2.1E+06 M**2

TIME = 3.2E+01 HOURS, MASS FRACTION OF EACH CUT REMAINING:
0.0E+00 3.8E-09 1.3E-02 4.1E-01 8.5E-01 9.7E-01 1.0E+00 1.0E+00 1.0E+00 1.0E+00 1.0E+00 1.0E+00 1.0E+00 1.0E+00
FRACTION (BASED ON MASS) REMAINING IN THE SLICK = 8.8E-01, AREA = 2.2E+06 M**2

TIME = 3.4E+01 HOURS, MASS FRACTION OF EACH CUT REMAINING:
0.0E+00 0.0E+00 1.0E-02 3.9E-01 8.4E-01 9.7E-01 1.0E+00 1.0E+00 1.0E+00 1.0E+00 1.0E+00 1.0E+00 1.0E+00 1.0E+00
FRACTION (BASED ON MASS) REMAINING IN THE SLICK = 8.8E-01, AREA = 2.2E+06 M**2

TIME = 3.5E+01 HOURS, MASS FRACTION OF EACH CUT REMAINING:
0.0E+00 0.0E+00 8.1E-03 3.7E-01 8.4E-01 9.7E-01 1.0E+00 1.0E+00 1.0E+00 1.0E+00 1.0E+00 1.0E+00 1.0E+00 1.0E+00
FRACTION (BASED ON MASS) REMAINING IN THE SLICK = 8.7E-01, AREA = 2.2E+06 M**2

TIME = 3.6E+01 HOURS, MASS FRACTION OF EACH CUT REMAINING:
0.0E+00 0.0E+00 6.4E-03 3.5E-01 8.3E-01 9.7E-01 1.0E+00 1.0E+00 1.0E+00 1.0E+00 1.0E+00 1.0E+00 1.0E+00 1.0E+00
FRACTION (BASED ON MASS) REMAINING IN THE SLICK = 8.7E-01, AREA = 2.3E+06 M**2

TIME = 3.7E+01 HOURS, MASS FRACTION OF EACH CUT REMAINING:
0.0E+00 0.0E+00 5.0E-03 3.4E-01 8.2E-01 9.7E-01 9.9E-01 1.0E+00 1.0E+00 1.0E+00 1.0E+00 1.0E+00 1.0E+00 1.0E+00
FRACTION (BASED ON MASS) REMAINING IN THE SLICK = 8.7E-01, AREA = 2.3E+06 M**2

TIME = 3.8E+01 HOURS, MASS FRACTION OF EACH CUT REMAINING:
0.0E+00 0.0E+00 3.9E-03 3.2E-01 8.1E-01 9.7E-01 9.9E-01 1.0E+00 1.0E+00 1.0E+00 1.0E+00 1.0E+00 1.0E+00 1.0E+00
FRACTION (BASED ON MASS) REMAINING IN THE SLICK = 8.7E-01, AREA = 2.3E+06 M**2

TIME = 3.9E+01 HOURS, MASS FRACTION OF EACH CUT REMAINING:
0.0E+00 0.0E+00 3.1E-03 3.0E-01 8.1E-01 9.6E-01 9.9E-01 1.0E+00 1.0E+00 1.0E+00 1.0E+00 1.0E+00 1.0E+00 1.0E+00
FRACTION (BASED ON MASS) REMAINING IN THE SLICK = 8.7E-01, AREA = 2.4E+06 M**2

STEP SIZE OF 1.087E+00 IS BASED ON CUT 4

TIME = 4.1E+01 HOURS, MASS FRACTION OF EACH CUT REMAINING:
0.0E+00 0.0E+00 2.0E-03 2.8E-01 7.9E-01 9.6E-01 9.9E-01 1.0E+00 1.0E+00 1.0E+00 1.0E+00 1.0E+00 1.0E+00 1.0E+00
FRACTION (BASED ON MASS) REMAINING IN THE SLICK = 8.7E-01, AREA = 2.4E+06 M**2

TIME = 4.2E+01 HOURS, MASS FRACTION OF EACH CUT REMAINING:
0.0E+00 0.0E+00 1.6E-03 2.6E-01 7.9E-01 9.6E-01 9.9E-01 1.0E+00 1.0E+00 1.0E+00 1.0E+00 1.0E+00 1.0E+00 1.0E+00
FRACTION (BASED ON MASS) REMAINING IN THE SLICK = 8.7E-01, AREA = 2.5E+06 M**2

TIME = 4.3E+01 HOURS, MASS FRACTION OF EACH CUT REMAINING:
0.0E+00 0.0E+00 1.2E-03 2.5E-01 7.8E-01 9.6E-01 9.9E-01 1.0E+00 1.0E+00 1.0E+00 1.0E+00 1.0E+00 1.0E+00 1.0E+00
FRACTION (BASED ON MASS) REMAINING IN THE SLICK = 8.7E-01, AREA = 2.5E+06 M**2

TIME = 4.4E+01 HOURS, MASS FRACTION OF EACH CUT REMAINING:
0.0E+00 0.0E+00 9.5E-04 2.4E-01 7.7E-01 9.6E-01 9.9E-01 1.0E+00 1.0E+00 1.0E+00 1.0E+00 1.0E+00 1.0E+00 1.0E+00
FRACTION (BASED ON MASS) REMAINING IN THE SLICK = 8.7E-01, AREA = 2.5E+06 M**2

TIME = 4.5E+01 HOURS, MASS FRACTION OF EACH CUT REMAINING:
0.0E+00 0.0E+00 7.4E-04 2.3E-01 7.6E-01 9.6E-01 9.9E-01 1.0E+00 1.0E+00 1.0E+00 1.0E+00 1.0E+00 1.0E+00 1.0E+00
FRACTION (BASED ON MASS) REMAINING IN THE SLICK = 8.7E-01, AREA = 2.5E+06 M**2

TIME = 4.7E+01 HOURS, MASS FRACTION OF EACH CUT REMAINING:
0.0E+00 0.0E+00 5.7E-04 2.1E-01 7.6E-01 9.5E-01 9.9E-01 1.0E+00 1.0E+00 1.0E+00 1.0E+00 1.0E+00 1.0E+00 1.0E+00

FRACTION (BASED ON MASS) REMAINING IN THE SLICK = 8.7E-01, AREA = 2.6E+06 M**2

TIME = 4.8E+01 HOURS, MASS FRACTION OF EACH CUT REMAINING:
0.0E+00 0.0E+00 4.4E-04 2.0E-01 7.5E-01 9.5E-01 9.9E-01 1.0E+00 1.0E+00 1.0E+00 1.0E+00 1.0E+00 1.0E+00 1.0E+00
FRACTION (BASED ON MASS) REMAINING IN THE SLICK = 8.6E-01, AREA = 2.6E+06 M**2

TIME = 4.9E+01 HOURS, MASS FRACTION OF EACH CUT REMAINING:
0.0E+00 0.0E+00 3.3E-04 1.9E-01 7.4E-01 9.5E-01 9.9E-01 1.0E+00 1.0E+00 1.0E+00 1.0E+00 1.0E+00 1.0E+00 1.0E+00
FRACTION (BASED ON MASS) REMAINING IN THE SLICK = 8.6E-01, AREA = 2.6E+06 M**2

TIME = 5.0E+01 HOURS, MASS FRACTION OF EACH CUT REMAINING:
0.0E+00 0.0E+00 2.5E-04 1.8E-01 7.3E-01 9.5E-01 9.9E-01 1.0E+00 1.0E+00 1.0E+00 1.0E+00 1.0E+00 1.0E+00 1.0E+00
FRACTION (BASED ON MASS) REMAINING IN THE SLICK = 8.6E-01, AREA = 2.7E+06 M**2

TIME = 5.1E+01 HOURS, MASS FRACTION OF EACH CUT REMAINING:
0.0E+00 0.0E+00 1.9E-04 1.7E-01 7.3E-01 9.5E-01 9.9E-01 1.0E+00 1.0E+00 1.0E+00 1.0E+00 1.0E+00 1.0E+00 1.0E+00
FRACTION (BASED ON MASS) REMAINING IN THE SLICK = 8.6E-01, AREA = 2.7E+06 M**2

TIME = 5.2E+01 HOURS, MASS FRACTION OF EACH CUT REMAINING:
0.0E+00 0.0E+00 1.5E-04 1.6E-01 7.2E-01 9.5E-01 9.9E-01 1.0E+00 1.0E+00 1.0E+00 1.0E+00 1.0E+00 1.0E+00 1.0E+00
FRACTION (BASED ON MASS) REMAINING IN THE SLICK = 8.6E-01, AREA = 2.7E+06 M**2

TIME = 1.0E+02 HOURS, MASS FRACTION OF EACH CUT REMAINING:
0.0E+00 0.0E+00 1.7E-11 6.0E-03 4.6E-01 8.5E-01 9.8E-01 1.0E+00 1.0E+00 1.0E+00 1.0E+00 1.0E+00 1.0E+00 1.0E+00
FRACTION (BASED ON MASS) REMAINING IN THE SLICK = 8.4E-01, AREA = 3.7E+06 M**2

STEP SIZE OF 3.511E+00 IS BASED ON CUT 5

TIME = 1.5E+02 HOURS, MASS FRACTION OF EACH CUT REMAINING:
0.0E+00 0.0E+00 0.0E+00 7.7E-05 1.8E-01 7.5E-01 9.6E-01 9.9E-01 1.0E+00 1.0E+00 1.0E+00 1.0E+00 1.0E+00 1.0E+00
FRACTION (BASED ON MASS) REMAINING IN THE SLICK = 8.3E-01, AREA = 4.5E+06 M**2

TIME = 2.1E+02 HOURS, MASS FRACTION OF EACH CUT REMAINING:
0.0E+00 0.0E+00 0.0E+00 3.0E-07 6.9E-02 6.4E-01 9.3E-01 9.9E-01 1.0E+00 1.0E+00 1.0E+00 1.0E+00 1.0E+00 1.0E+00
FRACTION (BASED ON MASS) REMAINING IN THE SLICK = 8.2E-01, AREA = 5.2E+06 M**2

TIME = 2.6E+02 HOURS, MASS FRACTION OF EACH CUT REMAINING:
0.0E+00 0.0E+00 0.0E+00 9.0E-10 2.3E-02 5.3E-01 9.1E-01 9.9E-01 1.0E+00 1.0E+00 1.0E+00 1.0E+00 1.0E+00 1.0E+00
FRACTION (BASED ON MASS) REMAINING IN THE SLICK = 8.1E-01, AREA = 5.8E+06 M**2

TIME = 3.1E+02 HOURS, MASS FRACTION OF EACH CUT REMAINING:
0.0E+00 0.0E+00 0.0E+00 0.0E+00 6.8E-03 4.3E-01 8.8E-01 9.8E-01 1.0E+00 1.0E+00 1.0E+00 1.0E+00 1.0E+00 1.0E+00
FRACTION (BASED ON MASS) REMAINING IN THE SLICK = 8.1E-01, AREA = 6.3E+06 M**2

STEP SIZE OF 1.160E+01 IS BASED ON CUT 6

TIME = 3.6E+02 HOURS, MASS FRACTION OF EACH CUT REMAINING:
0.0E+00 0.0E+00 0.0E+00 0.0E+00 1.8E-03 3.4E-01 8.5E-01 9.8E-01 1.0E+00 1.0E+00 1.0E+00 1.0E+00 1.0E+00 1.0E+00
FRACTION (BASED ON MASS) REMAINING IN THE SLICK = 8.0E-01, AREA = 6.7E+06 M**2

TIME = 4.2E+02 HOURS, MASS FRACTION OF EACH CUT REMAINING:
0.0E+00 0.0E+00 0.0E+00 0.0E+00 3.8E-04 2.6E-01 8.2E-01 9.7E-01 1.0E+00 1.0E+00 1.0E+00 1.0E+00 1.0E+00 1.0E+00

```
 FRACTION (BASED ON MASS) REMAINING IN THE SLICK =  8.0E-01, AREA =  7.2E+06 M**2

 TIME =  4.8E+02 HOURS, MASS FRACTION OF EACH CUT REMAINING:
 0.0E+00  0.0E+00  0.0E+00  0.0E+00  6.8E-05  2.0E-01  7.0E-01  9.6E-01  1.0E+00  1.0E+00  1.0E+00  1.0E+00  1.0E+00  1.0E+00
 FRACTION (BASED ON MASS) REMAINING IN THE SLICK =  7.9E-01, AREA =  7.7E+06 M**2

THE FINAL MASS FRACTIONS FOR THE SLICK AT  5.0E+02 HOURS ARE:
 0.000E+00  0.000E+00  0.000E+00  0.000E+00  2.299E-05  1.635E-01  7.581E-01  9.595E-01  9.965E-01  9.990E-01  1.000E+00
 1.000E+00  1.000E+00  1.000E+00
 FRACTION (BASED ON MASS) REMAINING IN THE SLICK =  7.9E-01, AREA =  7.9E+06 M**2

**********************************************************
```

CRUDE OIL CHARACTERIZATION AND PSEUDOCOMPONENT EVAPORATION MODEL
IDENTIFICATION: PRUDHOE BAY, ITEM 9, SAMPLE 77011

VAPOR PRESSURE IN ATMOSPHERES AT 3.200E+01 DEG F

	VP
1	3.784E-02
2	1.006E-02
3	2.584E-03
4	5.643E-04
5	1.128E-04
6	1.955E-05
7	3.176E-06
8	4.635E-07
9	6.603E-08
10	5.303E-09
11	2.092E-10
12	3.826E-11
13	4.512E-13
14	1.364E-14

MEAN MOLECULAR WEIGHT OF THE CRUDE = 2.730E+02

OVER-ALL MASS-TRANSFER COEFFICIENTS

WIND SPEED = 4.000E+01 KNOTS, OR 7.412E+04 M/HR
INITIAL SLICK DIAMETER = 7.116E+02 M, OR AREA = 3.975E+05 M**2

OVER-ALL MASS-TRANSFER COEFFICIENT FOR COMENE = 4.500E+01 M/HR

CUT	M/HR	G-MOLES/(HR)(ATM)(M**2)	SPGR OF CUT
1	4.903E+01	2.190E+03	6.929E-01
2	4.830E+01	2.157E+03	7.230E-01
3	4.771E+01	2.131E+03	7.519E-01
4	4.718E+01	2.100E+03	7.728E-01
5	4.671E+01	2.087E+03	7.901E-01
6	4.628E+01	2.067E+03	8.068E-01
7	4.594E+01	2.052E+03	8.179E-01
8	4.564E+01	2.039E+03	8.358E-01
9	4.541E+01	2.028E+03	8.509E-01
10	4.513E+01	2.016E+03	8.729E-01
11	4.481E+01	2.002E+03	8.911E-01
12	4.469E+01	1.997E+03	8.973E-01
13	4.440E+01	1.983E+03	9.100E-01
14	4.423E+01	1.976E+03	9.188E-01

FOR THIS SPILL OF 5.000E+04 BARRELS, THE MASS IS 7.062E+03 METRIC TONNES

VOLUME FROM SUMMING THE CUTS = 7.9E+03 M**3, OR 5.000E+04 BARRELS

KINEMATIC VISCOSITY OF THE BULK CRUDE FROM THE CUTS = 4.8E+00 CENTISTOKES AT 122 DEG F

KINEMATIC VISCOSITY OF THE BULK CRUDE FROM THE CUTS = 8.8E+00 AT T = 32.0 DEG F

COUNT THE CUTS IN THE FOLLOWING OUTPUT FROM LEFT TO RIGHT

THE INITIAL MOLES IN THE SLICK ARE:
1.305E+06 1.481E+06 1.848E+06 1.741E+06 1.634E+06 1.395E+06 1.581E+06 1.637E+06 1.601E+06 8.267E+05 1.683E+06
1.699E+06 1.305E+06 1.466E+06 4.791E+06

THE INITIAL MASSES IN THE SLICK ARE:
1.164E+08 1.504E+08 2.105E+08 2.225E+08 2.338E+08 2.242E+08 2.613E+08 3.299E+08 3.403E+08 1.955E+08 4.508E+08
4.400E+08 4.367E+08 5.438E+08 2.875E+09

CUT 1 GOES AWAY IN MINUTES, THEREFORE IT WAS DELETED AND THE CUTS RENUMBERED

STEP SIZE OF 1.325E-01 IS BASED ON CUT 1

TIME = 1.1E+00 HOURS, MASS FRACTION OF EACH CUT REMAINING:
6.1E-01 8.9E-01 9.8E-01 1.0E+00 1.0E+00 1.0E+00 1.0E+00 1.0E+00 1.0E+00 1.0E+00 1.0E+00 1.0E+00 1.0E+00
FRACTION (BASED ON MASS) REMAINING IN THE SLICK = 9.7E-01, AREA = 3.7E+05 M**2

TIME = 2.1E+00 HOURS, MASS FRACTION OF EACH CUT REMAINING:
3.2E-01 7.6E-01 9.4E-01 9.9E-01 1.0E+00 1.0E+00 1.0E+00 1.0E+00 1.0E+00 1.0E+00 1.0E+00 1.0E+00 1.0E+00
FRACTION (BASED ON MASS) REMAINING IN THE SLICK = 9.6E-01, AREA = 3.9E+05 M**2

TIME = 3.2E+00 HOURS, MASS FRACTION OF EACH CUT REMAINING:
1.4E-01 6.3E-01 9.1E-01 9.8E-01 1.0E+00 1.0E+00 1.0E+00 1.0E+00 1.0E+00 1.0E+00 1.0E+00 1.0E+00 1.0E+00
FRACTION (BASED ON MASS) REMAINING IN THE SLICK = 9.3E-01 AREA = 8.1E+05 M**2

TIME = 4.2E+00 HOURS, MASS FRACTION OF EACH CUT REMAINING:
5.0E-02 5.1E-01 8.7E-01 9.7E-01 1.0E+00 1.0E+00 1.0E+00 1.0E+00 1.0E+00 1.0E+00 1.0E+00 1.0E+00 1.0E+00
FRACTION (BASED ON MASS) REMAINING IN THE SLICK = 9.0E-01, AREA = 9.6E+05 M**2

TIME = 5.3E+00 HOURS, MASS FRACTION OF EACH CUT REMAINING:
2.1E-02 4.0E-01 8.2E-01 9.6E-01 9.9E-01 1.0E+00 1.0E+00 1.0E+00 1.0E+00 1.0E+00 1.0E+00 1.0E+00 1.0E+00 1.0E+00
FRACTION (BASED ON MASS) REMAINING IN THE SLICK = 9.4E-01, AREA = 9.9E+05 M**2

STEP SIZE OF 1.974E-01 IS BASED ON CUT 2

TIME = 6.5E+00 HOURS, MASS FRACTION OF EACH CUT REMAINING:
5.9E-03 3.0E-01 7.7E-01 9.5E-01 9.9E-01 1.0E+00 1.0E+00 1.0E+00 1.0E+00 1.0E+00 1.0E+00 1.0E+00 1.0E+00 1.0E+00
FRACTION (BASED ON MASS) REMAINING IN THE SLICK = 9.3E-01, AREA = 1.1E+06 M**2

TIME = 7.7E+00 HOURS, MASS FRACTION OF EACH CUT REMAINING:
1.5E-03 2.2E-01 7.2E-01 9.4E-01 9.9E-01 1.0E+00 1.0E+00 1.0E+00 1.0E+00 1.0E+00 1.0E+00 1.0E+00 1.0E+00 1.0E+00
FRACTION (BASED ON MASS) REMAINING IN THE SLICK = 9.3E-01, AREA = 1.2E+06 M**2

TIME = 8.9E+00 HOURS, MASS FRACTION OF EACH CUT REMAINING:
3.4E-04 1.5E-01 6.7E-01 9.2E-01 9.9E-01 1.0E+00 1.0E+00 1.0E+00 1.0E+00 1.0E+00 1.0E+00 1.0E+00 1.0E+00 1.0E+00
FRACTION (BASED ON MASS) REMAINING IN THE SLICK = 9.2E-01, AREA = 1.2E+06 M**2

TIME = 1.0E+01 HOURS, MASS FRACTION OF EACH CUT REMAINING:
7.1E-05 1.1E-01 6.2E-01 9.1E-01 9.8E-01 1.0E+00 1.0E+00 1.0E+00 1.0E+00 1.0E+00 1.0E+00 1.0E+00 1.0E+00 1.0E+00
FRACTION (BASED ON MASS) REMAINING IN THE SLICK = 9.2E-01, AREA = 1.3E+06 M**2

TIME = 1.1E+01 HOURS, MASS FRACTION OF EACH CUT REMAINING:
1.3E-05 7.1E-02 5.7E-01 8.9E-01 9.8E-01 1.0E+00 1.0E+00 1.0E+00 1.0E+00 1.0E+00 1.0E+00 1.0E+00 1.0E+00 1.0E+00
FRACTION (BASED ON MASS) REMAINING IN THE SLICK = 9.2E-01, AREA = 1.4E+06 M**2

TIME = 1.2E+01 HOURS, MASS FRACTION OF EACH CUT REMAINING:
2.3E-06 4.7E-02 5.2E-01 8.8E-01 9.8E-01 1.0E+00 1.0E+00 1.0E+00 1.0E+00 1.0E+00 1.0E+00 1.0E+00 1.0E+00 1.0E+00
FRACTION (BASED ON MASS) REMAINING IN THE SLICK = 9.1E-01, AREA = 1.4E+06 M**2

TIME = 1.4E+01 HOURS, MASS FRACTION OF EACH CUT REMAINING:
3.6E-07 3.1E-02 4.7E-01 8.6E-01 9.7E-01 1.0E+00 1.0E+00 1.0E+00 1.0E+00 1.0E+00 1.0E+00 1.0E+00 1.0E+00 1.0E+00
FRACTION (BASED ON MASS) REMAINING IN THE SLICK = 9.1E-01, AREA = 1.5E+06 M**2

TIME = 1.5E+01 HOURS, MASS FRACTION OF EACH CUT REMAINING:
5.3E-08 1.9E-02 4.3E-01 8.5E-01 9.7E-01 1.0E+00 1.0E+00 1.0E+00 1.0E+00 1.0E+00 1.0E+00 1.0E+00 1.0E+00 1.0E+00
FRACTION (BASED ON MASS) REMAINING IN THE SLICK = 9.1E-01, AREA = 1.5E+06 M**2

TIME = 1.6E+01 HOURS, MASS FRACTION OF EACH CUT REMAINING:
7.1E-09 1.2E-02 3.9E-01 8.3E-01 9.7E-01 9.9E-01 1.0E+00 1.0E+00 1.0E+00 1.0E+00 1.0E+00 1.0E+00 1.0E+00 1.0E+00
FRACTION (BASED ON MASS) REMAINING IN THE SLICK = 9.1E-01, AREA = 1.6E+06 M**2

TIME = 1.7E+01 HOURS, MASS FRACTION OF EACH CUT REMAINING:
0.0E+00 7.5E-03 3.5E-01 8.1E-01 9.6E-01 9.9E-01 1.0E+00 1.0E+00 1.0E+00 1.0E+00 1.0E+00 1.0E+00 1.0E+00 1.0E+00
FRACTION (BASED ON MASS) REMAINING IN THE SLICK = 9.0E-01, AREA = 1.6E+06 M**2

TIME = 1.8E+01 HOURS, MASS FRACTION OF EACH CUT REMAINING:
0.0E+00 4.5E-03 3.1E-01 7.9E-01 9.6E-01 9.9E-01 1.0E+00 1.0E+00 1.0E+00 1.0E+00 1.0E+00 1.0E+00 1.0E+00 1.0E+00
FRACTION (BASED ON MASS) REMAINING IN THE SLICK = 9.0E-01, AREA = 1.7E+06 M**2

STEP SIZE OF 5.215E-01 IS BASED ON CUT 3

TIME = 2.0E+01 HOURS, MASS FRACTION OF EACH CUT REMAINING:
0.0E+00 2.5E-03 2.7E-01 7.8E-01 9.6E-01 9.9E-01 1.0E+00 1.0E+00 1.0E+00 1.0E+00 1.0E+00 1.0E+00 1.0E+00 1.0E+00
FRACTION (BASED ON MASS) REMAINING IN THE SLICK = 9.0E-01, AREA = 1.7E+06 M**2

TIME = 2.1E+01 HOURS, MASS FRACTION OF EACH CUT REMAINING:
0.0E+00 1.6E-03 2.5E-01 7.6E-01 9.5E-01 9.9E-01 1.0E+00 1.0E+00 1.0E+00 1.0E+00 1.0E+00 1.0E+00 1.0E+00 1.0E+00
FRACTION (BASED ON MASS) REMAINING IN THE SLICK = 9.0E-01, AREA = 1.8E+06 M**2

TIME = 2.2E+01 HOURS, MASS FRACTION OF EACH CUT REMAINING:
0.0E+00 9.6E-04 2.2E-01 7.4E-01 9.5E-01 9.9E-01 1.0E+00 1.0E+00 1.0E+00 1.0E+00 1.0E+00 1.0E+00 1.0E+00 1.0E+00
FRACTION (BASED ON MASS) REMAINING IN THE SLICK = 9.0E-01, AREA = 1.8E+06 M**2

TIME = 2.3E+01 HOURS, MASS FRACTION OF EACH CUT REMAINING:
0.0E+00 5.8E-04 2.0E-01 7.3E-01 9.5E-01 9.9E-01 1.0E+00 1.0E+00 1.0E+00 1.0E+00 1.0E+00 1.0E+00 1.0E+00 1.0E+00
FRACTION (BASED ON MASS) REMAINING IN THE SLICK = 9.0E-01, AREA = 1.9E+06 M**2

TIME = 2.4E+01 HOURS, MASS FRACTION OF EACH CUT REMAINING:
0.0E+00 3.5E-04 1.8E-01 7.1E-01 9.4E-01 9.9E-01 1.0E+00 1.0E+00 1.0E+00 1.0E+00 1.0E+00 1.0E+00 1.0E+00 1.0E+00
FRACTION (BASED ON MASS) REMAINING IN THE SLICK = 9.0E-01, AREA = 1.9E+06 M**2

TIME = 2.5E+01 HOURS, MASS FRACTION OF EACH CUT REMAINING:
0.0E+00 2.1E-04 1.6E-01 7.0E-01 9.4E-01 9.9E-01 1.0E+00 1.0E+00 1.0E+00 1.0E+00 1.0E+00 1.0E+00 1.0E+00 1.0E+00
FRACTION (BASED ON MASS) REMAINING IN THE SLICK = 8.9E-01, AREA = 1.9E+06 M**2

TIME = 2.6E+01 HOURS, MASS FRACTION OF EACH CUT REMAINING:
0.0E+00 1.2E-04 1.4E-01 6.8E-01 9.4E-01 9.9E-01 1.0E+00 1.0E+00 1.0E+00 1.0E+00 1.0E+00 1.0E+00 1.0E+00 1.0E+00
FRACTION (BASED ON MASS) REMAINING IN THE SLICK = 8.9E-01, AREA = 2.0E+06 M**2

TIME = 2.7E+01 HOURS, MASS FRACTION OF EACH CUT REMAINING:
0.0E+00 7.0E-05 1.3E-01 6.7E-01 9.3E-01 9.9E-01 1.0E+00 1.0E+00 1.0E+00 1.0E+00 1.0E+00 1.0E+00 1.0E+00 1.0E+00
FRACTION (BASED ON MASS) REMAINING IN THE SLICK = 8.9E-01, AREA = 2.0E+06 M**2

TIME = 2.8E+01 HOURS, MASS FRACTION OF EACH CUT REMAINING:
0.0E+00 4.0E-05 1.1E-01 6.5E-01 9.3E-01 9.9E-01 1.0E+00 1.0E+00 1.0E+00 1.0E+00 1.0E+00 1.0E+00 1.0E+00 1.0E+00
FRACTION (BASED ON MASS) REMAINING IN THE SLICK = 8.9E-01, AREA = 2.0E+06 M**2

TIME = 2.9E+01 HOURS, MASS FRACTION OF EACH CUT REMAINING:
0.0E+00 2.3E-05 9.9E-02 6.3E-01 9.2E-01 9.9E-01 1.0E+00 1.0E+00 1.0E+00 1.0E+00 1.0E+00 1.0E+00 1.0E+00 1.0E+00
FRACTION (BASED ON MASS) REMAINING IN THE SLICK = 8.9E-01, AREA = 2.1E+06 M**2

TIME = 3.0E+01 HOURS, MASS FRACTION OF EACH CUT REMAINING:
0.0E+00 1.3E-05 8.8E-02 6.2E-01 9.2E-01 9.9E-01 1.0E+00 1.0E+00 1.0E+00 1.0E+00 1.0E+00 1.0E+00 1.0E+00 1.0E+00
FRACTION (BASED ON MASS) REMAINING IN THE SLICK = 8.9E-01, AREA = 2.1E+06 M**2

TIME = 3.1E+01 HOURS, MASS FRACTION OF EACH CUT REMAINING:
0.0E+00 7.1E-06 7.7E-02 6.0E-01 9.2E-01 9.9E-01 1.0E+00 1.0E+00 1.0E+00 1.0E+00 1.0E+00 1.0E+00 1.0E+00 1.0E+00
FRACTION (BASED ON MASS) REMAINING IN THE SLICK = 8.9E-01, AREA = 2.2E+06 M**2

TIME = 3.2E+01 HOURS, MASS FRACTION OF EACH CUT REMAINING:
0.0E+00 3.9E-06 6.8E-02 5.9E-01 9.1E-01 9.9E-01 1.0E+00 1.0E+00 1.0E+00 1.0E+00 1.0E+00 1.0E+00 1.0E+00 1.0E+00
FRACTION (BASED ON MASS) REMAINING IN THE SLICK = 8.9E-01, AREA = 2.2E+06 M**2

TIME = 3.3E+01 HOURS, MASS FRACTION OF EACH CUT REMAINING:
0.0E+00 2.1E-06 6.0E-02 5.7E-01 9.1E-01 9.0E-01 1.0E+00 1.0E+00 1.0E+00 1.0E+00 1.0E+00 1.0E+00 1.0E+00 1.0E+00
FRACTION (BASED ON MASS) REMAINING IN THE SLICK = 8.9E-01, AREA = 2.2E+06 M**2

TIME = 3.4E+01 HOURS, MASS FRACTION OF EACH CUT REMAINING:
0.0E+00 1.1E-06 5.2E-02 5.6E-01 9.0E-01 9.0E-01 1.0E+00 1.0E+00 1.0E+00 1.0E+00 1.0E+00 1.0E+00 1.0E+00 1.0E+00
FRACTION (BASED ON MASS) REMAINING IN THE SLICK = 8.8E-01, AREA = 2.2E+06 M**2

TIME = 3.5E+01 HOURS, MASS FRACTION OF EACH CUT REMAINING:
0.0E+00 6.1E-07 4.5E-02 5.4E-01 9.0E-01 9.0E-01 1.0E+00 1.0E+00 1.0E+00 1.0E+00 1.0E+00 1.0E+00 1.0E+00 1.0E+00
FRACTION (BASED ON MASS) REMAINING IN THE SLICK = 8.8E-01, AREA = 2.3E+06 M**2

TIME = 3.6E+01 HOURS, MASS FRACTION OF EACH CUT REMAINING:
0.0E+00 3.2E-07 4.0E-02 5.3E-01 9.0E-01 9.0E-01 1.0E+00 1.0E+00 1.0E+00 1.0E+00 1.0E+00 1.0E+00 1.0E+00 1.0E+00
FRACTION (BASED ON MASS) REMAINING IN THE SLICK = 8.8E-01, AREA = 2.3E+06 M**2

TIME = 3.7E+01 HOURS, MASS FRACTION OF EACH CUT REMAINING:
0.0E+00 1.7E-07 3.4E-02 5.1E-01 8.9E-01 9.8E-01 1.0E+00 1.0E+00 1.0E+00 1.0E+00 1.0E+00 1.0E+00 1.0E+00 1.0E+00
FRACTION (BASED ON MASS) REMAINING IN THE SLICK = 8.8E-01, AREA = 2.3E+06 M**2

TIME = 3.8E+01 HOURS, MASS FRACTION OF EACH CUT REMAINING:
0.0E+00 8.7E-08 3.0E-02 5.0E-01 8.9E-01 9.8E-01 1.0E+00 1.0E+00 1.0E+00 1.0E+00 1.0E+00 1.0E+00 1.0E+00 1.0E+00
FRACTION (BASED ON MASS) REMAINING IN THE SLICK = 8.8E-01, AREA = 2.4E+06 M**2

TIME = 3.9E+01 HOURS, MASS FRACTION OF EACH CUT REMAINING:
0.0E+00 4.5E-08 2.6E-02 4.9E-01 8.8E-01 9.8E-01 1.0E+00 1.0E+00 1.0E+00 1.0E+00 1.0E+00 1.0E+00 1.0E+00 1.0E+00
FRACTION (BASED ON MASS) REMAINING IN THE SLICK = 8.8E-01, AREA = 2.4E+06 M**2

TIME = 4.1E+01 HOURS, MASS FRACTION OF EACH CUT REMAINING:
0.0E+00 2.3E-08 2.2E-02 4.7E-01 8.8E-01 9.8E-01 1.0E+00 1.0E+00 1.0E+00 1.0E+00 1.0E+00 1.0E+00 1.0E+00 1.0E+00
FRACTION (BASED ON MASS) REMAINING IN THE SLICK = 8.8E-01, AREA = 2.4E+06 M**2

TIME = 4.2E+01 HOURS, MASS FRACTION OF EACH CUT REMAINING:
0.0E+00 1.1E-08 1.9E-02 4.6E-01 8.7E-01 9.8E-01 1.0E+00 1.0E+00 1.0E+00 1.0E+00 1.0E+00 1.0E+00 1.0E+00 1.0E+00
FRACTION (BASED ON MASS) REMAINING IN THE SLICK = 8.8E-01, AREA = 2.5E+06 M**2

TIME = 4.3E+01 HOURS, MASS FRACTION OF EACH CUT REMAINING:
0.0E+00 5.7E-09 1.7E-02 4.5E-01 8.7E-01 9.8E-01 1.0E+00 1.0E+00 1.0E+00 1.0E+00 1.0E+00 1.0E+00 1.0E+00 1.0E+00
FRACTION (BASED ON MASS) REMAINING IN THE SLICK = 8.8E-01, AREA = 2.5E+06 M**2

TIME = 4.4E+01 HOURS, MASS FRACTION OF EACH CUT REMAINING:
0.0E+00 0.0E+00 1.4E-02 4.3E-01 8.7E-01 9.8E-01 1.0E+00 1.0E+00 1.0E+00 1.0E+00 1.0E+00 1.0E+00 1.0E+00 1.0E+00
FRACTION (BASED ON MASS) REMAINING IN THE SLICK = 8.8E-01, AREA = 2.5E+06 M**2

TIME = 4.5E+01 HOURS, MASS FRACTION OF EACH CUT REMAINING:
0.0E+00 0.0E+00 1.2E-02 4.2E-01 8.6E-01 9.8E-01 1.0E+00 1.0E+00 1.0E+00 1.0E+00 1.0E+00 1.0E+00 1.0E+00 1.0E+00
FRACTION (BASED ON MASS) REMAINING IN THE SLICK = 8.8E-01, AREA = 2.5E+06 M**2

TIME = 4.6E+01 HOURS, MASS FRACTION OF EACH CUT REMAINING:
0.0E+00 0.0E+00 1.0E-02 4.1E-01 8.6E-01 9.8E-01 1.0E+00 1.0E+00 1.0E+00 1.0E+00 1.0E+00 1.0E+00 1.0E+00 1.0E+00
FRACTION (BASED ON MASS) REMAINING IN THE SLICK = 8.8E-01, AREA = 2.6E+06 M**2

TIME = 4.7E+01 HOURS, MASS FRACTION OF EACH CUT REMAINING:
0.0E+00 0.0E+00 9.0E-03 4.0E-01 8.5E-01 9.7E-01 1.0E+00 1.0E+00 1.0E+00 1.0E+00 1.0E+00 1.0E+00 1.0E+00 1.0E+00
FRACTION (BASED ON MASS) REMAINING IN THE SLICK = 8.0E-01, AREA = 2.6E+06 M**2

TIME = 4.8E+01 HOURS, MASS FRACTION OF EACH CUT REMAINING:
0.0E+00 0.0E+00 7.6E-03 3.8E-01 8.5E-01 9.7E-01 1.0E+00 1.0E+00 1.0E+00 1.0E+00 1.0E+00 1.0E+00 1.0E+00 1.0E+00
FRACTION (BASED ON MASS) REMAINING IN THE SLICK = 8.0E-01, AREA = 2.6E+06 M**2

TIME = 4.9E+01 HOURS, MASS FRACTION OF EACH CUT REMAINING:
0.0E+00 0.0E+00 6.5E-03 3.7E-01 8.4E-01 9.7E-01 1.0E+00 1.0E+00 1.0E+00 1.0E+00 1.0E+00 1.0E+00 1.0E+00 1.0E+00
FRACTION (BASED ON MASS) REMAINING IN THE SLICK = 8.7E-01, AREA = 2.7E+06 M**2

TIME = 5.0E+01 HOURS, MASS FRACTION OF EACH CUT REMAINING:
0.0E+00 0.0E+00 5.5E-03 3.6E-01 8.4E-01 9.7E-01 1.0E+00 1.0E+00 1.0E+00 1.0E+00 1.0E+00 1.0E+00 1.0E+00 1.0E+00
FRACTION (BASED ON MASS) REMAINING IN THE SLICK = 8.7E-01, AREA = 2.7E+06 M**2

TIME = 5.1E+01 HOURS, MASS FRACTION OF EACH CUT REMAINING:
0.0E+00 0.0E+00 4.7E-03 3.5E-01 8.3E-01 9.7E-01 1.0E+00 1.0E+00 1.0E+00 1.0E+00 1.0E+00 1.0E+00 1.0E+00 1.0E+00
FRACTION (BASED ON MASS) REMAINING IN THE SLICK = 8.7E-01, AREA = 2.7E+06 M**2

TIME = 5.2E+01 HOURS, MASS FRACTION OF EACH CUT REMAINING:
0.0E+00 0.0E+00 4.0E-03 3.4E-01 8.3E-01 9.7E-01 1.0E+00 1.0E+00 1.0E+00 1.0E+00 1.0E+00 1.0E+00 1.0E+00 1.0E+00
FRACTION (BASED ON MASS) REMAINING IN THE SLICK = 8.7E-01, AREA = 2.7E+06 M**2

STEP SIZE OF 1.555E+00 IS BASED ON CUT 4

TIME = 1.0E+02 HOURS, MASS FRACTION OF EACH CUT REMAINING:
0.0E+00 0.0E+00 2.2E-07 4.9E-02 5.9E-01 9.2E-01 9.9E-01 1.0E+00 1.0E+00 1.0E+00 1.0E+00 1.0E+00 1.0E+00 1.0E+00
FRACTION (BASED ON MASS) REMAINING IN THE SLICK = 8.5E-01, AREA = 3.7E+06 M**2

TIME = 1.5E+02 HOURS, MASS FRACTION OF EACH CUT REMAINING:
0.0E+00 0.0E+00 4.6E-13 3.7E-03 3.8E-01 8.6E-01 9.8E-01 1.0E+00 1.0E+00 1.0E+00 1.0E+00 1.0E+00 1.0E+00 1.0E+00
FRACTION (BASED ON MASS) REMAINING IN THE SLICK = 8.4E-01, AREA = 4.0E+06 M**2

STEP SIZE OF 5.200E+00 IS BASED ON CUT 5

TIME = 2.1E+02 HOURS, MASS FRACTION OF EACH CUT REMAINING:
0.0E+00 0.0E+00 0.0E+00 1.4E-04 2.2E-01 7.0E-01 9.6E-01 9.9E-01 1.0E+00 1.0E+00 1.0E+00 1.0E+00 1.0E+00 1.0E+00
FRACTION (BASED ON MASS) REMAINING IN THE SLICK = 8.3E-01, AREA = 5.2E+06 M**2

TIME = 2.6E+02 HOURS, MASS FRACTION OF EACH CUT REMAINING:
0.0E+00 0.0E+00 0.0E+00 3.8E-06 1.2E-01 7.1E-01 9.5E-01 9.9E-01 1.0E+00 1.0E+00 1.0E+00 1.0E+00 1.0E+00 1.0E+00
FRACTION (BASED ON MASS) REMAINING IN THE SLICK = 8.3E-01, AREA = 5.8E+06 M**2

TIME = 3.1E+02 HOURS, MASS FRACTION OF EACH CUT REMAINING:
0.0E+00 0.0E+00 0.0E+00 7.2E-08 5.8E-02 6.3E-01 9.4E-01 9.9E-01 1.0E+00 1.0E+00 1.0E+00 1.0E+00 1.0E+00 1.0E+00
FRACTION (BASED ON MASS) REMAINING IN THE SLICK = 8.2E-01, AREA = 6.3E+06 M**2

TIME = 3.6E+02 HOURS, MASS FRACTION OF EACH CUT REMAINING:
0.0E+00 0.0E+00 0.0E+00 9.4E-10 2.8E-02 5.6E-01 9.2E-01 9.9E-01 1.0E+00 1.0E+00 1.0E+00 1.0E+00 1.0E+00 1.0E+00
FRACTION (BASED ON MASS) REMAINING IN THE SLICK = 8.2E-01, AREA = 6.8E+06 M**2

```
 TIME =  4.2E+02 HOURS, MASS FRACTION OF EACH CUT REMAINING:
 0.0E+00  0.0E+00  0.0E+00  0.0E+00  1.2E-02  4.9E-01  9.0E-01  9.9E-01  1.0E+00  1.0E+00  1.0E+00  1.0E+00  1.0E+00  1.0E+00
 FRACTION (BASED ON MASS) REMAINING IN THE SLICK =  8.1E-01, AREA =  7.3E+06 M**2


 TIME =  4.7E+02 HOURS, MASS FRACTION OF EACH CUT REMAINING:
 0.0E+00  0.0E+00  0.0E+00  0.0E+00  5.2E-03  4.3E-01  8.0E-01  9.8E-01  1.0E+00  1.0E+00  1.0E+00  1.0E+00  1.0E+00  1.0E+00
 FRACTION (BASED ON MASS) REMAINING IN THE SLICK =  8.1E-01, AREA =  7.7E+06 M**2


 STEP SIZE OF  1.778E+01 IS BASED ON CUT   6

THE FINAL MASS FRACTIONS FOR THE SLICK AT  5.1E+02 HOURS ARE:
 0.000E+00  0.000E+00  0.000E+00  0.000E+00  1.942E-03  3.655E-01  8.642E-01  9.795E-01  9.983E-01  9.999E-01  1.000E+00
 1.000E+00  1.000E+00  1.000E+00
 FRACTION (BASED ON MASS) REMAINING IN THE SLICK =  8.0E-01, AREA =  8.1E+06 M**2

*****************************************************************
```

CRUDE OIL CHARACTERIZATION AND PSEUDOCOMPONENT EVAPORATION MODEL
IDENTIFICATION: PRUDHOE BAY, ITEM 9, SAMPLE 71011

VAPOR PRESSURE IN ATMOSPHERES AT 4.200E+01 DEG F

	VP
1	5.192E-02
2	1.555E-02
3	3.968E-03
4	9.029E-04
5	1.878E-04
6	3.435E-05
7	5.868E-06
8	9.034E-07
9	1.356E-07
10	1.160E-08
11	5.055E-10
12	9.601E-11
13	1.297E-12
14	4.340E-14

MEAN MOLECULAR WEIGHT OF THE CRUDE = 2.730E+02

OVER-ALL MASS-TRANSFER COEFFICIENTS

WIND SPEED = 1.000E+01 KNOTS, OR 1.853E+04 M/HR
INITIAL SLICK DIAMETER = 7.116E+02 M, OR AREA = 3.975E+05 M**2

OVER-ALL MASS-TRANSFER COEFFICIENT FOR CUMENE = 1.653E+01 M/HR

CUT	M/HR	G-MOLES/(HR)(ATM)(M**2)	SLCK OF CUT
1	1.663E+01	7.200E+02	6.929E-01
2	1.638E+01	7.171E+02	7.230E-01
3	1.613E+01	7.004E+02	7.519E-01
4	1.600E+01	7.005E+02	7.728E-01
5	1.584E+01	6.936E+02	7.901E-01
6	1.570E+01	6.872E+02	8.008E-01
7	1.558E+01	6.820E+02	8.179E-01
8	1.548E+01	6.776E+02	8.358E-01
9	1.540E+01	6.742E+02	8.509E-01
10	1.531E+01	6.701E+02	8.729E-01
11	1.520E+01	6.653E+02	8.811E-01
12	1.516E+01	6.636E+02	8.973E-01
13	1.506E+01	6.593E+02	9.100E-01
14	1.500E+01	6.567E+02	9.188E-01

FOR THIS SPILL OF 5.000E+04 BARRELS, THE MASS IS 7.062E+03 METRIC TONNES

VOLUME FROM SUMMING THE CUTS = 7.9E+03 M**3, OR 5.000E+04 BARRELS

KINEMATIC VISCOSITY OF THE BULK CRUDE FROM THE CUTS = 4.8E+00 CENTISTOKES AT 122 DEG F

KINEMATIC VISCOSITY OF THE BULK CRUDE FROM THE CUTS = 8.1E+00 AT T = 42.0 DEG F

COUNT THE CUTS IN THE FOLLOWING OUTPUT FROM LEFT TO RIGHT

THE INITIAL MOLES IN THE SLICK ARE:
1.303E+06 1.481E+06 1.848E+06 1.741E+06 1.634E+06 1.395E+06 1.581E+06 1.637E+06 1.601E+06 8.267E+05 1.683E+06
1.699E+06 1.305E+06 1.466E+06 4.791E+06

THE INITIAL MASSES IN THE SLICK ARE:
1.164E+08 1.504E+08 2.105E+08 2.225E+08 2.338E+08 2.242E+08 2.813E+08 3.209E+08 3.403E+08 1.955E+08 4.580E+08
4.880E+08 4.367E+08 5.438E+08 2.873E+09

STEP SIZE OF 8.651E-02 IS BASED ON CUT 1

TIME = 1.0E+00 HOURS, MASS FRACTION OF EACH CUT REMAINING:
4.7E-01 8.0E-01 9.5E-01 9.9E-01 1.0E+00 1.0E+00 1.0E+00 1.0E+00 1.0E+00 1.0E+00 1.0E+00 1.0E+00 1.0E+00 1.0E+00
1.0E+00
FRACTION (BASED ON MASS) REMAINING IN THE SLICK = 9.9E-01, AREA = 5.7E+05 M**2

TIME = 2.1E+00 HOURS, MASS FRACTION OF EACH CUT REMAINING:
1.7E-01 6.0E-01 8.8E-01 9.7E-01 9.9E-01 1.0E+00 1.0E+00 1.0E+00 1.0E+00 1.0E+00 1.0E+00 1.0E+00 1.0E+00 1.0E+00
1.0E+00
FRACTION (BASED ON MASS) REMAINING IN THE SLICK = 9.7E-01, AREA = 7.0E+05 M**2

TIME = 3.1E+00 HOURS, MASS FRACTION OF EACH CUT REMAINING:
5.1E-02 4.2E-01 8.0E-01 9.5E-01 9.9E-01 1.0E+00 1.0E+00 1.0E+00 1.0E+00 1.0E+00 1.0E+00 1.0E+00 1.0E+00 1.0E+00
1.0E+00
FRACTION (BASED ON MASS) REMAINING IN THE SLICK = 9.6E-01, AREA = 8.1E+05 M**2

TIME = 4.2E+00 HOURS, MASS FRACTION OF EACH CUT REMAINING:
1.3E-02 2.8E-01 7.2E-01 9.3E-01 9.9E-01 1.0E+00 1.0E+00 1.0E+00 1.0E+00 1.0E+00 1.0E+00 1.0E+00 1.0E+00 1.0E+00

1.0E+00
FRACTION (BASED ON MASS) REMAINING IN THE SLICK = 9.6E-01, AREA = 9.1E+05 M**2

STEP SIZE OF 1.169E-01 IS BASED ON CUT 2

TIME = 5.3E+00 HOURS, MASS FRACTION OF EACH CUT REMAINING:
2.4E-03 1.7E-01 6.4E-01 9.0E-01 9.8E-01 1.0E+00 1.0E+00 1.0E+00 1.0E+00 1.0E+00 1.0E+00 1.0E+00 1.0E+00 1.0E+00
1.0E+00
FRACTION (BASED ON MASS) REMAINING IN THE SLICK = 9.5E-01, AREA = 1.0E+06 M**2

TIME = 6.3E+00 HOURS, MASS FRACTION OF EACH CUT REMAINING:
4.2E-04 1.0E-01 5.6E-01 8.0E-01 9.7E-01 1.0E+00 1.0E+00 1.0E+00 1.0E+00 1.0E+00 1.0E+00 1.0E+00 1.0E+00 1.0E+00
1.0E+00
FRACTION (BASED ON MASS) REMAINING IN THE SLICK = 9.5E-01, AREA = 1.1E+06 M**2

TIME = 7.4E+00 HOURS, MASS FRACTION OF EACH CUT REMAINING:
6.4E-05 5.8E-02 4.9E-01 8.5E-01 9.7E-01 9.9E-01 1.0E+00 1.0E+00 1.0E+00 1.0E+00 1.0E+00 1.0E+00 1.0E+00 1.0E+00
1.0E+00
FRACTION (BASED ON MASS) REMAINING IN THE SLICK = 9.4E-01, AREA = 1.1E+06 M**2

TIME = 8.4E+00 HOURS, MASS FRACTION OF EACH CUT REMAINING:
8.6E-06 3.2E-02 4.2E-01 8.2E-01 9.6E-01 9.9E-01 1.0E+00 1.0E+00 1.0E+00 1.0E+00 1.0E+00 1.0E+00 1.0E+00 1.0E+00
1.0E+00
FRACTION (BASED ON MASS) REMAINING IN THE SLICK = 9.4E-01, AREA = 1.2E+06 M**2

TIME = 9.5E+00 HOURS, MASS FRACTION OF EACH CUT REMAINING:
1.0E-06 1.7E-02 3.6E-01 7.9E-01 9.5E-01 9.9E-01 1.0E+00 1.0E+00 1.0E+00 1.0E+00 1.0E+00 1.0E+00 1.0E+00 1.0E+00
1.0E+00
FRACTION (BASED ON MASS) REMAINING IN THE SLICK = 9.4E-01, AREA = 1.3E+06 M**2

TIME = 1.1E+01 HOURS, MASS FRACTION OF EACH CUT REMAINING:
1.1E-07 8.7E-03 3.0E-01 7.6E-01 9.5E-01 9.9E-01 1.0E+00 1.0E+00 1.0E+00 1.0E+00 1.0E+00 1.0E+00 1.0E+00 1.0E+00
1.0E+00
FRACTION (BASED ON MASS) REMAINING IN THE SLICK = 9.3E-01, AREA = 1.3E+06 M**2

TIME = 1.2E+01 HOURS, MASS FRACTION OF EACH CUT REMAINING:
9.0E-09 4.3E-03 2.5E-01 7.3E-01 9.4E-01 9.9E-01 1.0E+00 1.0E+00 1.0E+00 1.0E+00 1.0E+00 1.0E+00 1.0E+00 1.0E+00
1.0E+00
FRACTION (BASED ON MASS) REMAINING IN THE SLICK = 9.3E-01, AREA = 1.4E+06 M**2

STEP SIZE OF 2.813E-01 IS BASED ON CUT 3

TIME = 1.3E+01 HOURS, MASS FRACTION OF EACH CUT REMAINING:
0.0E+00 2.0E-03 2.1E-01 7.0E-01 9.3E-01 9.9E-01 1.0E+00 1.0E+00 1.0E+00 1.0E+00 1.0E+00 1.0E+00 1.0E+00 1.0E+00
1.0E+00
FRACTION (BASED ON MASS) REMAINING IN THE SLICK = 9.3E-01, AREA = 1.4E+06 M**2

TIME = 1.4E+01 HOURS, MASS FRACTION OF EACH CUT REMAINING:
0.0E+00 8.9E-04 1.7E-01 6.7E-01 9.2E-01 9.9E-01 1.0E+00 1.0E+00 1.0E+00 1.0E+00 1.0E+00 1.0E+00 1.0E+00 1.0E+00
1.0E+00
FRACTION (BASED ON MASS) REMAINING IN THE SLICK = 9.2E-01, AREA = 1.5E+06 M**2

TIME = 1.5E+01 HOURS, MASS FRACTION OF EACH CUT REMAINING:
0.0E+00 3.0E-04 1.4E-01 6.4E-01 9.1E-01 9.9E-01 1.0E+00 1.0E+00 1.0E+00 1.0E+00 1.0E+00 1.0E+00 1.0E+00 1.0E+00

1.0E+00
FRACTION (BASED ON MASS) REMAINING IN THE SLICK = 9.2E-01, AREA = 1.6E+06 M**2

TIME = 1.6E+01 HOURS, MASS FRACTION OF EACH CUT REMAINING:
0.0E+00 1.6E-04 1.1E-01 6.1E-01 9.0E-01 9.8E-01 1.0E+00 1.0E+00 1.0E+00 1.0E+00 1.0E+00 1.0E+00 1.0E+00 1.0E+00
1.0E+00
FRACTION (BASED ON MASS) REMAINING IN THE SLICK = 9.2E-01, AREA = 1.6E+06 M**2

TIME = 1.7E+01 HOURS, MASS FRACTION OF EACH CUT REMAINING:
0.0E+00 6.2E-05 8.7E-02 5.8E-01 8.9E-01 9.8E-01 1.0E+00 1.0E+00 1.0E+00 1.0E+00 1.0E+00 1.0E+00 1.0E+00 1.0E+00
1.0E+00
FRACTION (BASED ON MASS) REMAINING IN THE SLICK = 9.2E-01, AREA = 1.7E+06 M**2

TIME = 1.8E+01 HOURS, MASS FRACTION OF EACH CUT REMAINING:
0.0E+00 2.4E-05 6.8E-02 5.5E-01 8.8E-01 9.8E-01 1.0E+00 1.0E+00 1.0E+00 1.0E+00 1.0E+00 1.0E+00 1.0E+00 1.0E+00
1.0E+00
FRACTION (BASED ON MASS) REMAINING IN THE SLICK = 9.2E-01, AREA = 1.7E+06 M**2

TIME = 1.9E+01 HOURS, MASS FRACTION OF EACH CUT REMAINING:
0.0E+00 9.0E-06 5.3E-02 5.2E-01 8.7E-01 9.8E-01 1.0E+00 1.0E+00 1.0E+00 1.0E+00 1.0E+00 1.0E+00 1.0E+00 1.0E+00
1.0E+00
FRACTION (BASED ON MASS) REMAINING IN THE SLICK = 9.1E-01, AREA = 1.8E+06 M**2

TIME = 2.1E+01 HOURS, MASS FRACTION OF EACH CUT REMAINING:
0.0E+00 3.3E-06 4.1E-02 4.9E-01 8.6E-01 9.7E-01 1.0E+00 1.0E+00 1.0E+00 1.0E+00 1.0E+00 1.0E+00 1.0E+00 1.0E+00
1.0E+00
FRACTION (BASED ON MASS) REMAINING IN THE SLICK = 9.1E-01, AREA = 1.8E+06 M**2

TIME = 2.2E+01 HOURS, MASS FRACTION OF EACH CUT REMAINING:
0.0E+00 1.2E-06 3.2E-02 4.6E-01 8.5E-01 9.7E-01 1.0E+00 1.0E+00 1.0E+00 1.0E+00 1.0E+00 1.0E+00 1.0E+00 1.0E+00
1.0E+00
FRACTION (BASED ON MASS) REMAINING IN THE SLICK = 9.1E-01, AREA = 1.8E+06 M**2

TIME = 2.3E+01 HOURS, MASS FRACTION OF EACH CUT REMAINING:
0.0E+00 4.0E-07 2.4E-02 4.3E-01 8.4E-01 9.7E-01 9.9E-01 1.0E+00 1.0E+00 1.0E+00 1.0E+00 1.0E+00 1.0E+00 1.0E+00
1.0E+00
FRACTION (BASED ON MASS) REMAINING IN THE SLICK = 9.1E-01, AREA = 1.9E+06 M**2

TIME = 2.4E+01 HOURS, MASS FRACTION OF EACH CUT REMAINING:
0.0E+00 1.3E-07 1.8E-02 4.1E-01 8.3E-01 9.7E-01 9.9E-01 1.0E+00 1.0E+00 1.0E+00 1.0E+00 1.0E+00 1.0E+00 1.0E+00
1.0E+00
FRACTION (BASED ON MASS) REMAINING IN THE SLICK = 9.1E-01, AREA = 1.9E+06 M**2

TIME = 2.5E+01 HOURS, MASS FRACTION OF EACH CUT REMAINING:
0.0E+00 4.3E-08 1.4E-02 3.8E-01 8.2E-01 9.6E-01 9.9E-01 1.0E+00 1.0E+00 1.0E+00 1.0E+00 1.0E+00 1.0E+00 1.0E+00
1.0E+00
FRACTION (BASED ON MASS) REMAINING IN THE SLICK = 9.1E-01, AREA = 2.0E+06 M**2

TIME = 2.6E+01 HOURS, MASS FRACTION OF EACH CUT REMAINING:
0.0E+00 1.4E-08 1.0E-02 3.6E-01 8.1E-01 9.6E-01 9.9E-01 1.0E+00 1.0E+00 1.0E+00 1.0E+00 1.0E+00 1.0E+00 1.0E+00
1.0E+00
FRACTION (BASED ON MASS) REMAINING IN THE SLICK = 9.1E-01, AREA = 2.0E+06 M**2

TIME = 2.7E+01 HOURS, MASS FRACTION OF EACH CUT REMAINING:
0.0E+00 4.3E-09 7.3E-03 3.4E-01 8.0E-01 9.6E-01 9.9E-01 1.0E+00 1.0E+00 1.0E+00 1.0E+00 1.0E+00 1.0E+00 1.0E+00

1.0E+00
FRACTION (BASED ON MASS) REMAINING IN THE SLICK = 9.0E-01, AREA = 2.0E+06 M**2

TIME = 2.0E+01 HOURS, MASS FRACTION OF EACH CUT REMAINING:
0.0E+00 0.0E+00 5.7E-03 3.1E-01 7.9E-01 9.6E-01 9.9E-01 1.0E+00 1.0E+00 1.0E+00 1.0E+00 1.0E+00 1.0E+00 1.0E+00
1.0E+00
FRACTION (BASED ON MASS) REMAINING IN THE SLICK = 9.0E-01, AREA = 2.1E+06 M**2

TIME = 3.0E+01 HOURS, MASS FRACTION OF EACH CUT REMAINING:
0.0E+00 0.0E+00 4.2E-03 2.9E-01 7.0E-01 9.6E-01 9.9E-01 1.0E+00 1.0E+00 1.0E+00 1.0E+00 1.0E+00 1.0E+00 1.0E+00
1.0E+00
FRACTION (BASED ON MASS) REMAINING IN THE SLICK = 9.0E-01, AREA = 2.1E+06 M**2

TIME = 3.1E+01 HOURS, MASS FRACTION OF EACH CUT REMAINING:
0.0E+00 0.0E+00 3.1E-03 2.7E-01 7.6E-01 9.5E-01 9.9E-01 1.0E+00 1.0E+00 1.0E+00 1.0E+00 1.0E+00 1.0E+00 1.0E+00
1.0E+00
FRACTION (BASED ON MASS) REMAINING IN THE SLICK = 9.0E-01, AREA = 2.2E+06 M**2

TIME = 3.2E+01 HOURS, MASS FRACTION OF EACH CUT REMAINING:
0.0E+00 0.0E+00 2.2E-03 2.5E-01 7.5E-01 9.5E-01 9.9E-01 1.0E+00 1.0E+00 1.0E+00 1.0E+00 1.0E+00 1.0E+00 1.0E+00
1.0E+00
FRACTION (BASED ON MASS) REMAINING IN THE SLICK = 9.0E-01, AREA = 2.2E+06 M**2

STEP SIZE OF 7.699E-01 IS BASED ON CUT 4

TIME = 3.3E+01 HOURS, MASS FRACTION OF EACH CUT REMAINING:
0.0E+00 0.0E+00 1.6E-03 2.4E-01 7.4E-01 9.5E-01 9.9E-01 1.0E+00 1.0E+00 1.0E+00 1.0E+00 1.0E+00 1.0E+00 1.0E+00
1.0E+00
FRACTION (BASED ON MASS) REMAINING IN THE SLICK = 9.0E-01, AREA = 2.2E+06 M**2

TIME = 3.4E+01 HOURS, MASS FRACTION OF EACH CUT REMAINING:
0.0E+00 0.0E+00 1.0E-03 2.1E-01 7.3E-01 9.4E-01 9.9E-01 1.0E+00 1.0E+00 1.0E+00 1.0E+00 1.0E+00 1.0E+00 1.0E+00
1.0E+00
FRACTION (BASED ON MASS) REMAINING IN THE SLICK = 9.0E-01, AREA = 2.3E+06 M**2

TIME = 3.6E+01 HOURS, MASS FRACTION OF EACH CUT REMAINING:
0.0E+00 0.0E+00 6.6E-04 1.9E-01 7.1E-01 9.4E-01 9.9E-01 1.0E+00 1.0E+00 1.0E+00 1.0E+00 1.0E+00 1.0E+00 1.0E+00
1.0E+00
FRACTION (BASED ON MASS) REMAINING IN THE SLICK = 9.0E-01, AREA = 2.3E+06 M**2

TIME = 3.7E+01 HOURS, MASS FRACTION OF EACH CUT REMAINING:
0.0E+00 0.0E+00 4.1E-04 1.7E-01 7.0E-01 9.4E-01 9.9E-01 1.0E+00 1.0E+00 1.0E+00 1.0E+00 1.0E+00 1.0E+00 1.0E+00
1.0E+00
FRACTION (BASED ON MASS) REMAINING IN THE SLICK = 8.9E-01, AREA = 2.4E+06 M**2

TIME = 3.9E+01 HOURS, MASS FRACTION OF EACH CUT REMAINING:
0.0E+00 0.0E+00 2.5E-04 1.5E-01 6.8E-01 9.3E-01 9.9E-01 1.0E+00 1.0E+00 1.0E+00 1.0E+00 1.0E+00 1.0E+00 1.0E+00
1.0E+00
FRACTION (BASED ON MASS) REMAINING IN THE SLICK = 8.9E-01, AREA = 2.4E+06 M**2

TIME = 4.1E+01 HOURS, MASS FRACTION OF EACH CUT REMAINING:
0.0E+00 0.0E+00 1.5E-04 1.4E-01 6.7E-01 9.3E-01 9.9E-01 1.0E+00 1.0E+00 1.0E+00 1.0E+00 1.0E+00 1.0E+00 1.0E+00
1.0E+00
FRACTION (BASED ON MASS) REMAINING IN THE SLICK = 8.9E-01, AREA = 2.5E+06 M**2

TIME = 4.2E+01 HOURS, MASS FRACTION OF EACH CUT REMAINING:
0.0E+00 0.0E+00 9.2E-05 1.2E-01 6.5E-01 9.2E-01 9.9E-01 1.0E+00 1.0E+00 1.0E+00 1.0E+00 1.0E+00 1.0E+00 1.0E+00
1.0E+00
FRACTION (BASED ON MASS) REMAINING IN THE SLICK = 8.9E-01, AREA = 2.5E+06 M**2

TIME = 4.4E+01 HOURS, MASS FRACTION OF EACH CUT REMAINING:
0.0E+00 0.0E+00 5.5E-05 1.1E-01 6.3E-01 9.2E-01 9.9E-01 1.0E+00 1.0E+00 1.0E+00 1.0E+00 1.0E+00 1.0E+00 1.0E+00
1.0E+00
FRACTION (BASED ON MASS) REMAINING IN THE SLICK = 8.9E-01, AREA = 2.5E+06 M**2

TIME = 4.5E+01 HOURS, MASS FRACTION OF EACH CUT REMAINING:
0.0E+00 0.0E+00 3.2E-05 9.8E-02 6.2E-01 9.2E-01 9.9E-01 1.0E+00 1.0E+00 1.0E+00 1.0E+00 1.0E+00 1.0E+00 1.0E+00
1.0E+00
FRACTION (BASED ON MASS) REMAINING IN THE SLICK = 8.9E-01, AREA = 2.6E+06 M**2

TIME = 4.7E+01 HOURS, MASS FRACTION OF EACH CUT REMAINING:
0.0E+00 0.0E+00 1.9E-05 8.7E-02 6.0E-01 9.1E-01 9.8E-01 1.0E+00 1.0E+00 1.0E+00 1.0E+00 1.0E+00 1.0E+00 1.0E+00
1.0E+00
FRACTION (BASED ON MASS) REMAINING IN THE SLICK = 8.9E-01, AREA = 2.6E+06 M**2

TIME = 4.8E+01 HOURS, MASS FRACTION OF EACH CUT REMAINING:
0.0E+00 0.0E+00 1.1E-05 7.7E-02 5.9E-01 9.1E-01 9.8E-01 1.0E+00 1.0E+00 1.0E+00 1.0E+00 1.0E+00 1.0E+00 1.0E+00
1.0E+00
FRACTION (BASED ON MASS) REMAINING IN THE SLICK = 8.9E-01, AREA = 2.7E+06 M**2

TIME = 5.0E+01 HOURS, MASS FRACTION OF EACH CUT REMAINING:
0.0E+00 0.0E+00 6.3E-06 6.8E-02 5.7E-01 9.0E-01 9.8E-01 1.0E+00 1.0E+00 1.0E+00 1.0E+00 1.0E+00 1.0E+00 1.0E+00
1.0E+00
FRACTION (BASED ON MASS) REMAINING IN THE SLICK = 8.9E-01, AREA = 2.7E+06 M**2

TIME = 5.1E+01 HOURS, MASS FRACTION OF EACH CUT REMAINING:
0.0E+00 0.0E+00 3.6E-06 6.0E-02 5.6E-01 9.0E-01 9.8E-01 1.0E+00 1.0E+00 1.0E+00 1.0E+00 1.0E+00 1.0E+00 1.0E+00
1.0E+00
FRACTION (BASED ON MASS) REMAINING IN THE SLICK = 8.8E-01, AREA = 2.7E+06 M**2

TIME = 5.3E+01 HOURS, MASS FRACTION OF EACH CUT REMAINING:
0.0E+00 0.0E+00 2.0E-06 5.2E-02 5.4E-01 9.0E-01 9.8E-01 1.0E+00 1.0E+00 1.0E+00 1.0E+00 1.0E+00 1.0E+00 1.0E+00
1.0E+00
FRACTION (BASED ON MASS) REMAINING IN THE SLICK = 8.8E-01, AREA = 2.8E+06 M**2

STEP SIZE OF 2.252E+00 IS BASED ON CUT 5

TIME = 1.0E+02 HOURS, MASS FRACTION OF EACH CUT REMAINING:
0.0E+00 0.0E+00 3.0E-16 3.0E-04 1.9E-01 7.4E-01 9.5E-01 9.9E-01 1.0E+00 1.0E+00 1.0E+00 1.0E+00 1.0E+00 1.0E+00
1.0E+00
FRACTION (BASED ON MASS) REMAINING IN THE SLICK = 8.6E-01, AREA = 3.0E+06 M**2

TIME = 1.6E+02 HOURS, MASS FRACTION OF EACH CUT REMAINING:
0.0E+00 0.0E+00 0.0E+00 2.9E-07 4.5E-02 5.7E-01 9.1E-01 9.9E-01 1.0E+00 1.0E+00 1.0E+00 1.0E+00 1.0E+00 1.0E+00
1.0E+00
FRACTION (BASED ON MASS) REMAINING IN THE SLICK = 8.3E-01, AREA = 4.6E+06 M**2

TIME = 2.1E+02 HOURS, MASS FRACTION OF EACH CUT REMAINING:
0.0E+00 0.0E+00 0.0E+00 7.6E-11 8.3E-03 4.2E-01 8.6E-01 9.8E-01 1.0E+00 1.0E+00 1.0E+00 1.0E+00 1.0E+00 1.0E+00

```
1.0E+00
FRACTION (BASED ON MASS) REMAINING IN THE SLICK =  8.4E-01, AREA =  5.3E+06 M**2


STEP SIZE OF  7.316E+00 IS BASED ON CUT   6

TIME =  2.6E+02 HOURS, MASS FRACTION OF EACH CUT REMAINING:
0.0E+00  0.0E+00  0.0E+00  0.0E+00  1.2E-03  3.0E-01  8.1E-01  9.7E-01  1.0E+00  1.0E+00  1.0E+00  1.0E+00  1.0E+00  1.0E+00
1.0E+00
FRACTION (BASED ON MASS) REMAINING IN THE SLICK =  8.4E-01, AREA =  5.9E+06 M**2

TIME =  3.1E+02 HOURS, MASS FRACTION OF EACH CUT REMAINING:
0.0E+00  0.0E+00  0.0E+00  0.0E+00  1.5E-04  2.0E-01  7.6E-01  9.6E-01  9.9E-01  1.0E+00  1.0E+00  1.0E+00  1.0E+00  1.0E+00
1.0E+00
FRACTION (BASED ON MASS) REMAINING IN THE SLICK =  8.3E-01, AREA =  6.4E+06 M**2

TIME =  3.6E+02 HOURS, MASS FRACTION OF EACH CUT REMAINING:
0.0E+00  0.0E+00  0.0E+00  0.0E+00  1.4E-05  1.3E-01  7.1E-01  9.5E-01  9.9E-01  1.0E+00  1.0E+00  1.0E+00  1.0E+00  1.0E+00
1.0E+00
FRACTION (BASED ON MASS) REMAINING IN THE SLICK =  8.3E-01, AREA =  6.9E+06 M**2

TIME =  4.1E+02 HOURS, MASS FRACTION OF EACH CUT REMAINING:
0.0E+00  0.0E+00  0.0E+00  0.0E+00  1.2E-06  8.4E-02  6.6E-01  9.4E-01  9.9E-01  1.0E+00  1.0E+00  1.0E+00  1.0E+00  1.0E+00
1.0E+00
FRACTION (BASED ON MASS) REMAINING IN THE SLICK =  8.2E-01, AREA =  7.3E+06 M**2

TIME =  4.6E+02 HOURS, MASS FRACTION OF EACH CUT REMAINING:
0.0E+00  0.0E+00  0.0E+00  0.0E+00  8.1E-08  5.2E-02  6.1E-01  9.3E-01  9.9E-01  1.0E+00  1.0E+00  1.0E+00  1.0E+00  1.0E+00
1.0E+00
FRACTION (BASED ON MASS) REMAINING IN THE SLICK =  8.2E-01, AREA =  7.7E+06 M**2

THE FINAL MASS FRACTIONS FOR THE SLICK AT  5.1E+02 HOURS ARE:
 0.000E+00  0.000E+00  0.000E+00  0.000E+00  4.020E-09  3.190E-02  5.551E-01  9.139E-01  9.866E-01  9.989E-01  1.000E+00
 1.000E+00  1.000E+00  1.000E+00  1.000E+00
FRACTION (BASED ON MASS) REMAINING IN THE SLICK =  8.2E-01, AREA =  8.1E+06 M**2

*****************************************************************
```

CODE LISTING: OCTOBER 1981

```
      C        ***** CUTVAP.FOR *****
      C
      C        GET YOUR OUTPUT FROM CUTVAP.OUT/FILE:FORTRAN
      C
               REAL*4 MW,MWI,KR,MTC1,MTC3,MASS,MOLES
               COMMON /COIL/ MWI,T01,VCI,PCI,CNUMI,VIS1
               COMMON /SPILL/ MTC3(30),VP(30),VLOG(30),RHO(30),Z,TERM2
     1,MW(30)
               COMMON /PCODE/ IOU
               DIMENSION TB(30),API(30),A(30),B(30),TBL(30),APIL(30),VC(30)
     1,TC(30),PC(30),CNUM(30),T10(30),HVAPI(30),HVAPZ(30)
     2,VOLL(30),VOL(30),MOLES(30),MTCI(30),VIS(30),VISE(30)
     3,VLOGK(30),SPGR(30),NC(30),NS(30)
               DIMENSION ANAME1(10),ANAME2(10)
               DATA ANAME2/'NORTH',' SLOP','E CRU','DE    ',6*'    '/
               DATA TBL/137.5,196.,220.,256.,283.,304.5,327.5,354.,380.5
     1,405.,426.5,449.5,470.,490.,509.5,528.,547.5,567.5,586.,602.
     2,621.,641.,650.,7*0./
               DATA APIL/71.6,59.7,55.,53.8,49.6,49.6,47.9,46.,44.,38.6
     1,38.8,37.2,35.4,33.9,33.1,32.2,31.8,31.6,30.7,29.6,28.,26.9
     2,14.6,7*0./
               DATA VOLL/1.5,2.1,2.,2.,2.,1.,2.,1.9,2.,2.,2.,2.,2.,2.
     1,2.,2.,2.,2.,2.1,2.,2.,1.8,55.,7*0./
               YI(X)=((1.-X)**0.38)/(X**X)
               OPEN(UNIT=32,DIALOG='DSKB:CUTVAP.OUT')
               IOU=32
               APIBL=25.7
               TYPE 501
      501      FORMAT(1X,'ENTER THE NUMBER OF TBP CUTS TO BE CHARACTERIZED
     1 ON 12')
               TYPE 502
      502      FORMAT(1X,'IF YOU HAVE NO INPUT DATA JUST ENTER 99')
               TYPE 503
      503      FORMAT(1X,'A 99 ENTRY WILL USE THE LIBRARY EXAMPLE')
               ICODE=1
               ACCEPT 504, NCUTS
      504      FORMAT(I2)
               IF(NCUTS.NE.99) GO TO 505
               ICODE=2
               NCUTS=23
               APIB=APIBL
               DO 507 I=1,10
               ANAME1(I)=ANAME2(I)
      507      CONTINUE
               GO TO 333
      505      TYPE 516
      516      FORMAT(1X,'ENTER THE IDENTIFICATION OF THE CRUDE')
               ACCEPT 517, (ANAME1(I),I=1,10)
      517      FORMAT(10A5)
               TYPE 521
      521      FORMAT(1X,'ENTER THE BULK API GRAVITY')
               ACCEPT 11, APIB
      333      DO 90 I=1,NCUTS
               GO TO (80,81), ICODE
      80       TYPE 10, I
      10       FORMAT(1X,'ENTER THE BOILING POINT AT 1 ATM TB IN DEG F
     1 FOR CUT',I3)
               ACCEPT 11, TB(I)
      11       FORMAT(F10.0)
               TYPE 12, I
      12       FORMAT(1X,'ENTER API GRAVITY FOR CUT',I3)
               ACCEPT 11, API(I)
               TYPE 13, I
      13       FORMAT(1X,'ENTER VOLUME PER CENT FOR CUT',I3)
               ACCEPT 11, VOL(I)
               GO TO 900
```

```
00670   81      TB(I)=TBL(I)
00680           API(I)=APIL(I)
00690           VOL(I)=VOLL(I)
00700   900     CONTINUE
00710   C
00720   C       DISPLAY THE CUTS BACK TO THE USER.
00730   C
00740           TYPE 681
00750   681     FORMAT(/,1X,'CUT',5X,'TB',9X,'API',9X,'VOL')
00760           DO 700 I=1,NCUTS
00770           TYPE 699, I,TB(I),API(I),VOL(I)
00780   699     FORMAT(1X,I2,3(2X,1PE10.3))
00790   700     CONTINUE
00800           TYPE 701
00810   701     FORMAT(1X,'DO YOU WANT TO CHANGE ANY?')
00820   712     ACCEPT 702, ANS
00830   702     FORMAT(A1)
00840           IF(ANS.EQ.'N') GO TO 713
00850           TYPE 703
00860   703     FORMAT(1X,'ENTER THE DATA POINT NUMBER TO BE CHANGED ON I2')
00870           ACCEPT 504, N
00880           TYPE 704
00890   704     FORMAT(1X,'ENTER 1 TO CHANGE TB, 2 FOR API, 3 FOR VOL%')
00900           ACCEPT 705, IC
00910   705     FORMAT(I1)
00920           TYPE 706
00930   706     FORMAT(1X,'ENTER THE CHANGED DATA')
00940           GO TO (707,708,709), IC
00950   707     ACCEPT 11, TB(N)
00960           GO TO 710
00970   708     ACCEPT 11, API(N)
00980           GO TO 710
00990   709     ACCEPT 11, VOL(N)
01000   710     TYPE 711
01010   711     FORMAT(1X,'DO YOU WANT TO CHANGE ANYMORE?')
01020           GO TO 712
01030   C
01040   C       ALWAYS RENORMALIZE THE INPUT VOLUMES TO 100%.
01050   C
01060   713     VTOTAL=0.
01070           DO 720 I=1,NCUTS
01080           VTOTAL=VTOTAL+VOL(I)
01090   720     CONTINUE
01100           DO 721 I=1,NCUTS
01110           VOL(I)=100.*VOL(I)/VTOTAL
01120   721     CONTINUE
01130   C
01140   C       NOW CHARACTERIZE ALL THE CUTS EXCEPT THE LAST ONE WHICH IS
01150   C       THE BOTTOM OF THE BARREL.  USE A VAPOR PRESSURE OF 0. AND A
01160   C       MOLECULARE WEIGHT OF 600.
01170   C
01180           MW(NCUTS)=600.
01190           VP(NCUTS)=0.
01200           NV=1
01210           NC1=NCUTS-1
01220           DO 1000 I=1,NCUTS
01230           APIN=API(I)
01240           TBN=TB(I)
01250           IF(I.EQ.NCUTS) NV=2
01260           CALL CHAR(APIN,TBN,AN,BN,NSN,NV)
01270   C
01280   C       THE CHARACTERIZATION SUBROUTINE RETURNS THE LOG10 OF THE
01290   C       KINEMATIC VISCOSITY (CENTISTOKES) AT 122 DEG F.
01300   C
01310           VISK(I)=10.**VIS1
01320           VLOGK(I)=ALOG(VISK(I))
```

```
01330                 GO TO (61,1000), NV
01340    61           NS(I)=NSN
01350                 A(I)=AN
01360                 B(I)=BN
01370                 MW(I)=MWI
01380                 TC(I)=TCI
01390                 TC(I)=TC(I)+459.
01400                 VC(I)=VCI
01410                 PC(I)=PCI
01420                 CNUM(I)=CNUMI
01430    C
01440    C            FIND THE TEMPERATURE AT WHICH THE VAPOR PRESSURE IS 10 MMHG
01450    C            BY USING NEWTON-RAPHSON WITH TB AS THE FIRST GUESS.
01460    C
01470                 NC(I)=0
01480                 YTEN=ALOG10(0.01315/PC(I))
01490                 X=(TB(I)+459.)/TC(I)
01500    140          EX=EXP(-20.*(X-B(I))**2)
01510                 Y=-A(I)*(1.-X)/X-EX
01520                 YOBJ=Y-YTEN
01530                 VP(I)=PC(I)*10.**Y
01540                 TEST=ABS(VP(I)-0.01315)
01550                 IF(TEST.LT.0.001315) GO TO 150
01560                 NC(I)=NC(I)+1
01570                 IF(NC(I).GT.20) GO TO 160
01580                 DY=A(I)/(X*X)+40.*(X-B(I))*EX
01590                 BI=YOBJ-DY*X
01600                 X=-BI/DY
01610                 GO TO 140
01620    C
01630    C            UNSUCCESSFUL EXIT FROM NEWTON-RAPHSON
01640    C
01650    160          TYPE 161, I,X,Y
01660    161          FORMAT(1X,'T10 FAILURE FOR',I4,' AT T = ',1PE10.3,' WHERE
01670           1 LOG10(P) = ',1PE10.3)
01680                 GO TO 9999
01690    C
01700    C            SUCCESSFUL EXIT FROM NEWTON-RAPHSON
01710    C
01720    150          T10(I)=X*TC(I)
01730    C
01740    C            CALCULATE THE HEAT OF VAPORIZATION AT 10 MMHG WITH THE
01750    C            CLAPEYRON EQUATION AND USE WATSONS METHOD FOR THE
01760    C            VAPOR PRESSURE BELOW 10 MMHG.
01770    C
01780                 TR2=T10(I)/TC(I)
01790                 EX=92.12*(TR2-B(I))*EXP(-20.*(TR2-B(I))**2)
01800                 HVAP=1.987*T10(I)*T10(I)*(2.303*A(I)/(TR2*TR2)+EX)/TC(I)
01810                 HVAPI(I)=HVAP/MW(I)
01820                 HVAPZ(I)=HVAP/(1.-TR2)**0.38
01830    1000         CONTINUE
01840    C
01850    C            END OF TBP CUTS CHARACTERIZATION
01860    C
01870                 WRITE (10U,162) (ANAME(I),I=1,10)
01880    162          FORMAT(1H1,'SUMMARY OF TBP CUTS CHARACTERIZATION FOR: '
01890           1,10A5)
01900                 WRITE (10U,163)
01910    163          FORMAT(/,8X,'TB',8X,'API',8X,'VOL',9X,'MW',9X,'TC',9X,'PC'
01920           1,9X,'VC',10X,'A',10X,'B',8X,'T10',8X,'VIS',5X,'NC NS')
01930                 DO 169 I=1,NCUTS
01940                 WRITE (10U,164) I,TB(I),API(I),VOL(I),MW(I),TC(I),PC(I),VC(I)
01950           1,A(I),B(I),T10(I),VISK(I),NC(I),NS(I)
01960    164          FORMAT(1X,I2,11(1X,1PE10.3),2(1X,I2))
01970    169          CONTINUE
01980                 WRITE (10U,180)
```

```
01990   180     FORMAT(//,1X,'TB = NORMAL BOILING TEMPERATURE, DEG F')
02000           WRITE (IOU,181)
02010   181     FORMAT(1X,'API = API GRAVITY')
02020           WRITE (IOU,182)
02030   182     FORMAT(1X,'VOL = VOLUME PER CENT OF TOTAL CRUDE')
02040           WRITE (IOU,183)
02050   183     FORMAT(1X,'MW = MOLECULAR WEIGHT')
02060           WRITE (IOU,184)
02070   184     FORMAT(1X,'TC = CRITICAL TEMPERATURE, DEG RANKINE')
02080           WRITE (IOU,185)
02090   185     FORMAT(1X,'PC = CRITICAL PRESSURE, ATMOSPHERES')
02100           WRITE (IOU,186)
02110   186     FORMAT(1X,'VC = CRITICAL VOLUME, CC/MOLE')
02120           WRITE (IOU,187)
02130   187     FORMAT(1X,'A AND B ARE PARAMETERS IN THE VAPOR PRESSURE
02140      1 EQUATION')
02150           WRITE (IOU,191)
02160   191     FORMAT(1X,'T10 IS THE TEMPERATURE IN DEG R WHERE THE VAPOR
02170      1 PRESSURE IS 10 MM HG')
02180           WRITE (IOU,192)
02190   192     FORMAT(1X,'VIS IS THE KINEMATIC VISCOSITY IN CENTISTOKES
02200      1 AT 122 DEG F')
02210           WRITE (IOU,188)
02220   188     FORMAT(1X,'NC = ERROR CODE, SHOULD BE LESS THAN 20')
02230           WRITE (IOU,189)
02240   189     FORMAT(1X,'NS = ERROR CODE, SHOULD BE EQUAL TO 1')
02250           WRITE (IOU,190) NCUTS
02260   190     FORMAT(1X,'IGNORE THE ERROR CODES FOR COMPONENT NUMBER ',I2)
02270   999     TYPE 153
02280   153     FORMAT(1X,'ENTER T IN DEG F FOR VP CALCULATION')
02290           ACCEPT 11, XSAVE
02300           TK=(XSAVE-32.)/1.8+273.
02310           IF(XSAVE.LT.0.) GO TO 999
02320           XPRINT=XSAVE
02330           XSAVE=XSAVE+459.
02340   C       CALCULATE THE VAPOR PRESSURE AT THE INPUT TEMPERATURE.
02350   C
02360   C       AT THIS POINT IF THE INPUT TEMPERATURE IS LESS THAN THE
02370   C       10 MMHG TEMPERATURE USE THE WATSON-CLAPEYRON EQUATION.
02380   C
02390   C       THE WATSON-CLAPEYRON EQUATION IS:
02400   C
02410   C       LN(P2/P1) = (HVAPZ/(R*TC))*INTEGRAL
02420   C
02430   C       WHERE P1 = PRESSURE AT TR1, P2 = PRESSURE AT TR2, HVAPZ IS
02440   C       THE HEAT OF VAPORIZATION AT ABSOLUTE ZERO,
02450   C       R = 1.987 BTU/(LBMOLE, DEG R),
02460   C       TC = CRITICAL TEMPERATURE AND INTEGRAL = VAPORIZATION
02470   C       INTEGRAL BETWEEN TR1 AND TR2.
02480   C
02490           WRITE (IOU,1001)
02500   1001    FORMAT(1H1,'CRUDE OIL CHARACTERIZATION AND PSEUDOCOMPONENT
02510      1 EVAPORATION MODEL')
02520           WRITE (IOU,1002) (ANAME1(I),I=1,10)
02530   1002    FORMAT(1X,'IDENTIFICATION: ',10A5,/)
02540           WRITE (IOU,1003) XPRINT
02550   1003    FORMAT(1X,'VAPOR PRESSURE IN ATMOSPHERES AT ',1PE10.3,' DEG F')
02560           WRITE (IOU,1004)
02570   1004    FORMAT(/,12X,'VP',/)
02580           DO 2000 I=1,NC1
02590           X=XSAVE
02600           IF(X.LT.T10(I)) GO TO 144
02610           X=X/TC(I)
02620           EX=EXP(-20.*(X-B(I))**2)
02630           Y=-A(I)*(1.-X)/X-EX
02640           VP(I)=PC(I)*10.**Y
```

```
02650                 GO TO 1999
02660      144        TR1=X/TC(I)
02670      C
02680      C         DO INTEGRAL BY SIMPSONS RULE WITH 21 POINTS
02690      C
02700                 TR2=T10(I)/TC(I)
02710                 DH=(TR2-TR1)/20.
02720                 RESULT=Y1(TR1)
02730                 TR=TR1
02740                 DO 142 K=1,10
02750                 TR=TR+DH
02760                 RESULT=RESULT+4.*Y1(TR)
02770                 TR=TR+DH
02780                 RESULT=RESULT+2.*Y1(TR)
02790      142        CONTINUE
02800                 TR=TR+DH
02810                 RESULT=RESULT+4.*Y1(TR)
02820                 TR=TR+DH
02830                 RESULT=DH*(RESULT+Y1(TR))/3.
02840                 P1=-4.33-HVAPZ(I)*RESULT/(1.987*TC(I))
02850                 VP(I)=EXP(P1)
02860      1999       WRITE (10U,16B) I,VP(I)
02870      16B        FORMAT(1X,I2,5X,1PE10.3)
02880      2000       CONTINUE
02890                 TYPE 550
02900      550        FORMAT(1X,'THE TBP CUTS HAVE BEEN CHARACTERIZED')
02910                 TYPE 551
02920      551        FORMAT(1X,'DO YOU WISH TO WEATHER THIS CRUDE?')
02930                 ACCEPT 702, ANS
02940                 IF(ANS.EQ.'N') GO TO 9999
02950                 TYPE 552
02960      552        FORMAT(1X,'ENTER THE SPILL SIZE IN BARRELS')
02970                 ACCEPT 11, BBL
02980                 TYPE 553
02990      553        FORMAT(1X,'ENTER WIND SPEED IN KNOTS PER HOUR')
03000                 ACCEPT 11, WIND5
03010                 TYPE 111
03020      111        FORMAT(1X,'ENTER NUMBER OF HOURS FOR OIL WEATHERING TO OCCUR')
03030                 ACCEPT 11, X2
03040      C
03050      C         NOW CALCULATE THE INITIAL GRAM MOLES FOR EACH COMPONENT TO
03060      C         GET THE INTEGRATION STARTED.
03070      C
03080                 BM=0.159*BBL
03090                 TMOLES=0.
03100                 DO 570 I=1,NCUTS
03110                 SPGR(I)=141.5/(API(I)+131.5)
03120                 AMASS=1532.*SPGR(I)*BBL*VOL(I)
03130                 MOLES(I)=AMASS/MW(I)
03140                 TMOLES=TMOLES+MOLES(I)
03150                 BIO(I)=100.*MOLES(I)/(BM*VOL(I))
03160      570        CONTINUE
03170      C
03180      C         CALCULATE THE MEAN MOLECULAR WEIGHT OF THE CRUDE
03190      C
03200                 SUM=0.
03210                 DO 170 I=1,NCUTS
03220                 SUM=SUM+MOLES(I)
03230      170        CONTINUE
03240                 WTMOLE=0.
03250                 DO 171 I=1,NCUTS
03260                 WTMOLE=WTMOLE+MW(I)*MOLES(I)/SUM
03270      171        CONTINUE
03280                 WRITE (10U,172) WTMOLE
03290      172        FORMAT(/,1X,'MEAN MOLECULAR WEIGHT OF THE CRUDE = ',1PE10.3)
03300      C
```

```
03310   C       CALCULATE AN AREA IN THE SAME WAY IT WILL BE CALCULATED
03320   C       AS THE SLICK WEATHERS.
03330   C
03340           Z=0.02
03350           VOLUM=0.
03360           DO 666 I=1,NCUTS
03370           VOLUM=VOLUM+MOLES(I)/RHO(I)
03380   666     CONTINUE
03390           AREA=VOLUM/Z
03400           DIA=SQRT(AREA/0.785)
03410   C
03420   C       CONVERT WIND SPEED TO M/HR.
03430   C
03440           WINDM=1652.9*WINDS
03450   C
03460   C       THE MASS TRANSFER COEFFICIENT IS CALCULATED ACCORDING TO TWO
03470   C       WAYS:  MTC1 IS ACCORDING TO MACKAY AND BASED ON CUMENE WITH
03480   C       A MOLECULAR WEIGHT OF 120.  KH IS CUMENE'S MASS TRANSFER
03490   C       COEFFICIENT.  THESE ARE OVER-ALL MASS-TRANSFER COEFFICIENTS.
03500   C
03510           TERM1=0.015*WINDM**0.78
03520           TERM2=DIA**(-0.11)
03530   C
03540   C       KH INCLUDES THE SCHMIDT NUMBER FOR CUMENE.
03550   C
03560           KH=TERM1*TERM2
03570           WRITE (10U,560)
03580   560     FORMAT(1H1,'OVER-ALL MASS-TRANSFER COEFFICIENTS')
03590           WRITE (10U,561) WINDS,WINDM
03600   561     FORMAT(/,1X,'WIND SPEED = ',1PE10.3,' KNOTS, OR ',1PE10.3
03610         1,' M/HR')
03620           WRITE (10U,616) DIA,AREA
03630   616     FORMAT(1X,'INITIAL SLICK DIAMETER = ',1PE10.3,' M, OR AREA = '
03640         1,1PE10.3,' M**2')
03650           WRITE (10U,562) KH
03660   562     FORMAT(/,1X,'OVER-ALL MASS-TRANSFER COEFFICIENT FOR CUMENE = '
03670         1,1PE10.3,' M/HR',/)
03680           WRITE (10U,579)
03690   579     FORMAT(3X,'CUT',12X,'M/HR',7X,'G-MOLES/(HR)(ATM)(M**2)'
03700         1,3X,'SPGR OF CUT')
03710           TEMP=(8.2E-05)*TK
03720           DO 564 I=1,NCt
03730           MTC1(I)=KH*0.93*SQRT((MW(I)+29.)/MW(I))
03740   C
03750   C       MTC3(I) IS THE OVER-ALL MASS-TRANSFER COEFFICIENT DIVIDED
03760   C       BY R*T.  R=82.06E+06 (ATM)(M**3)/(G-MOLE)(DEG K)
03770   C
03780           MTC3(I)=MTC1(I)/TEMP
03790           WRITE (10U,566) I,MTC1(I),MTC3(I),SPGR(I)
03800   566     FORMAT(2X,I3,3(10X,1PE10.3))
03810   564     CONTINUE
03820           SPGRB=141.5/(API8+131.5)
03830           MASS=0.1582*BBL*SPGRB
03840           WRITE (10U,565) BBL,MASS
03850   565     FORMAT(/,1X,'FOR THIS SPILL OF ',1PE10.3,' BARRELS, THE
03860         1 MASS IS ',1PE10.3,' METRIC TONNES')
03870           VOLUMB=VOLUM/0.159
03880           WRITE (10U,581) VOLUM,VOLUMB
03890   581     FORMAT(/,1X,'VOLUME FROM SUMMING THE CUTS = ',1PE9.1,' M**3
03900         1, OR ',1PE10.3,' BARRELS')
03910   C
03920   C       CALCULATE THE VISCOSITY OF THE CRUDE AT 122 DEG F AND THE
03930   C       ENTERED ENVIRONMENT TEMPERATURE.
03940   C
03950           VISMIX=0.
03960           DO 571 I=1,NCUTS
```

```
03970             VISMIX=VISMIX+MOLES(I)*VLOCK(I)/TMOLES
03980     571     CONTINUE
03990             VISMIX=EXP(VISMIX)
04000             WRITE (10U,572) VISMIX
04010     572     FORMAT(/,1X,'KINEMATIC VISCOSITY OF THE BULK CRUDE FROM
04020    1 THE CUTS = ',1PE8.1,' CENTISTOKES AT 122 DEG F')
04030             VISMIX=0.
04040             DO 573 I=1,NCUTS
04050             VIS(I)=VISK(I)*EXP(1923.*(1./XSAVE-0.001721))
04060             VLOC(I)=ALOG(VIS(I))
04070             VISMIX=VISMIX+MOLES(I)*VLOC(I)/TMOLES
04080     573     CONTINUE
04090             VISMIX=EXP(VISMIX)
04100             WRITE (10U,574) VISMIX,XPRINT
04110     574     FORMAT(/,1X,'KINEMATIC VISCOSITY OF THE BULK CRUDE FROM THE
04120    1 CUTS = ',1PE8.1,' AT T = ',0PF5.1,' DEG F',/)
04130             NEQ=NCUTS
04140     C
04150     C       PRINT EVERY XP TIME INCREMENT.
04160     C
04170             XP=1.
04180             X1=0.
04190             MOLES(NCUTS+1)=AREA
04200             CALL BRKG4(MOLES,X1,X2,XP,NEQ)
04210             TYPE 590
04220     590     FORMAT(1X,'DO IT AGAIN?')
04230             ACCEPT 702, ANS
04240             IF(ANS.EQ.'Y') GO TO 999
04250     9999    CONTINUE
04260             END
04270             SUBROUTINE CHAR(API,TB,A,B,NS,NV)
04280             REAL*4 MW1
04290             COMMON /COIL/ MW1,TC1,VC1,PC1,CNUM1,VIS1
04300             DIMENSION C(2,6),T(2,6),P(4),V(2,6)
04310             DATA ((C(I,J),J=1,6),I=1,2)/6.241E+01,-4.595E-02,-2.836E-01
04320            1,3.256E-03,4.570E-04,5.279E-04
04330            1,4.260E+02,-1.007,-7.449,1.30E-02,1.047E-03,2.621E-02/
04340               DATA ((T(I,J),J=1,6),I=1,2)/4.055E+02,1.337,-2.662,-2.169E-03
04350            1,-4.943E-04,1.454E-02
04360            1,412.2,1.276,-2.865,-2.0UUE-03,-3.707E-04,2.UUUE-02/
04370               DATA P/1.237E-02,0.2516,4.039E-02,-4.024E-02/
04380               DATA ((V(I,J),J=1,6),I=1,2)/ -0.4400,-9.344E-04,0.01583
04390            1,-5.219E-05,5.260E-06,1.536E-04
04400            1,-0.6019,1.793E-03,-3.159E-03,-5.1E-06,9.067E-07,3.522E-05/
04410     C
04420     C       THIS SUBROUTINE CHARACTERIZES A CUT OF CRUDE OIL WITH RESPECT
04430     C       TO VAPOR PRESSURE.  THE INPUT REQUIRED IS API GRAVITY AND THE
04440     C       BOILING POINT AT 1 ATMOSPHERE.  THE OUTPUT IS A SWITCH NS
04450     C       WHERE NS=1 MEANS THE VAPOR PRESSURE EQUATION CAN BE USED DOWN TO
04460     C       10 MM HG AND NS=2 MEANS THE CLAPEYRON EQUATION SHOULD BE USED.
04470     C
04480     C       THE VAPOR PRESSURE EQUATION IS:
04490     C
04500     C       LOG10(PR) = -A*(1.-TR)/TR - EXP(-20*(TR-B)**2)
04510     C
04520     C       WHERE PR = REDUCED PRESSURE, TR = REDUCED TEMPERATURE AND
04530     C       A AND B ARE RETURNED BY THIS SUBROUTINE.
04540     C
04550     C       API = GRAVITY, TB = BOILING POINT AT 1 ATMOSPHERE IN DEG F.
04560     C       CALCULATE CRITICAL TEMPERATURE AND MOLECULAR WEIGHT.
04570     C
04580             API2=API*API
04590             TB2=TB*TB
04600             CROSS=API*TB
04610     C
04620     C       CALCULATE THE VISCOSITY OF THE CUT.
```

```
04630   C
04640           I=1
04650           IF(API.GT.35.) I=2
04660           VIS1=V(I,1)+V(I,2)*TB+V(I,3)*API+V(I,4)*CROSS+V(I,5)*TB2
04670          1+V(I,6)*API2
04680           GO TO (99,101), NV
04690   99      I=1
04700           IF(TB.GT.500.) I=2
04710           MW1=C(I,1)+C(I,2)*TB+C(I,3)*API+C(I,4)*CROSS+C(I,5)*TB2
04720          1+C(I,6)*API2
04730           TC1=T(I,1)+T(I,2)*TB+T(I,3)*API+T(I,4)*CROSS+T(I,5)*TB2
04740          1+T(I,6)*API2
04750           TCK=(TC1+459.)/1.8
04760   C
04770   C       CALCULATE THE VISCOSITY OF THE CUT.
04780   C
04790           I=1
04800           IF(API.GT.35.) I=2
04810           VIS1=V(I,1)+V(I,2)*TB+V(I,3)*API+V(I,4)*CROSS+V(I,5)*TB2
04820          1+V(I,6)*API2
04830   C
04840   C       CALCULATE THE CARBON NUMBER
04850   C
04860           CNUM1=(MW1-2.)/14.
04870           X=ALOG10(CNUM1)
04880   C
04890   C       CALCULATE B FOR THE VAPOR PRESSURE EQUATION
04900   C
04910           BPRIME=P(1)+X*(P(2)+X*(P(3)+X*P(4)))
04920           B=BPRIME-0.02
04930   C
04940   C       CALCULATE THE CRITICAL VOLUME, CC/GMOLE
04950   C
04960           VW=1.88+2.44*CNUM1
04970           VC1=VW/0.044
04980   C
04990   C       CALCULATE THE CRITICAL PRESSURE IN ATMOSPHERES
05000   C
05010           PCP=20.8*TCK/(VC1-8.)
05020           PC1=PCP+10.
05030           TR=(TB+459.)/(TC1+459.)
05040           PR=1./PC1
05050           NS=1
05060           IF(TR.LE.B) GO TO 100
05070           A=(ALOG10(PR)+EXP(-20.*(TR-B)**2))*TR/(TR-1.)
05080           GO TO 101
05090   100     NS=2
05100   101     RETURN
05110           END
05120           SUBROUTINE BRKG4(Y,X1,X2,XP,NEQ)
05130           REAL*4 K1,K2,K3,K4,MTC3I,MW,MWU
05140           COMMON /SPILL/ MTC3(30),VP(30),VLOC(30),RHO(30),Z,TERM2
05150          1,MW(30)
05160           COMMON /PCODE/ 100
05170           COMMON /TALK/ NEQ1
05180           DIMENSION Y(30),YARG(30),K1(30),K2(30),K3(30),K4(30)
05190           DIMENSION YSAVE(30),YP(30),YMSAVE(30),YN(30),MWU(30)
05200   C
05210   C       RUNGA-KUTTA 4-TH ORDER NUMERICAL INTEGRATION FOR SIMULTANEOUS
05220   C       DIFFERENTIAL EQUATIONS.  SEE C.R. WYLIE, PAGES 108-117 OR
05230   C       D. GREENSPAN, PAGES 113-115.
05240   C
05250   C       THIS SUBROUTINE DOES THE PRINTING, THE INITIAL AND FINAL VALUES
05260   C       ARE ALWAYS PRINTED.  PRINT THE RESULTS EVERY XP INCREMENT
05270   C       IN X.
05280   C
```

```
05290 C       THE USER MUST WRITE SUBROUTINE FXYZ WHICH CALCULATES THE
05300 C       K1, K2, K3, AND K4 VECTORS AS A FUNCTION OF X AND THE
05310 C       CURRENT Y VECTOR.  INTEGRATION FOLLOWS THE REFERENCES AND
05320 C       WAS TEST ON PROBLEM 5, PAGE 116 IN WYLIE.
05330 C
05340 C       THE FIRST NCUTS POSITIONS IN THE Y VECTOR ARE THE MOLES
05350 C       OF THE COMPONENTS, POSITION NCUTS+1 IS THE AREA OF THE
05360 C       SLICK.
05370 C
05380         NEQ1=NEQ+1
05390         NS=1
05400         IN=1
05410         IKEEP=1
05420         TOTAL=0.
05430         TSAVE=0.
05440         DO 30 I=1,NEQ
05450         YSAVE(I)=Y(I)
05460         YMSAVE(I)=Y(I)*MW(I)
05470         MWU(I)=MW(I)
05480         TSAVE=TSAVE+YMSAVE(I)
05490         TOTAL=TOTAL+Y(I)
05500 30      CONTINUE
05510         NDEL=0
05520         NFAST=0
05530         X=X1
05540         XW=X+XP
05550         WRITE (10U,933)
05560 933     FORMAT(/,1X,'COUNT THE CUTS IN THE FOLLOWING OUTPUT FROM LEFT
05570        1 TO RIGHT',/)
05580         WRITE (10U,931)
05590 931     FORMAT(1X,'THE INITIAL MOLES IN THE SLICK ARE:')
05600         WRITE (10U,900) (Y(I),I=1,NEQ)
05610 900     FORMAT((1(1X,1PE10.3)))
05620         WRITE (10U,932)
05630 932     FORMAT(/,1X,'THE INITIAL MASSES IN THE SLICK ARE:')
05640         WRITE (10U,900) (YMSAVE(I),I=1,NEQ)
05650         WRITE (10U,902)
05660 902     FORMAT(/)
05670 C
05680 C       CALCULATE DY/DX AND SET THE STEP SIZE TO APPROXIMATE
05690 C       A 5% CHANGE IN THE MOST RAPIDLY CHANGING Y.  WHEN THIS
05700 C       Y DECREASES BY A FACTOR OF 20, RESET THE STEP SIZE
05710 C       ACCORDING TO THE NEXT Y.
05720 C       SOME Y'S WILL CHANGE SO FAST THAT THEY WILL BE GONE
05730 C       IN A FEW MINUTES.  THESE ARE DELETED BEFORE INTEGRATION
05740 C       STARTS AND NOTED ON THE PRINTED RESULTS.
05750 C
05760 899     NFAST=NFAST+1
05770 890     CALL FXYZ(X,Y,K1,NEQ)
05780         H=0.05*Y(NFAST)/K1(NFAST)
05790         YOLD=Y(NFAST)
05800         H=ABS(H)
05810         H2=H/2.
05820         GO TO (801,898), IN
05830 801     IF(H.GT.0.05) GO TO 886
05840 C
05850 C       Y(NFAST) CHANGES TOO FAST TO CALCULATE, DELETE IT AND MOVE
05860 C       EVERYBODY ONE SPACE TO THE LEFT.
05870 C
05880 C       WHEN YOU MOVE THE AREA BE SURE TO SUBTRACT THE CONTRIBUTION
05890 C       OF THE CUT JUST DELETED.
05900 C
05910         ISTART=1
05920         NFAST=1
05930         NDEL=NDEL+1
05940         NEQ=NEQ-1
```

```
05950           AD=Y(I)/RHO(I)/Z
05960           DO 850 I=1,NEQ
05970           II=I+1
05980           Y(I)=Y(II)
05990           VP(I)=VP(II)
06000           MTC3(I)=MTC3(II)
06010           YSAVE(I)=YSAVE(II)
06020           VLOC(I)=VLOC(II)
06030           RHO(I)=RHO(II)
06040           MWU(I)=MWU(II)
06050           YMSAVE(I)=YMSAVE(II)
06060   850     CONTINUE
06070           Y(NEQ+1)=Y(NEQ+2)-AD
06080           WRITE (10U,849) NDEL
06090   849     FORMAT(1X,'CUT ',I2,' GOES AWAY IN MINUTES, THEREFORE IT WAS
06100          1 DELETED AND THE CUTS RENUMBERED',/)
06110           GO TO 890
06120   886     IN=2
06130           NEQ1=NEQ+1
06140   898     WRITE (10U,871) H,NFAST
06150   871     FORMAT(/,2X,'STEP SIZE OF ',1PE10.3,' IS BASED ON CUT ',I3,/)
06160   897     IF(X.LT.XW) GO TO 901
06170           XW=X+XP
06180           YTOT=0.
06190           TMASS=0.
06200           DO 31 I=1,NEQ
06210           YF(I)=Y(I)/YSAVE(I)
06220           YTOT=YTOT+Y(I)
06230           YM(I)=Y(I)*MWU(I)
06240           TMASS=TMASS+YM(I)
06250           YM(I)=YM(I)/YMSAVE(I)
06260   31      CONTINUE
06270           WRITE (10U,432) X
06280   432     FORMAT(2X,'TIME = ',1PE8.1,' HOURS, MASS FRACTION OF EACH
06290          1 CUT REMAINING:')
06300           WRITE (10U,911) (YM(I),I=1,NEQ)
06310   911     FORMAT(14(1X,1PE8.1))
06320   C
06330   C       WHEN THE FRACTION REMAINING OF COMPONENT I GETS LOW,
06340   C       SET ITS VAPOR PRESSURE AND MOLES EQUAL TO ZERO.
06350   C
06360           DO 631 I=ISTART,NEQ
06370           IF(YF(I).GT.1.0E-0B) GO TO 631
06380           IKEEP=I+1
06390           VP(I)=0.
06400           Y(I)=0.
06410   631     CONTINUE
06420           ISTART=IKEEP
06430           CONE=TMASS/TSAVE
06440           WRITE (10U,922) CONE,Y(NEQ1)
06450   922     FORMAT(2X,'FRACTION (BASED ON MASS) REMAINING IN THE SLICK
06460          1 = ',1PE8.1,', AREA = ',1PE8.1,' M**2')
06470           WRITE (10U,902)
06480   C
06490   C       INCREASE XP TO 50 HOURS AFTER 50 HOURS OF WEATHERING.
06500   C
06510           GO TO (701,901), NS
06520   701     IF(X.LT.50.) GO TO 901
06530           NS=2
06540           XP=50.
06550   C
06560   C       TAKE A STEP IN TIME
06570   C
06580   901     XARG=X
06590           DO 101 I=1,NEQ1
06600           YARG(I)=Y(I)
```

```
06610  101     CONTINUE
06620           CALL FXYZ(XARG,YARG,K1,NEQ)
06630           XARG=X+H2
06640           DO 102 I=1,NEQ1
06650           YARG(I)=Y(I)+H*K1(I)/2.
06660  102     CONTINUE
06670           CALL FXYZ(XARG,YARG,K2,NEQ)
06680           DO 103 I=1,NEQ1
06690           YARG(I)=Y(I)+H*K2(I)/2.
06700  103     CONTINUE
06710           CALL FXYZ(XARG,YARG,K3,NEQ)
06720           XARG=X+H
06730           DO 104 I=1,NEQ1
06740           YARG(I)=Y(I)+H*K3(I)
06750  104     CONTINUE
06760           CALL FXYZ(XARG,YARG,K4,NEQ)
06770           DO 105 I=1,NEQ1
06780           Y(I)=Y(I)+H*(K1(I)+2.*(K2(I)+K3(I))+K4(I))/6.
06790  105     CONTINUE
06800  C
06810  C       RECALCULATE THE OVER-ALL MASS-TRANSFER COEFFICIENTS OUTSIDE
06820  C       THE DERIVATIVE SUBROUTINE.  THE DIAMETER DEPENDENCE IS VERY
06830  C       SLOW.  TERM2 IS THE OLD DIA**(-0.11).  SO DIVIDE THE OLD
06840  C       COEFFICIENT BY TERM2 AND MULTIPLY IN THE NEW ONE.
06850  C
06860           DIA=SQRT(Y(NEQ1)/0.785)
06870           TNEW=DIA**(-0.11)
06880           ADJUST=TNEW/TERM2
06890           DO 115 I=1,NEQ
06900           MTC3(I)=MTC3(I)*ADJUST
06910  115     CONTINUE
06920           TERM2=TNEW
06930           IF(X.GE.X2) GO TO 106
06940           X=XARG
06950           TEST=ABS(Y(NFAST)/YOLD)
06960           IF(TEST.LT.0.01) GO TO 899
06970           GO TO 897
06980  106     WRITE (10U,930) X
06990  930     FORMAT(1X,'THE FINAL MASSES FOR THE SLICK AT ',1PE8.1
07000        1,' HOURS ARE:')
07010           TMASS=0.
07020           DO 913 I=1,NEQ
07030           YM(I)=Y(I)*MWU(I)
07040           TMASS=TMASS+YM(I)
07050           YM(I)=YM(I)/YMSAVE(I)
07060  913     CONTINUE
07070           CONE=TMASS/TSAVE
07080           WRITE (10U,900) (YM(I),I=1,NEQ)
07090           WRITE (10U,922) CONE,Y(NEQ1)
07100           RETURN
07110           END
07120           SUBROUTINE FXYZ(XARG,MOLES,K,NEQ)
07130           REAL*4 MOLES,K,MTC3,MW
07140           COMMON /SPILL/ MTC3(30),VP(30),VLOG(30),RHO(30),Z,TERM2
07150        1,MW(30)
07160           COMMON /TALK/ NEQ1
07170           DIMENSION MOLES(30),K(30)
07180  C
07190  C       THE THICK AREA IS MOLES(NEQ+1).
07200  C
07210           SUM=0.
07220           DO 100 I=1,NEQ
07230           SUM=SUM+MOLES(I)
07240  100     CONTINUE
07250           DO 200 I=1,NEQ
07260           K(I)=MTC3(I)*MOLES(NEQ1)*VP(I)*MOLES(I)/SUM
```

```
07270               K(I)=-K(I)
07280     200       CONTINUE
07290               VOL=0.
07300               DO 300 I=1,NEQ
07310               VOL=VOL+MOLES(I)/RHO(I)
07320     300       CONTINUE
07330               Z=VOL/MOLES(NEQ1)
07340               K(NEQ1)=(5.4E+05)*(Z**1.33)*MOLES(NEQ1)**0.33
07350               RETURN
07360               END
```

CODE FLOW CHART; OCTOBER 1981

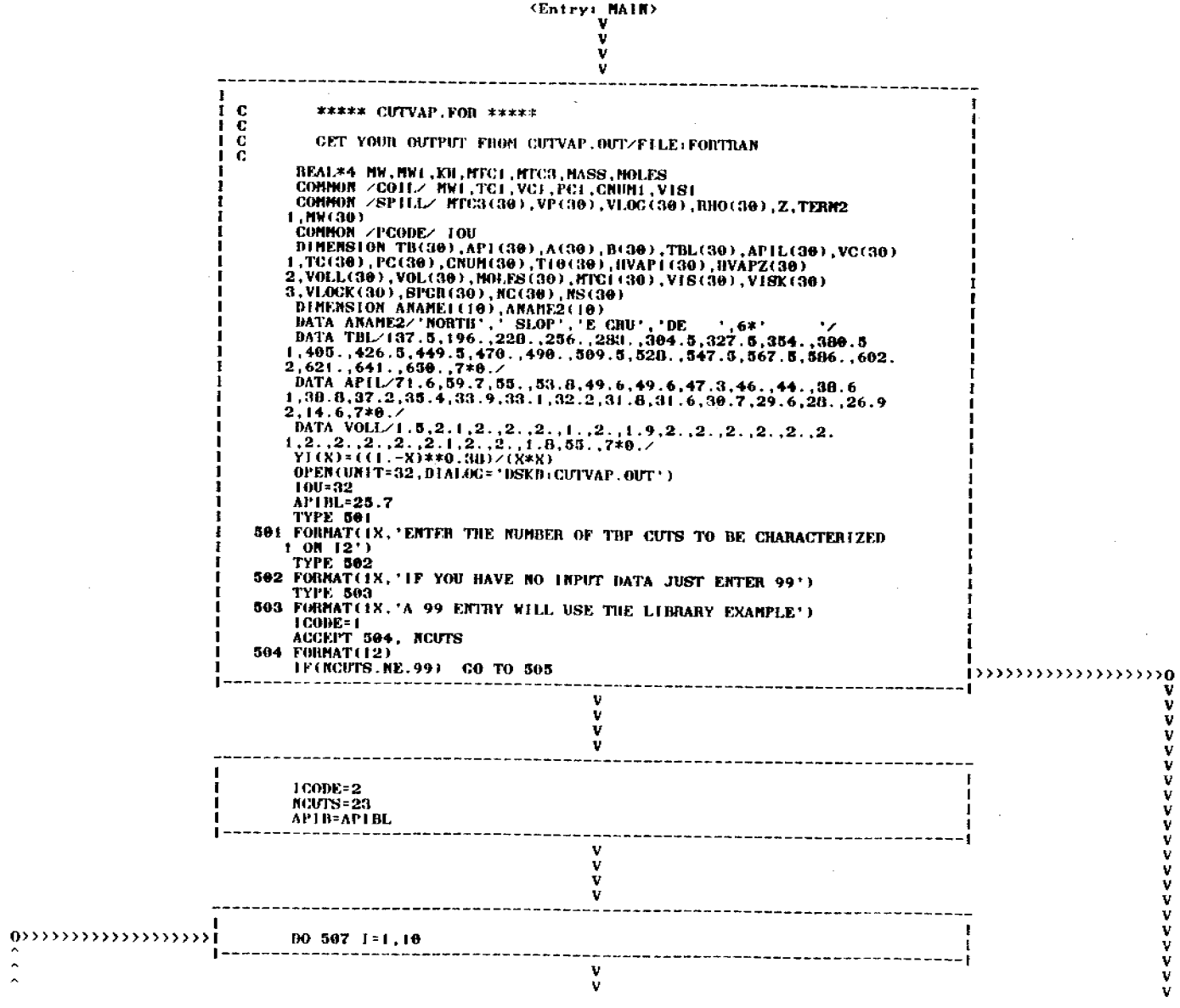
<Entry: MAIN>
C ***** CUTVAP.FOR *****
C
C GET YOUR OUTPUT FROM CUTVAP.OUT/FILE:FORTRAN
C
REAL*4 MW,MW1,KH,MTC1,MTC3,MASS,MOLES
COMMON /COIL/ MW1,TC1,VC1,PC1,CNUM1,VIS1
COMMON /SPILL/ MTC3(30),VP(30),VLOC(30),RHO(30),Z,TERM2
1,MW(30)
COMMON /PCODE/ IOU
DIMENSION TB(30),API(30),A(30),B(30),TBL(30),APIL(30),VC(30)
1,TC(30),PC(30),CNUM(30),TI0(30),HVAPI(30),HVAPZ(30)
2,VOLL(30),VOL(30),MOLES(30),MTC1(30),VIS(30),VISK(30)
3,VLOCK(30),SPGR(30),NC(30),NS(30)
DIMENSION ANAME1(10),ANAME2(10)
DATA ANAME2/'NORTH',' SLOP','E CRU','DE ',6*' '/
DATA TBL/137.5,196.,228.,256.,283.,304.5,327.5,354.,380.5
1,405.,426.5,449.5,470.,490.,509.5,528.,547.5,567.5,586.,602.
2,621.,641.,658.,7*0./
DATA APIL/71.6,59.7,55.,53.8,49.6,49.6,47.3,46.,44.,38.6
1,38.8,37.2,35.4,33.9,33.1,32.2,31.8,31.6,30.7,29.6,28.,26.9
2,14.6,7*0./
DATA VOLL/1.5,2.1,2.,2.,2.,1.,2.,1.9,2.,2.,2.,2.,2.,2.
1,2.,2.,2.,2.,2.1,2.,2.,1.8,55.,7*0./
YI(X)=((1.-X)**0.38)/(X*X)
OPEN(UNIT=32,DIALOG='DSKB:CUTVAP.OUT')
IOU=32
APIBL=25.7
TYPE 501
501 FORMAT(1X,'ENTER THE NUMBER OF TBP CUTS TO BE CHARACTERIZED
1 ON 12')
TYPE 502
502 FORMAT(1X,'IF YOU HAVE NO INPUT DATA JUST ENTER 99')
TYPE 503
503 FORMAT(1X,'A 99 ENTRY WILL USE THE LIBRARY EXAMPLE')
ICODE=1
ACCEPT 504, NCUTS
504 FORMAT(I2)
IF(NCUTS.NE.99) GO TO 505
ICODE=2
NCUTS=23
APIB=APIBL
DO 507 I=1,10

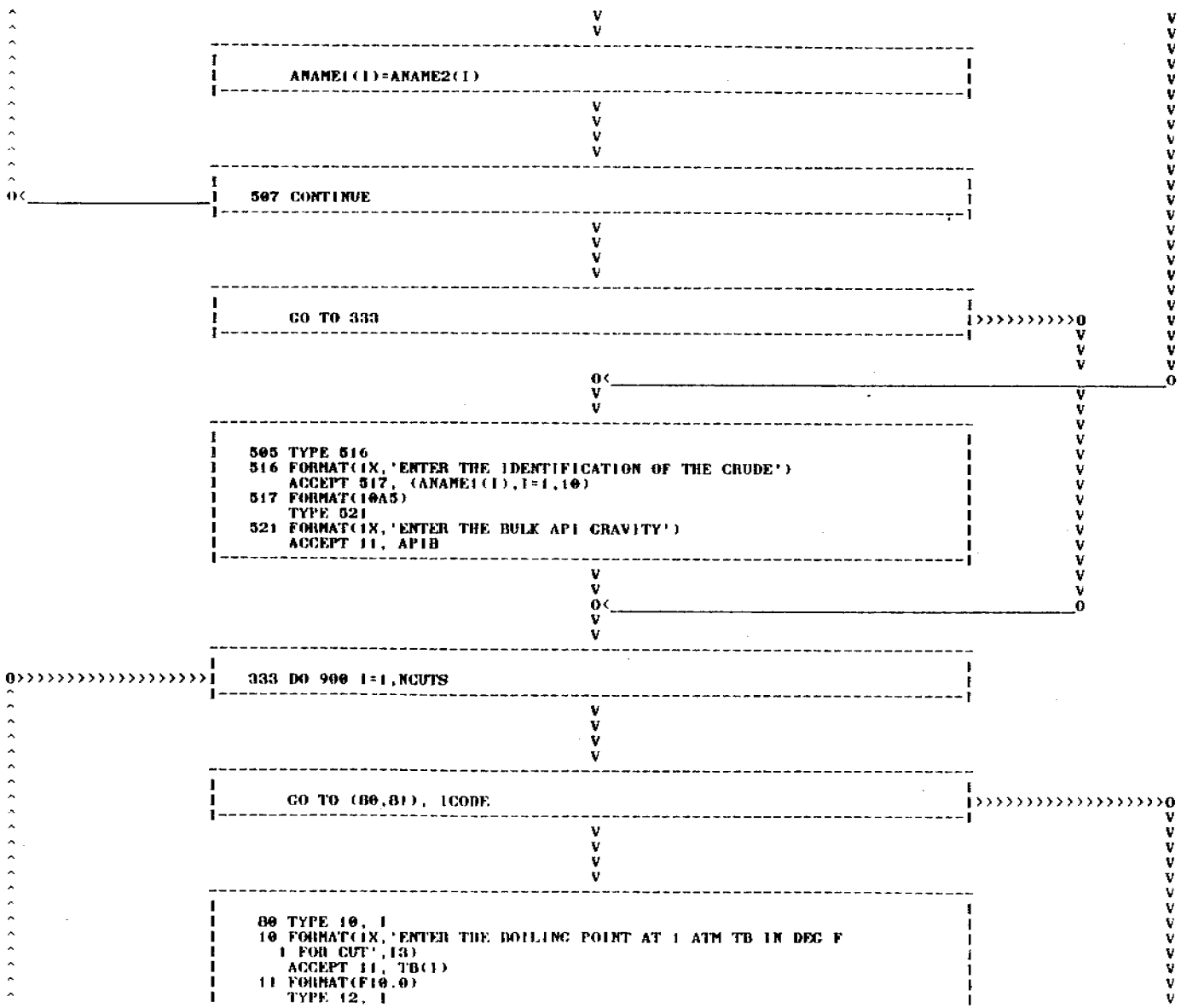
ANAME1(I)=ANAME2(I)
507 CONTINUE
GO TO 333
505 TYPE 516
516 FORMAT(1X,'ENTER THE IDENTIFICATION OF THE CRUDE')
ACCEPT 517, (ANAME1(I),I=1,10)
517 FORMAT(10A5)
TYPE 521
521 FORMAT(1X,'ENTER THE BULK API GRAVITY')
ACCEPT 11, APIB
333 DO 900 I=1,NCUTS
GO TO (80,81), ICODE
80 TYPE 10, I
10 FORMAT(1X,'ENTER THE BOILING POINT AT 1 ATM TB IN DEG F
1 FOR CUT',I3)
ACCEPT 11, TB(I)
11 FORMAT(F10.0)
TYPE 12, I

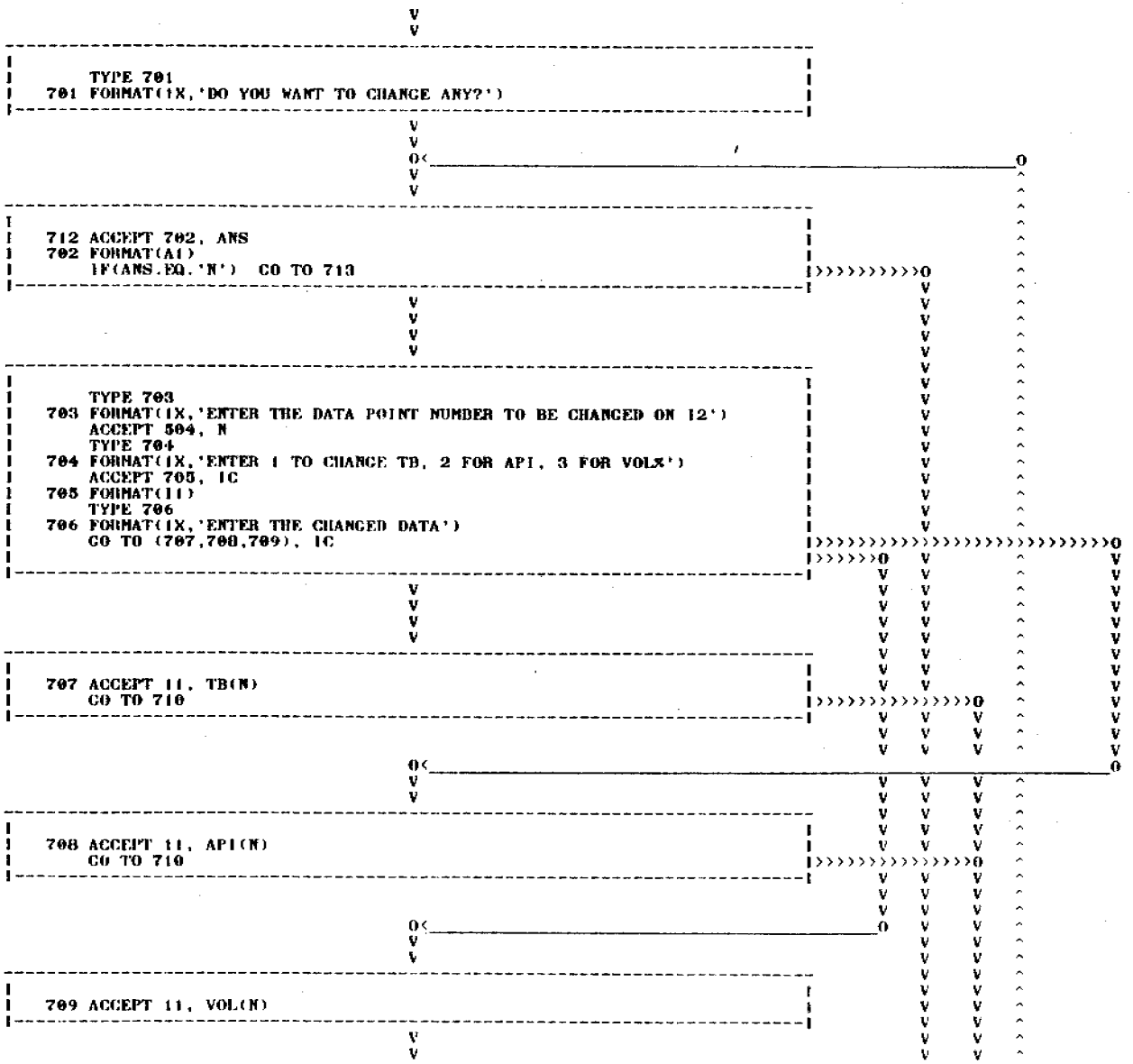
TYPE 701
701 FORMAT(1X,'DO YOU WANT TO CHANGE ANY?')
712 ACCEPT 702, ANS
702 FORMAT(A1)
IF(ANS.EQ.'N') GO TO 713
TYPE 703
703 FORMAT(1X,'ENTER THE DATA POINT NUMBER TO BE CHANGED ON 12')
ACCEPT 504, N
TYPE 704
704 FORMAT(1X,'ENTER 1 TO CHANGE TB, 2 FOR API, 3 FOR VOLX')
ACCEPT 705, IC
705 FORMAT(I1)
TYPE 706
706 FORMAT(1X,'ENTER THE CHANGED DATA')
GO TO (707,708,709), IC
707 ACCEPT 11, TB(N)
GO TO 710
708 ACCEPT 11, API(N)
GO TO 710
709 ACCEPT 11, VOL(N)

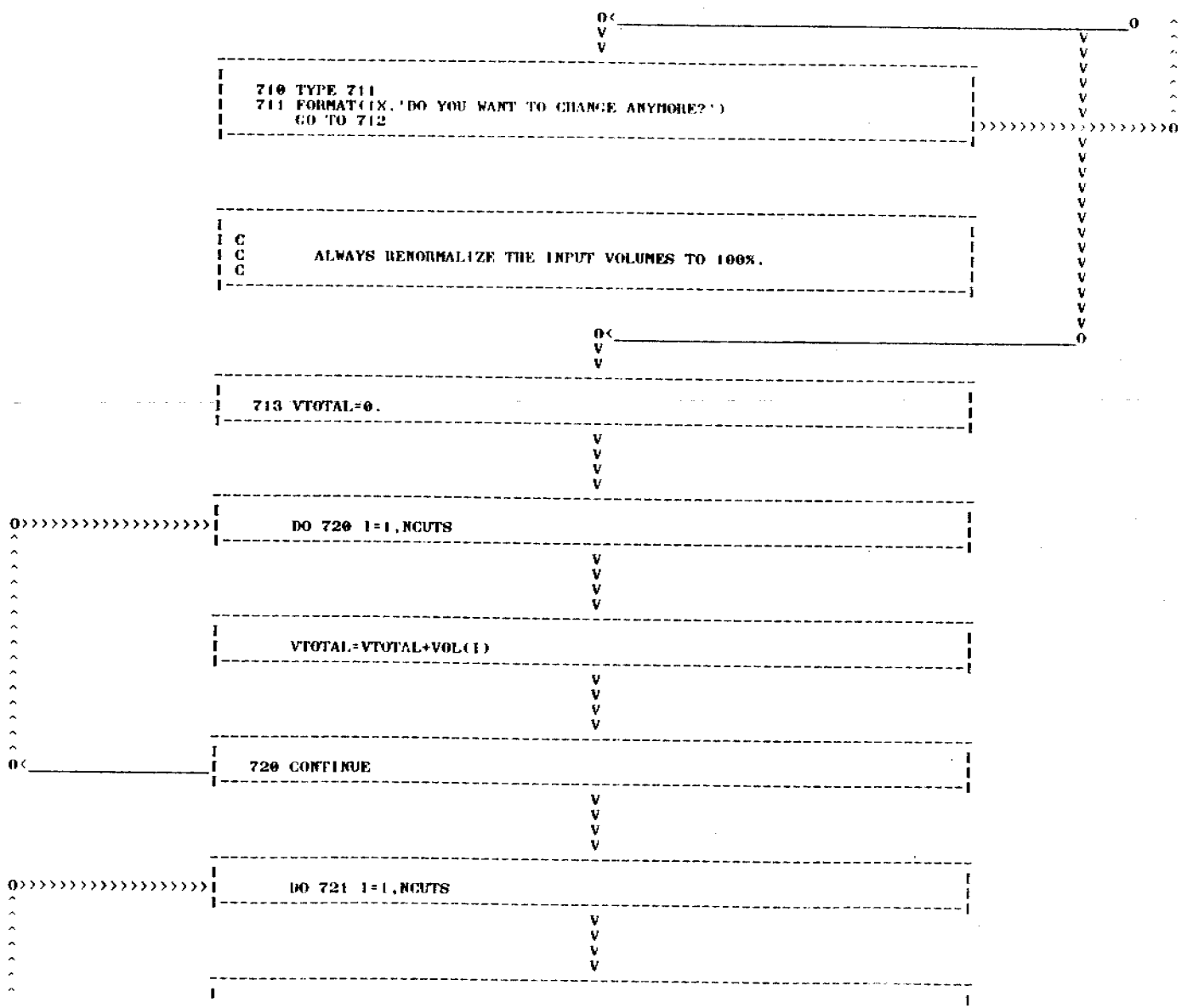
710 TYPE 711
711 FORMAT(1X,'DO YOU WANT TO CHANGE ANYMORE?')
GO TO 712
C
C ALWAYS RENORMALIZE THE INPUT VOLUMES TO 100%.
C
713 VTOTAL=0.
DO 720 I=1,NCUTS
VTOTAL=VTOTAL+VOL(I)
720 CONTINUE
DO 721 I=1,NCUTS

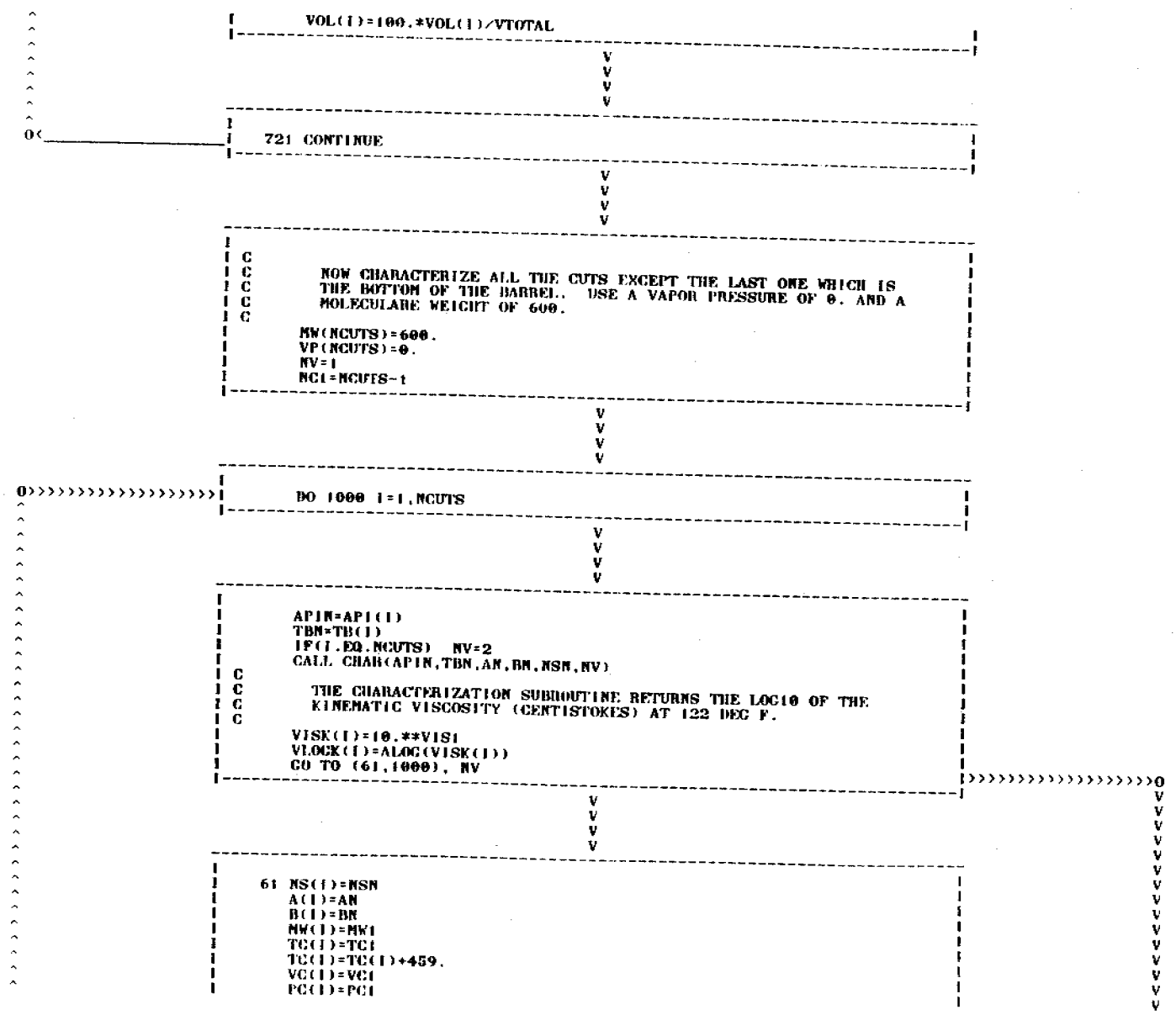
VOL(I)=100.*VOL(I)/VTOTAL
721 CONTINUE
C
C NOW CHARACTERIZE ALL THE CUTS EXCEPT THE LAST ONE WHICH IS
C THE BOTTOM OF THE BARREL. USE A VAPOR PRESSURE OF 0. AND A
C MOLECULARE WEIGHT OF 600.
C
MW(NCUTS)=600.
VP(NCUTS)=0.
NV=1
NCI=NCUTS-1
DO 1000 I=1,NCUTS
APIN=API(I)
TBN=TB(I)
IF(I.EQ.NCUTS) NV=2
CALL CHAR(APIN,TBN,AN,BN,NSN,NV)
C
C THE CHARACTERIZATION SUBROUTINE RETURNS THE LOG10 OF THE
C KINEMATIC VISCOSITY (CENTISTOKES) AT 122 DEG F.
C
VISK(I)=10.**VISI
VLOCK(I)=ALOG(VISK(I))
GO TO (61,1000), NV
61 NS(I)=NSN
A(I)=AN
B(I)=BN
MW(I)=MWI
TC(I)=TCI
TC(I)=TC(I)+459.
VC(I)=VCI
PC(I)=PCI

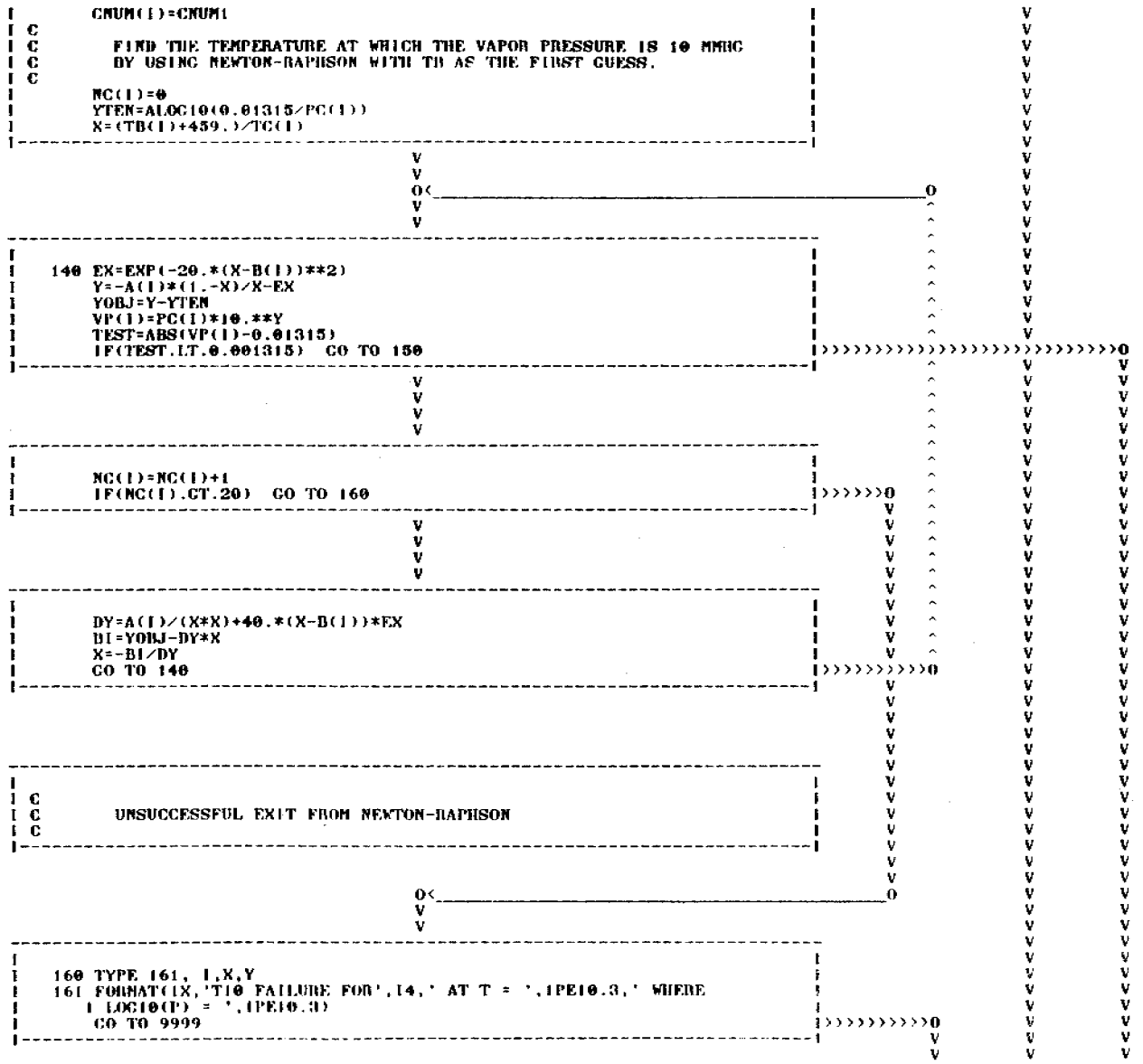
CNUM(I)=CNUM1
C
C FIND THE TEMPERATURE AT WHICH THE VAPOR PRESSURE IS 10 MMHG
C BY USING NEWTON-RAPHSON WITH TB AS THE FIRST GUESS.
C
NC(I)=0
YTEN=ALOG10(0.01315/PC(I))
X=(TB(I)+459.)/TC(I)
140 EX=EXP(-20.*(X-B(I))**2)
Y=-A(I)*(1.-X)/X-EX
YOBJ=Y-YTEN
VP(I)=PC(I)*10.**Y
TEST=ABS(VP(I)-0.01315)
IF(TEST.LT.0.001315) GO TO 150
NC(I)=NC(I)+1
IF(NC(I).GT.20) GO TO 160
DY=A(I)/(X*X)+40.*(X-B(I))*EX
BI=YOBJ-DY*X
X=-BI/DY
GO TO 140
C
C UNSUCCESSFUL EXIT FROM NEWTON-RAPHSON
C
160 TYPE 161, I,X,Y
161 FORMAT(1X,'T10 FAILURE FOR',I4,' AT T = ',1PE10.3,' WHERE
1 LOC10(P) = ',1PE10.3)
GO TO 9999

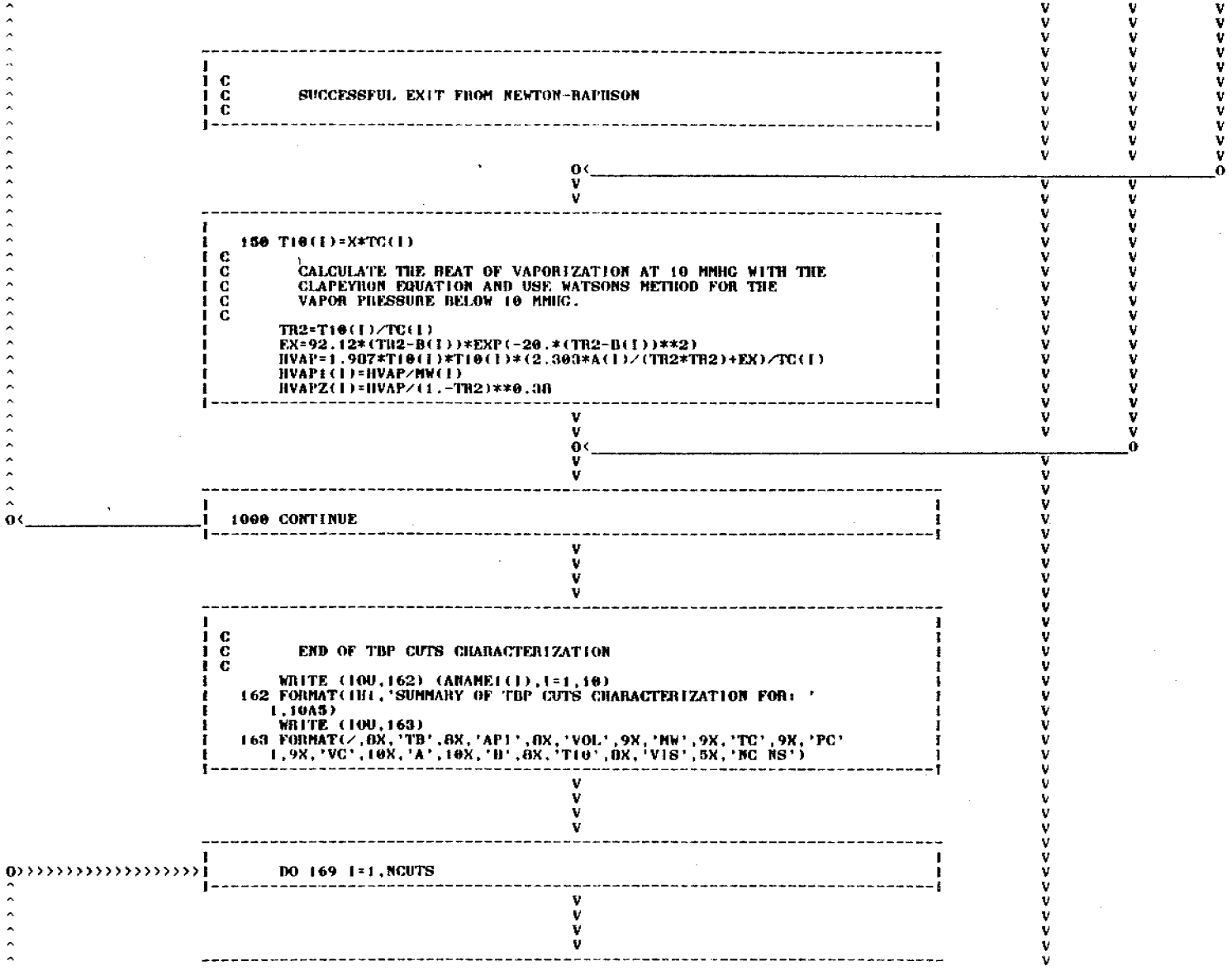
C
C SUCCESSFUL EXIT FROM NEWTON-RAPHSON
C
150 T10(I)=X*TC(I)
C
C CALCULATE THE HEAT OF VAPORIZATION AT 10 MMHG WITH THE
C CLAPEYRON EQUATION AND USE WATSONS METHOD FOR THE
C VAPOR PRESSURE BELOW 10 MMHG.
C
TR2=T10(I)/TC(I)
EX=92.12*(TR2-B(I))*EXP(-20.*(TR2-B(I))**2)
HVAP=1.987*T10(I)*T10(I)*(2.303*A(I)/(TR2*TR2)+EX)/TC(I)
HVAPI(I)=HVAP/MW(I)
HVAPZ(I)=HVAP/(1.-TR2)**0.38
1000 CONTINUE
C
C END OF TBP CUTS CHARACTERIZATION
C
WRITE (IOU,162) (ANAME1(I),I=1,10)
162 FORMAT(1H1,'SUMMARY OF TBP CUTS CHARACTERIZATION FOR: '
1,10A5)
WRITE (IOU,163)
163 FORMAT(/,8X,'TB',8X,'API',8X,'VOL',9X,'MW',9X,'TC',9X,'PC'
1,9X,'VC',10X,'A',10X,'B',8X,'T10',8X,'VIS',5X,'NC NS')
DO 169 I=1,NCUTS

```
      WRITE (IOU,164) I,TB(I),API(I),VOL(I),MW(I),TC(I),PC(I),VC(I),A(I)
     1,B(I),T10(I),VISK(I),NC(I),NS(I)
  164 FORMAT(1X,I2,11(1X,1PE10.3),2(1X,I2))
```

```
  169 CONTINUE
```

```
      WRITE (IOU,180)
  180 FORMAT(//,1X,'TB = NORMAL BOILING TEMPERATURE, DEG F')
      WRITE (IOU,181)
  181 FORMAT(1X,'API = API GRAVITY')
      WRITE (IOU,182)
  182 FORMAT(1X,'VOL = VOLUME PER CENT OF TOTAL CRUDE')
      WRITE (IOU,183)
  183 FORMAT(1X,'MW = MOLECULAR WEIGHT')
      WRITE (IOU,184)
  184 FORMAT(1X,'TC = CRITICAL TEMPERATURE, DEG RANKINE')
      WRITE (IOU,185)
  185 FORMAT(1X,'PC = CRITICAL PRESSURE, ATMOSPHERES')
      WRITE (IOU,186)
  186 FORMAT(1X,'VC = CRITICAL VOLUME, CC/MOLE')
      WRITE (IOU,187)
  187 FORMAT(1X,'A AND B ARE PARAMETERS IN THE VAPOR PRESSURE
     1 EQUATION')
      WRITE (IOU,191)
  191 FORMAT(1X,'T10 IS THE TEMPERATURE IN DEG R WHERE THE VAPOR
     1 PRESSURE IS 10 MM HG')
      WRITE (IOU,192)
  192 FORMAT(1X,'VIS IS THE KINEMATIC VISCOSITY IN CENTISTOKES
     1 AT 122 DEG F')
      WRITE (IOU,188)
  188 FORMAT(1X,'NC = ERROR CODE, SHOULD BE LESS THAN 20')
      WRITE (IOU,189)
  189 FORMAT(1X,'NS = ERROR CODE, SHOULD BE EQUAL TO 1')
      WRITE (IOU,190) NCUTS
  190 FORMAT(1X,'IGNORE THE ERROR CODES FOR COMPONENT NUMBER ',I2)
```

```
  999 TYPE 153
  153 FORMAT(1X,'ENTER T IN DEG F FOR VP CALCULATION')
      ACCEPT 11, XSAVE
      TK=(XSAVE-32.)/1.8+273.
      IF(XSAVE.LT.0.)  GO TO 999
```

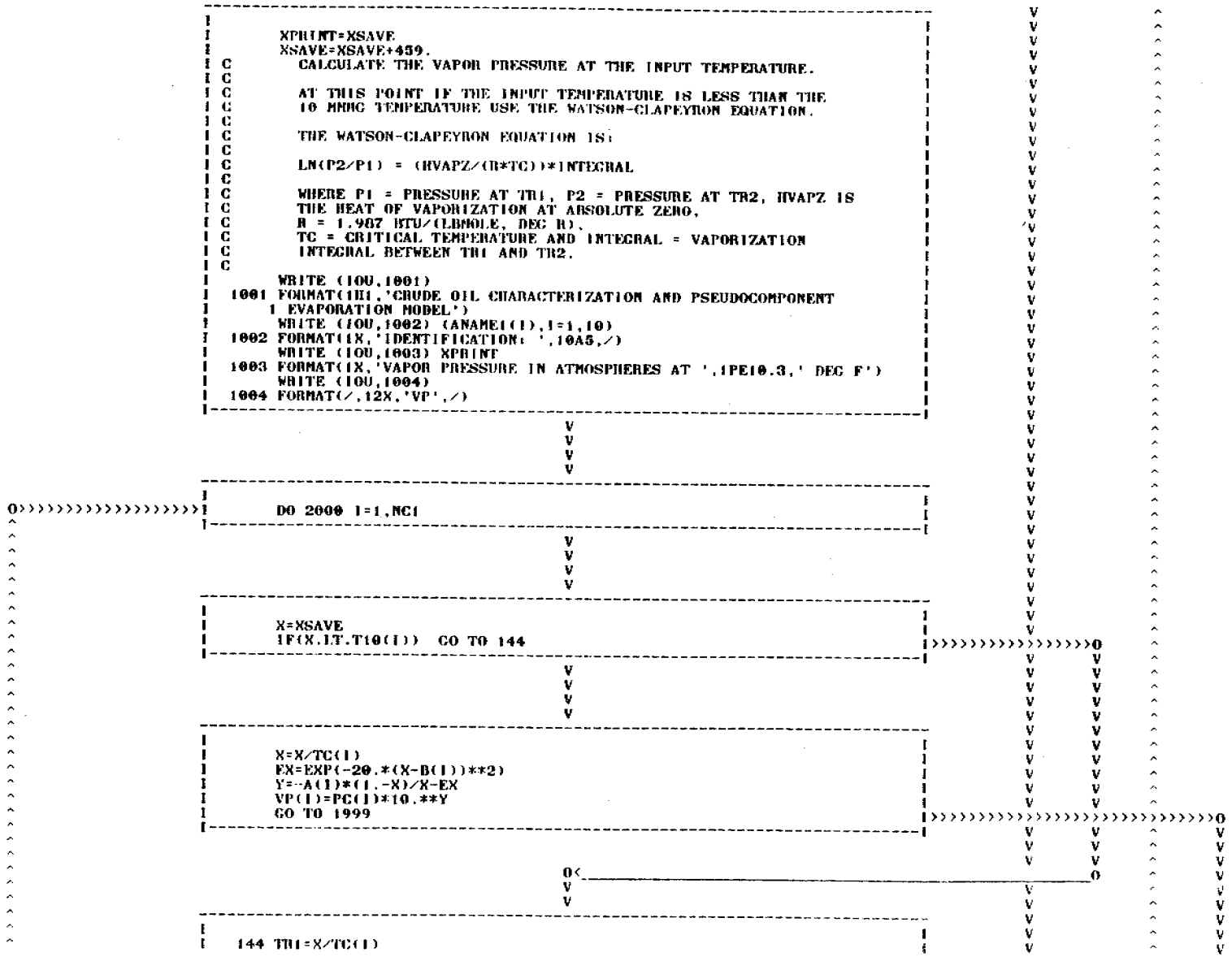
XPRINT=XSAVE
XSAVE=XSAVE+459.
C CALCULATE THE VAPOR PRESSURE AT THE INPUT TEMPERATURE.
C
C AT THIS POINT IF THE INPUT TEMPERATURE IS LESS THAN THE
C 10 MMHG TEMPERATURE USE THE WATSON-CLAPEYRON EQUATION.
C
C THE WATSON-CLAPEYRON EQUATION IS:
C
C LN(P2/P1) = (HVAPZ/(R*TC))*INTEGRAL
C
C WHERE P1 = PRESSURE AT TR1, P2 = PRESSURE AT TR2, HVAPZ IS
C THE HEAT OF VAPORIZATION AT ABSOLUTE ZERO,
C R = 1.987 BTU/(LBMOLE, DEG R),
C TC = CRITICAL TEMPERATURE AND INTEGRAL = VAPORIZATION
C INTEGRAL BETWEEN TR1 AND TR2.
C
WRITE (IOU,1001)
1001 FORMAT(1H1,'CRUDE OIL CHARACTERIZATION AND PSEUDOCOMPONENT
1 EVAPORATION MODEL')
WRITE (IOU,1002) (ANAME1(I),I=1,10)
1002 FORMAT(1X,'IDENTIFICATION: ',10A5,/)
WRITE (IOU,1003) XPRINT
1003 FORMAT(1X,'VAPOR PRESSURE IN ATMOSPHERES AT ',1PE10.3,' DEG F')
WRITE (IOU,1004)
1004 FORMAT(/,12X,'VP',/)
DO 2000 I=1,NC1
X=XSAVE
IF(X.LT.T10(I)) GO TO 144
X=X/TC(I)
EX=EXP(-20.*(X-B(I))**2)
Y=-A(I)*(1.-X)/X-EX
VP(I)=PC(I)*10.**Y
GO TO 1999
144 TR1=X/TC(I)

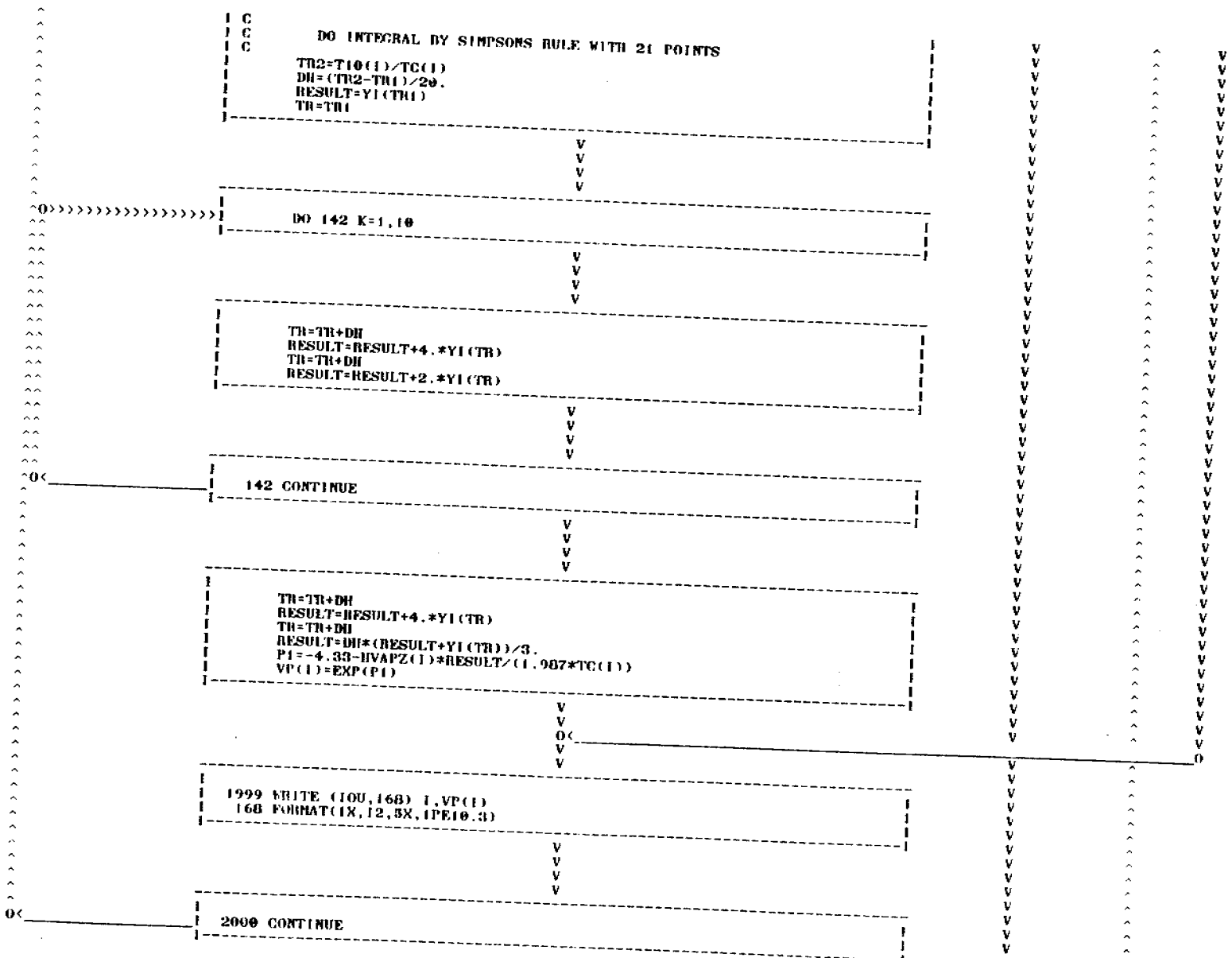
C
C
C DO INTEGRAL BY SIMPSONS RULE WITH 21 POINTS
TR2=T10(I)/TC(I)
DH=(TR2-TR1)/20.
RESULT=YI(TR1)
TR=TR1
DO 142 K=1,10
TR=TR+DH
RESULT=RESULT+4.*YI(TR)
TR=TR+DH
RESULT=RESULT+2.*YI(TR)
142 CONTINUE
TR=TR+DH
RESULT=RESULT+4.*YI(TR)
TR=TR+DH
RESULT=DH*(RESULT+YI(TR))/3.
P1=-4.33-HVAPZ(I)*RESULT/(1.987*TC(I))
VP(I)=EXP(P1)
1999 WRITE (IOU,168) I,VP(I)
168 FORMAT(1X,I2,5X,1PE10.3)
2000 CONTINUE

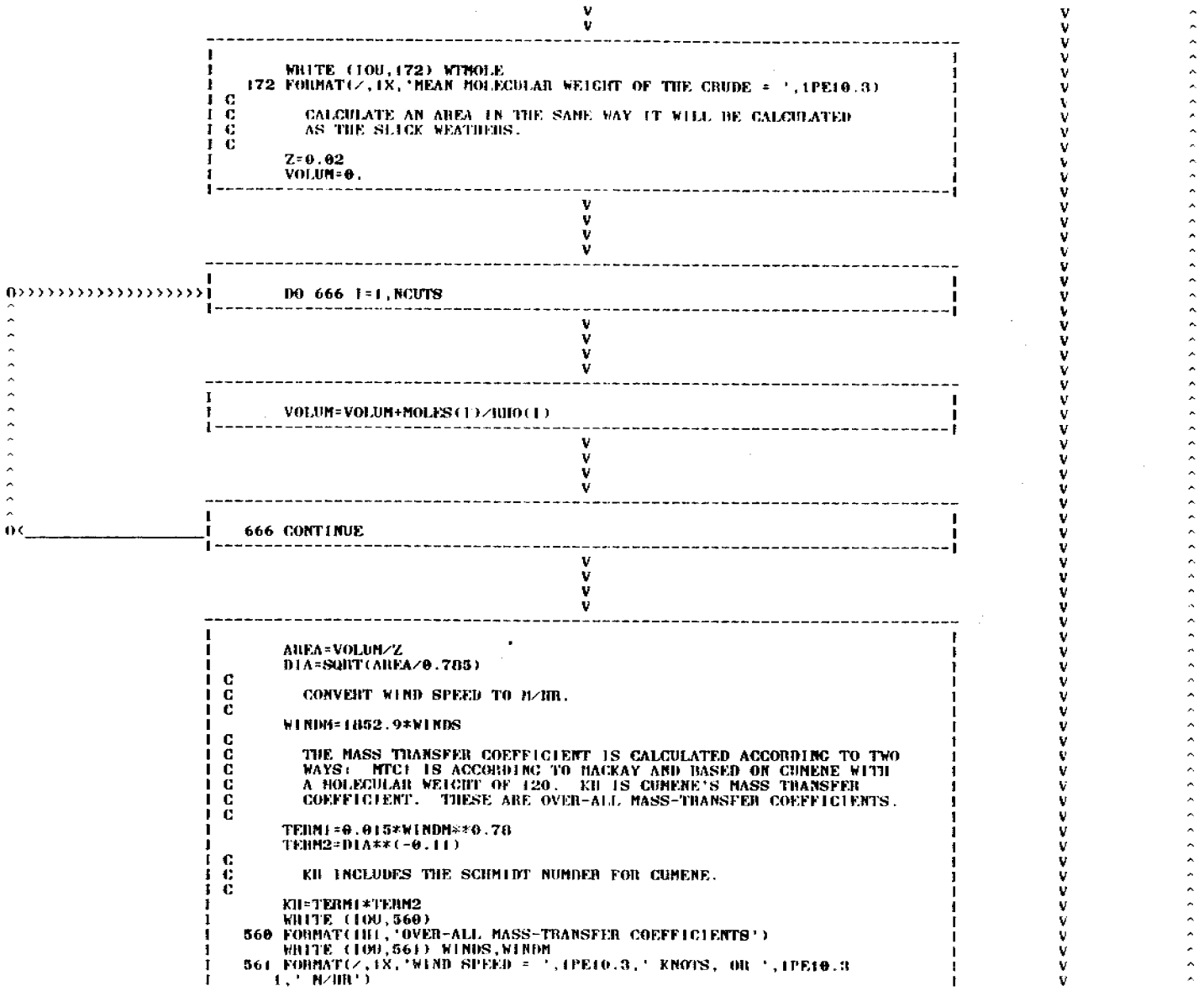
WRITE (IOU,172) WTMOLE
172 FORMAT(/,1X,'MEAN MOLECULAR WEIGHT OF THE CRUDE = ',1PE10.3)
C
C CALCULATE AN AREA IN THE SAME WAY IT WILL BE CALCULATED
C AS THE SLICK WEATHERS.
C
Z=0.02
VOLUM=0.
DO 666 I=1,NCUTS
VOLUM=VOLUM+MOLES(I)/RHO(I)
666 CONTINUE
AREA=VOLUM/Z
DIA=SQRT(AREA/0.785)
C
C CONVERT WIND SPEED TO M/HR.
C
WINDM=1852.9*WINDS
C
C THE MASS TRANSFER COEFFICIENT IS CALCULATED ACCORDING TO TWO
C WAYS: MTC1 IS ACCORDING TO MACKAY AND BASED ON CUMENE WITH
C A MOLECULAR WEIGHT OF 120. KH IS CUMENE'S MASS TRANSFER
C COEFFICIENT. THESE ARE OVER-ALL MASS-TRANSFER COEFFICIENTS.
C
TERM1=0.015*WINDM**0.78
TERM2=DIA**(-0.11)
C
C KH INCLUDES THE SCHMIDT NUMBER FOR CUMENE.
C
KH=TERM1*TERM2
WRITE (IOU,560)
560 FORMAT(1H1,'OVER-ALL MASS-TRANSFER COEFFICIENTS')
WRITE (IOU,561) WINDS,WINDM
561 FORMAT(/,1X,'WIND SPEED = ',1PE10.3,' KNOTS, OR ',1PE10.3
1,' M/HR')

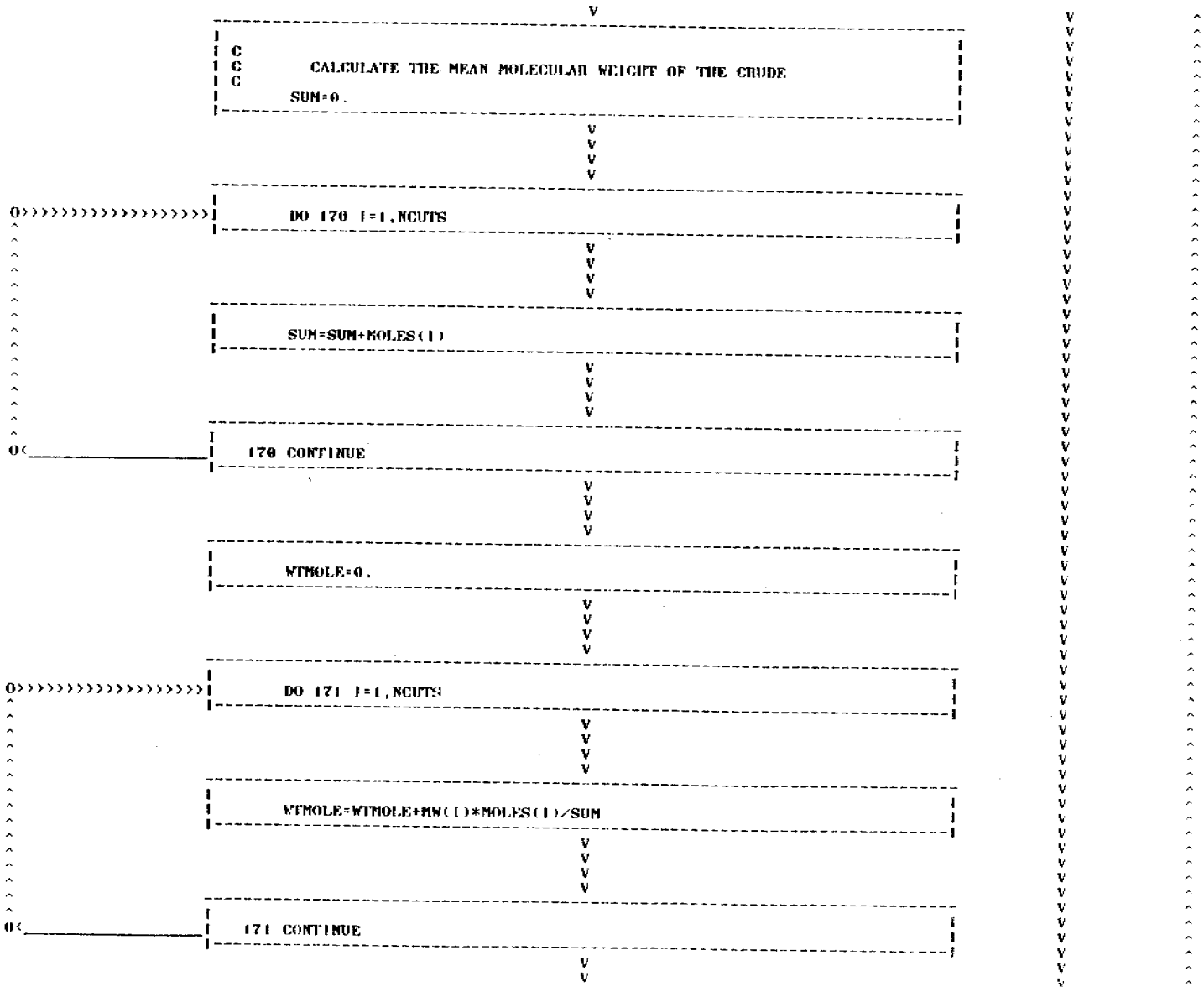
C
C CALCULATE THE MEAN MOLECULAR WEIGHT OF THE CRUDE
C
SUM=0.
DO 170 I=1,NCUTS
SUM=SUM+MOLES(I)
170 CONTINUE
WTMOLE=0.
DO 171 I=1,NCUTS
WTMOLE=WTMOLE+MW(I)*MOLES(I)/SUM
171 CONTINUE

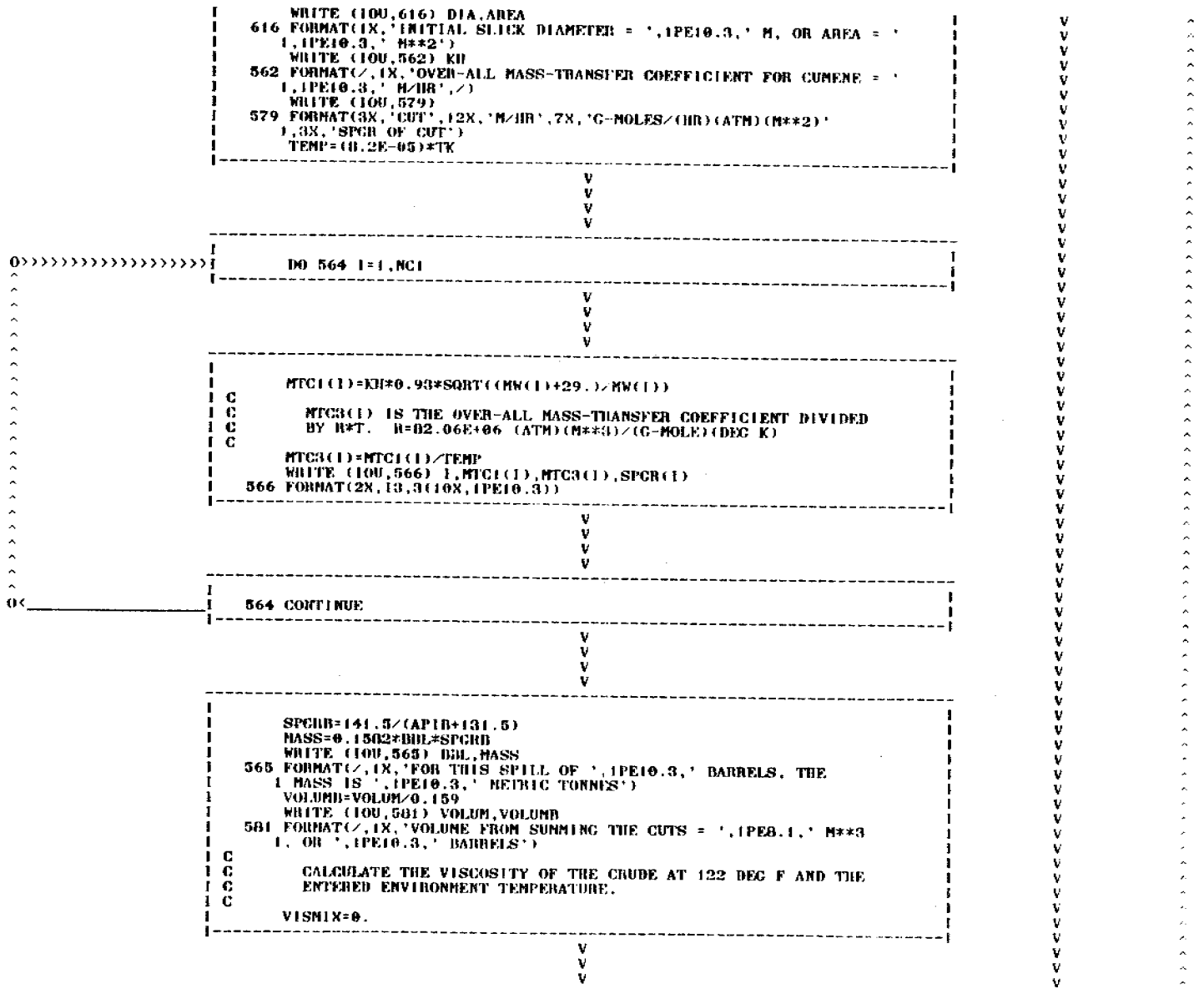
WRITE (IOU,616) DIA,AREA
616 FORMAT(1X,'INITIAL SLICK DIAMETER = ',1PE10.3,' M, OR AREA = '
1,1PE10.3,' M**2')
WRITE (IOU,562) KH
562 FORMAT(/,1X,'OVER-ALL MASS-TRANSFER COEFFICIENT FOR CUMENE = '
1,1PE10.3,' M/HR',/)
WRITE (IOU,579)
579 FORMAT(3X,'CUT',12X,'M/HR',7X,'G-MOLES/(HR)(ATM)(M**2)'
1,3X,'SPGR OF CUT')
TEMP=(8.2E-05)*TK
DO 564 I=1,NCI
MTC1(I)=KH*0.93*SQRT((MW(I)+29.)/MW(I))
C
C MTC3(I) IS THE OVER-ALL MASS-TRANSFER COEFFICIENT DIVIDED
C BY R*T. R=82.06E+06 (ATM)(M**3)/(G-MOLE)(DEG K)
C
MTC3(I)=MTC1(I)/TEMP
WRITE (IOU,566) I,MTC1(I),MTC3(I),SPGR(I)
566 FORMAT(2X,I3,3(10X,1PE10.3))
564 CONTINUE
SPGRB=141.5/(APIB+131.5)
MASS=0.1502*BBL*SPGRB
WRITE (IOU,565) BBL,MASS
565 FORMAT(/,1X,'FOR THIS SPILL OF ',1PE10.3,' BARRELS, THE
1 MASS IS ',1PE10.3,' METRIC TONNES')
VOLUMB=VOLUM/0.159
WRITE (IOU,581) VOLUM,VOLUMB
581 FORMAT(/,1X,'VOLUME FROM SUMMING THE CUTS = ',1PE8.1,' M**3
1, OR ',1PE10.3,' BARRELS')
C
C CALCULATE THE VISCOSITY OF THE CRUDE AT 122 DEG F AND THE
C ENTERED ENVIRONMENT TEMPERATURE.
C
VISMIX=0.

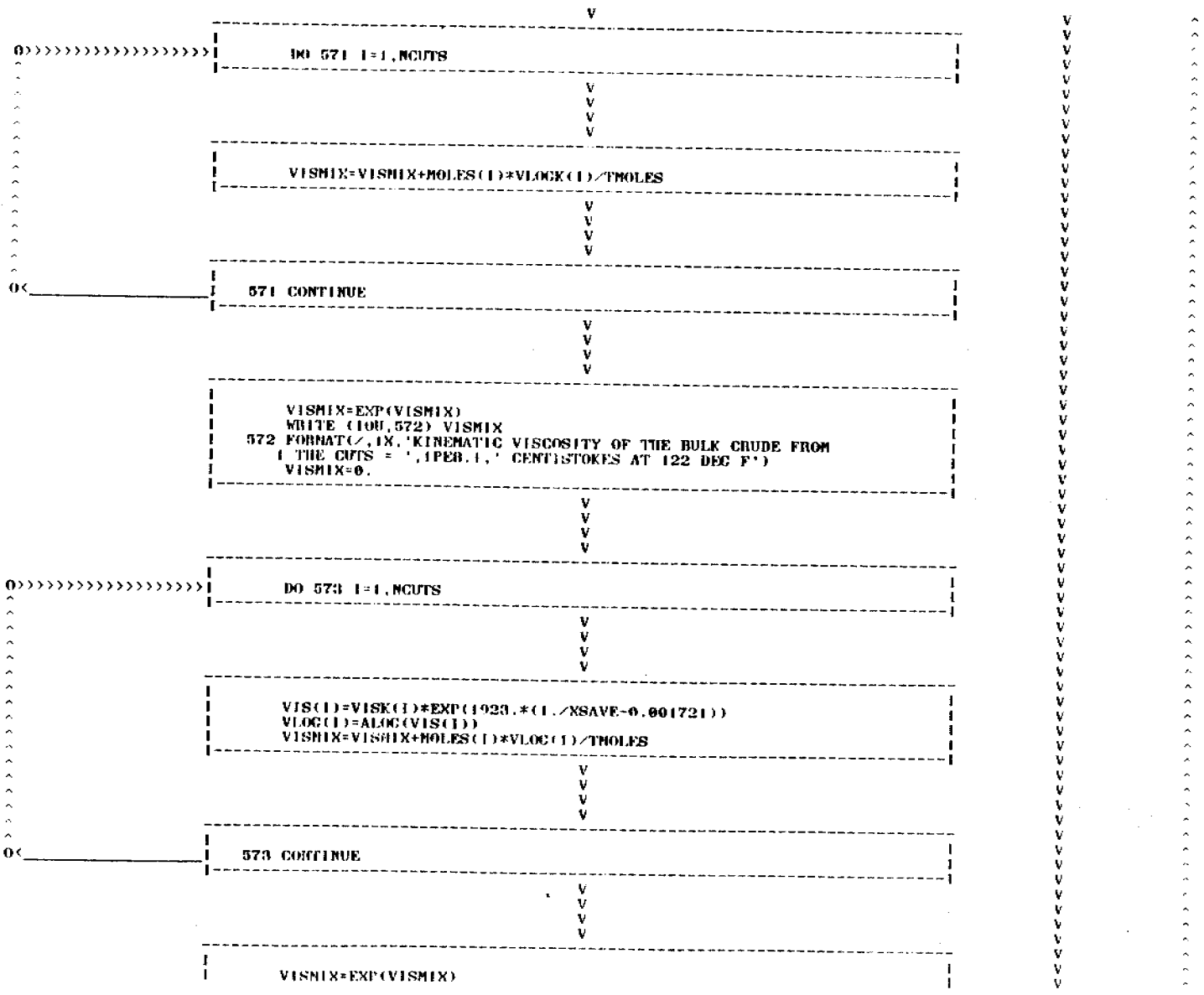
DO 571 I=1,NCUTS
VISMIX=VISMIX+MOLES(I)*VLOCK(I)/TMOLES
571 CONTINUE
VISMIX=EXP(VISMIX)
WRITE (IOU,572) VISMIX
572 FORMAT(/,1X,'KINEMATIC VISCOSITY OF THE BULK CRUDE FROM
THE CUTS = ',1PE8.1,' CENTISTOKES AT 122 DEG F')
VISMIX=0.
DO 573 I=1,NCUTS
VIS(I)=VISK(I)*EXP(1923.*(1./XSAVE-0.001721))
VLOC(I)=ALOG(VIS(I))
VISMIX=VISMIX+MOLES(I)*VLOC(I)/TMOLES
573 CONTINUE
VISMIX=EXP(VISMIX)

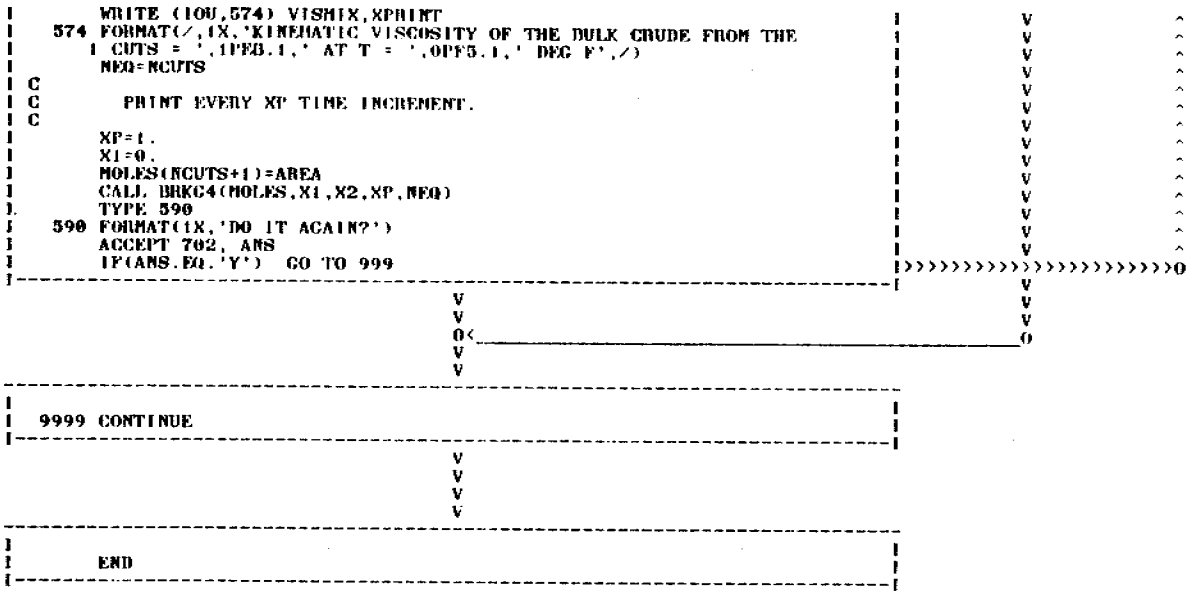

No source errors.
9 K CORE USED

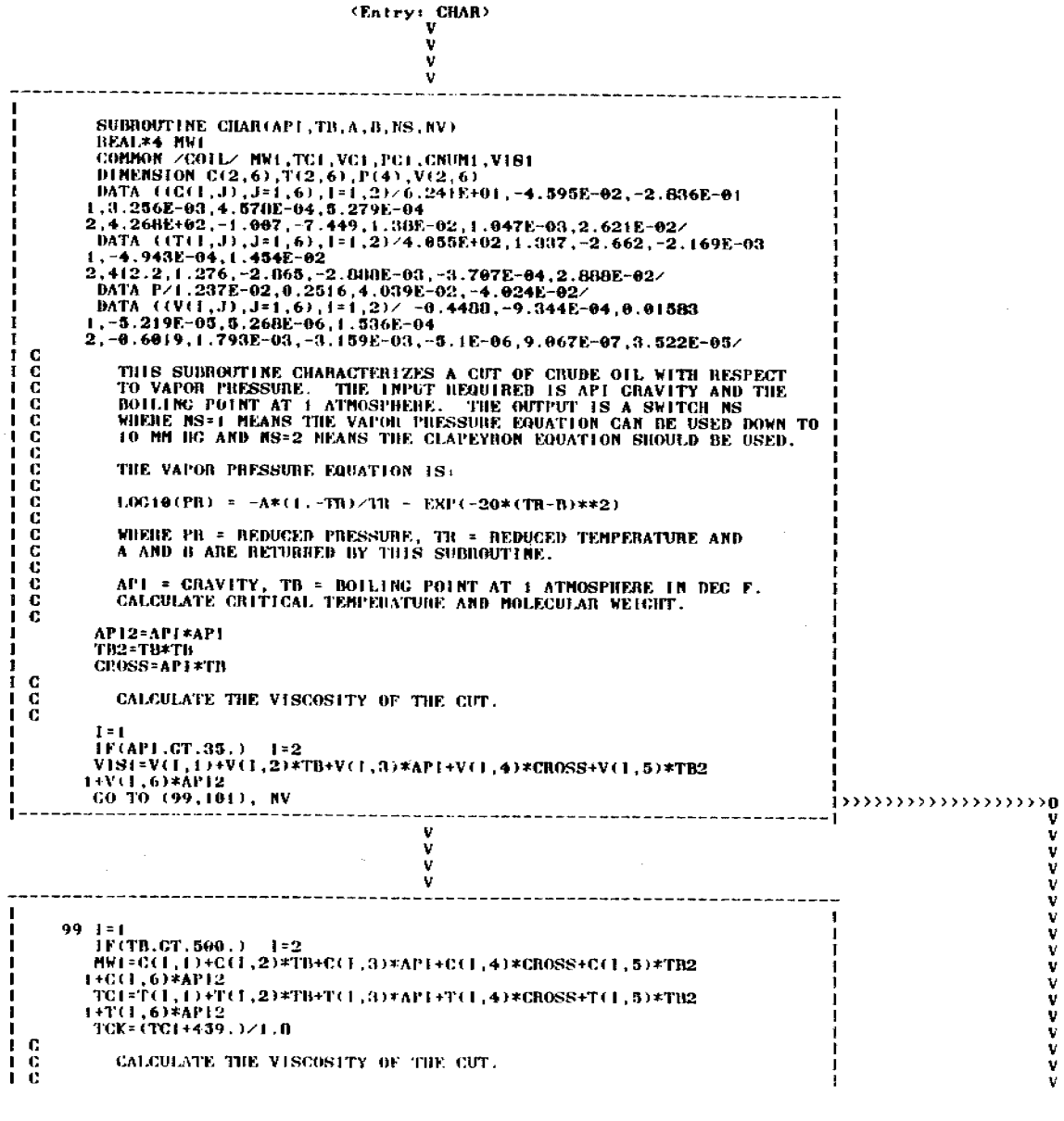
(Entry: CHAR)
SUBROUTINE CHAR(API,TB,A,B,NS,NV)
REAL*4 MW1
COMMON /COIL/ MW1,TC1,VC1,PC1,CNUM1,VIS1
DIMENSION C(2,6),T(2,6),P(4),V(2,6)
DATA ((C(I,J),J=1,6),I=1,2)/6.241E+01,-4.595E-02,-2.836E-01
1,3.256E-03,4.570E-04,5.279E-04
2,4.268E+02,-1.007,-7.449,1.38E-02,1.047E-03,2.621E-02/
DATA ((T(I,J),J=1,6),I=1,2)/4.055E+02,1.937,-2.662,-2.169E-03
1,-4.943E-04,1.454E-02
2,412.2,1.276,-2.065,-2.800E-03,-3.707E-04,2.888E-02/
DATA P/1.237E-02,0.2516,4.039E-02,-4.024E-02/
DATA ((V(I,J),J=1,6),I=1,2)/ -0.4400,-9.344E-04,0.01583
1,-5.219E-05,5.268E-06,1.536E-04
2,-0.6019,1.793E-03,-3.159E-03,-5.1E-06,9.067E-07,3.522E-05/
C
C THIS SUBROUTINE CHARACTERIZES A CUT OF CRUDE OIL WITH RESPECT
C TO VAPOR PRESSURE. THE INPUT REQUIRED IS API GRAVITY AND THE
C BOILING POINT AT 1 ATMOSPHERE. THE OUTPUT IS A SWITCH NS
C WHERE NS=1 MEANS THE VAPOR PRESSURE EQUATION CAN BE USED DOWN TO
C 10 MM HG AND NS=2 MEANS THE CLAPEYRON EQUATION SHOULD BE USED.
C
C THE VAPOR PRESSURE EQUATION IS:
C
C LOG10(PR) = -A*(1.-TR)/TR - EXP(-20*(TR-B)**2)
C
C WHERE PR = REDUCED PRESSURE, TR = REDUCED TEMPERATURE AND
C A AND B ARE RETURNED BY THIS SUBROUTINE.
C
C API = GRAVITY, TB = BOILING POINT AT 1 ATMOSPHERE IN DEG F.
C CALCULATE CRITICAL TEMPERATURE AND MOLECULAR WEIGHT.
C
API2=API*API
TB2=TB*TB
CROSS=API*TB
C
C CALCULATE THE VISCOSITY OF THE CUT.
C
I=1
IF(API.GT.35.) I=2
VIS1=V(I,1)+V(I,2)*TB+V(I,3)*API+V(I,4)*CROSS+V(I,5)*TB2
1+V(I,6)*API2
GO TO (99,101), NV
99 I=1
IF(TB.GT.500.) I=2
MW1=C(I,1)+C(I,2)*TB+C(I,3)*API+C(I,4)*CROSS+C(I,5)*TB2
1+C(I,6)*API2
TC1=T(I,1)+T(I,2)*TB+T(I,3)*API+T(I,4)*CROSS+T(I,5)*TB2
1+T(I,6)*API2
TCK=(TC1+439.)/1.8
C
C CALCULATE THE VISCOSITY OF THE CUT.
C

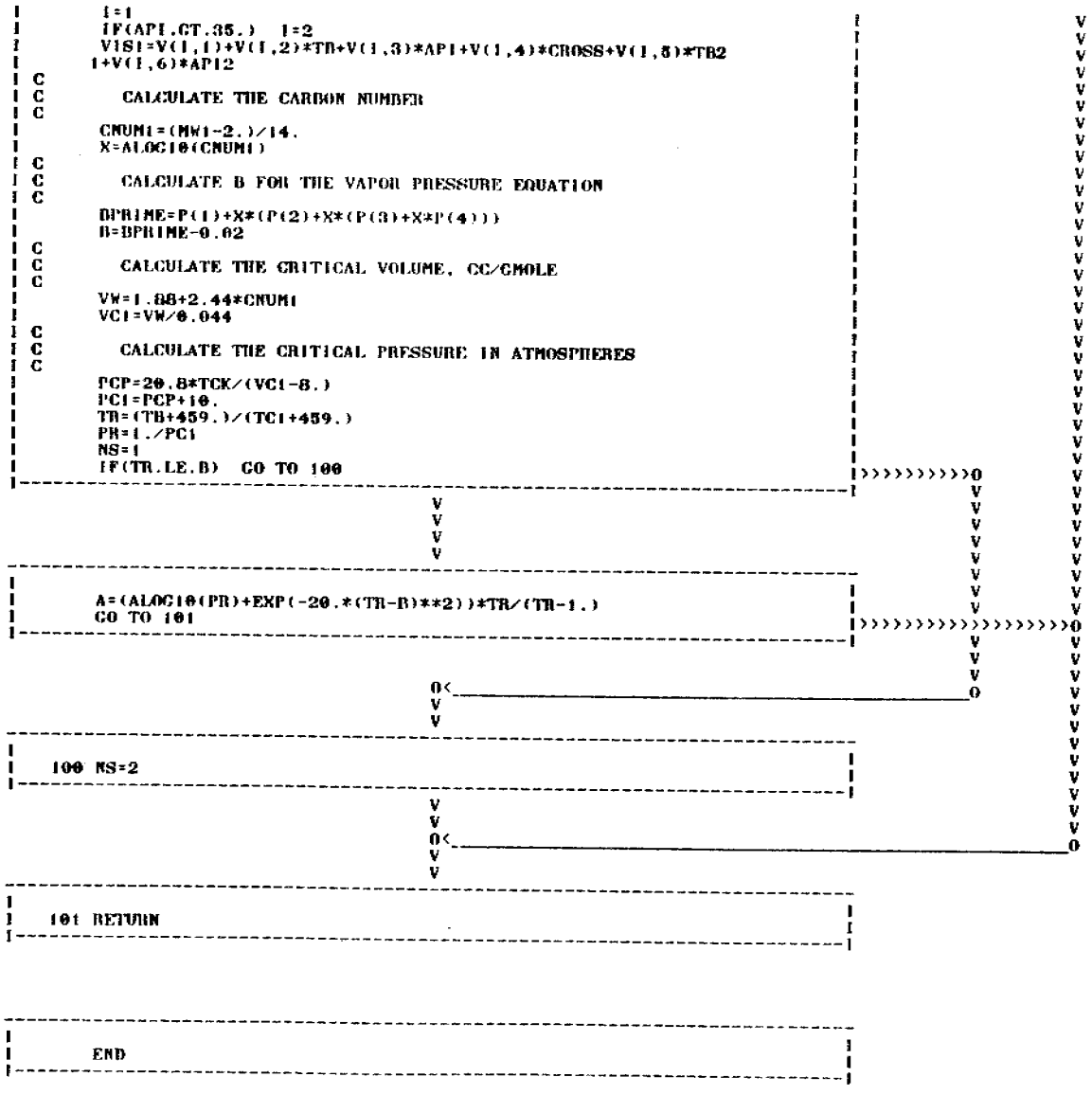
I=1
IF(API.GT.35.) I=2
VIS1=V(I,1)+V(I,2)*TR+V(I,3)*API+V(I,4)*CROSS+V(I,5)*TB2
1+V(I,6)*API2
C
C CALCULATE THE CARBON NUMBER
C
CNUM1=(MW1-2.)/14.
X=ALOG10(CNUM1)
C
C CALCULATE B FOR THE VAPOR PRESSURE EQUATION
C
BPRIME=P(1)+X*(P(2)+X*(P(3)+X*P(4)))
B=BPRIME-0.02
C
C CALCULATE THE CRITICAL VOLUME, CC/GMOLE
C
VW=1.88+2.44*CNUM1
VC1=VW/0.044
C
C CALCULATE THE CRITICAL PRESSURE IN ATMOSPHERES
C
PCP=20.8*TCK/(VC1-8.)
PC1=PCP+10.
TR=(TB+459.)/(TC1+459.)
PR=1./PC1
NS=1
IF(TR.LE.B) GO TO 100
A=(ALOG10(PR)+EXP(-20.*(TR-B)**2))*TR/(TR-1.)
GO TO 101
100 NS=2
101 RETURN
END

```
No source errors.
8 K CORE USED
```

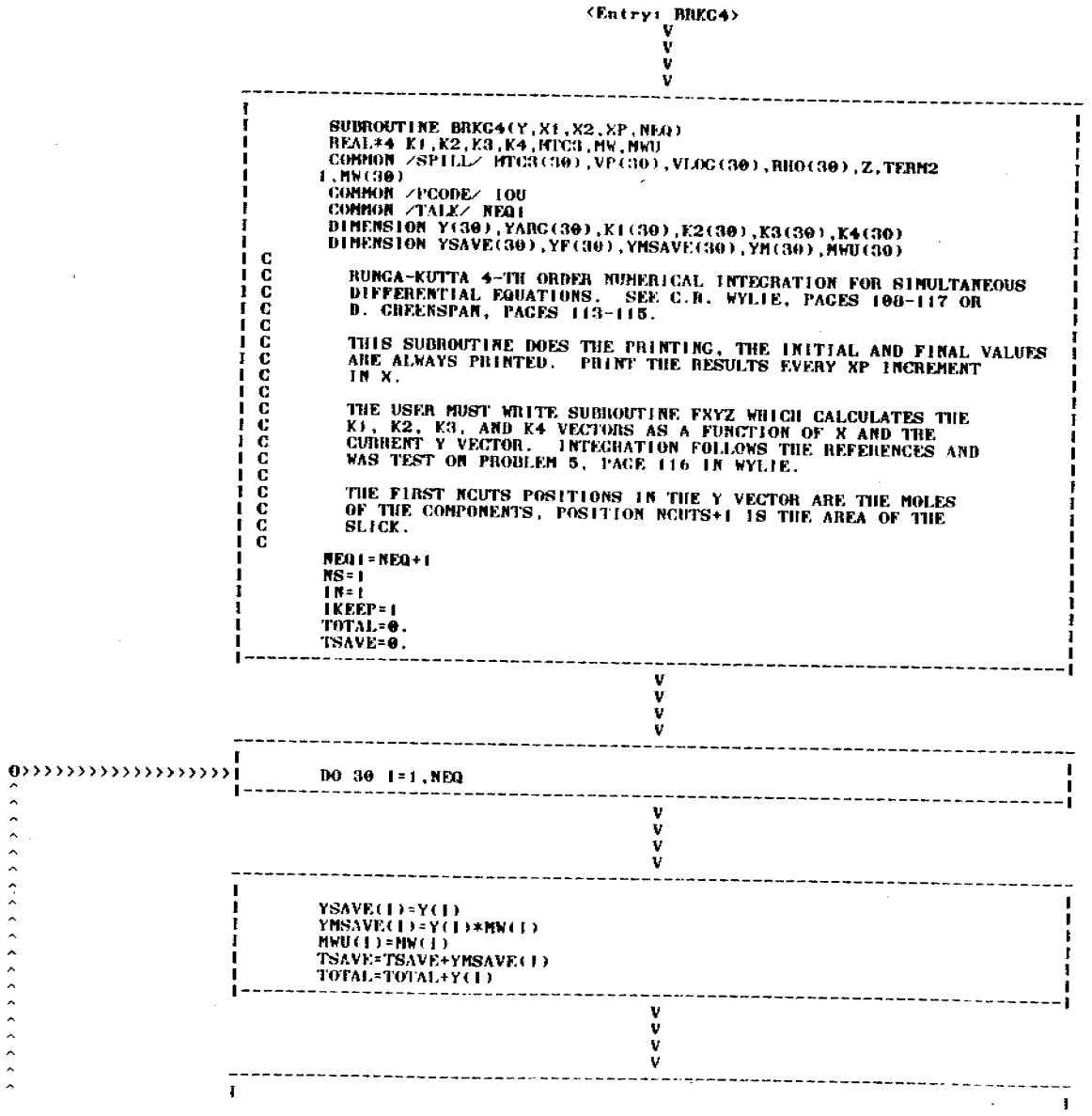
<Entry: BRKG4>
SUBROUTINE BRKG4(Y,X1,X2,XP,NEQ)
REAL*4 K1,K2,K3,K4,MTC3,MW,MWU
COMMON /SPILL/ MTC3(30),VP(30),VLOC(30),RHO(30),Z,TERM2
1,MW(30)
COMMON /PCODE/ IOU
COMMON /TALK/ NEQ1
DIMENSION Y(30),YARG(30),K1(30),K2(30),K3(30),K4(30)
DIMENSION YSAVE(30),YP(30),YMSAVE(30),YM(30),MWU(30)
C
C RUNGA-KUTTA 4-TH ORDER NUMERICAL INTEGRATION FOR SIMULTANEOUS
C DIFFERENTIAL EQUATIONS. SEE C.R. WYLIE, PAGES 108-117 OR
C D. GREENSPAN, PAGES 113-115.
C
C THIS SUBROUTINE DOES THE PRINTING, THE INITIAL AND FINAL VALUES
C ARE ALWAYS PRINTED. PRINT THE RESULTS EVERY XP INCREMENT
C IN X.
C
C THE USER MUST WRITE SUBROUTINE FXYZ WHICH CALCULATES THE
C K1, K2, K3, AND K4 VECTORS AS A FUNCTION OF X AND THE
C CURRENT Y VECTOR. INTEGRATION FOLLOWS THE REFERENCES AND
C WAS TEST ON PROBLEM 5, PAGE 116 IN WYLIE.
C
C THE FIRST NCUTS POSITIONS IN THE Y VECTOR ARE THE MOLES
C OF THE COMPONENTS, POSITION NCUTS+1 IS THE AREA OF THE
C SLICK.
C
NEQ1=NEQ+1
NS=1
IN=1
IKEEP=1
TOTAL=0.
TSAVE=0.
0>>>>>>>>>>>>>>>>>>>>
DO 30 I=1,NEQ
YSAVE(I)=Y(I)
YMSAVE(I)=Y(I)*MW(I)
MWU(I)=MW(I)
TSAVE=TSAVE+YMSAVE(I)
TOTAL=TOTAL+Y(I)

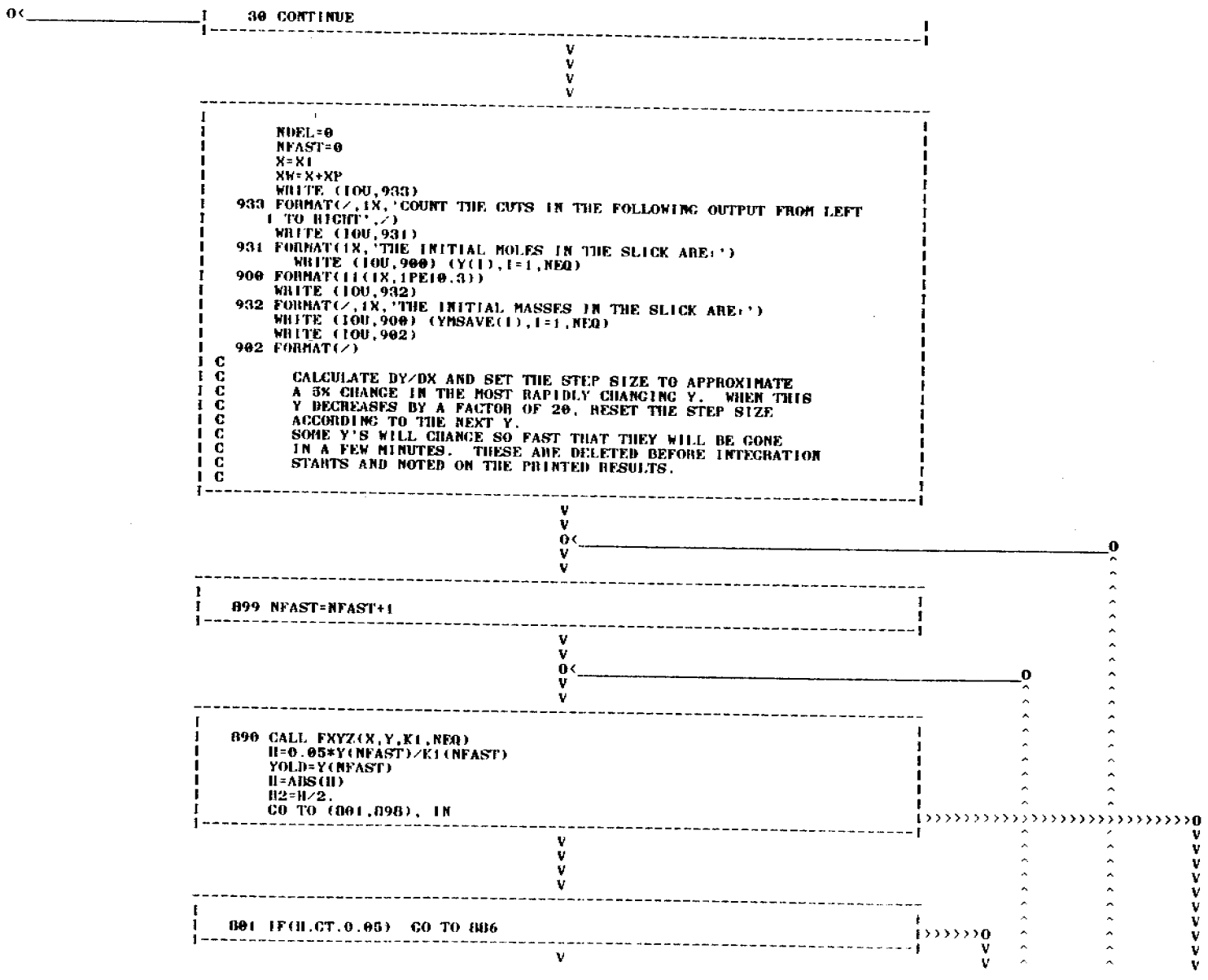
30 CONTINUE
NDEL=0
NFAST=0
X=X1
XW=X+XP
WRITE (IOU,933)
933 FORMAT(/,1X,'COUNT THE CUTS IN THE FOLLOWING OUTPUT FROM LEFT
1 TO RIGHT',/)
WRITE (IOU,931)
931 FORMAT(1X,'THE INITIAL MOLES IN THE SLICK ARE:')
WRITE (IOU,900) (Y(I),I=1,NEQ)
900 FORMAT(1(1X,1PE10.3))
WRITE (IOU,932)
932 FORMAT(/,1X,'THE INITIAL MASSES IN THE SLICK ARE:')
WRITE (IOU,900) (YMSAVE(I),I=1,NEQ)
WRITE (IOU,902)
902 FORMAT(/)
C
C CALCULATE DY/DX AND SET THE STEP SIZE TO APPROXIMATE
C A 5% CHANGE IN THE MOST RAPIDLY CHANGING Y. WHEN THIS
C Y DECREASES BY A FACTOR OF 20, RESET THE STEP SIZE
C ACCORDING TO THE NEXT Y.
C SOME Y'S WILL CHANGE SO FAST THAT THEY WILL BE GONE
C IN A FEW MINUTES. THESE ARE DELETED BEFORE INTEGRATION
C STARTS AND NOTED ON THE PRINTED RESULTS.
C
899 NFAST=NFAST+1
890 CALL FXYZ(X,Y,K1,NEQ)
H=0.05*Y(NFAST)/K1(NFAST)
YOLD=Y(NFAST)
H=ABS(H)
H2=H/2.
GO TO (801,898), IN
801 IF(H.GT.0.05) GO TO 806

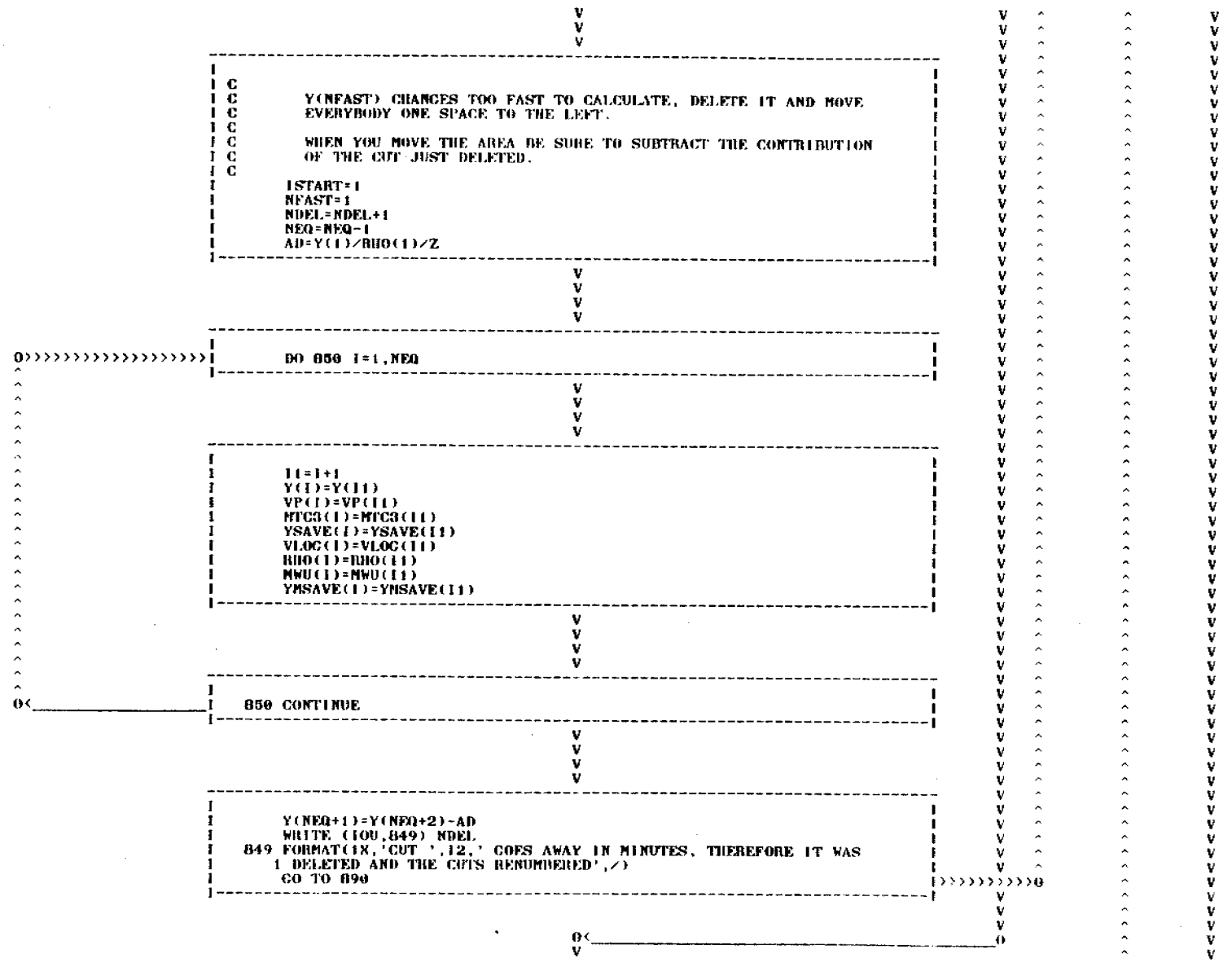
C
C Y(NFAST) CHANGES TOO FAST TO CALCULATE, DELETE IT AND MOVE
C EVERYBODY ONE SPACE TO THE LEFT.
C
C WHEN YOU MOVE THE AREA BE SURE TO SUBTRACT THE CONTRIBUTION
C OF THE CUT JUST DELETED.
C
ISTART=1
NFAST=1
NDEL=NDEL+1
NEQ=NEQ-1
AD=Y(1)/RHO(1)/Z
DO 850 I=1,NEQ
II=I+1
Y(I)=Y(II)
VP(I)=VP(II)
MTC3(I)=MTC3(II)
YSAVE(I)=YSAVE(II)
VLOC(I)=VLOC(II)
RHO(I)=RHO(II)
MWU(I)=MWU(II)
YMSAVE(I)=YMSAVE(II)
850 CONTINUE
Y(NEQ+1)=Y(NEQ+2)-AD
WRITE (IOU,849) NDEL
849 FORMAT(1X,'CUT ',I2,' GOES AWAY IN MINUTES, THEREFORE IT WAS
1 DELETED AND THE CUTS RENUMBERED',/)
GO TO 890

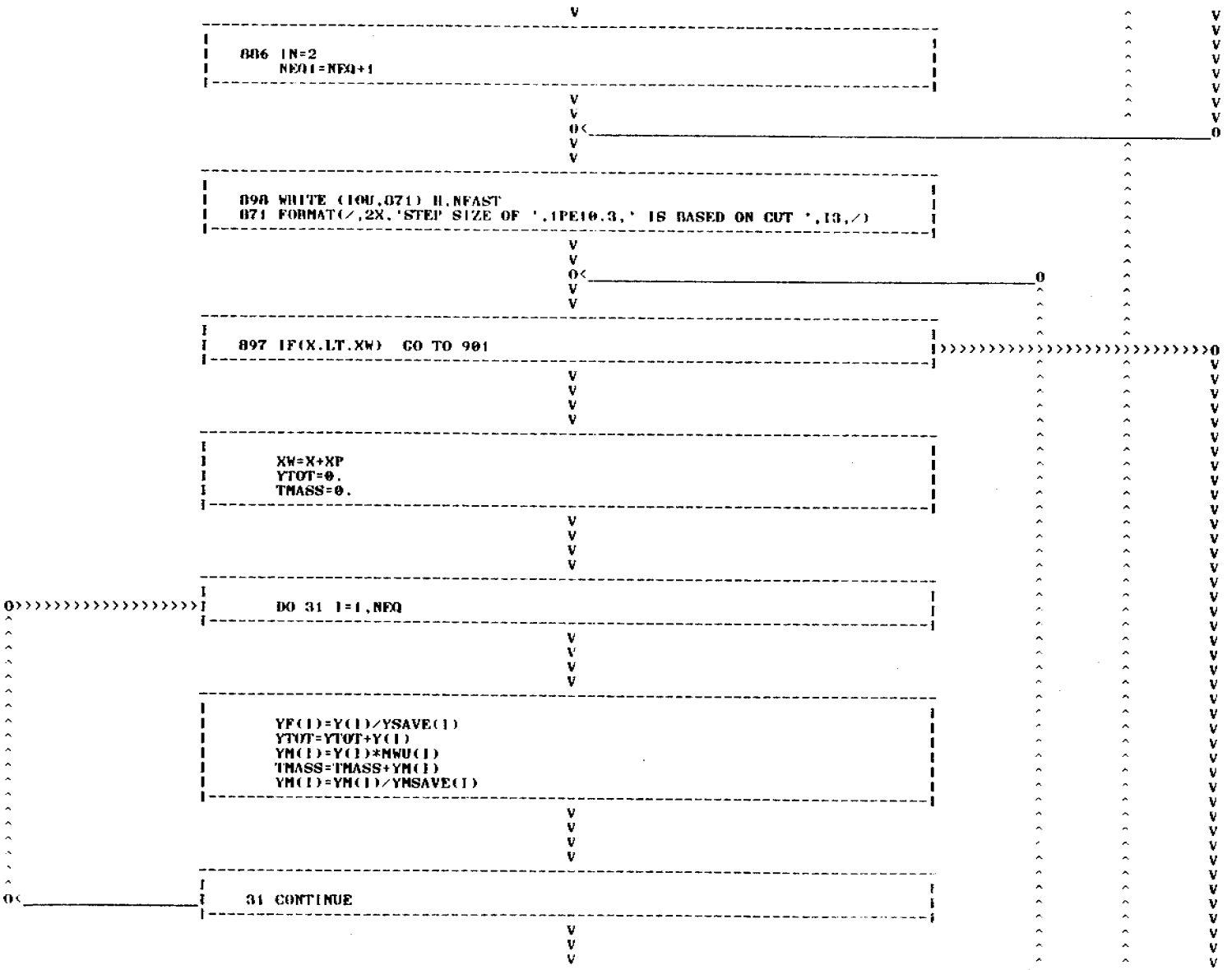
806 IN=2
NEQ1=NEQ+1
898 WRITE (10U,871) H,NFAST
871 FORMAT(/,2X,'STEP SIZE OF ',1PE10.3,' IS BASED ON CUT ',I3,/)
897 IF(X.LT.XW) GO TO 901
XW=X+XP
YTOT=0.
TMASS=0.
DO 31 I=1,NEQ
YF(I)=Y(I)/YSAVE(I)
YTOT=YTOT+Y(I)
YM(I)=Y(I)*MWU(I)
TMASS=TMASS+YM(I)
YM(I)=YM(I)/YMSAVE(I)
31 CONTINUE

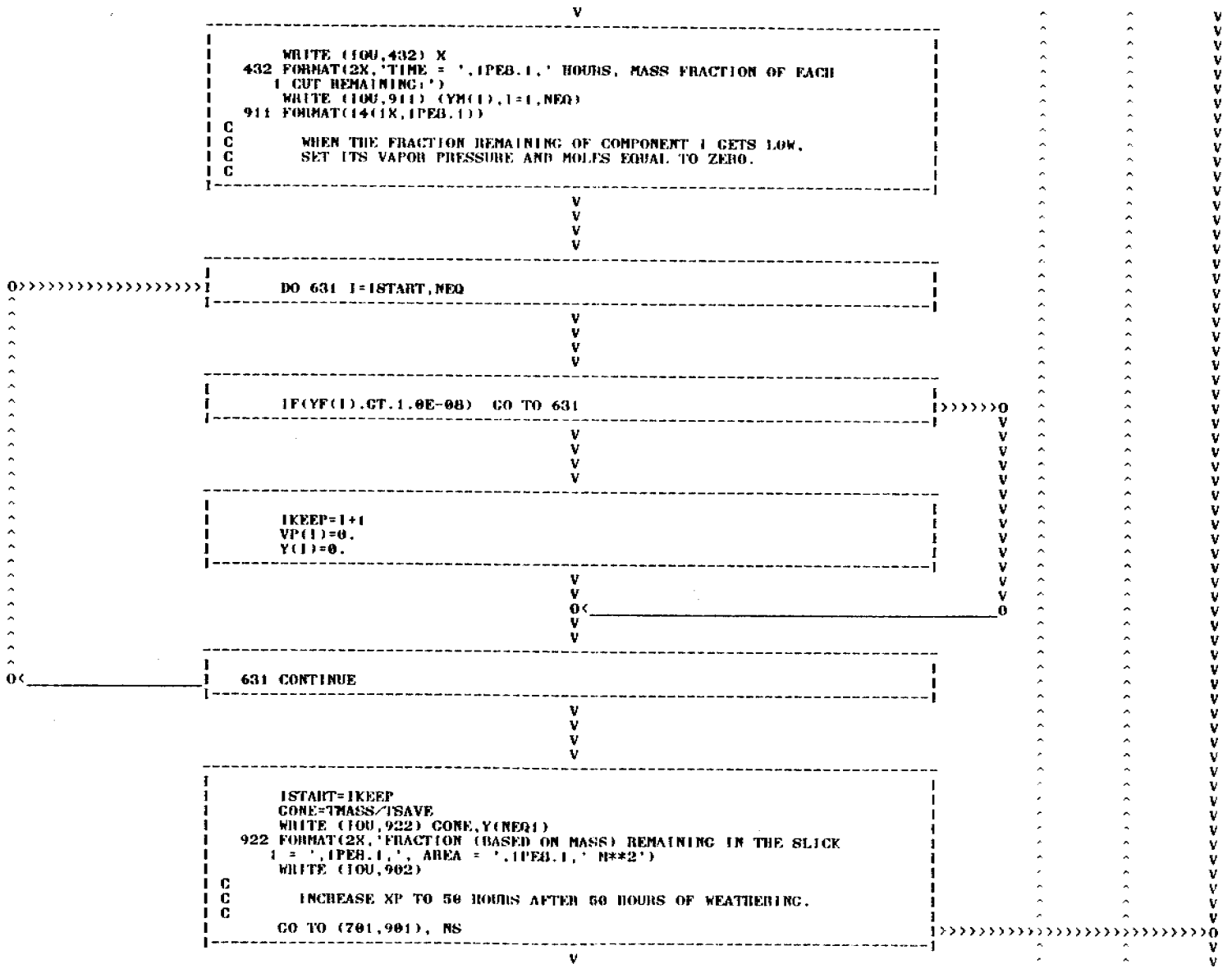
WRITE (IOU,432) X
432 FORMAT(2X,'TIME = ',1PE8.1,' HOURS, MASS FRACTION OF EACH
1 CUT REMAINING:')
WRITE (IOU,911) (YM(I),I=1,NEQ)
911 FORMAT(14(1X,1PE8.1))
C
C WHEN THE FRACTION REMAINING OF COMPONENT I GETS LOW,
C SET ITS VAPOR PRESSURE AND MOLES EQUAL TO ZERO.
C
DO 631 I=ISTART,NEQ
IF(YF(I).GT.1.0E-08) GO TO 631
IKEEP=I+1
VP(I)=0.
Y(I)=0.
631 CONTINUE
ISTART=IKEEP
CONE=TMASS/TSAVE
WRITE (IOU,922) CONE,Y(NEQ1)
922 FORMAT(2X,'FRACTION (BASED ON MASS) REMAINING IN THE SLICK
1 = ',1PE8.1,', AREA = ',1PE8.1,' M**2')
WRITE (IOU,902)
C
C INCREASE XP TO 50 HOURS AFTER 50 HOURS OF WEATHERING.
C
GO TO (701,901), NS

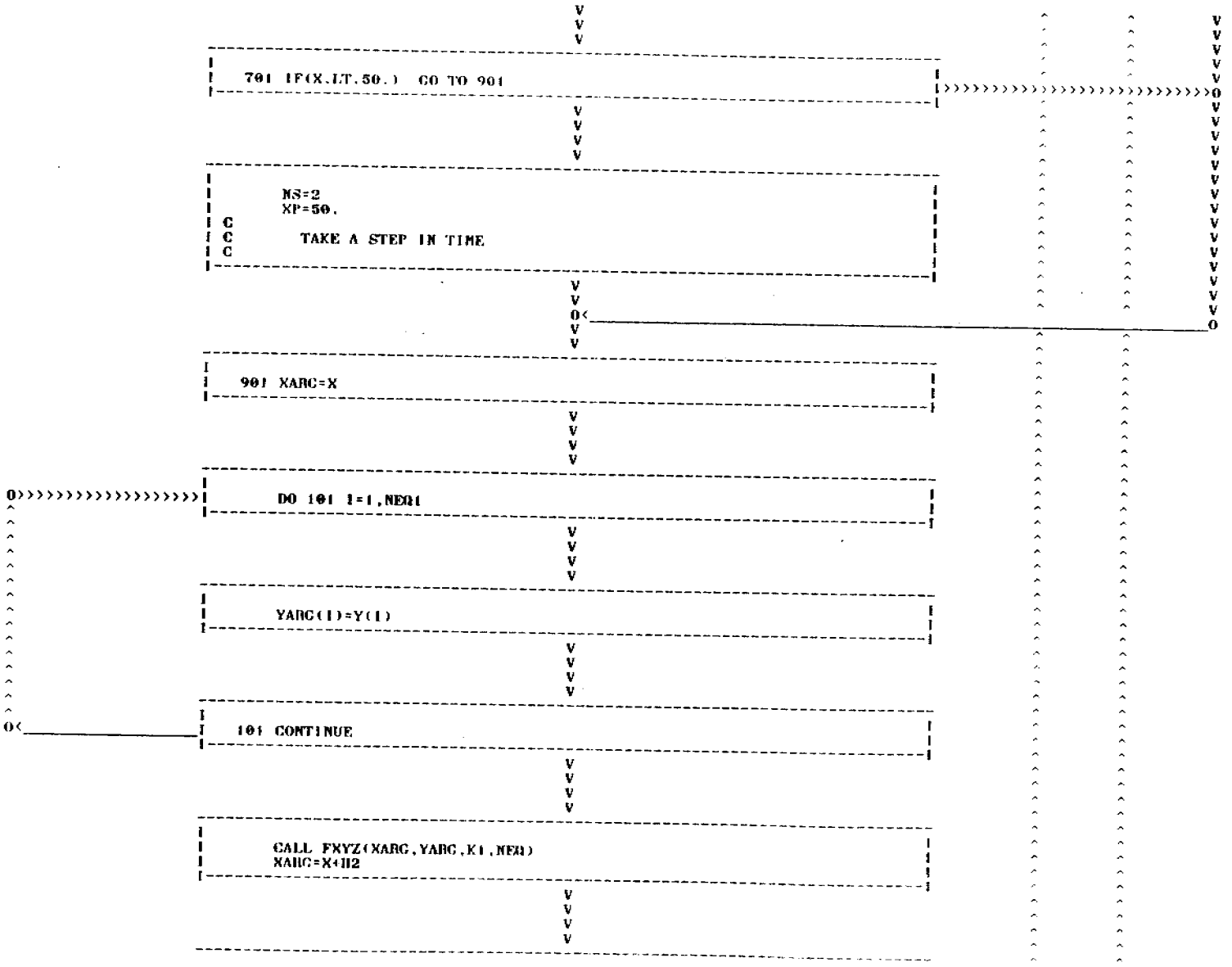
701 IF(X.LT.50.) GO TO 901
NS=2
XP=50.
C
C TAKE A STEP IN TIME
C
901 XARG=X
DO 101 I=1,NEQ1
YARG(I)=Y(I)
101 CONTINUE
CALL FXYZ(XARG,YARG,K1,NEQ)
XARG=X+H2

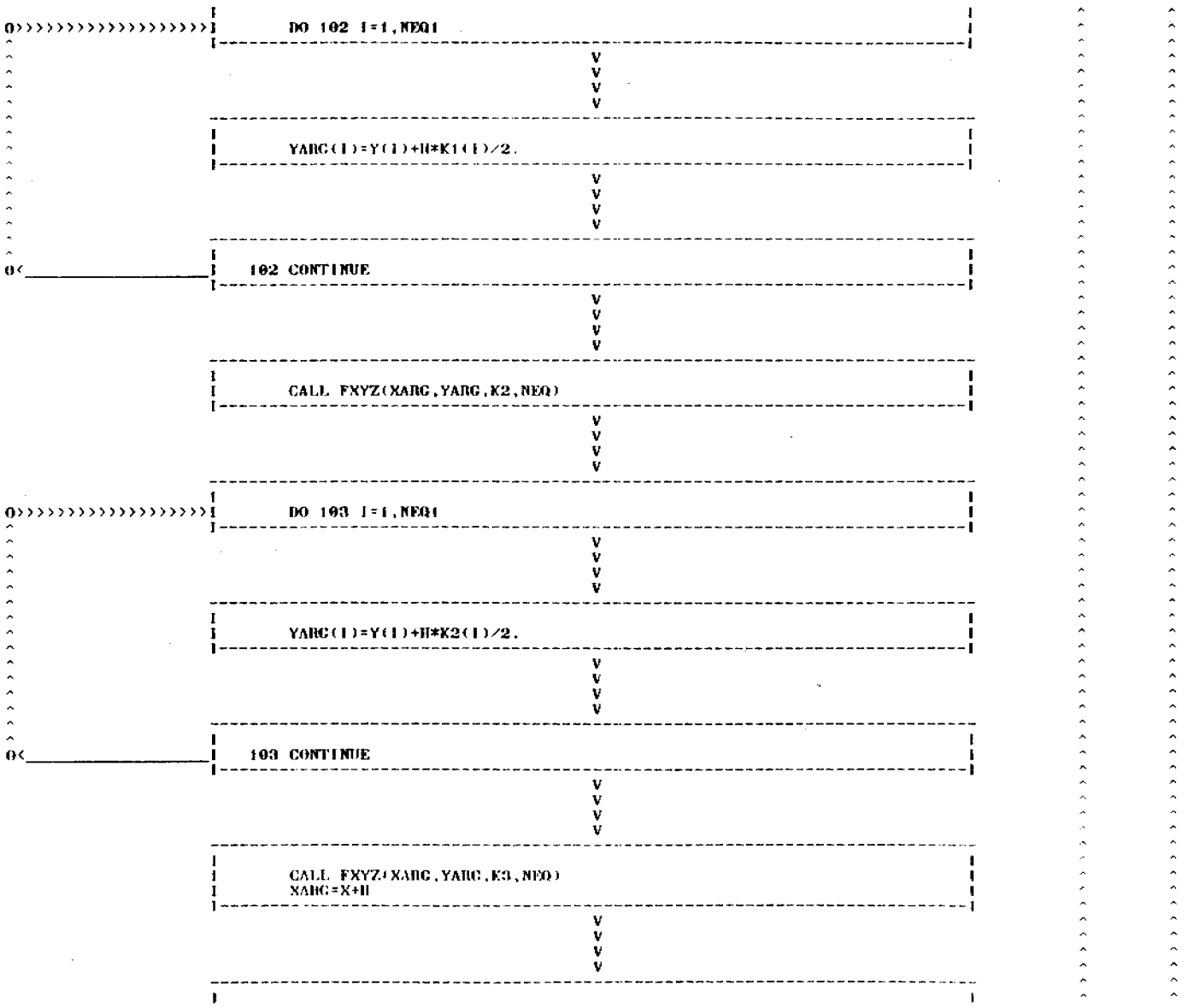
DO 102 I=1,NEQ1
YARG(I)=Y(I)+H*K1(I)/2.
102 CONTINUE
CALL FXYZ(XARG,YARG,K2,NEQ)
DO 103 I=1,NEQ1
YARG(I)=Y(I)+H*K2(I)/2.
103 CONTINUE
CALL FXYZ(XARG,YARG,K3,NEQ)
XARG=X+H

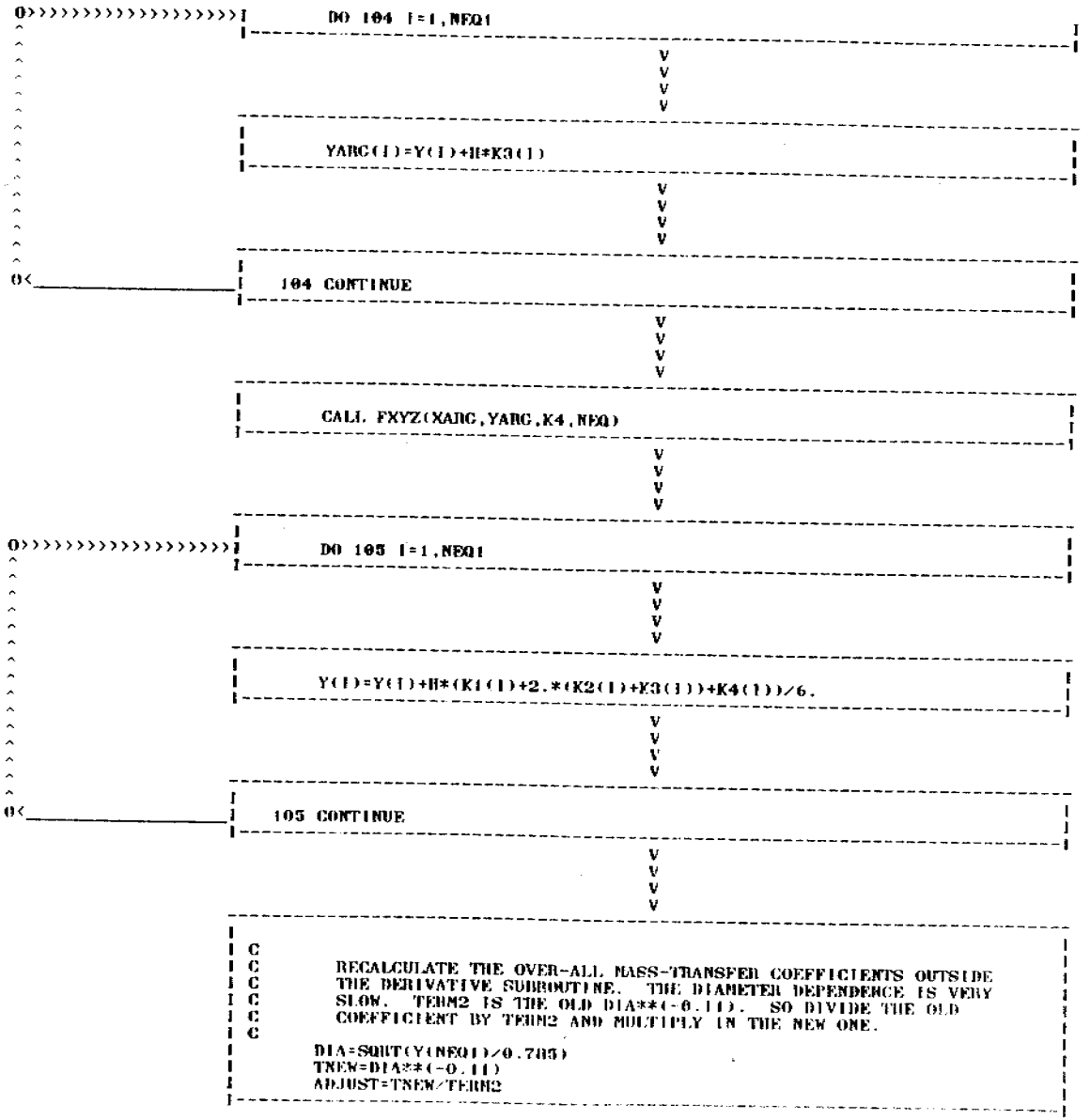
DO 104 I=1,NEQ1
YARG(I)=Y(I)+H*K3(I)
104 CONTINUE
CALL FXYZ(XARG,YARG,K4,NEQ)
DO 105 I=1,NEQ1
Y(I)=Y(I)+H*(K1(I)+2.*(K2(I)+K3(I))+K4(I))/6.
105 CONTINUE
C
C RECALCULATE THE OVER-ALL MASS-TRANSFER COEFFICIENTS OUTSIDE
C THE DERIVATIVE SUBROUTINE. THE DIAMETER DEPENDENCE IS VERY
C SLOW. TERM2 IS THE OLD DIA**(-0.11). SO DIVIDE THE OLD
C COEFFICIENT BY TERM2 AND MULTIPLY IN THE NEW ONE.
C
DIA=SQRT(Y(NEQ1)/0.785)
TNEW=DIA**(-0.11)
ADJUST=TNEW/TERM2

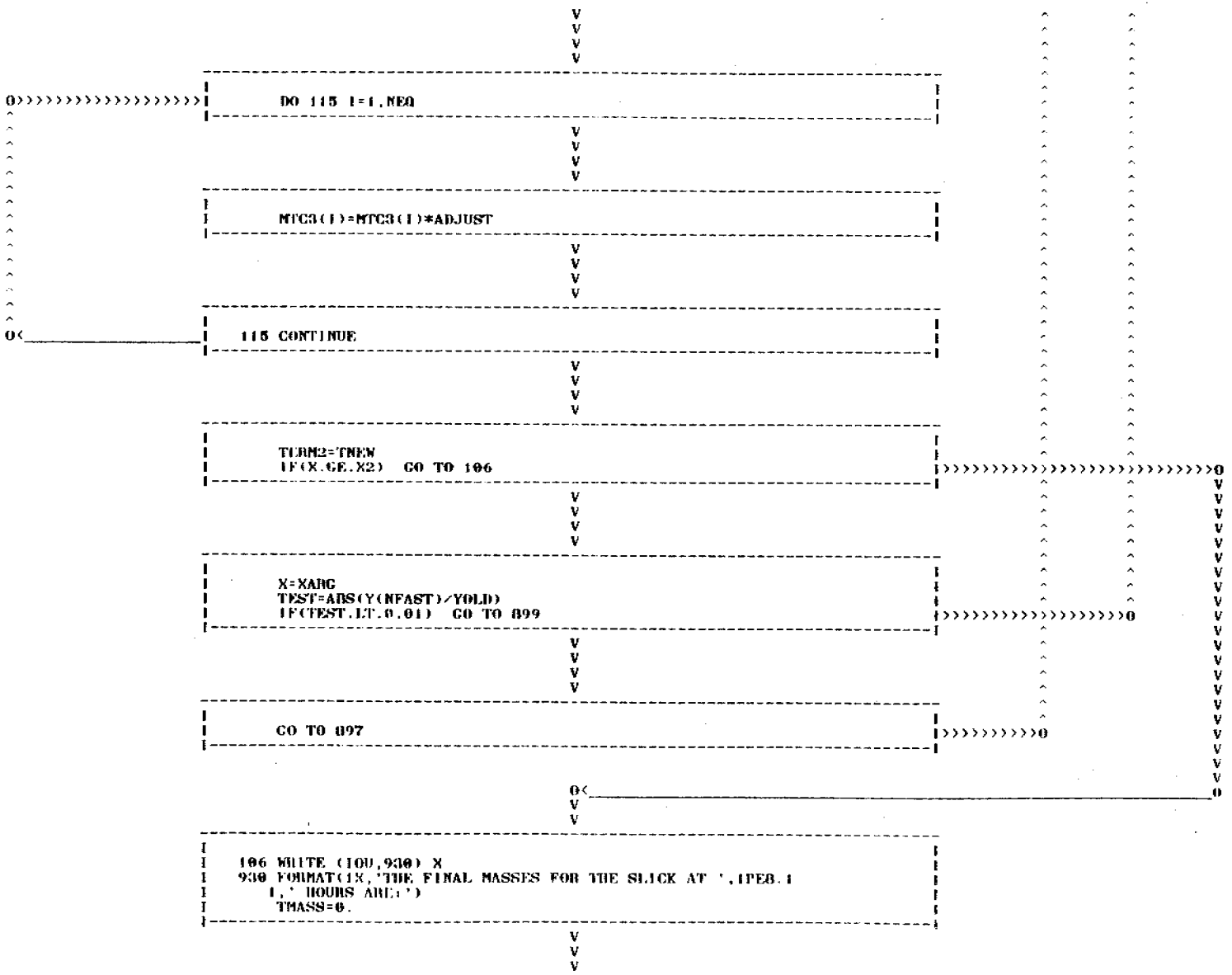
DO 115 I=1,NEQ
MTC3(I)=MTC3(I)*ADJUST
115 CONTINUE
TURM2='NEW
IF(X.GE.X2) GO TO 106
X=XARG
TEST=ABS(Y(NFAST)/YOLD)
IF(TEST.LT.0.01) GO TO 899
GO TO 897
106 WRITE (IOU,930) X
930 FORMAT(1X,'THE FINAL MASSES FOR THE SLICK AT ',1PE8.1
1,' HOURS ARE:')
TMASS=0.

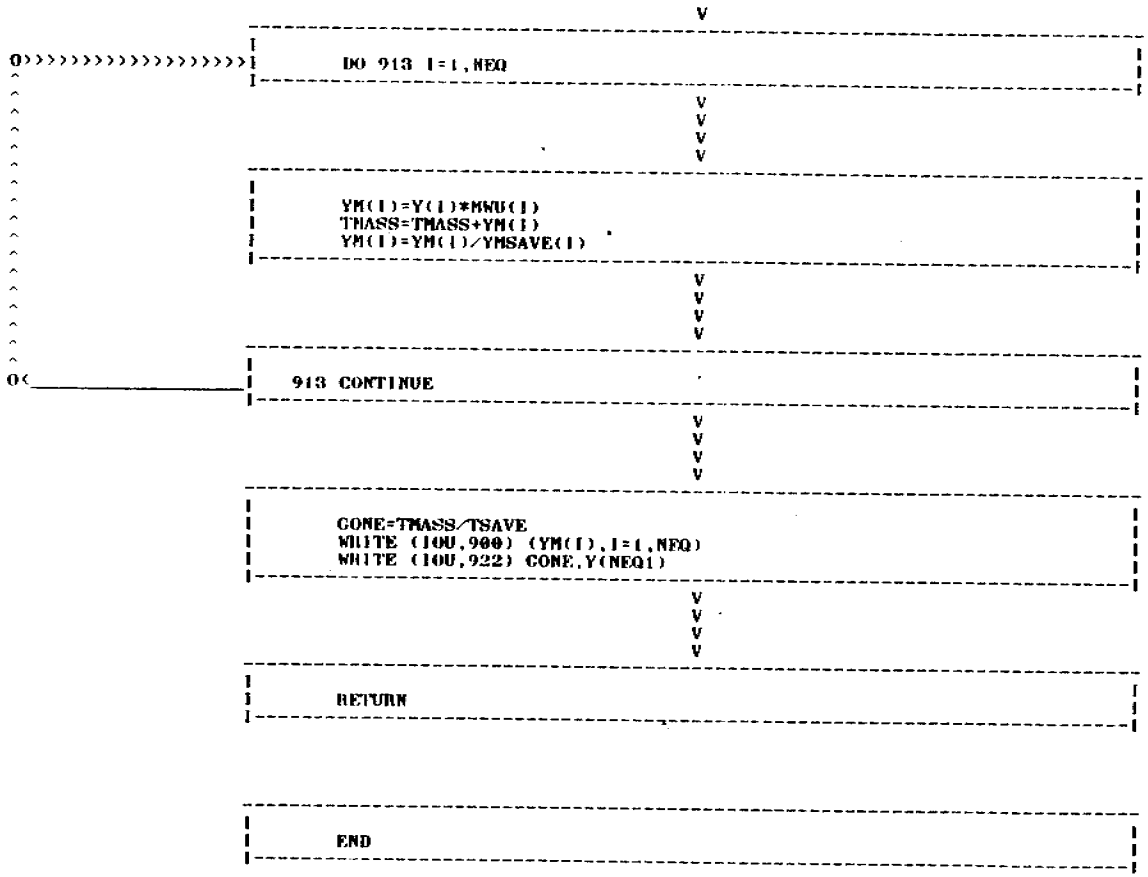

No source errors.
8 K CORE USED

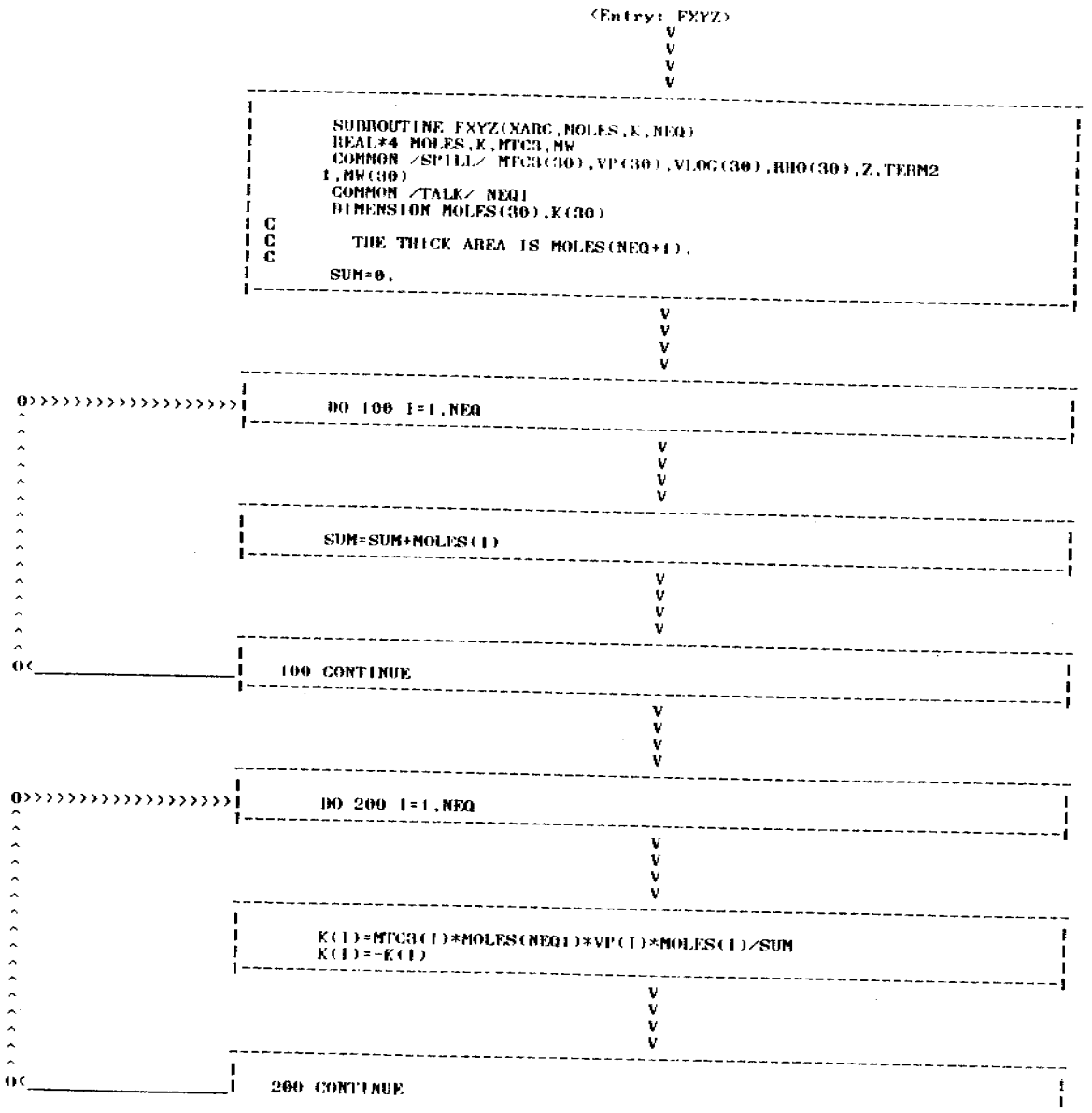
<Entry: FXYZ>
SUBROUTINE FXYZ(XARG,MOLES,K,NEQ)
REAL*4 MOLES,K,MTC3,MW
COMMON /SPILL/ MTC3(30),VP(30),VLOC(30),RHO(30),Z,TERM2
1,MW(30)
COMMON /TALK/ NEQ1
DIMENSION MOLES(30),K(30)
C
C THE THICK AREA IS MOLES(NEQ+1).
C
SUM=0.
DO 100 I=1,NEQ
SUM=SUM+MOLES(I)
100 CONTINUE
DO 200 I=1,NEQ
K(I)=MTC3(I)*MOLES(NEQ1)*VP(I)*MOLES(I)/SUM
K(I)=-K(I)
200 CONTINUE

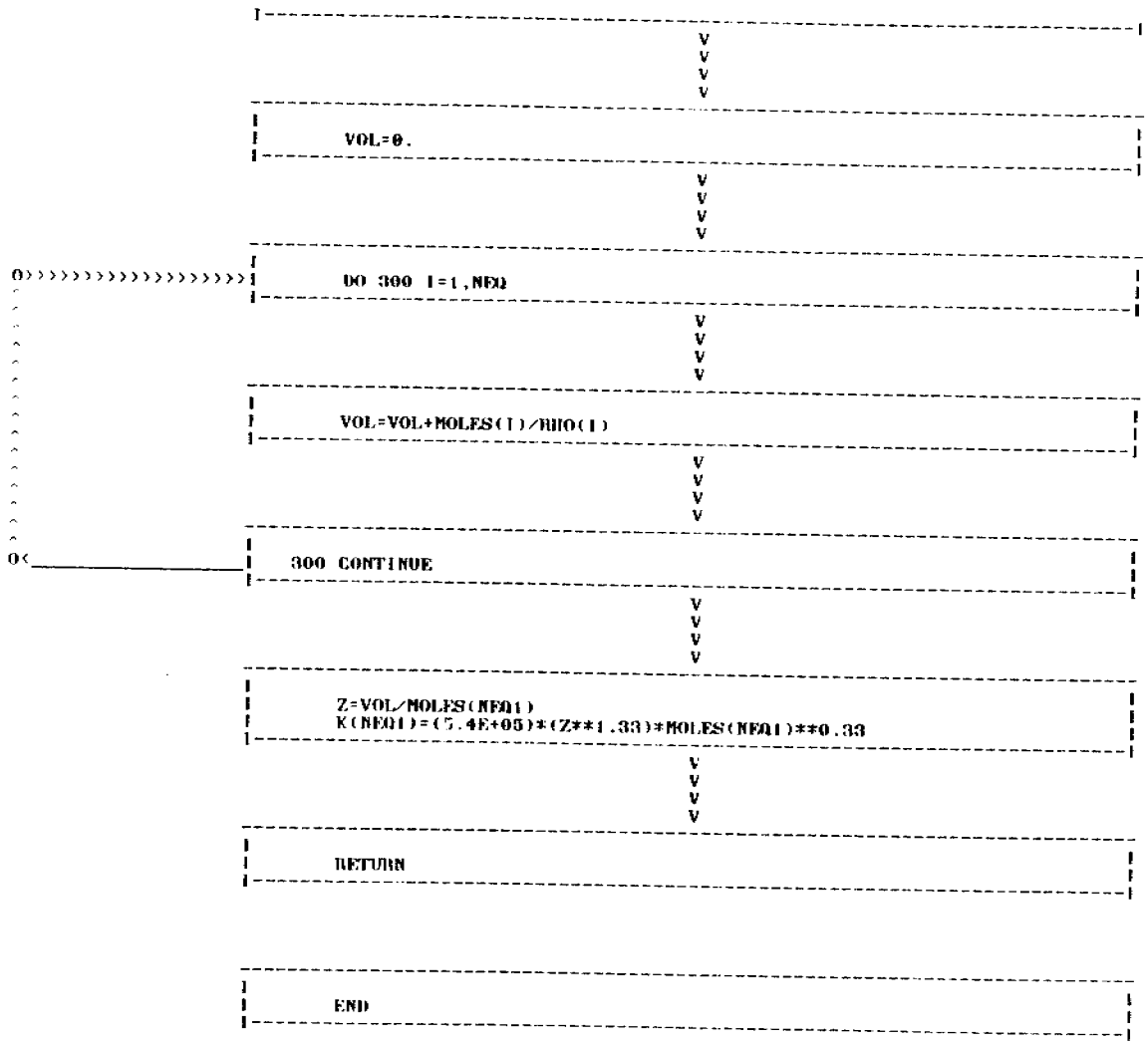

No source errors.
8 K CORE USED

APPENDIX B

METHODS FOR MICROBIAL DEGRADATION STUDIES

^{14}C-Hydrocarbon Mineralization Assay

Three ^{14}C-labeled hydrocarbon substrates were utilized for the determination of hydrocarbon degradation potential, defined here as the percent mineralization to $^{14}CO_2$: n(1-^{14}C) hexadecane (53.6 mCi/mmol, Amersham), (1(4,5,8)-^{14}C) naphthalene (5 mCi/mmol, Amersham), and (1(4,5,8)-^{14}C) methylnaphthalene (5 mCi/mmol, Bionuclear). Working solutions were prepared with hexane or benzene as solvents to give 0.1 μCi/ μl activities, stored at 4°C, and assayed weekly for radioactivity to insure consistency in the concentrations of substrates. Seawater aliquots (50 ml) from each of the experimental tanks and the incoming seawater were transferred to 100 ml sterile serum bottles and spiked with 0.5 μCi of the ^{14}C-labeled hydrocarbons, one compound per sample with each sample prepared in duplicate. Controls were killed with 1 μM $HgCl_2$ prior to spiking with the labeled compound.

The spiked seawater samples were capped with sleeve stoppers and incubated in the dark for 24 hours at in situ temperatures in a seawater bath. After the incubation period the stoppers were replaced with identical stoppers fitted with a polypropylene "center well" containing a 25-mm by 30-mm rectangle of Whatman No. 1 filter paper folded into an accordian-pleated array and wetted with 200 μl of 1N NaOH. The samples were then acidified to pH 2.0 by injection of 0.5 ml of 1 N H_2SO_4 (through the sleeve stopper) with a hypodermic syringe. After 2 hours the filter paper was transferred to a second 100 ml serum bottle containing 1 ml of 1N H_2SO_4 which was quickly capped with a sleeve stopper fitted with a center well (as before) and a wick which had been wetted with 200 μl of phenethylamine.

After 12-14 hours the phenethylamine wicks were transferred to a scintillation vial containing 10 ml of Beta-Phase cocktail (West Chem Products) and assayed for radioactivity on a Beckman LS100C scintillation counter.

The resulting counts for duplicates were averaged and corrected for the control counts prior to further data treatment. The data (in counts per minute) were converted to μg/liter·day by the following equation.

$$\mu g/\ell \cdot day = (cpm)\left(\frac{1\ dpm}{0.9\ cpm}\right)\left(\frac{1\ \mu Ci}{2.22 \times 10^6\ dpm}\right)\left(S.A.^{-1}\right)\left(m.w.\right)\left(\frac{1000\ ml}{1\ \ell}\right)\left(\frac{1}{50\ ml}\right)\left(\frac{1}{day}\right)$$

where a counting efficiency of 90% was utilized, SA is the specific activity in μCi/μ mole, and M.W. is the molecular weight of the particular labeled substrate.

References: WATSON et al. (1971); CAPARELLO and LA ROCK (1975); WALKER and COLWELL (1976); HODSON et al. (1977).

^{3}H-Thymidine Incorporation

Thymidine (methyl-^{3}H) solutions were stored as supplied (20 Ci/mmol, New England Nuclear) in 70% aqueous ethanol for maximum stability. Working solutions were prepared by evaporating to dryness the appropriate volume under a stream of dry filtered air and reconstituting with distilled water. These solutions were stored at 4°C and checked weekly for radioactivity.

Duplicate seawater aliquots (10 ml) from each experimental aquarium and the incoming seawater were spiked with 5nM of labeled thymidine and incubated in the dark at *in situ* temperatures for 1 hour. Incubation uptake was terminated by filtration through a 25-mm dia. type HA membrane (0.45 μm nominal pore size, Millipore Corp.). After filtration the vacuum was stopped and 10 ml of ice-cold (< 5°C) filtered (sterile) seawater was added to cool the filter. This was filtered through and the vacuum was stopped prior to addition of 15 ml ice-cold (< 5°C) 5% trichloroacetic acid (TCA) to extract the soluble thymidine pools from the cells. Temperature control is critical during the extraction as a temperature rise above 10°C for TCA will hydrolyse DNA and allow incorporated label to solubilize and pass through the filter. After

3 min. the vacuum was started and the filter was rinsed twice with ~5 ml ice-cold 5%, TCA, and then placed in a scintillation vial. Ethyl acetate (1 ml) was added to dissolve the filter; 10 ml of Beta-Phase cocktail was added and the radioactivity was assayed by liquid scintillation spectrometry.

The resulting counts for duplicates were averaged and corrected for poisoned controls (1 μM $HgCl_2$) and a counting efficiency of 35%. The data were converted to nmoles/liter day of incorporation by the formula:

$$\text{n moles}/\ell\cdot\text{day} = (\text{cpm})\left(\frac{1\ \text{dpm}}{0.35\ \text{cpm}}\right)\left(\frac{1\ \text{Ci}}{2.22 \times 10^{12}\ \text{dpm}}\right)\left(\frac{1\ \text{m mol}}{20\ \text{Ci}}\right)\left(\frac{10^6\ \text{n mol}}{\text{m mol}}\right)\left(\frac{24\ \text{hr}}{\text{day}}\right)\left(\frac{1}{0.015\ \ell}\right)\left(\frac{1}{1\ \text{hr}}\right)$$

References: FUHRMAN and AZAM (1980); FUHRMAN et al. (1980); FUHRMAN and AZAM (in press, 1981)

^{3}H-Leucine and ^{3}H-Glucose Uptake

The procedure for both substrates was identical except for the amino acid leucine, in that a larger sample was prepared such that an aliquot could be saved and preserved for the autoradiography procedure (details in this section).

Working solutions of ^{3}H-Leucine (60 Ci/mmol, New England Nuclear) were prepared by diluting an aliquot of the stock solution into distilled water. The ^{3}H-Glucose solutions (30 Ci/mmol, New England Nuclear) were prepared by evaporating an aliquot under a stream of dry, filtered air followed by reconstitution in distilled water. All solutions were stored at 4°C and assayed weekly for radioactivity to check stability.

Each experimental aquarium and the incoming seawater was sampled in duplicate and controls were killed with 1 M $HgCl_2$ prior to addition of radiolabeled substrate. To each sample (10 ml for ^{3}H-Glucose; 15 ml for ^{3}H-Leucine) 50 μl (1.5 μCi) of radiolabeled compound was added, followed by incubation for 2 hr. in the dark at in situ temperature.

The incubation was terminated by sample filtration through a HA membrane (0.45 μm nominal pore size, Millipore Corp.), followed by several washes with filter-sterilized seawater to remove any nonincorporated label. After filtration, each filter was placed in a scintillation vial, and 1 ml Ethyl acetate added to dissolve the membrane. After approximately 10 min., 10 ml of Beta-Phase cocktail was added and the sample assayed for radioactivity by liquid scintillation spectrometry. Duplicates were averaged and corrected for control blanks, and the resulting counts were converted to uptake in nmoles/liter day with the formula:

$$\text{n moles}/\ell\cdot\text{day} = (\text{cpm})\left(\frac{1\ \text{dpm}}{0.35\ \text{cpm}}\right)\left(\frac{1\ \text{Ci}}{2.22 \times 10^{12}\ \text{dpm}}\right)(\text{S.A.}^{-1})\left(\frac{10^6\ \text{n mol}}{\text{m mol}}\right)\left(\frac{24\ \text{hr}}{\text{day}}\right)\left(\frac{1}{2\ \text{hr}}\right)\left(\frac{1}{0.015\ \ell}\right)$$

where a counting efficiency of 35% was utilized and S.A. is the specific activity (in Ci/mmol) for the labeled substrate.

References: AZAM and HOLM-HANSEN (1973); FUHRMAN et al. (1980).

Epifluorescence Enumeration

Seawater samples (10-15 ml) from each experimental aquarium and the incoming seawater were immediately preserved with 4% filter-sterilized formalin (buffered with $Na_2B_4O_7$), and the cellular DNA was stained to fluoresce with Acridine orange (0.01%, 2 min.) prior to filtration. The Nucleopore polycarbonate filters were stained prior to use with Irgalan black (to eliminate autofluorescence) and a type AA (0.8 μm, Millipore) membrane was

used as a back filter to distribute the vacuum evenly. After filtration, the filter was mounted on a microscope slide with a cover slip affixed with paraffin oil. Blanks were prepared in a similar fashion except that filter-sterilized seawater (GS, 0.2 μm, Millipore Corp.) was preserved and stained.

The slides were examined by epifluorescence microscopy and counted in a random fashion by grids. All counts for each grid were averaged (10 grids per slide) for duplicate slides and the data converted to cells x 10^6/ml seawater.

References: HOBBIE et al. (1977); FUHRMAN and AZAM (1980).

Autoradiography Assay

The micro-autoradiographic technique provides for simultaneous examination by phase contrast microscopy of bacterial cells stained with acridine orange and labeled with developed silver grains. The method of preparation provides for orientation of bacteria between the photographic emulsion and the microscope objective to prevent visual interference by the silver grains.

The 5 ml aliquots from the ^{3}H-leucine uptake assays (preserved with 4% formalin) were stained with sterile-filtered 0.01% acridine orange for 1 min., followed by filtration through a 0.2 μm pore size nucleospore membrane (25 mm dia.). A type AA filter (0.8 μm, Millipore) was used as a back filter for even vacuum distribution. The filter was rinsed with sterile, filtered, distilled water, and kept damp for subsequent transfer of cells onto the surface of a mounted gelatin-coated coverslip. (Details of the gelatin-coated coverslip preparation are presented elsewhere - see References below).

Resulting autoradiograms were prepared in total darkness with Kodak NTB2 Nuclear track emulsion coating, dried, and exposed at 4°C. After the appropriate exposure time, the autoradiograms were developed, fixed and further prepared as detailed elsewhere (see References below). Bacteria were

counted by epifluorescence microscopy and silver gain clusters were counted by transmitted phase contrast microscopy.

References: MEYER-REIL (1978); FUHRMAN and AZAM (in press, 1981).

METHODS FOR HYDROCARBON ANALYSES AND PHOTOCHEMICAL/MICROBIAL OXIDATION PRODUCT CHARACTERIZATION

Volatile Hydrocarbon Analyses

Volatile hydrocarbons are sampled from the air above the slick in the evaporation/dissolution chamber (or the flow-through outdoor tanks in Alaska) by vacuum-pumping measured volumes of air through 1/8 in. ID x 12 in. long stainless tubes packed with Tenax® GC polymer. For each sample, two tubes are connected in series with Swagelok fittings, and prior to and immediately after sampling, all tubes are sealed with Swagelok endcaps and plugs. Sampling is achieved by use of a Gast Mfg. Corp. vacuum pump attached to the Tenax® traps via flow regulators and flexible Teflon tubing. Air velocities above the slick in the evaporation/dissolution chamber are measured with a Kurz air velocity meter 4m above the oil/seawater interface.

Before each sample is obtained, the Tenax® trap's flow velocity is checked with a bubble flow meter. Approximately 60 second samples are generally obtained at flow rates ranging from 20 to 30 ml/min; thus, sample volumes ranged from 20-30 ml.

Water samples for analysis of dissolved lower-molecular-weight aliphatic and aromatic hydrocarbons are taken in Pierce septum-capped vials for subsequent purge and trap analysis by GC/MS techniques similar to those developed by Bellar and Lichtenberg (1974) and others.

Following collection, the water samples are refrigerated (no preservatives are added), and they are maintained at 3°C until analysis. Capped stainless-steel Tenax® traps are stored at ambient temperature until analysis.

The Tenax® air samples are analyzed by heat desorption followed by Flame Ionization Detector (FID) gas chromatography on a Hewlett Packard 57330A

instrument or gas chromatography/mass spectrometry (GC/MS) using a Finnigan 4021 quadrupole instrument. The heat desorption is accomplished by installing the Tenax® traps in a Tekmar liquid sample concentrator (LSC-2) interfaced to the injection port system of either the FID GC or GC/MS (PAYNE et al., 1980b).

At the time of desorption (5 min. at 180°C at 20 ml/min He flow) the gas chromatographic column (packed 6 ft. x 22 mm I.D. SP-1000) and oven are cryogenically cooled to 30°C. Following desorption, the oven is programmed rapidly (30°C/min) to 100°C and then from 100°C to 200°C at 10°C/min. The final temperature of 200°C is held for the duration of the chromatographic run. A GC column flow rate of 20 ml/min He is also used and the injector temperature is held at 200°C.

The effluent from the gas chromatograph is then analyzed by FID on the HP-GC or it is passed through a glass jet separator for enrichment and then directly into the ion source of the GC/MS (operated in the electron impact-mode at 300°C). Spectra are acquired by operating the ion source at 70eV from 35 to 300 amu in 1.95 sec. A hold time of 0.05 sec is used to allow the electronics to stabilize before the next scan. The ion source is tuned for maximum sensitivity with perfluorotributylamine and the ion fragments at m/e 69 and m/e 219 are calibrated to give a 2.5:1 ratio; the electron multiplier is operated at 1600V with the preamplifier gain at 10^{-7} amps/volt. GC/MS data acquisition is initiated at the moment of desorption. Typically, 900-1000 scans are acquired for each data file.

The water samples stored in Pierce vials are allowed to come to room temperature and 5-ml aliquots are withdrawn and injected into the purge device of the LSC-2. Before purging in mass spectrometry operations, 100 ng each of three internal standards, dichlorobutane (m/e 55), bromochloromethane (m/e 130), and bromochloropropane (m/e 77) are added. This allows correction of recovered values for matrix effects and corrects for differences in ionization potential, lens voltage, etc., among runs. Instrumental conditions are identical to those described for Tenax® column analysis.

Before analyses with either instrument, response factors are determined for 10-12 target aliphatic and aromatic compounds of interest by spiking several known mixed standards into salt water blanks which are then analyzed as samples (PAYNE et al., 1980b).

Higher Molecular Weight Petroleum Hydrocarbon Analyses

Water sediment and oil/mousse samples are analyzed by procedures which basically involve: 1) extraction, 2) fractionation into aliphatic, aromatic and polar constituents by liquid/solid (SiO_2) column chromatography and analysis by FID capillary gas chromatrography and capillary gas chromatography/mass spectrometry. Specific details with regard to these analytical procedures (including instrument calibrations, sensitivity, data reduction, etc.) are presented in Appendix C to this report (Methods Section, page 4 of "Chemical Weathering of Petroleum Hydrocarbons in Sub-Artic Sediments: Results of Chemical Analyses of Naturally Weathered Sediment Plots Spiked with Fresh and Artificially Weathered Cook Inlet Crude Oil").

Water samples from the flow-through seawater systems are collected in 20-liter carboys and pH was adjusted to 2.0. Three hundred-fifty ml of methylene chloride is then added to each carboy (approximately 200 ml of methylene chloride goes into solution on the first addition) and the mixture is stirred vigorously for 3 minutes. The methylene chloride is removed by pressurizing the carboys with N_2 and forcing the methylene chloride through a stainless steel syphon tube into a separatory funnel. This procedure is repeated two more times. The methylene chloride extract is concentrated to 100 ml in K-D concentrators and then passed through sodium sulfate to remove the residual water. The anhydrous methylene chloride extract is then concentrated to 2 ml and solvent-exchanged to hexane. The concentrate is then fractionated on silica gel using the three fraction schemes described in Appendix C, page 4 of "Chemical Weathering of Petroleum Hydrocarbons in Sub-Artic Sediments: Results of Chemical Analyses of Naturally Weathered Sediment Parts Spiked with Fresh and Artificially Weathered Cook Inlet Crude Oil".

APPENDIX C

CHEMICAL WEATHERING OF PETROLEUM HYDROCARBONS IN SUB-ARCTIC SEDIMENTS: RESULTS OF CHEMICAL ANALYSES OF NATURALLY WEATHERED SEDIMENT PLOTS SPIKED WITH FRESH AND ARTIFICALLY WEATHERED COOK INLET CRUDE OILS

Report Submitted to:

Dr. Robert Griffith
Department of Microbiology
Oregon State University
Corvallis, Oregon

by:

James R. Payne, Gary S. Smith, James L. Lambach and Paul J. Mankiewicz

Division of Environmental
Chemistry and Geochemistry
Science Applications, Inc.
476 Prospect Street
La Jolla, California 92038

December, 1980

TABLE OF CONTENTS

LIST OF TABLES

LIST OF FIGURES

LIST OF FIGURES (CONTINUED)

OBJECTIVES

The primary goal of this program was to examine the biological and chemical impact of fresh and weathered crude oil after its incorporation into sub-arctic sedimentary regimes. The experiments that were used in this program were designed by Dr. Robert Griffith and his colleagues at Oregon State University to study one-year time series changes in biological productivity, recruitment and recolonization as a function of the chemical composition of the oil within the sedimentary study plots.

In an effort to assist Dr. Griffith in this program, the Environmental Chemistry and Geochemistry Division of Science Applications, Inc. (SAI) undertook detailed chemical analyses of the sediment samples used in these experiments. Specifically, hydrocarbon profiles (concentrations) were determined in control and experimental sedimentary plots which had been spiked with three different levels of fresh and artificially weathered Cook Inlet Crude Oil. These sediments were examined: first, after the initial spiking, and second, after one year of natural weathering in the sedimentary regime at Kasitsna Bay, Alaska. Additional studies were also undertaken in Sadie Cove, Alaska, where oiled sediments were spiked with Chiton and starch before deployment into the field, to determine if biotic weathering processes were controlled by limited nutrient concentrations.

Results of the hydrocarbon analyses from these experiments are presented in this section.

IMPLICATIONS FOR OFF-SHORE OIL AND GAS DEVELOPMENT

Many investigators have long suspected that spilled oil on the water surface or in the water column does not constitute as great an environmental threat as oil which has been incorporated into sedimentary regimes. Ironically, in the case of most major oil spills and laboratory studies, the sediments have been found to be the ultimate repository or sink for the bulk of the higher molecular weight components in the released oil (Jordan and Payne, 1980, D'Oxouville et al., 1979; Meyers, 1978; Mayo et al., 1978; Gearing et al., 1979; Winters 1978; Meyers and Quinn 1973; Zurcher and Thuer 1978; Bassin and Ichiye 1977). Once incorporated into the sediments, many of the unweathered toxic components of oil are retained unaltered for extended periods (Teal et al., 1978; Mayo et al., 1978) causing a variety of long term pertibations to plants, organisms and the physical (areobic vs. an aerobic) nature of the sediment itself. If contaminant concentrations reach high enough levels, the biological productivity of an entire area may be completely destroyed immediately after the spill impact, and residual toxic levels may prevent recolonization of native species for a number of years (American Institute of Biological Sciences, 1978). This is a significant problem in areas of high productivity or in sedimentary regimes critical to the survival of juvenile species. Alternately, competing species with different degrees of tolerance to oil could opportunistically recolonize an area, thus further altering the biological balance at the spill site for years.

In these experiments, we attempted to determine the levels or concentrations of oil in sub-Arctic sediments that could cause limited recovery or long term damage to an area. We also sought to determine concentrations and conditions under which specific compounds in the complex hydrocarbon mixture are selectively removed due to biotic and abiotic processes after incorporation of oil into the sediments. The results of these studies indicate that spiked levels of oil approaching 50 parts per thousand (ppt) (total oil wt/wt) cause extensive and significant long term damage to sub-Arctic sediments, and that little or no significant additional weathering (removal of toxic components) occurs at least up to one year following initial exposure. This was observed when both fresh and artificially weathered crude oils were spiked into the sedimentary matrix at the 50 ppt level. Similar trends were observed at the 1 ppt level, but some evidence of selective lower molecular weight hydrocarbon degradation after one year was found. The experimental results also suggest that at levels of oil approaching 50 ppt, the biotic utilization of specific hydrocarbon components is not inhibited by limited nutrient levels but rather by the toxicity of the oil itself.

A recommendation which can be drawn from these results is that in oil spill prevention, mitigation, and clean-up efforts, every attempt should be made to prevent oil from reaching sub-Arctic sediments particularly in low energy nearshore subtidal regimes where high biological productivity is observed.

METHODS

Techniques for artificially weathering Cook Inlet Crude Oil and subsequent spiking, homogenization, and deployment of sediment into the experimental trays for in situ weathering are described elsewhere. Subsamples of the spiked and control sediments from the experimental trays were frozen at the initiation of the experiment and again after one year in the field. All frozen sediment samples were shipped on ice to SAI's Trace Environmental Chemistry Laboratory in one lot on 17 October 1980, where they were subsequently stored at $-4^{\circ}C$ until analyses were begun.

Extraction

Each sediment sample was extracted using a shaker-table procedure which is similar to that described by Payne et al. (1978) and Brown et al. (1980) and which has been shown to yield comparable results to Soxhlet extraction (MacLeod and Fischer, 1980; and Payne et al., 1979). Briefly, the thawed sediment was placed in tared 500 ml Teflon jars and a wet weight was determined. Approximately 50 ml of methanol was added to the sediment for water removal, and the jars were sealed and agitated on a shaker table for 15 minutes. The jars were then centrifuged at 3000 rpm for 20 minutes at room temperature and the supernatant was decanted off and saved, and the drying procedure was repeated. After the second drying step, 150 ml of methylene chloride (CH_2Cl_2) and methanol (65:35 v/v) were added to the jars and agitation

was continued for 12 hours. The samples were centrifuged, the supernatant saved, and the procedure was repeated with the agitation occurring for a period of 6 hours. The methanol-water washes and the methanol-methylene chloride extracts were combined in a separatory funnel and back extracted with 400-500 ml of saturated sodium chloride in distilled water which had been previously extracted with hexane. The lower layer (CH_2Cl_2) was removed and the water phase was back extracted with three additional 100 ml aliquots of CH_2Cl_2. The combined CH_2Cl_2 extracts were concentrated to approximately 100 ml using a Kuderna-Danish (K-D) apparatus, and dried by passage through a column of sodium sulfate followed by additional elution with CH_2Cl_2. The dried extract was concentrated to about 10 ml using a K-D apparatus and solvent exchanged (3x) into hexane, followed by solvent reduction to 1-2 ml in preparation for column chromatography.

Liquid Column Chromatography

To fractionate the sediment extracts, a three-part fractionation scheme was employed to separate the aliphatic, aromatic, and polar compounds (Payne, et al., 1980). A 10 mm I.D. x 23 cm long column with a 16 ml pore volume was packed with 1.5 cm of activated copper at the base of the column (to remove elemental sulfur), followed by a hexane slurry of 60/200-mesh silica gel that had been cleaned with CH_2Cl_2 and activated at 210°C for 24 hours. The elution scheme was as follows:

Fraction/Solvent	Amount	Compound Class
1. Hexane	30 ml	Aliphatic hydrocarbons
2. Hexane:Benzene 50:50	45 ml	Aromatic hydrocarbons
3. 50% CH_3OH in CH_2Cl_2	60 ml	Polar compounds

Gas Chromatographic Analysis

All gas chrmatographic results were obtained on a Hewlett-Packard 5840A gas chromatograph equipped with an 18835A glass capillary inlet system and flame ionization detector. The microprocessor-based instrument was interfaced to a Texas Instruments Silent 700 ASR data terminal equipped with casette tape drive, allowing permanent storage of calibration data, retention times, and peak areas required for the data reduction system.

A 30-meter J&W Scientific Co. SE-54 wall-coated open tubular fused silica capillary column was utilized for the desired chromatographic separations. Temperature programming used with this column included:

Initial Temperature	50°C for 5 minutes
Program Rate	3.5°C/min
Final Temperature	275° for 60 minutes

The injection port and detector were maintained at 280° and 350°C, respectively. All injections were made in the splitless mode of operation with an injection port backflush 1 minute into the run.

Constant injection volumes of 1.0 µl were analyzed automatically using a Hewlett-Packard model 7671A Automatic Liquid Sampler, increasing precision substantially relative to manual injection.

Gas Chromatogram Data Reduction

Hydrocarbon concentrations for individual resolved peaks in each gas chromatogram were calculated on a DEC-10 System Computer using the formula given in equation 1. This particular example is of the program used for seawater analysis. Operator-controlled modification of the DEC-10 program allows similar data reduction on sediments, tissues, or individual oil (mousse) samples.

$$\mu g \text{ compound X/L seawater} = (A_x) \times (R.F.) \times \left[\frac{P.I.V. + 2}{Inj.S.Vol.} \cdot \frac{Pre\text{-}C.S.\ Vol.}{Post\text{-}C.S.Vol.} \cdot \frac{100}{\%NSL \text{ on } LC} \times \frac{100}{\%DW/FW} \times \frac{1}{liters}\right] \quad (1)$$

where:

A_x = the area of peak X as integrated by the gas chromatograph (in arbitrary GC area units)

R.F. = the response factor (in units of µg/GC area unit)

P.I.V. + 1 = the post-injection volume (in µl) from which a 1-µl aliquot had been removed for analysis by GC (measured by syringe immediately following sample injection)

Inj.S.Vol. = the volume of sample injected into the GC (always 1.0 µl as measured by an HP Automatic Liquid Sampler)

Pre-C.S.Vol. & Post-C.S. Vol.	= the total solvent volumes before and after an aliquot is removed for gravimetric analysis on a Cahn electrobalance
%NSL on LC	= the percent of sample non-saponifiable lipid used for SiO_2 column chromatography
%DW/FW	= the percent dry weight of wet weight in the sediment tissue, or oil sample being analyzed
liters	= liters of seawater initially extracted (or grams wet weight of oil or sediment).

During analysis of the extracts, the 5840A gas chromatograph was recalibrated after every 8 to 10 injections, and individual response factors were calculated for all detected even and odd n-alkanes between nC_8 and nC_{32}. Concentrations of other components (e.g., branched and cyclic) that eluted between the major n-alkanes were calculated by linear interpolation of the adjacent n-alkane response factors and the unknown compound peak's KOVAT index. By incorporating the post-injection volume (PIV) into the calculation, the amount of hydrocarbons measured in the injected sample were converted to the total hydrocarbon concentration in the sample.

Unresolved complex mixtures (UCM's) were measured in triplicate by planimetry; the planimeter area was converted to the gas chromatograph's standard area units at a given attenuation and then quantitated using the average response factors of all the n-alkanes occurring within the range of the UCM, as shown in equation 2.

$$\frac{\mu g\ UCM}{liter} = Area_p \times (Conf.\ F) \times \frac{S.\ Att.}{Ref.\ Att.} \times (\overline{R.F.}_{a-b}) \times [\ldots] \quad (2)$$

where:

Area	= UCM area in arbitrary planimeter units,
Conv. F.	= a factor for converting arbitrary planimeter units to GC area units at a specific GC attentuation,
S. Att. and Ref. Att.	= the GC attenuation at which the sample chromatogram was run and the reference attenuation to determine the conversion factor (Conv. F.), respectively,
$R.F._{a-b}$	= the mean response factor for all sequential n-alkanes (with carbon numbers a to b) whose retention times fall within the retention time window of the UCM, and
[...]	= the same parameters enclosed in brackets in equation 1.

Confirmation of KOVAT index assignment to n-alkanes was done by computer correlation with n-alkane standard retention times and direct data-reduction-operator input.

Assignment of a KOVAT index to each branched or cyclic compound eluting between the n-alkanes was done by interpolation using the unknown compound and adjacent n-alkane retention times. Assignment of KOVAT indices to peaks in the aromatic fraction was made by direct correlation of unknown peaks with retention times from the n-alkane and aromatic standard runs completed prior to sample injection (Payne, et al., 1978b).

Capillary Gas Chromatography Mass Spectrometry

Selected extractable organic compounds previously analyzed by fused silica capillary column-FID GC were also subjected to fused silica capillary gas chromatography/mass spectrometry (GC/MS). A 30-meter J&W Scientific Co. SE-54 capillary column (0.25-mm I.D. with a film thickness of 25 μm was used to achieve chromatographic separation in a Finnigan 4021 quadrupole mass spectrometer. The capillary system was operated in the splitless (Grob-type) mode. The static time upon injection was 0.8 min, after which time the injection port was backflushed with the split and septum sweep flows at a combined rate of 35 ml/min. Linear velocity was set at 35 cm/sec, which gave a flow rate of 1.18 ml/min. The GC was programmed to remain isothermal at 30°C for 1.5 min following injection, elevated at 4°C/min from 30 to 160°, and 8°C/min from 160-275°, after which the oven was held isothermally at 275°C for approximately 20 minutes.

The flexible fused silica column was routed directly into the ion source of the mass spectrometer, which was operated in the electron impact mode at 70eV with the lens potentials optimized for maximum ion transmission. The quadrupole offset and offset programs were adjusted to yield a fragmentation ratio for perfluorotributylamine m/e 69-to-219 of 4:1. This tuning yields quadrupole electron impact spectra that are comparable to magnetic sector electron impact spectra, thereby allowing optimal matches in the computer search routines used in the INCOS data system that scans the quadrupole rods from 35-475 amu in

0.95 sec. A hold time of 0.05 sec between scans allows the electronics to stabilize prior to the next scan. The mass spectrometer was tuned at the beginning of each day using perfluorotributylamine. A calibration was accomplished with a routine diagostic fit of 2% mass accuracy. Prior to analysis of samples, standard mixtures of n-alkanes, pristane, phytane, and mixed aromatic hydrocarbons were injected.

RESULTS AND DISCUSSION

Time Zero Samples

Figure 1 presents the FID capillary gas chromatograms obtained on the control sediment samples taken from Kasitsna Bay at the beginning of the spiked sediment experiments. The most characteristic feature in the aliphatic fraction chromatogram, A, is the predominance of odd numbered n-alkanes in the molecular weight range of nC_{21} to nC_{29}, (RT 56.53; 62.12; 67.03; 71.93; 78.77) reflecting biogenic input. The sample also contains very low levels of nC_{17} and pristane (RT 44.55; 44.75) and nC_{18} and phytane (RT 47.40; 47.83). The three major components at retention times 31.21, 35.77 and 43.08 are internal spikes and a GC recovery standard (triisopropylbenzene, 31.21; n-decylcyclohexane, 43.08; and hexamethylbenzene, 35.77, respectively). There is no apparent evidence of any petroleum contamination and there appears to be a small cluster of branched and unsaturated biogenic hydrocarbons between nC_{20} and nC_{21}. The aromatic fraction chromatogram, B, from this

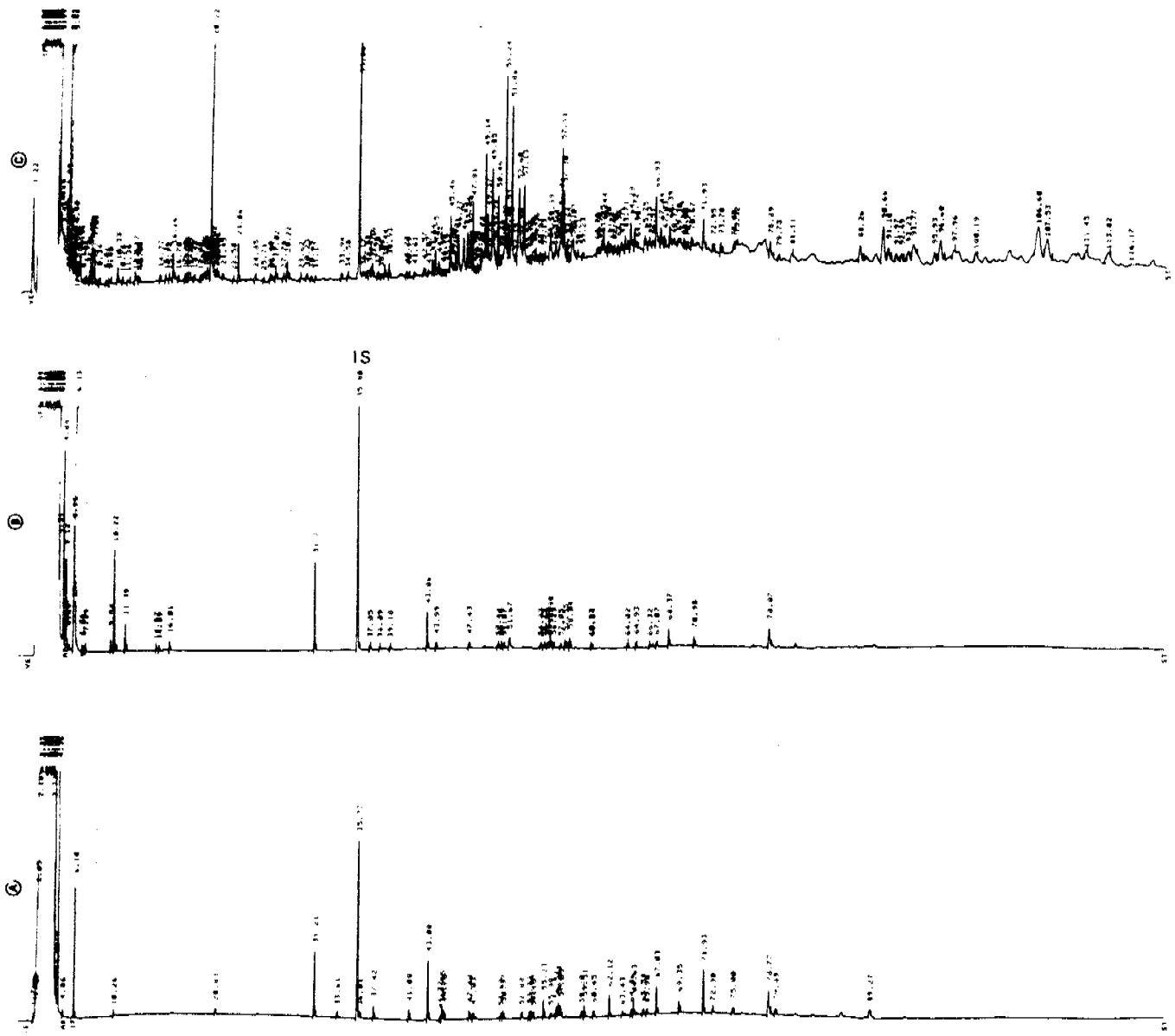

Figure 1. Flame Ionization Detector capillary gas chromatograms of: A, the aliphatic fraction; B, the aromatic fraction and C, the polar fraction extracts obtained from time zero control sediment samples from Kasitsna Bay.

sample shows very little contamination of any kind, with only sub-nanogram per gram-dry-weight components present. The polar fraction chromatogram, C, does show evidence of several polar materials which are currently underoing analysis by GC/MS. From GC/MS analyses of similar sediment samples, the identities of these peaks are suspected to be long chain fatty acid esters of biogenic origin.

Tables 1 and 2 present the reduced quantitative data obtained from the capillary FID gas chromatographic runs of these and all the other sediment samples analyzed as part of this program. The data in Tables 1 and 2 illustrate several interesting quantitative aspects which should be considered when interpreting the results. First, the background levels of hydrocarbons in the control samples from Kasitsna Bay at times zero and one year were both extremely low. In neither case was an Unresolved Complex Mixture (UCM) present, and the highest hydrocarbon concentration in these two samples was only six micrograms per gram dry weight. The odd to even n-alkane ratios for these samples (1 and 625) were high, ranging from 5.2 to 7.9, reflecting predominance of the odd n-alkanes of biogenic origin.

Figures 2 and 3 present gas chromatograms of the hexane and benzene fractions from the fresh Cook Inlet crude oil and the artificially weathered Cook Inlet crude oil used to spike the sediment samples, respectively. Figure 2A clearly shows a high degree of complexity in the lower molecular weight range from nC_8 through nC_{12},

Table 1. Reduced Aliphatic Hydrocarbon Data Derived from Flame Ionization Detector Capillary GC Analyses

Sediment Sample	OSU ID No	Time in Field (years)	Total Resolved ug/g	Total UCM* ug/g	Σ n-alkanes ug/g	Σ even n-alkanes ug/g	Σ odd n-alkanes ug/g	pristane + phytane / n-alkanes	odd alk / even alk	prist / nC_{17}	phy / nC_{18}	prist / phyt	n-alk / branched
KASITSNA BAY CONTROL	1	0	5.89	0.	2.76	0.449	2.31	0.0157	5.15	0.758	0.	4--	0.883
KASITSNA BAY CONTROL	625	1	1.22	0.	0.533	0.06	0.473	0	7.86	0.	0.	0.	0.776
FRESH CRUDE SPIKE 50ppt	5	0	2840.	4090.	1460.	742.	722.	0.0749	0.973	0.681	0.343	2.63	1.06
FRESH CRUDE SPIKE 1ppt	4	0	83.3	154.	52.8	24.2	28.6	0.055	1.18	0.630	0.411	2.18	0.690
FRESH CRUDE SPIKE 0.1ppt	3	0	11.3	12.8	5.03	2.11	2.92	0.596	1.39	0.601	0.380	2.40	0.803
WEATHERED CRUDE SPIKE 50	14	0	1530.	3020.	945.	460.	485.	0.104	1.06	0.721	0.326	2.75	1.62
WEATHERED CRUDE SPIKE 1	12	0	62.2	136.	40.3	19.3	21.0	0.0871	1.09	0.645	0.371	2.27	1.84
FRESH CRUDE SPIKE 50ppt	628	1R	2430.	1740.	1080.	560.	515.	0.0861	0.921	0.761	0.354	2.63	0.796
FRESH CRUDE SPIKE 50ppt	629	1R	2700.	3770.	1250.	645.	605.	0.0799	0.934	0.700	0.386	2.43	0.860
FRESH CRUDE SPIKE 50ppt	630	1R	2060.	3010.	950.	494.	458.	0.0832	0.927	0.708	0.357	2.41	0.862
FRESH CRUDE SPIKE 1ppt	631	1	21.3	98.1	10.9	4.89	6.04	0.144	1.24	1.28	0.709	2.40	1.06
FRESH CRUDE SPIKE 0.1ppt	634	1	3.29	13.1	1.09	0.179	0.912	0.0320	5.10	0.800	0.	3--	0.496
WEATHERED CRUDE SPIKE 50	637	1	1530.	3710.	949.	449.	499.	0.109	1.11	0.926	0.463	2.40	1.64
WEATHERED CRUDE SPIKE 1	640	1	14.3	319.	2.81	0.	2.81	0.	2--	0.	0.	0.	0.243
SADIE COVE CONTROL	206	0	26.1	0.	10.7	1.37	9.33	0.	6.81	0.	0.	0.	0.773
SADIE COVE OIL & STARCH	782	1	3760.	5200.	1605.	837.	768.	0.071	0.917	0.762	0.391	2.55	0.743
SADIE COVE OIL	779	1	4730.	6100.	1920.	983.	932.	0.0838	0.948	0.880	0.420	2.75	0.681
SADIE COVE OIL & CHITIN	780	1	4700.	6670.	1986.	1020.	968.	0.0630	0.951	0.626	0.345	2.14	0.732
COOK INLET CRUDE OIL													
FRESH	-	N.A.	84000	77600	33000	18300	14700	0.0703	0.804	0.673	0.331	2.41	0.648
WEATHERED	-	N.A.	38700.	54500.	24500.	11600.	12900.	0.0989	1.12	0.654	0.380	2.23	1.73

*UCM = Unresolved Complex Mixture

Table 2. Reduced Aromatic Hydrocarbon Data Derived from Flame Ionization Detector Capillary GC Analyses.

Sediment Sample	OSU ID No	Time in Field (years)	Total Resolved ug/g	Total UCM* ug/g	Naphthalene (1185)**	2 Methyl-naphthalene (1295)	1 Methyl-naphthalene (1313)	Biphenyl (1381)	2,6 Dimethyl naphthalene (1404)	Fluorene (1586)	Phenan-threne (1786)	Anthracene	1 Methyl-phenanthrene	Fluoranthene	Pyrene
KASITSNA BAY CONTROL	1	0	3.08	0.	nd	nd	nd	nd	nd	nd	0.0262	nd	nd	nd	0.0392
KASITSNA BAY CONTROL	625	1	1.212	0.	nd	nd	nd	nd	nd	nd	nd	nd	nd	nd	nd
FRESH CRUDE SPIKE 50ppt	5	0	1460.	1740.	58.0	137.	94.9	16.2	65.4	32.5	56.6	nd	18.0	nd	nd
FRESH CRUDE SPIKE 1ppt	4	0	12.2	22.3	0.363	0.960	0.570	0.0418	0.469	0.120	0.190	nd	0.0658	nd	nd
FRESH CRUDE SPIKE 0.1ppt	3	0	0.0289	0.0259	0.00025	0.00064	0.00037	nd	0.0032	nd	0.00032	nd	nd	0.0021	0.00012
WEATHERED CRUDE SPIKE 50	14	0	210.	824.	nd	5.59	4.77	nd	11.7	4.88	8.65	nd	nd	1.47	nd
WEATHERED CRUDE SPIKE 1	12	0	10.7	40.62	0.152	0.513	0.334	nd	0.467	0.150	0.255	nd	nd	nd	0.0376
FRESH CRUDE SPIKE 50ppt	628	1	469.	1235.	15.3	39.6	23.7	1.48	19.2	4.84	6.7	nd	2.48	1.00	nd
FRESH CRUDE SPIKE 50ppt	629	1	428.	880.	13.3	35.2	21.0	1.17	17.9	4.27	5.98	nd	2.40	0.840	nd
FRESH CRUDE SPIKE 50ppt	630	1	300.	2020.	9.75	30.4	18.6	nd	17.5	4.44	7.15	nd	2.95	nd	nd
FRESH CRUDE SPIKE 1ppt	631	1	9.33	29.7	0.163	0.517	0.433	0.0311	0.383	0.107	0.129	nd	0.0621	nd	nd
FRESH CRUDE SPIKE 0.1ppt	634	1	2.23	3.98	nd	0.0257	nd	nd	0.0321	nd	0.0307	nd	nd	nd	0.0185
WEATHERED CRUDE SPIKE 50	637	1	288.	901.	nd	5.19	4.07	nd	9.58	3.71	6.80	nd	nd	nd	nd
WEATHERED CRUDE SPIKE 1	640	1	12.28	51.84	0.0429	0.243	0.134	0.0234	0.420	0.195	0.137	nd	0.116	0.032	0.0297
SADIE COVE CONTROL	206	0	2.92	0	nd	nd	nd	nd	nd	nd	0.10258	nd	nd	0.02803	0.21073
SADIE COVE OIL & STARCH	782	1	781.	2010.	22.2	51.0	29.5	1.21	22.2	4.50	8.37	nd	2.64	nd	nd
SADIE COVE OIL	779	1	872.	2440.	32.6	75.0	43.2	nd	32.3	6.27	10.2	nd	5.71	2.04	nd
SADIE COVE OIL & CHITIN	780	1	1070.	1660.	33.8	77.8	45.7	1.80	31.0	6.24	9.99	nd	6.66	nd	nd
COOK INLET CRUDE OIL															
FRESH	-	N.A.	34700.	41600.	484.	1110.	644.	nd	540.	nd	190.	nd	nd	nd	nd
WEATHERED	-	N.A.	15400.	31400.	nd	nd	nd	nd	223.	102.	235.	nd	nd	nd	nd

* Unresolved complex mixture.
** Kovat indices in parentheses.
nd = not detected.

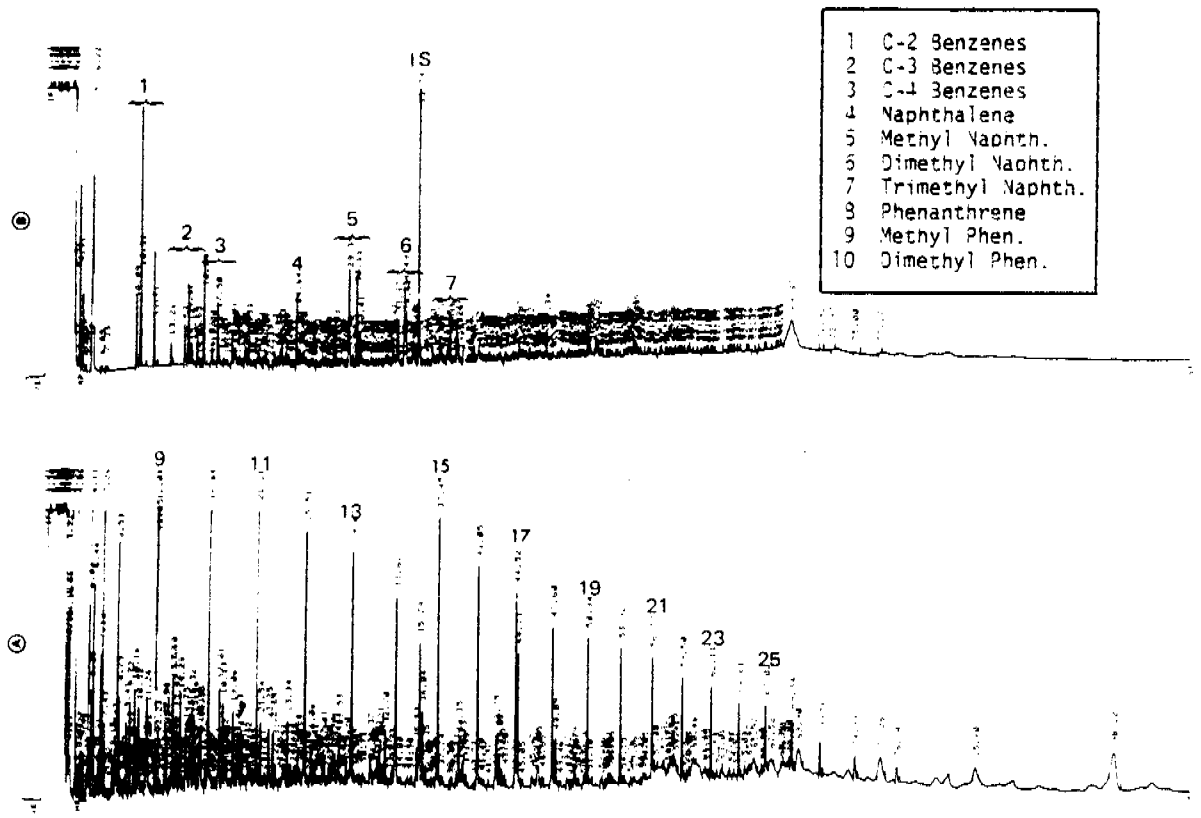

Figure 2. Flame Ionization Detector capillary gas chromatograms of: A, the aliphatic fraction, and B, the aromatic fraction extracts obtained on the fresh Cook Inlet Crude Oil used to spike the Kasitsna Bay sediment samples.

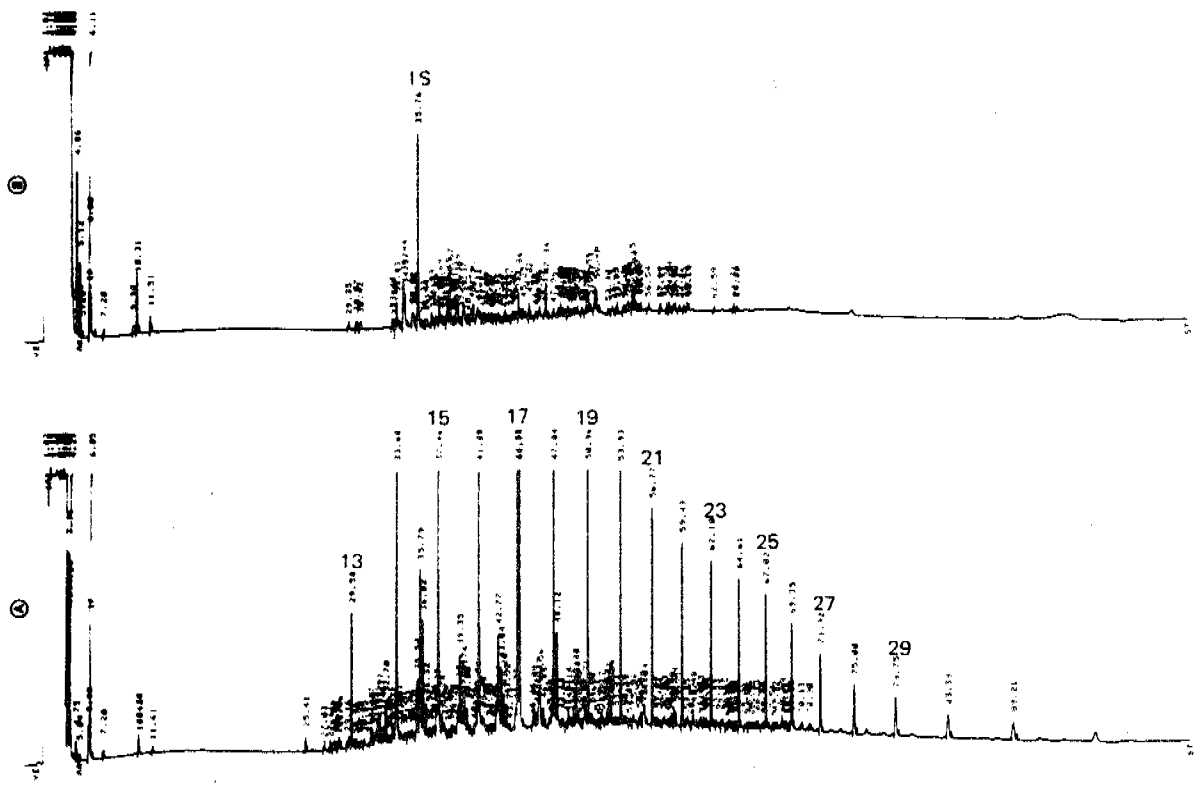

Figure 3. Flame Ionization Detector capillary gas chromatograms of: A, the aliphatic fraction, and B, the aromatic fraction extracts obtained from the Artifically Weathered Cook Inlet Crude Oil used to spike the Kasitsna Bay sediment samples.

although the aliphatic fraction is characterized in general, by n-alkanes from nC_8 through nC_{32}. The aromatic fraction shows a number of lower molecular weight aromatic compounds in the range of KOVAT index 800 to KOVAT index 1500 (RT 10.09 to 35.79). These compounds were identified by GC/MS as alkyl substituted benzenes such as xylenes, ethylbenzene, trimethylbenzene and propylbenzenes. The large peak at RT 35.79 is the GC internal standard hexamethylbenzene. Also in this sample are peaks identified as napthalene (RT 24.64), 2-methylnapthalene (RT 29.38), 1-methylnapthalene (RT 30.11), 2,6-dimethylnapthalene (RT 33.87), and several low level alkyl substituted phenanthrenes, as shown by the data in Table 2.

Figure 3 shows the gas chromatograms of artificially weathered crude oil used to spike the sediment samples. Clearly the aliphatic fraction, Figure 3A, shows loss of the lower molecular weight n-alkanes below nC_{13}; however, the higher molecular weight materials are present at approximately the same ratios as in the starting crude oil. This is illustrated by the consistency in the pristane/phytane, pristane/nC_{17}, and phytane/nC_{18} ratios for the fresh and weathered crude oils, as shown by the data in Table 1. The aromatic fraction of the artificially weathered crude shows nearly complete dimunition of the lower molecular weight hydrocarbons below dimethylnapthalene; however, there still are several higher molecular weight polynuclears present. These are primarily phenanthrene at RT 47.34 (KOVAT 1790), 1-methylphenanthrene at RT 51.97 (KOVAT 1933), and fluoranthene at RT 55.45 (KOVAT 2070). Higher

molecular weight compounds such as benz(a)anthracene, benzo(e)pyrene, benzo(a)pyrene and perylene are not apparently present in either the starting or weathered Cook Inlet crude oil to an appreciable degree.

Figure 4 shows the gas chromatograms of the aliphatic, aromatic and polar fractions obtained on the Kasitsna Bay time zero sample spiked with fresh crude oil at 1.0 ppt. The chromatograms obtained on the sediments spiked at 50 ppt were essentially identical in appearance to those in Figure 4, and thus the heavier spiked sample's chromatograms are not shown here. Further, the concentrations of crude oil in the 50 ppt samples were at such a high level that only approximately 2% of the extractable materials could be effectively applied to the liquid chromatography columns for separation into aliphatic, aromatic and polar fractions. This allowed accurate quantitation of the materials but did not figuratively show the presence of the lower molecular weight compounds to the same degree as the lower level spiked samples where the entire sample could be fractionated and analyzed without prior dilution.

With regard to the chromatograms in Figure 4, the aliphatic fraction, A, is nearly identical to the aliphatic fraction of the starting fresh Cook Inlet Crude oil shown in Figure 2. This is reflected qualitatively in the chromatograms presented in the figures and also quantitatively by the pristane/phytane, pristane/nC_{17} and phytane/nC_{18} ratio data presented in Table 1. The suite of nC_{20}-nC_{21} branched/unsaturated compounds in the background control sample are completely masked in the spiked sediment samples. The aromatic fractions of the spiked

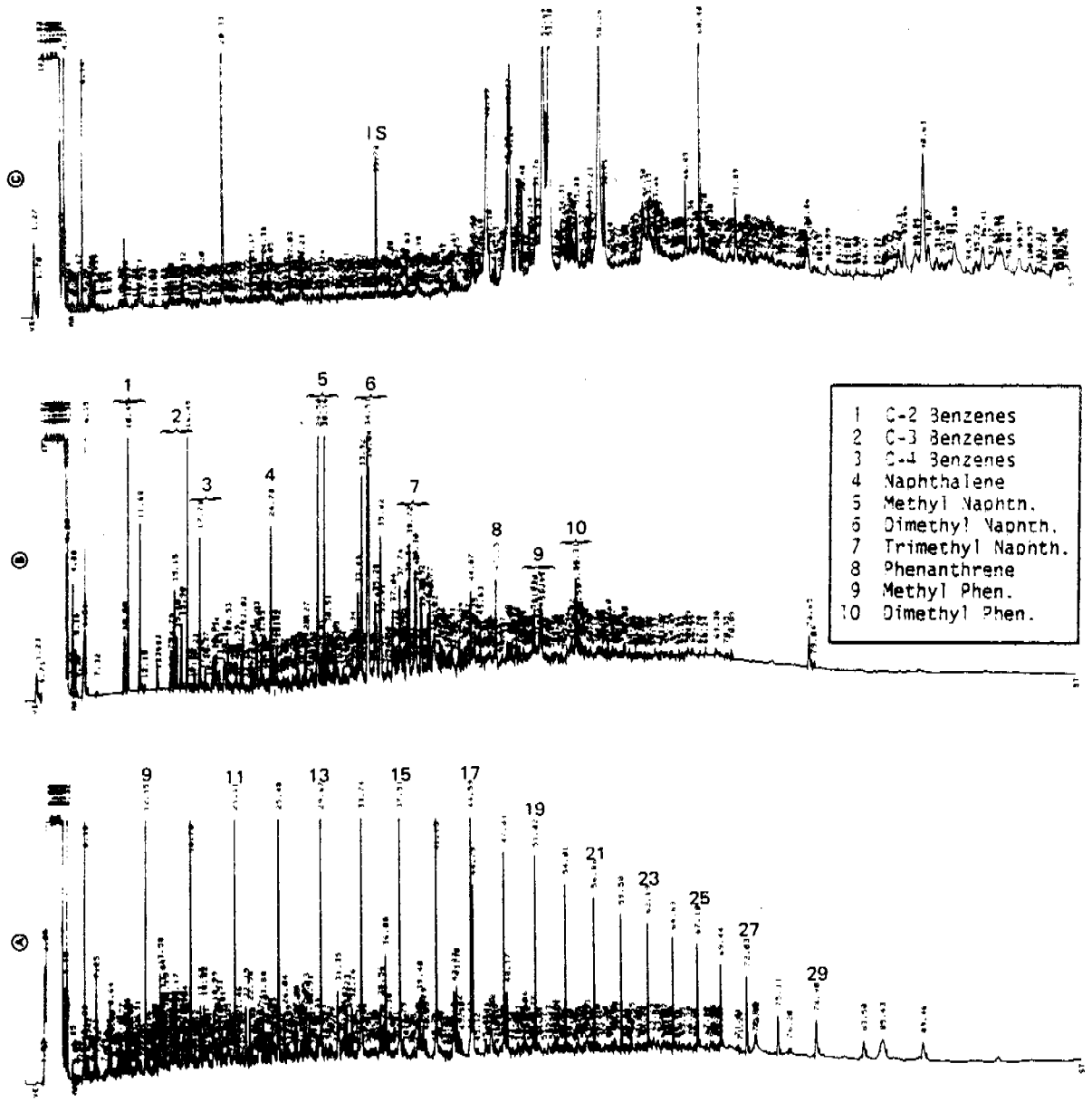

Figure 4. Flame Ionization Detector capillary gas chromatograms of: A, the aliphatic fraction, B, the aromatic fraction, and C, the polar fraction extracts obtained from time zero Kasitsna Bay sediment samples which had been spiked with fresh Cook Inlet Crude Oil at 1 ppt.

sample show many of the same aromatic compounds in the napthalene (KOVAT 1185) to pyrene (KOVAT 2124) range and the alkyl-substituted aromatic compounds at KOVAT indices 800 to1012 as in the starting crude oil. The polar fraction of the fresh spiked sediment at time zero shows many of the same biogenic compounds as in the Kasitsna Bay control sediment. This is particularly true of the compounds between retention times 46.99 and 68.40. These compounds are present at a greater apparent concentration in the spiked sediment sample; however, examination of reduced chromatographic data output shows that this primarily reflects a smaller final sample extract volume resulting in more material being loaded on the fused silica capillary column.

Figure 5 presents the capillary chromatograms obtained on the time zero sediment samples spiked with artificially weathered crude oil. The chromatograms are qualitatively very similar to those shown in Figure 3 which presented the weathered Cook Inlet crude used to spike the sediment samples. Aliphatics are virtually absent below nC_{13} as are aromatic compounds with KOVAT indices below 1300. A number of higher molecular weight polynuclear aromatic compounds can be identified in the weathered crude, and these are 2-methylnaphthalene at 29.38, 1-methylnapthalene at 30.11, 2,6-dimethylnapthalene at 33.88, fluorene at 40.61, phenanthrene at 47.41, 1-methylphenanthrene at 51.85 and fluoranthene at 55.45. There appear to be no polynuclear aromatic hydrocarbons with molecular weights greater than chrysene in the time zero artifically weathered sediment sample.

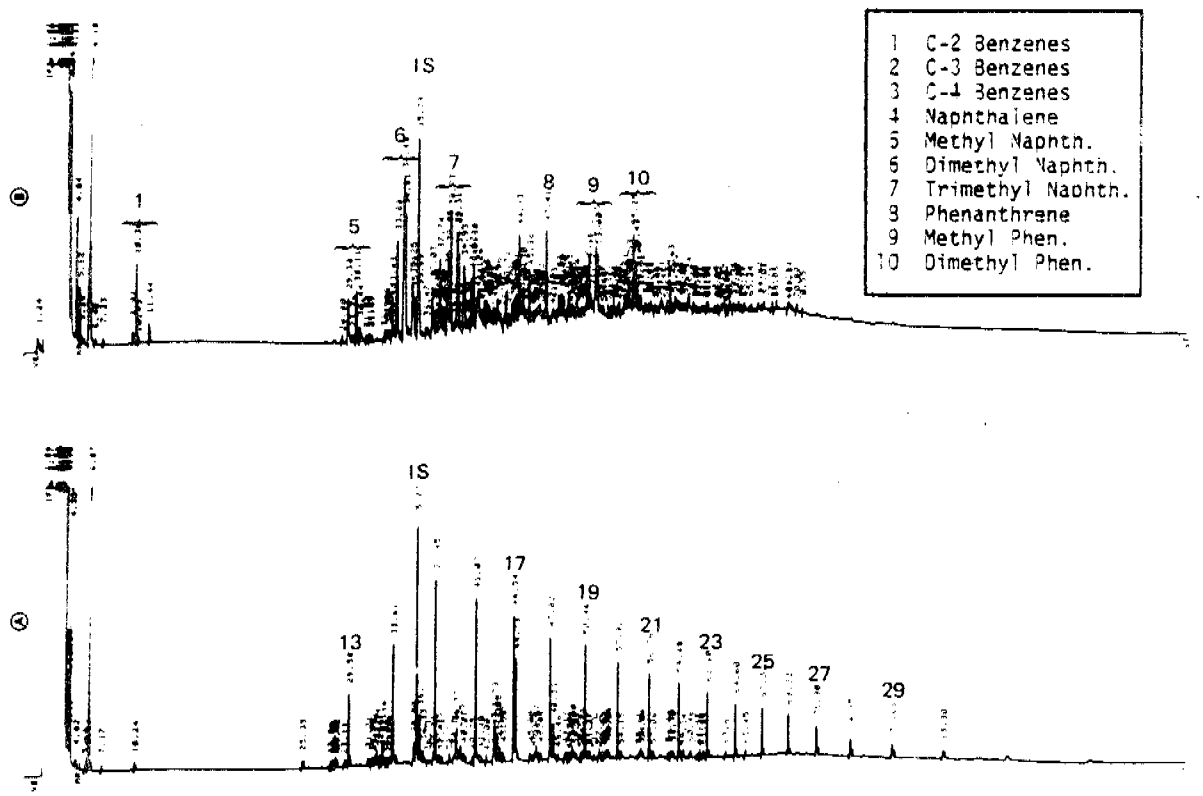

Figure 5. Flame Ionization Detector capillary gas chromatograms of: A, the aliphatic fraction and B, the aromatic fraction extracts obtained from time zero Kasitsna Bay sediment samples spiked with Artifically Weathered Cook Inlet Crude Oil at 50 ppt.

Time One Year Samples

Each sediment sample was spiked and placed in a sediment tray; the sediment samples were deployed at various depths in Kasitsna Bay and Sadie Cove. After one year of exposure the trays were retrieved and subsamples of the sediments were collected. Figure 6 shows the chromatograms obtained on the aliphatic fraction of A, the 50 ppt fresh crude oil spiked into the sediment at time zero, and B, C, and D, the triplicate samples examined after one year of natural weathering. Several features are significant in this figure. The first and most obvious feature is the lack of any appreciable weathering of the oil at this high level of concentration. This is reflected in the qualitative appearance of the chromatograms and in the data presented in Table 1. Specifically, the lower molecular weight n-alkanes from nC_8 through nC_{12}, and the branched and cyclic compounds occurring between KOVAT index 900 and 1000 appear to be nearly identical in all four samples.

Figure 7 graphically presents the concentration abundance of the n-alkanes in the 50 ppt spiked sediment sample at time zero and again after one year of weathering in Kasitsna Bay. Note that in addition to the concentrations of the time zero and one year samples being very similar, the overall trends showing decreases in the higher molecular weight compounds are nearly identical for both samples, illustrating the lack of any appreciable selective weathering.

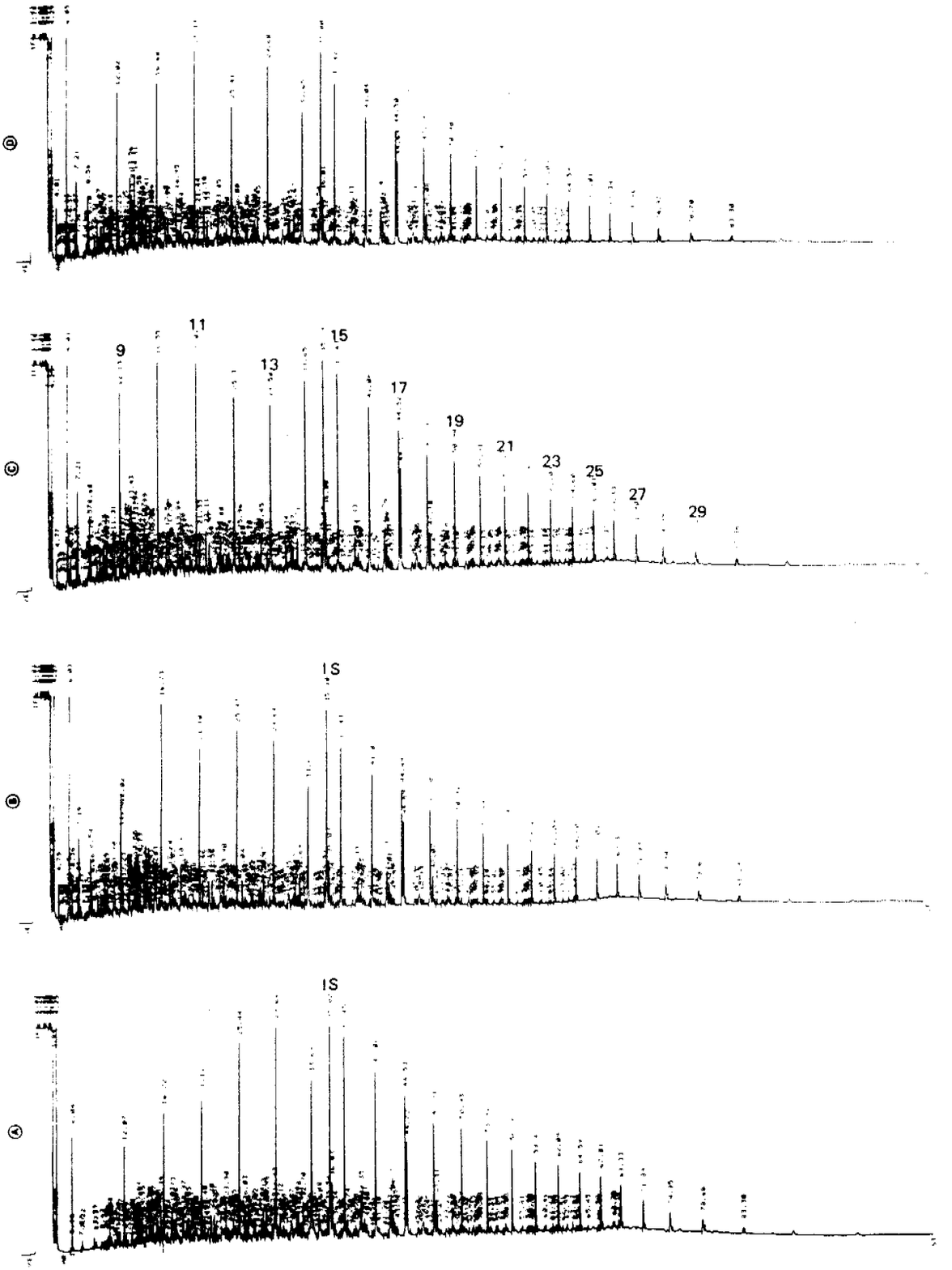

Figure 6. Flame Ionization Detector capillary gas chromatograms of: A, the aliphatic fraction of the 50 ppt fresh Cook Inlet Crude Oil spiked into the sediment at time zero, and B, C, and D, the aliphatic fractions of the triplicate samples examined after one year of natural weathering in Kasitsna Bay.

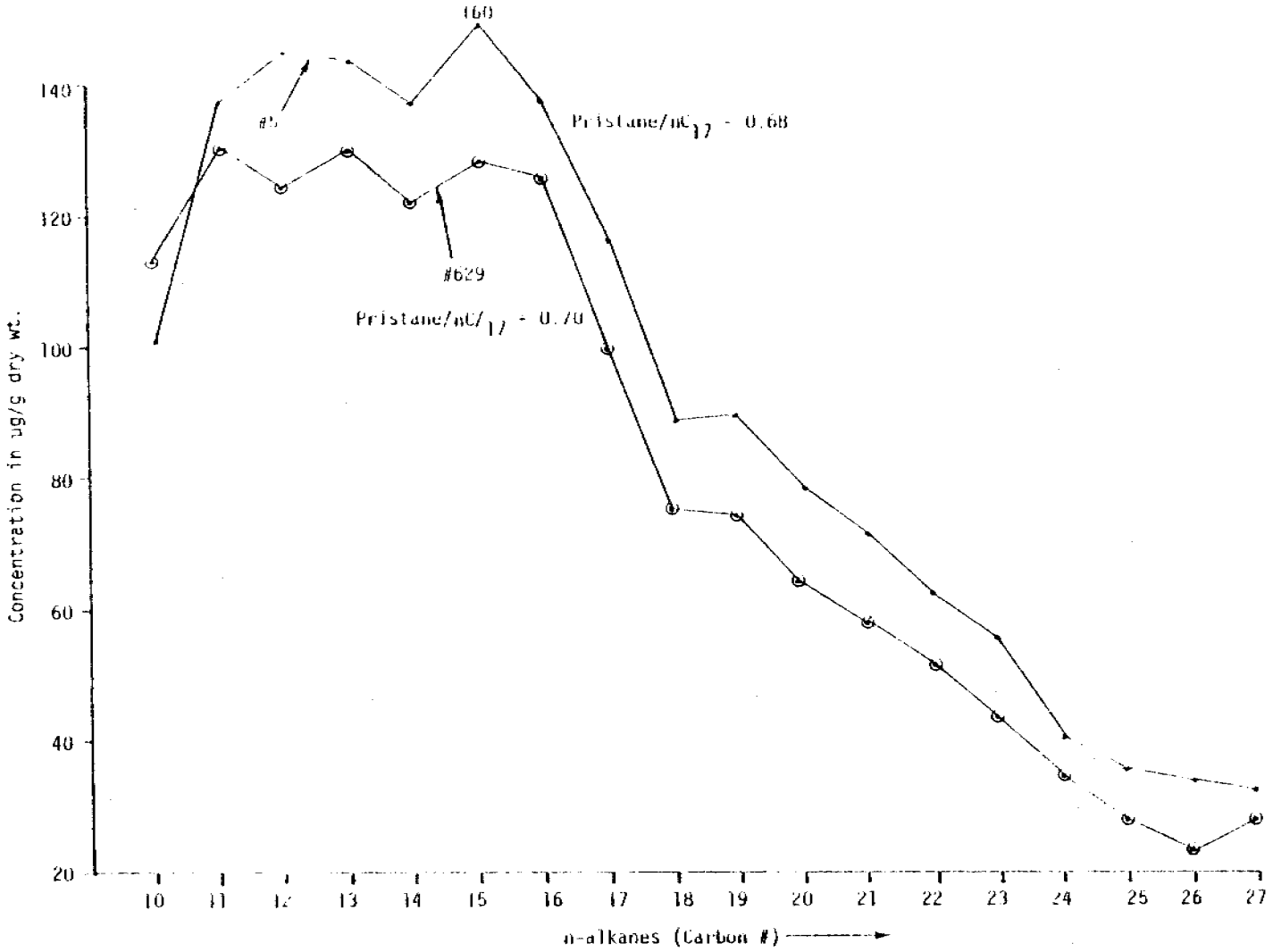

Figure 7. Concentration abundance of the n-alkanes in a sediment sample spiked with 50 parts per thousand fresh crude illustrating the time zero sample (·) and sample after one year of weathering (⊙).

The similarity of the pristane/nC_{17} and phytane/nC_{18} ratios, as observed qualitatively in Figure 6 and Table 1, also illustrates the lack of any appreciable biotic or abiotic weathering in these samples. The chromatographic profiles are essentially superimposable, reflecting the homogeniety of the initial spiked sediment, the replicability of the weathering process in the field and the precision of the analytical method. Individual values for these three fractions are presented in Table 1, and the agreement of such features as the total n-alkanes, sum of odd n-alkanes, even n-alkanes, pristane/phytane ratios, etc., is evident of consideration.

Figure 8 presents the gas chromatograms of the aromatic fractions obtained on the 50 ppt fresh Cook Inlet-spiked sediment at time zero (A) and the replicate fractions (B, C and D) obtained from analysis of the triplicate sediment samples after one year of natural weathering. As in Figure 6, there does not appear to be any selective weathering of the individual components present; however, examination of the reduced data in Table 2 and Figure 9 shows that some decreases in aromatic hydrocarbon concentrations did occur after 1 year. The apparent lower levels of material in chromatogram A (Figure 8) only reflect a larger final sample extract volume from which an aliquot was removed for analysis by GC. Figure 9A presents a graphical representation of the concentrations of eight selected aromatic compounds in the fresh 50 ppt

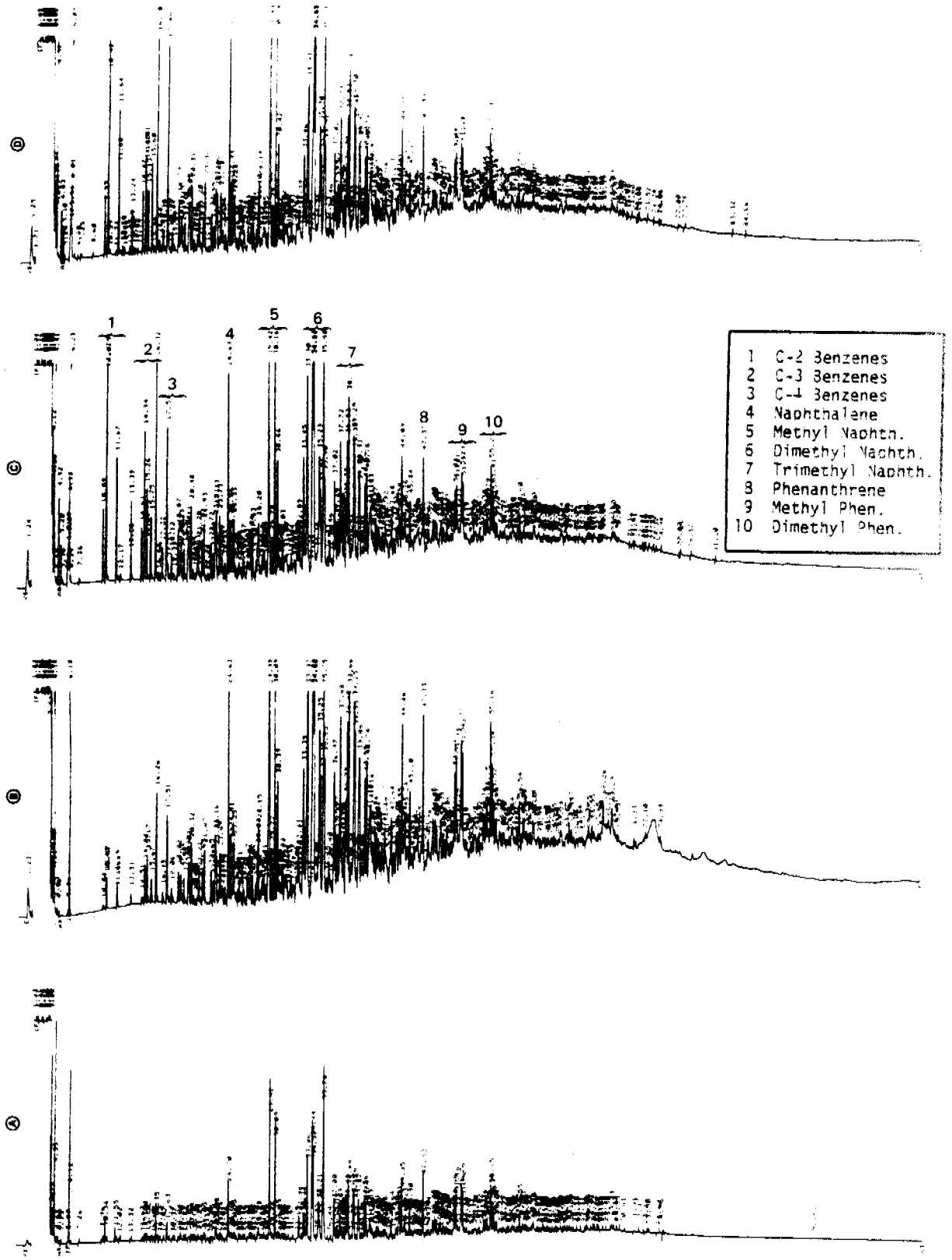

Figure 8. Flame Ionization Detector gas chromatograms of: A, the aromatic fraction of the 50 ppt fresh Cook Inlet Crude Oil spiked into the sediment at time zero and B, C, and D, the aromatic fractions of the triplicate samples examined after one year of natural weathering in Kasitsna Bay.

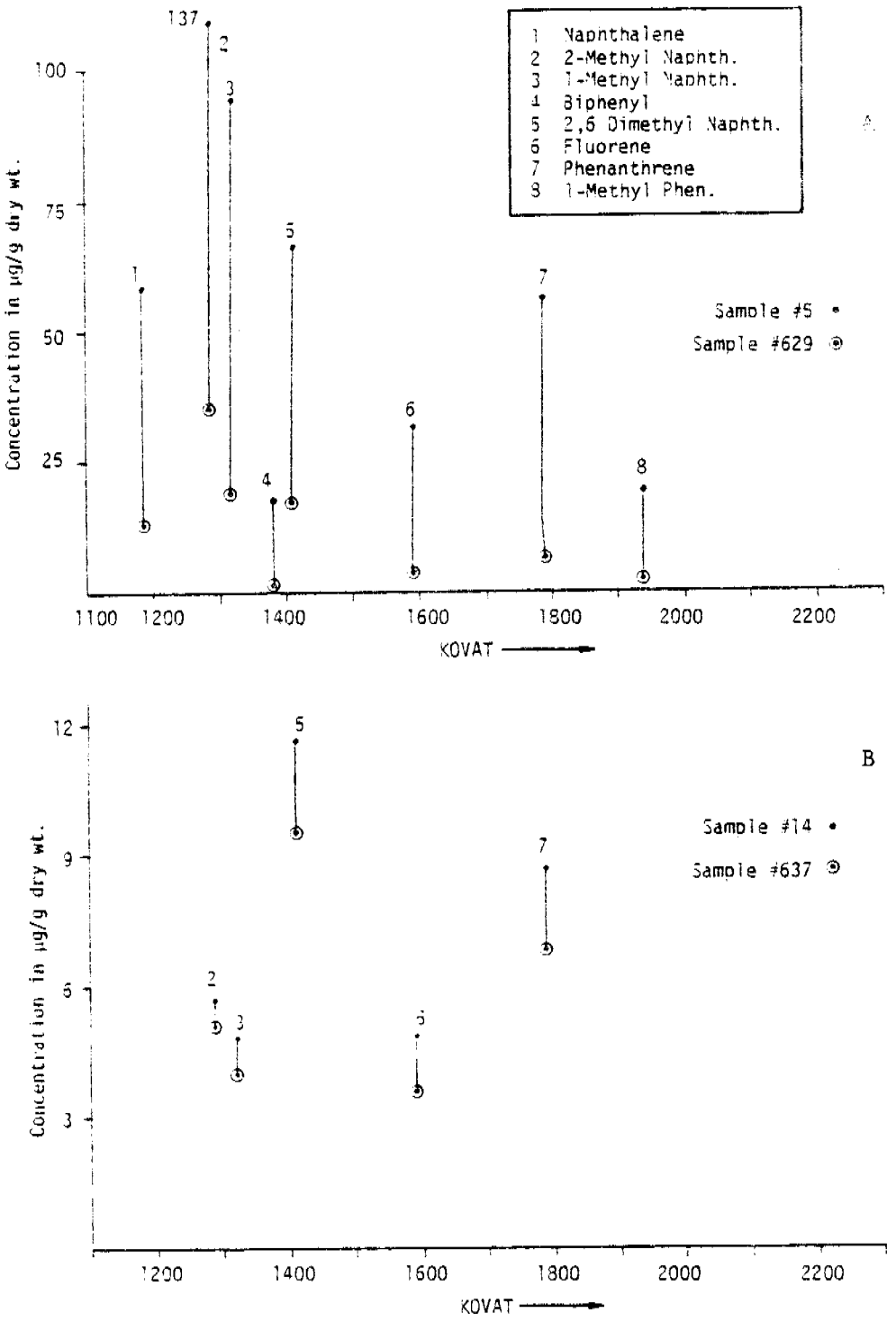

Figure 9. Concentration abundance of selected aromatic hydrocarbons from a 50 parts per thousand spike of fresh crude (Top) showing the time zero sample (•) and sample after one year of weathering (⊙), and bottom, a 50 ppt spike of artifically weathered crude at time zero (•) and after one year of weathering (⊙).

spiked sediments at time zero and time one year. While time zero levels of individual aromatic compounds ranged from 50 to 137 micrograms per gram dry weight (for napthalene through 2,6-dimethylnapthalene), after one year these compounds were present at concentrations ranging from 15 to 40 micrograms per gram dry weight. The decreases in aromatic compounds from Kovat indices 1100 to 1500 were greater than the decreases in aromatics with Kovat indices ranging from 1500 to 2000. This presumably reflects two things: 1) the greater volatility and water solubility of the lower molecular weight aromatic compounds, and 2) the lower relative abundance of the higher molecular weight aromatics in the crude oil to begin with.

Figure 9B shows the relative losses of aromatic hydrocarbons in the artifically weathered crude oil spiked into the Kasitsna Bay sediments at time zero and time one year. This figure illustrates that much smaller relative changes occurred over the one year period after the oil was spiked into the sediment. That is, the starting concentrations of aromatic compounds such as 2-methylnaphthalene through phenanthrene ranged between only 6 and 12 micrograms per gram dry weight of sediment when artifically weathered crude was used to spike the sample at time zero. These levels were not significantly reduced after one year of weathering in the sediments of Kasitsna Bay: the most significant weathering occurred while the oil was "artifically weathered" on the surface of a

salt water aquarium before the oil was spiked into the sediment. Nevertheless, once these compounds are introduced into the sediments, they are not as rapidly removed as they would be from simple dissolution in the starting oil itself.

Figure 10 presents the gas chromatograms of the aliphatic and aromatic fractions obtained on the 1 ppt fresh-crude oil spiked sediment after one year of weathering in Kasitsna Bay. In comparison with Figure 4 which shows the starting 1.0 ppm spiked material, it is clear that significant weathering of the sample has occurred. This is reflected first in the significantly greater relative loss of the lower molecular weight alkanes below nC_{13}, presumably due to a combination of biological and abiotic (dissolution) processes. Evidence of biochemical degradation is shown in examining the pristane/nC_{17} and phytane/nC_{18} levels in the aliphatic fraction in Figure 10 compared to the aliphatic fraction in Figure 4, and by examining the numerical values for these ratios in Table 1. Clearly the straight chain alkanes have been preferentially removed relative to the branched chain isoprenoids. The overall levels of other aliphatic hydrocarbons are also significantly reduced as illustrated qualitatively in Figure 10 and by the data in Table 1. Figure 11 graphically presents the concentration abundance of n-alkanes in the 1.0 ppt fresh crude oil sediment spike at time zero and after one year of natural weathering. Clearly all of the lower molecular weight alkanes below nC_{18} are reduced by a factor of from 2 to 5 and the higher molecular weight n-alkanes are reduced by at least a factor of 2 compared to the sample taken at time zero. For the 1 ppt sample the total

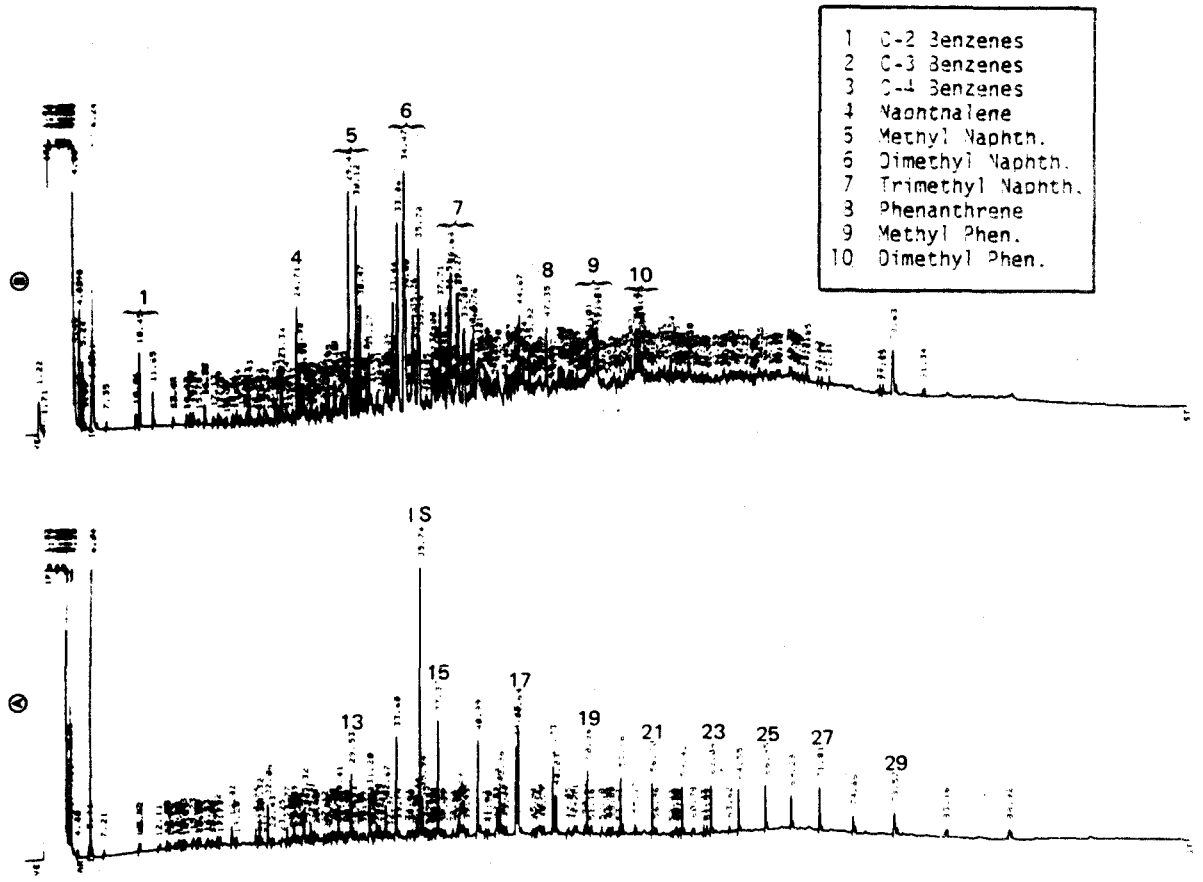

Figure 10. Flame Ionization Detector gas chromatograms of: A, the aliphatic fraction and B, the aromatic fraction extracts obtained from 1 ppt fresh Cook Inlet Crude Oil spiked sediments after one year of weathering in Kasitsna Bay.

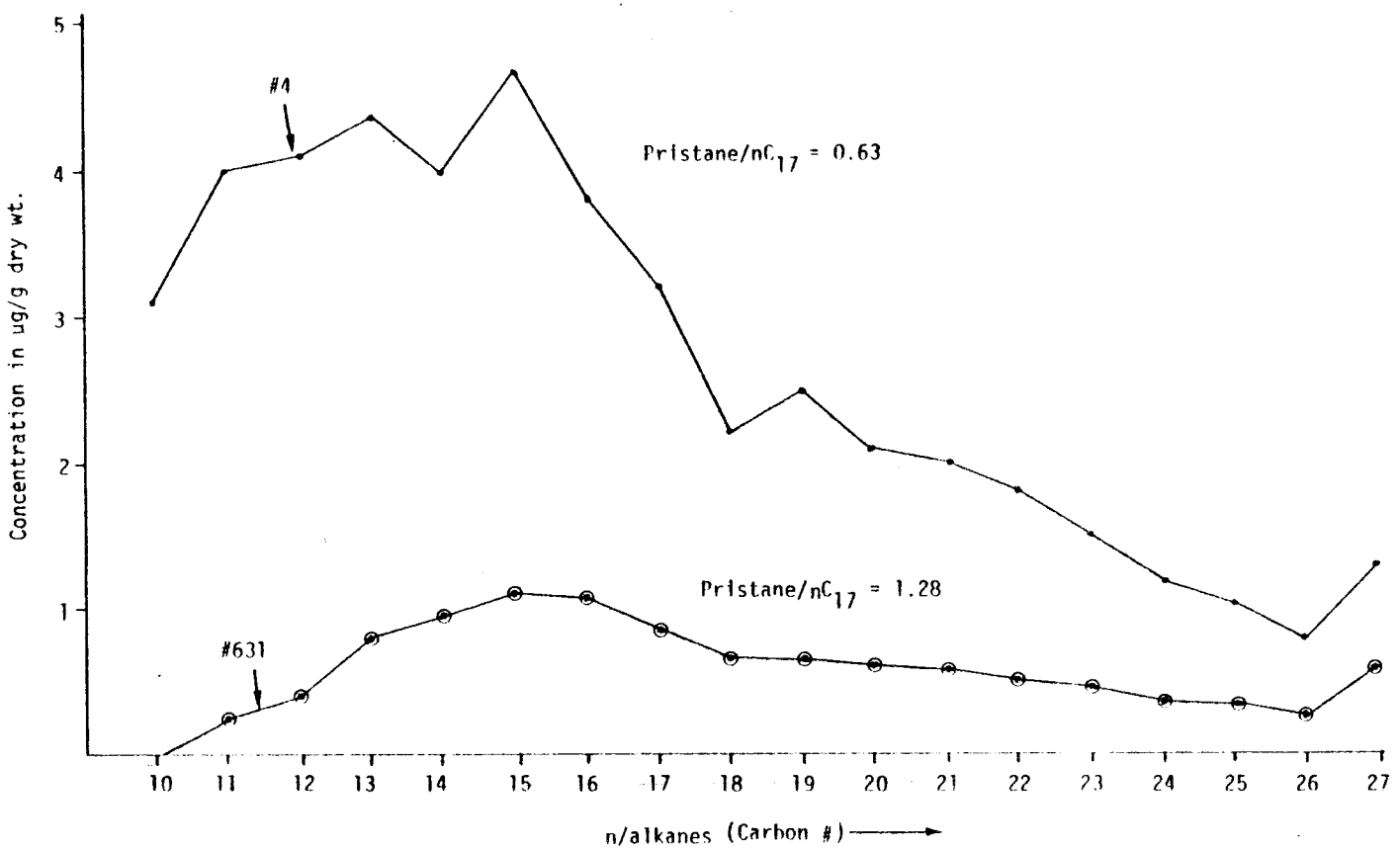

Figure 11. Concentration abundance of the n-alkanes for a sediment oil spike of 1.0 part per thousand fresh crude illustrating the time zero sample (•) and sample after one year of weathering (⊙).

resolved hydrocarbons decreased from 83 to 21 μg/g dry weight during the year of exposure and the unresolved complex mixture decreased from 154 to 98 μg/g dry weight.

The aromatic fraction data in Figure 10B show somewhat less degradation compared to the aliphatic fraction. Compounds with molecular weights less than naphthalene (KOVAT < 1185) are obviously removed due to a combination of biological and abiotic factors (dissolution and evaporation); however, compounds with molecular weights greater than 1-methylnapthalene (KOVAT > 1315) appear to be present in relatively identical concentrations compared to the starting materials. That is, while overall levels are slightly reduced as illustrated by the data in Table 2, the relative concentrations of the individual polynuclear aromatics are very similar in the time zero and time one year samples. This is also reflected quite obviously by the qualitative appearance of the aromatic fractions shown in Figures 4B and 10B, respectively, and by the data presented in Figure 12A. Figure 12A graphically presents the relative concentration abundance of selected aromatic hydrocarbons from the 1 ppt spike of fresh crude oil at time zero and after one year. Clearly while the relative range of concentrations of all of the compounds in the time zero and one year samples are lower compared to the 50 ppt sample shown in Figure 9A, the overall concentrations of the time zero and naturally weathered 1 ppt samples are still relatively similar. This is particularly true of the higher molecular weight compounds, bi-phenyl, fluorene, phenanthrene and

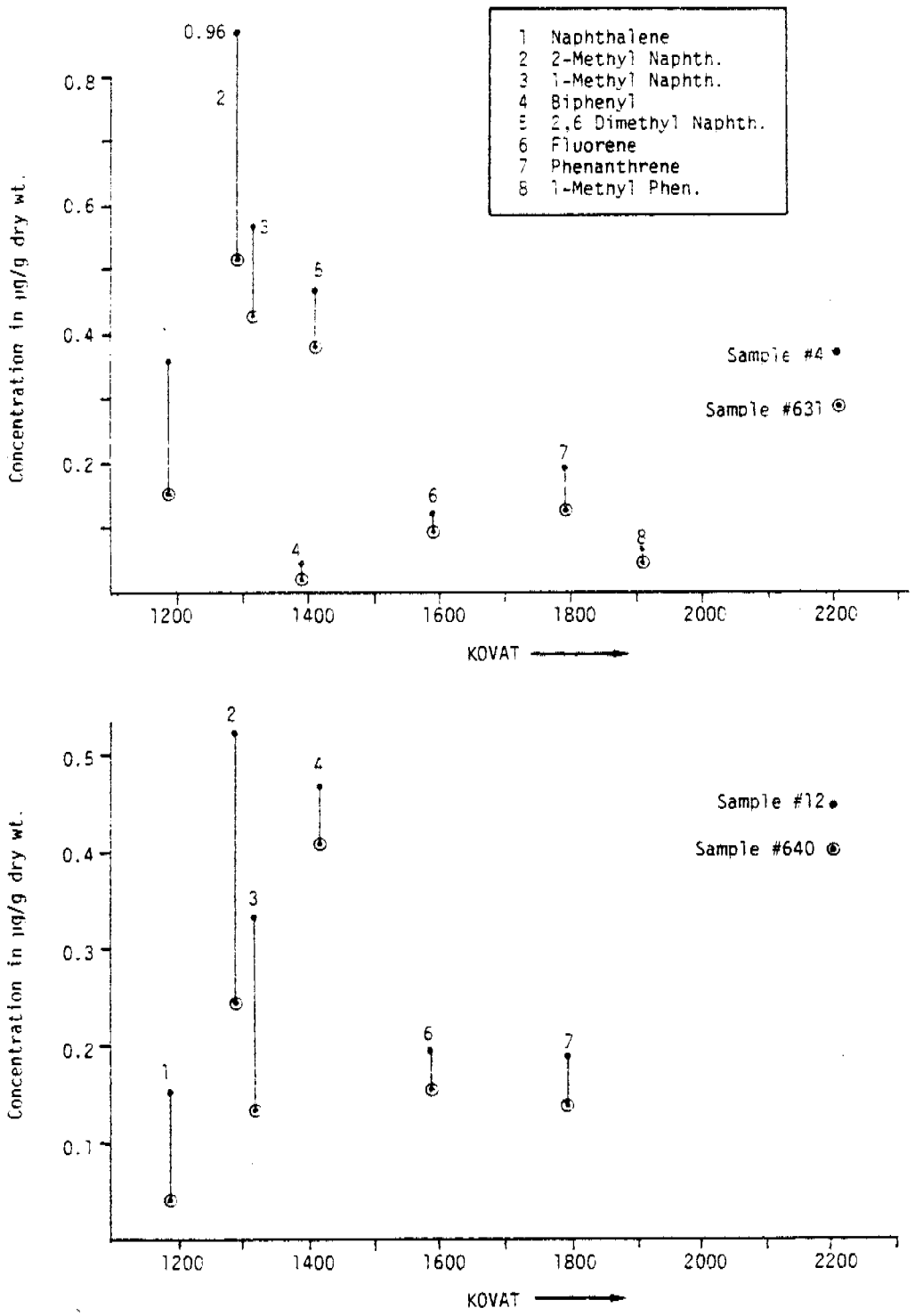

Figure 12. Concentration abundance of selected aromatic hydrocarbons from a 1.0 part per thousand spike of fresh crude (Top) showing the time zero sample (•) and sample after one year of weathering (⊙). Bottom shows a 1.0 ppt spike of artifically weathered crude for the time zero sample (•) and sample after one year of weathering (⊙).

1-methylphenanthrene. As in Figure 9A and B, the relative concentrations of artifically weathered aromatic compounds from the 1.0 ppt sample shown in 12B show that concentrations are in the same range in the artifically weathered sample as in the fresh sample after it had been weathered for a full year.

Clearly, while biological degradation of the aliphatic hydrocarbons (primarily n-alkane) occurred at the 1 ppt level, concommitant degradation of the higher molecular weight polynuclear aromatics compounds with molecular weights above that of methylnapthalene did not occur at a significant level.

This lack of degradation of higher molecular weight PNA's at the 1.0 ppt level is also illustrated in Figure 13, which presents the aromatic fraction chromatograms of: A) the 1 part per thousand fresh crude spiked into the sediment at time zero; B) the aromatic fraction obtained from the 1 ppt sediment after one year of in situ weathering in Kasitsna Bay; and C) the aromatic fraction of the 1 ppt sediment spiked with artificially weathered crude oil after one year of additional weathering in Kasitsna Bay. Clearly, examination of chromatograms 13A and B shows that some loss of the lower molecular weight alkyl substituted benzenes at retention times 10.45, 11.68, 15.15, 15.90, 16.49 and 17.71 has occurred due to either evaporation or dissolution. Compounds with molecular weights greater than that of 1-methylnapthalene at retention time 29.41 (B) are present in nearly identical relative concentrations. The chromatogram in 13C shows that the same compounds were also

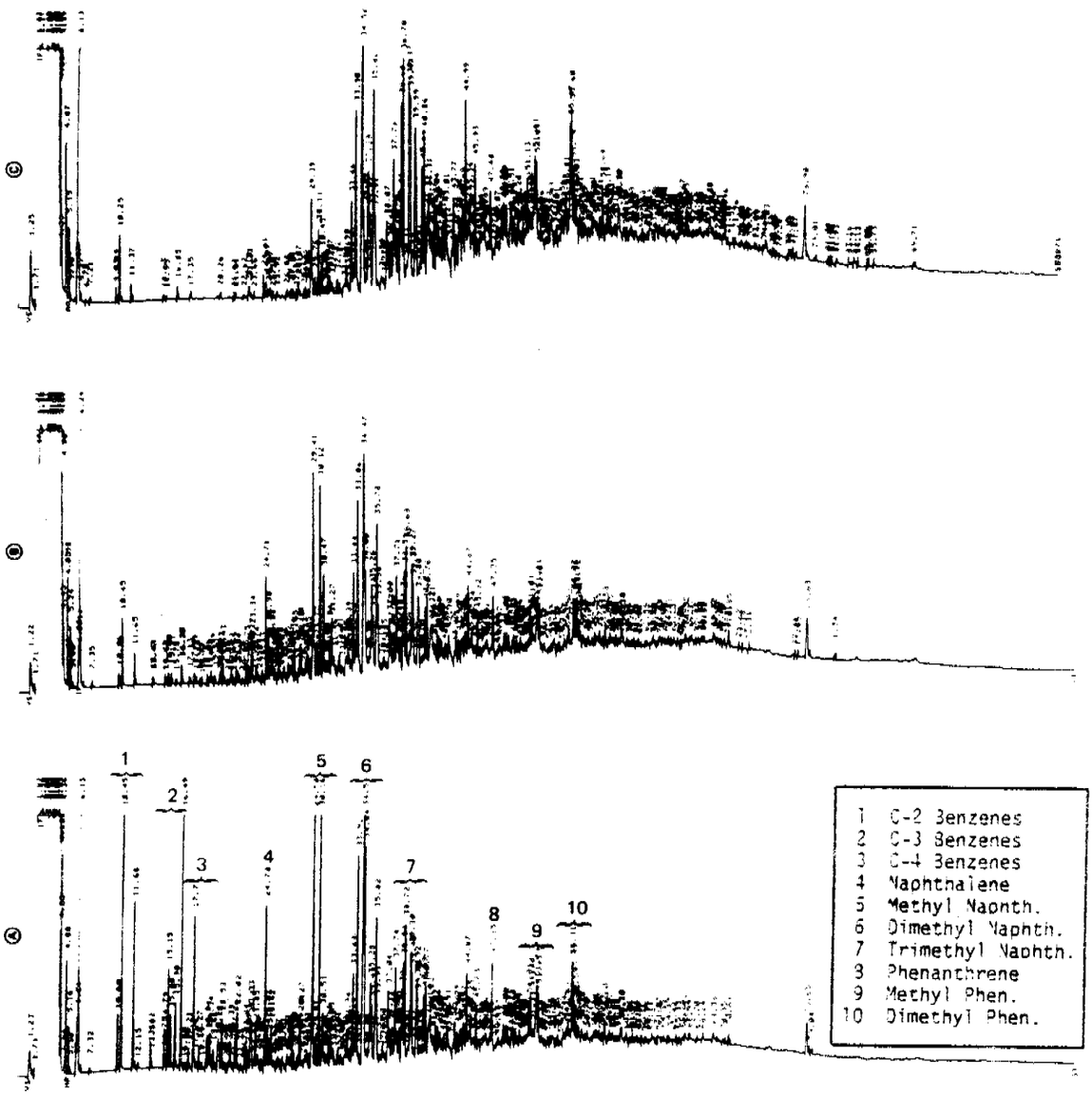

Figure 13. Flame Ionization Detector gas chromatograms of extracts of the aromatic fractions obtained from: A, the sediment spiked with 1 ppt fresh crude oil at time zero; B, the 1 ppt fresh crude sample after one year of natural weathering in Kasitsna Bay and C, the 1 ppt sediment sample spiked with artifically weathered crude oil after one year of additional weathering in Kasitsna Bay.

present in the "artificially weathered" oil which was spiked into the sediment after an additional year of natural weathering. This suggests that although many lower molecular weight aromatic compounds are removed from natural weathering of spilled oil while the oil is still at the surface, once the less water soluble and volatile higher molecular weight PNA's are incorporated into the sediment, additional degradative processes are extremely slow. Thus, while the relatively non-toxic aliphatic hydrocarbons are significantly degraded by biological processes in the sediments at 1 ppt, the more toxic aromatic compounds appear to be longer lived when introduced to the sediment from either fresh or weathered crude oil at similar levels.

Figure 14 presents the aliphatic, aromatic and polar fraction chromatograms obtained on the 0.1 ppt fresh crude oil spiked into the sediment at time zero (a) and after one year of weathering in the sediments of Kasitsna Bay (b, aliphatic fraction; c, aromatic fraction; d, polar fraction). Clearly, almost all of the n-alkanes in the starting oil are no longer present in the sediment after one year of weathering. In fact, the only compounds of any significance in the aliphatic fraction of the fully weathered sediment are higher molecular weight odd n-alkanes, nC_{23}, nC_{25}, nC_{27}, and nC_{29}. These same compounds are also predominant in the fresh crude sample shown in Figure 14A. That is, instead of seeing a regular decrease in higher molecular weight n-alkanes from nC_{22} through nC_{32}, the odd carbons at 23, 25 and 27 from biogenic input are clearly present. These are the only compounds which

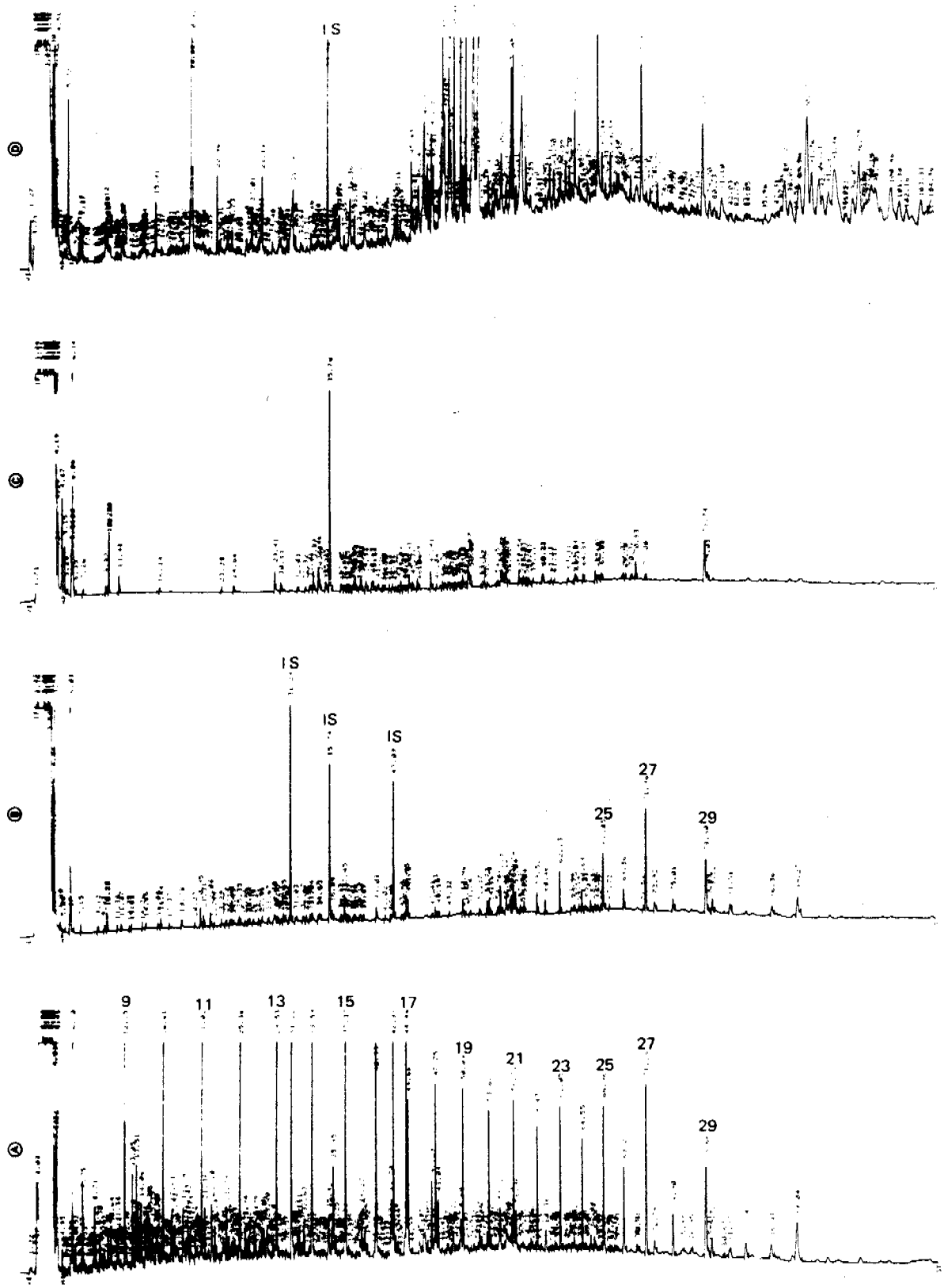

Figure 14. Flame Ionization Detector capillary gas chromatograms of: A, the aliphatic fraction of the sediment spiked with 0.1 ppt Fresh Crude Oil at time zero and B, the aliphatic fraction, C, the aromatic fraction, and D, the polar fraction extracts obtained on the 0.1 ppt Fresh Crude Oil spiked sample after one year of Natural Weathering in Kasitsna Bay.

remain in the sediment after one year, although there is some evidence that several unsaturated compounds between KOVAT indices 1900 and 2200 are present in Figure 14B. The aromatic fraction 14C shows only extremely low levels of residual materials with some evidence of pyrene perhaps remaining in the sediment at retention time 78.70. This compound was not detected in the starting crude oil to an appreciable degree, however, so its presence may reflect input from some other source. GC/MS characterization of the compounds in the polar fraction, 14D, is being completed at this time.

Figure 15 shows the chromatograms of the aliphatic and aromatic fractions of the 50 ppt artificially weathered crude oil spiked into the sediment after one year of additional degradation in the sediment plots in Kasitsna Bay. Comparison of the sediments spiked with the weathered crude oil at time zero, as shown in Figure 5, shows little or no change in the oil composition after one year of additional weathering. This is perhaps better illustrated in Figure 16, which presents the concentration abundance of the n-alkanes in the sediment spike at 50 ppt of the artifically weathered crude oil in the time zero sample and after one year of additional natural weathering. The data illustrate that all compounds below the level of nC_{14} are drastically reduced in both the starting material and the residual oil isolated after one year of natural weathering; however, the higher molecular weight compounds are not significantly altered. The corresponding data for the aromatic fraction of the 50 ppt spike of artifically weathered crude are shown in Figure 9B. These

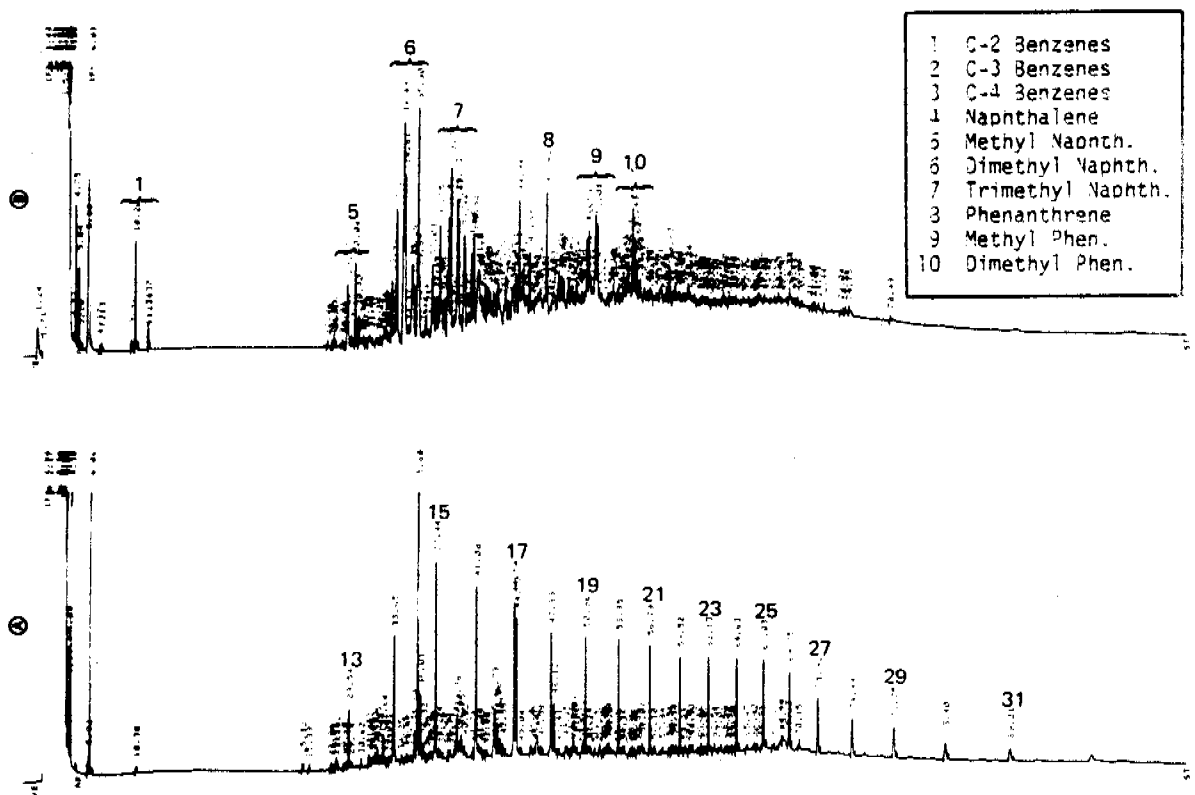

Figure 15. Flame Ionization Detector capillary gas chromatograms of: A, the aliphatic fraction and B, the Aromatic fraction extracts obtained from the time one year Kasitsna Bay sample spiked with Artifically Weathered Cook Inlet Crude Oil at 50 ppt.

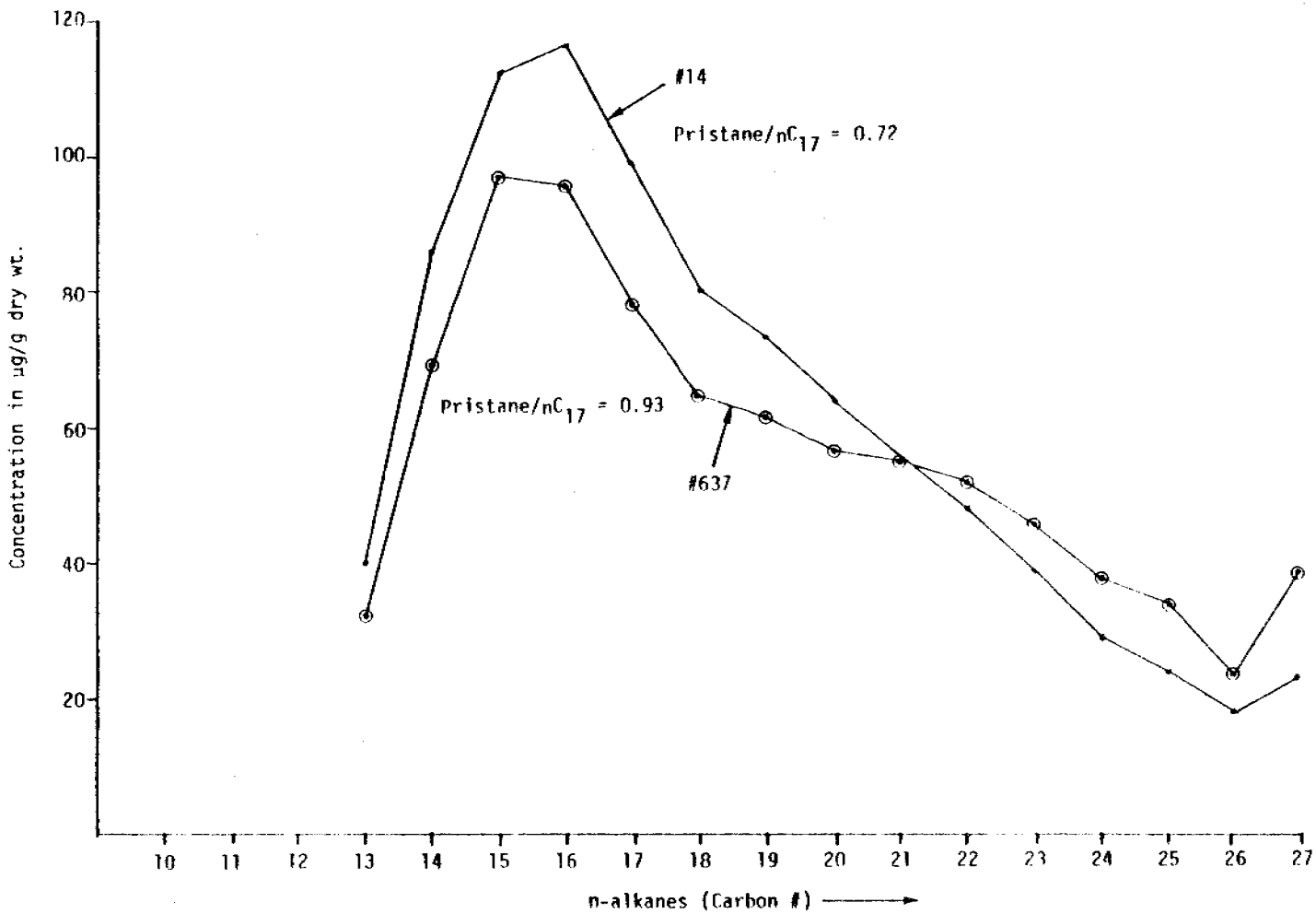

Figure 16. Concentration abundance of the n-alkanes for a sediment oil spike of 50 parts per thousand artifically weathered crude illustrating the time zero sample (•) and sample after one year of weathering (⊙).

show that while the overall concentrations of the lower molecular weight mono and di-cyclic aromatic compounds were reduced in the weathered crude oil compared to the fresh crude oil, once the artifically weathered oil reached the sediment, further degradation and loss of the aromatic compounds did not occur.

When 1.0 ppt weathered crude oil was spiked into the sediments, much greater degradation and loss of the lower molecular weight n-alkanes occurred as illustrated by the data in Figure 17. In Figure 17 the loss of lower molecular weight aliphatic compounds can clearly be observed in the artifically weathered oil as it was spiked into the sediments. The sample collected after one year of weathering at Kasistna Bay contained essentially no aliphatic hydrocarbons below nC_{24}. This was very similar to the case when 1.0 ppt fresh crude oil was spiked into the sediments and similar decreases in the aliphatic fraction were observed. The data in Figure 12B, however, show that the relative concentrations of aromatics in the 1.0 ppt weathered crude did not decrease significantly over the year period after the oil was introduced into the sediment. Quite clearly from these results, after fresh or weathered oil is incorporated into the sub-Arctic sedimentary regime at concentrations greater than 1.0 ppt, only limited additional degradation of the aromatic fraction occurs, at least in periods up to one year.

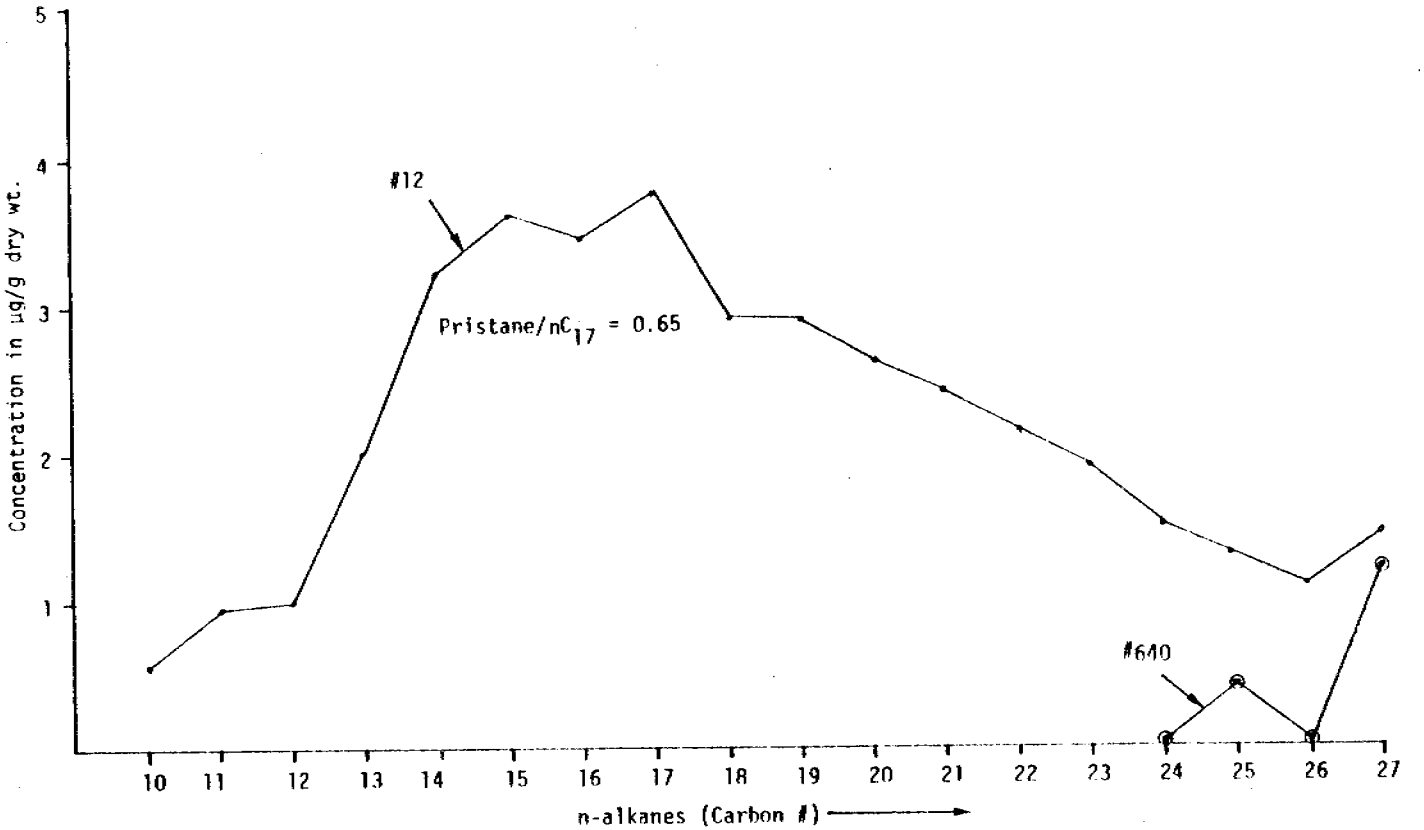

Figure 17. Concentration abundance of the n-alkanes for a sediment oil spike of 1.0 parts per thousand artifically weathered crude illustrating the time zero sample (•) and sample after one year of weathering (⊙).

Sadie Cove Oil/Nutrient Spiked Experiments

Figure 18 presents the aliphatic fraction chromatograms obtained on a) the 50 ppt oil plus starch b) 50 ppt oil alone and c) 50 ppt oil plus Chiton samples from Sadie Cove. The three chromatograms are essentially identical showing that little or no degradation of the oil occurred at the 50 ppt level. This is also reflected quantitatively by comparing the numbers in Table 1 for samples No.s 782, 779 and 780. These data suggest that the total reoslved hydrocarbons and unresolved complex mixtures are essentially identical in the three samples. Other similarities include the odd/even hydrocarbon ratios, the ratio of the sum of pristane plus phytane to the total n-alkanes, and the pristane/nC_{17} and phytane/nC_{18} ratios. Essentially, these data suggest that at the 50 ppt level degradation is not nutrient limited. Figure 19 presents the aromatic fraction chromatograms obtained on the same three Sadie Cove sediment samples: a) oil plus starch, b) oil alone and c) oil plus Chiton. As the data in Table 2 illustrate, the aromatic compounds which were identified appear to be essentially the same in all three samples, although there may be some decrease in the levels of aromatic compounds in the oil and starch sample (a). Replicate analyses would be required to determine if the subtle difference in overall aromatic compound levels is statistically significant. Alternatively, it may be prudent to examine 1.0 ppt oil spikes in the presence and absence of nutrients to determine if enhanced aromatic hydrocarbon degradation can be induced to lower overall hydrocarbon levels where the inherent toxicity may be reduced.

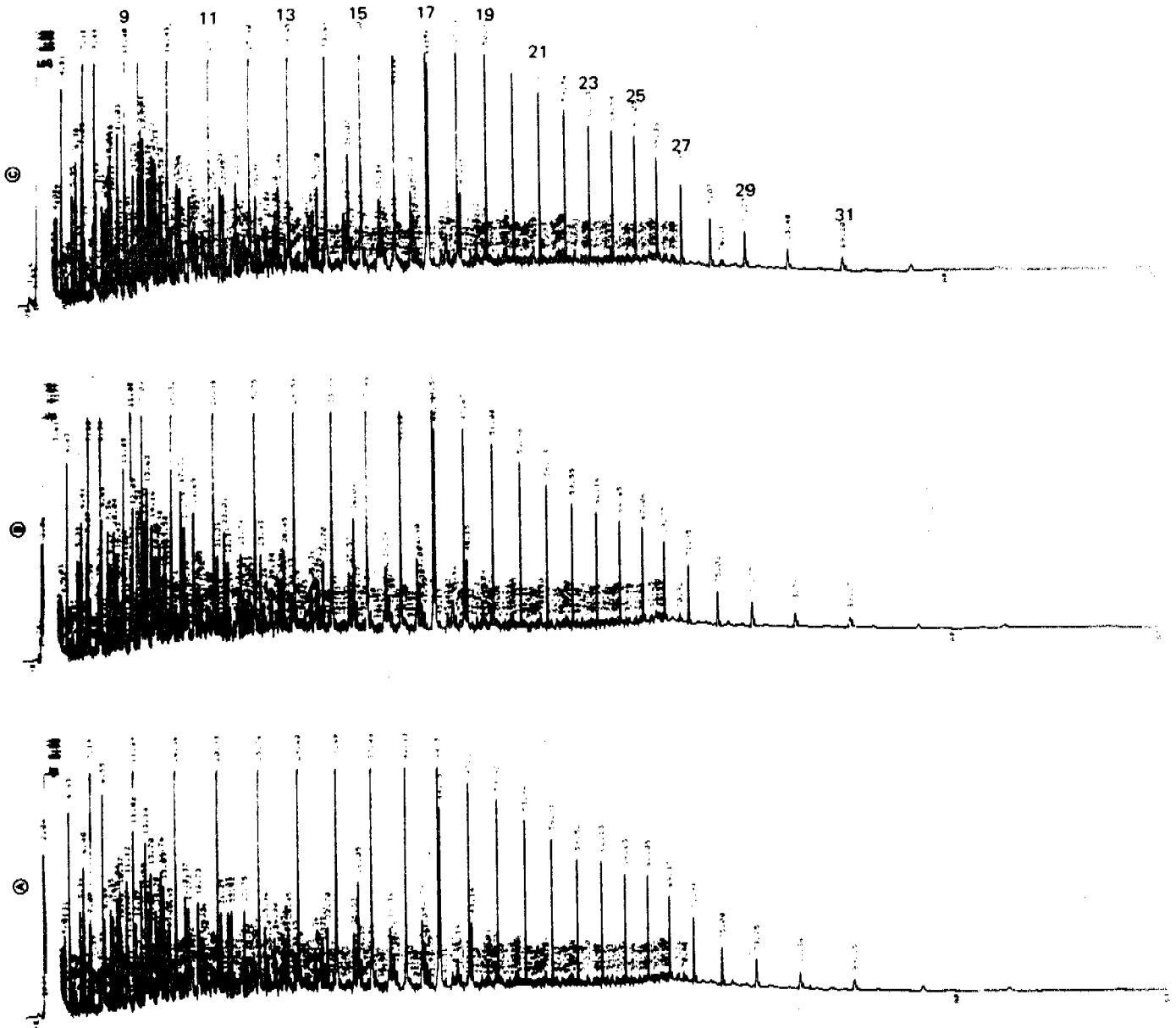

Figure 18. Flame Ionization Detector capillary gas chromatograms of aliphatic fraction extracts obtained on: A, 50 ppt fresh Oil plus starch, B, 50 ppt fresh Oil alone, and C, 50 ppt fresh Oil plus Chitin after one year of natural weathering in the sediments of Sadie Cove.

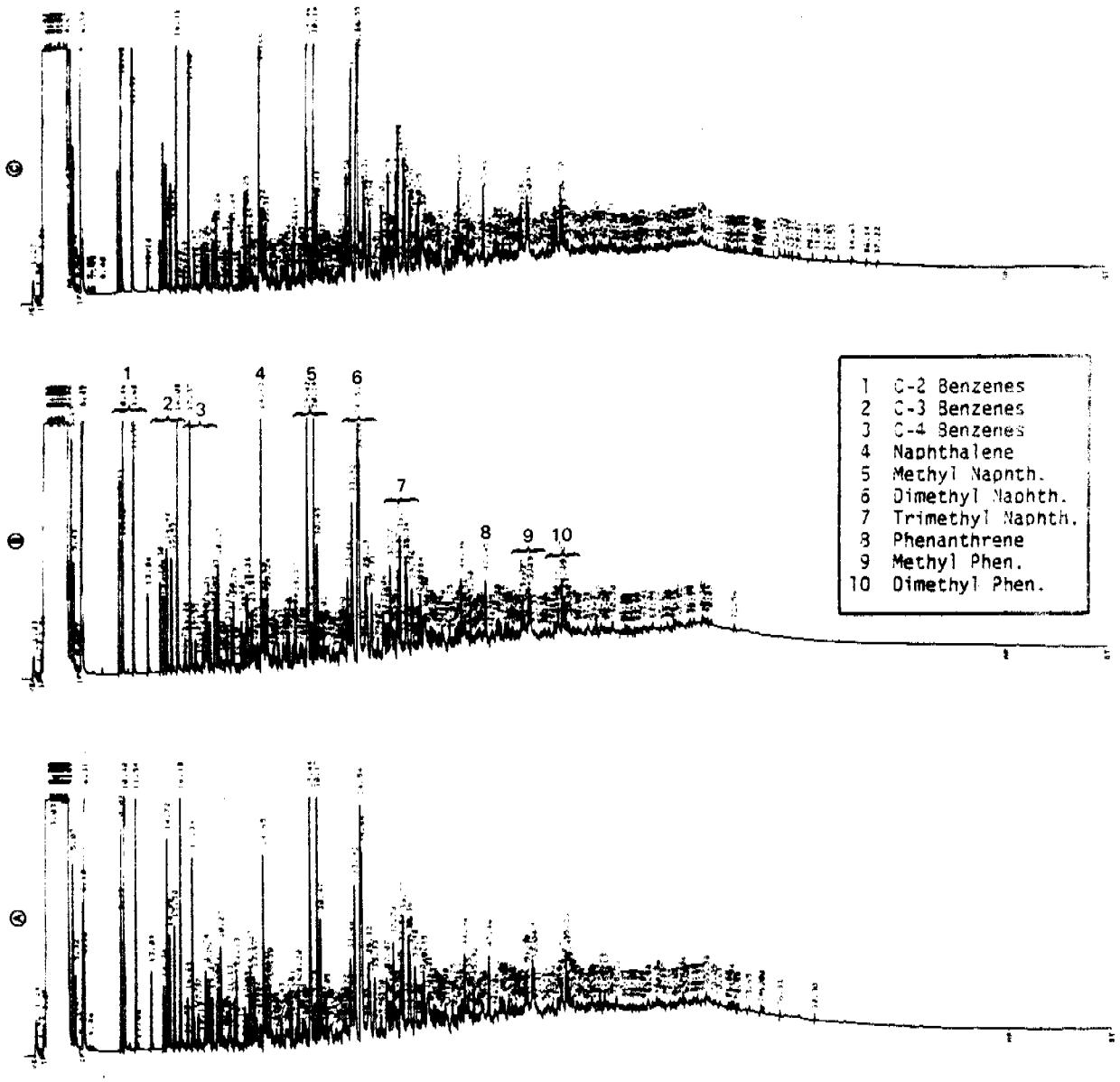

Figure 19. Flame Ionization Detector capillary gas chromatograms of aromatic fraction extracts obtained on: A, 50 ppt fresh Oil plus starch, B, 50 ppt Oil alone, and C, 50 ppt fresh Oil plus Chitin after one year of natural weathering in the sediments of Sadie Cove.

SUMMARY

The results presented here support the conclusion that in a major oil spill event in the sub-Arctic marine environment, the most significant weathering of the oil will occur at the air/sea interface or in the water column before the oil is incorporated into the sedimentary regime. This is particularly true in fine-grain sediment matrices in low-energy environments. Once levels of fresh and weathered Cook Inlet Crude oil reached concentrations in excess of 1 ppt in the sediment plots examined in the study, very little additional weathering or loss of higher molecular weight aromatic hydrocarbons occurred. At spiked levels of 50 ppt with both fresh and weathered crude oil, nearly complete inhibition of microbiological utilization or selective removal of aliphatic hydrocarbons was also observed, especially for those sediments spiked with fresh crude. Recovery of biological activity and selective utilization of aliphatic hydrocarbons did occur in the samples spiked with fresh and weathered crude at 1 ppt, and in the 0.1 ppt spiked samples, there was little or no evidence of either aliphatic or aromatic petroleum hydrocarbon contamination after one year. At that time, the 0.1 ppt spiked samples appeared to contain only the same biogenic hydrocarbons observed in the non-spiked control sediment samples from Kasitsna Bay.

In the study plots which were spiked with 50 ppt oil plus added nutrients (starch and Chitin), there was no evidence of any enhanced biotic recovery or selective hydrocarbon utilization with either fresh or weathered crude oil. This suggests inhibition of biological processes

from the high levels of toxic aromatic compounds in the oil itself rather than inhibition from limited nutrient concentrations. To more accurately address the role of added nutrients in oil degradation, detailed analyses should be completed on lower spiked oil concentrations in the presence and absence of nutrients. Also, experiments to assess the role of dissolved oxygen, grain-size, the energy (tidal and wave) input to the sedimentary environment, total organic carbon content and other factors such as total bio-mass, could be considered in future studies.

From the results obtained on the fresh and weathered crude oils and the sediment samples examined in this program, it appears that the maximum amount of weathering and removal (dissolution and evaporation) of toxic components can be achieved if spill clean up and treatment efforts are designed to prolong the time that the oil remains on the water surface or suspended in the water column. This may suggest limited use of dispersants or detergents in certain spill situations, particularly if damage to coastal zones is not imminent. Containment and recovery of the residual higher molecular weight materials should take precedence over other strategies such as chemical dispersal which may result in higher sub-tidal sediment loadings.

REFERENCES

American Institute of Biological Sciences, 1978. The Proceedings of the Conference on Assessment of Ecological Impacts of Oil Spills, Keystone, Colorado, 14-17 June 1980, 936 pgs.

Bassin, J.J., T. Ichiye. 1977. Flocculation behavior of suspended sediments and oil emulsions. Journal of Sedimentary Petrology 47(2): 671-677.

Brown, D.W., L.S. Ramos, M.Y. Uyeda, A.J. Friedman, and W.D. MacLeod, Jr. (1980): Ambient-temperature extraction of hydrocarbons from marine sediments--comparison with boiling-solvent extractions. In: Petroleum in the Marine Environment, L. Petrakis and F.T. Weiss (Eds.), Advances in Chemistry Series 185, American Chemical Society, Washington, DC, pp. 313-326.

D'Oxouville, L., M.O. Hayes, E.R. Gundlach, W.J. Sexton, and J. Michel. 1979. Occurrence of oil in offshore bottom sediments at the AMOCO CADIZ oil spill site, In: Proceedings of the 1979 Oil Spill Conference, March 19-22, Los Angeles, CA, p. 187-192.

Gearing, J.N., P.J. Gearing, T. Wade, J.G. Quinn, H. B. McCarty, J. Farrington and R.F. Lee. 1979. The rates of transport and fates of petroleum hydrocarbons in a controlled marine ecosystem and a note on analytical variability, p. 555-564. In: Proceedings of the 1979 Oil Spill Conference (Prevention, Behavior, Control, Cleanup) 19-22 March 1979, Los Angeles, Calif.

Jordon, R.E. and J.R. Payne, Fate and Weathering of Petroleum Spills in the Marine Environment: A Literature Review and Synopsis. Ann Arbor Science Publishers Inc., Ann Arbor, Michigan. 1980. 175 pp.

MacLeod, W.D., Jr. and J.R. Fisher, 1980. Intercalibration of Analytical Laboratories. Manuscript presented at the Researcher/Pierce IXTOC-1 Symposium, Miami, Florida, 9-11 June, 1980. 7 pp.

Mayo, D.W., D.S. Page, J. Cooley, E. Sorenson, F. Bradley, E.S. Gilfillan, F.A. Hanson. 1978. Weathering characteristics of petroleum hydrocarbons deposited in fine clay marine sediments, Searsport, Maine, Journal of Fisheries Research Board of Canada, 35(5):552-565.

Meyers, P.A. 1976. Sediments--sources of sinks for petroleum hydrocarbons? In: Sources, Effects and Sinks of Hydrocarbons in the Aquatic Environment; Proceedings of the Symposium, American University, Washington, D.C., 9-11 August, 1976 (American Institute of Biological Sciences 1977).

Meyers, P.A. and J.G. Quinn. 1973. Association of hydrocarbons and mineral particles in saline solutions. Nature 244:23-4.

National Academy of Sciences. 1975. Petroleum in the marine environment, Washington, D.C., 107 pp.

Parker, P.L. and S. Macko. 1978. An intensive study of the heavy hydrocarbons in the suspended particulate matter of seawater, ch. 11 of South Texas Outer-Continental Shelf BLM Study.

Payne, J.R., P.J. Mankiewicz, J.R. Nemmers, R.E. Jordan, I.R. Kaplan, M.I. Venkatesan, S. Brenner, J. Bonilla, D. Meredith, B. Meyers, B. Haddad, A.L. Burlingame, A. Ensminger, G. Gould, and M.L. Moberg. 1978 a. High molecular weight petroleum hydrocarbon analytical procedures. Southern California Baseline Study, Benthic Year II. Volume III, Report 5.0. Final report submitted to the Bureau of Land Management, Department of Interior, Washington, D.C. by Science Applications, Inc.

Payne, J.R., J.R. Clayton, Jr., B.W. de Lappe, P.L. Millikin, J.S. Parkin, R.K. Okazaki, E.F. Letterman, and R.W. Risebrough. Hydrocarbons in the Water Column. Southern California Baseline Study, Vol. III, Report 3.2.3., p. 1-207. 1978 b. Final Report, submitted to the Bureau of Land Management, Washington D.C. by the University of California Bodega Marine Laboratory, Bodega Bay, California, and Science Applications, Inc., La Jolla, California.

Payne, J.R., J.E. Nemmers, R.E. Jordan, P.J. Mankiewicz, A.D. Oesterle, S. Laughon, and G. Smith. Measurement of petroleum hydrocarbon burdens in marine sediments by three commonly accepted procedures: results of a NOAA inter-laboratory calibration exercise, Fall, 1978. Submitted to Dr. John A. Calder, Staff Chemist, OCSEAP, U.S. Department of Commerce, National Oceanic and Atmospheric Administration, Environmental Research Laboratory, Boulder, CO, January 1979. pp. 1-34, plus appendix.

Payne, J.R., G.S. Smith, P.J. Mankiewicz, R.F. Shokes, N.W. Flynn, W. Moreno and J. Altamirano. Horizontal and Vertical Transport of Dissolved and Particulate-Bound Higher Molecular Weight Hydrocarbons from the IXTOC-1 Blowout. Manuscript presented at the RESEARCHER/PIERCE IXTOC-I Symposium, Miami, Florida, June 9-11, 1980. 47 pp.

Teal, J.M., C. Burns, and J. Farrington. 1978. Analysis of aromatic hydrocarbons in intertidal sediments, resulting in two spills of Number 2 Fuel Oil in Buzzard's Bay, Massachusetts. Journal of Fisheries Research Board of Canada 35(5):510-520.

Winters, J.K. 1978. Fate of petroleum derived aromatic compounds in seawater held in outdoor tanks and South Texas Outer-continental Shelf Study-BLM, ch. 12. Draft final report.

Zurcher, F. and M. Thuer. 1978. Rapid weathering processes of fuel oil in natural waters. Analysis and interpretations. Environmental Science and Tech. 12(7):838-843.

U.S. Department of Commerce
National Oceanic & Atmospheric Administration
Office of Marine Pollution Assessment
Alaska Office, RD/MPF24
P.O. Box 1808
Juneau, Alaska 99802